Cretaceous to Paleogene Palinspastic Reconstruction of the East Coast Basin, New Zealand

A critical constraint for the reconstruction of the Zealandia continent, and its evolution from the breakup of Gondwana to the present.

PhD Thesis presented by

Benjamin R. Hines

February 2018

Submitted in fulfilment of the degree of Doctor of Philosophy (PhD)
School of Geography, Environment and Earth Sciences
Victoria University of Wellington

FRONTISPIECE

View over Swale Stream and Coverham, Clarence Valley.

Dedicated to

all the pick axes and boots that were destroyed

during the making of this thesis

Sampling Karekare Formation in Mangaotane Stream, Raukumara Ranges.

ABSTRACT

The East Coast Basin is a Cretaceous-Cenozoic sedimentary basin that largely formed within a passive margin setting, and has subsequently evolved through the Neogene in a convergent margin setting. The position of the basin prior to the inception of the modern boundary between the Pacific and Australian plates has, for many decades, been a contentious issue in paleogeographic reconstructions of Zealandia and the southwest Pacific region. The sedimentary, tectonic and paleoenvironmental development of the basin have substantial importance in understanding the evolution of Zealandia, and resource exploration in the region. However, the pre-Neogene position, orientation and internal deformation of the basin is poorly constrained. To date, paleogeographic reconstructions have utilised the East Coast Basin to accommodate an unknown volume of deformation, with substantial variability between reconstructions. This thesis combines a number of methods and approaches to produce a rigorously tested, palinspastic model for the Cretaceous to Paleogene East Coast Basin that is integrated within the wider Zealandia paleogeographic and tectonic framework.

Late Cretaceous–Eocene marine successions in the basin are dominated by thick, often lithologically monotonous sedimentary units. Moderate- to high-resolution geochemical analysis applied to 1100 samples from late Cretaceous to Eocene stratigraphic sections across Hawke's Bay, Wairarapa and Marlborough, provide a framework for chemostratigraphic correlations across the basin to supplement bio- and lithostratigraphic studies. The Waipawa Formation holds particular interest, as it forms an important isochronous unit, making it possible to establish facies relationships and correlations between multiple sections in various environmental settings and lithostratigraphic associations across the basin. Trace metal indices and organic carbon relationships reveal evidence of shifting paleo-redox conditions during the Late Paleocene, associated with enhanced preservation of terrestrial organic matter. The increased preservation occurs in tandem with increased sedimentation rates, suggesting that sediment supply and burial rate are controlling factors in the source and preservation of organic matter.

Recently developed rigid-plate reconstructions for Zealandia are integrated with geological and geophysical datasets to emplace constraints on the Neogene deformation of the basin. To facilitate reconstruction, the basin was subdivided along major basement-penetrating faults to produce a micro-plate model. Lineations in basement terranes provide piercing points for the base reconstruction, which are utilised in conjunction with paleomagnetic constraints on the rotation

and fault movements of, and between, individual structural blocks to retroactively remove Neogene deformation. Removal of shortening, rotation and lateral displacements establishes a foundation upon which a series of Cretaceous-Paleogene palinspastic reconstructions can be built. These palinspastic reconstructions are then translated into a suite of paleoenvironmental maps through the integration of various datasets, including litho-, bio- and chemostratigraphic and sedimentological measurements, and heavy mineral and detrital grain studies. These data provide insight into environmental and sediment provenance characteristics that are incorporated into paleogeographic reconstructions, in addition to enabling compilation of a composite section used for the identification and interpretation of second- and third-order (1–10 Myr) sequence stratigraphic cycles from the Motuan to Bortonian (c. 105–40 Ma). The joint assessment of multiple provenance indicators informs of sediment sources, supply routes and hinterland tectonics, and basement unroofing and exhumation, contributing to geodynamic models of basin development. A series of paleogeographic maps have been developed for important time-slices through the late Cretaceous to late Eocene, namely the Ngaterian, Piripauan, Haumurian, K-Pg boundary, Teurian, Mangaorapan and Bortonian stages, providing basin-wide temporal and spatial perspectives of ancient depositional environments in a consistent and reproducible format. Information derived from these palinspastic maps has implications for the petroleum prospectivity of the East Coast region, and broader applicability to paleotectonic, paleoclimate, and paleoceanographic research.

TABLE OF CONTENTS

Digital Appendices

LIST OF FIGURES

Chapter One

Chapter Two

2.10 Representative outcrop of Tangaruhe Formation in Mangawarawara Stream.

2.11 A) Rakauroa Member in Pukemuri Stream. B) Rakauroa Member cropping out in Mangahouanga Stream.

2.12 A) Porangahau Member at Old Hill Road, comprised of sandstone-dominated, decimetre-bedded alternating sandstone-mudstone. B) Porangahau Member cropping out at Whangai Bluff, Waimarama, comprised of mudstone dominated, green to dark grey, decimetre-bedded alternating fine sandstone-mudstone.

2.13 A) Upper Calcareous Member cropping out in a road cutting on Ongaonga Road. B) Upper Calcareous Member cropping out at Riversdale.

2.14 Te Uri Member of the Whangai Formation cropping out in the upper Akitio River (Tawanui) section.

2.15 A) Waipawa Formation cropping out in a road cut on Angora Road (Taylor White). B) Waipawa Formation at Kerosene Bluff. C) Waipawa Formation at Te Kaukau Point ('Cleft Section'). D) Waipawa Formation at Kerosene Bluff, showing iron oxides and jarosite on weathered surface. E) Waipawa Formation at Taylor White, showing *Bathysiphon* sp. tubes, and bioturbation trace.

2.16 A) Bortonian-aged Wanstead Formation outcrop at Aropito. B) Mangaorapan Wanstead Formation cropping out at Tawanui. C) Outcrop of Bortonian Wanstead Formation in Pukemuri Stream. D) Slumped, deformed mudstone in Pukemuri Stream.

2.17 Manurewa Formation in Pukemuri Stream.

2.18 A) Dip slopes of the lower Awhea Formation cropping out in Pukemuri Stream. B) Decimetre-bedded, sand-dominated flysch at the base of the Awhea Formation, Te Oroi Stream. C) Mud-dominated, decimetre-bedded flysch in the upper part of the Awhea Formation, Te Oroi Stream.

2.19 A) Mungaroa Limestone cropping out in Pukemuri Stream. B) Channel deposit within the Mungaroa Limestone at Te Kaukau Point. C) The upper micritic limestone member at Te Kaukau Point.

2.20 A) Alternating fine sandstone-mudstone of the Awheaiti Formation in Pukemuri Stream. B) Cross-cutting relationships in Awheaiti Formation, Pukemuri Stream.

2.21 A) Pebbly mudstone at the base of the Pukemuri Siltstone in Pukemuri Stream. B) Rafted sediment blocks in the lower Pukemuri Silstone, Pukeuri Stream. C). Typical Pukemuri Siltstone in Awheaiti Stream (BR34/087020). Hammer for scale. D) Richly-glauconitic sandstone with siderite concretions, amongst pale brown, laminated mudstone in the Pukemuri Siltstone, Pukemuri Stream.

2.22 A) Tectonic melange of the Champagne Formation in Wharekiri Stream. B) Champagne Formation in Ouse Gorge. C) Basal conglomerate of the Champagne Formation in Clarence River. D) Disturbed alternating sandstone-mudstone beds within the Champagne Formation in Ouse Stream.

2.23 A) Outcrop in Wharekiri Stream demonstrating decimetre-bedded Split Rock Formation onlapping onto massive sandstone of the Pahau Terrane. B) Decimetre-bedded, alternating sandstone and mudstone typical of Split Rock Formation in Wharekiri Stream.

Chapter Three

Chapter Four

Chapter Five

Chapter Eight

LIST OF TABLES

LIST OF ENCLOSURES

List of Acronyms

CCP	Cretaceous-Cenozoic Programme
DOP	Degree of Pyritization
DSDP	Deep Sea Drilling Project
ECA	East Coast Allochthon
ECB	East Coast Basin
EF	Enrichment Factor
FID	Flame Ionisation Detector
FRF	Fossil Record File
GSB	Great South Basin
GTS	Geological Timescale
HI	Hydrogen Index
HST	Highstand Systems Tract
ICP-AES	Inductively Coupled Plasma Atomic Emission Spectrometry
ICP-MS	Inductively Coupled Plasma Mass Spectrometry
LOD	Limit of Detection
LOQ	Limit of Quantification
LST	Lowstand Systems Tract
MBIE	Ministry of Business, Innovation and Employment
MFS	Maximum Flooding Surface
MOM	Marine Organic Matter
MRS	Marine Ravinement Surface
NA	Northland Allochthon
NZGTS	New Zealand Geological Timescale
ODP	Ocean Drilling Project
OI	Oxygen Index
OM	Organic Matter
OMZ	Oxygen Minimum Zone
PC	Principle Component
PCA	Principle Components Analysis
POM	Porangahau Member, Whangai Formation
PSF	Petroleum Source Rocks and Fluids
pXRF	Portable X-Ray Florescence
RAK	Rakauroa Member, Whangai Formation
RSE	Regressive Surface of Erosion
RST	Regressive Systems Tract
SAR	Sediment Accumulation Rate
SB	Sequence Boundary
SRA	Source Rock Analyser
TE	Trace Elements
TOC	Total Organic Carbon
TOM	Terrestrial Organic Matter
TSE	Transgressive Surface of Erosion
TST	Transgressive Systems Tract
TUM	Te Uri Member, Whangai Formation
UCM	Upper Calcareous Member, Whangai Formation
XRD	X-Ray Diffraction
XRF	X-Ray Florescence

ACKNOWLEDGEMENTS

This thesis has by no means been a solo effort – from my supervisory team, to the friends who helped out with field work, analyses, editing, or general distractions – all have helped me get to this point and I wish to acknowledge you all. Particular thanks must go to James Crampton, who bore the brunt of my odd questions and requests, and who often ended up in the position of playing both good cop and bad cop – eventually banning me from any further field work! Likewise to Kyle Bland, who was a laid-back and easy-going as you could possibly wish for in a supervisor, yet still managed to produce ridiculously detailed revisions. Thanks to these tolerant supervisors who let me disappear for months at a time on voyages, into the bush, kayaking the Cook Strait, various overseas adventures from the Himalayas, to the Arabian Desert, to tropical seas, to the Rockies, the Italian Alps… and never said a word. Couldn't ask for better. Couldn't have done this without you. I would like to express my gratitude to Diane Seward, who oversaw the fission track component of this study, it is an incredible dataset and will certainly be published in the future.
So much thanks needs to be given to Katie Collins. She was always there to lend a hand (even when she's in Chicago), and helped enormously with editing manuscripts, applied statistics, and general enthusiasm (so much enthusiasm) for my research. Thanks to Michael Gazley, without whom, this thesis would have taken a very different direction, and I probably would have never produced the geochemical dataset presented herein. Thanks to Hannu Seebeck, who in many regards acted as an additional supervisor while working through the tectonic reconstruction. Thanks to Mike Hannah, who in James' and Katie's general absence had to deal with the daily 'look what I did' (I just wish you'd actually pin the pictures on the fridge).

Thanks to Mum and Dad, who never tire of asking "when will it be done?", but who are also always there to support me in whatever way. I am grateful to my sister Laura, whose continued support, interest and enthusiasm in what I do was greatly appreciated. And cheers to my brother Wally, who's decided that now that I'm finished, it's now my turn to work on the farm!

To Kelly, Daniel, Elliot, Max, Bella, Steven, Danny, Trace, Valerie, Ann, Lauren, Matt and Dez, and all the others over the past few years, who kept me distracted, be it fishing and diving throughout the summer, and mountains in the winter, squash, football or a few beers, it was all welcomed. Jenni and Georgia, I could always count on you to be up for coffee, beer, or whiskey, whenever it was called for, regardless of the time of day. You guys got me through!

I would like to express my gratitude to the technical and office staff, who have been extremely helpful through the course of this thesis, and at the end of the day, are always keen to sit back and have a beer. It's appreciated!

Special thanks to Jordy, who has patiently put up with the field trips, the absences, and the long hours. Thank you for all you've done, you've been truly amazing. I'm looking forward to our future adventures and endeavours now that I'm unencumbered by this little beastie. Despite the time it's kept me away, if it wasn't for this thesis, we probably wouldn't have met!

Perhaps the greatest thanks might have to go to my various office mates throughout this thesis (Melissa, Marcel, Tom and Jürgen), who have somehow survived the various experiments with gravity (and mass flow mechanisms) that I routinely conduct in the office. Thanks for tolerating the chaos and the carnage.

Particular thanks to Des Darby and GNS Science for awarding me the Sarah Beanland Memorial Scholarship – this research would not have happened without it. Thanks to OMV New Zealand, who funded the final few months of my PhD research, and to the Geoscience Society of New Zealand, who awarded me the travel grant that got me to Italy.

I would like to take a moment to acknowledge all those beneficial discussions, particularly with Hugh Morgans, Chris Clowes and Nick Mortimer, but also Harry Rowe, Alan Clare, Andy Nicol, Peter King, Richard Sykes, and Brad Field. You've all contributed to the construction of this manuscript in various ways.

Chapter One

INTRODUCTION

"The area covered by this paper is so great, and the country so broken and difficult to access, that a complete survey would occupy more than one season of continuous work."

-J. Allan Thomson (1913). Results of field work. New Zealand Geological Survey 7th annual report 122-123.

Northeast-facing view from Castlepoint over the East Coast, North Island.

Page intentionally left blank for formatting purposes

Chapter One

INTRODUCTION

1.1 Rationale

This study presents a comprehensive, multi-disciplinary, tectono-, chemo-, and sequence-stratigraphic investigation into the geological evolution of the Late Cretaceous to Eocene sedimentary succession in the Hawke's Bay, Wairarapa and Marlborough regions of the East Coast Basin, eastern New Zealand. The main aim is to reconstruct the paleogeography of the pre-Neogene East Coast Basin by assessing the stratigraphic architecture, the organic- and inorganic geochemical properties of the basin fill, and paleoenvironmental (water depth and oceanicity) changes through time. Paleoenvironmental information is combined with a retro-deformed block model of the East Coast region that accounts for structural deformation and dislocation associated with the Neogene development of the Hikurangi subduction margin. The resulting integration of the discrete tectonic and sequence stratigraphic frameworks facilitate the production of a series of spatially- and temporally-constrained, palinspastic paleogeographic maps.

Sedimentary fill in the East Coast Basin records the final stages of subduction beneath eastern Gondwana in the Early Cretaceous, the separation of Zealandia from Gondwana in the mid-Cretaceous, a phase of passive thermal subsidence, the re-inception of subduction beneath eastern North Island, and ongoing convergent-margin tectonics. Because of this, many phases in the evolution of the Pacific-Australia plate margin can be constrained through analysis of the basin's outcropping stratigraphy. Reconstruction of the Cretaceous to Paleogene East Coast Basin allows us to better understand the conditions prior to the development of the modern Hikurangi subduction margin, and the progressive development of the margin. Historically, there has been a lack of consensus on the relative geographical position or configuration of the East Coast Basin in pre-Neogene times. This partly stems from the absence of clear piercing points that would constrain fault offsets east of the Esk Head Melange—a unit of basement rocks—whereas elsewhere in New Zealand, prominent basement markers and lineations provide a clear basis for reconstructions.

Parts of the East Coast Basin contain thick sedimentary sequences that have previously not been interpreted in a sequence stratigraphic framework. The facies architecture of the basin can contribute to global models of sea-level variability prior to the development of large-scale ice sheets and the associated cyclical sea-level variability they induce. In addition, better understanding of

the basin's facies architecture provides insights into pre-Neogene tectonic signals, useful for the comparison of regional- and inter-basinal events. Furthermore, understanding the depositional setting of the pre-Neogene basin fill, and the oceanic conditions into which such rocks were deposited, provides critical new insights into the properties and potential of petroleum source rocks (primarily the late Paleocene Waipawa Formation) within the East Coast Basin.

This project culminates in the production of a series of palinspastic reconstructions for the East Coast Basin, which have been developed using a multi-disciplinary approach. Four primary research outcomes of this project are:

1. Definition of spatial and temporal relationships between depositional environments for the Late Cretaceous to late Paleogene succession of the East Coast Basin.
2. Derivation of a sequence stratigraphic framework for the East Coast Basin, following on from point 1.
3. Constraints on the extent of Neogene deformation on the pre-Miocene sedimentary succession, and the development of a tectonic model for the East Coast region.
4. Integration of the tectonic model (point 3) with stratigraphic data (points 1 & 2) as a base for paleogeographic reconstructions and production of a series of 'time-slice' palinspastic maps for the East Coast Basin.

1.2 Geographic Setting

The East Coast Basin, North Island, New Zealand, lies across the onshore and marine realms, and covers approximately 75,000 km^2, from East Cape in North Island, through to the Kaikoura Peninsula in South Island (Figure 1.1; Field, Uruski *et al.,* 1997; King *et al.*, 1999). The basin reaches elevations of up to 2880 m above sea level, and occurs in water depths of *ca.* 1000 m below sea level (Leckie *et al.*, 1992). The northern and western boundaries are marked by the North Island axial ranges (Figure 1.2), with an offshore continuation along the East Cape Ridge (the Raukumara, Ruahine, Tararua, and Rimutaka ranges; Cashman *et al.*, 1992; Davey *et al.*, 1997; Sutherland *et al.*, 2009). The Raukumara Basin lies to the north and west of the East Cape Ridge (Figure 1.1). The western boundary of the East Coast Basin in North Island is delineated by the Wairarapa and Wellington-Mohaka-Whakatane Fault systems along the eastern margins of the axial ranges (Figure 1.2; Beanland *et al.*, 1998; Nicol *et al.*, 2007). The eastern and southern boundary of the basin is demarcated offshore by the Hikurangi subduction interface (Figure 1.2; Uruski *et al.* 2005; Uruski

et al. 2006; Bland *et al.*, 2015). Onshore, the southern boundary is marked by a structural high, the Hurunui High, which is effectively a westward extension of the Chatham Rise that separates the Pegasus and Canterbury basins (Figure 2.1; Field & Browne *et al.*, 1989; Crampton *et al.*, 2003).

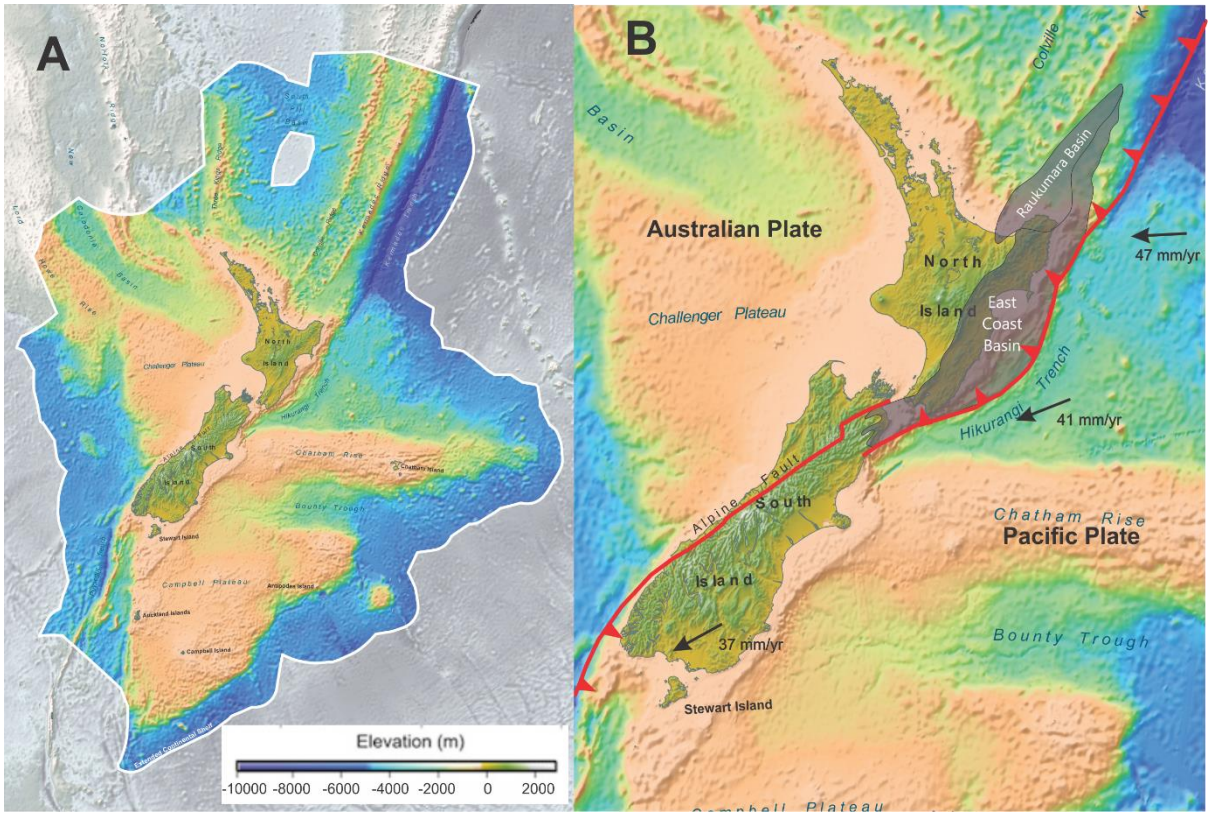

Figure 1.1: A) Map of New Zealand and bathymetric features, with the New Zealand exclusive economic zone outlined. B) Location of the East Coast Basin, and the Raukumara Basin; vectors indicate direction and magnitude of modern Pacific Plate convergence relative to the Australian Plate. Source GNS Science (left), adapted from GNS Science (right).

The East Coast Basin has been deformed extensively, having been dissected, dislocated and re-oriented following the inception of the Hikurangi subduction margin through the basin in the Late Oligocene–Early Miocene. Different authors have applied different terminology to describe essentially the same structural and physiographic divisions of the East Coast Basin (e.g., Pettinga, 1982; Berryman *et al.*, 1989; Ballance, 1993a; Lewis & Pettinga, 1993). The basin is partitioned into four major physiographic divisions that reflect the modern tectonic regime (from west to east): the North Island axial ranges, the forearc basin, the coastal ranges, and the continental slope. The North Island axial ranges mark the boundary from compressional deformation in the east into

strike slip deformation to the west, whereas the coastal ranges mark the onshore expression of the accretionary wedge, with the intervening area forming the present-day forearc (Figure 1.2).

The age of the sedimentary fill within the basin ranges from latest-Early Cretaceous through to Quaternary, and is of the order of 10,000 m-thick in the thickest and most complete sections of the basin (Grindley, 1960; Field, Uruski *et al.*, 1997; Begg & Johnston, 2000; Lee & Begg, 2002). Within the basin, the Cretaceous to Paleogene succession has been divided into two northeast-southwest oriented, elongate, geographic/spatial domains, the eastern and western sub-belts, characterised by distinct stratigraphic motifs, based on facies changes within early-Late Cretaceous to Paleocene strata, the distribution of late Cretaceous volcanogenic units and the degree of tectonic deformation (Figure 1.2; Moore *et al.*, 1986; Moore, 1988a, 1988b; Crampton *et al.*, 2006). In addition to the sub-belt scheme, Moore (1988b) also defined a series of structural blocks, divided on the basis of lithological affinities and bounded by major structures. The Marlborough region is widely accepted as falling within the western sub-belt, on the basis of lithological characteristics (Crampton, 1997; Field, Uruski *et al.*, 1997; Crampton *et al.*, 2003, 2006).

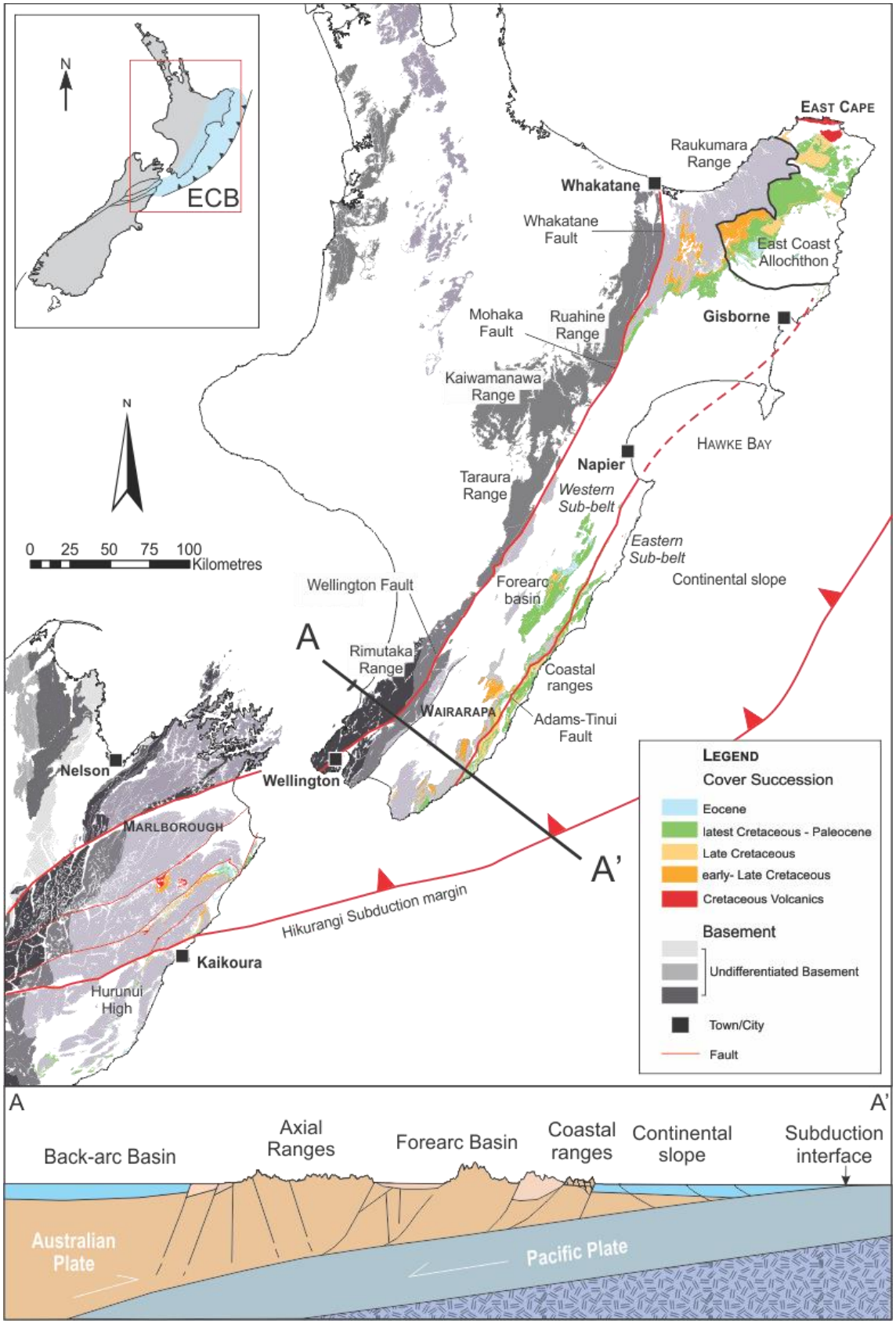

Figure 1.2: Major tectonic and physiographic features of the East Coast Basin (ECB). Sub-belt boundaries from Moore (1988a). Cross section A-A' modified from Hines et al. (2013). Data for base map sourced from Heron (2014).

1.3 Geological History & Tectonic Setting

The Torlesse Composite Terrane (comprised of the Rakaia, Kaweka and Pahau basement terranes) and Murihiku basement terranes that underlie eastern New Zealand originated in association with a subduction zone along the eastern Gondwana margin during the Permian to latest Early Cretaceous, providing an inherited structural lineation of basement fabrics (Sutherland, 1999a, 1999b; Mortimer, 2014; Lamb *et al.*, 2016). The Late Jurassic to Early Cretaceous period, as recorded by the Pahau Terrane in eastern New Zealand, likely developed within a series of depositional basins along a section of the accretionary wedge on the convergent margin of eastern Gondwana (Bassett & Orlowski, 2004; Adams *et al.*, 2013a). Subduction at the margin of Gondwana continued until the Early Cretaceous (110–100 Ma; Davy *et al.*, 2008), with the East Coast Basin developing subsequently as one of several near-continuous basin depocentres oriented margin-parallel at this time (the other basins being the Raukumara, Pegasus and Canterbury basins).

The Gondwana margin was deformed and uplifted in the latest Jurassic to earliest Cretaceous, due to the arrival and collision of the Hikurangi Plateau at the westward dipping Chatham Rise subduction trench. The plateau is interpreted as mass of unusually thick (12–15 km) oceanic basaltic crust, which effectively choked the subduction zone at *ca.* 105 Ma, resulting in a substantial plate reorganisation (Davy *et al.*, 2008; Collot *et al.*, 2009; Adams *et al.*, 2013a). Cessation of subduction on at least the Chatham Rise sector of the Gondwana margin resulted in paleogeographic and paleotectonic changes during the earliest Late Cretaceous, including widespread Late Cretaceous extension, with rifting of the old Gondwana margin centred on the modern-day Tasman Sea (Kamp, 1986; King *et al.*, 1999; Strogen *et al.*, 2017). Subduction in parts of the East Coast Basin may have continued until ~85 Ma (Mazengarb & Harris, 1994; Kamp, 1999; 2000; Crampton *et al.*, *in prep.*). Plate reconfiguration resulted in the breakup of Gondwana, and the proto-New Zealand subcontinent (Zealandia) was completely separated from the rest of Gondwana by the Late Cretaceous (e.g., Kamp, 1986; King *et al.*, 1999; Strogen *et al.*, 2017). During this time, the abandoned trench in the east was progressively infilled, forming the base of the cover sequence and the foundations for the East Coast Basin (Crampton, 1997; Field & Uruski *et al.*, 1997).

Seafloor spreading in the Tasman Sea region resulted in the rifting of proto-New Zealand from the eastern Australian margin in the Late Cretaceous, and continued through to the late Paleocene (Gaina *et al.*, 1998). Progressive migration away from the active rift zone resulted in the thermal relaxation and gradual subsidence of the New Zealand region (Ballance, 1993b). Consequently, the

Late Cretaceous–Paleogene strata of the East Coast Basin are dominated by thick successions of largely homogenous, fine-grained, deep marine sedimentary rocks characteristic of a passive margin depositional setting (Moore, 1988a; Field & Uruski *et al.*, 1997; King, 2000a, 2000b; Mazengarb & Speden, 2000; Lee & Begg, 2002; Lee *et al.* 2011).

The East Coast region remained relatively quiescent until the middle to late Eocene, when a major plate reorganisation affected the entire southwest Pacific between 50 and 40 Ma, possibly a consequence of the collision of the Indian Plate with Southeast Asia (Hall, 2002). This reorganisation initiated the development of the modern Australia–Pacific plate boundary through the New Zealand region. Ophiolite obduction in New Caledonia, north of New Zealand, suggests that instigation of convergent tectonics commenced on the margin during the mid-Eocene (48 Ma; Aitchison *et al.*, 1995; Cluzel *et al.*, 2006; 2010). The plate boundary began to evolve in southern New Zealand during the middle to late Eocene in response to sea-floor spreading and the formation of oceanic crust in the Emerald Basin, and the development of a zone of actively subsiding, extensional basins that propagated northwards from the southwestern South Island to the southern Taranaki Basin (Sutherland, 1995, 1999a; King & Thrasher, 1996; King, 2000a; Sutherland *et al.*, 2000; Cande & Stock, 2004). The nature of the Eocene plate boundary in the intervening area between the Emerald Basin and New Caledonia is poorly constrained at this time (Sutherland, 1995; Mortimer, 2014).

The southeast migration of the Australian-Pacific plate Euler pole from 30 Ma (Sutherland, 1995), resulted in the southward propagation of the subduction margin into the New Zealand region in the late Oligocene–Early Miocene. Subduction had initiated beneath Northland by the early Miocene (Isaac *et al.*, 1994), and initiation of subduction along the Hikurangi margin is marked by the obduction of the Northland and East Coast allochthons between 20–23 Ma (Stoneley, 1968; Balance & Spörli, 1979; Rait *et al.*, 1991; Mazengarb & Harris, 1994; Isaac *et al.*, 1994, 1996; Herzer, 1995; Field, Uruski *et al.*, 1997; Mortimer *et al.*, 2003; Bradshaw, 2004; Schellart, 2007), along with coeval thrusting and the emplacement of olistostromes in the Wairarapa and Marlborough regions (Chanier & Ferriere, 1991; Delteil *et al.*, 1996, 2006). The developing subduction zone propagated south during the Miocene, likely in response to slab roll back of the Pacific Plate (Schellart *et al.*, 2006). The exact orientation and configuration of the Early Miocene plate boundary in northern New Zealand remains a contentious issue, with widely varied interpretations and reconstructions for the East Coast region (Figure 1.3). However, several lines of geological evidence provide constraints on the aspects of the development of the plate margin, including south-westward transport directions for the Northland and East Coast allochthons (Stoneley, 1968; Rait, 2000), and the trend of the Northland Arc (Herzer, 1995). However, the fold-thrust belt associated with

initiation of Neogene subduction, along with structural data from basement terranes, have a northeast–southwest trend, indicating that this portion of the margin has rotated ≥90° to its current orientation since the Early Miocene, consistent with vertical axis rotation derived from paleomagnetic studies of the region (Walcott, 1989, 1998; Rowan *et al.*, 2005; Rowan & Roberts, 2006; Hall *et al.*, 2004; Randall *et al.*, 2011; Lamb, 2011). Either underplating of buoyant continental crust in the southern end of the Hikurangi subduction margin (Walcott, 1989; Barnes & Lepinay, 1997), and/or the Chatham Rise impinging on the South Island (e.g., Wallace *et al.*, 2004) has been suggested as the cause for the locking of the plate interface, providing a coupling around which the Hikurangi margin has rotated clockwise through the Neogene.

Despite these understandings, it remains difficult to reconcile the estimated ≥90° of vertical-axis rotation on the Hikurangi margin with deformation trends within the New Zealand region (Nicol *et al.*, 2007). Such a substantial rotation would require significant shortening in the southern Hikurangi margin, yet seismic interpretation and balanced cross sections indicate only ~30 km of Neogene shortening in southern Wairarapa (Nicol & Bevan, 2003; Nicol *et al.*, 2007). Similarly, the relatively low metamorphic grade of basement strata exposed in the East Coast Basin and the North Island axial ranges (e.g., Jiao *et al.*, 2015), is inconsistent with a high amount of Neogene rotation and shortening.

The Neogene structural style is primarily compressional, including the Early Miocene emplacement of thrust sheets in East Cape, southern Hawke's Bay and Marlborough (Rait *et al.*, 1991; Delteil *et al.*, 2006). Compressional and dextral strike-slip faulting has continued to the present, with the largest proportion of dextral faulting occurring since the Late Miocene (Cashman *et al.*, 1992; Beanland *et al.*, 1998; Barnes *et al.*, 2002; Kamp, 1987; Bland & Kamp, 2006; Nicol & Wallace, 2007). The transition of arc volcanism from the Kaimai-Tauranga volcanic centre and associated onset of extension within the Taupo Volcanic Zone at 2 Ma (Wilson & Rowland, 2016), and the initiation of dextral strike-slip displacements on the North Island Dextral Fault Belt (Beanland, 1995; Beanland *et al.*, 1998) resulted in further changes, to produce the current tectonic regime.

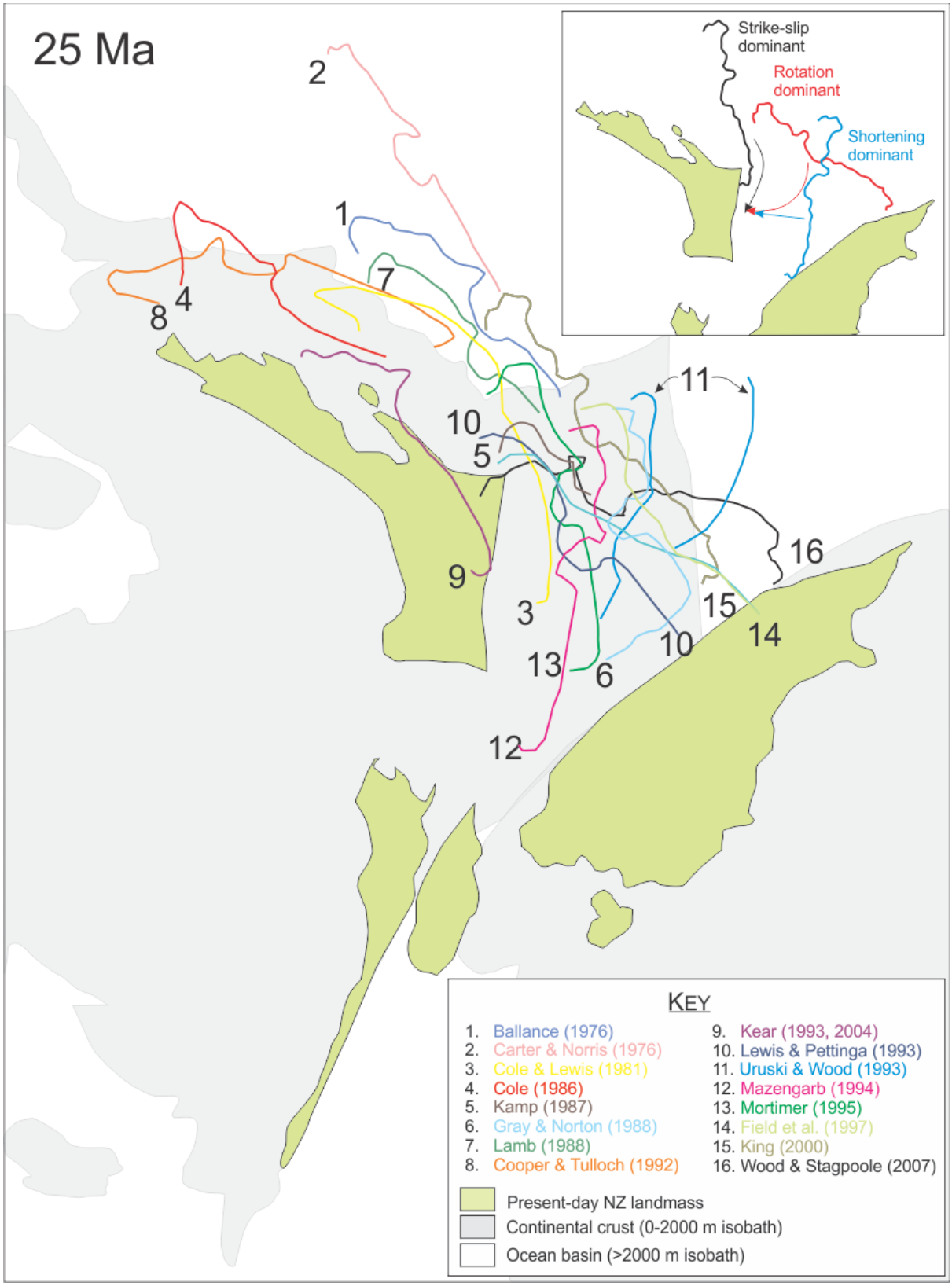

Figure 1.3: Location of the eastern North Island in various pre-Miocene reconstructions of the proto-New Zealand subcontinent. Inset shows the outcome of the relative position of eastern North Island based on the dominant mode of deformation adopted by any particular reconstruction. Figure modified from King (2000a) and Wood & Stagpoole (2007).

1.4 Specific Research Questions

1) *Can constraints be placed on paleoenvironmental changes through time, across structural divisions, to assist in the development of paleogeographic reconstructions for the East Coast Basin?*

In order to reconstruct the development of the basin, the outcropping late Cretaceous–Paleogene stratigraphic succession has been interrogated to provide paleoenvironmental information that can supplement and support paleogeographic reconstructions (e.g., water depth, continental slope direction, water current direction). This component of the study included detailed logging of measured sections, and interpretation of facies, paleoenvironments, and depositional relationships. In addition, extensive databases of existing measured sections, including the East Coast Cretaceous-Cenozoic Programme (CCP) and published sections were also used. Characterisation of rapid vertical and lateral facies changes, and the application of revised age control has been important for the determination of paleogeographic and paleoenvironmental boundaries.

2) *Can bulk-rock geochemistry be applied to resolve changes in provenance, paleo-redox conditions and paleoenvironmental settings?*

The development of portable X-ray florescence technology enables the rapid and accurate collection of large bulk-rock geochemical datasets. Whereas this methodology is typically applied in industry-based studies of metamorphic and igneous ore bodies, there are studies that suggest the integration of this approach with conventional organic and inorganic geochemical analyses may provide useful insights into provenance and paleo-redox states and, by association, paleoenvironmental setting and conditions. Applying this method at a basin-wide scale allows the development of a chemostratigraphic framework, within which conventional lithostratigraphic, provenance (detrital zircon, heavy minerals assemblages) and source rock analyses may be placed. Integrating these chemostratigraphic approaches into the existing stratigraphic framework provides new constraints on Late Cretaceous–Eocene paleoenvironmental conditions and provides a new tool for correlating lithologically monotonous mudstone formations prospective for petroleum resources in the sedimentary basins of New Zealand.

3) *Can Neogene deformation be back-stripped to produce a pre-Miocene structural reconstruction of the East Coast Basin?*

Regional paleogeographic reconstructions typically treat the East Coast Basin simply as a single crustal block (e.g., King, 2000a). The approach of Crampton *et al.* (2003) and Lamb (2011) in dividing the region into component structures provides a more realistic means of determining the degree and nature of Neogene deformation that can then be back-stripped, and integrated into regional paleogeographic reconstructions. The palinspastic reconstruction of Crampton *et al.* (2003), for the late Cretaceous–Paleogene Marlborough region of the East Coast Basin, acts as a model for the approach of this study. However, more recent and comprehensive paleomagnetic datasets for the region (e.g., Randall *et al.*, 2011; Lamb, 2011; Dallanave *et al.*, 2015, 2016) are now available, making a review of this reconstruction and a basin-wide expansion of the model timely. Integration of recent paleomagnetism studies, along with rotation and fault slip information for pre-Neogene strata, provide constraints on the rotation and lateral displacement of structural blocks. This then allows for the retro-active back-stripping of Neogene deformation, ultimately cumulating in a pre-Neogene base model that facilitates paleogeographic reconstructions for the late Cretaceous–late Paleogene East Coast Basin (Figure 1.4).

4) *Can the signatures of global eustastic sea-level change be discriminated from tectonics in the Cretaceous-Paleogene stratigraphic successions in the East Coast Basin?*

Previous studies have failed to determine a long-ranging sequence stratigraphic framework in the New Zealand Cretaceous-Paleogene succession that has resolved events below the 10–100 Ma period. Through the application of detailed stratigraphic analysis and identification of key surfaces, is it possible to resolve a meso-scale (1–10 Ma frequency) sequence stratigraphy for the Cretaceous–Paleogene succession of the East Coast Basin? This is particularly important in determining the depositional controls within the basin - is sedimentation governed by sea level variability, local and/or regional tectonics, or a combination thereof? The application of apatite fission-track modelling in tandem with 1-dimensional basin modelling help to constrain the timing of tectonic controls in the basin, particularly the onset of passive margin thermal subsidence.

5) How has the Paleogeography of the East Coast Basin evolved through the Cretaceous–Paleogene?

The broad structural divisions of the North Island sector of the East Coast Basin, as defined by Moore (1988a), the regional paleogeographic reconstructions of King (2000a), Strogen *et al.* (2017) Arnot & Bland *et al.* (2016), Sahoo & Bland *et al.* (2017), and the palinspastic models of the Marlborough region produced by Crampton *et al.* (2003), provide a starting framework for this present study. Integration of the pre-Neogene structural reconstruction and a base layer for the addition of stratigraphic and paleoenvironmental datasets enables the development of a series paleogeographic reconstructions. These reconstructions are presented as a series of 'time-slice'-style palinspastic maps for selected intervals to reveal the Cretaceous–Paleogene evolution of the basin. Additional insights into the evolution of the basin obtained from paleoenvironmental and provenance information are integrated into and projected onto these palinspastic reconstructions.

1.5 Study Design

This thesis synthesizes disparate strands of new and existing research to produce an integrated paleogeographic study of the Cretaceous-Paleogene stratigraphy of the East Coast Basin. Stratigraphic sections provide archives recording environmental histories that vary spatially and temporally. To utilise these records, detailed examination of existing measured sections, in particular sections from the East Coast CCP (Field & Uruski *et al.*, 1997), as well as Moore (1988a; 1988b) and Crampton (1997), have been used to identify important sections for this study. Supplementary sections were measured and sampled in various localities, to characterise the abrupt vertical and lateral facies changes that are known to occur in the Cretaceous–Paleogene succession, and to identify any unknown and unquantified relationships across structural boundaries (e.g., Moore *et al.*, 1986; Moore 1988a; 1988b; Crampton, 1997; Laird *et al.*, 2003; Hines *et al.*, 2013). Detailed sample suites through stratigraphic columns were then analysed, primarily using bulk rock geochemical analytical methods (XRF, pXRF, XRD, SRA, and ICP-MS), to provide information on provenance and environmental characteristics, allowing the definition and distinction of important intervals for use in paleogeographic reconstructions (Figure 1.4). Detrital zircon and heavy mineral assemblage and compositional studies provide information about hinterland uplift, erosion, source regions and depositional pathways.

A tectonic model for the East Coast Basin and the wider New Zealand region was constructed in the open-source GPlates software (Boyden *et al.,* 2011; Qin *et al.*, 2012), through the application of retroactive deformations across a series of timeplanes between the present and the late Eocene.

This resulted in a structural model that has had all Neogene deformation removed, acting as a template for paleogeographic reconstructions for late Cretaceous-Paleogene depositional environments. Development of the structural model was an iterative process, incorporating vertical axis rotations, basement marker piercing points, definition of structural blocks (based on major structural divisions), strike-slip estimates, and shortening estimates (Figure 1.4).

Revised age control, and a basin-wide assessment of facies trends, paleoenvironments and stratigraphic relationships, have enabled the development of a sequence stratigraphic framework. When these datasets are incorporated into the pre-Neogene structural model for the East Coast Basin, a series of palinspastic reconstructions through the Late Cretaceous to Paleogene are produced.

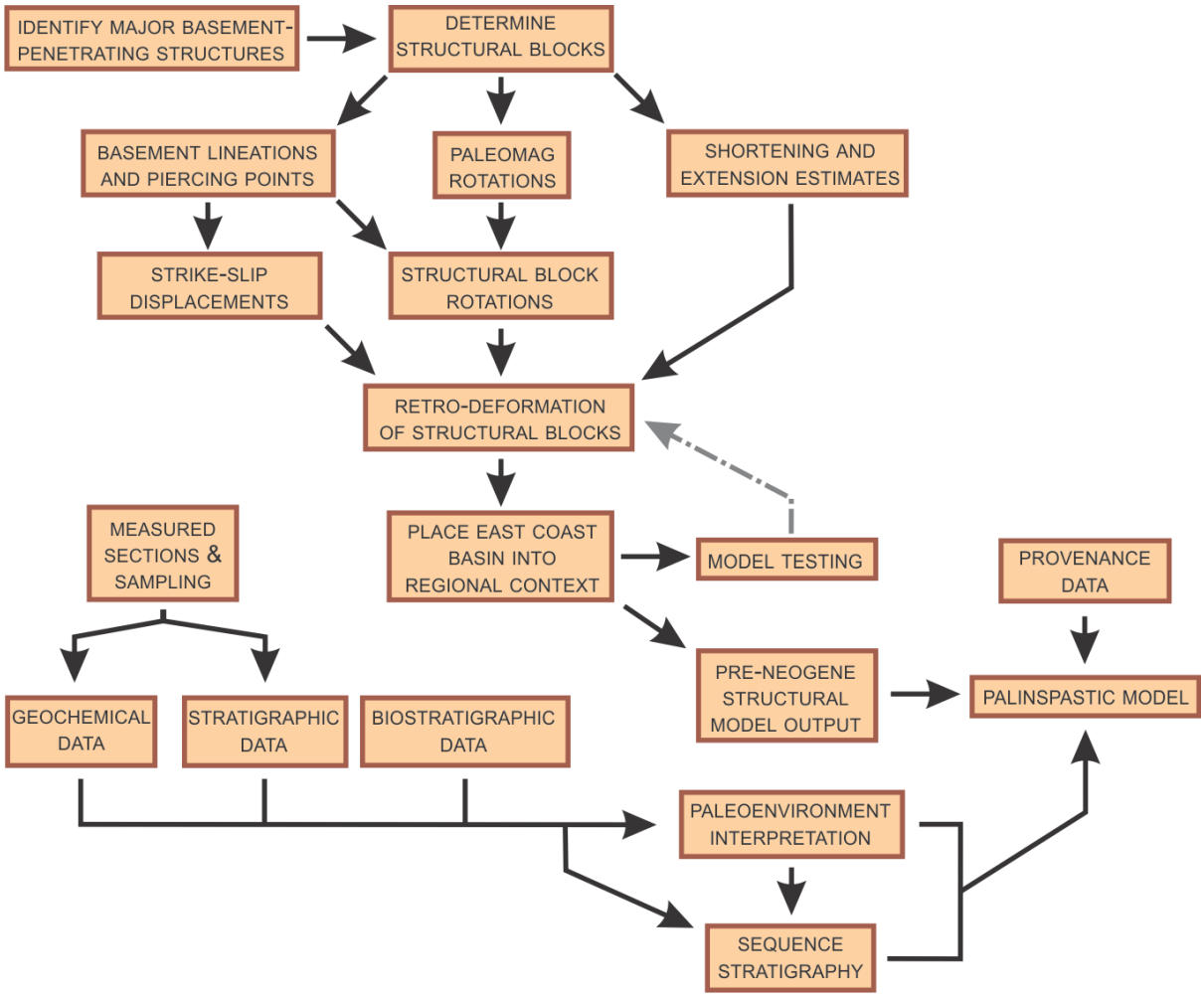

Figure 1.4: Generalised workflow for the various components of this thesis, culminating in the development of a palinspastic reconstruction for the East Coast Basin.

1.6 Thesis Objectives

Specific objectives and aims determined for this project include:

1) Establish a revised lithostratigraphy for the Hawke's Bay, Wairarapa and Marlborough regions of the East Coast Basin. This draws upon recently acquired paleontological age control (Chapter Two).
2) Identify and characterise a surface suitable for correlation across structural blocks (Chapters Three & Four).
3) Characterise the internal variability and facies architecture of the latest Cretaceous to Eocene passive margin succession (Chapters Three, Four, & Seven).
4) Determine a sequence stratigraphic framework for the late Cretaceous to Eocene sedimentary succession of the East Coast Basin (Chapter Seven).
5) Develop a tectonic reconstruction for the East Coast Basin that honours geophysical, lithostratigraphic, biostratigraphic and paleoenvironmental constraints (Chapter Five).
6) Apply paleoenvironmental data to the tectonic reconstruction of the East Coast Basin to reconstruct the paleogeographic development of the basin, including global sea-level changes and regional tectonic events, ultimately to produce a series of palinspastic, time-slice maps (Chapter Eight).

1.7 Research Outcomes

Research undertaken during the course of this thesis has resulted in a new depositional model for the Whangai, Waipawa and Wanstead formations, of which the Whangai and Waipawa formations form important prospective source rocks in the East Coast Basin (e.g., Moore *et al.*, 1987; Moore, 1989a; Killops *et al.*, 2000; Hollis *et al.*, 2006, 2014; Sykes *et al.*, 2012). Data collection during the course of this thesis has resulted in the doubling of the available source rock analyses of the prospective Waipawa Formation, and the development of moderate- to high-resolution organic and inorganic geochemical datasets through detailed measured sections, in a manner that has not previously been applied to the East Coast Basin. Sampling, analyses and data interpretation have contributed towards objectives (PSF Task 1.5) of the GNS Science Source Rocks and Fluids programme. Source rock, sequence and chemo-stratigraphic analyses, tectonic reconstructions and the series of palinspastic maps produced during this thesis have made important contributions towards the Petroleum Basins Research Frontiers Taskforce project at GNS Science.

In addition to this, the development of a third-order sequence stratigraphic framework for the East Coast Basin has informed depositional models for the region, as well as allowing the identification and differentiation of sea level and tectonic events, and the characterisation of latest Cretaceous and Paleogene stratigraphic architecture. Furthermore, detailed assessment of the stratigraphy in the southern Wairarapa and Marlborough has improved stratigraphic correlations across Cook Strait.

The primary outcome of this thesis is a series of palinspastic maps for the East Coast Basin across selected intervals that can be integrated with existing reconstructions for the Reinga, Northland, Taranaki, and Deepwater Taranaki basins, and the Canterbury-Great South basins (Strogen *et al.*, 2014, 2017; Arnot & Bland *et al.*, 2016; Sahoo & Bland *et al.,* 2017). These maps contribute to the GNS Science Cretaceous paleogeographic mapping programme ('Zmap').

1.8 Conventions Applied in this Thesis

A combination of international and New Zealand stages are used throughout the thesis. Use of New Zealand stages reflects the dominantly biostratigraphic age control on the sedimentary succession, and the often largely endemic fossil faunas in the New Zealand region (Cooper, 2004), which are tied to the New Zealand geological timescale (NZGTS; Figure 1.5; Crampton *et al.*, 2004a; Raine *et al.*, 2015). Cretaceous sedimentary rocks of the East Coast Basin typically contain no, to few age-diagnostic foraminifera, so biostratigraphic age control is often entirely reliant on inoceramid and *Aucellina* bivalves, and dinoflagellate assemblages (e.g., Roncaglia *et al.*, 1999; Crampton *et al.*, 2000, 2001, 2004a; Schiøler *et al.*, 2002). Conversely, Paleogene strata of the East Coast Basin generally lack macrofossils, but produce reasonable microfossil faunas (foraminifera, dinoflagellates and calcareous nannofossils; e.g., Moore & Morgans, 1987; Strong *et al.*, 1995; Crouch *et al.*, 2014; Kulhaneek *et al.*, 2015; Morgans, 2016). Biostratigraphic data has been primarily sourced from the Fossil Record Electronic Database (FRED), which has been an invaluable resource in the determination of age and paleoenvironmental information for this study.

In some instances, Cretaceous–Paleocene strata have dinoflagellate or calcareous nannofossil age control that can be correlated to the international timescale. Local stages are given preference herein, although in the circumstances where the local stages are particularly long-ranging (e.g., the Haumurian, 22.4 Ma; Figure 1.5), international stages are applied if they provide a useful subdivision. Throughout this study, geological ages are given in terms of the latest New Zealand geological timescale (NZGTS; Raine *et al.*, 2015; Figure 1.5), which has been calibrated to the International Geological Timescale (GTS; Gradstein *et al.*, 2012). Age-dependent data from older publications has been calibrated to the GTS12. When referring to geological periods, epochs, and stages, the qualifiers Early, Middle and Late (capitalised) are used when such periods have been formally defined. The use of early, middle, and late (lower case), infers an informal use of the terms. In this thesis, a widely used example of this is "mid-Cretaceous", which has no formal definitions, but is a convenient informal qualifier to denote the approximate initiation of the cover succession in the East Coast Basin.

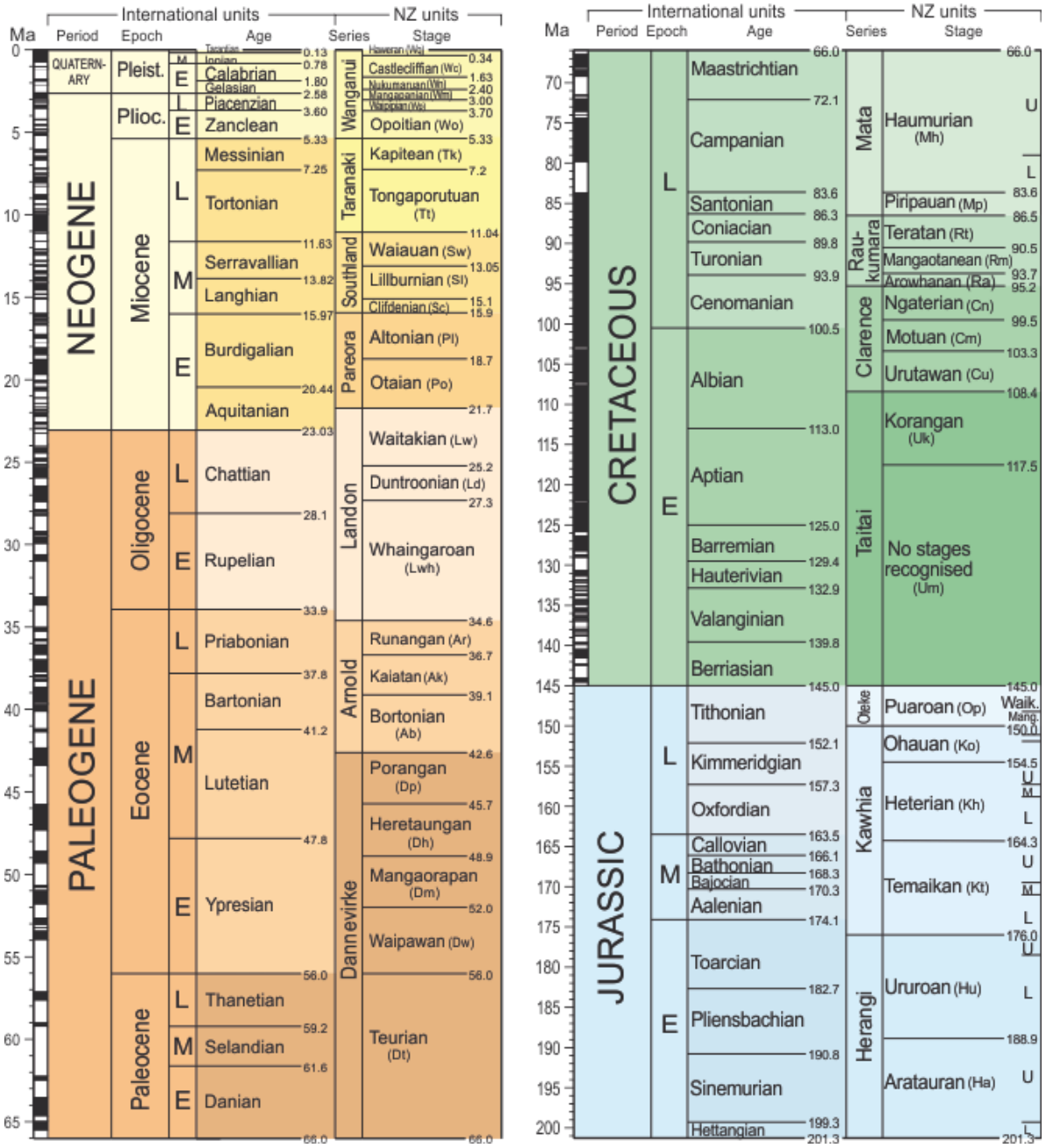

Figure 1.5: The New Zealand Geological Timescale (NZGTS15), alongside the international geological timescale of Gradstein *et al.* (2012). Figure modified from Raine *et al.* (2015).

Indicators of paleoenvironmental conditions useful for palinspastic reconstruction include paleocurrent and paleoslope indicators (Figure 1.6). Paleocurrent directions can be determined from long-axis orientation of clasts, belemnites (Figure 1.6A), turritellid gastropods (Figure 1.6B), large elongate foraminifera (e.g. *Bathysiphon* spp.), or measurement of flute casts, parting current lineations, and asymmetric ripples. Paleoslope directions are determined from the orientation of the axial plane of syn-depositional slump folds, formed by the plastic deformation of soft sediment

(Figure 1.6C, D). All estimates of paleocurrent and paleoslope have been corrected for local tilting and folding of strata using stereographic projection.

The East Coast CCP (Field, Uruski *et al.*, 1997) is referred to extensively throughout this thesis, providing summary of much of the initial framework that this study is largely built upon. The CCP was a project of the New Zealand Geological Survey (now GNS Science) to describe the (then) known Cretaceous and Cenozoic sedimentary basins around New Zealand. Description and identification of basement divisions is based on the basement terrane nomenclature of Mortimer *et al.* (2014), and is applied throughout the thesis.

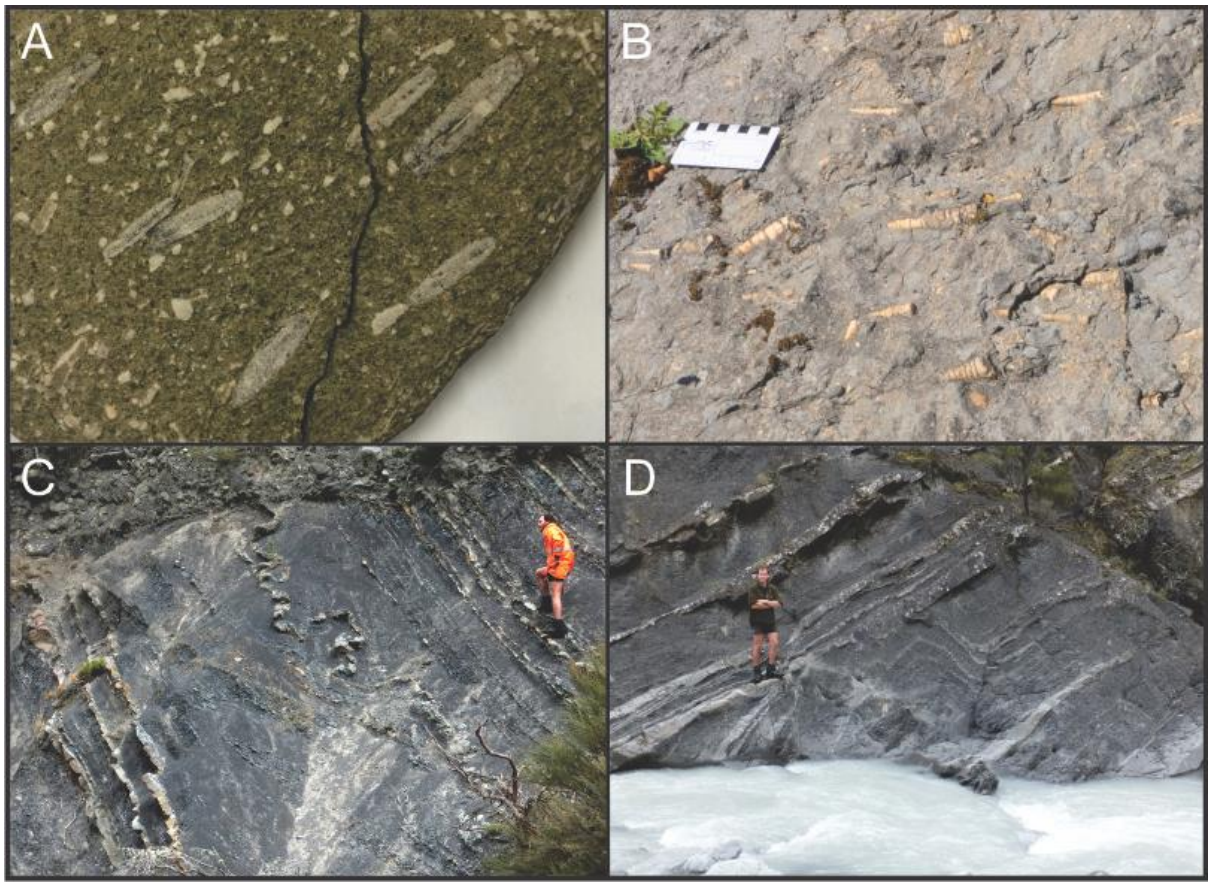

Figure 1.6: Examples of paleoenvironmental indicators of paleocurrent and paleoslope direction. A) Current oriented belemnites in Glenburn Formation from Pukemuri Stream. B) Current oriented turretellid gastropods in Takiritini Formation, Bellis Quarry, Tinui. C) Disturbed bedding, bounded by coherent sediment packages, indicative of syn-sedimentary slumping in Split Rock Formation, Wharekiri Stream. Photo supplied by J. Crampton. D) Syn-sedimentary slump fold, bounded by coherent, pararllel-bedded sediment on either side, occurring in Split Rock Formation, Wahrekiri Stream. Note the axial plane is tilted to the right-hand side, indicating the down-slope direction. Photo supplied by J. Crampton.

1.9 Statement of the Contributions to this Thesis by the Author & Collaborators

Data Analysis

Because of the broad scope of this study and use of diverse methods and approaches, some components of the thesis have relied on input from specialist collaborators, although the primary author is responsible for all aspects of study design and analysis. Any results that are the work of collaborators are identified clearly and attributed. In particular:

- Hannu Seebeck (GNS) – Development of G-Plates model. Refer to Chapter Five.
- Katie Collins (VUW, University of Chicago) – Multivariate statistical analyses of geochemical and heavy mineral/provenance datasets, specifically: principal components analysis of pXRF data, hierarchical cluster analysis of detrital zircon age distributions and heavy mineral populations. Refer to Chapters Three and Six.
- Michael Gazley (CSIRO, VUW) – Provision of pXRF devices used in this study, pXRF data reduction, XRD analysis and spectra interpretation. Refer to Chapters Three, Four and Six.
- G. Todd Ventura (GNS) – Bulk pyrolysis source rock analyses. Refer to Chapters Three and Four.
- Yulia Urarova (CSIRO) – XRD analyses and spectra interpretation. Refer to Chapters Four and Six.

Funding

My time and university fees were largely covered by the GNS Science Sarah Beanland Memorial Scholarship for the duration of this PhD thesis. Supplementary funding was also awarded by:

- New Zealand Geoscience Society: *Young Researchers Travel Grant* – Funds contributed towards international conference travel expenses.
- OMV New Zealand Limited: *Post-graduate scholarship* – Funds contributed to completion of geochemical analyses of prospective source and reservoir rocks in the East Coast Basin.
- GNS Science: *Petroleum Source Rocks and Fluids Programme* (MBIE Contract C05X0302) – Covered bulk pyrolysis source rock analyses of samples collected in this study.
- GNS Science: *Petroleum Basins Research programme, Frontiers Task Force project* – External geochemical analyses of 20 bulk rock samples.

1.10 Outline of Thesis Chapters

The results of this thesis have been presented in a mixture of paper and thesis chapter formats, with two results chapters (Chapters Three and Four) written in a paper-style format, and included between traditional thesis-style chapters. The two paper-style chapters are either submitted (Chapter Three) or in advanced preparation for submission (Chapter Four) to international journals, and as such are presented in the style required by the respective journals they have been submitted to (*Chemical Geology*, and *Marine and Petroleum Geology*, respectively).

Chapter Two: Geological Setting and Lithostratigraphy

Overview of the geological setting of the study area, and a summary of the existing lithostratigraphic framework for the Cretaceous to Oligocene East Coast Basin. Revised ages and formation synonymies are presented and discussed.

Chapter Three: Ocean Redox Conditions of the Paleocene Southwest Pacific

The late Paleocene Waipawa Formation provides the most widespread and accessible approximation of an "isochronous" stratigraphic horizon known currently in the East Coast Basin. The purpose of this chapter is to establish the base paleo-environmental and paleo-depositional conditions of 'typical' Waipawa Formation, which can then be used to assess lateral correlatives of the Waipawa Formation in different facies associations across the East Coast Basin in chapter Four. Chapter Three considers the depositional setting of the Whangai, Waipawa and Wanstead formations, and produces environmental and oceanographic interpretations that inform model development in Chapters Four, Five, Seven and Eight. Datasets presented in this chapter include the use and verification of novel methods in rapid, economical and reproducible geochemical data collection and the application of multivariate statistical methods in the assessment of large, varied datasets. This paper is presented as a manuscript that has been submitted to the journal *Chemical Geology*.

Chapter Four: Sequence and Chemo-stratigraphic Framework for the Waipawa Formation and Correlatives

This chapter draws on findings from Chapter Three to produce a working model of the environmental and depositional conditions of all lateral correlatives of the Waipawa Formation across the East Coast Basin. The Waipawa Formation and correlatives forms an apparently near-isochronous plane of chronostratigraphically restricted duration across the entire basin, providing

an important surface for tying sequence stratigraphic and paleogeographic model development, as well as informing conditions for the production of a late Paleocene palinspastic model. This chapter draws on disparate datasets, including measured sections, sedimentological interpretations, organic and inorganic bulk rock geochemical analyses, and foraminiferal biostratigraphy.

Chapter Five: Tectonic Reconstruction

This chapter discusses the development of a tectonic reconstruction for the East Coast Basin, and considers previous models, datasets that can aid the development and testing of a model, and model development. The base model discussed in this chapter will form the basis of the paleogeographic and palinspastic reconstructions presented in Chapters Six and Seven.

Chapter Six: Sequence Stratigraphy of the East Coast Basin

Using interpretations drawn from Chapters Two, Three and Four, along with information from fieldwork conducted during the course of this study, combined with measured sections from the East Coast CCP and published literature, this chapter presents a third-order sequence-stratigraphic framework for the late Cretaceous–Paleogene sedimentary succession in the East Coast Basin.

Chapter Seven: Sequence Stratigraphic Framework for the East Coast Basin

Stratigraphic, paleoenvironmental and geochemical data from Chapter Two, Three, and Four are integrated to provide a composite third-order sequence stratigraphic framework for the East Coast Basin that is compared with global records, as well as records from the New Zealand region.

Chapter Eight: Synthesis and Conclusions

Data and interpretations derived from Chapters Two, Three, Four, Six and Seven, along with field observations and published data, are applied to the tectonic reconstruction developed in Chapter Five. The results are presented as a series of time-slice style maps, ranging from the early Late Cretaceous to the Eocene, showing progressive paleo-environmental changes over six time planes through the development of the East Coast Basin. The thesis concludes with summary of the primary findings of this study, much of which are presented as the reconstructed paleogeographic timeslice maps, and areas with potential for future work are identified.

1.11 Papers Presented During Thesis Research

During the course of this thesis research, the author has presented preliminary results as either poster or oral presentations at both national and international conferences. Manuscripts have been published in peer-reviewed journals, and contributions have been made to field trip guides and scientific reports. These are referenced below. A number of additional presentations have been given to interest groups at GNS Science, Victoria University of Wellington, the Ministry of Business, Innovation and Employment, OMV New Zealand Limited, and the Geological Society of New Zealand.

Peer-Reviewed Journal Articles

Hines, B. R., Kulhanek, D. D., Hollis, C. J., Atkins, C. B. & Morgans, H. E. G. (2013). The Paleogene stratigraphy and paleoenvironment of Tora, southeast Wairarapa, New Zealand. *New Zealand Journal of Geology and Geophysics*. DOI: 10.1080/00288306.2013.836112

Hines, B. R., Hollis, C. J., Atkins, C. B., Baker, J. A., Morgans, H. E. G., Strong, C. P. (2017). Reduction of oceanic temperature gradients in the Early Eocene Southwest Pacific Ocean. *Palaeogeography, Palaeoclimatology, Palaeoecology 475,* 41-54. DOI*:* 10.1016/j.palaeo.2017.02.037.

Dallanave, E., Bachtadse, V., Crouch, E. M., Tauxe, L., Shepherd, C. L., Morgans, H. E. G., Hollis, C. J., **Hines, B. R**., Sugisaki, S. (2016). Constraining early to middle Eocene climate evolution of the southwest Pacific and Southern Ocean. *Earth and Planetary Science Letters.* DOI: 10.1016/j.epsl.2015.11.010.

Dallanave, E., Agnini, C., Bachtadse, V., Muttoni, G., Crampton, J. S., Strong, C. P., **Hines, B. R**. & Hollis, C. J. (2015). Early to middle Eocene magneto-biochronology of the southwest Pacific Ocean and climate influence on sedimentation: Insights from Mead Stream section, New Zealand. *The Geological Society of America Bulletin*. B31147-1.

Hollis, C.J., **Hines, B. R.**, Littler, K., Villasante-Marcos, V., Kulhanek, D. K., Strong, C. P., Zachos, J.C., Eggins, S. M., Northcote, L., & Phillips, A. (2015). Onset of the Paleocene–Eocene Thermal Maximum in the southern Pacific Ocean (DSDP Site 277, Campbell Plateau). *Climates of the Past Discussions*, 11, 243-278.

Rainsley, E., Turney, C. S., Golledge, N. R., Wilmshurst, J. M., McGlone, M. S., Hogg, A. G., Thomas, Z. A., Flett, V., Palmer, J. G., Jones, R. T., de Wet, G., Hutchinson, D. K., Lipson, M. J., Fenwick, P., **Hines, B. R.,** Binetti, U., Fogwill, C. J. (2016). Pleistocene glacial history of the New Zealand subantarctic islands. *Climate of the Past.* DOI: 10.5194/cp-2018-52.

Turney, C., McGlone, M., Palmer, J. Fogwill, C., Hogg, A., Thomas, Z., Lipson, M., Wilmshurst, J., Fenwick, P., Jones, R., **Hines, B. R.,** & Clark, G. (2015). Intensification of Southern Hemisphere Westerly Winds during the First Millennium CE: Evidence from the Subantarctic Campbell and Auckland Islands (50-52˚S). *Journal of Quaternary Science,* DOI: 10.1002/jqs.2828

Conference Papers

Hines, B. R. & Collins. K. S. (2013). Determination of Neogene Mg/Ca seawater ratios and Mg/Ca calibrations for extinct foraminiferal lineages. *New Zealand Geosciences Conference*, Christchurch, New Zealand. 24th-27th November 2013.

Hines, B. R., Gazley, M., Crampton, J. S., Bland, K. & Seward, D. (2014). Developing a chemostratigraphic framework for the Whangai Formation. *New Zealand Geosciences Conference*, New Plymouth, New Zealand. 24th-27th November 2014.

Hines, B. R., Collins, K. S., Neil, H. L. & Gazley, M. F. (2015). Cenozoic sea temperature exhibited by crassatellid molluscs. *New Zealand Geosciences Conference*, Wellington, New Zealand. 23rd-25th November 2015.

Hines, B. R., Gazley, M. F., Bland, K., Ventura, G. T., Crampton, J. S., Collins, K. S. (2015). Geochemical insights into the depositional conditions of prospective Late Cretaceous – Paleogene marine source rocks of the East Coast Basin, New Zealand. *American Association of Petroleum Geologists workshop: Analogues for Modern depositional environments*. Wellington, New Zealand. 19th-23rd April 2015.

Hines, B. R., Gazley, M. F., Collins, K. S., Crampton, J. S., Ventura, G. T., Bland, K. J. & Seward, D. (2015). Crossing the Strait: Reconciling Paleogene stratigraphic linkages between Wairarapa and Marlborough. *New Zealand Geosciences Conference*, Wellington, New Zealand. 23rd-25th November 2015.

Hines, B. R., Ventura, G. T., Gazley, M. F., Bland, K. J., Crampton, J. S., Collins, K. S. (2015). Chemostratigraphic framework for changing depositional conditions of prospective Late

Cretaceous – Paleogene marine source rocks of the East Coast Basin, New Zealand**.** American Association of Petroleum Geologists: *East Australian Basins Symposium*. Melbourne, Australia. 2015.

Hines, B. R., Crampton, J. S., Bland, K. J. & Seward, D. (2016). Palispastic reconstruction of the East Coast Basin, New Zealand. *Geological Society of America Annual Meeting*, Denver, Colorado. 25th-28th September 2016.

Hines, B. R., Gazley, M. F., Ventura, G. T., Collins, K. S., Bland, K. J. & Crampton, J. S. (2016). Sequence and chemo-stratigraphic framework for the Waipawa Formation, East Coast Basin, New Zealand: controls on Paleocene black shale deposition in the southwest Pacific. *Geological Society of America Annual Meeting*, Denver, Colorado. 25th-28th September 2016.

Hines, B. R., Seebeck, H., Crampton, J. S., Bland, K. J. (2017). Filling the blank wedge of Zealandia: Cretaceous to Paleogene reconstruction of the East Coast Basin. *New Zealand Geosciences Conference*, Auckland, New Zealand. 6th-8th December 2017.

Bache F., Sutherland R., Stagpoole V., Browne G., Lawrence M. J. F., Mortimer N., Herzer R., Black J., **Hines B. R**., Roop H., Flowers M., Roullard P., Collot J., Patriat M. (2014). Geological overview of the Reinga Basin, NW New Zealand: key observations and new constraints. *Advantage 2014 Conference, Wellington, 1st - 4th April 2014*.

Bland, K., Clowes, C., Field, B., **Hines, B**. **R**., Ventura, T, Morgans, H., Strogen, D. & Sykes, R. (2016). Onshore petroleum seeps in the southern East Coast Basin, and their stratigraphic occurrences: an overview from recent fieldwork. *Petroleum Geoscience Workshop*, Lower Hutt, New Zealand. 22-23rd September 2016.

Dallanave, E., Agnini, C., Bachtadse, V., Muttoni, G., Crampton, J. S., Strong, P., **Hines, B. R**., Hollis, C. J. & Slotnick, B. S. (2014). Early to middle Eocene magneto-biochronology of the southwest Pacific Ocean and climate influence on sedimentation: new data from the Mead Stream section (Marlborough, New Zealand**).** *AGU Fall Meeting Abstracts 2014*.

Field, B. D., **Hines, B. R**., Clowes, C., Rechden, R., Ventura, G. T., Hollis, C. J. & Sykes, R. (2016) Using Milankovitch cyclicity for stratigraphic correlation and prediction of petroleum generative potential in the Waipawa Formation, East Coast Basin. *Advantage NZ Conference*, Auckland, New Zealand. April 2016.

Gazley, M. F., Collins, K. S., **Hines., B. R**., Fisher, L. A. & McFarlane, A. (2015). Application of multivariate statistics and cluster analysis to mineral exploration and mine geology. *NZAusIMM Conference*. Perth, Australia. 2015.

Hollis, C. J., Pascher, K., **Hines. B. R**., Littler, K., Kulhanek, D. K., Strong, C. P., Zachos, J. C., Eggins, S. M. & Phillips, A. (2014). Was the Early Eocene ocean unbearably warm or are the proxies unbelievably wrong? *Rend. Online Soc. Geol. It.,* Vol. 31 (2014), pp. 109-110, *Società Geologica Italiana, Roma 2014*. (doi: 10.3301/ROL.2014.71)

Hollis, C. J., Pascher, K., Shepard, C., **Hines, B. R**., Morgans, H. E. G., Strong, C. P., Naafs, D. & Pancost, R. (2016). The tolerable warmness of the Eocene hyperthermal ocean. *International Conference on Paleoceanography*, Utrecht, the Netherlands. 29th August – 2nd September 2016.

Kulhanek, D K., Hollis, C. J., **Hines, B. R**., Littler, K., Strong, C. P., Zachos, J. C. & Vilasante-Marcos, V. (2015). A new Paleocene-Eocene Thermal Maximum record from Deep Sea Drilling Project Site 277 (Campbell Plateau): A window into calcareous nannofossil response in the southern high latitudes. *International Nannoplankton Association meeting*, March 2015.

Ventura, G. T., **Hines, B. R**., Field, B. D., Bland, K. J., Strogen, D. P., Clowes, C. & Sykes, R. (2015). Paleoenvironmental and diagenetic controls on the petroleum generation characteristics of the Late Paleocene Waipawa Formation of the East Coast Basin, New Zealand. *New Zealand Geosciences Conference*, Wellington, New Zealand. 23rd-25th November 2015.

Science and Consultancy Reports

Bache, F., Sutherland, R., Mortimer, N., Browne, G. H., Lawrence, M. J. F., Black, J. A., Flowers, M., Rouillard, P., Pallentin, A., Woelz, S., Wilcox, S., **Hines, B**. **R**., Jury, S., Roop, H. (2014). Tangaroa TAN1312 Voyage Report: dredging Reinga and Aotea basins to constrain seismic stratigraphy and petroleum systems (DRASP), NW New Zealand. *GNS Science report 2014/05*. 136 p.

Bland, K. J., Ventura, G. T., **Hines, B. R**. &. Crampton, J. S. (2013). Record of sample collection from a potential Waipawa Formation outcrop at the Opouwae River Mouth, Te Kaukau Point, southeastern Wairarapa, 31 July 2013, for micropalentological and source rock analyses. *GNS Science Internal Report 2013/09*. 26p.

Bland, K. J., Morgans, H. E. G., **Hines, B. R**. & Crampton, J. S. (2014). Outcrop analogues for the offshore East Coast and Pegasus basins: field trip to the southern Hawke's Bay-Wairarapa areas, 28th-31st January 2014. *GNS Science Consultancy Report 2014/12*. 81 p.

Clowes, C. D., Bland, K. J., Morgans, H. E. G., **Hines, B. R.** (2016). Record of geological observations and sample collection from Late Cretaceous- Early Miocene strata in southern Hawke's Bay, 04-08 April 2016. *GNS Science Internal Report 2016/14*. 56 p.

Ventura, G.T.; **Hines, B. R.;** Clowes, C.D. (2016). Source rock pyrolysis properties of four Waipawa Formation sections in Wairarapa and southern Hawke's Bay: interim results, *GNS Science Internal Report 2016/06*. 12p + 1 appendix.

Ventura, G.T.; **Hines, B. R**.; Clowes, C.; Field, B.D. (2016). Section log, initial micropaleontological and geochemical analyses, and gamma ray scintillometer data for the Whangai and Waipawa formations at Okau Stream, eastern Wairarapa, *GNS Science Internal Report 2016/05*. 48 p.

Field Trip Guides

Hines, B. R. (2015). Paleogene stratigraphy and paleoenvironment of the Tora coast. In: Atkins, C., (ed.) Fieldguides Geosciences 2015, Wellington, Geoscience Society of New Zealand Miscellaneous Publication No. 143b. ISBN: 978-1-877480-50-8

Chapter Two

REVISION OF THE CRETACEOUS–PALEOCENE STRATIGRAPHIC NOMENCLATURE OF THE EAST COAST BASIN

"*The Jurassic is grey, the Cretaceous is green*"

- George Grindley on East Coast Basin stratigraphy,

M. Isaac, (2017). Tributary to George Grindley, *GSNZ Newsletter No. 22*.

View eastward over Sawpit Gully (foreground), Coverham (middle distance) and the Inland Kaikoura Ranges (far distance).

Page intentionally left blank for formatting purposes

PREFACE TO CHAPTER TWO

Chapter Structure

- The stratigraphy of main regions (Raukumara to Wairarapa, Tora, and Marlborough) are introduced. Areas are divided on the basis of commonality within sedimentary successions, typically age, lithofacies, and the presence of bounding structures. Sedimentary units are described in each area in chronological order.
- This is followed by a discussion on synonymous stratigraphic units and correlations of units across the previously defined regions.
- This leads into a division of a first- to second-order sequence stratigraphic framework across the basin.

Overview

- Thirty sections were logged during this thesis, 34 localities were sampled, and an additional 25 localities were visited during the course of this thesis (Figure 2.1)
- My own outcrop observations (Figure 2.2) are integrated with published works to inform revision and correlation of stratigraphic units within the East Coast Basin.
- Recent dinoflagellate zonation schemes are applied to faunal assemblages from the Fossil Record file Electronic Database (FRED) to assess chronostratigraphic trends.
- Chronostratigraphic and lithostratigraphic frameworks are summarised as a first- to second-order sequence stratigraphy for the East Coast Basin, enabling comparison with the King (2000) megasequence and the Zealandia megasequence of Mortimer *et al.* (2014). This provides a basis to refine a third-order sequence stratigraphy in Chapter Seven.
- The stratigraphic observations, correlations, and environmental interpretations covered within this chapter provide the base dataset for the palinspastic maps presented in Chapter Eight.

Note: Following the November 2016 Kaikoura earthquake, many of the Marlborough sections described herein have since been either destroyed, buried by landslides, or submerged in dammed catchments.

Aerial view of damage to two important sections considered during this study. Photos: Dougal Townsend/GNS Science.

Chapter Two

REVISION OF THE CRETACEOUS–PALEOCENE STRATIGRAPHIC NOMENCLATURE OF THE EAST COAST BASIN

2.1 Introduction

The primary goals outlined for this thesis require the assessment and the application of a large amount of stratigraphic data from a number of sections (Figures 2.1 & 2.2). A series of stratigraphic patterns have been recognised in the East Coast Basin that broadly represent an integrated sequence stratigraphic and tectono-stratigraphic response to sedimentary trends within the Cretaceous to Miocene cover strata of the basin (Pettinga, 1982; Moore *et al.*, 1986). The sedimentary rocks of the East Coast Basin comprise an overall fining-upwards succession from late Cretaceous sandstone to Paleocene–Eocene mudstone and muddy limestone, equivalent to the first-order cycle of King (2000b) (Figure 2.3). Moore *et al.* (1986), following the divisions of Pettinga (1982), divided the Cretaceous–Paleogene stratigraphy of the East Coast Basin into four broad sedimentation phases. These were subsequently adopted by Field and Uruski *et al.* (1997) in a review of the stratigraphy of the East Coast Basin, and are approximately equal to the second-order divisions of King *et al.* (1999) and King (2000b). These are divided as follows:

1. Cretaceous rifting and drifting – deposition of predominantly clastic sandstone, mudstone, conglomerate and flysch successions.

2. Paleocene–Eocene thermal subsidence phase – Deposition of a fine-grained, siliciclastic succession that becomes increasingly calcareous upwards, forming a transition interval.

3. Further subsidence – late Eocene to Oligocene deposition of a fine-grained, calcareous succession, comprised of smectitic mudstone, micritic limestone, and glauconitic sandstone.

4. Renewed tectonism during the Oligocene, related to the development of the modern plate boundary – deposition of calcareous turbidites, mass-flow deposits, and massive mudstones and sandstones.

The earliest cycle recognised by King (2000b) is mid-Cretaceous non-marine and marine transgressive deposits overlying a Ngaterian unconformity. This unconformity is widely recognised across New Zealand sedimentary basins, but in the East Coast Basin, the base of the cover

sequence is older; for example, the Split Rock Formation is Urutawan at its base in Marlborough, and in the Raukumara area there are sedimentary cover rocks of Urutawan-Motuan age (Mazengarb & Speden, 2000; Crampton *et al.*, 2003, 2004b; Leonard *et al.*, 2010). In western sedimentary basins and parts of the East Coast Basin (particularly Marlborough; Crampton & Laird, 1997) the early depositional phases of this sedimentary cycle occurred within normal fault-controlled grabens (Laird, 1992). This extensional phase began between 108–103 Ma (King *et al.*, 1999; Davy *et al.*, 2008). In the East Coast Basin, this extension is generally recognised around the base of the Motuan at 105 Ma (Moore & Speden, 1984; Laird & Bradshaw, 2004). This sequence is widely represented in many places across the East Coast Basin by the deposition of a coarse-grained basal facies that is superseded by marine sandstones and mudstones. An intra-Piripauan unconformity is recognised widely across the East Coast and Canterbury basins (Field & Browne *et al.*, 1989; Crampton *et al.*, 2006), and together, these two unconformities constrain a single second order cycle.

The second cycle in the King (2000b) mega-sequence was deposited from the Haumurian to Teurian, and is marked by regional marine transgression. In many parts of New Zealand this included a coarse basal facies marking transgression onto basement, associated with the onset of passive margin subsidence. Over the top of these units, passive margin deposition prevailed throughout the Haumurian and Teurian. By the end of the Paleocene a post-rift passive margin had developed around Zealandia, and the entire region is considered to have been tectonically quiescent (King, 2000b).

Seafloor spreading of the Tasman Sea ceased around 52 Ma (Gaina *et al.*, 1998), although Zealandia continued to drift further from Antarctica in the Early to Middle Eocene, and consequently was isolated from any plate boundary. This resulted in an extended period of widespread tectonic quiescence, whereby sedimentation was characterised by post-rift cooling and passive margin thermal subsidence (Ballance, 1993b; King, 2000b). In the East Coast Basin, this period is dominated by progressive transgression across the basin, with a notable deepening, and an increase in carbonate-dominated sedimentation (Hollis *et al.*, 2005a; Hines *et al.*, 2013), representing the third cycle of King *et al.* (1999).

An intra-cycle Porangan unconformity has been identified in the Taranaki, Great South and Canterbury basins, corresponding to a basinward facies shift, and the lowering of base level (King, 2000b). However, at this time there is a notable rise in base level in parts of the West Coast, western Southland (King, 2000b) and the East Coast Basin (Hines *et al.*, 2013). These changes are correlated with the onset of seafloor spreading and extension in the Emerald Basin, south of Zealandia,

marking initiation of the development of the modern New Zealand plate boundary zone (King, 2000b).

The fourth second-order cycle identified by King (2000b) spans the Oligocene to earliest Miocene, and corresponds to peak submersion of Zealandia. This cycle is dominated by the widespread deposition of carbonates, both on submerged shallow marine platforms and in deep marine settings. The base of this cycle corresponds to the regional flooding surface of the first order mega-cycle, and greensands are commonly observed at this horizon, indicating a substantial reduction in clastic sediment supply caused by the onset of marine transgression (King, 2000b). This surface typically coincides approximately with the Eocene-Oligocene boundary.

The Oligocene is widely considered to represent the peak of marine transgression and passive margin development around Zealandia (e.g., Landis *et al.,* 2008). However, in southwestern New Zealand, the slow regional subsidence was being overprinted by localised tectonism associated with the development of the modern plate boundary. North of New Zealand, the subduction of the Pacific Plate was already established (Bache *et al.*, 2012). This increase in tectonic activity is likely to be at least partially responsible for the numerous unconformities within this second order cycle (King, 2000). In addition to this, the Oligocene saw the development of permanent Antarctic ice sheets and the associated deep water formation, resulting in the development of a deep western boundary current along the eastern margin of Zealandia and the consequent, widespread development of the Marshall Paraconformity in the East Coast and Canterbury basins (Carter *et al.*, 2004).

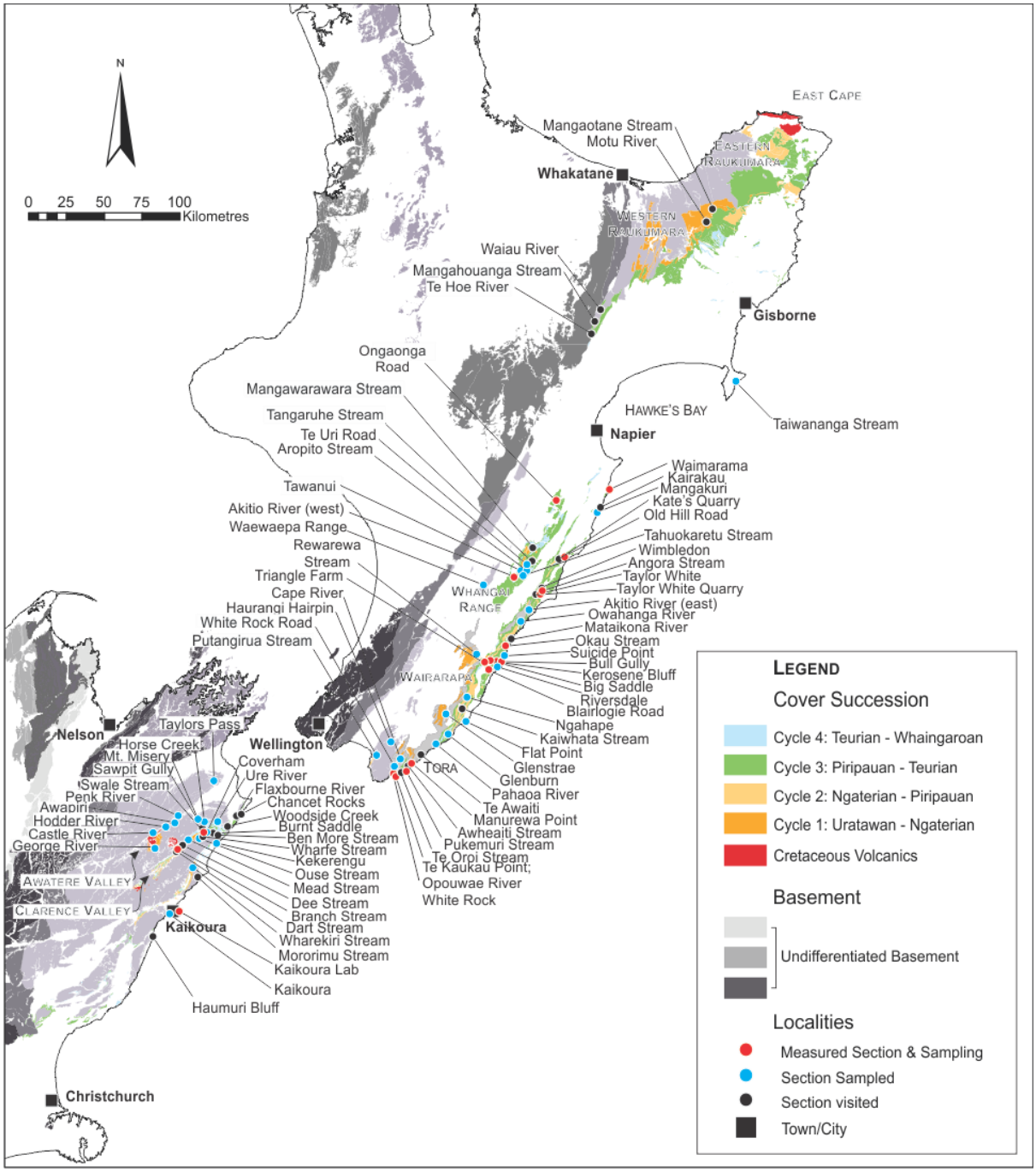

Figure 2.1: Localities and sections that were logged, sampled and/or visited during the course of this study. Base map data from Heron (2014). Geological units are coloured by a second-order sequence- and tectono-stratigraphic framework modified after King (2000b) (discussed later in this chapter) for direct comparison to key localities referred to in this chapter (Figure 2.2).

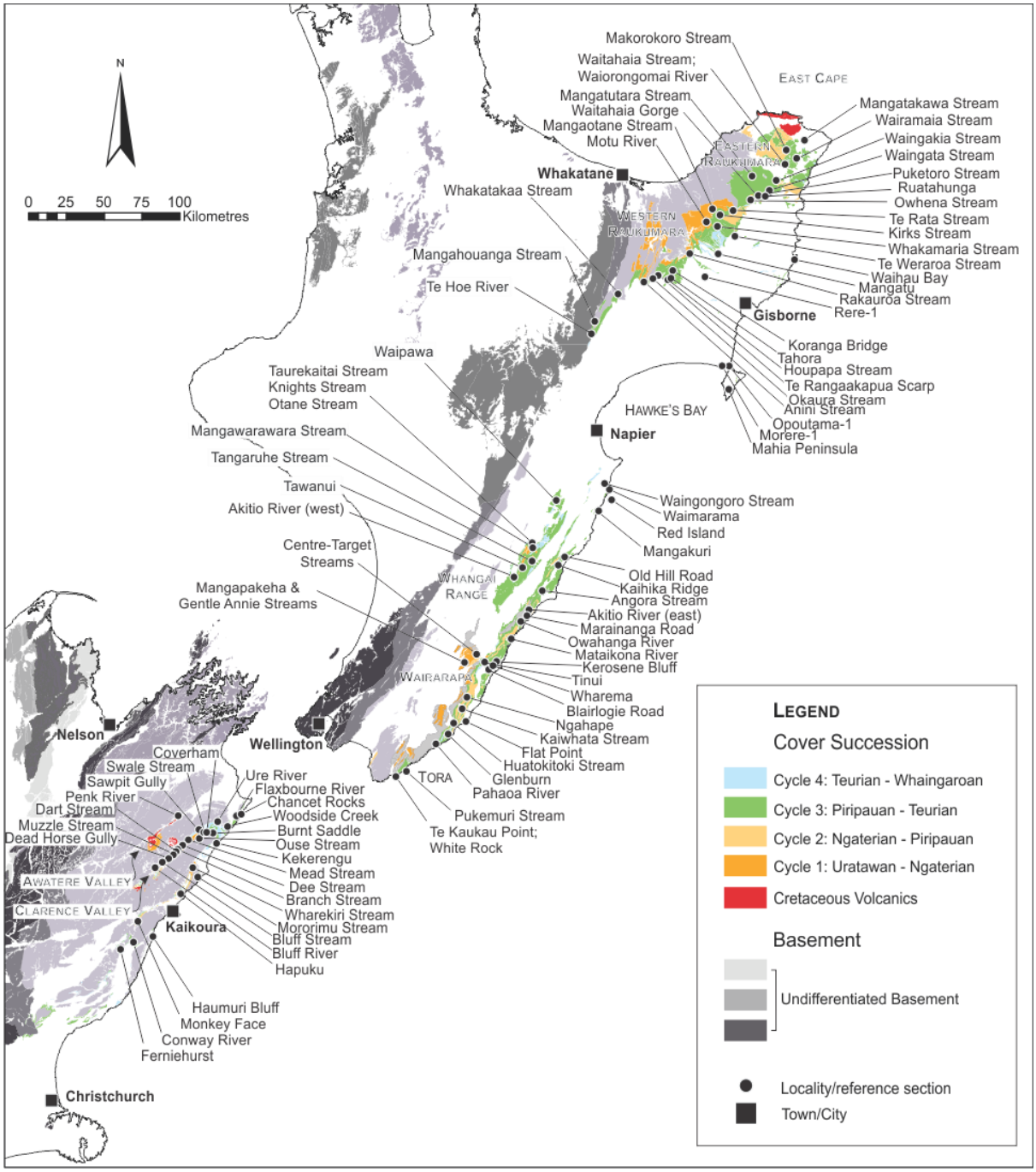

Figure 2.2: Sections and localities referred to in text. Base map data from Heron (2014). Geological units are coloured by a second-order sequence- and tectono-stratigraphic framework modified after King (2000) (discussed in Chapter Seven).

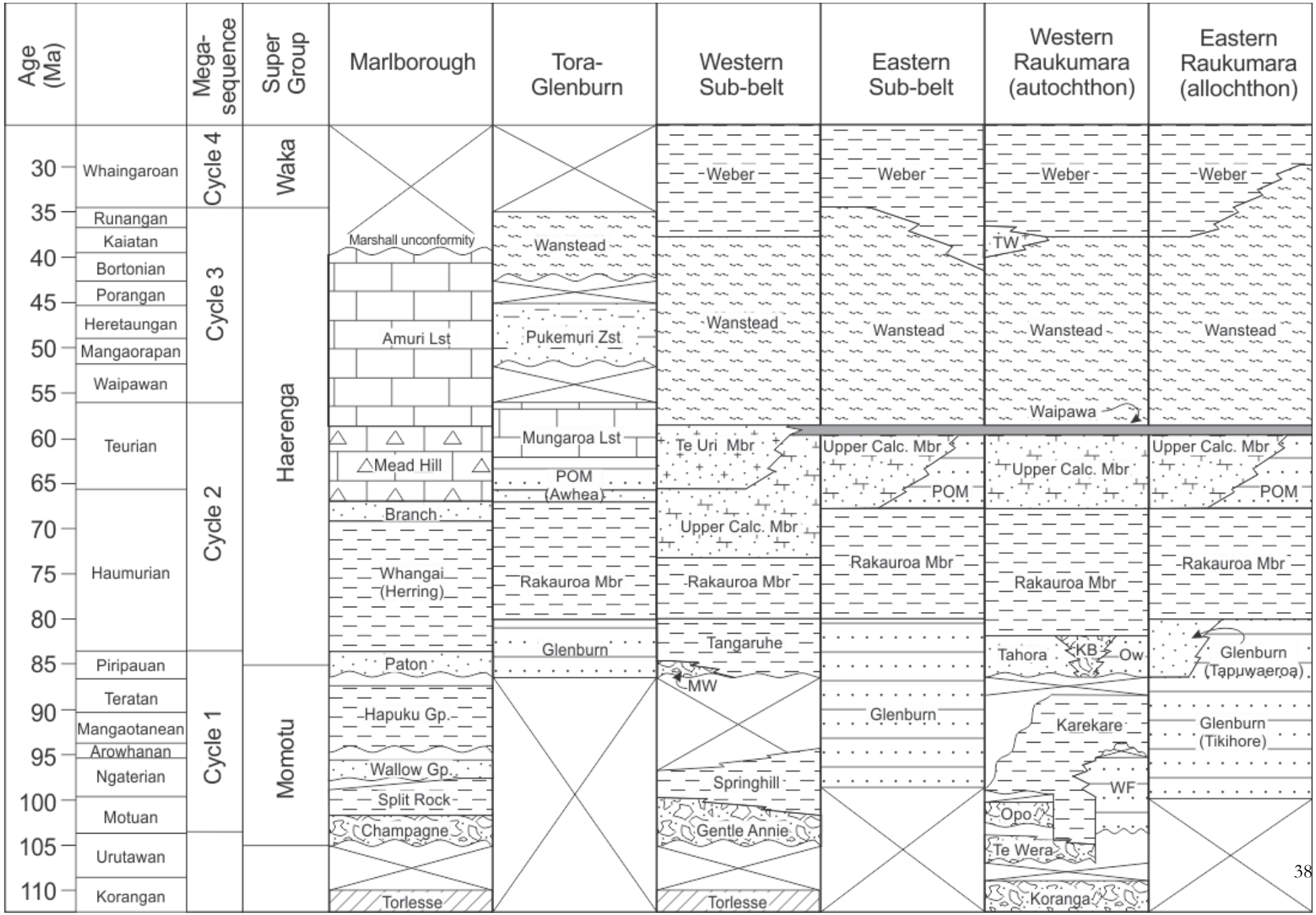
Age (Ma)
Mega-sequence
Super Group
Marlborough
Tora-Glenburn
Western Sub-belt
Eastern Sub-belt
Western Raukumara (autochthon)
Eastern Raukumara (allochthon)
30
35
40
45
50
55
60
65
70
75
80
85
90
95
100
105
110
Whaingaroan
Runangan
Kaiatan
Bortonian
Porangan
Heretaungan
Mangaorapan
Waipawan
Teurian
Haumurian
Piripauan
Teratan
Mangaotanean
Arowhanan
Ngaterian
Motuan
Urutawan
Korangan
Cycle 4
Cycle 3
Cycle 2
Cycle 1
Waka
Haerenga
Momotu
Marshall unconformity
Amuri Lst
Mead Hill
Branch
Whangai (Herring)
Paton
Hapuku Gp.
Wallow Gp.
Split Rock
Champagne
Torlesse
Wanstead
Pukemuri Zst
Mungaroa Lst
POM (Awhea)
Rakauroa Mbr
Glenburn
Weber
Wanstead
Te Uri Mbr
Upper Calc. Mbr
Rakauroa Mbr
Tangaruhe
MW
Springhill
Gentle Annie
Torlesse
Weber
Wanstead
Upper Calc. Mbr
POM
Rakauroa Mbr
Glenburn
Weber
TW
Wanstead
Waipawa
Upper Calc. Mbr
Rakauroa Mbr
Tahora
KB
Ow
Karekare
WF
Opo
Te Wera
Koranga
Weber
Wanstead
Upper Calc. Mbr
POM
Rakauroa Mbr
Glenburn (Tapuwaeroa)
Glenburn (Tikihore)

2.2 Basement-Cover Transition

Whereas the contact between Torlesse Composite Terrane basement and mid-Cretaceous cover may be difficult to pinpoint in some locations (Mazengarb & Harris, 1994), in most places there is an angular unconformity and a marked decrease in induration and deformation between basement and cover. Although there is a widespread mid-Cretaceous unconformity across New Zealand (King, 2000b, Rattenbury *et al.*, 2006), in the East Coast Basin the event that caused this unconformity was short-lived with little, if any, hiatus, and with little to no change in metamorphic grade, making it difficult to pinpoint. In the Raukumara region, the contact between Korangan basement rocks and cover strata is variably marked by a fault, a high angle unconformity, a series of unconformities, an olistostrome melange, or a channelized contact (Mazengarb & Speden, 2000; Laird & Bradshaw, 2004; Leonard *et al.*, 2010). In the southern Hawke's Bay-Wairarapa regions, Motuan Pahaoa Group basement (uppermost Pahau Terrane), is overlain by Motuan cover strata (Moore & Speden, 1984; Lee & Begg, 2002; Lee *et al.*, 2011). Zircons from above and below the basement-cover unconformity in Wairarapa give a c. 100 Ma age, suggesting derivation from the same or similar aged rocks, or recycling of zircons (Laird & Bradshaw, 2004; Rattenbury *et al.*, 2006; Adams *et al.*, 2013a). In Marlborough, the basement-cover contact cannot be reliably identified on the basis of metamorphic grade, changes in induration, or clastic composition (Rattenbury *et al.*, 2006). The uppermost Pahau Terrane in Marlborough is poorly dated, although Field & Uruski *et al.* (1997) identify an intra-Motuan unconformity. Conversely, Crampton *et al.* (2004b) show no significant stratigraphic break in the Motuan succession in the Coverham area, although they identify an earlier, intra-Uratawan unconformity. The diachronous nature of the basement-cover unconformity in the Marlborough and Raukumara regions is probably indicative of deposition in localised, syntectonic basins (Rattenbury *et al.*, 2006).

Figure 2.3: Existing stratigraphic relationships across broad regional divisions of the East Coast Basin, covered by this study. Formations discussed here are labelled. Bracketed formation names are considered synonymous with other formations. Western and Eastern Sub-belts generally refer to the modern forearc basin and the accretionary high, which demonstrate distinct differences in Cretaceous–Paleogene stratigraphy. Revised age control is presented at the end of this chapter. Modified after Moore (1988a) and Field & Uruski *et al.* (1997). MW = Mangawarawara Member, WF = Waitahaia Formation, Opo = Oponae Melange, OW = Owhena Formation, KB = Kirks Breccia Member, TW = Te Waka Greensand, POM = Porangahau Member. Megasequences are adopted from Mortimer *et al.* (2014). Cycles are modified after King *et al.* (1999).

2.3 Raukumara

2.3.1 Koranga Formation

The Koranga Formation has a restricted distribution in a narrow north–northeast-trending belt between Koranga and Motu (Field & Uruski *et al.*, 1997). The formation forms the base of the Matawai Group (Isaac, 1977; Moore *et al.*, 1986), and the type section is Maccoyella Ridge (Speden, 1975; Field & Uruski *et al.*, 1997). The Koranga Formation marks the coarse basal facies of the cover succession in this part of the East Coast Basin.

Lithostratigraphy

The Koranga Formation unconformably overlies Pahau Terrane with a marked angular unconformity (Figure 2.3). The formation comprises indurated sandstone, conglomerate, intraformational breccia, and minor siltstone (Speden, 1975; Isaac, 1977). Conglomerate clasts include sandstone and siltstone, along with pebbles of fine-grained acid volcanics and granite (Speden, 1975). The formation is up to 250 m-thick.

Paleontology and Age

Macrofossils are common in some localities, with over 30 species collected from the type section at Maccoyella Ridge (Field & Uruski *et al.*, 1997). Plant fragments are pervasive throughout the formation. The age of the formation is Korangan by definition (forms the type section for the Korangan Stage), and this stage is defined on the presence of *Aucellina* and *Maccoyella* bivalve species present (Speden, 1975).

Depositional Setting

The Koranga Formation was interpreted as being deposited in a shallow-marine environment, adjacent to a rapidly eroding landmass of significant relief (Speden, 1975; Isaac, 1977). However, Laird and Bradshaw (1996) interpreted the Koranga Formation as representing a deep-marine environment, dominated by debris flows and turbidites. This study follows the shallow marine environmental interpretation of Speden (1975).

2.3.2 Te Wera Formation

The Te Wera Formation is restricted to the Koranga River area (Leonard *et al.*, 2010). The formation belongs to the Matawai Group (Mazengarb & Speden, 2000), and was originally defined by Speden (1973; 1975). The type section is Koranga. Although separated by an unconformity, the Koranga Formation and Te Wera Formation are part of the same sedimentary cycle (Speden, 1973). The Te Wera Formation can be correlated with other sedimentary melanges and conglomeratic units at the base of the cover succession in the East Coast Basin, including the Gentle Annie Formation and the Champagne Formation.

Lithostratigraphy

The Te Wera Formation unconformably overlies both Pahau Terrane metasedimentary basement rocks and the Koranga Formation (Speden, 1975). The formation is comprised of moderately indurated, well-bedded conglomerate, breccia, grit, coarse to fine sandstone and minor siltstone (Field & Uruski *et al.*, 1997). Conglomerate beds are confined to the base of the formation, and are overlain by metre-scale cross-beds. Sandstone often contains mudstone rip-up clasts, and glauconite is common in some units (Moore, 1978). The formation has a maximum-thickness of 250 m.

Paleontology and Age

Macrofossils and carbonaceous material are common throughout the formation, with macrofossils including *Aucellina gryphaeoides,* and *Maccoyella* n. sp., indicating an Urutawan age (Speden, 1973, 1975; Moore, 1978).

Depositional Setting

The Te Wera Formation has been interpreted as being deposited in a high-energy, inner-shelf environment, in which sand bars and banks developed (Speden, 1975; Isaac, 1977; Mazengarb, 1993). Conglomerate beds are interpreted as basal lag deposits, and overlying cross-bedding interpreted as either storm or tidal deposits (Speden, 1975; Mazengarb, 1993). However, Laird and Bradshaw (1996) suggest a submarine fan-channel system environment for the formation. Here, the Te Wera Formation is considered as a shelf deposit, following Speden (1975) and Mazengarb (1993).

2.3.3 Oponae Melange

The Oponae Melange has a very restricted distribution, and is only known from near Oponae in the Waioeka Gorge in western Raukumara, although a larger area of melange is documented west of the Motu River (Field & Uruski *et al.*, 1997; Leonard *et al.*, 2010). The melange is included in the Matawai Group (Mazengarb & Speden , 2000). The age, thickness and lithology of the formation are comparable to the Gentle Annie Formation (see below).

Lithostratigraphy

In places the Oponae Melange unconformably overlies Pahau Terrane metasedimentary basement, and is interpreted as an olistostrome deposit (Mazengarb, 1993). Elsewhere, it is apparently in fault contact with both Pahau Terrane and younger cover deposits (Leonard *et al.*, 2010). The melange is comprised of angular blocks and rounded pebbles of sandstone, mudstone, marble, bedded chert, coal and igneous rocks, within a matrix of folded and sheared mudstone and fine sandstone. The melange is over 200 m-thick.

Paleontology and Age

Macrofossils are rare, although the Motuan Stage index fossil, *Aucellina euglypha*, has been identified within the formation (Speden, 1973, 1976; Leonard *et al.*, 2010), thereby indicating a Motuan age for the formation. The overlying Karekare Formation is also Motuan in age.

Depositional Setting

The depositional environment for the Oponae Melange has not been constrained. The formation is interpreted to have been deposited as an olistostrome in association with tectonism in a localised basin (Leonard *et al.*, 2010). Deposition occurred within a marine setting, but paleodepth cannot be determined (Field & Uruski *et al.*, 1997).

2.3.4 Waitahaia Formation

The Waitahia Formation crops out predominantly in eastern Raukumara, and is restricted to the area between Mangatau Stream, Mangatutara Valley and the Waingakia Stream area (Mazengarb, 1988; Mazengarb & Speden, 2000). The formation belongs to the Matawai Group. The Waitahaia Formation was defined by Moore *et al.* (1986), and a reference section nominated along the Waitahaia River (Phillips, 1985). The formation interfingers with the Karekare Formation (Figure 2.3).

Lithostratigraphy

The Waitahaia Formation typically unconformably overlies Pahau Terrane, although in the central Raukumara region the formation interfingers with Ngaterian Karekare Formation. The formation is comprised of a thick succession of indurated, centimetre- to metre-bedded alternating sandstone-mudstone, with minor conglomerate, tuff, chert and intraformational slump packets (Field & Uruski *et al.*, 1997). The oldest strata are comprised of indurated, mudstone-dominated, centimetre to decimetre interbedded sandstone and mudstone (Mazengarb & Speden, 2000; Crampton *et al.*, 2001). Sandstones are typically fine grained, carbonaceous, graded, and display sole marks (Field & Uruski *et al.*, 1997). Channel structures are present in places, and intraformational slumping is common (Field & Uruski *et al.*, 1997). The formation has a maximum known thickness of 1400 m (Mazengarb & Speden, 2000).

Paleontology and Age

Fossil faunas from the formation are poorly preserved. Rare *Inoceramus* aff. *wairakius* and *Inoceramus ipuanus-kapuus* suggest a Urutawan to Motuan age for the base of the formation (Phillips, 1985; Mazengarb, 1988). A number of possible *Inoceramus hakarius-fyfei* imply a likely Ngaterian age for the formation (Phillips, 1985). The Waitahaia Formation at Mangaotane Stream includes *Inoceramus fyfei* and *Magadiceramus rangatira haroldi*, indicating a Ngaterian to Arowhanan age for the top of the formation in western Raukumara (Crampton *et al.*, 2001).

Depositional Setting

The Waitahaia Formation is interpreted as the lower to middle fan deposits of a major submarine fan complex (Mazengarb, 1993). Submarine slumping suggests emplacement in slope or base-of-slope environments (Field & Uruski *et al.*, 1997). Paleocurrent orientations are north–south (Mazengarb, 1988). Conversely, Phillips (1985) interpreted a shelfal depositional setting for the Waitahaia Formation. Herein, the Waitahaia Formation is considered a deep marine, slope depositional environment, following Mazengarb (1993), Mazengarb & Harris (1994), and Field & Uruski *et al.* (1997).

2.3.5 Karekare Formation

The Karekare Formation crops out extensively in the Raukumara area. The Karekare Formation is included in the Matawai Group (Mazengarb & Speden, 2000). The type section for the Karekare Formation is Mangaotane Stream and was first described by Speden (1975). The Karekare

Formation interfingers with the Waitahaia Formation, and is correlated with the Springhill Formation (Hawke's Bay–Wairarapa) and the Swale Siltstone of the Split Rock Formation (Clarence Valley).

Lithostratigraphy

Urutawan-aged Karekare Formation unconformably overlies steeply dipping Pahau Terrane rocks in northern Hawke's Bay and western Raukumara (Field & Uruski *et al.*, 1997). Across the Motu Fault and in eastern Raukumara, the lower Karekare Formation unconformably overlies the Waitahaia Formation, with the former having a latest Ngaterian to Arowhanan age (Phillips, 1985; Crampton *et al.*, 2001). Karekare Formation is comprised dominantly of moderately indurated, massive grey siltstone and mudstone (Figure 2.4A), along with occasional thin-bedded fine sandstone and rare lenses of pebble conglomerate (Leonard *et al.*, 2010). Siltstones and mudstones are commonly bioturbated, fossiliferous, and rich in plant fragments. In western Raukumara, the Karekare Formation is up to 3000 m-thick (Field & Uruski *et al.*, 1997; Leonard *et al.*, 2010), and in eastern Raukumara, the formation ranges from 350 to 1200 m thick (Speden, 1975; Moore *et al.*, 1989; Mazengarb & Speden, 2000; Crampton *et al.*, 2001). A carbon isotope excursion across red mudstones in the Karekare Formation (Figure 2.4B) have been used to identify the Cretaceous Ocean Anoxic Event 2 at the Cenomanian/Turonian boundary section in Mangaotane Stream (Hasegawa *et al.*, 2013).

Paleontology and Age

The long sedimentary record represented by the Karekare Formation includes a number of inoceramiid bivalves (Figure 2.4 C, D), including; *I. fyfei*, *Magadiceramus rangatira haroldi*, *M. rangatira rangatira*, *Cremnoceramus bicorrugatus matamuus*, *C. bicorrugatus bicorrugatus*, *I. spedeni*, *I. opetius*, *I. pacificus* and *I. australis* (Crampton *et al.*, 2001). Macrofossils (inoceramid and *Aucellina* bivalves), foraminifera and dinoflagellate assemblages indicate a Uratawan to Teratan age for the formation in western Raukumara (Mazengarb & Speden, 2000; Crampton *et al.*, 2001; Schiøler *et al.*, 2001). In eastern Raukumara, the formation is notably younger, ranging from Arowhanan to Teratan in age (Phillips, 1985; Field & Uruski *et al.*, 1997).

Depositional Setting

The depositional environment for the Karekare Formation is interpreted as ranging from shallow shelf to bathyal marine conditions (Crampton *et al.*, 2001). The base of the Karekare Formation (Ngaterian to Arowhanan) in the Motu River area is interpreted as being deposited in a bathyal environment (400-1500 m), whereas the upper Karekare Formation (Mangaotanean to Piripauan)

is interpreted as being deposited in bathyal to outer shelf depths (Crampton *et al.*, 2001). In eastern Raukumara, a deepening at the base of the Karekare Formation, followed by a shallowing upwards trend through the Arowhanan is inferred (Phillips, 1985).

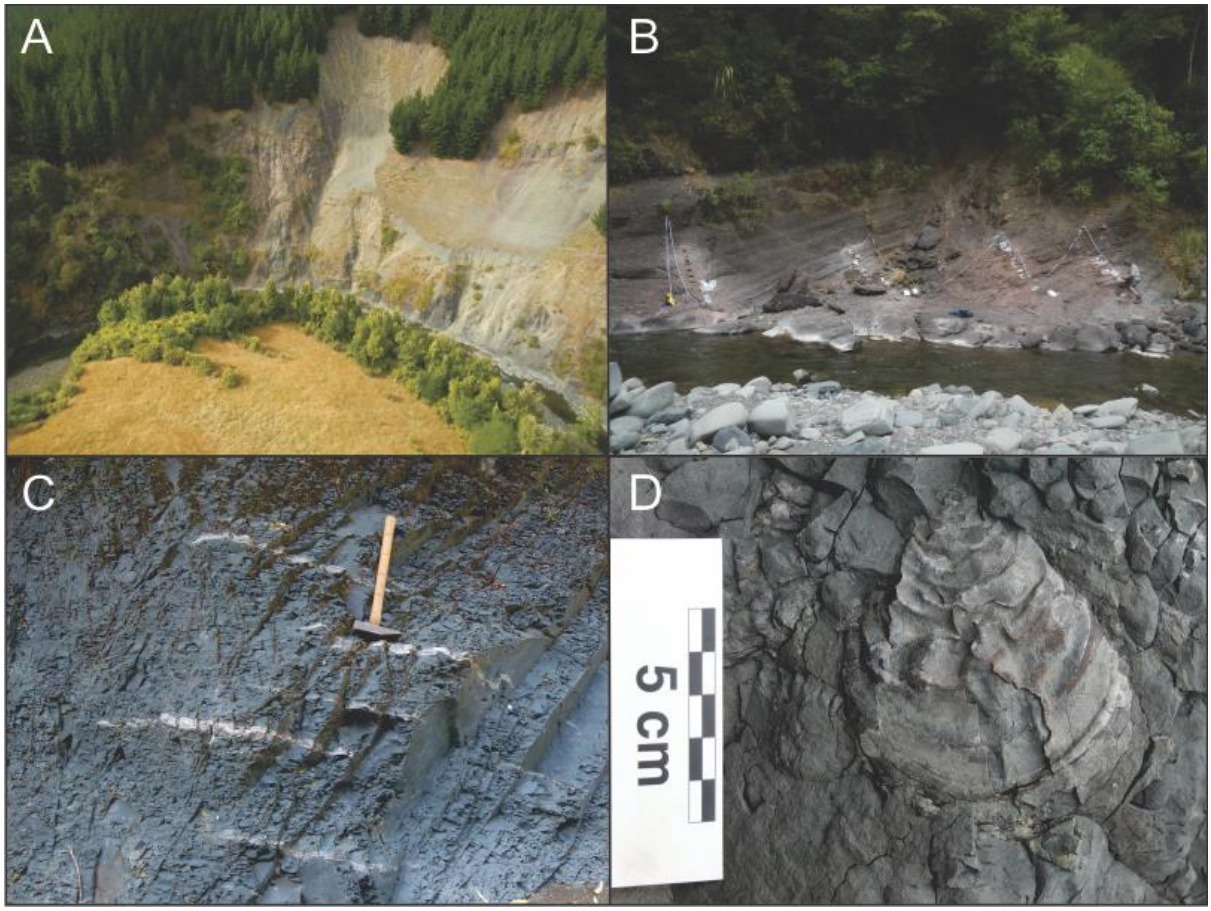

Figure 2.4: A) Aerial view of a large outcrop of Karekare Formation in Mangaotane Stream (BE42/173703). B) Cenomanian-Turonian boundary section in Mangaotane Stream, through section of 'red beds' (BE42/176704). Figure for scale. C) Examples of cross-sections through individuals of *M. rangatira* in Arowhanan Karekare Formation in Mangaotane Stream (BE42/192688). Hammer for scale. Hammer handle is 0.5 m long. Photo supplied by J. Crampton. D) *I. opetius* in Karekare Formation in Mangaotane Stream (BE42/195682). Photo supplied by J. Crampton.

2.3.6 Tapuwaeroa Formation

The Tapuwaeroa Formation, part of the Ruatoria Group (Mazengarb, 1993), is mapped between the Waikuru River and Rangitakia (Mazengarb & Speden, 2000). The Tapuwaeroa Formation was originally used by Lillie (1953) and Wellman (1959). The type section for the formation is the Waiorongomai River (Mazengarb, 1993). The Tapuwaeroa Formation is laterally equivalent to the Tikihore and Glenburn formations, and is synonymised with the Taiporutu Formation on Mahia Peninsula (Mazengarb, 1993; Mazengarb & Harris, 1994).

Lithostratigraphy

The Tapuwaeroa Formation gradationally overlies, and is laterally equivalent to upper parts of the Tikihore Formation (Figure 2.3; Field & Uruski *et al.*, 1997). It is comprised of moderately indurated, decimetre- to metre-bedded sandstone, grit, conglomerate, glauconitic sandstone and grey mudstone. Conglomerate beds are rare, but reach up to 4 m-thick. Sandstone beds are up to 6 m-thick, and are typically fine grained, graded, and display Bouma sequences. Plant fragments and carbonaceous laminae are common. The formation reaches up to 1150 m thick in the Waiorongomai River (Mazengarb, 1993).

Paleontology and Age

The Tapuwaeroa Formation is Piripauan to early Haumurian in age (Field & Uruski *et al.*, 1997).

Depositional Setting

The Tapuwaeroa Formation is interpreted to have been deposited in more proximal paleoenvironments than the laterally equivalent bathyal setting of the Tikihore Formation, though still likely at slope depths (Field & Uruski *et al.*, 1997). Paleocurrent orientations indicate flow to the northwest (Field & Uruski *et al.*, 1997). The lithology, age and environmental interpretation of the Tapuwaeroa Formation is very similar to the 'Te Mai facies' of the uppermost Glenburn Formation (e.g., Moore, 1980; Crampton, 1997).

Synonymy & Correlation

The Tapuwaeroa Formation (and Taiporutu Formation; Mahia) is herein considered synonymous with the upper Glenburn Formation (Piripauan-lower Haumurian) as expressed in the southern Hawke's Bay – Wairarapa. This is based on the equivalent age of the units, and the distinctive lithological similarities between the units, despite the large distance between them.

2.3.7 Tahora Formation

The Tahora Formation is restricted to the northern Hawke's Bay-Raukumara region. The formation marks the base of the Tinui Group, and the type section is Houpapa Stream (Isaac *et al.*, 1991). The Owhena Formation is considered a deeper, lateral equivalent of the Tahora Formation (Isaac *et al.*, 1991).

Lithostratigraphy

The Tahora Formation unconformably overlies Torlesse Composite Terrane basement, and Arowhanan Karekare Formation, separated by the Motu Fault (Crampton & Moore, 1990; Isaac *et al.*, 1991). The Tahora Formation is comprised of massive to well-bedded, quartzose fine to coarse sandstone, containing minor siltstone, greensand, conglomerate and breccia (Figure 2.5A, B; Leonard *et al.*, 2010). Sandstones typically contain abundant plant fragments. The Maungataniwha Sandstone Member is comprised of massive to poorly-bedded quartzose fine sandstone and is best-known as a source of marine reptile and dinosaur bones (Wiffen & Moisley, 1986; Leonard *et al.*, 2010; Young & Hannah, 2010). The base of the member is marked by a conglomerate and breccia interbedded with sandstone (Cutten, 1994) and grades upwards into shelly and concretionary sandstone and mudstone. An eastern facies of the Tahora Formation, the Mutuera Member, consists of poorly bedded glauconitic siltstone, and is less than 50 m thick (Isaac *et al.*, 1991; Field & Uruski *et al.*, 1997). The Houpapa Member is comprised of alternating sandstone-mudstone and minor conglomerate, and has a very restricted distribution. The Tahora Formation has a maximum-thickness of 400 m in the Te Hoe River area, although decreases to 50 m thick eastwards at Tahora (Isaac *et al.*, 1991).

Paleontology and Age

Maungataniwha Sandstone Member has produced diverse macro- and microfaunas, including, bivalves, gastropods, scaphopods, belemnites, ammonites, annelids, nautiloids (Figure 2.5C, D; Crampton, 1990; Crampton and Moore, 1990), crinoids (Eagle, 1994), crustaceans (Glaessner, 1980; Feldmann, 1993), beetles (Craw & Watt, 1987), shark and fish remains (Keyes, 1977; Wiffen, 1983), the remains of marine reptiles (Figure 2.5C), pterosaurs and turtles (Wiffen, 1980; 1981; 1990a, b; Wiffen & Moisley, 1986; Wiffen & Molnar, 1988; Cutten, 1994; Wiffen *et al.*, 1995), in addition to sauropod, ankylosaur and theropod remains (Molnar, 1981; Scarlett & Molnar, 1984; Molnar & Wiffen, 1994; 2007), along with various plant remains (Wiffen, 1980; 1996; Raine, 1990; Pole, 2008).

Diverse mollusc and dinoflagellate faunas have been recovered from the formation, indicating a Piripauan to Haumurian age (Young & Hannah, 2010; Crampton & Moore, 1990; Schiøler *et al.*, 2001). In places the base of the Tahora Formation is Piripauan (e.g., Te Hoe River, Vajda & Raine, 2010; Whakatakaa, Moore *et al.*, 1988; Crampton & Moore, 1990; Te Rangaakapua, Moore *et al.*, 1989), or Lower Haumurian (e.g., Koranga, Crampton *et al.*, 2006; Anini-Okaura Stream; Speden 1973), suggestive of the time-transgressive nature of this unit. At Tahora, foraminifera indicate the top of the Tahora Formation is early Haumurian in age (Joass, 1987; Isaac *et al.*, 1991), with a mid-Upper Haumurian age (Campanian to early Maastrichtian) identified for the top of the formation in the Maungahouanga Stream (Young & Hannah, 2010).

Depositional Setting

The basal 60 m of the Tahora Formation in the Te Hoe River–Mangahouanga Stream area is conglomeratic, interpreted as an alluvial depositional setting by Browne (1991). Stratigraphically above this, a rocky shore fauna was identified by Crampton (1988a) and Crampton & Moore (1990) in the westernmost extent of the formation, providing a Late Cretaceous paleo-shoreline, which deepens to shallow-marine, inner-shelf depositional environments eastwards (Crampton & Moore, 1990; Schiøler *et al.*, 2001; Young & Hannah, 2010). The Mutuera Member is considered to be a deeper-water facies of the Tahora Formation, whereas the Houpapa member is interpreted as localised channel fill and gravity flow deposits (Isaac *et al.*, 1991; Field & Uruski *et al.*, 1997). The Tahora Formation is the basal unit of the Late Cretaceous to Paleogene transgressive succession in the East Coast Basin (Isaac *et al.*, 1991; Cutten, 1994; Crampton *et al.*, 2006).

Figure 2.5: A) Outcrop of the Maungataniwha sandstone in the Maungataniwha area (BH39/385927). B) Thick-bedded sandstones of the lower Tahora Formation in the Koranga River at Koranga Bridge (BF41/748409). Photo supplied by James Crampton. C) Marine reptile vertebrae fossils in a float block of Maungataniwha Sandstone Member, Mangahouanga Stream (BH39/319855). D) Marine molluscs, including inoceramid prisms and Aporrhaid gastropods in the Tahora Formation (BH39/349880). Field of view is approximately 30 cm.

2.3.8 Owhena Formation

The Owhena Formation has a restricted outcrop distribution between Ruatahunga and Waingata Stream in the Raukumara region. Previously the formation was referred to as the 'Mata Sandstone'. The Owhena Formation was first defined by Phillips (1985), who nominated the Waitahaia River as the type section, and Owhena Stream as a reference section. The Owhena Formation is considered a lateral equivalent of the Tahora Formation and the Tapuwaeroa Formation (Phillips, 1985; Isaac *et al.*, 1991).

Lithostratigraphy

In the Waitahaia River, the Owhena Formation unconformably overlies the Karekare Formation (Figure 2.6A; Webb, 1971; Webb, 1985; Isaac *et al.*, 1991). The Owhena Formation consists of a fining-upwards succession of sandstone, siltstone and mudstone (e.g., Phillips, 1985; Crampton *et al.*, 2006), which extends northeast from near Ruatahunga Station (BE43/346734) to Waingata Stream, where it thins out (Phillips, 1985). The base of the formation is dominated by decimetre-bedded, alternating sandstone and mudstone (Figure 2.6B; Phillips, 1985). The most complete section is in Waitahaia River, where it is 100 m-thick.

Paleontology and Age

The formation is assigned a late Piripauan to early Haumurian age on the basis of foraminifera and dinoflagellate assemblages (Phillips, 1985). The Owhena Formation is early Piripauan (lower Santonian) in the Waitahaia River area based on dinoflagellate assemblages (Y16/f165, Y16/f166) (Crampton *et al.*, 2006).

Depositional Setting

The Owhena Formation is interpreted as being deposited at shelf depths, with a gradual transgression during deposition of the Owhena Formation, with a transition from shelfal to upper bathyal sediments (Phillips, 1985).

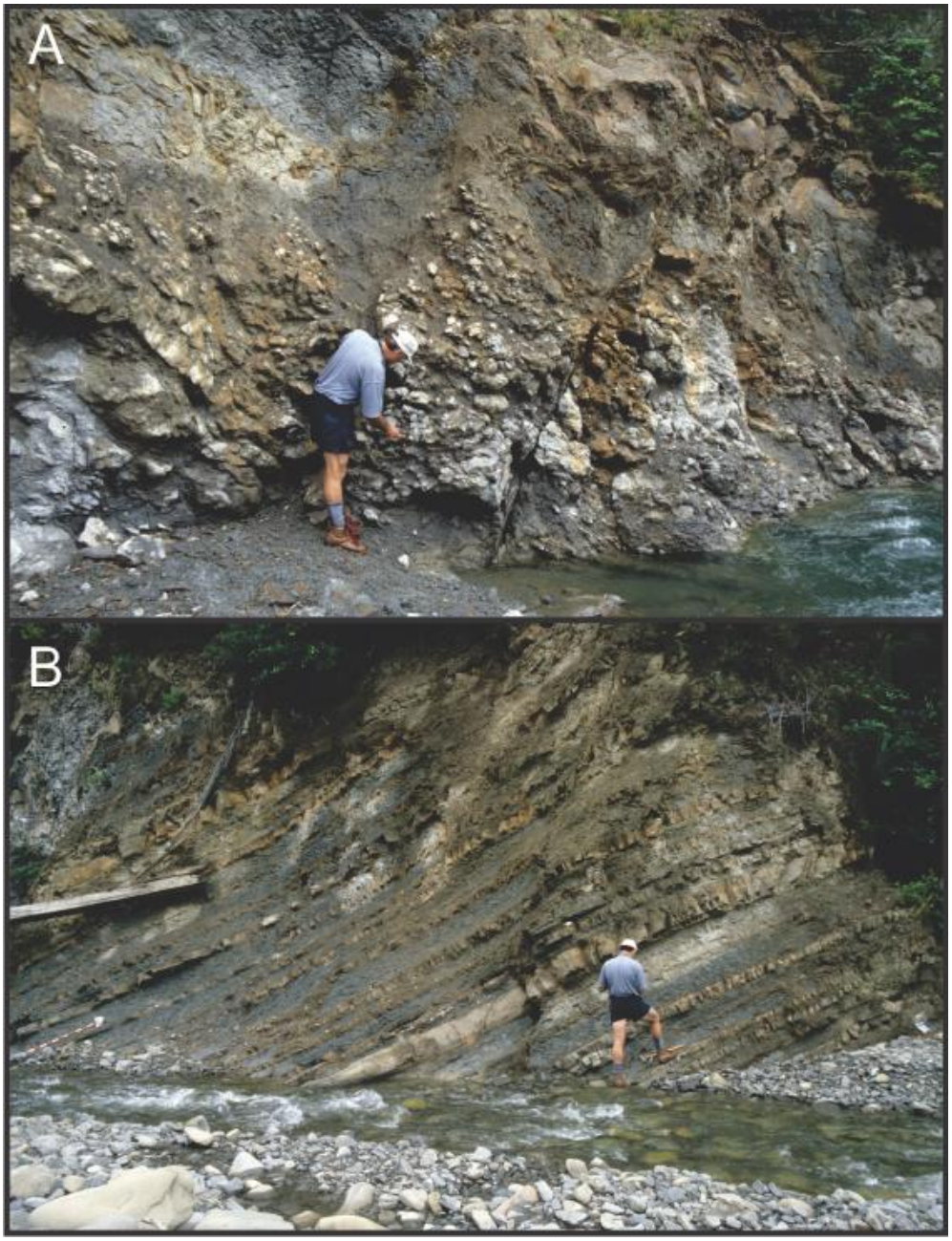

Figure 2.6: A) Nodular horizon marking the contact between the Karekare Formation (below) and the Owhena Formation (above) in Waitahaia River (BE43/361751). B) Alternating sandstone-mudstone of typical Owhena Formation in Waitahaia River (BE43/360751). Photos supplied by J. Crampton.

2.4 Hawke's Bay – Wairarapa

2.4.1 Gentle Annie Formation

The Gentle Annie Formation is a sedimentary breccia unit, of Urutawan-Motuan age, that extends from the Tora-White Rock area to the Whangai Range (Moore & Speden, 1979; 1984). The Gentle Annie Formation forms the base of the Mangapurupuru Group (Begg & Johnston, 2000; Lee & Begg, 2002; Lee *et al.*, 2011), and was initially described by Johnston (1975; 1980), from type sections in the Mangapakeha and Gentle Annie Streams in the Tinui area. The Gentle Annie Formation is correlated with other, disparate mid-Cretaceous sedimentary breccias and melanges in the East Coast Basin, including the Oponae Melange and Champagne Formation, and approximately coeval with the Te Wera Formation.

Lithostratigraphy

Gentle Annie Formation unconformably overlies Pahaoa Group (uppermost Pahau Terrane) metasedimentary basement rocks. The formation is comprised of green-grey, massive, poorly-sorted pebbly mudstone with minor intervals of moderately fossiliferous, well-bedded sandstone-mudstone and massive sandstone (Crampton, 1997). Clasts within this sedimentary melange are typically rounded, and pebble-sized or smaller, although blocks >10 m are common, and megaclasts >100 m are present (Figure 2.7; Crampton, 1997). Pebble-sized clasts often have polished surfaces, and are commonly comprised of indurated sandstone and locally common igneous clasts, with lesser mudstone and calcareous concretions (Crampton, 1997). The measured thickness of the Gentle Annie Formation is ~400 m in the Whangai Range area (Crampton, 1989), ~600 m in the Tinui area, and up to 700 m-thick in the Tora-White Rock area (Moore & Speden, 1984).

Paleontology and Age

Fossil faunas are poorly preserved and often reworked from older strata (Moore & Speden, 1979, 1984). The identification of *Aucellina euglypha* indicate a Urutawan-Motuan age, although Moore & Speden (1979) consider the formation to be dominantly Motuan.

Depositional Setting

Moore and Speden (1984) argue that the formation was likely deposited in a shelf environment, although Barnes (1988) considers that the Gentle Annie Formation and associated units were deposited in a trench-slope basin. The Gentle Annie Formation likely represents an initial period of rapid basin infill associated with rapid basin subsidence of uplift of the hinterland, at slope

depths or deeper, based on the overlying Springhill Formation (Crampton, 1997). The Gentle Annie Formation is interpreted as an olistostrome deposited by multiple, discrete debris flows adjacent to a fault-controlled basin margin (Crampton, 1989; Moore & Speden, 1979; 1984). The restricted stratigraphic range but wide distribution, including correlative units in Raukumara (Oponae Melange) and Marlborough (Champagne Formation) suggest that deposition was associated with an intra-Motuan tectonic event throughout the basin (Crampton, 1989; 1997).

Figure 2.7: Sheared clasts within a sandy mudstone matrix in an outcrop of the Gentle Annie Formation on White Rock Road (BQ34/047065).

2.4.2 Springhill Formation

The Springhill Formation has been mapped from the Whangai Range area through to the Tora-White Rock area (Moore & Speden, 1979; 1984). The Springhill Formation is included in the Mangapurupuru Group, and the type section for the formation extends from Centre Stream to Rewa Stream (Johnston, 1975; Moore & Speden, 1979). The Springhill Formation is considered an equivalent of the Karekare Formation in the Raukumara region, and the Swale Siltstone of Marlborough (Field & Uruski *et al.*, 1997).

Lithostratigraphy

The Springhill Formation gradationally overlies the Gentle Annie Formation. It is dominated by macro- and microfossiliferous mudstone, but also includes alternating sandstone-mudstone, minor conglomerate, thick-bedded sandstones, tuffs, and glauconitic grit (Figure 2.8; Crampton, 1997). The true stratigraphic thickness is difficult to determine due to deformation, although thickness estimates range from 750 m in the Whangai Range area to >650–2200 m in the Tinui area (Johnston, 1975; 1980; Crampton, 1989; 1997).

Paleontology and Age

The Springhill Formation was deposited between the Motuan and the Ngaterian, based on common *Aucellina euglpha* and *Mytiloides ipuanus* and *I. kapuus*, although deposition extended into the Arowhanan in the Tinui area based on the identification of *M. rangatira* (Moore & Speden, 1979, 1984; Crampton, 1989; 1997; Neef, 1995).

Depositional Setting

Paleoenvironmental indicators are poorly represented in the Springhill Formation. Foraminifera from the base of the formation indicate deposition within outer shelf to bathyal depths (Crampton, 1997), whilst foraminiferal assemblages from higher in the formation indicate deposition at middle to outer shelf depths (Hornibrook *et al.*, 1989; Adams, 1985; Crampton, 1997). Similarly, dinoflagellates from the Springhill Formation suggest deposition within near-shore to mid-shelf depths (Crampton, 1997). On this basis, Crampton (1997) interprets the Springhill Formation as being deposited at outermost shelf to slope depths via sediment gravity flows with progressively decreasing sedimentation rates and shallowing up-section.

Figure 2.8: Springhill Formation (at base), overlain by Tangaruhe Formation in Mangawarawara Stream (BM37/867439). Contact is ~10 cm above hammer handle. Hammer for scale – handle is 0.5 m long. Photo supplied by James Crampton.

2.4.3 Glenburn Formation

The Glenburn Formation is restricted to the eastern sub-belt, cropping out from Tora in the south to Waimarama in the north. The formation forms the top of the Mangapurupuru Group (Moore & Speden, 1979), and a type section is designated in Smokey Gully and Mataikona River (Johnston, 1975, 1980; Crampton, 1997). The age-equivalent Tikihore Formation, present within thrust sheets of the East Coast Allochthon, crops out between Waihau Bay and Mahia Peninsula, and has also been identified in the Opoutama-1 drillhole (Field & Uruski *et al.*, 1997; Ian Brown Associates Ltd, 2004). The Tikihore Formation is included in the Ruatoria Group (e.g. Mazengarb & Speden, 2000). Both the Glenburn and Tikihore formations are comprised of thick successions of centimetre- to metre-bedded, alternating sandstone and mudstone (Figure 2.9A, B). The Tikihore Formation is Arowhanan to Piripauan in age in the lower Mata River area, where it reaches 1060 m thick, with near-continuous exposure (Mazengarb & Speden, 2000).

Lithostratigraphy

The basal contact of the Glenburn Formation has not been observed, although Uratawan-Motuan volcanics at Red Island and Hinemahanga Rocks in Hawke's Bay may in part represent basement to Glenburn Formation, and elsewhere it is likely top overlie Pahaoa Group sediments (Moore *et al.,* 1986; Crampton, 1997). However, Urutawan to Motuan volcanics at Red Island and Himetanga Rocks, near Waimarama, may represent basement locally (Crampton, 1997; Field & Uruski *et al.*, 1997).

The Glenburn Formation consists of non-calcareous, interbedded sandstone, siltstone and mudstone, with decimetre to metre bedding (Figure 2.9 C, D, E). Sandstone beds are typically sharp-based and fine to medium grained, with flute casts at the base of some beds. Sedimentary structures include Bouma T_{bc} and T_{abc} beds, with some convolute bedding and dewatering structures (Leckie *et al.*, 1992). Mudstones are typically bioturbated, as are the upper surfaces of some sandstone beds. The uppermost Glenburn Formation (Te Mai Formation of Moore, 1980; Neef, 1992, 1995), is sandstone and flysch dominated, and contains a number of normal and reverse-graded conglomeratic beds of metre-scale thickness (Figure 2.9F). Sandstone beds are commonly carbonaceous, display convolute lamination, and fragments of *Inoceramus* (Neef, 1992; Laird *et al.*, 2003; Hines *et al.*, 2013; Hines, 2015). The formation has a minimum thickness of 1200 m in the Kaiwhata River and Mataikona River areas, although the base of the formation is never observed (Crampton, 1997).

Paleontology and Age

A reasonable bivalve macrofauna, dominantly comprising inoceramids, has been documented from the Glenburn Formation, along with occasional belemnites and ammonites. Samples from the Glenburn Formation rarely return foraminiferal faunas (H. E. G. Morgans, C. P. Strong pers. comm.), although a sample from the upper Glenburn Formation in Angora Stream (U24/f538) returned a reasonably diverse, entirely agglutinated, flysch-type foraminiferal fauna (Leckie *et al.*, 1992). Dinoflagellate floras are also moderately diverse (Schiøler & Crampton, 2014).

The base of the Glenburn Formation has not been identified or dated. However, the oldest observed inoceramid assemblages indicate a Ngaterian age at the minimum (Crampton, 1997; Schiøler & Crampton, 2014). The upper Glenburn Formation is considered to be Piripauan to Haumurian in age (Neef, 1992; Crampton, 1997; Laird *et al.*, 2003). A late Piripauan (Santonian) age for the upper Glenburn Formation at Tora is determined from inoceramid and dinoflagellate assemblages (Laird *et al.*, 2003), although in the Riversdale area, the uppermost portion of the

formation gives a lower Haumurian age (Early Campanian–early Maastrichtian) based on dinoflagellate assemblages (Lee, 1996). Similarly, the top of the formation at Huatokitoki Stream gives a late Piripauan to lower Haumurian age (mid- to late Santonian to early Campanian) based on dinoflagellates (Lee, 1996). The top of the Glenburn Formation at Angora Stream gives a late Haumurian age based on dinoflagellate assemblages (Crampton *et al.*, 2006).

Depositional Setting

The Glenburn Formation represents a widespread and long ranging submarine fan system deposited at bathyal depths (Crampton, 1997). This is supported by the presence of the foraminferan *Glomospira charoides* in the upper Glenburn Formation at Angora Stream, indicating deposition at bathyal depths (Leckie *et al.*, 1992). Neef (1995) interprets the base of the Glenburn Formation as representing distal turbidite deposition at bathyal depths during the Mangaotanean to Teratan ("Kipihana Formation" lithofacies), which are then overlain by more proximal turbidites in the Piripauan succession ("Te Mai Formation" lithofacies). Flute structures in the upper Glenburn Formation indicate a northeastern paleocurrent direction (055°; Neef, 1992).

Synonymy & Correlation

The Tikihore and Glenburn formations are synonymised herein, on the basis of similarities in age, lithology, depositional setting and thickness (Figure 2.9). The Glenburn Formation was first proposed by Eade (1966), and the name has since been applied widely by Johnston (1975) and Crampton (1997). Tikihore Formation was first used by Black (1980), and using the principle of precedence, the name Glenburn Formation is used here. Similarly, the Tapuwaeroa Formation that overlies the Tikihore Formation in eastern Raukumara shares a number of age, lithological and environmental characteristics with the uppermost Glenburn Formation of Piripauan to Haumurian age ("Te Mai facies" of Moore, 1980). The upper Glenburn Formation is characterised by a coarsening-upwards trend, and including distinctive cross-bedding and a high terrestrial organic carbon content, which also characterises the Tapuwaeroa Formation (Black, 1980).

The Kipihana and Te Mai Formations applied by Neef (1992, 1995) are also synonymised with the Glenburn Formation here, being comprised of Mangaotanean to Teratan, decimetre-bedded alternating sandstone and mudstone that coarsens upwards from the Teratan to Piripauan to decimetre- to metre-bedded alternating sandstone and mudstone, and conglomerates (Te Mai Formation *sensu* Neef, 1992, 1995). The southern part of the area (Mataikona River) mapped by Neef (1995), was included in a detailed assessment of the Glenburn Formation by Crampton (1997), who also identified Glenburn Formation of Teratan to Piripauan age north of the Neef

(1992, 1995) map area. The Te Mai Formation (largely Piripauan decimetre-bedded alternating sandstone and mudstone in the Glenburn area) has also used previously by Moore (1980) and was included by Crampton (1997) as the upper part of the Glenburn Formation.

Figure 2.9: A) Glenburn (previously referred to as Tikihore) Formation at Orete Point, East Cape (BD43/331268). Figure for scale. Photo supplied by J. Crampton. B) Glenburn Formation cropping out in the Mata River (BE44/539854), showing a syn-sedimentary slump unit at Mangaotanean-Teratan boundary. Photo supplied by J. Crampton. C) Glenburn Formation of Arowhanan age on the shore platform at Horewai Point, Glenburn (BQ35/381209), younging to the left. Photo supplied by James Crampton. D) Thick-bedded sandstones within the Glenburn Formation at Mangakuri Beach (BQ35/381209), younging to the left. Jacob Staff (1.5 m long) for scale. Photo Supplied by James Crampton. E) Outcrop of Piripauan Glenburn Formation near the mouth of Pukemuri Stream (BR34/076989). Figure for scale. F) Large-scale cross-bedding and pebble conglomerate within the Glenburn Formation on the Tora coast (BR34/070986). Note the lithological similarities between the Glenburn Formation in Raukumara (A, B) and the Glenburn Formation in eastern Wairarapa (C, D, E, F).

2.4.4 Tangaruhe Formation

The Tangaruhe Formation is restricted to the Western Sub-belt, and extends from Otane Stream, southern Hawke's Bay, to Tinui, in the Wairarapa region (Crampton, 1997). The formation is defined from a type section in Tangaruhe Stream in the Whangai Range, and is assigned to the Tinui Group (e.g. Moore, 1988a; Lee & Begg, 2002). The Tangaruhe Formation is laterally equivalent to the Tapuwaeroa and Te Mai formations of Lillie (1953) and Johnston (1975), respectively, the latter now incorporated within the Glenburn Formation (see discussion above).

Lithostratigraphy

The Tangaruhe Formation unconformably overlies the Springhill Formation (Figure 2.8). The formation is a glauconitic, alternating sandstone-mudstone to massive, more-or-less sandy mudstone that demonstrates rapid vertical and lateral facies transitions (Figure 2.10; Adams, 1985; Crampton, 1989; 1997). The base of the formation is characterised by coarse lithologies; either alternating sandstone-mudstone or pebbly sandstone and mudstone, referred to as the Mangawarawara Member, which reaches up to 180 m thick (Crampton, 1997; Field & Uruski *et al.*, 1997). The upper part of the formation is comprised of massive to well-bedded sandstone, siltstone and mudstone, and is typically grey-green to green-black, strongly bioturbated mudstone with minor sandstone, and less than 3% glauconite (Crampton, 1997), although the upper contact with the Whangai Formation is marked by thick-bedded sandstone. In the Tinui area, a few metre-thick beds of volcanogenic mudstone crop out within the formation (Crampton, 1997). The thickness of the Tangaruhe Formation is laterally variable, reaching a maximum of 280 m thick in the Whangai Range area (Crampton, 1997).

Paleontology and Age

Foraminifera are abundant and diverse within the formation (Adams, 1985; Crampton, 1997). The Tangaruhe Formation was deposited in the Piripauan to early Haumurian (Crampton, 1997). Fish teeth are common in grain mounts (this study). Macrofossils include *Inoceramus* bivalves, disarticulated brachiopods, belemnites and ammonites (Crampton, 1997).

Depositional Setting

The coarse, variable sedimentation of the lower part of the Mangawarawara Member is interpreted to represent either a coarse channel-fill facies, or alternately a base-of-slope debris apron (Crampton, 1997). The upper part of the formation is dominated by strongly bioturbated mudstone and siltstone, indicating deposition in a lower energy environment (Crampton, 1997). Foraminifera indicate deposition at depths greater than 200 m (Adams, 1985; Crampton, 1997).

Figure 2.10: Representative outcrop of Tangaruhe Formation in Mangawarawara Stream (BM37/865440). Photo supplied by James Crampton.

2.4.5 Whangai Formation

The Whangai Formation has a wide temporal range in addition to being widespread, and is typically dominated by a fine-grained sedimentary succession that spans the breadth of the East Coast Basin and beyond, with lateral correlatives identified in New Caledonia, Northland, Canterbury, and Great South Basins (Moore, 1988a). The Whangai Formation is subdivided into five members on the basis of lithology; the Kirks Breccia, Rakauroa, Porangahau, Upper Calcareous and Te Uri members (Moore *et al.*, 1986; Moore, 1988a, b). The Whangai Formation and its various members form the bulk of the Tinui Group. The late Piripauan to early Teurian Whangai Formation consists of 30 to ~600 m of primarily micaceous and argillaceous siltstone (Moore, 1988a; Field & Uruski *et al.*, 1997).

2.4.5.1 Kirks Breccia Member, Whangai Formation

The Kirks Breccia Member occurs as isolated outcrops in the Raukumara region (Moore, 1988a; Moore, 1989b), and has not been observed in the Hawke's Bay, Wairarapa, or Marlborough regions. The Kirks Breccia Member marks the base of the Whangai Formation in the northern East Coast Basin. Its type section is in Kirks Clearing on the Motu River (Moore, 1988a). Deposition of the Kirks Breccia Member was coeval with the deposition of the Tahora and Owhena formations. The member may possibly be coeval with the Mangawarawara Member of the Tangaruhe Formation, both of which outcrop out in the Western Sub-belt (Figure 2.2).

Lithostratigraphy

The Kirks Breccia Member infills a single, large channel structure incised into the underlying Karekare Formation with a sharp, channelised basal contact. The Kirks Breccia Member is a poorly-sorted matrix to clast supported breccia. Clasts are comprised of fine sandstone, light- and dark-grey mudstone, and concretions. The breccia is a coarse, matrix- to clast-supported breccia-conglomerate, with an unsorted, random distribution of larger clasts throughout the unit (Moore, 1989b). Clasts are typically pebble to cobble sized, but included larger slabs of rafted material, including sandstone clasts and concretions up to 3 m in diameter. Clasts are composed of angular to sub-rounded fine sandstone, light-grey mudstone, dark-grey mudstone and calcareous concretions within a matrix of micaceous mudstone. The Kirks Breccia varies from 30 to 200 m thick, and grades upwards into the Rakauroa Member of the Whangai Formation (Moore, 1989b).

Paleontology and Age

Dinoflagellate assemblages from the Kirks Breccia Member place it as late Piripauan to early Haumurian in age (Moore, 1989b). Fragments of *Magadiceramus rangatira* are included in sandstone clasts within the member, suggesting that a proportion of the clasts are derived from the underlying Arowhanan Karekare Formation (Moore, 1989b).

Depositional Setting

The Kirks Breccia is interpreted as being deposited in a channel at shelfal depths, most likely outer shelf, and fed by locally derived material rather than sediment reworked from a near-shore source.

The Kirks Breccia is Piripauan in age, and is suggested as evidence that there was ongoing deformation in the region at this time that may correlate with other examples in western Raukumara in the Late Cretaceous (Isaac, 1977; Moore, 1978; Moore, 1989b). The member is folded around a steeply plunging anticline (Moore, 1989b).

2.4.5.2 Rakauroa Member, Whangai Formation

The Rakauroa Member is found across much of the North Island East Coast Basin, from the Raukumara Peninsula to Tora. The member was originally named the Rakauroa Formation (Jablonski, 1934; Lillie, 1953), and incorporated into the Whangai Formation by Moore *et al.* (1986). The type section for the Rakauroa Member is in Rakauroa Stream (Moore, 1988a). The Rakauroa Member is typically the lowermost observed member of the Whangai Formation (Moore, 1989b).

Lithostratigraphy

The base of the Rakauroa Member is considered conformable in most sections. At Owhena Stream, the Owhena Formation grades into the Whangai Formation, with the base of the Rakauroa Member marked by a 5–10 m-thick nodular concretionary horizon (Figure 2.6; Phillips, 1985; Moore, 1988a; Crampton *et al.*, 2006). In many sections the base of the formation is marked by a 4–5 m-thick bed of sandstone (e.g. Akitio River, Packtrack Stream, Angora Stream; Leckie *et al.*, 1992; Crampton, 1997; Francis, 1999; 2001; Crampton *et al.*, 2006). Neef (1995) noted onlap of the Rakauroa Member onto basement strata (Mangapokia Formation, of the uppermost Pahau Terrane) near Marainanga Road, where basal strata of the Rakauroa Member is represented by fine sandstone and mudstone containing scattered bivalves. In the Ngahape area of Wairarapa, Moore (1980) describes a thick, bioturbated sandstone containing numerous concretions at the base of the Rakauroa Member, with the basal contact marked by a 5–40 cm-thick conglomerate of weathered igneous clasts. Similarly, Crampton *et al.* (2001) note a thin conglomerate at the base of the Rakauroa Member in Mangaotane Stream.

The Rakauroa Member primarily comprises indurated, poorly-bedded to massive, rusty-orange weathering, medium-grey, siliceous, non-calcareous, micaceous mudstone (Figure 2.11A, B; Moore, 1988a). Occasionally the formation may contain centimetre- to decimetre-thick greensand beds, sedimentary dikes, laminated beds, calcareous concretions, and pyrite nodules (Moore, 1988a; Leckie *et al.*, 1992). The base of the unit is commonly sandy, and fines upwards, with sandstone beds decreasing in thickness and frequency up-section, and rare above the basal 25 m. Sedimentary structures include wavy and parallel lamination, climbing ripples, and ripple cross-stratification (Leckie *et al.*, 1992). Cone in cone structures are commonly observed in sandstone beds (Leckie *et al.*, 1992). In some sections, the base of the Rakauroa Member is marked by centimetre- to decimetre-bedded, alternating dark- and light-coloured siltstone, referred to as "thin-bedded Rakauroa" (Leckie *et al.*, 1995).

The Rakauroa Member ranges from 40 to 400 m-thick, although is typically 200–300 m-thick in most sections. The Rakauroa Member ranges from 40–70 m-thick in the Raukumara Peninsula area, and 350 m in southern Wairarapa at Tora although here the basal contact with the Glenburn Formation is faulted (Moore, 1988a; Wasmuth, 1996; Laird *et al.*, 2003; Hines *et al.*, 2013).

Paleontology and Age

Macrofossils are rare in the Rakauroa Member, but those found include ammonites, belemnites, echinoid spines, and fish vertebrae, teeth and scales, *Inoceramus* sp. *Nuculana* sp., *Lucina* c.f. *canterburiensis* and possible *Callistina* sp. bivalves (Moore, 1988a). *Terebellina* (*Bathysiphon*) are common in some localities (Moore, 1980; 1988a; Francis, 1999, 2001). The degree of bioturbation is variable, ranging from rare to intense, with only *Zoophycos* accurately recognised (Moore, 1987a). The formation is dominantly Haumuarian in age. However, detailed assessment of the temporal and spatial trends of the formation across the basin show that the base of the Whangai Formation is time-transgressive (Crampton *et al.*, 2003; 2006).

Depositional Setting

Foraminifera from lower in the formation indicate deposition at shelf depths, possibly with reduced oxygen levels (Moore, 1988b). In western Raukumara, Moore (1989b) considers that the Rakauroa Member was deposited at no deeper than outer shelf depths. Neef (1995) interprets the basal strata as representing neritic conditions, with the remainder of the formation deposited at bathyal depths, consistent with the interpretation of marine transgression through the Whangai Formation.

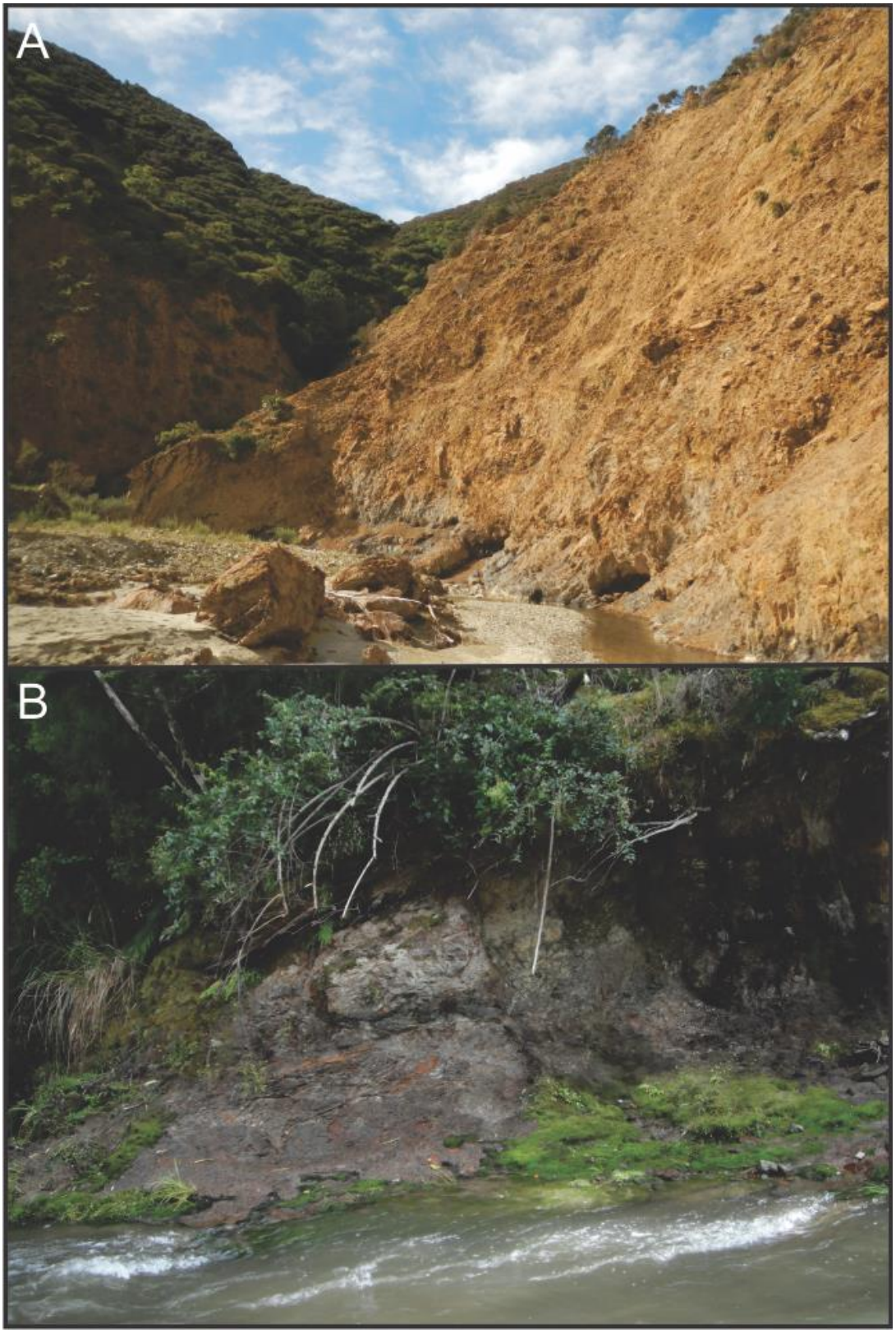

Figure 2.11: Typical outcrops of the Rakauroa Member. A) Well-exposed Rakauroa Member in Pukemuri Stream, southeast Wairarapa (BR34/077000). The orange-brown weathering is characteristic of the formation. Field of view is approximately 30 m. B) Rakauroa Member cropping out in Mangahouanga Stream, northwest Hawke's Bay (BH39/316857). Field of view approximately 5 m.

2.4.5.3 Porangahau Member, Whangai Formation

As defined by Moore (1988a), the Porangahau Member has a restricted distribution, occurring in outcrop only between Akitio River and Angora Stream in the southern Hawke's Bay, and Mangatakawa Stream in eastern Raukumara. The Porangahau Member was included in the Whangai Formation by Moore *et al.* (1986). The type section for the member is Kaihika Ridge (BM38/029297) near Porangahau, southern Hawke's Bay (Moore, 1988a).

Lithostratigraphy

The Porangahau Member conformably overlies the Rakauroa Member. It consists of well-bedded, decimetre-thick beds of grey to green-grey, calcareous alternating sandstone and mudstone (Figure 2.12, A, B; Moore, 1988a). Sandstone interbeds are fine to coarse grained and are up to 30 cm thick, and commonly contain glauconite. Mudstone beds are occasionally red-brown and green (Leckie *et al.*, 1992). Fine sandstone beds contain planar- and climbing-ripples, parallel laminations and antidune bedding. Some beds contain ball and pillow structures. Coarse sandstone beds up to 10 cm-thick pinch out laterally. Bioturbation varies from slight to moderate. In places, regular decimetre-thick interbedded light- and dark-grey mudstone occur, which are are referred to as the 'zebra beds' lithofacies (Figure 2.12B; Moore 1988a). The member ranges from 20 to 300 m thick.

Paleontology and Age

No macrofossils are recorded from the Porangahau Member, but *Zoophycos* and *Chondrites* traces are noted by Moore (1988a). The Porangahau Member is of early Teurian age based on foraminiferal faunas (Leckie *et al.*, 1992). Where present, the Porangahau Member typically spans the K/Pg boundary.

Depositional Setting

Foraminiferal faunas indicate deposition in bathyal water depths (Leckie *et al.*, 1992). The absence of Porangahau Member between the Rakauroa and Upper Calcareous members in the Puketoro, Mataikona, and Waipawa-Otane areas, suggests that the Porangahau Member likely represents a series of disparate submarine fans, rather than a single margin-wide system.

Synonymy & Correlation

The Porangahau Member is a potential lateral correlative of the Awhea Formation at Glenburn and Tora, and the Butts Formation in northern Marlborough. The Awhea Formation is coeval with the Porangahau Member (Hines *et al.*, 2013; Crouch *et al.*, 2014) and shares distinct lithological similarities. This was suggested in Hines *et al.* (2013), and is discussed further within this chapter.

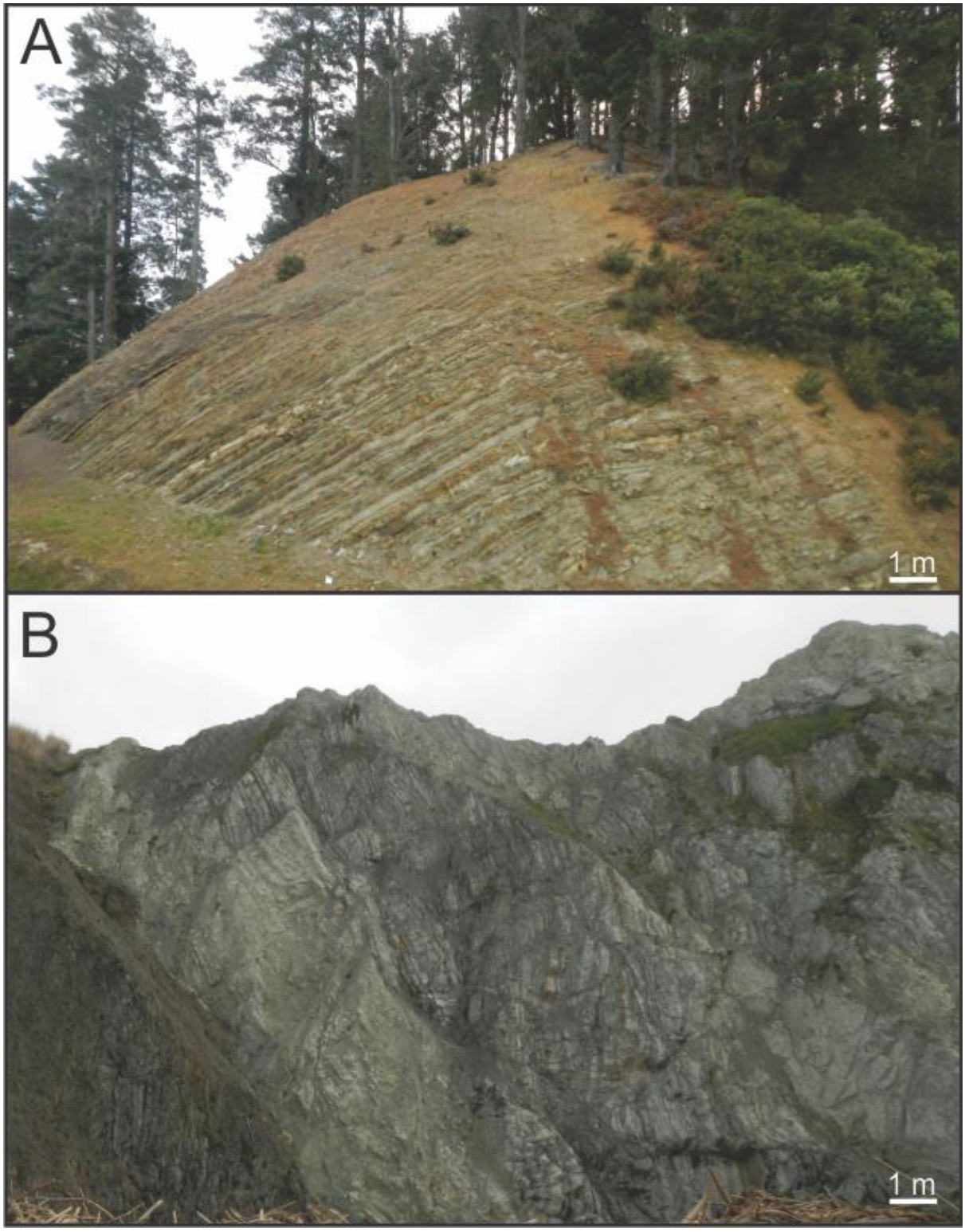

Figure 2.12: A) Porangahau Member at Old Hill Road (BM38/062337), here comprised of sandstone-dominated, decimetre-bedded alternating sandstone-mudstone. B) Porangahau Member cropping out at Whangai Bluff, Waimarama (BL39/427823), here comprised of mudstone-dominated, green to dark-grey, decimetre-bedded alternating fine sandstone-mudstone.

2.4.5.4 Upper Calcareous Member, Whangai Formation

The Upper Calcareous Member was defined in Moore *et al.* (1986). It occurs extensively across the North Island East Coast Basin, from eastern Raukumara to the Ngahape area of central Wairarapa. The formation does not crop out further south in the Glenburn and Tora areas. The type section of the member is located in Tangaruhe Stream (Moore, 1988a). The Upper Calcareous Member in the Eastern Sub-belt is coeval with the Kaiwhata and Mungaroa limestones in southern Wairarapa, and the Mead Hill Formation in Marlborough.

Lithostratigraphy

The base of the Upper Calcareous Member conformably overlies either the Rakauroa Member or Porangahau Member. The Upper Calcareous Member consists of poorly-bedded to massive, intensely bioturbated, calcareous (1–15% $CaCO_3$; Moore, 1988a), micaceous mudstone (Figure 2.13A, B). Carbonate content increases upwards through the formation (Leckie *et al.*, 1992). In places, the member may also contain concretions, pyrite nodules, glauconitic sandstone beds and brecciated beds, and isolated, possibly rafted pebbles (Leckie *et al.*, 1992; 1995). Bedding, where present, comprises 0.5 to 4 cm-thick light- and dark-coloured alternating mudstone beds. In places, delicate millimetre-scale laminations are preserved.

Kenny (1986) further subdivided the Upper Calcareous Member, incorporating a flinty interval containing chert nodules, and an uppermost muddy limestone, as the "Waingata Limestone". The observation of a chert interval midway through the Upper Calcareous Member is consistent with outcrops in the southern Hawke's bay (e.g., Mara Quarry; Moore, 1988a; Neef, 1995). Similarly, muddy limestone in the uppermost Upper Calcareous Member is coeval with the Mungaroa Limestone in southern Wairarapa. Neef (1995) notes chert and siltstone couplets in the middle of the Upper Calcareous Member, previously described by Moore (1988a) in the Mara Quarry. The Upper Calcareous Member reaches to 520 m-thick in the Owahanga–Akitio River area of northeast Wairarapa (Neef, 1992), although the thickness of the member is more commonly 50–200 m thick (Rogers *et al.*, 2001).

Paleontology and Age

Although rare, a diverse range of macrofossils have been identified from the Upper Calcareous Member, including; a Podocarpacae frond and *Araucaria haasti* (plant), echinoid spines, fish scales, *Terebellina* (*Bathysiphon*), and a number the bivalves c.f. *Limopsis*, c.f. *Hypoxytoma*, *Entolium* c.f. *membranaceum*, *Ostrea* c.f. *dichotoma* and c.f. *Pycnodonte* (Moore, 1988a). In addition to these, seven species of ammonites were identified by Isaac (1977) in Late Cretaceous, weakly calcareous

siltstones that Moore (1988a) attributes to the Upper Calcareous Member. The Upper Calcareous Member is late Haumurian to early Teurian in age, based on macrofossil, and dinoflagellate and foraminiferal faunas (Moore, 1988a). In Angora Stream, southern Hawke's Bay, the Upper Calcareous Member is Teurian in age and intensely bioturbated, with the burrow forms of the *Cruziana-Zoophycos* ichnofacies (Leckie *et al.*, 1992). In the Tawanui section, Akitio River (southern Hawke's Bay), the Upper Calcareous Member is of late Haumurian, restricted to the *Manumiella druggii* dinoflagellate zone and the *Globotruncata circumnodifer* foraminiferal assemblage zone (Wilson *et al.*, 1989). At Tawanui, the Upper Calcareous Member is moderately to intensely burrowed, including *Chondrites*, and foraminiferal faunas an outer neritic to upper bathyal depth (Leckie *et al.*, 1992).

Depositional Setting

Although an outer shelf environment is favoured by Moore (1988a), the Upper Calcareous Member was likely deposited in an upper to middle bathyal environment based on molluscan and foraminiferal faunas presented in Moore (1988a). Foraminiferal faunas for the formation indicate a minimum 200 m paleodepth for the member, and Moore (1988a) notes a deepening trend between the Western and Eastern sub-belts.

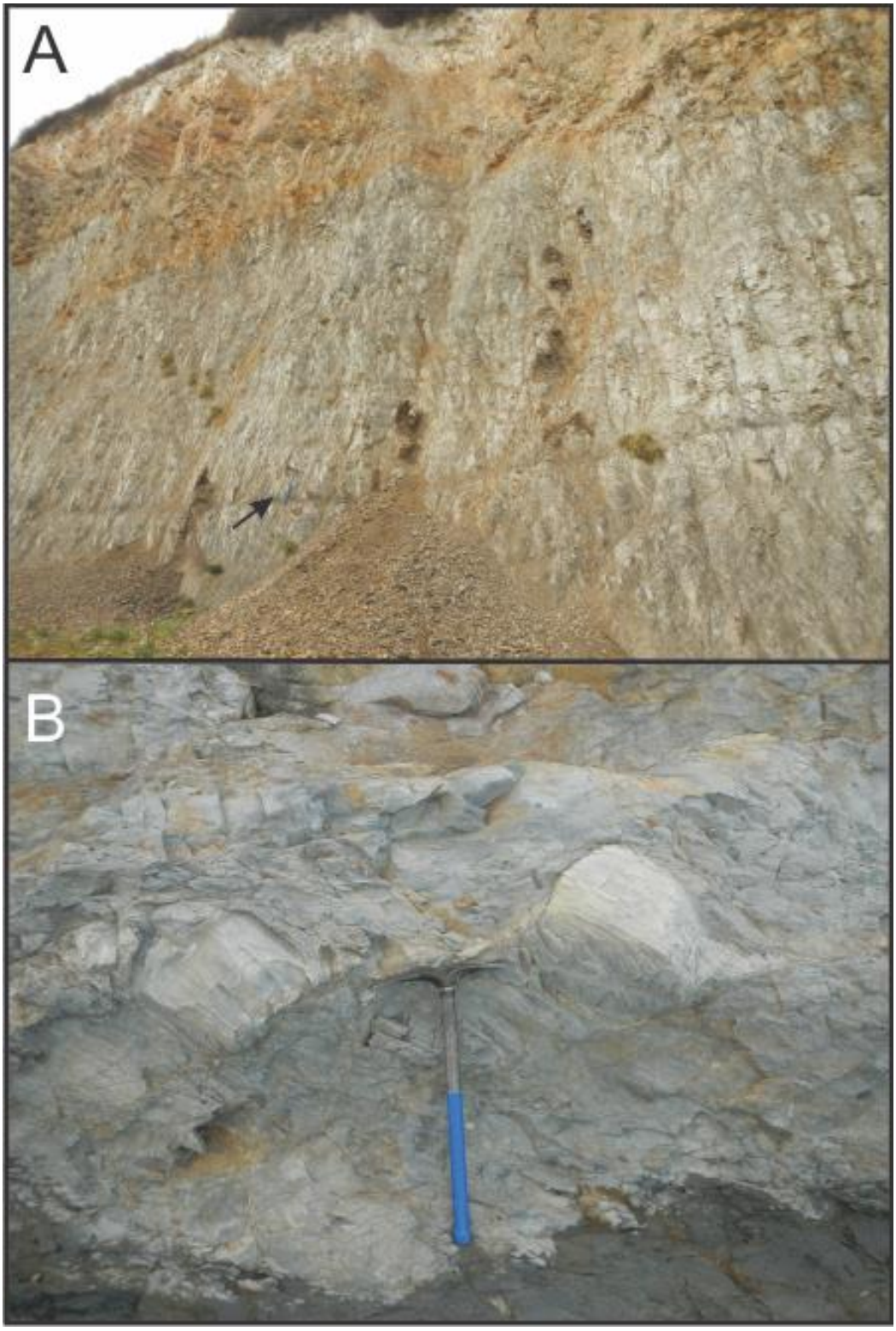

Figure 2.13: A) Upper Calcareous Member cropping out in a road cutting on Ongaonga Road, central Hawke's Bay (BL38/031720). Hammer for scale (arrowed) – handle is 70 cm long. B) Upper Calcareous Member cropping out at Riversdale, eastern Wairarapa (BP36/592481). Hammer for scale – handle is 70 cm long.

2.4.5.5 Te Uri Member, Whangai Formation

The Te Uri Member has a restricted distribution, and has only been identified at Te Hoe River (northwest Hawke's Bay), and in the Whangai Range (southern Hawke's Bay). The Te Uri Member was defined by Moore (1988a), who nominated Tangaruhe Stream as the type section. The uppermost portion of the Te Uri Member has been geochemically correlated with the Waipawa Formation (Rogers *et al.*, 2001).

Lithostratigraphy

The base of the Te Uri Member is conformable with underlying strata (Figure 2.14). The Te Uri Member consists of poorly- to well-bedded glauconitic sandstone and mudstone (Figure 2.14). In outcrops of alternating sandstone-mudstone, sandstone beds are sharp-based, typically 5 to 55 cm-thick, and vary from fine- to coarse-grained. The sharp bases to sandstone beds load onto the *Planolites* burrowed surfaces of underlying mudstones (Rogers *et al.*, 2001). Clasts are dominantly quartzose, with some clasts of sandstone and mudstone up to 2 mm diameter, and glauconite is quite common (Leckie *et al.*, 1992). Fine sandstone beds contain uni-directional ripple cross-lamination and antidune bedding, and the bases of some sandstone beds contain tool marks with a 30–210° orientation (Leckie *et al.*, 1992). Coarse sandstone beds are observed to pinch out laterally, and are overlain by very fine sandstone beds that are parallel and ripple laminated (Leckie *et al.*, 1992). Minor ball and pillow structures and convolute bedding are observed. The mudstone is variable in nature, varying from intensely bioturbated to non-bioturbated, with fine laminations preserved (Leckie *et al.*, 1992). The Te Uri Member is sandier than the underlying units, and dominated by moderately bedded, highly bioturbated, glauconitic sandstone and mudstones, and where present, varies from 3 to 40 m thick.

Paleontology and Age

With the exception of shark teeth (K. Bland, pers. comm. 2018), and fish teeth identified in mineral separates (this study), no macrofossils have been reported from the Te Uri Member. The uppermost Te Uri Member is typically intensely bioturbated with *Planolites*, *Zoophycos*, *Thallasinoides, Teichichus* and *Skolithos* (Moore, 1987a; Leckie *et al.*, 1992). The member lies immediately above the K/Pg boundary (Figure 2.14), and spans much of the Teurian stage based on foraminiferal, calcareous nannofossil and dinoflagellate assemblages (Leckie *et al.*, 1992; Rogers *et al.*, 2001; Crouch *et al.*, 2014; Kulhanek *et al.*, 2015).

Depositional Setting

The occurrence of *Zoophycos* and *Teichichnus* bioturbation indicates an assemblage of opportunists that colonise inhospitable zones on the limit of habitability (Bromley, 1990; Leckie *et al.*, 1992). *Zoophycos* and *Chondrites* are indicative of bathyal, oxygen depleted environments (Ekdale, 1985; Leckie *et al.*, 1992). The Te Uri Member, through comparison with the modern Canterbury Shelf, was interpreted by Leckie *et al.* (1992) as a sand body on the shelf edge that was subjected to prolonged winnowing and glaucony during a sea-level lowstand. Sedimentary structures described in the Te Uri Member by Leckie *et al.* (1992), including tool marks, cross-bedding and bioturbation, are consistent with a shallow-marine setting. The top 4 m of the Te Uri Member at Tawanui has been geochemically correlated with the Waipawa Formation (Rogers *et al.*, 2001; Hollis *et al.*, 2014). The paleoenvironmental interpretation of this unit and stratigraphic relationships of the various members of the Whangai Formation are reviewed in Chapters Four and Seven.

Figure 2.14: Te Uri Member of the Whangai Formation cropping out in the upper Akitio River (Tawanui) section (BM37/867246). Sharp contact in the centre of the photo is the basal contact of the Te Uri Member (left) with the Upper Calcareous Member (right), approximating the Cretaceous-Paleogene boundary. Photo supplied by K. Bland.

2.4.6 Waipawa Formation

The Waipawa Formation generally follows the outcrop distribution of the Whangai Formation in the North Island, with the exception of the Whangai Range area. Outcrops of the Waipawa Formation have been identified in the southern Wairarapa (Hines *et al.*, 2013; Hollis *et al.*, 2014; Kulhanek *et al.*, 2015) , Mead Stream in Marlborough (Strong *et al.*, 1995; Hollis *et al.*, 2005a, 2014), and Northland (Isaac *et al.*, 1994). The Waipawa Formation marks the top of the Tinui Group in North Island (Moore, 1988a), and is included within Muzzle Group rocks in Marlborough (Reay, 1993). The type section for the Waipawa Formation occurs in the Waipawa River near Waipawa Township, central Hawke's Bay. The Waipawa Formation has been correlated with the uppermost Te Uri Member, along with the upper Waipara Greensand in the Canterbury Basin, and the Tartan Formation in the Great South Basin on the basis of geochemistry (Rogers *et al.*, 2001; Schiøler *et al.*, 2010; Hollis *et al.*, 2014). Two thin, dark-grey mudstone beds have been identified in Dee Stream (Clarence Valley, Marlborough), which may correlate with the Waipawa Formation at Mead Stream (Hancock *et al.*, 2003).

Lithostratigraphy

The Waipawa Formation conformably overlies the Whangai Formation. At Te Hoe River, the Waipawa Formation overlies Te Uri Member, whereas elsewhere the formation typically gradationally overlies the Upper Calcareous Member, although it conformably overlies the Porangahau Member in several localities, and at Rakauroa Stream the formation unconformably overlies the Rakauroa Member on a sharp, burrowed contact (Moore, 1988a). In Mead Stream, the Waipawa Formation conformably overlies the Mead Hill Formation (Strong *et al.*, 1995; Hollis *et al.*, 2005a). The Waipawa Formation typically comprises poorly-bedded, dark-brown to grey to brownish-black micaceous, carbonaceous mudstone (Figure 2.15A, B, C) with moderate to high total organic carbon (TOC = 0.5–13%; Moore, 1988a; 1989). The Waipawa Formation varies considerably in thickness, from 1.5 m-thick at Tora (Figure 2.15C; Hines *et al.*, 2013), to 70 m-thick at Kerosene Bluff (Moore, 1988a; 1989). The formation is typically around 10–30 m-thick, and weathered surfaces commonly show jarosite, iron oxides and/or gypsum (Figure 2.15D).

Paleontology and Age

Macrofossils from the Waipawa Formation are rare, and include *Thyasira* sp. and *Conchocoele* sp. bivalves, fish vertebrae, locally abundant *Terebellina* (*Bathysiphon*) and small decalcified bivalve fragments (Figure 2.15E; Moore, 1987b, 1988a; 1989a). Biostratigraphic data suggests that deposition of the Waipawa Formation occurred during the late Teurian Stage, in the upper part of

NZP5 Dinoflagellate Zone and calcareous nannofossil zones NP5–NP7, indicating a Selandian to Thanetian age (Late Paleocene; Crouch, 2001; Kulhanek *et al.*, 2015), likely restricted to 59.4–58.7 Ma (Hollis *et al.*, 2014).

Depositional Setting

It has been argued that the Waipawa Formation represents dysoxic to anoxic seafloor conditions, on the basis of increased total organic carbon (TOC) preservation (0.5–13 % TOC), in comparison to the immediately-underlying Whangai Formation (0–~1.5 % TOC), as well as poor to absent foraminiferal and macrofaunas, and outcrop appearance of the Waipawa Formation (Moore, 1988a; Killops *et al.*, 2000; Rogers *et al.*, 2001; Hollis & Manzno-Kareah, 2005; Hollis *et al.*, 2014). There is substantial debate around the depositional environment and conditions for this formation, which are reviewed in detail in Chapters 3 and 4.

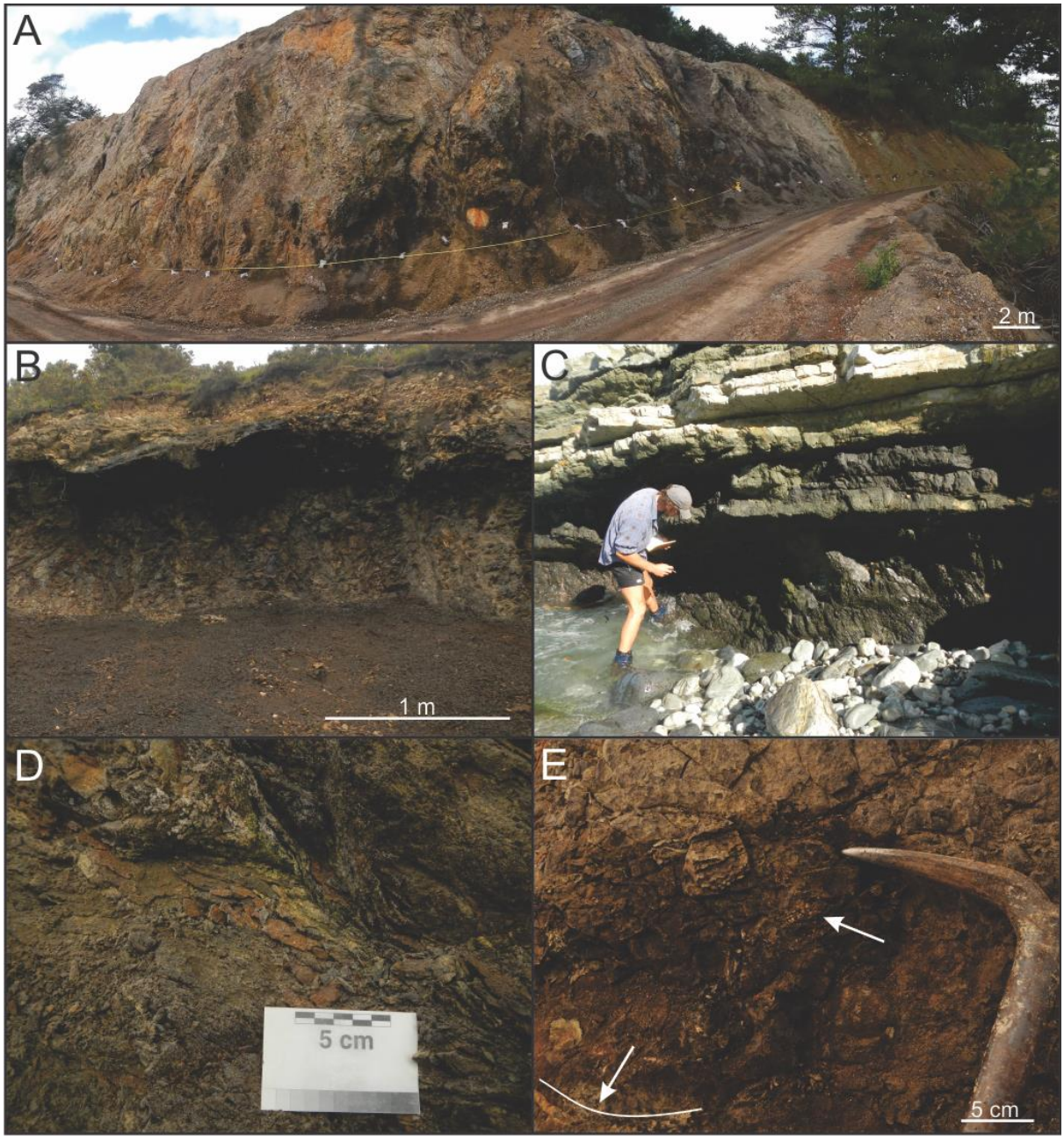

Figure 2.15: A) Waipawa Formation cropping out in a road cut on Angora Road, named the Taylor White section (BM37/944150). Note the concretion in the centre of the photo, and the contact with the overlying green-grey Wanstead Formation on the right hand side of the photo. B) Waipawa Formation at Kerosene Bluff (BP36/685714). C) Waipawa Formation at Te Kaukau Point ('Cleft Section', BR33/025950), where the Waipawa Formation is 1.8 m-thick, and deposited in association with the Mungaroa Limestone (refer to Chapter Four). D) Typical Waipawa Formation at Kerosene Bluff, showing iron oxides and jarosite on weathered surface. E) Waipawa Formation at Taylor White, showing *Bathysiphon* sp. tubes (small pale dots, arrowed), and bioturbation trace (outlined and arrowed, bottom left corner). Note the absence of bedding in all photos.

2.4.7 Wanstead Formation

The Wanstead Formation is widely distributed throughout the North Island East Coast Basin, and generally follows the outcrop distribution of the Whangai Formation (Moore *et al.*, 1986; Moore, 1988a). The Wanstead Formation is the basal unit of the Mangatu Group (Moore *et al.*, 1986; Mazengarb & Speden, 2000), and was originally described by Ongley (1941), who designated a type section in road cuts at Wanstead (southern Hawke's Bay). This type section was revised by Lillie (1953) to include Te Uri Stream.

Lithostratigraphy

The Wanstead Formation is commonly poorly exposed, with slumping and slope instability frequent due to the smectitic clay-rich nature of the formation. In the Whangai Range area, the Wanstead Formation conformably overlies the Te Uri Member of the Whangai Formation. At Huatokitoki Stream, the Wanstead Formation conformably overlies the Kaiwhata Limestone (Lee & Begg, 2002), although further south at Tora, the base of the Wanstead Formation is unconformable, attributed to local submarine channel and fan development (Hines *et al.*, 2013). The base of the Wanstead Formation may be unconformable in some localities in the Eastern Subbelt where flysch facies of the Wanstead Formation overlies the Waipawa Formation. This flysch facies is locally restricted to the Wimbledon to Whareama Valley area (southern Hawke's Bay–eastern Wairarapa). Elsewhere, the Wanstead Formation is apparently conformable with either Te Uri Member or Waipawa Formation (depending on locality). In southern Hawke's Bay-Wairarapa, the base of the Wanstead Formation is marked by alternating fine sandstone and mudstone (Neef, 1995; others, pers. obs.). Elsewhere, the base beds of the Wanstead Formation comprise grey, generally massive, calcareous mudstone (Figure 2.16A, B, C). A friable, quartzose, glauconitic sandstone crops out 10 m above the Waipawa Formation at Blairlogie Road (eastern Wairarapa), and a similar unit is observed 30 m above the Waipawa Formation at Old Hill Road, near Porangahau (southern Hawke's Bay).

A 1 m-thick, clast supported, polymict basal conglomerate, comprised of poorly-sorted, pebble- to boulder-sized, moderately to well-rounded clasts, overlies the unconformable contact with the Pukemuri Siltstone at Tora. Sharply overlying the conglomerate is green-grey to blue-grey, highly calcareous mudstone with occasional grey mudstone layers and minor glauconitic sandstone, typical of the Wanstead Formation (Figure 2.16C). The mudstone tends to be mottled, indicative of pervasive bioturbation.

The Wanstead Formation is at least 300 m-thick in Waingongoro Stream and, in the upper reaches of the Mataikona River, the Wanstead Formation is comprised of at least 450 m of massive mudstone (Neef, 1995). At Te Hoe River, the Wanstead Formation is 250 m-thick (Moore, 1987). The Wanstead Formation is up to 490 m thick (Field & Uruski *et al.*, 1997), though is more typically 100–200 m thick (Lee & Begg, 2002; Hines *et al.*, 2013). The formation is typically slumped and/or sheared (Figure 2.16D), making true estimates of thickness and lithological variability difficult to characterise.

Paleontology and Age

No macrofossils have been reported from the Wanstead Formation, except for a single *Perploma* bivalve from the Mataikona River (Neef, 1995). The Wanstead Formation does provide diverse and well-preserved foraminifera faunas, returning Teurian to Runangan ages (late Paleocene to latest Eocene) for the formation, though more typically Teurian to Bortonian (late Paleocene to middle Eocene; Moore & Morgans, 1987; Field & Uruski *et al.*, 1997).

Foraminiferal assemblages recovered from the Wanstead Formation at Tora give a Bortonian to late Kaiatan age (middle to late Eocene) based on calcareous nannofossil assemblages, giving a more restricted age range than Wanstead Formation in northern Wairarapa and Hawke's Bay (Hines *et al.*, 2013).

Depositional Setting

Benthic foraminiferal faunas indicate a mid- to lower-bathyal depositional depth for the Wanstead Formation. The formation progressively youngs and deepens southwards (Hines *et al.*, 2013). The deepwater Wanstead Formation indicates that submarine canyons debouched into the Akitio area (Neef, 1992). Flute casts in this section indicate that turbidite currents were directed to the northeast (Neef, 1995). The conglomeratic unit at the base of the formation at Tora is interpreted as deep marine debris flow, and related to a similar conglomerate at Akitio, northeast Wairarapa (Hines *et al.*, 2013). The calcareous mudstones of the Wanstead Formation record hemipelagic deposition with pervasive bioturbation indicative of basin-floor deposition (Hines *et al.*, 2013). Benthic foraminiferal assemblages indicate lower bathyal to abyssal paleodepths (2000–3500 m) in the middle Eocene at Tora (Hines *et al.*, 2013).

Synonymy & Correlation

The Wanstead Formation can be correlated with the Huatokitoki Formation (e.g. Lee & Begg, 2002) and the Pukemuri Siltstone (Hines *et al.*, 2013), and is coeval with the Amuri Limestone in Marlborough.

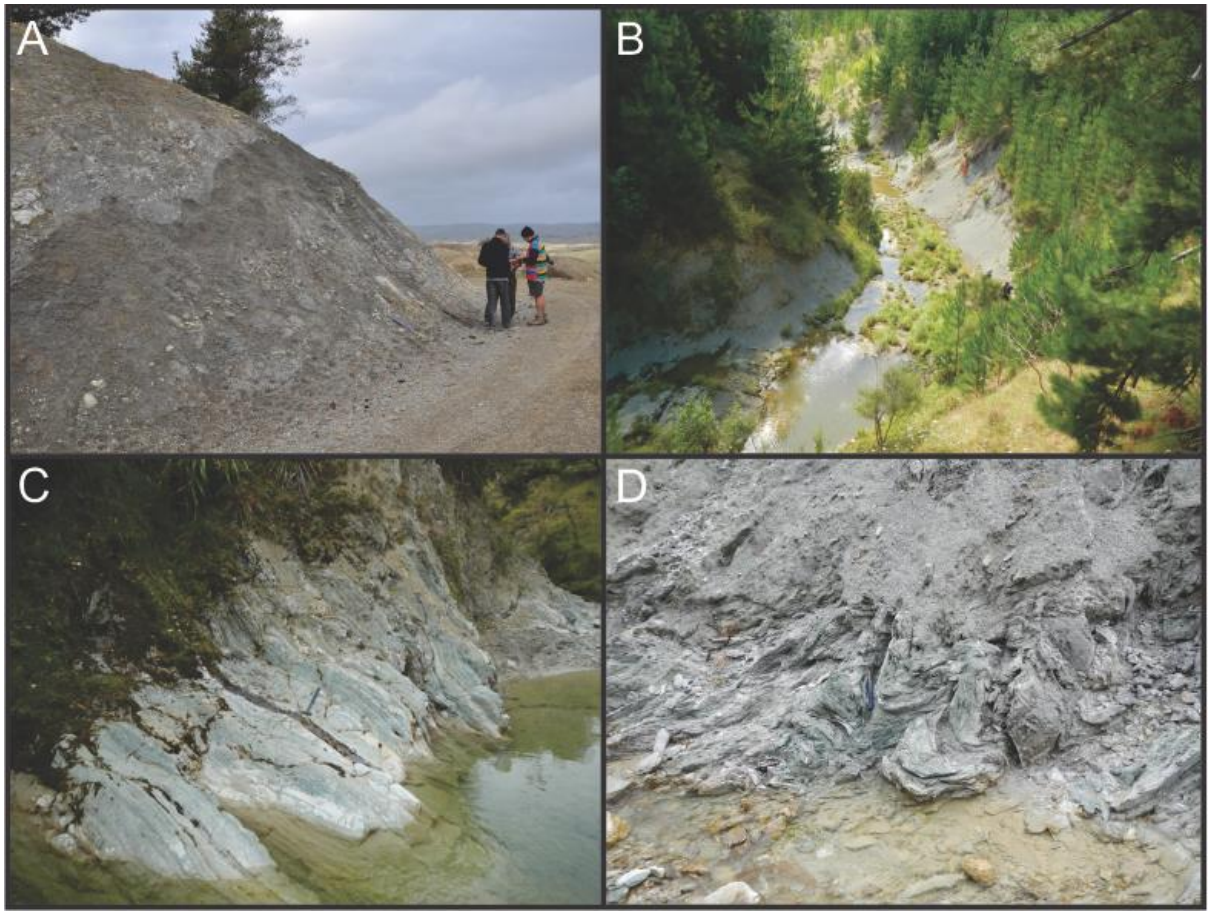

Figure 2.16: A) Bortonian-aged Wanstead Formation outcrop at Aropito, southern Hawke's Bay (BM37/890298). B) Mangaorapan Wanstead Formation cropping out at the Tawanui section, upper Akitio River (southern Hawke's Bay; BM37/874248). C) Outcrop of Bortonian Wanstead Formation in Pukemuri Stream, southeast Wairarapa (BR34/067009). D) Deformed mudstone in Pukemuri Stream (BR34/066010), characteristic of the Wanstead Formation in many outcrops.

2.4.8 Weber Formation

The Weber Formation extends from the Raukumara Peninsula to northern Wairarapa, but does not crop out south of the Carterton Fault (Lee & Begg, 2002). The Weber Formation is included in the Mangatu Group, and was originally named by Ongley & Willianson (1931). Ongley (1941) designated a type section for the formation in the Akitio River. The basal greensand lithofacies identified by Leckie *et al.* (1992) in the southern Hawke's Bay possibly correlates with the Te Waka Greensand (Black, 1980; Kenny, 1984) in Raukumara. The formation has been extensively revised recently by Morgans (2016).

Lithostratigraphy

In western Raukumara, the Weber Formation overlies the Wanstead Formation across a low-angle unconformity (Leonard *et al.*, 2010). Kenny (1984) describes the base of the Weber Formation as marked by a gradation from the Te Waka Greensand lithofacies of the Mangatu Group in the eastern Raukumara area (Figure 2.3). In southern Hawke's Bay, the Weber Formation conformably overlies the Wanstead Formation, and may be poorly- to well-bedded, bioturbated, light-grey calcareous mudstone (Leckie *et al.*, 1992; Neef, 1995; Rogers *et al.*, 2001). However, in parts of the Weber area, the Weber Formation unconformably overlies the Whangai Formation, with the Wanstead Formation removed entirely, although in nearby localities the Wanstead Formation is thin (~30 m), and highly deformed (Lee & Begg, 2002; Clowes, *in prep.*; Morgans, 2016). Carbonate content ranges from 23–70%, averaging 40–50% (Leckie *et al.*, 1992). The Weber Formation can be subdivided into four informal lithofacies; the glauconitic lithofacies, the limestone, lithofacies, the flysch lithofacies, and the siltstone lithofacies (Leckie *et al.*, 1992; Morgans, 2016).

The basal, glauconitic lithofacies is characterised by intensely bioturbated, fine-grained, calcareous sandstone that grades up from the Wanstead Formation into glauconitic, medium-grey, muddy siltstone with common *Zoophycos* (Leckie *et al.*, 1992). The limestone lithofacies consists of massive, light-grey, very calcareous, slightly glauconitic, muddy siltstone, that characterises 'typical' Weber Formation. The carbonate content ranges from 40–70% (i.e. muddy limestone), and there are thin, discontinuous sandstone beds within the top 23 m of the lithofacies (Leckie *et al.*, 1992). The flysch lithofacies grades upwards from the limestone facies and consists of 80 m of light grey, hard, calcareous fine sandstone and muddy siltstone (Leckie *et al.*, 1992). The siltstone lithofacies is determined to sit above the flysch lithofacies on the basis of biostratigraphic data; no outcrop relationship between these two units has been observed. The siltstone lithofacies consists of soft, green-grey, calcareous, muddy siltstone (Leckie *et al.*, 1992). The Weber Formation is up to 370 m thick (Leckie *et al.*, 1992), although Johnston (1980) estimated the formation to be 720 m-thick,

and is more typically 200–340 m-thick (Moore *et al.*, 1986; Morgans, 2016). In western Raukumara, the Weber Formation reaches 170 m-thick (Leonard *et al.*, 2010; Morgans, 2016).

Paleontology and Age

The Weber Formation ranges from Runangan to Waitakian age (late Eocene to early Miocene), but is more commonly Kaiatan to Duntroonian in age (late Eocene to Oligocene; Neef, 1995; Rogers *et al.*, 2001; Lee & Begg, 2002; Morgans, 2016). The basal glauconitic lithofacies is Kaiatan to lower Whainaroan in age, whereas the limestone lithofacies is lower to upper Whaingaroan in age (Leckie *et al.*, 1992). The flysch lithofacies has an upper Whaingaroan to Duntroonian age, and the siltstone lithofacies is of lower Waitakian age (Leckie *et al.*, 1992; Morgans, 2016).

In Raukumara, the formation has a Whaingaroan to Duntroonian age (Kenny, 1984; Morgans, 2016). This age, in tandem with the Bortonian age more commonly applied to the Te Waka Greensand lithofacies (Field & Uruski *et al.*, 1997), may correspond with the base of the Weber Formation in the southern Hawke's Bay, which is better described, with finer age control.

Depositional Setting

Foraminiferal faunas indicate an upper- to lower bathyal depositional depth for the Weber Formation (Moore & Morgans, 1987; Field & Uruski *et al.*, 1997; Morgans, 2016).

2.5 Tora

2.5.1 Manurewa Formation

The Manurewa Formation has a limited distribution, being restricted to the Tora area of southeast Wairarapa (Laird *et al.*, 2003; Hines *et al.*, 2013). As currently defined, the Manurewa Formation is included within the Awhea Group (Begg & Johnston, 2000). The formation was first described by Waterhouse & Bradley (1957), who designated Pukemuri Stream as the type. The base of the Manurewa Formation is coeval with the base of the Porangahau Member of the Whangai Formation, and approximately coeval with the Branch Sandstone in Marlborough. Based on the age, lithology and depositional setting of the Awhea Formation, it is considered synonymous with the Porangahau Member of the Whangai Formation. This synonymy would also suggest that the formation be placed within the Tinui Group.

Lithostratigraphy

The Manurewa Formation overlies the Whangai Formation with a sharp, channelised lower contact (Hines *et al.*, 2013). The formation is divided into two members (Waterhouse & Bradley, 1957), which exhibit considerable lateral facies variation (Hines *et al.*, 2013). The Lower Member is comprised of thinly bedded, alternating glauconitic sandstone and mudstone, and may grade into centimetre- to decimetre-bedded impure micritic limestone (Figure 2.17; Hines *et al.*, 2013). The Upper Member consists of massive to laminated greensand that contains abundant pyrite nodules, and includes a conglomeratic interval. The basal contact of the Upper Member is channelised into underlying strata, either the Lower Member or Whangai Formation (Figure 2.17).

Paleontology and Age

Bioturbation traces include *Nereites*, c.f. *Chondrites*, *Ophiomorpha* and *Zoophycos* (Hines *et al.*, 2013). Foraminiferal assemblages contain long-ranging Late Cretaceous–Paleocene (Haumurian–Teurian) assemblages, and several studies have identified the Cretaceous-Paleogene boundary at the base of the Upper Member (Wasmuth, 1996; Laird *et al.*, 2003; Vellekoop, 2010). Dinoflagellate assemblages from the Lower Member are assigned to the latest Cretaceous *Manumiella druggii* Zone, whereas the Upper Member contains an assemblage that is correlated to the early Paleocene *Trithyrodinium evitii* Zone (Laird *et al.*, 2003).

Depositional Setting

The Manurewa Formation is reinterpreted in this study as deposits from a submarine-fan system dominated by channelised and mass-emplaced conglomerate and sandstone facies within an otherwise low-energy, bathyal depositional environment. The channelised contact between the Lower and Upper members of the Manurewa Formation (Wasmuth, 1996; Laird *et al.*, 2003) is consistent with the continuation of channel incision, deposition and lobe development, within a submarine-fan setting. Furthermore, the Manurewa Formation is a localised unit restricted to the Tora area (Laird *et al.*, 2003), consistent with the interpretation of early-stage fan development with limited lateral extent.

Figure 2.17: Manurewa Formation cropping out in Pukemuri Stream (BR34/075001) Rakauroa Member of the Whangai Formation crops out on the left-hand side, and the lower member of the Manurewa Formation (grey, centre of image). The channelized contact at the base of the upper member is at head height on the figure.

2.5.2 Awhea Formation

The Awhea Formation is restricted to the Tora and Glenburn areas of coastal Wairarapa. The formation was originally described by Waterhouse & Bradley (1957) and is was included within the Awhea Group by Begg & Johnston (2000). The type section for the formation is Pukemuri Stream (Figure 2.18A). The Awhea Formation is here synonymised with the Porangahau Member of the Whangai Formation on the basis of age, thickness, and lithological characteristics.

Lithostratigraphy

The Awhea Formation has a conformable, gradational contact with the underlying Manurewa Formation (Laird *et al.*, 2003; Hines *et al.*, 2013). The Awhea Formation is comprised of well-bedded alternating sandstone and mudstone (Figure 2.18A, B). In the lower part of the formation, 20–50 cm-thick, green-grey, glauconitic fine sandstone beds are separated by thin mudstone beds (Figure 2.18A; Hines *et al.*, 2013). Bedding surfaces are extensively bioturbated and burrows are

commonly infilled by pyrite (Hines *et al.*, 2013). In the upper part of the formation the sandstone beds display normal grading and become increasingly fine-grained and thinly bedded, less glauconitic, and less bioturbated (Figure 2.18C; Hines *et al.*, 2013). The stratigraphic thickness of the Awhea Formation thins northwards, from 290 m at Tora to 47 m near the Pahaoa River mouth at Glenburn (Tayler, 2011).

Paleontology and Age

Extensive bioturbation in the lower part of the Awhea Formation includes *Nereites*, *Paleodictyon*, *Ophiomorpha*, *Scolicia* and *Planolites*. Foraminiferal faunas from the Awhea Formation indicate an early Teurian age (Hines *et al.*, 2013).

Depositional Setting

Foraminiferal faunas indicate a middle to lower bathyal depositional environment (Hines *et al.*, 2013). The underlying Upper Member of the Manurewa Formation grades into the alternating bedded sandstones and mudstones of the Awhea Formation, interpreted as turbidite deposition in a submarine fan setting (Hines *et al.*, 2013). The Awhea Formation displays a thinning upwards sequence of turbidites, which may indicate gradual lobe shifting or more distal turbidite deposition.

Synonymy & Correlation

Jointly, the Manurewa and Awhea formations are considered synonymous with the Porangahau Member of the Whangai Formation on the basis of strong lithological similarities to the Porangahau Member, and the restricted, coeval age range of both units (upper *M. druggii* zone to NP3; Laird *et al.*, 2003; Hines *et al.*, 2013; Crouch *et al.*, 2014; Kulhanek *et al.*, 2015). The Butt Formation in Chancet Rocks area of northeastern Marlborough has a similar lithological expression to the Awhea Formation, but is slightly older (upper Haumurian, possibly *M. druggii* zone), although age control on the formation is poor (Strong, 2000). Herein, the Butt Formation is considered as a correlative of the Porangahau Member.

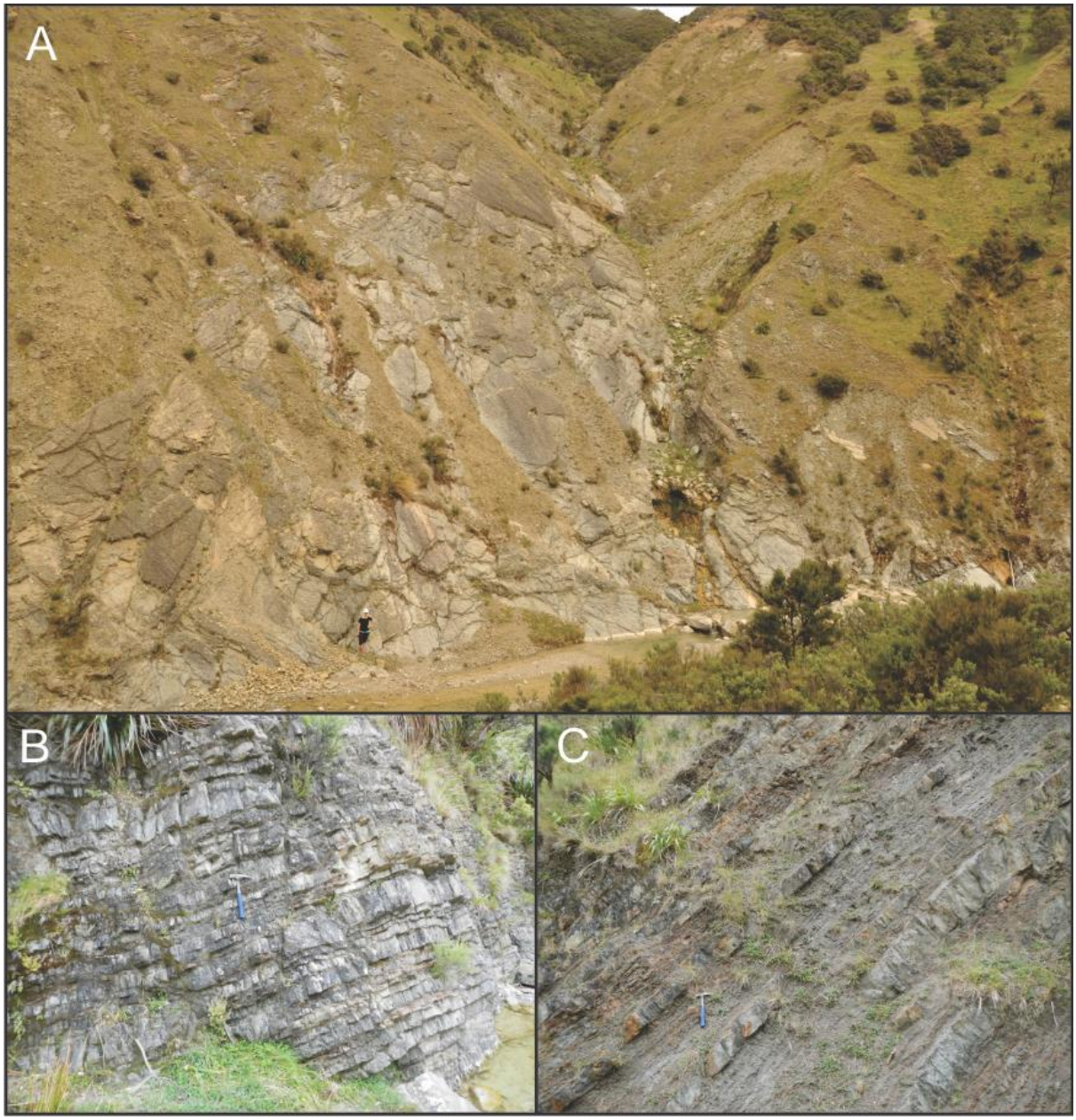

Figure 2.18: A) Dip slopes of the lower Awhea Formation cropping out in Pukemuri Stream (BR34/074001). Figure for scale at base of slope. B) Decimetre-bedded, sand-dominated flysch at the base of the Awhea Formation, Te Oroi Stream (BR34/047975). Hammer for scale. C) Mud-dominated, decimetre-bedded flysch in the upper part of the Awhea Formation, Te Oroi Stream (BR34/044979).

2.5.3 Mungaroa Limestone

The Mungaroa Limestone is restricted to the Tora area of southeast Wairarapa, and is included in the Awhea Group by Begg & Johnston (2000). The formation was originally described by Waterhouse & Bradley (1957), who designated Mungaroa Hill and Pukemuri Stream as the type

section. The formation is in part coeval with the Mead Hill Formation in Marlborough, and is synonymous with the Kaiwhata Limestone at Glenburn.

Lithostratigraphy

The Mungaroa Limestone is divided into three informal members: a lower calcareous mudstone, a middle alternating sandstone-mudstone, and an upper porcellaneous limestone. The white, weakly bedded, calcareous mudstone of the lower member gradationally overlies the Awhea Formation. The lower member grades into the middle member, which consists of decimetre-bedded, grey-green, sandstone alternating with thinner mudstone (Figure 2.19A). In northern sections, a channelized contact removes the upper member, and at Te Kaukau Point, infilled channel structures and apparent in the gradational zone from the middle to upper members (Figure 2.19B). A gradational contact separates the middle member from the upper member, the latter being comprised of well-bedded, white micritic limestone (Figure 2.19C). Bedding is uniform, with an average bed thickness of 10 cm and sharp contacts between beds, infrequent chert nodules, and common decimetre- to metre-thick glauconitic sandstone beds. Syn-sedimentary slump folding and sedimentary dykes are observed in the formation (Kirk, 1966; Browne, 1987; Hines *et al.*, 2013). The Mungaroa Limestone thins northwards, from 85 m thick at Tora (Hines *et al.*, 2013), to 28 m at Glenburn (Tayler, 2011).

Paleontology and Age

Zoophycos and *Planolites* occur throughout the formation, becoming extensive in the upper micritic limestone member. Calcareous nannofossil assemblages from the lower member indicate Nannofossil Zone NP4 (62.82–60.48 Ma) of Martini (1971) (Hines *et al.*, 2013). Calcareous nannofossil assemblages from the middle member of the Mungaroa Limestone place it in Upper Zone NP5 (60.48–59.17 Ma; Hines *et al.*, 2013). The upper micritic limestone member and an interbedded dark mudstone at Te Kaukau Point are placed in Radiolarian Zone RP5 (61–59 Ma; Hollis, 2002; Hines *et al.*, 2013).

Depositional Setting

The Mungaroa Limestone was deposited at middle to lower bathyal depths (800–1500 m; Hines *et al.*, 2013). The well-bedded character of the middle member with sharp basal contacts, cross-bedding and normal grading indicates deposition by turbidity currents. The upper member of the Mungaroa Limestone primarily reflects pelagic deposition with minor terrigenous input, with occasional influx of glauconitic sands as redeposited sediments within this otherwise low-energy pelagic environment (Browne, 1987).

The abrupt transition to the upper limestone member suggests a rapid, regional reduction in the deposition of clastic sediment during the middle Paleocene (Nannofossil Zone NP5) and potentially a northwards extension of the pelagic facies of the southern East Coast Basin. Deformation and slump structures indicate paleoslope movements and syn-sedimentary deformation of sediments. Paleo-channel erosion at the base of overlying units has resulted in a reduced thickness of the formation (20 – 100 m) in some sections at Tora (Hines *et al.*, 2013).

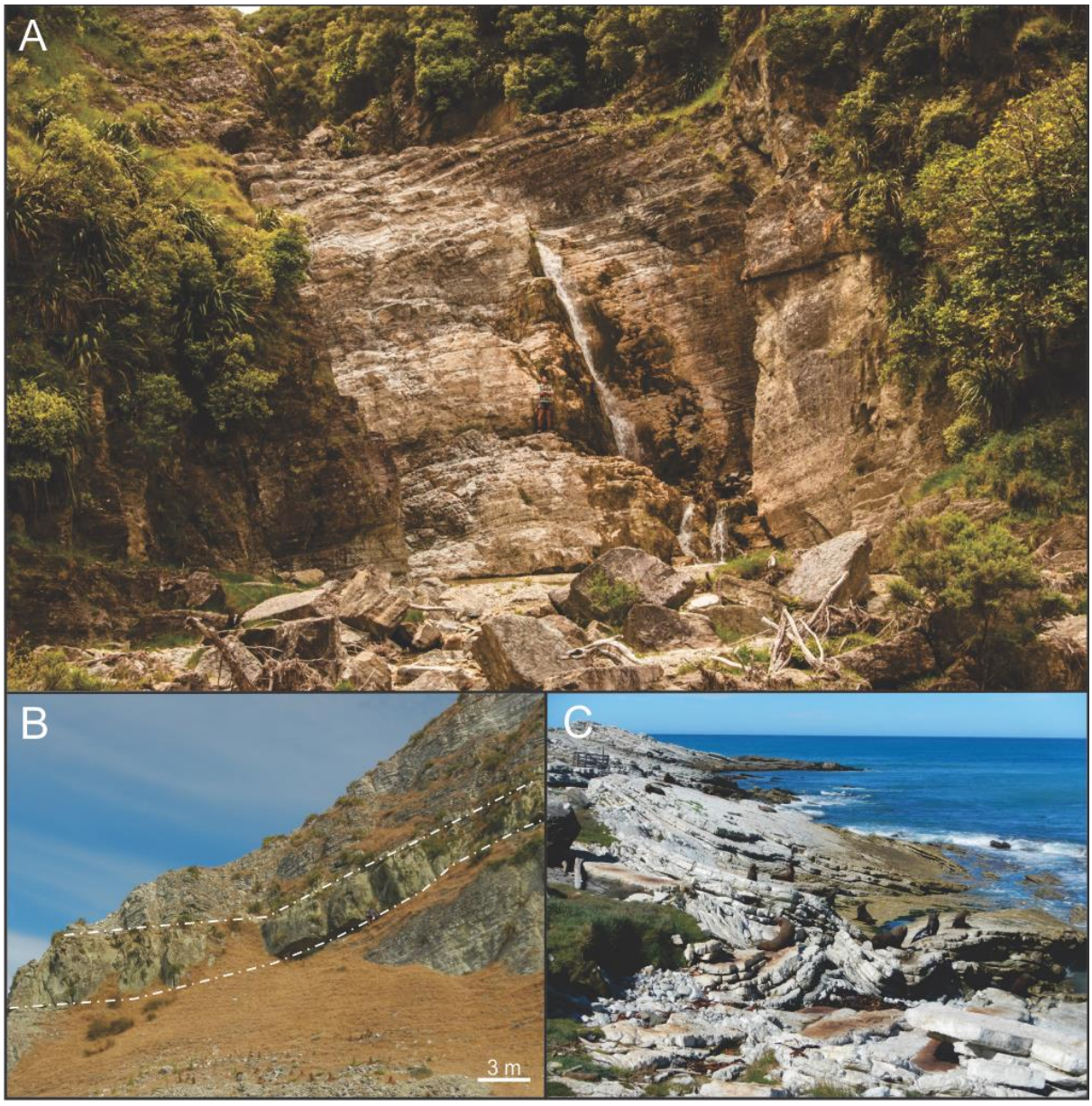

Figure 2.19: A) Mungaroa Limestone cropping out in Pukemuri Stream (BR34/071005). Figure for scale (centre of image). B) Channel deposit within the Mungaroa Limestone at Te Kaukau Point (BR33/026951), at the base of the upper micritic limestone member. C) The upper micritic limestone member at Te Kaukau Point (BR33/024951). Seals for scale. Note soft sediment deformation.

2.5.4 Awheaiti Formation

The Awheaiti Formation is restricted in outcrop to the Pukemuri and Te Oroi Streams, and was included within the Tora Group by Hines *et al.* (2013). The formation was first described by Waterhouse (1955) and Waterhouse & Bradley (1957), who designated Pukemuri Stream as the type section for the formation. The Awheaiti Formation is considered synonymous with parts of the Wanstead Formation elsewhere in the Hawke's Bay – Wairarapa, suggesting it should be placed in the Mangatu Group.

Lithostratigraphy

The Awheaiti Formation is variably channelised into the underlying Mungaroa Limestone (Hines *et al.*, 2013). In Pukemuri Stream, the type section, channelisation at the base of the formation has removed much of the upper micritic limestone member of the underlying Mungaroa Limestone (Hines *et al.*, 2013). The formation is comprised of decimetre-bedded, alternating fine sandstone and mudstone, and contains large-scale cross-bedding within channel structures (Figure 2.20A, B). The formation is 8 m-thick in Pukemuri Stream.

Paleontology and Age

Calcareous nannofossil assemblages indicate a latest Teurian (Paleocene) age for the formation (NP7; Hines *et al.*, 2013). Foraminiferal assemblages indicate a Teurian to Waipawan (Paleocene–early Eocene) age for the formation. Large *Bathysiphon* foraminifera are common.

Depositional Setting

The formation is interpreted as representing localised channel and overbank deposits of a submarine-fan system (Hines *et al.*, 2013). Oriented *Bathysiphon* foraminifera demonstrate a northeast current lineation in bedding planes.

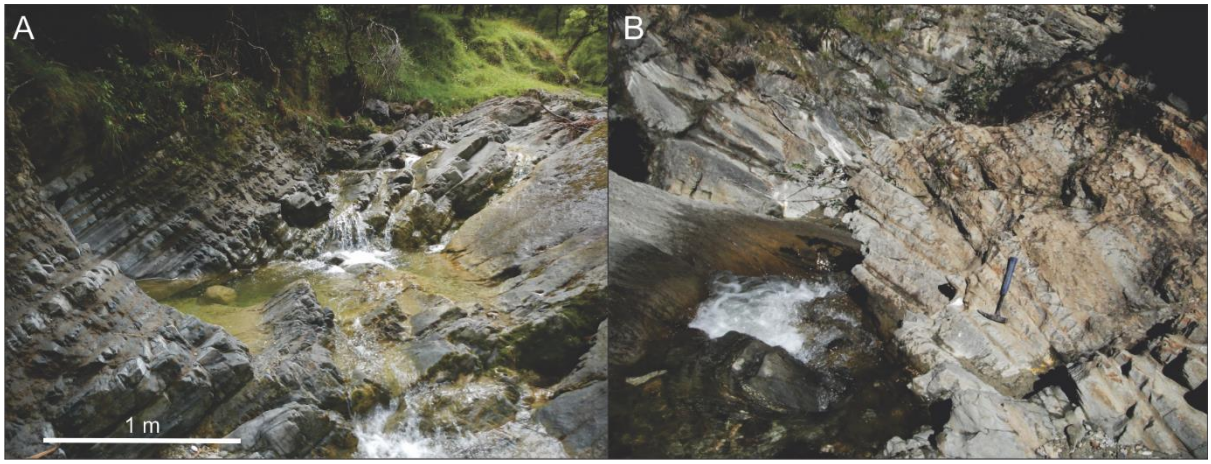

Figure 2.20: A) Alternating fine sandstone-mudstone of the Awheaiti Formation in Pukemuri Stream (BR34/071006). B) Cross-cutting relationships within the Awheaiti Formation Hammer for scale. Hammer handle is 30 cm long.

2.5.5 Pukemuri Siltstone

The Pukemuri Siltstone is restricted to the Tora area, and forms the uppermost unit of the Tora Group (Begg & Johnston, 2000). The formation was initially described by Waterhouse & Bradley (1957), who nominated Pukemuri Stream as the type section. The Pukemuri Siltstone is coeval with the Huatokitoki Formation and the Wanstead Formation (Moore, 1980; Field & Uruski *et al.*, 1997), and should be considered part of the Wanstead Formation.

Lithostratigraphy

The Pukemuri Siltstone overlies the Awheaiti Formation with an unconformable, angular discordance of 15–20° (Hines *et al.*, 2013). The base of the formation is comprised of 30 m of pebbly mudstone (Figure 2.21A). Clasts become scattered and less abundant towards the top of the unit, where it grades into 25 m of blue-grey, faintly cm-bedded mudstone, with intraformational slumping and convolute bedding within coherent bedding packages. The upper portion of this interval also contains megaclasts (≤6 m) and rafted sediment (Figure 2.21B). Above this is a 40 m-thick interval of massive, flaggy, grey mudstone (Figure 2.21C), which is overlain by purple-brown mudstone and 30 m of decimetre-bedded alternating sandstone-mudstone at the top of the formation. A thin, 20 cm thick bed of exceptionally glauconitic sandstone (80–90% glauconite) containing siderite concretions can be traced laterally for approximately 10 kilometres (Figure 2.21D). The formation ranges from 110 to 170 m thick in the Tora area.

Paleontology and Age

Foraminiferal and calcareous nannofossil biostratigraphy indicate a Mangaorapan to Heretaungan age for the formation (early to middle Eocene, Nannofossil Zones NP12–14; Hines *et al.*, 2013).

Depositional Setting

The pebbly mudstone of the lower Pukemuri Siltstone is interpreted as a marine debris flow deposit. The depositional system reverted to a slope environment during the late-early to early-middle Eocene. The mudstone that overlies the basal pebbly mudstone is characterised by syn-sedimentary folding, suggesting a slope depositional setting (Hines *et al.*, 2013). Foraminiferal faunas are indicative of a mid- to lower-bathyal paleodepth. The low foraminiferal abundance in samples collected in the lower Pukemuri Siltstone, in conjunction with slumped, convolute bedding, may be due to high sediment supply, whilst higher in the section, greater foraminiferal abundances and laminated bedding may indicate reduced sedimentation rates.

Figure 2.21: A) Pebbly mudstone at the base of the Pukemuri Siltstone in Pukemuri Stream (BR34/070007). B) Rafted sediment blocks in the lower Pukemuri Silstone, Pukeuri Stream (BR34/070007). Photo supplied by C. Atkins. Figure for scale. C). Typical Pukemuri Siltstone in Awheaiti Stream (BR34/087020). Hammer for scale. D) Richly-glauconitic sandstone with siderite concretions, amongst pale brown, laminated mudstone in the Pukemuri Siltstone, Pukemuri Stream (BR34/069007).

2.6 Marlborough

2.6.1 Champagne Formation

The Champagne Formation marks the base of the cover succession in the Marlborough region. The Champagne Formation crops out within the Clarence Valley in a narrow 10 km-long band from Ouse Stream to Dee Stream, as well as within Wharekiri Stream (Rattenbury *et al.*, 2006), and the Kekerengu River (pers. obs.). The Champagne Formation was originally described as the Champagne Member of the Split Rock Formation by Ritchie (1986), although was mapped in Rattenbury *et al.* (2006) a separate formation. The formal application of formation would be consistent with the widespread outcrop distribution, distinct lithology and unconformable surfaces

bounding the unit above and below. The Champagne Formation forms the base of the Coverham Group, and the type section is Ouse Stream, Coverham (Crampton *et al.*, 2004b).

Lithostratigraphy

The Champagne Formation (and correlatives) unconformably overlie Pahau Terrane basement, typically with a strong angular discordance (Reay, 1980, 1993; Crampton *et al.*, 1998; Rattenbury *et al.*, 2006). The formation is comprised of highly deformed sandstone, mudstone and conglomerate (Figure 2.22), and demonstrates boudinage of sandstone beds, asymmetric folding, and soft-sediment deformation structures (Figure 2.22B, D; Crampton *et al.*, 1998). In Wharekiri Stream, exposures of 'broken formation' melange are present within the formation (Figure 2.22A). In the middle Clarence valley, thickness varies from 20 to 275 m (Reay, 1993). The Champagne Formation in the Coverham area was logged as 200 m thick by Ritchie (1986).

Paleontology and Age

A Trigoniid in reworked greywacke boulders in the Tentpoles Conglomerate Member of the Split Rock Formation indicates a maximum Korangan age (Early Cretaceous) for the base of the formation (Reay, 1993). Hall (1963) identified *Inoceramus kapuus* above the basal conglomerate of the Split Rock Formation, suggesting a Urutawan age for the unit. Ritchie (1966) considered the age of the Champagne Formation to be Urutawan to Ngaterian based on fossil collections that include; *Inoceramus ipuanus-kapuus,* foraminifera and echinoid spines and plates. Fossils from the base of the formation give Uruatawan–Motuan ages, whilst the fossils from upper parts of the formation give Ngaterian ages (Ritchie, 1986). Plant material increases up section in the Champagne Formation (Ritchie, 1986). In the type section, Ouse Stream, Crampton *et al.* (2004b) consider the formation to be entirely Urutawan.

Depositional Setting

The coarse-grained and olistostromal deposits of the Champagne Formation are interpreted as being deposited as mass transport deposits, derived of locally sourced material, and infilling existing, complex and substantial topography, likely infilling 600–800 m-deep pre-existing canyons in Torlesse Composite Terrane (Laird, 1981, 1982; Lewis & Laird, 1986). Olistostrome deposits in Penk Stream are interpreted as being deposited in a bathyal setting (Field & Uruski *et al.*, 1997), although elsewhere the formation is interpreted as being deposited by debris flows, possibly stimulated by adjacent or nearby fault scarps (Reay, 1993). An increase in the proportion of plant matter up section in the Champagne Formation in the Clarence River area is interpreted by Ritchie (1986) as representing shallow water deposition in a prodelta, muddy shelf environment.

Synonymy & Correlation

The Champagne Formation (Crampton & Laird, 1997; Crampton *et al.*, 2004), at the base of the Split Rock Formation in the northern Clarence Valley, Wharekiri Stream and Awatere Valley is synonymous with the Tentpoles Conglomerate Member of the Split Rock Formation identified by Reay (1993) in the middle Clarence Valley. Olistostrome deposits in Penk River, along with the Gladstone Formation (Challis, 1966) in the Awatere Valley, and the Tentpoles Conglomerate and Bluff Dump members of Reay (1987, 1993) in the middle Clarence Valley, are considered synonymous with the Champagne Formation. The Tentpoles Conglomerate Member is equivalent to the basal conglomerate of the Champagne Formation, and the Bluff Dump Member is likely equivalent to the disturbed sandstones and mudstones higher in the Champagne Formation. The Totara Formation in the Awatere Valley has a similar lithology and composition, and may be equated with the Champagne Formation (Montague, 1981; Ritchie, 1986).

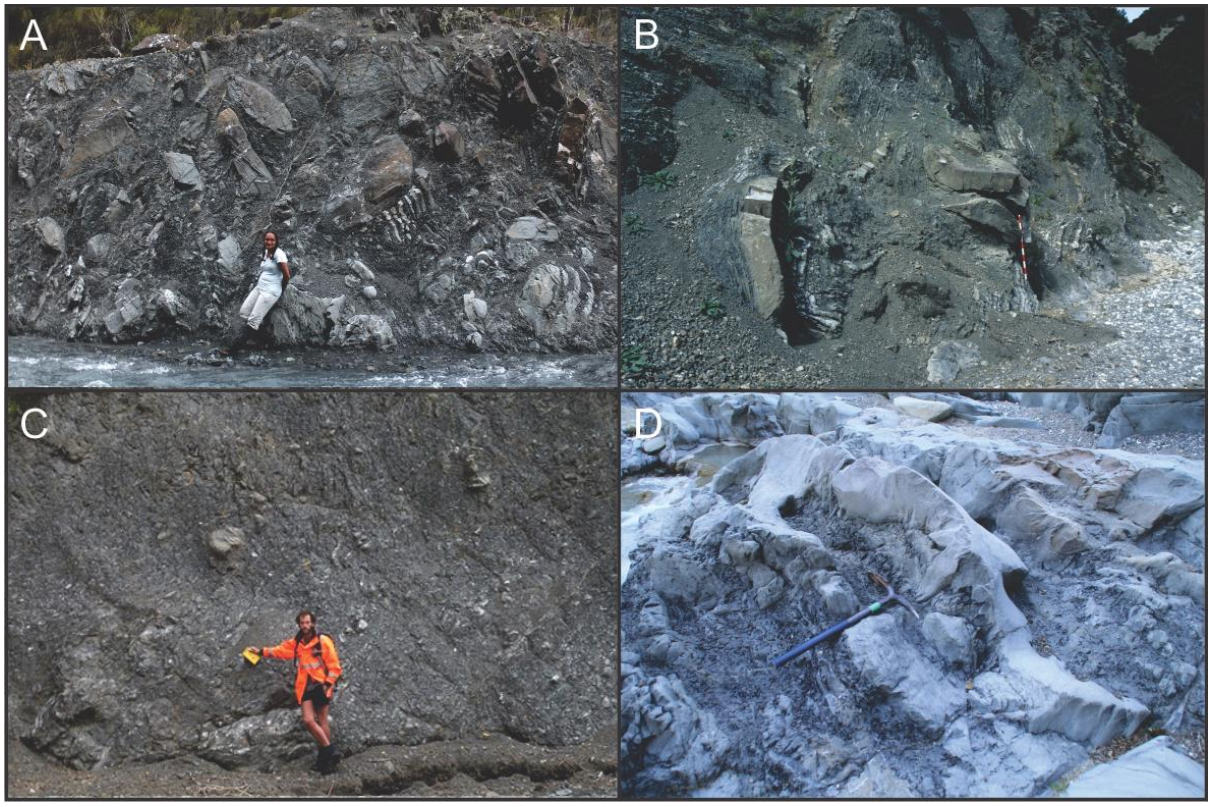

Figure 2.22: A) Tectonic melange ('broken formation') of the Champagne Formation in Wharekiri Stream (BT28/666304). Photo provided by J. Crampton. B) Champagne Formation in Ouse Gorge (BS28/701529). Jacob Staff for scale (1.5 m long). Photo supplied by J. Crampton. C) Basal conglomerate of the Champagne Formation in Wharekiri Stream (BT28/666305). Photo provided by J. Crampton. D) Disturbed alternating sandstone-mudstone beds within the Champagne Formation in Ouse Stream (BS28/716544). Hammer for scale – handle is 70 cm long. Photo supplied by K. Bland.

2.6.2 Split Rock Formation *(undifferentiated)*

The Split Rock Formation is a widespread unit in the Marlborough region. It is often divided into several members, although in many instances this is not possible, in part due to the wide range of depositional settings across the distribution of the formation. Members are identified where possible in this study, otherwise they are attributed to undifferentiated Split Rock Formation.

Outcrops of Split Rock Formation occur in much of the Marlborough region, except the Kaikoura and Haumuri Bluff area where the base of the cover succession is Piripauan in age. The Split Rock Formation is assigned to the Coverham Group, and was originally defined by Suggate (1958), who nominated a type section between Split Rock and Black Rock Streams. Ritchie (1986) divided the formation into four members after revising the stratigraphy of Hall (1963): the Champagne Member (described as separate formation above), the Ouse Siltstone, Wharf Sandstone and Swale Siltstone in the Coverham area. In the central Clarence Valley, Reay (1993), divided the Split Rock Formation into the Tentpoles Conglomerate, Cold Stream, and Black Rock members, which have comparable lithostratigraphic characteristic as the members identified by Ritchie (1986). Each of these members could easily be described as individual formations, having a substantial stratigraphic thickness attributed to each member, and being recognisable over a large area, however are retained as members due to the undifferentiated nature of the Split Rock Formation in some localities. Sedimentary strata of the Winterton and Gladstone formations of the Awatere Valley (Challis, 1966), and a number of unnamed correlatives in the Marlborough region, are included in undifferentiated Split Rock Formation.

Lithostratigraphy

The basal Split Rock Formation unconformably overlies the Pahau Terrane. In places Motuan to Ngaterian strata of the Split Rock Formation onlap Pahau Terrane (e.g., Wharekiri Stream; Figure 2.23A). Basal deposits vary locally, although almost all are coarse grained, and dominantly consist of clast- or matrix-supported conglomerate (Field & Uruski *et al.*, 1997). The alternating sandstones and siltstones to laminated mudstones of the Split Rock Formation unconformably overly the conglomerates of the Champagne Formation (Figure 2.23B; Laird, 1992; Reay, 1993; Morris, 1987). The Split Rock Formation locally reaches thicknesses of over 2000 m, although thicknesses vary considerably across the Marlborough region.

Paleontology and Age

The Split Rock Formation spans the Urutawan to latest Ngaterian age based on the presence of *Inoceramus ipuanus-kapuus* and *Aucellina euglypha*. The top of the formation is difficult to precisely place, and may extend to the Arowhanan (J. Crampton, pers. comm.).

Depositional Setting

The Split Rock Formation is interpreted as part of a fan-delta complex, infilling distributary channels (Reay, 1980, 1993; Morris, 1987). Paleocurrent directions vary widely: in the Awatere Valley they indicate flow towards the northeast-southwest, in Coverham they indicate flow towards the southwest and northwest, and in the middle Clarence valley they indicate flow towards the northeast (Reay, 1993; Field & Uruski *et al.*, 1997; Crampton *et al.*, 1998, 2003). Paleoslope indicators, where available, suggest slope directions towards the northeast in the Clarence and Awatere valleys, although at Mororimu Stream they are directed to the southwest, and to the west at Coverham (Reay, 1993; Field & Uruski *et al.*, 1997).

In the Coverham area, the depositional setting is interpreted as a slope basin environment (Ritchie, 1986). However, in the Awatere Valley, common ripple marks in the Cam River indicate deposition occurred at or above storm wave base (Field & Uruski *et al.*, 1997). Shallow-marine deposits have been identified in the Hapuku drillhole (Laird, 1982), although no correlative strata are known south of this location suggesting the borehole's location marks the edge of the basin during this time. Altogether these various environmental indicators suggest a complex topography for the basal Split Rock Formation. In places, deposition is also inferred to have occurred in half-grabens in response in intermittent movement on the bounding faults (Lewis & Laird, 1986; Laird, 1992).

Synonymy & Correlation

Formal subdivisions of the Split Rock Formation include; the Ouse Siltstone, Wharf Sandstone, and Swale Siltstone (Morris, 1987; Reay, 1980, 1993; Crampton & Laird, 1997). The Ouse Siltstone is equivalent to the Cold Stream Member (Ritchie, 1986). The Black Rock Member of Reay (1993) can be correlated with the Wharf Sandstone on the basis of age, thickness, lithology, and stratigraphic relationships. The Ouse Siltstone and Wharf Sandstone members are equivalent with the Gladstone, Lower Winterton and Upper Winterton formations in the Awatere Valley (Montague, 1981; Ritchie, 1986).

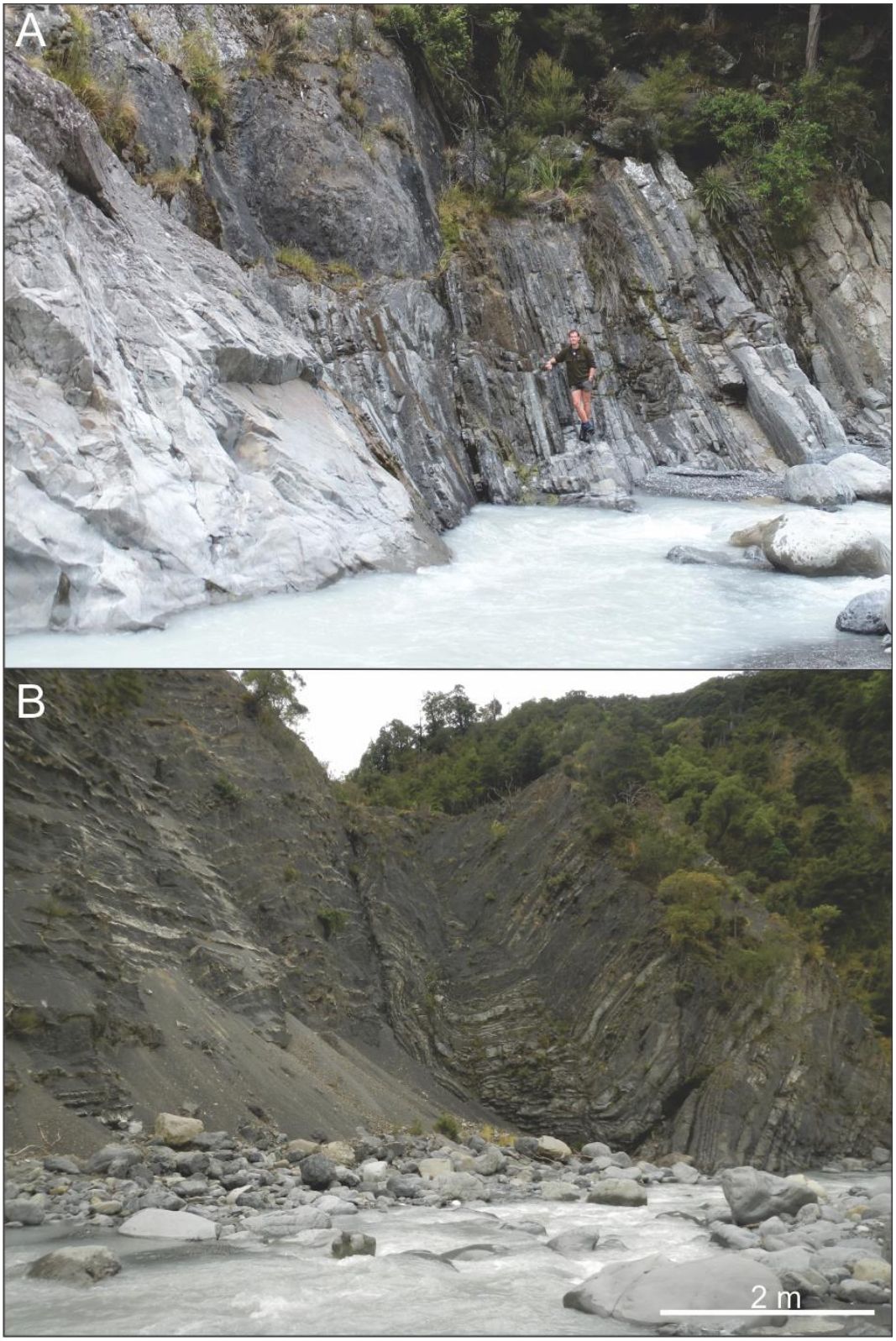

Figure 2.23: A) Outcrop in Wharekiri Stream (BT28/682325) demonstrating the basal unconformity of the Split Rock Formation, where decimetre-bedded Motuan or Ngaterian Split Rock Formation (right-hand side) onlaps massive sandstone of the Pahau Terrane (left-hand side). Image provided by J. Crampton. B) Decimetre-bedded, alternating sandstone and mudstone typical of Split Rock Formation in Wharekiri Stream.

2.6.2.1 Ouse Siltstone Member, Split Rock Formation

Lithostratigraphy

The Ouse Siltstone disconformably overlies the Champagne Formation in the Coverham area of the Clarence Valley (Ritchie, 1986). The Ouse Siltstone includes packages of massive siltstone and alternating flysch-like sequences of sandstone and siltstone (Figure 2.24A, B; Ritchie, 1986). The upper part of the Ouse Siltstone shows abundant evidence for large-scale soft-sediment deformation in places, particularly in the upper part of the formation in Ouse Stream (Figure 2.24B). The Ouse Siltstone is 300 m-thick in the type section in Ouse Stream. The Ouse Siltstone is comparable to the Winterton Formation in the Awatere Valley of the same age (Challis, 1966).

Paleontology and Age

The lower Ouse Siltstone is moderately and locally richly fossiliferous, and include *Mytiloides ipuanus*, *I. urius* and *Aucellina euglypha*, giving a Motuan age, although the upper part of the member is essentially barren of fossil material (Figure 2.24A; Ritchie, 1986; Crampton *et al.*, 2004). Foraminifera and rare ammonites have also been retrieved from the unit (Ritchie, 1986).

Depositional Setting

Ritchie (1986) interprets the Ouse Siltstone as being deposited by mass-flow processes in a slope basin. The Cold Stream Member is interpreted as suspension deposits (Reay, 1993).

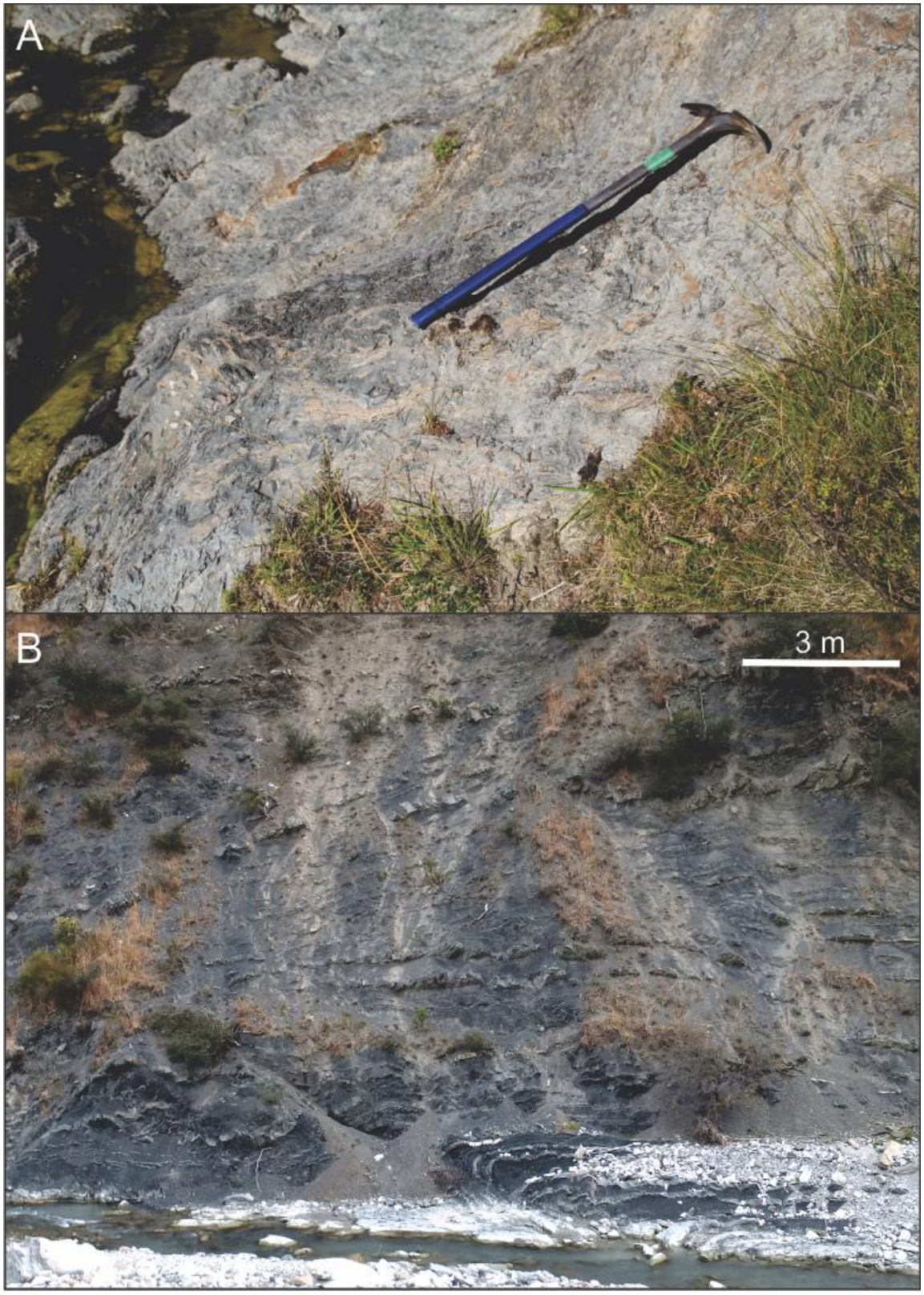

Figure 2.24: A) *Mytiloides ipuanus* shellbed at the base of the Ouse Siltstone of the Split Rock Formation cropping out in Ouse Stream (BS28/718548), just above the basal conglomerate. Cross-sections through individual shells are apparent as pink-orange colouration in the outcrop. Hammer for scale – handle is 70 cm long. Image supplied by K. Bland. B) Upper Ouse Siltstone in Ouse Stream (BS28/692535) showing packages of slumped and discordant bedding. Photo supplied by J. Crampton.

2.6.2.2 Wharf Sandstone Member, Split Rock Formation

Lithostratigraphy

The Wharf Sandstone gradationally overlies the Ouse Siltstone, and is comprised of decimetre- to metre-bedded, alternating sandstone-mudstone with well-developed Bouma A–D sequences (Figure 2.25; Ritchie, 1986; Crampton *et al*., 2004b). Carbonaceous material forming thin coal lenses is common, as is bioturbation in the upper surfaces of bedding sequences. Sedimentary structures are common, and include flute casts, wavy lamination, convoluted bedding, slumping, sandstone dikes and flame structures (Ritchie, 1986). The unit has a maximum thickness of 128 m in Ouse Stream.

Paleontology and Age

The Wharf Sandstone Member is essentially barren of macrofossils, although the bivalve *Aucellina euglypha* in the Wharf Sandstone (Reay, 1993; his Black Rock Member), indicating that the top of the formation is no younger than Motuan. Also present are *Dimitobelus superstes* belemnites and a fragment of an ammonite (Reay, 1993). *Aucellina euglypha* was also identified by Ritchie (1986) in addition to microflora assemblages that also indicate a Motuan age for the Wharf Sandstone.

Depositional Setting

Paleocurrent orientations from the Wharf Sandstone indicate a southwesterly current direction, although this evolves ups-section to a dominantly northwest orientation in the upper half of the formation (Ritchie, 1986; Crampton *et al*., 1998). The Wharf Sandstone Member is interpreted as being deposited by sediment gravity flows on a submarine fan lobe (Ritchie, 1986). The Black Rock Member is interpreted as deltaic-turbiditic current channel fill deposits (Reay, 1993).

Figure 2.25: Wharf Sandstone in Wharf Stream (BS28/726551). Figure for scale. Photo from K. Bland.

2.6.2.3 Swale Siltstone Member, Split Rock Formation

Lithostratigraphy

The Swale Siltstone is a thick, widespread unit that gradationally overlies the Wharf Sandstone (Figure 2.26). The Swale Siltstone is comprised of massive siltstone, with rare sandstone beds, and lensoidal and spherical concretions that form along bedding planes and often contain *Inoceramids* (Figure 2.26). The mudstone massive to metre-bedded, and in places displays evidence of extensive syn-sedimentary slumping. Fossils and large septarian concretions up to 2 m in diameter are abundant locally (Field & Uruski *et al.*, 1997). Fine sandstone occurs in beds up to 5 m-thick. Thick beds typically lack any internal structure, whilst thinner beds are commonly graded and preserve partial Bouma sequences (Field & Uruski *et al.*, 1997). Based on age and lithological similarities, this formation is comparable to the Karekare Formation in Raukumara. The Swale Siltstone is at least 1000 m-thick (Field & Uruski *et al.*, 1997).

Paleontology and Age

Good inoceramid faunas are recovered from the Swale Siltstone, including *Inoceramus* sp. C indicating a Ngaterian age (Crampton *et al.*, 2004b), in addition to diverse but sparse fauna of other molluscs, corals, ichthyosaurs and ammonites. The Swale Siltstone is largely Ngaterian in age.

Depositional Setting

The Swale Siltstone is interpreted as being deposited by hemipelagic sedimentation at slope depths (Ritchie, 1986).

Figure 2.26: A) Swale Siltstone cropping out in Nidd Stream, Coverham (BS28/728559). Note occasional bedding (e.g. top, centre of frame) and abundant concretions. Field of view is approximately 50 m. Photo supplied by J. Crampton.

2.6.3 Warder Formation

The Warder Formation is restricted in outcrop to the middle Clarence Valley, Awatere Valley, and Monkey Face areas (Crampton, 1988b; Reay, 1993; Beu *et al.*, 2014). The Warder Formation was originally defined as the Warder Coal Measure Member of the Gridiron Formation (Suggate, 1958; Lensen, 1978), but was elevated to formation status and included in the Wallow Group by Reay

(1993). The type section for the formation is in upper Seymour Stream, along the eastern side of the Seaward Kaikoura Range. The Warder Formation represents the terrestrial, southern extent of the Bluff Sandstone-Hapuku Group sedimentary system, and it interfingers with the Gridiron Volcanics (Browne & Reay, 1993; Reay, 1993; Beu *et al.*, 2014).

Lithostratigraphy

The Warder Formation unconformably overlies Torlesse Composite Terrane basement, and locally the Split Rock Formation (Reay, 1993). The Warder Formation is comprised of carbonaceous sandstone, mudstone and conglomerate, with considerable vertical and lateral facies variation (Reay, 1993). Conglomerate within the Warder Formation typically occurs as thin lenses several metres long and up to a metre thick (Reay, 1993). Sandstone of the formation is typically light-grey, moderately-indurated and fine grained (Figure 2.27; Reay, 1993). Mudstone within the Warder Formation is generally light-grey to blue-grey, moderately-indurated, and may be massive or laminated, limonitic, carbonaceous, concretionary, kaolinitic and jarositic. Thin lenses of sulphurous, sub-bituminous coal up to 0.5 m-thick occur within the formation. Sandstone beds are generally massive, although in places may be normally graded, and show shallow channel structures, trough cross-bedding and truncated herring-bone stratification, slump structures, symmetric and asymmetric ripples, along with sand volcanoes and liquefaction structures (Reay, 1993; Browne & Reay, 1993). The formation ranges from 2–170 m-thick in the middle Clarence Valley (Reay, 1993), and up to 20 m-thick in the Monkey Face area (Crampton, 1988b).

Paleontology and Age

The Warder Formation contains a diverse paleoflora, including, fossil roots, *in situ* stumps, branches and leaves or various identified and unidentified species, in addition to rare freshwater molluscs (Reay, 1993; Parrish *et al.*, 1998; Beu *et al.*, 2014). The Warder Formation is assigned a Ngaterian age (early-Late Cretaceous) based on its stratigraphic position and interfingering relationship with the Gridiron Volcanics (Figure 2.27; Reay, 1993).

Depositional Setting

The Warder Formation is interpreted as being deposited subaerially on a coastal flood plain. The formation's lithology, paleontology, and sedimentary structures indicate a variety of sub-environments including streams, lakes and estuaries (Reay, 1993). Most paleocurrent orientations obtained from sedimentary structures indicate a spread of directions between NNE and SW, with the dominant flow direction being to the southeast (Reay, 1993).

Figure 2.27: Warder Formation cropping out in Seymour Stream (BT26/339235), beneath a thick basaltic lava flow belonging to the interfingering Gridiron Volcanics. Figure for scale. Photo supplied by J. Crampton.

2.6.4 Bluff Sandstone

The Bluff Sandstone extends from the middle Clarence Valley as far north as Sawpit Gully, and southeast to the Monkey Face area. The Bluff Sandstone was originally defined as the Bluff Sandstone Member of the Gridiron Formation (Suggate, 1958; Lensen, 1978), but was elevated to formation status and included in the Wallow Group by Reay (1993). The type section for the formation is in upper Seymour Stream. The Bluff Sandstone is considered the marine, lateral equivalent of the Warder Formation and interfingers with the Gridiron Volcanics (Browne & Reay, 1993).

Lithostratigraphy

The Bluff Sandstone ranges from thick-bedded sandstone, to alternating sandstone-mudstone, and minor conglomerate and siltstone that interfingers with the Warder Formation and Gridiron Volcanics in the middle Clarence Valley, and overlies Torlesse Composite Terrane or Split Rock Formation across a strong angular unconformity elsewhere (Crampton, 1988b; Browne & Reay, 1993; Reay, 1993; Field & Uruski *et al.*, 1997; Beu *et al.*, 2014). Where the formation interfingers

with the Gridiron Volcanics, the Bluff Sandstone is interstratified with the uppermost lava flows (Reay, 1993).

Where the Bluff Sandstone overlies Torlesse basement, conglomerate or breccia is always present, and typically consists of 1–2 m of normally graded, well-rounded, pebble to cobble polymict, including Torlesse basement-derived sandstone, chert, quartz, jasper, rhyolite, granite and basalt, fining upwards from 100–200 mm clasts at the base to 5 mm at the top. The conglomerate is typically clast supported. Bedding and channelling in the thick-bedded sandstone is shown by accumulations of macrofossil debris and/or exotic granules and pebbles (Figure 2.28A, B). Alternating sandstone-mudstone typically occurs as 10–15 m-thick centimetre to decimetre-bedded packets. Sandstone beds are typically fine-grained, laterally continuous, and have sharp bases and tops, and contain angular mudstone rip-up clasts (Figure 2.28B). The lithotype varies from sandstone dominated to mudstone dominated. In Bluff Stream, 5–6 m-thick packets of slump-folded sandstone and convolute sandstone are interbedded. Current parting lineations and cross-bedding are prevalent throughout much of the formation. Ripple types include symmetric ripples, flaser bedding, and asymmetric ripples. Hummocky cross-stratification, small load structures, dewatering structures and convolute bedding occur locally, and flute casts are present of the base of some sandstone beds (Crampton, 1988b; Reay, 1993). Channelling is common and ranges from shallow decimetre-scale scours to 2 m-deep siltstone-filled channels. The thick-bedded sandstone is massive to indistinctly laminated, light-grey friable to indurated well-sorted fine sandstone that is locally carbonaceous, and contains sideritic concretions, pyrite nodules and calcite veins (Crampton, 1988b; Reay, 1993). The formation reaches over 500 m thick at Dead Horse Gully, but thins to a few metres in the northern Clarence Valley (Figure 2.28C) and to the southeast at Wharekiri Stream (Reay, 1993).

Paleontology and Age

Fossils in the Bluff Sandstone are uncommon, but include *M. rangatira rangatira*, *Inoceramus concentricus,* and *Eselaevitrigonia wellmani.* The Bluff Sandstone ranges between Ngaterian and Arowhanan in age based on the presence of *Inocermus tawhanus* and *M. rangatira rangatira.* Radiometric dating of the interfingering Gridiron Volcanics indicated that the Ngaterian-Arowhanan boundary lies immediately above the volcanics (Reay, 1993). Crampton (1988b) suggests that the age of basal Bluff Sandstone may be diachronous, being late Motuan in the east (in the Monkey Face area), Ngaterian in the west (middle Clarence Valley), and Arowhanan in the Coverham area.

Depositional Setting

The Warder Formation represents the terrestrial age-equivalent southern extent of the Bluff Sandstone and Hapuku Group. Transgression resulted in the deposition of the shallow-marine Bluff Sandstone over top of the Warder Formation in the Arowhanan. The Bluff Sandstone is inferred to have been deposited in a marginal- to shallow-marine setting, in an asymmetrically subsiding basin (Crampton, 1988; Reay, 1993). Fossil faunas are indicative of high-energy, inner- to mid-shelf environments, and various sedimentological characteristics indicate the localised presence of channels, channel bars, and deltaic deposits (Reay, 1993). Sedimentary structures indicate paleocurrents varied over 297°, ranging from WSW to south (Reay, 1993). Crampton (1988) interpreted the Bluff Sandstone as being deposited in a wave-dominated coastal setting.

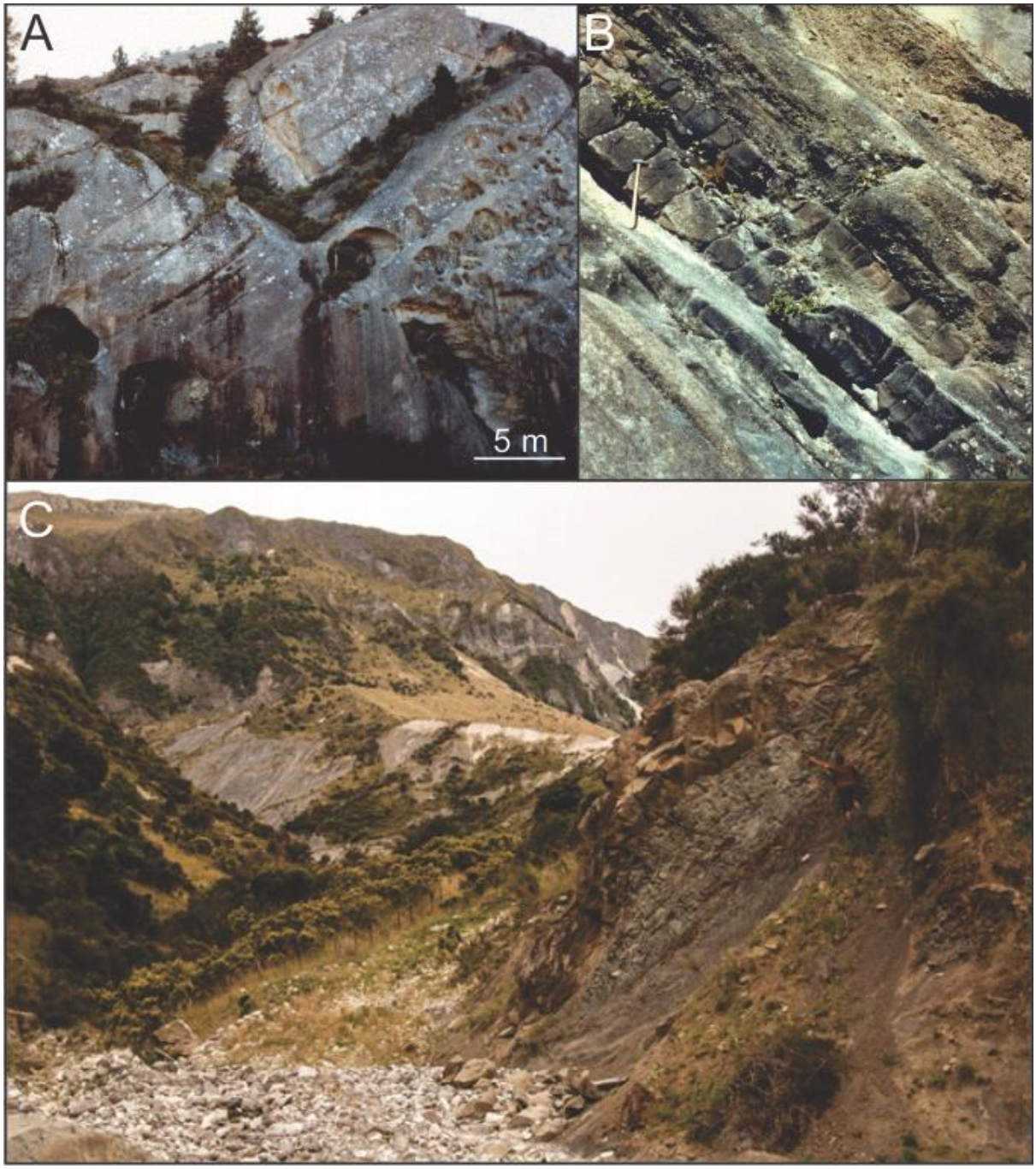

Figure 2.28: A) Outcrop of Ngaterian Bluff Sandstone in the Monkey Face (Tuku Tuku Iwi) area (BT26/343029). B) Detail of bedding in Ngaterian Bluff Sandstone in the Monkey Face area (BT26/343029), showing decimetre-bedded sandstone and conglomerate. Hammer for scale (50 cm long). C) Arowhanan-aged Bluff Sandstone cropping out in Sawpit Gully (Clarence Valley; BS28/726565), true left of stream (right-hand side of photo). Figure for scale.

2.6.5 Nidd Formation (Hapuku Group)

The Nidd Formation is preserved in fault-bound slivers southeast of the Clarence Fault. Elsewhere in Marlborough sedimentary strata of the same age are generally referred to as undifferentiated Hapuku Group (Laird, 1992; Crampton & Laird, 1997; Field & Uruski *et al.*, 1997; Crampton *et al.*, 2003). Hapuku Group sediments are poorly exposed and as such, are generally poorly described (Field & Uruski, *et al.*, 1997). The Hapuku Group, for the most part, comprises poorly- and undescribed sedimentary units of Ngaterian to Piripauan age (Rattenbury *et al.*, 2006). The type/reference sections for the Nidd Formation are in Nidd Stream or Sawpit Gully.

Lithostratigraphy

The lower contact of the Nidd Formation is gradational with the Swale Siltstone. The formation is comprised of moderately indurated concretionary siltstone, silty sandstone and sandstone (Figure 2.29A; Hasegawa *et al.*, 2013). Tubular septarian and cannonball concretions occur in the Sawpit Gully section. The Nidd Formation is richly-fossiliferous in places (Figure 2.29B), and is commonly weakly-bedded, glauconitic, and bioturbated. Mapped outcrops of the Nidd Formation are usually truncated by faults (Rattenbury *et al.*, 2006), although a there is an estimated minimum thickness of ~200 m in the Sawpit Gully area.

Hapuku Group sediments are 37 m thick in the Hapuku River, and at least 98 m thick in Wharekiri Stream (Field & Uruski *et al.*, 1997). In most instances the Hapuku Group rests unconformably on the sediments of the Wallow Group (Reay, 1993; Field & Uruski *et al.*, 1997). A few metres of non-marine conglomerate containing plant material is present at the base of the group in the extreme southwest of the Clarence Valley, forming the Willows Formation (Reay, 1993; Field & Uruski *et al.*, 1997). This sedimentary succession changes rapidly vertically and laterally into fossiliferous, shallow marine sandstones and mudstones of the Nidd Formation in the Coverham area, which are coeval with the Bluff Sandstone of the middle Clarence Valley (Reay, 1993; Field & Uruski *et al.*, 1997). The Hapuku Group is quite variable lithologically, but extensive bioturbation, especially *Ophiomorpha*, is a common and widespread characteristic (Field & Uruski *et al.*, 1997). The primary lithology of the group is indistinctly bedded, purple-brown siltstone and fine grained muddy sandstone. Glauconite is common towards the east, in Bluff Stream, Mororimu Stream and Wharekiri Stream (Field & Uruski *et al.*, 1997).

Paleontology and Age

Inoceramid bivalves are common in the formation, particularly the lower section (Figure 2.28B), and include *M. rangatira rangatira*, and *Crenoceramus bicorrugatus matamuus* and *C. bicorrugatus bicorrugatus*, indicating an Arowhanan to Teratan age (Hasegawa *et al.*, 2013). In addition to Inoceramid bivalves, other macrofossils include belemnites, ammonites, decapod crustaceans, corals, and cf. *Chondrites* bioturbation have been observed in the formation (Feldmann, 1993; pers. obs.). The Ocean Anoxic Event 2 (OAE 2) event has been identified in this section (Hawegawa *et al.*, 2013), and is marked by a fossil barren zone that occurs above the greatest carbon isotope excursion. The Hapuku Group includes strata from the latest Ngaterian to Teratan age, with local unconformities and stages absent (Field & Uruski *et al.*, 1997).

Depositional Setting

The depositional environment for the Nidd Formation is poorly constrained, but is inferred to have been at mid- to outer shelf depths on the basis of paleontological and sedimentological evidence (Hasegawa *et al.*, 2013). The Hapuku Group is broadly interpreted as a condensed succession of Arowhanan to Teratan (upper Cenomanian to lower Coniacian) non- to shallow-marine clastic sedimentary rocks (Reay, 1993; Schiøler *et al.*, 2002).

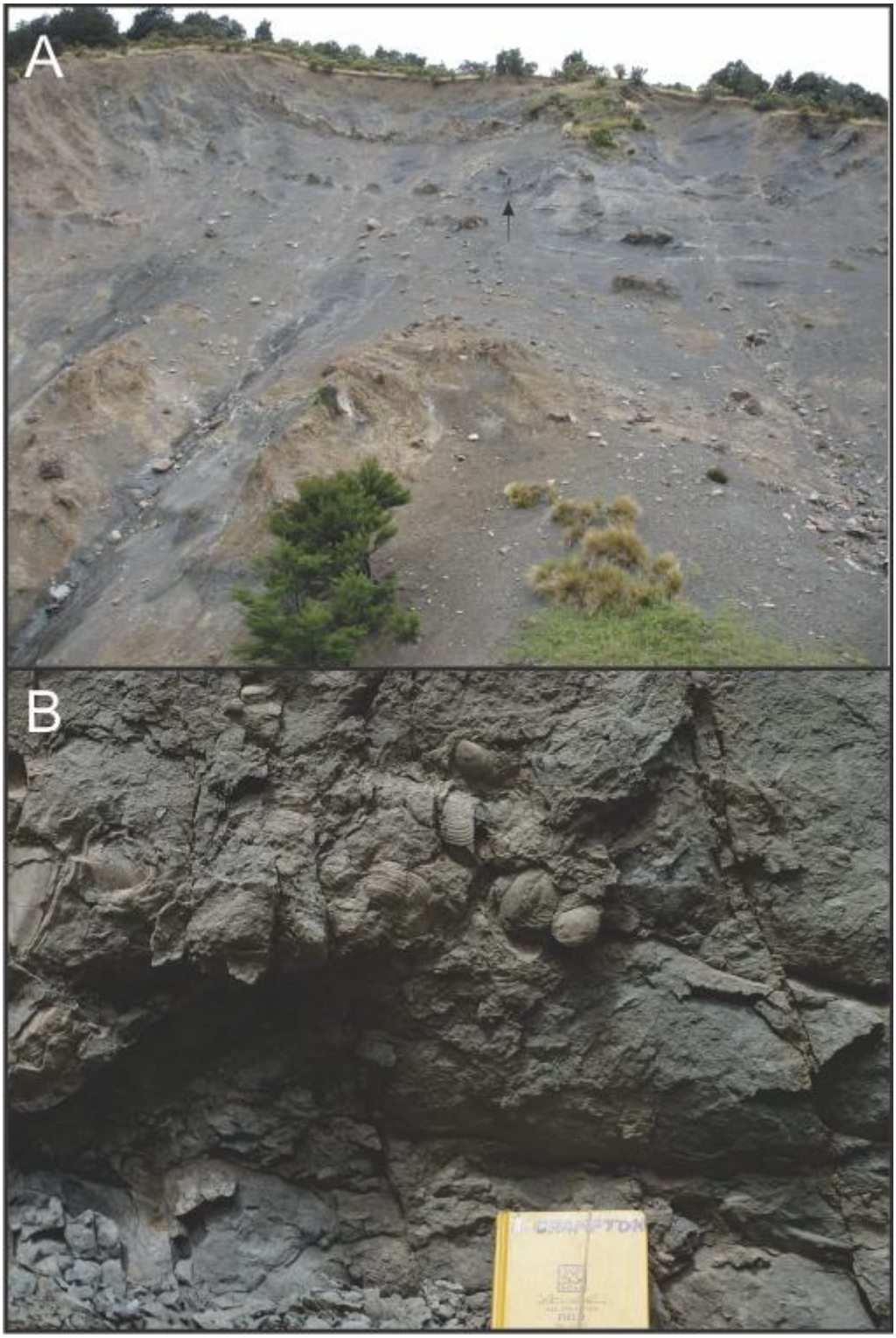

Figure 2.29: A) Well-exposed Nidd Formation in Sawpit Gully (BS28/726567). Figure for scale (arrowed). Photo supplied by J. Crampton. B) Shellbed of *Cremnoceramus bicorrugatus* in Sawpit Gully. Photo supplied by J. Crampton.

2.6.6 Burnt Creek Formation

The Burnt Creek Formation has a restricted distribution between the Ouse Fault and the Kekerengu River in the northern Clarence Valley area. The Burnt Creek Formation is included in the Coverham Group (Ritchie, 1986; Morris, 1987). The type section is the southwestern branch of Burnt Stream (Hall, 1963; Crampton & Laird, 1997). The formation is distinctly different to the coeval Nidd Formation, in that it is comprised of conglomerate and pebbly mudstone, and lacks the common bioturbation observed in the Nidd Formation/Hapuku Group (Crampton & Laird, 1997; Field & Uruski *et al.*, 1997).

Lithostratigraphy

Basal Burnt Creek Formation rests unconformably on Pahau Terrane. The formation is comprised of a thick conglomerate of Pahau Terrane-derived pebbles and boulders, overlain by pebbly mudstone, alternating graded sandstone and mudstone, and increasingly thick mudstones towards the top of the formation (Figure 2.30; Crampton & Laird, 1997). The formation is at least 200 m thick, and may have had an original maximum-thickness of >470 m (Crampton & Laird, 1997).

Paleontology and Age

Inoceramids are abundant, including *I. madagascariensis* and *I. opetius* indicating a Mangaotanean to Teratan age for the formation. This demonstrates that the basal unconformity is strongly diachronous over a short distance (Crampton & Laird, 1997). In Burnt Stream, inoceramids are observed to be glauconised and pyritised (this study).

Depositional Setting

The Burnt Creek Formation is very different to the coeval Nidd Formation, which occurs northwest of the Ouse Fault. Based on this, Crampton & Laird (1997) suggest that the Burnt Creek Formation represents the onlap and infilling of an incised valley or deposition adjacent to an active syn-sedimentary fault, and that the Ouse Fault was a major normal fault during the Clarence and Raukumara series. A depositional depth of outer shelf to upper bathyal is inferred by Crampton & Laird (1997). Paleocurrent directions range between 45° and 100° in Mangaotanean strata, and 305° to 008° in Teratan strata (Crampton & Laird, 1997).

Figure 2.30: Burnt Creek Formation, cropping out in Wharf Stream (BS28/748557). Figure for scale (centre of image). Photo supplied by J. Crampton.

2.6.7 Paton Formation

The Paton Formation crops out from Muzzle Stream (Clarence Valley) to Kekerengu (coastal Marlborough), although a number of Piripauan-aged greensands further south may be correlated with the formation (e.g. Crampton *et al.*, 1988; Laird, 1993; Reay, 1993; Schiøler *et al.*, 2002). The formation forms the base of the Seymour Group. The Paton Formation was originally introduced by Hall (1963), who designated Burnt Saddle as the type section. The Paton Formation passes southwards into the Okarahia Sandstone (Schiøler & Wilson, 1998).

Lithostratigraphy

The Paton Formation unconformably overlies the Bluff Sandstone with a sharp contact at Muzzle Stream, but elsewhere it unconformably overlies Nidd Formation (Morris, 1987; Crampton, 2003), or conformably overlies and interfingers with Burnt Creek Formation (Figure 2.31; Crampton & Laird, 1997).

The Paton Formation is typically a dark-green to green-grey, decimetre-bedded to massive, strongly-bioturbated, glauconitic, normally graded, fine to medium sandstone (Figure 2.31; Reay, 1993; Crampton & Laird, 1997; Schiøler *et al.*, 2002). Bedding is defined in places by fossil debris, angular mudstone rip-up clasts, basalt granules and carbonaceous laminae. Localised centimetre-scale bedding, shallow channels, load structures and current parting lineations are present (Reay, 1993). The formation is mildly to moderately glauconitic in places, and concretions are common.

Crampton (pers. comms.) notes difficulty in distinguishing Paton Formation from the underlying Nidd Formation in fresh outcrop. The "glauconite" referred to by several authors in the Paton Formation is likely to be chlorite. Chloritised sediments are common in the late Cretaceous strata of the East Coast Basin, including the Tangaruhe Formation in the Whangai Range (J. Crampton, Pers. Comm.). The Paton Formation is 18 m thick at Muzzle Station and thickens to the northeast to 320 m in the Kekerengu Valley, although is typically 2–20 m-thick (Reay, 1993; Crampton & Laird, 1997; Field & Uruski *et al.*, 1997; Schiøler *et al.*, 2002).

Paleontology and Age

Fragmentary and complete inoceramid bivalves are common, and typically not in life position. Shellbeds of disarticulated individuals are present at a few levels in the formation. *Inoceramus* sp. and wood fragments are common, and dinoflagellate cysts are abundant, providing a Piripauan to early Haumurian age for the formation (Reay, 1993). The Paton Formation has a Teratan to early Haumurian age, based on inoceramid bivalves and dinoflagellate assemblages (Schiøler & Wilson, 1998; Crampton *et al.*, 2000; Schiøler *et al.*, 2002).

The formation has proven barren for calcareous foraminifera and nannofossils, though the presence of the agglutinated foraminifera genus *Glomopsira* suggests minimum water depths of 100–150 m (Schiøler *et al.*, 2002). Diverse macrofossil faunas have been recovered from the Paton Formation, including belemnites, ammonites, *I. opetius*, *I. pacificus,* and *I. australis* (Schiøler & Wilson, 1998; Crampton *et al.*, 2000; this study).

Depositional Setting

The Paton Formation is inferred to have been deposited in a shallow-marine (perhaps inner shelf) setting, possibly a restricted, shallow-shelf setting (Reay, 1993; Schiøler *et al.*, 2002). Palynofacies analysis suggests that Paton Formation was deposited under oxic conditions in a nearshore environment, although foraminiferal assemblages suggest that deposition occurred under sub-oxic conditions (Schiøler & Wilson, 1998; Crampton *et al.*, 2000).

Synonymy & Correlation

The 'Formation A' described by Crampton (1988) in the in the Monkey Face area fits the description and stratigraphic position of the Paton Formation. Dinoflagellate assemblages from 'Formation A' suggest a Piripauan or earliest Haumurian age (Crampton, 1988), comparable to the age of the Paton Formation, and it may therefore be a southern extension of this unit. The Okarahira Sandstone in the Haumuri Bluff area (Roncaglia *et al.*, 1999; Crampton *et al.*, 2000), likely represent a nearshore to marginal marine correlative of the Paton Formation.

Figure 2.31: Outcrop of Paton Formation on the Coverham road (BS28/740557). The thick sandstone bed in the centre of the frame marks the contact between the underlying Burnt Creek Formation and the Paton Formation. Photo provided by J. Crampton.

2.6.8 Whangai Formation ('Herring facies')

The Whanagi Formation (Herring facies) and lateral correlatives crop out from Chancet Rocks to Conway River mouth and is included in the Seymour Group (Reay, 1993; Crampton *et al.*, 2003). The Herring Formation was originally used by Webb (1971). Bluff Stream and Dead Horse Gully were designated as lectotype sections for the formation by Reay (1993).

Lithostratigraphy

The Whangai Formation typically rests on a sharp, undulating contact with the underlying Paton Formation, and is comprised of massive to decimetre-bedded, dark-grey, micaceous, siliceous, sulphurous silty mudstone that is interbedded with minor fine sandstone layers (Figure 2.32A, B;

Laird, 1992; Reay, 1993; Schiøler *et al.*, 2002). The formation contains large ovoid concretions. The formation thickens to the northwest, ranging from 45 m at Dart Stream, to 285 m at Dead Horse Gully, to 700 m at Woodside Creek (Reay, 1993; Field & Uruski *et al.*, 1997). In Nidd Stream, a ~10 cm-thick nodular horizon marks the base of the formation (Figure 2.32C), corresponding with a sedimentary hiatus (Schiøler *et al.*, 2002). In Nidd Stream and Isolation Creek, the Mead Hill Formation rests on the Whangai Formation (Figure 2.32D), although elsewhere, these formations are separated by the Branch Sandstone (Figure 2.33 & 2.34A; Reay & Strong, 1992). The top of the Whangai Formation in the central Clarence Valley, particularly in Dead Horse Gully, is demarcated by a nodular pyrite horizon (O30/f0237; FRED).

Paleontology and Age

Sparse microfaunal assemblages are typical of the Whangai Formation, most species are arenaceous or siliceous benthic forms, and *Terebelina* (*Bathysiphon*) tubes are common (Reay, 1993). Foraminifera and dinoflagellates indicate a Haumurian age. Dinoflagellate assemblages indicate that the age of the base of the formation is diachronous across Marlborough, from late Santonian to middle Campanian (~84–79 Ma; Crampton *et al.*, 2003).

Depositional Setting

Based on the poor foraminiferal and ichnofaunas present, the Whangai Formation is inferred by Reay (1993) to have been deposited in a poorly oxygenated, shallow-marine environment. Localised cross-bedding in the formation indicates a dominantly southeasterly current direction.

Synonymy & Correlation

Within the Marlborough region, the Whangai Formation can be correlated with the Conway Siltstone south of Kaikoura, and the Woolshed, Butt and Mirza formations elsewhere Marlborough, and is considered synonymous with these formations, and with the Whangai Formation of the North Island East Coast (Laird & Schiøler, 2005; Rattenbury *et al.*, 2006). Herein, the Herring Formation is synonymised with the Whangai Formation, specifically the Rakauroa Member, on the basis of age, lithological and geochemical affinities, discussed later in this thesis (Chapters Four, Six and Seven).

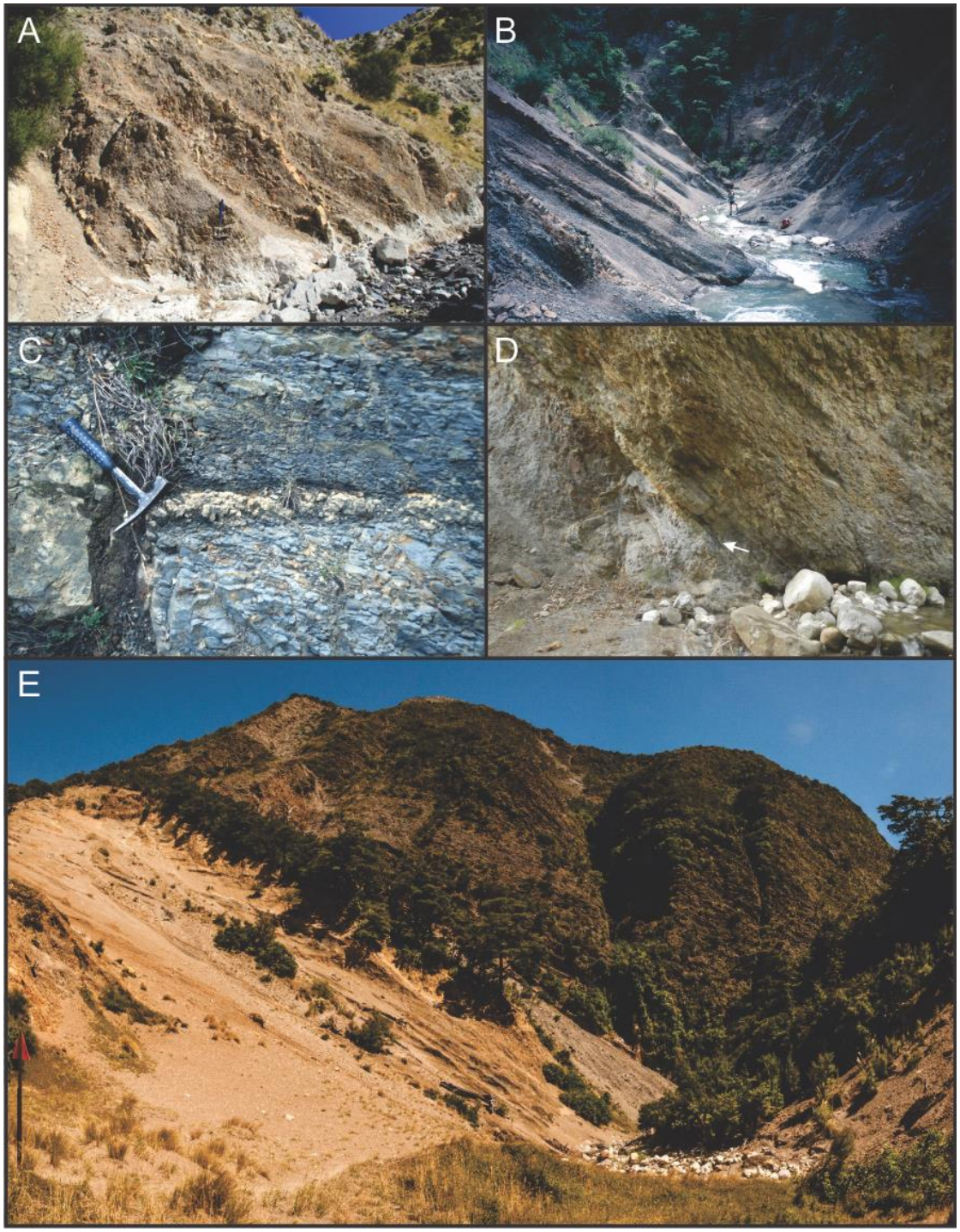

Figure 2.32: A) Whangai Formation (Herring facies) cropping out in a tributary of the Dart Stream (BS27/561441). Hammer for scale – handle is 70 cm long. Photo from K. Bland. B) Whangai Formation in Nidd Stream (BS28/737567). Figure for scale. Photo from J. Crampton. C) Nodular horizon marking the contact between Paton Formation and Whangai Formation in Nidd Stream (BS28/756579). Hammer for scale (25 cm long). Photo supplied by J. Crampton. D) Contact between the Whangai Formation and the overlying Mead Hill Formation in Nidd Stream (BS28/737567). Nodule bed is in lower left-hand corner of image. Hammer for scale on contact (arrowed). E) Whangai Formation cropping out in Isolation Creek (foreground; BS28/818610), overlain by chert-dominated Mead Hill Formation.

2.6.9 Branch Sandstone

The Branch Sandstone and correlatives is present from Haumuri Bluff to Branch Stream. Further north, it is either faulted out, or absent. The Branch Sandstone marks the top of the Seymour Group. The type section for the Branch Sandstone is Branch Stream (Reay & Strong, 1992; Reay, 1993).

Lithostratigraphy

The Branch Sandstone conformably overlies the Whangai Formation with a sharp, planar contact (Figure 2.33). Locally the contact is burrowed, or represented by a basal conglomerate (Reay, 1993). The formation is dominantly a massive, light brown grey, well-sorted fine sandstone, with minor carbonaceous siltstone, lignite and conglomerate (Figure 2.33), that is generally well- to moderately-indurated, but rarely cemented (Reay, 1993). At Bluff Stream, the basal 30 cm of the formation is matrix-supported pebble-conglomerate, of which 50% of clasts show a phosphatised outer margin, and shark teeth are common (Reay, 1993). The Branch Sandstone is generally massive, and bedding and sedimentary structures are rare. Locally, slump structures, centimetre-scale low-rank coal seams, dish structures, intrusive sandstone dikes (Figure 2.33), and convolute bedding may be present (Reay, 1993). The formation varies in thickness, from 3 m-thick at Bluff River, to 9 m-thick at Mororimu Stream, with an average thickness of 11 m (Reay, 1993).

Paleontology and Age

Many outcrops are extensively bioturbated, producing a mottled texture, with the dominant ichnogenus being *Thallasinoides* (Reay, 1993). The only macrofauna recovered from the formation is a rugose coral (*Dasmosilia*) and shark teeth (Reay, 1993). Foraminiferal and dinoflagellate assemblages indicate a Haumurian age for the formation.

Depositional Setting

The Branch Sandstone is interpreted as a deposit of a paralic environment, as suggested by foraminiferal assemblages and algal borings on phosphatised clasts. This latter observation suggests deposition occurred within the photic zone (Reay, 1993). The formation is interpreted as migrating barrier sandbar by Reay & Strong (1992). Deposition in high-energy, well-oxygenated bottom waters is suggested by the well-sorted sandstone, low organic carbon accumulation, and the very active infaunal bioturbation (Reay, 1993). The localised presence of carbonaceous siltstone and coal in the thickest, and most-westward section of the Branch Sandstone suggests possible subaerial emergence (Reay, 1993).

Synonymy & Correlation

The Branch Sandstone is synonymous with the Claverley Sandstone that overlies the Conway Formation in the Haumuri Bluff and Conway River area (Morris, 1987; Reay, 1993).

Figure 2.33: Sharp contact (red arrow) between the Whangai Formation (left) and the overlying Branch Sandstone (right) in Wharekiri Stream (BT28/647296). Figure for scale (lower centre of image; white arrow), marking intrusive sandstone dike. Photo supplied by J. Crampton.

2.6.10 Mead Hill Formation

The Mead Hill Formation is a geographically extensive formation, occurring across large parts of the Marlborough area, from Chancet Rocks (near Ward) to Kaikoura. The Mead Hill Formation forms the base of the Muzzle Group. The first use of the formation is attributed to Webb (1966, 1971), who nominated Mead Stream as the stratotype section. Reay (1993) nominated Muzzle Stream as a hypostratotype for the formation. The Mungaroa and Kaiwhata limestones of southern

North Island (see descriptions in previous sections) have been suggested as lateral correlatives of the Mead Hill Formation. Given the age discrepancy, these formations are kept separate here.

Lithostratigraphy

The Mead Hill Formation conformably overlies either the Branch Sandstone or the Whangai (Herring) Formation (depending on location) with a sharp contact (Figure 2.32D, 2.34A; Reay, 1993; Hollis *et al.*, 2005b; this study). The Mead Hill Formation is a strongly cemented, chert-rich, decimetre-bedded, grey to white, muddy, foraminiferal micritic limestone interbedded with medium dark-grey, poorly indurated calcareous mudstone. With the exception of bioturbation and the consistent decimetre bedding, primary sedimentary structures are absent from the formation. Styolites are present in the formation in places. Chert is present in varying quantities throughout the formation and commonly occurs as elliptical nodules, becoming more prevalent above the Cretaceous-Paleogene boundary (Figure 2.34B). These nodules form the centre of beds, and may comprise over 90% of the host bed, in which case the lithology is described as siliceous limestone (Reay, 1993). Commonly, nodules appear to have coalesced to form continuous bands, referred to as the ribbon cherts (Figure 2.34C), generally found above the Cretaceous-Paleogene boundary (Strong *et al.*, 1995). The top of the formation is marked by either the sub-Teredo Limestone Member unconformity, or the deposition of the Waipawa Formation (Figure 2.34D; Hollis *et al.*, 2005b, 2014). The formation increases in thickness northeast-wards from ~10 m at Kaikoura, to 18 m at Bluff River, 40 m at Muzzle Stream, 79 m at Dart Stream, to ~200 m thick at Mead Stream, where the basal contact is faulted out (Reay, 1993; Strong *et al.*, 1995; Hollis *et al.*, 2005a).

Paleontology and Age

Age control for the Mead Hill Formation is based on foraminiferal and radiolarian assemblages, which provided a latest Haumurian to early Teurian age (Reay, 1993; Strong *et al.*, 1995; Hollis *et al.*, 2003a; 2005a, 2005b). In several sections the K/Pg boundary is well-preserved, including Mead Stream, Woodside Creek and Flaxbourne River. At the latter two sites a boundary clay, and in some instances an iridium anomaly, have been identified (Strong, 1977, 2000; Strong *et al.*, 1995; Hollis *et al.*, 2003a, 2003b).

The formation is moderately bioturbated, and trace fossils are generally indistinct below the Cretaceous-Tertiary boundary, although small *Thallasinoides*, and rare *Teichichnus* and *Planolites* burrows were noted by Reay (1993). The intensity and diversity of bioturbation increases across the Cretaceous-Paleogene boundary (Reay, 1993).

Depositional Setting

Reay (1993) interprets the base of the Mead Hill Formation as being deposited at shelf depths, with progressive deepening and increasing exposure to oceanic circulation during the late Haumurian, with the upper portion of the formation deposited at bathyal depths. In the Clarence Valley and Ward areas, the Mead Hill Formation deepens from an outer shelf setting in the latest Cretaceous to an upper bathyal to middle bathyal depositional setting (Strong *et al.*, 1995; Hollis *et al.*, 2005a).

At the time of the K/Pg boundary, the Mead Hill Formation is interpreted as being outer shelf to upper bathyal in the Branch Stream and Woodside Creek sections, and middle bathyal in the Mead Stream and Flaxbourne River sections (Hollis *et al.*, 2003a, 2003b). No outcrops of Cretaceous Mead Hill Formation occur south of Branch Stream in the Clarence Valley (Crampton *et al.*, 2003). Reay (1993) infers time-transgressive relationships for the base of the Mead Hill Formation, suggesting that the base youngs southwards.

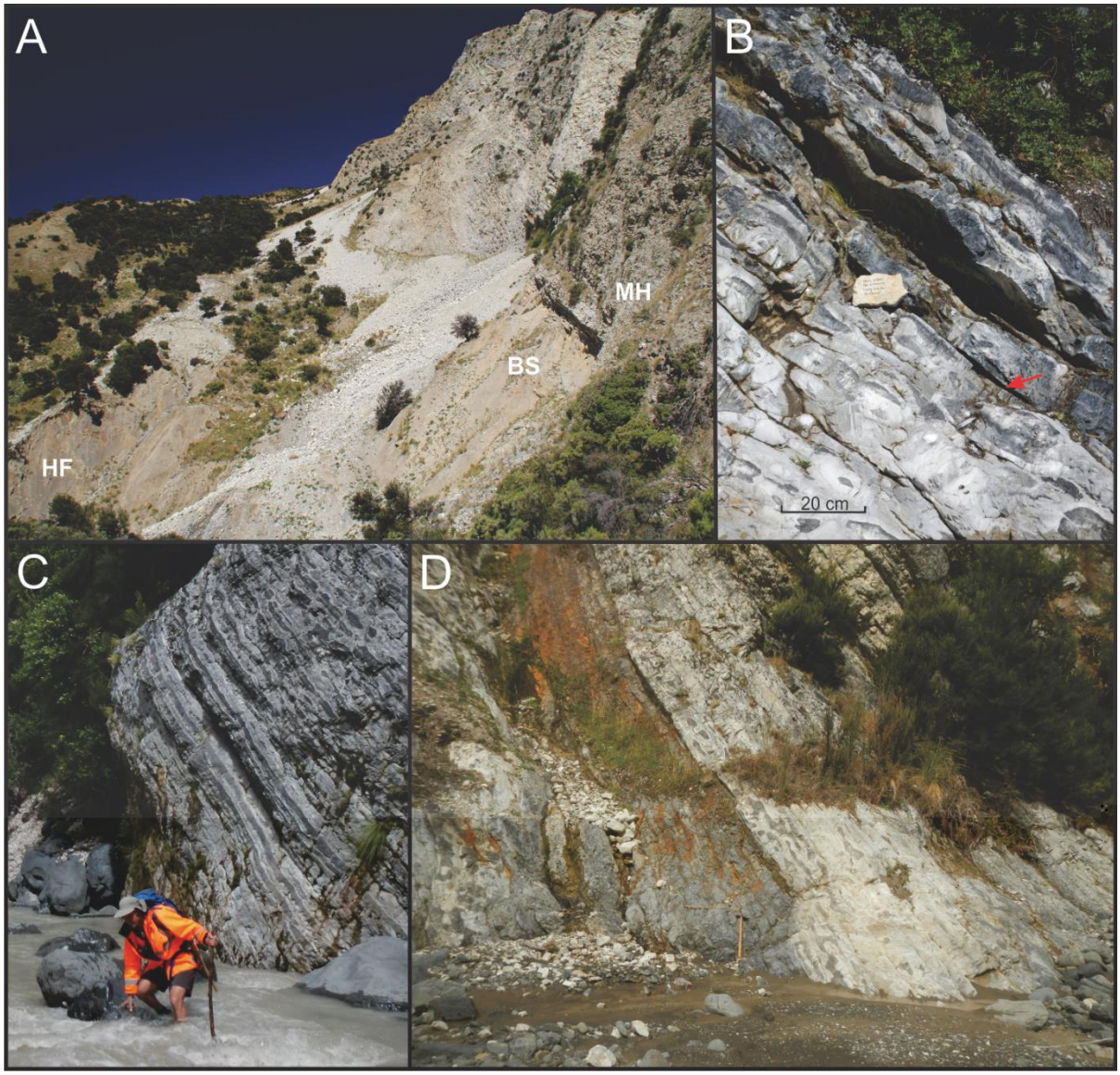

Figure 2.34: A) Basal contact of the Mead Hill Formation (MH), overlying Branch Sandstone (BS), over top of Whangai (Herring) Formation (HF) in Dart Stream (BS27/561440). Photo supplied by K. Bland. B) Cretaceous-Paleogene boundary in Mead Stream (BS28/661542). Boundary clay is indicated by the arrow. Note the transition to dominantly siliceous (black) composition above the boundary. C) Ribbon cherts, characteristic of the much of the Paleocene Mead Hill Formation and the Lower Limestone member of the Amuri Limestone, in Mead Stream (BS28/660544). Figure for scale. D) Waipawa Formation cropping out in Mead Stream (BS28/658543), separating the Mead Hill Formation from the Amuri Limestone. Hammer for scale (centre, base of outcrop). Hammer handle is 0.5 m long.

2.6.11 Amuri Limestone

The Amuri Limestone is an extensive unit across the Marlborough region, cropping out from the Clarence Valley to Chancet Rocks, and south to Haumuri Bluff. The formation is particularly well-exposed in the Clarence Valley (Figure 2.35A). The Amuri Limestone belongs to the Muzzle Group, and can be subdivided into seven informal members; the Teredo Limestone, Dee Marl, Lower Limestone, Lower Marl, Upper Limestone, Fells Greensand, and Upper Marl (Reay, 1993; Strong *et al.*, 1995; Hollis *et al.*, 2005a, 2005b; Nicolo *et al.*, 2010). The first use of Amuri Limestone is attributed to Hutton (1874). Reay (1993) nominated Dart Stream as the hypostratotype section. The Amuri Limestone is coeval with the Wanstead Formation of the North Island East Coast Basin. Amuri Limestone is also recognised in the northern Canterbury Basin, though has a notable younger age than the Amuri Limestone in Marlborough (e.g., Browne & Field, 1985; Lewis, 1992).

2.6.11.1 Teredo Limestone Member, Amuri Limestone

Lithostratigraphy

The Teredo Limestone Member ranges from Haumuri Bluff, south of Kaikoura to Muzzle Stream in the middle Clarence Valley. In sections where it is absent, there is a small unconformity, or as at Mead Stream, the Waipawa Formation is present (Reay, 1993; Hollis *et al.*, 2005a, 2005b, 2014). The Teredo Limestone is a calcareous and glauconitic, sandy limestone that marks the base of the Amuri Limestone, although is not present north of Dart Stream. In southwestern area of the middle Clarence Valley, the Teredo Limestone Member overlies the Whangai (Herring) Formation with an unconformable contact (Reay, 1993). The base of the member is marked by a low-angle (~2°) angular unconformity, removing part of the underlying Mead Hill Formation (Reay, 1993; Hollis *et al.*, 2005b). The Teredo Limestone Member is a moderately hard, massive, poorly-sorted, muddy, silty, glauconitic, phosphatic, calcareous sandstone (Figure 2.35B). The base of the member may be marked by *Thallasinoides* bioturbation and/or phosphatic nodules, as at exposures on the Kaikoura shore platform (Rattenbury *et al.*, 2006). Elsewhere, the base of the member is often marked by a 20 cm-thick basal breccia, and sparse angular, matrix-supported phosphatised limestone clasts are scattered throughout (Reay, 1993). The formation is typically massive, though occasional low-angle stratification may be observed infilling broad, shallow channels (Reay, 1993). The member ranges from a 16 cm-thick bed in Muzzle Stream, to 20 m thick at Seymour Stream, to 7 m thick at Kaikoura (Reay, 1993; Hines, unpublished data). South of Muzzle and Bluff streams, the Teredo Limestone Member consists of two distinct units, a lower unit up to 20 m

thick that consists of massive to cross-bedded calcareous greensand, and an upper unit of highly bioturbated, very glauconitic, calcareous sandstone (Reay 1993; Hollis *et al.*, 2005b).

Paleontology and Age

The Teredo Limestone Member is named for a series of borings that resemble Teredo worm/bivalve borings, where it outcrops on the shore platform at Kaikoura. Individual and clustered horizontal and vertical calcite tubes are abundant through the limestone, and were originally identified as Teredo borings by Hector (1874) (Figure 2.35B). These were reclassified as Clavagellid bivalve tubes by Warren & Speden (1978). Macrofossils from the Teredo Limestone Member consist of a crinoid stem, spatangoid echinoid, mollusc fragments, fish, shark and cetacean teeth and phosphatised vertebrae and other bones (Reay, 1993).

Microfossils are generally well preserved in the Teredo Limestone Member. The base of the member is diachronous, with foraminifera, calcareous nannofossils and dinoflagellates, indicating that the formation ranges from early Teurian (early Paleocene) in the northern middle Clarence Valley, to early Waipawan (early Eocene) in the south at Kaikoura and Haumuri Bluff (Reay, 1993; Hollis *et al.*, 2005b). A significant hiatus occurs below the Teredo Limestone Member in the central Clarence Valley, with 6 Myr missing at Muzzle Stream and at least 10 Myr missing at Bluff Stream (Hollis *et al.*, 2005b). At the Kaikoura Lab section (Kaikoura township), Haumurian-aged Mead Hill Formation is overlain by late Teurian to early Waipawan Teredo Limestone Member, that in turn is overlain early Waipawan to Mangaorapan Amuri Limestone (Lower Marl) (C. Hollis, unpublished data, this study).

Depositional Setting

Foraminiferal evidence suggest that the member was deposited in an inner-shelf environment (Reay, 1993). Abundant glauconite, phosphate nodules and pervasive bioturbation suggest low to absent sedimentation under low-energy conditions. Paleocurrent directions from Seymour Stream indicate a southwesterly current direction (Reay, 1993).

2.6.11.2 Lower Limestone Member, Amuri Limestone

Lithostratigraphy

The Lower Limestone Member is present from the northern Clarence Valley as far south as Wallow Stream, where it wedges out. The Lower Limestone Member conformably overlies the Teredo Limestone Member (Hollis *et al.*, 2005b) or the Waipawa Formation (Strong *et al.*, Hollis *et*

al., 2005a) where either are present, or else lies unconformably on the Mead Hill Formation (Reay, 1993). The Lower Limestone Member is dominated by decimetre-bedded siliceous limestone separated by marly partings (Hollis *et al.*, 2005a, 2005b). There are thin stringers of chert within the lower limestone, and the upper ribbon chert immediately above the Dee Marl Member marks the highest occurrence of chert on the Amuri Limestone (Hollis *et al.*, 2005a). The Lower Limestone Member reaches a maximum-thickness of 82 m at Dart Stream, although it thins northwards (76 m at Mead Stream, Hollis *et al.* 2005a), and thins southwards to 8.5 m at Muzzle Stream (Hollis *et al.*, 2005b), before wedging out between the Bluff and Gentle Annie streams (Reay, 1993; Hollis *et al.*, 2005b).

Paleontology and Age

No macrofossils have yet been recorded from this member. Trace fossils include *Planolites* and *Teichichnus* traces, rare *Thallasinoides*, and abundant *Zoophycos* (Morris, 1987). *Teichichnus* traces were only observed at the base of the Lower Limestone Member at Muzzle Stream and further south (Morris, 1987). The Lower Limestone Member contains numerous forms of bioturbation including *Zoophycos* (Nicolo *et al.*, 2010). The Lower Limestone Member is late Paleocene (Teurian) to Waipawan (early Eocene) in age (Strong *et al.*, 1995).

Depositional Setting

A gradual change in the proportion of glauconite in the Lower Limestone Member immediately overlying the Teredo Limestone Member implies a gradual change in environmental conditions (Hollis *et al.*, 2005b). The Lower Limestone Member was deposited in a mid-bathyal environment (Strong *et al.*, 1995; Hollis *et al.*, 2005a; Nicolo *et al.*, 2010). Sediment accumulation rates (SAR) of 20 m/Myr reflect the low terrigenous supply during deposition of the member (Dallanave *et al.*, 2015).

2.6.11.3 Dee Marl Member, Amuri Limestone

Lithostratigraphy

The Dee Marl Member has a restricted distribution, and crops out between the Muzzle and Mead Stream sections (Nicolo *et al.*, 2010). The Dee Marl occurs within the Lower Limestone Member and is interpreted to represent the Palecoene–Eocene Thermal Maximum (PETM; Nicolo *et al.*, 2010). The lower contact is conformable. The Dee Marl Member refers to a collection of marl beds that then grade progressively upwards into the limestone (Figure 2.35C; Nicolo *et al.*, 2010).

A briefly exposed section at the base of the Dee Marl Member showed a 20 cm-thick laminated dark mudstone that had previously not been observed (Figure 2.35C). The Dee Marl Member is 80 cm thick at Muzzle Stream, 1 m thick in Dee Stream, and 1.89 m thick in Mead Stream (Hollis *et al.*, 2005a, 2005b; Nicolo *et al.*, 2010).

Paleontology and Age

Ichnofossil assemblages are dominated by *Chondrites* and *Zoophycos* (Nicolo *et al.*, 2010). Foraminifera and calcareous nannofossil assemblages suggest the marl sits across the Palecoene-Eocene boundary (Hancock *et al.*, 2003; Hollis *et al.*, 2005a; Nicolo *et al.*, 2010).

Depositional Setting

The Dee Marl Member records a benthic foraminifera extinction event at the base, along with the short-lived occurrences of warm-water planktic foraminifera and calcareous nannofossils, and a prominent carbon isotope excursion (PETM; Hancock *et al.*, 2003; Hollis *et al.*, 2005a; Nicolo *et al.*, 2010). Benthic foraminifera faunas indicate dysaerobic conditions (Hancock *et al.*, 2003; Nicolo *et al.*, 2010), which may relate to a recently observed dark-brown shale at the base of the formation. This is a significant observation as the PETM is presented by an organic-rich shale in many northern hemisphere sites (e.g., Boucsein & Stein, 2009; Gavrilov *et al.*, 2011; Schulte *et al.*, 2013), but no such shales have previously been identified in the New Zealand region across the Paleocene-Eocene boundary.

2.6.11.4 Lower Marl Member, Amuri Limestone

Lithostratigraphy

The Lower Marl Member is present throughout the Marlborough region, from northern Clarence Valley to Kaikoura. The Lower Marl Member conformably overlies the Teredo Limestone Member to the south with a relatively sharp basal contact (Reay, 1993). North of the Bluff River, the Lower Marl Member gradationally overlies the Lower Limestone Member, marked by an increasing abundance of marl beds, and diminishing frequency of micritic limestone beds (Figure 2.35D; Reay, 1993; Strong *et al.*, 1995; Hollis *et al.*, 2005b). The Lower Marl Member consists of alternating, hard, pale greenish-grey limestone and softer greenish-grey marl (Figure 2.35D, E, F; Strong *et al.*, 1995). Marl is more dominant than limestone, with marl forming beds from 20 cm to 1.5 m thick, and limestone forming beds 10 cm to 1 m thick (Strong *et al.*, 1995; this study). The Lower Marl Member is differentiated from the Upper Marl Member by its thicker limestone-marl

alternations and greater hardness contrast between limestone and marl (Strong *et al.*, 1995). In the central Clarence Valley, the Lower Marl Member is 40 m thick (Hollis *et al.*, 2005b). The Lower Marl Member is 75 m thick at Swale Stream (this study), 112 m thick at Mead Stream (Strong *et al.*, 1995), 103 m thick at Branch Stream (this study), and ~30 m thick at Kaikoura (this study).

Paleontology and Age

The only macrofossil identified in the Lower Marl Member is a *Propeamussium* sp. bivalve, however the formation also contains bioturbation traces of *Planolites* and *Zoophycos* (Morris, 1987). The Lower Marl Member is Waipawan to Heretaungan (early to middle Eocene) in age (Strong *et al.*, 1995).

Depositional Setting

The Lower Marl Member is interpreted as representing the main phase of the Early Eocene Climatic Optimum and the associated increased terrigenous sediment flux (SAR=50 m/Myr; Hollis *et al.*, 2005; Slotnick *et al.*, 2012, 2015; Dallanave *et al.*, 2015).

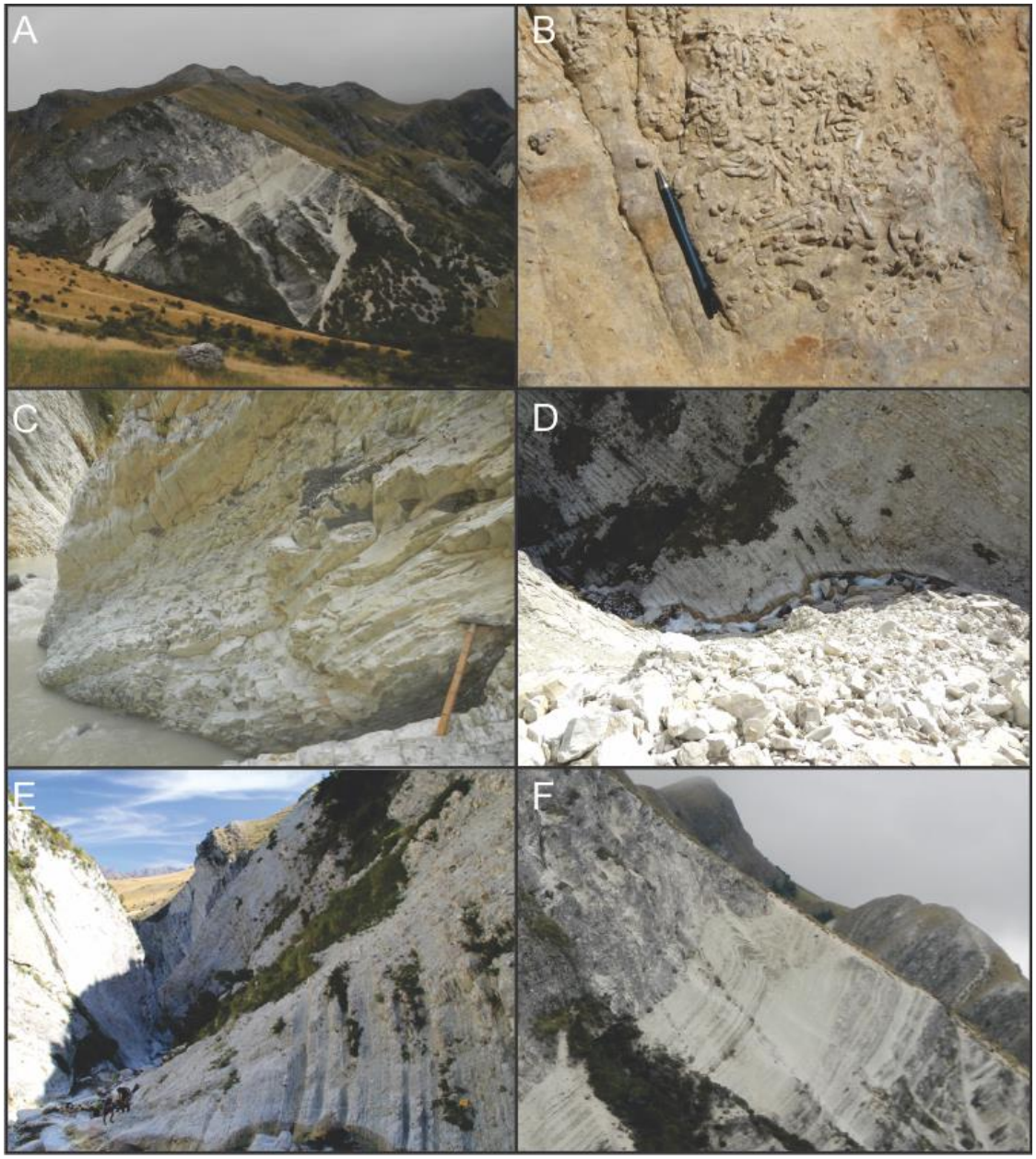

Figure 2.35: A) View of much of the Amuri Limestone in the Coverham area (BS28/705572), showing the Lower Limestone Member at the lower right of the cliff outcrop, overlain by the Lower Marl Member (white band), in turn overlain by Upper Limestone Member. The Upper Marl Member is hidden beneath tussock in the top-left of image. View is from Mead Hill looking into Swale Stream. White band in photo is approximately 40 m wide. B) Clavigellid bivalve tubes exposed in a bedding surface of the Teredo Limestone Member at Haumuri Bluff (BU27/421885). Pen for scale is approximately 13 cm long. Photo supplied by James Crampton. C) Outcrop of Dee Marl in Mead Stream (BS28/658544), with previously unexposed dark-coloured shale at the base (near hammer). Hammer is 0.5 m long. D) Outcrop of the Lower Marl Member in Branch Stream. Figures for scale (centre of image). E) Lower Marl Member in Branch Stream (BS27/585467), displaying the decimetre-scale alternation of limestone and marl. Figures for scale. Image supplied by K. Bland. F) Possible syn-sedimentary slumping in the Lower Marl Member cropping out in Swale Stream (BS28/705572), immediately below the Upper Limestone Member. Field of view is approximately 80 m.

2.6.11.5 Upper Limestone Member, Amuri Limestone

Lithostratigraphy

The Upper Limestone Member conformably overlies the Lower Marl, although in most exposures in the Clarence Valley the contact between the Lower Marl and Upper Limestone Member is disrupted (e.g., Hollis *et al.*, 2005b; Figure 2.35F). The Upper Limestone Member consists of uniform, dense, white weathering, light-grey limestone with centimetre to decimetre bedding (Strong *et al.*, 1995). The Upper Limestone Member is 75 m thick at Mead Stream (Strong *et al.*, 1995), 48 m thick at Branch Stream (This study), and 31 m thick at Haumuri Bluff, where it overlies the Teredo Limestone Member (Morris, 1987).

Paleontology and Age

Macrofossils in this member include pectenids, *Prionocidaris* aff. *marshalli* and echinoid spines, along with the trace fossils *Thallasinoides* and *Chondrites* (Morris, 1987). The Upper Limestone Member is Heretaungan to Porangan (middle Eocene) in age (Strong *et al.*, 1995).

Depositional Setting

The Upper Limestone Member was deposited in a mid- to lower-bathyal environment (Strong *et al.*, 1995), during a period of low terrestrial weathering. Sediment accumulation rates in the Upper Limestone Member are lower than those of the Lower Limestone Member (SAR=10 m/Myr; Dallanave *et al.*, 2015).

2.6.11.6 Upper Marl Member, Amuri Limestone

Lithostratigraphy

The Upper Marl Member is present from the northern Clarence Valley as far south as Dart Stream. South of Dart Stream, the Upper Marl Member is truncated by the Fells Greensand. The Upper Marl Member conformably overlies the Upper Limestone Member. The middle Eocene top of the formation is unconformably overlain by the early Miocene Weka Pass Formation with a strongly bioturbated contact marking the Marshall Paraconformity (Figure 2.36; Reay, 1993; Strong *et al.*, 1995; Hollis *et al.*, 2005a). The Upper Marl Member consists of approximately equal proportions of marl and limestone, alternating as 0.2–0.75 m-thick beds (Figure 2.36; Strong *et al.*, 1995). The Upper Marl Member is 125 m thick in Mead Stream (Strong *et al.*, 1995), and 84 m thick at Branch Stream (this study).

Paleontology and Age

A number of indeterminate oysters have been recovered from the Upper Marl Member at Kaikoura, along with a *Terebratulid* brachiopod and a crinoid stem (Morris, 1987). Ichnofauna includes *Planolites*, *Chondites*, *Zoophycos*, and *Thallasinoides* (Morris, 1987). The Upper Marl Member is Bortonian (middle Eocene) in age (Strong *et al.*, 1995).

Depositional Setting

The Upper Marl Member of the Amuri Limestone is interpreted to have been deposited at lower bathyal depths, greater than 1300 m, based on foraminiferal faunas (Strong *et al.*, 1995). The timing of the deposition of the Upper Marl Member is coincident with the Middle Eocene Climatic Optimum (MECO), and with an increase in terrigenous sediment supply (SAR=40 m/Myr; Dallanave *et al.*, 2015).

2.6.11.7 Fells Greensand, Amuri Limestone

Lithostratigraphy

The Fells Greensand has a restricted distribution in the central Clarence Valley, between Seymour Stream and Dart Stream, the lower Awatere Valley, and from Kekerengu to the Ure River in coastal Marlborough (Morris, 1987; Reay, 1993; Townsend & Little, 1998). The greensand is locally intercalated between the Upper Limestone and Upper Marl (Morris, 1987). The Fells Greensand consists of centimetre- to decimetre-bedded greensand beds. Flute casts are rarely preserved on the soles of beds. Internal structures include laminations, normal grading and possible hummocky cross-stratification (Morris, 1987). The type section is in Bluff Stream where it reaches 11.4 m thick (Morris, 1987).

Paleontology and Age

Thallasinoides is the only ichnotaxa identified in the Fells Greensand (Morris, 1987). The Fells Greensand is early to mid-Bortonian (middle Eocene) in age (Morris, 1987).

Depositional Setting

The Fells Greensand was deposited in bathyal settings with a low sediment accumulation rate.

Figure 2.36: Upper Marl Member of the Amuri Limestone (Bortonian/middle Eocene), overlain by the Weka Pass Limestone (Early Miocene) in Mead Stream (BS28/654546). Figure for scale. Image supplied by K. Bland.

2.7 Haumuri Bluff

2.7.1 Okarahia Sandstone

The Okarahia Sandstone has a distribution restricted to the Haumuri Bluff area. The formation is included in the Eyre Group, and the type section is at Haumuri Bluff (Warren & Speden, 1978; Browne & Field, 1985).

Lithostratigraphy

The Okarahia Sandstone unconformably overlies Pahau Terrane basement, and consists of weakly indurated, quartzose sandstone (Warren & Speden, 1978; Crampton *et al.*, 2000). The formation is approximately 80 m thick (Roncaglia *et al.*, 1999; Crampton *et al.*, 2000).

Paleontology and Age

Inoceramid bivalves indicate a Piripauan mid-Late Cretaceous age for the formation, with *Inoceramus pacificus* identified at the base of the formation, indicating a Teratan to earliest Piripauan (late Coniacian) age for the base of the formation, and *Inoceramus australis* indicating an early Piripauan (late Coniacian to middle Santonian) age for the top of the formation (Warren & Speden, 1978; Roncaglia *et al.*, 1999). Dinoflagellate faunas restrict the age of the formation to late Teratan to early Piripauan (late Coniacian to early Santonian; Roncaglia *et al.*, 1999).

Depositional Setting

The formation is interpreted to have been deposited in a high-energy, nearshore, paralic to inner-shelf depositional environment (Warren & Speden, 1978; Roncaglia *et al.*, 1999). Palynomorphs suggest deposition in a marginal-marine environment (Crampton *et al.*, 2000).

2.7.2 Tarapuhi Grit

The formation has a distribution restricted from Ferniehurst (Canterbury) to Kaikoura (Browne & Field, 1985). The formation is included in the Eyre Group, and the type section is Haumuri Bluff (Browne & Field, 1985).

Lithostratigraphy

The Tarapuhi Grit unconformably overlies the Okarahia Sandstone, and is comprised of green-grey, calcareous, glauconitic, fine sandstone with granule-sized polished quartz and chert clasts (Roncaglia *et al.*, 1999). The formation is 4 m thick at Haumuri Bluff, and is conformably overlain by the Conway Formation (Roncaglia *et al.*, 1999).

Paleontology and Age

The bivalves *Inoceramus matotorus* and *Ostrea lapillicola,* and the belemnite *Dimitobelus hectori*, suggest an early Haumurian age for the Tarapuhi Grit (Warren & Speden, 1978). This is consistent with dinoflagellate assemblages that indicate an early-middle Campanian age for the Tarapuhi Grit (Roncaglia *et al.*, 1999).

Depositional Setting

The formation is interpreted as having been deposited in a shallow-marine, nearshore environment (Warren & Speden, 1978).

2.7.3 Conway Siltstone

The Conway Siltstone extends from Haumuri Bluff to the Waipara River area in northern Canterbury. The formation belongs to the Eyre Group (Field & Browne, 1985; Field & Browne *et al.*, 1989), with the Conway River mouth designated as the type section (Warren & Speden, 1978). The Conway Siltstone is synonymous with the Whangai, Mirza, Woolshed and Herring formations (e.g., Crampton *et al.*, 2000). The unit has been of significant interest, particularly at Haumuri Bluff, due its rich macrofossil faunas, particularly marine reptiles. This has resulted in the formation being called a number of names over the past century, including; Saurian Sands (Haast, 1871a; Wilson, 1963), Septaria Clays (Haast, 1871b), Sulphur Sands (Hector, 1874; Thomson, 1920; Mason, 1941; Wilson, 1963), Boulder Sands (Hector, 1874; McKay, 1877a), Saurian Beds (McKay, 1877b; Thomson, 1920; Wellman, 1959; Wilson, 1963), Concretionary Sands (Mason, 1941), Laidmore Formation (Webb, 1966, 1971; Welles & Gregg, 1971), and Conway Formation (Browne & Field, 1985).

Lithostratigraphy

The Conway Siltstone conformably overlies the Tarapuhi Grit at Haumuri Bluff, though further south, at Waipara River, the formation overlies the Broken River Formation (Warren & Speden, 1978; Browne & Field, 1985; Roncaglia *et al.*, 1999). The formation is soft, medium-grey, massive, jarositic, slightly glauconitic, siltstone or silty sandstone (Roncaglia *et al.*, 1999; Crampton *et al.*, 2000; Wilson *et al.*, 2005). Bioturbation is pervasive, and has destroyed primary sedimentary structures in most outcrops (Wilson *et al.*, 2005). The unit contains a number of large, sub-spherical concretions up to 5 m in diameter, which are a characteristic feature of the formation, approximately 25% of which are reported to contain reptile bone (Warren & Speden, 1978; Wilson *et al.*, 2005). The formation is typically 100–300 m thick (Roncaglia *et al.*, 1999).

Paleontology and Age

The formation is richly fossiliferous in many localities, particularly Haumuri Bluff, where plesiosaur and mosasaur bone, shark teeth, ammonites, belemnites and various molluscs are common (Wilson *et al.*, 2005). In other outcrops of the Conway Siltstone, the formation is quite decalcified, and calcareous-shelled invertebrates, brachiopods, fish remains, and plant fragments are less common (Wilson *et al.*, 2005). Foraminifera are rare in the formation (Webb, 1966), although rich, well-preserved dinoflagellate assemblages are present (Roncaglia *et al.*, 1999).

There is good control on the age of the Conway Siltstone due to rich dinoflagellate assemblages. The base of the formation at Waipara River identified as younger (*A. acutulum* zone; c. 71.3–69.4 Ma) than at Haumuri Bluff (*V. spinulosa* zone; c. 80.5–79 Ma) (Roncaglia *et al.*, 1999).

Depositional Setting

In the Haumuri Bluff area, the Conway Siltstone is interpreted to have been deposited in an offshore, likely outer shelf environment, but with a high influx of terrestrial organic material (Roncaglia *et al.*, 1999). Further up the section, an increase in leaf cuticles and terrestrial organic matter suggests progradation of the coastline (Roncaglia *et al.*, 1999). In the Waipara River area, the Conway Siltstone is interpreted as representing the transition from a non-marine to nearshore environment with occasional marine intrusions (Broken River Formation), to a marginal- to shallow-marine environment (Roncaglia *et al.*, 1999).

2.7.4 Claverley Sandstone

The Claverley Sandstone extends from Kaikoura to Conway River, though as discussed previously in this chapter, it is a lateral correlative of the Branch Sandstone mapped in the Clarence Valley. The formation belongs to the Eyre Group Field & Browne, 1985), and the north side of Haumuri Bluff was designated the type section (Warren & Speden, 1978). The Claverley Sandstone is regarded here as being synonymous with the Branch Sandstone (e.g., Morris, 1987).

Lithostratigraphy

The Claverley Sandstone gradationally overlies the Conway Siltstone (Browne & Field, 1985). The formation is a moderately indurated, locally calcareous, bioturbated, glauconitic, poorly-sorted, quartzose, fine sandstone (Warren & Speden, 1978; Browne & Field, 1985). The formation is 45 m thick at Conway River mouth, thinning to 32 m thick at Haumuri Bluff (Browne & Field, 1985; Crampton *et al.*, 2000). At Haumuri Bluff the Claverley Sandstone is unconformably overlain by the Teredo Limestone Member (Roncaglia *et al.*, 1999).

Paleontology and Age

Foraminiferal and dinoflagellate faunas indicate a middle to late Campanian (latest Cretaceous/Haumurian) age for the formation (Browne & Field, 1985; Roncaglia *et al.*, 1999).

Depositional Setting

The formation is interpreted as being deposited in a shallow-marine environment (Warren & Speden, 1978). The Claverley Sandstone records fully marine conditions, coastal progradation, and shallowing up-section with a nearby source of terrestrial debris (Roncaglia & Schiøler, 1997).

2.8 Discussion

2.8.1 Overview

A scarcity of calcareous benthic taxa and the general absence of planktic foraminifera is typical of latest Cretaceous and Paleocene sedimentary rocks of eastern New Zealand. These absences are apparently independent of the water depth in which the rocks were deposited (Moore 1988b; Schiøler *et al.*, 2010). In the absence of age-definitive foraminiferal faunas, the presence of dinoflagellates, and the finer-scale division offered by their Cretaceous biostratigraphic zonation, provide a useful tool for assigning ages to the Whangai and associated formations. Recent revisions to the dinoflagellate zonation scheme (Figure 2.37; Schiøler & Wilson, 1998; Roncaglia *et al.*, 1999; Schiøler *et al.*, 2002; Crampton *et al.*, 2004a, 2004b; Schiøler & Crampton, 2014), now enable diachronous transitions between and within formations to be resolved.

The adopted age and lithostratigraphic relationships between formations in the East Coast Basin across three transects (Figure 2.38) are presented as chronostratigraphic panels in Figures 2.39, 2.40 and 2.41. Where resolved utilising the best-available biostratigraphy, unconformities have been identified on the chronostratigraphic panels. In a number of places there is lithological evidence for unconformities or paraconformities (e.g., condensed shellbeds, coarse basal facies, manganese, siderite and phosphate nodular horizons, dolomitised or phosphatised horizons, greensands), but unconformities are often not resolved at the resolution of the biostratigraphic evidence in a particular area. These features are noted, and referred to in the sequence stratigraphic divisions presented in Chapter Seven. A number of intra-zone and intraformational unconformities are likely to be present, particularly within formations that span broad time intervals (e.g., Karekare, Glenburn, Whangai, and Wanstead formations), but are not resolved at the sampling resolution available (Crampton *et al.*, 2006).

2.8.2 Synonymy & Revised Age Control

Stratigraphic nomenclature throughout the East Coast Basin has been complicated by successive generations of geological mapping, applying individual names to sedimentary packages based on restricted locations or restricted mapping areas. Revision of the stratigraphic nomenclature across the East Coast Basin has drawn parallels between a number of similar units, as well as drawing upon recommendations and correlations of previous authors in the region. Moore (1988a) completed a detailed review of the latest Cretaceous succession throughout the East Coast Basin, which is largely adhered to here. As such, many of the synonymies identified here are in the Cretaceous succession, or arising from a recent, detailed review of the stratigraphy of the Tora-

Glenburn area (Hines *et al.*, 2013), and correlating this with the Paleogene succession elsewhere in the East Coast Basin. The Champagne Formation (Crampton *et al.*, 2004b; Rattenbury *et al.*, 2006) and the Tentpoles Conglomerate and Bluff Dump members of the Split Rock Formation identified by Reay (1980, 1993) in the middle Clarence Valley are synonymised as the Champagne Formation herein. The Ouse Siltstone Member of Ritchie (1986) and the Cold Stream Member of Reay (1993) are synonymised here as the Ouse Siltstone Member. Likewise, the Wharf Sandstone Member of Ritchie (1986) is synonymised with the Black Rock Member of Reay (1993).

The Glenburn and Tikihore Formations are considered synonymous herein, on the basis of age and lithological characteristics (Figure 2.9). Likewise, the Tapuwaeroa Formation that overlies the Tikihore Formation is considered synonymous with the Glenburn Formation in this study, as it shares a number of age, lithological and environmental characteristics with the uppermost Glenburn Formation of Piripauan to Haumurian age ("Te Mai facies" of Moore, 1980). The upper Glenburn Formation is characterised by a coarsening-upwards trend, and including distinctive cross-bedding and a high terrestrial organic carbon content (Crampton, 1997; Laird *et al.*, 2003).

The Rakauroa Member is herein considered as synonymous with the Herring, Woolshed and Conway Siltstone formations in the Marlborough region (as per, Field & Uruski *et al.*, 1997; Crampton *et al.*, 2000, 2003, 2006; Figures 2.39, 2.41). This stratigraphic interval represents a period of widespread sedimentation of siliceous, micaceous sediments into a broadly passive-margin setting. Two distinct age modes are apparent in palynological studies of the Claverley sandstone at Conway River; a late Campanian, and a late Maastrichtian age (e.g. Roncaglia *et al.*, 1999; Wilson *et al.*, 2005; Crampton *et al.*, 2006). There is little evidence for an unconformity, although there is a thin mudstone unit separating the distinct ages. Although previously not differentiated, here, the lower, older sandstone is correlative to the Whangai (Herring) Formation in deeper parts of the basin, and the upper sandstone is tentatively correlated with the Branch Sandstone of the same age. Therefore, the name Claverley Sandstone is retained for the lower, older unit, and Branch Sandstone is used to describe the substantially young, upper sandstone unit at Conway River (e.g. Morris, 1987; Reay, 1993).

In the Tora area of southeastern Wairarapa, the Manurewa and Awhea Formations represent a locally restricted submarine-fan environment (Hines *et al.*, 2013) that may correlate with the late Haumurian-aged Butt Formation in northeast Marlborough (Figure 2.41). The Manurewa Formation is equated with the initial progradation and development of the Awhea Formation submarine-fan system, that initiated with avulsion and channelisation apparent in the Manurewa Formation, and are considered here as a single, continuous complex (Figure 2.39; Hines *et al.*,

2013). Herein, the Porangahau Member (Whangai Formation) and the Manurewa and Awhea formations in the Tora area are considered synonymous, both being bathyal flysch facies that span the latest Maastrichtian *M. druggii* dinoflagellate zone (latest Cretaceous) to the early Teurian *T. evittii* zone (earliest Paleocene) and the calcareous nannofossil NP1–3 zones (Figure 2.39; Laird *et al.*, 2003; Hines *et al.*, 2013; Crouch *et al.*, 2014; Kulhanek *et al.*, 2015).

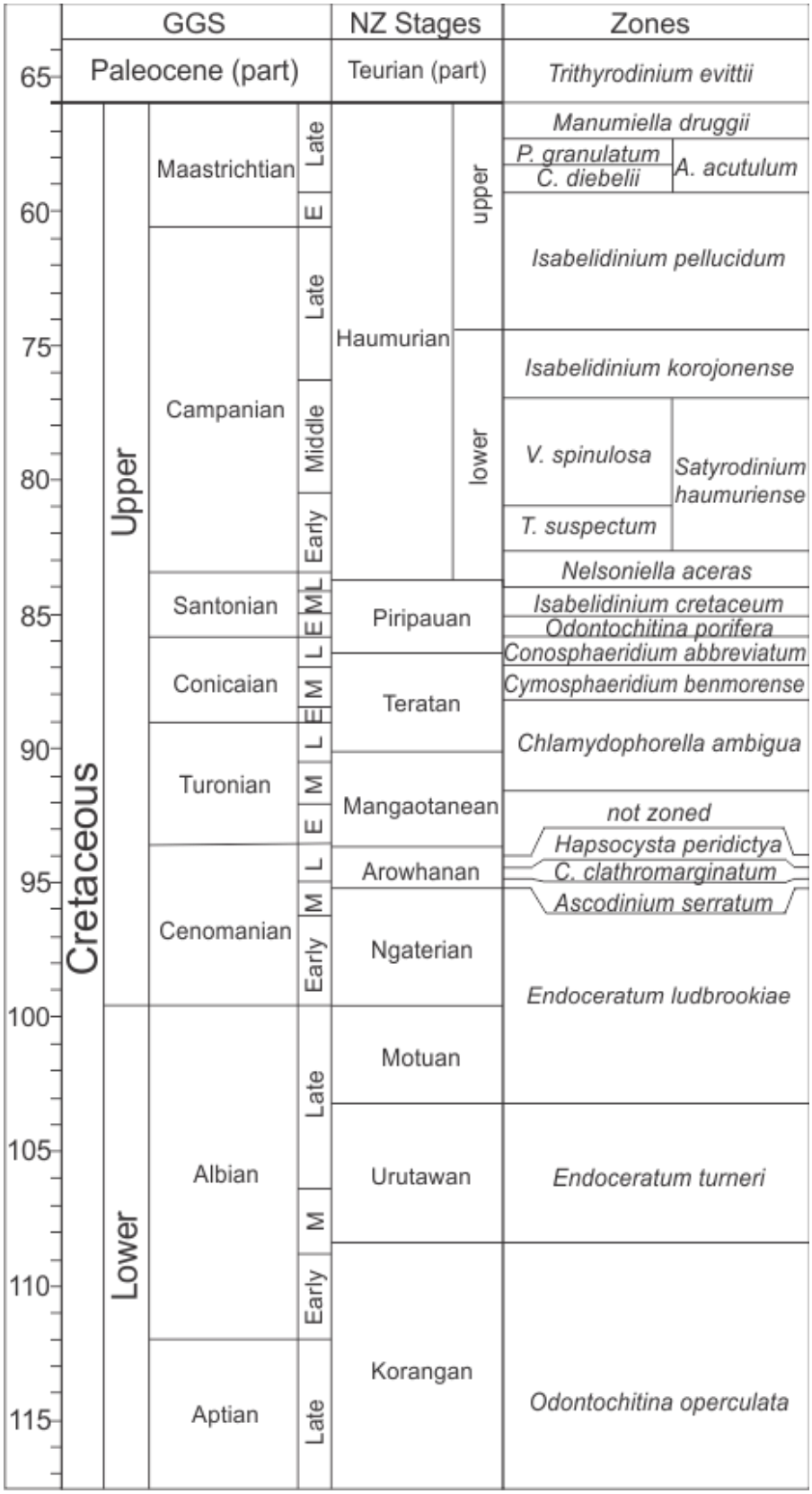

Figure 2.37: Late Cretaceous to early Paleocene international timescale from Gradstein *et al.* (2012) alongside the New Zealand geological stages (Raine *et al.*, 2015), showing the revised dinoflagellate biozones used herein (Roncaglia *et al.*, 1999; Crampton *et al.*, 2000, 2001, 2004, Schiøler et al., 2002; Schiøler & Crampton, 2014; Raine *et al.*, 2015).

This study agrees that the Mungaroa Limestone in the Tora area, and the Kaiwhata Limestone in the Glenburn area, are synonymous, as previously suggested by a number of authors (van de Hueval, 1960; Webby, 1969; Browne, 1987; Field & Uruski *et al.*, 1997; Lee & Begg, 2002; Hines *et al.*, 2013). These rocks likely represent a northward thinning and lateral extension of the Mead Hill Formation from the Marlborough region in to southern North Island (Browne, 1987; Hines *et al.*, 2013).

Immediately above the Waipawa Formation in a number of sections in the southern Hawke's Bay and southern Wairarapa, lies late Teurian, poorly-calcareous, variably glauconitic flysch at the base of the Wanstead Formation (Figure 2.39). Late Teurian flysch also occurs at Tora, associated with the deposition of the Awheaiti Formation, which has a limited thickness and a restricted distribution. The Awheaiti Formation occurs at approximately the same stratigraphic position (i.e. late Teurian, above the Waipawa Formation), leading to the interpretation that this unit may represent the basal facies of the Wanstead Formation. Immediately overlying the Awheati Formation is the mud-rich facies of the Pukemuri Siltstone, (and Huatokitoki Formation further north) in the Tora-Glenburn area of southeast Wairarapa, that are generally included in the broadly defined Wanstead Formation (Figure 2.39; Field & Uruski *et al.* 1997; Lee & Begg, 2002; Begg & Johnston, 2000; Hines *et al.*, 2013). The Wanstead Formation spans late Paleocene to late Eocene time, and incorporates a wide range of lithofacies such as non-calcareous mudstone, smectitic marl, and flysch. The Pukemuri Siltstone at Tora is considered here to be a coarser, syn-sedimentary slump-affected facies of the Wanstead Formation. In places there are significant intra-formational unconformities within the Wanstead Formation and correlatives. For example, Waipawan and Porangan-aged strata are largely removed from the Tora area (Figure 2.41; Hines *et al.*, 2013). Likewise at Pahaoa River mouth (coastal southeast Wairarapa) is lies within calcareous nanofossil zone NP9 (Kulhanek *et al.*, 2015).These unconformities are discussed in detail in the sequence stratigraphy chapter (Chapter Seven).

2.8.3 Implications of Revised Age Control

Reassessment of the New Zealand Late Cretaceous timescale and particularly dinoflagellate zonation (Roncaglia *et al.*, 1999; Crampton *et al.*, 2000, 2001, 2004) has allowed this study to provide a higher-resolution assessment of the diachroneity at the base of the Rakauroa Member (Whangai Formation). Application of the revised dinoflagellate zonation demonstrates that the base of the

Rakauroa Member is strongly diachronous across the basin, ranging from early Campanian to Maastrichtian (NZ Haumurian Stage; ~82 Ma to ~70 Ma, Figure 2.39). The base of the Whangai Formation often demonstrates an unconformable surface, marked by nodular horizons (e.g. Owhena Stream, Nidd Stream), thick sandstone beds (e.g., Angora Stream, Packtrack Stream; Francis, 2001; Crampton *et al.*, 2006), or conglomerate beds (Mangaotane Stream, Glenburn area; Moore, 1980, 1988a; Schiøler *et al.*, 2001). Similarly, the base of the Conway Siltstone is diachronous between Haumuri Bluff and Waipara River (Roncaglia *et al.*, 1999).

The geographical distribution of the Porangahau Member is partitioned by, and overlain by the background sedimentary processes represented by the Upper Calcareous Member (Whangai Formation), suggesting the Porangahau Member represents a series of discrete fans. The basal progradation of the Porangahau Member fan systems occur during the lower *M. druggii* zone (Laird *et al.*, 2003; FRED), coincident with the deposition of the Branch Sandstone between the Whangai ("Herring") and Mead Hill formations in Marlborough (Figure 2.41). This has sequence stratigraphic implications discussed in Chapter Seven (Sequence Stratigraphy).

Deposition of the Mungaroa Limestone occurred in the Paleocene between calcareous nannofossil zones NP3–4 and NP6 (Figure 2.39; Hines *et al.*, 2013; Kulhanek *et al.*, 2015), occupying the same temporal range as the Upper Calcareous Member in sections where it overlies the Porangahau Member (e.g., Angora Stream, southern Hawke's Bay; Crouch *et al.*, 2014; Kulhanek *et al.*, 2015; Figure 2.39). The implication is that eastern areas of the basin are marked by deposition of calcareous sediments between NP3–4 and the NP6, suggesting an increase in carbonate productivity or a decrease in terrigenous sedimentation. This is consistent with the composition of lower parts of the Te Uri Member in the Whangai Range, which are characterised by glauconitic sandstones and mudstones between NP4–5 (Figure 2.40; Leckie *et al.*, 1992; Rogers *et al.*, 2001; Kulhanek *et al.*, 2015), indicative of reduced terrigenous sedimentation. The late Paleocene Waipawa Formation marks a distinct transition from the siliceous and weakly calcareous facies of the Whangai Formation to the more calcareous mudstones typical of the Wanstead Formation. A similar transition is observed in Marlborough, where the strongly siliceous facies of the Mead Hill Formation grades into the pure micrites and marls of the Amuri Limestone. The age of the Waipawa Formation, and by definition the above-mentioned lithofacies transition, has been refined to 58.7–59.4 Ma (Hollis *et al.*, 2014).

The 6–10 million year extent of Cretaceous–Paleogene erosion at the base of the Amuri Limestone, marked by the distinctive Teredo Limestone Member (Amuri Formation; Figure 2.41) can be determined with the aid of refined dinoflagellate biostratigraphy for the Haumurian

(Roncaglia *et al.* 1999; Crampton *et al.*, 2000 Schiøler *et al.*, 2002), and detailed biostratigraphy across the Muzzle Group (Strong *et al.*, 1995; Hancock *et al.*, 2003; Hollis *et al.*, 2003a, 2005a, 2005b, 2014; Dallanave *et al.*, 2015).

In the Whangai Range (southern Hawke's Bay) and Mangatu (Raukumara Peninsula) areas, the boundary between the Wanstead and Weber formations is generally marked by a basal greensand facies of Bortonian to Kaiatan age (Kenny, 1984, 1986; Leckie *et al.*, 1992; Field & Uruski *et al.*, 1997; Morgans, 2016; Clowes, *in prep.*). This interval corresponds to peak paleodepths in the Wanstead Formation during the Bortonian (Hines *et al.*, 2013). The latest Eocene to early Oligocene represents peak transgression and maximum flooding of the New Zealand region (Black, 1980; Field & Uruski *et al.*, 1997; King, 2000b; Landis *et al.*, 2008).

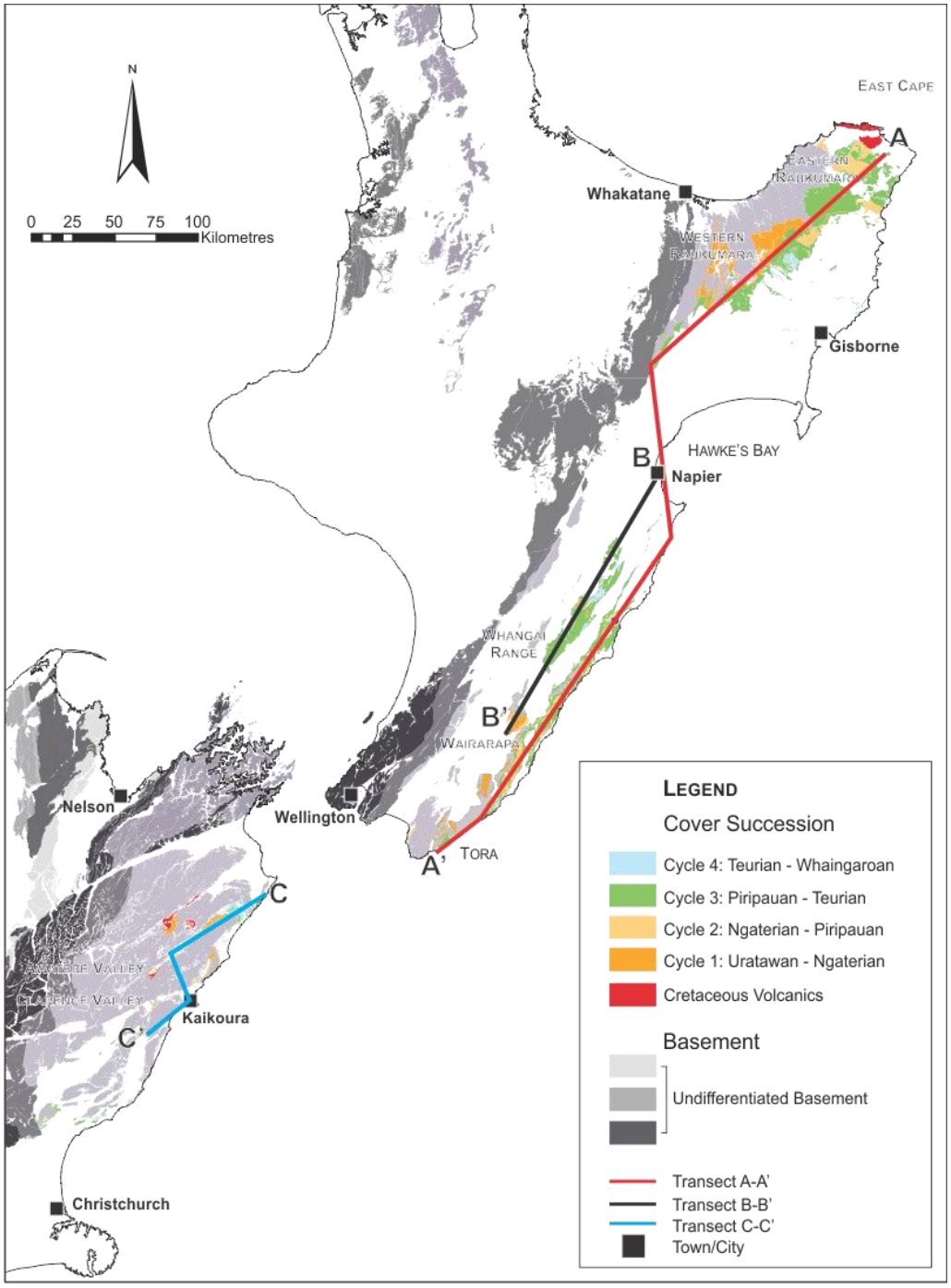

Figure 2.38: Transects for chronostratigraphic panels in Figures 2.39, 2.40 and 2.41.

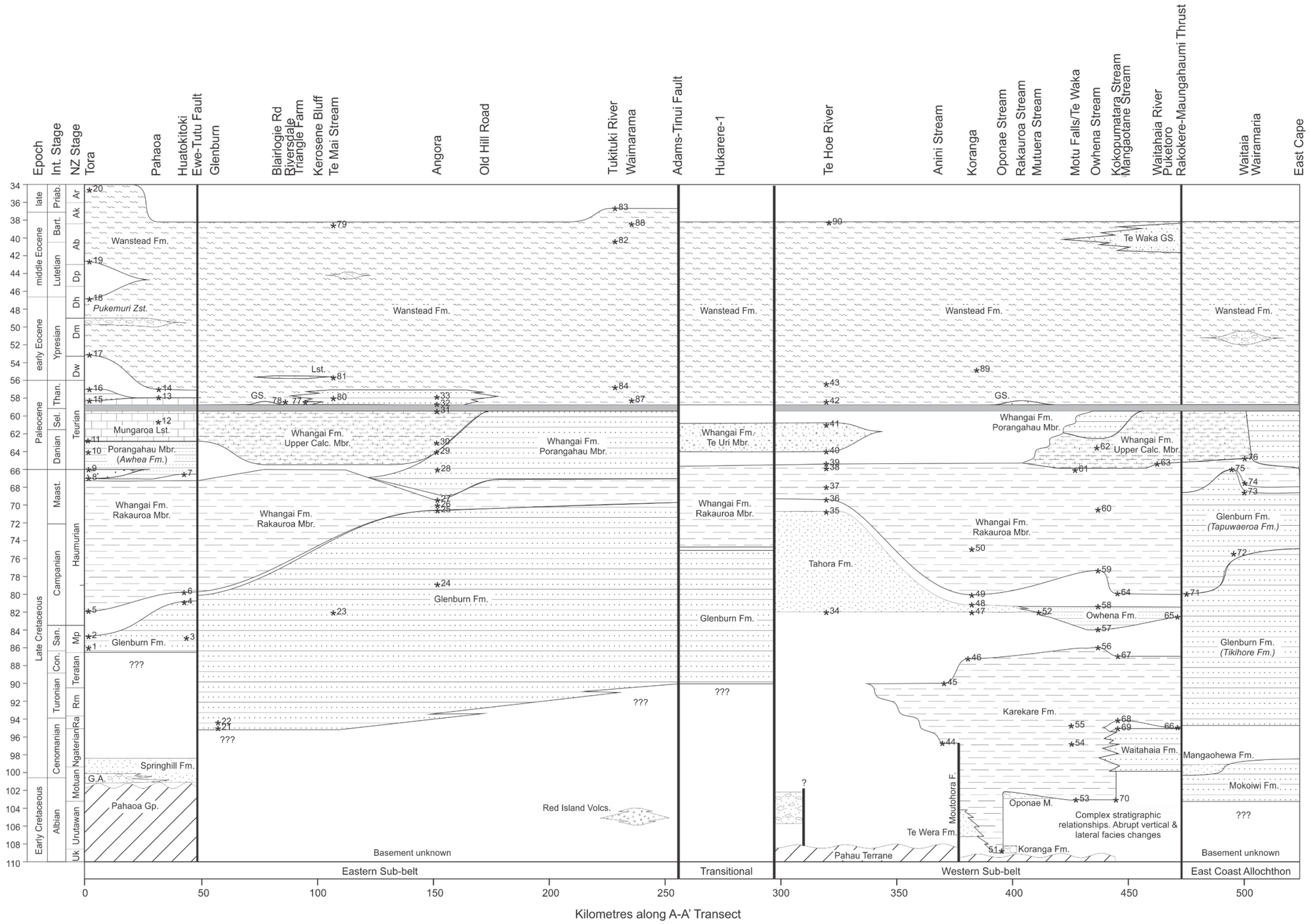

Figure 2.39: Chronostratigraphic panel for the North Island East Coast Basin transect A-A' (Figure 2.38). Italicised names refer to synonymised formations (see discussion in text). Asterisked numbers refer to the complied revised age control in Appendix 1. Hukarere-1 data sourced from Westech Energy New Zealand Ltd (2001).

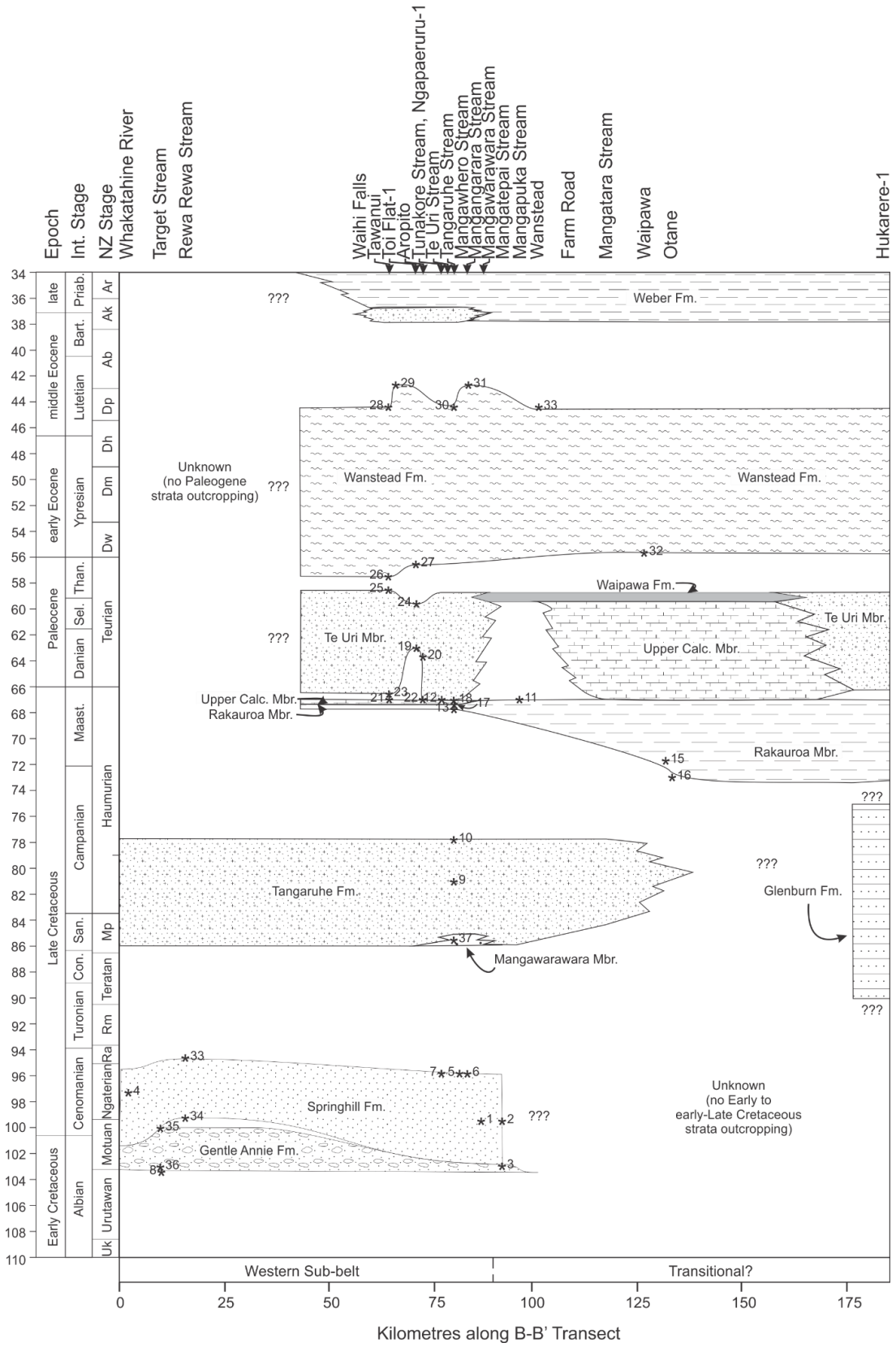

Figure 2.40: Chronostratigraphic panel for the Whangai Range area, transect B-B' (Figure 2.38). Italicised names refer to synonymised formations (see discussion in text). Asterisked numbers refer to the complied revised age control in Appendix 1. Hukarere-1 data from Westech Energy New Zealand Ltd (2001).

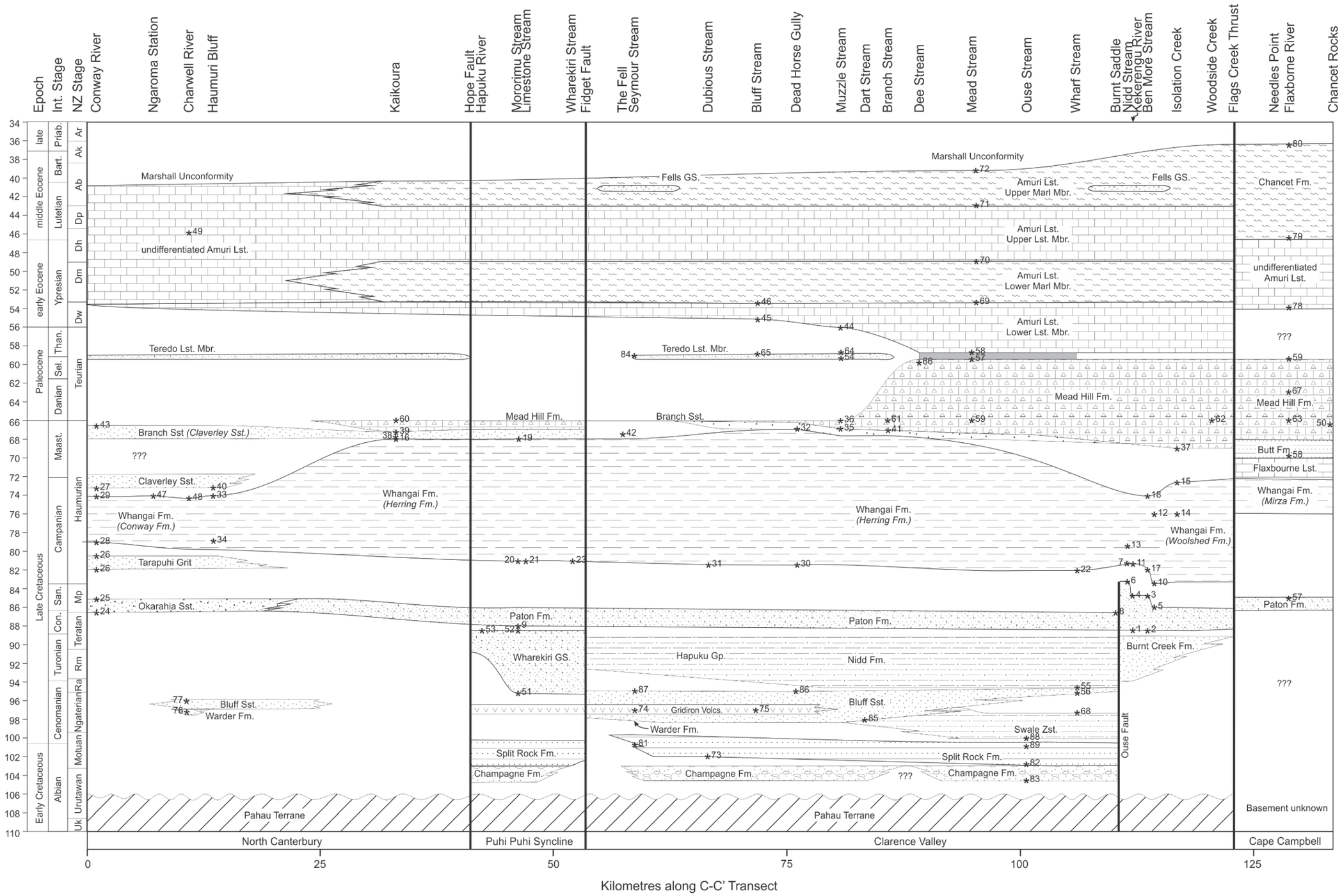

Figure 2.41: Chronostratigraphic panel for the Marlborough area, transect C-C' (Figure 2.38). Italicised names refer to synonymised formations (see discussion in text). Asterisked numbers refer to the complied revised age control in Appendix 1.

2.8.4 Stratigraphic Variation between the Eastern & Western Sub-belts

Early to mid-Cretaceous formations in the East Cape and Marlborough areas occur in disparate outcrops that demonstrate abrupt vertical and lateral facies transitions, attributed to local deposition in restricted, tectonically controlled basins (Field & Uruski *et al.*, 1997; Laird & Bradshaw, 2004). The stratigraphy of the East Coast Basin, particularly the Late Cretaceous stratigraphy, has historically been divided into two characteristic motifs that occur in two fault-bounded, elongate, northeast–southwest-oriented domains named the Eastern Sub-belt and Western Sub-belt (Moore, 1988a; Crampton, 1997; Crampton *et al.*, 2006). The division into the Eastern and Western sub-belts was based on notable changes in lithofacies and stratigraphic relationships in the Late Cretaceous–Paleogene succession, as well as the distribution of Cretaceous volcanic units (Moore *et al.*, 1986; Moore, 1988b). Conventionally, the Eastern Sub-belt is considered to comprise sedimentary strata of the East Coast Allochthon and strata east of the Adams-Tinui Fault, whereas the Western Sub-belt comprised autochthonous sedimentary rocks in western Raukumara and west of the Adams-Tinui Fault (Moore 1988b). Marlborough has conventionally been considered part of the Western Sub-belt (Crampton, 1997; Field & Uruski *et al.*, 1997; Crampton *et al.*, 2003), based largely on lithological affinities between the Karekare, Springhill, and Swale Siltstone formations of Late Cretaceous age. However, within the Paleogene succession, rocks of the Eastern Sub-belt, particularly those in southern Wairarapa, share the greatest lithological affinities between the Mead Hill Formation and the Mungaroa Limestone and the Awhea and Butt formations.

The identification of both the Glenburn Formation and Te Uri Member (Whangai Formation) in Hukarere-1 (Figures 2.39, 2.40; Westech Energy New Zealand Ltd, 2001), a petroleum exploration drillhole located at Port of Napier, has indicated a previously unresolved transition between the Eastern and Western sub-belts. Traditionally, the Te Uri Member is a key defining unit of the Western Sub-belt (e.g., Moore, 1988a), whereas the Glenburn Formation is considered restricted to the Eastern Sub-belt (e.g., Crampton, 1997). Other formations and members, such as the Rakauroa and Upper Calcareous Members (Whangai Formation), and the Waipawa and Wanstead formations extend across both sub-belts, with little apparent lithological differentiation or change.

There is a pronounced contrast between the approximately coeval Ngaterian Springhill and Glenburn formations across the western and eastern sub-belts. The Springhill and Glenburn formations likely record deposition in shelf and slope setting, respectively, and the juxtaposition of these formations across sub-belt boundaries may arise from some degree of Neogene shortening. This transition is better preserved in the western sub-belt in western Raukumara, where

the transition between shelf to slope settings is more intact, coherent and stratigraphic relationships are better preserved, with shelfal mudstones of the Karekare Formation interfingering with the flysch facies of the Waitahaia Formation (Mazengarb & Harris, 1994; Mazengarb & Speden, 2000; Crampton *et al.*, 2001)

Some of the strongest stratigraphic basis for the division of the Eastern and Western sub-belts in the Hawke's Bay-Wairarapa regions are the differentiation of the Tangaruhe Formation, Cretaceous Upper Calcareous Member and the Paleocene Te Uri Member (Whangai Formation), all of which are largely restricted to the Whangai Range area (Figure 2.40). The Upper Calcareous Member is diachronous across its east–west extent, being Late Cretaceous (Haumurian) in the west, and Paleocene (early Teurian) in the east of the basin (Figures 2.39, 2.40), under the prevailing stratigraphic framework for the Whangai Formation established by Moore (1988a). Assessment of regional stratigraphic relationships and unconformable surfaces in this study, along with a review of existing data, suggest that this is simply a sedimentary response to facies variations, rather than diachronous deposition across the basin. Cretaceous-aged Upper Calcareous Member within the Western Sub-belt only occurs in the Whangai Range. Elsewhere, including the Western Sub-belt, the Upper Calcareous Member is of Paleocene age (e.g., at the Waipawa Standard section, Puketoro; Kenny, 1986; Moore 1988a). This contrast may explain differences in the carbonate content of the Upper Calcareous Member across the basin; the Cretaceous Upper Calcareous Member in the Whangai Range has notably lower carbonate content (<3%; Moore, 1988a), compared to the Paleocene Upper Calcareous Member (10–20% carbonate; Moore, 1988a). Where the Paleocene Upper Calcareous Member is not present, the stratigraphic interval is instead represented by the Te Uri Member, or in sections where the Waipawa Formation immediately overlies the Rakauroa Member, there is often several metres of greensand that likely corresponds to the Te Uri Member, such as at Te Hoe River (northwest Hawke's Bay), and Mangawarawara and Otane streams (central Hawke's Bay), or an unconformity between the Rakauroa Member and the Waipawa Formation (e.g., Rakauroa Stream (Raukumara Peninsula); Moore, 1988a; 1989a).

The likely interpretation to explain the above stratigraphic relationships is that, in North Island, the Sub-belt boundary represents a zone of likely Neogene shortening, resulting in the juxtaposition of dominantly shallow-marine (Western Sub-belt) with deeper-marine (Eastern Sub-belt) strata. This is certainly the case across the Raukorere Thrust, where there has been tens to hundreds of kilometres of shortening across the basal decollement of the East Coast Allochthon (Rait *et al.*, 1991; Mazengarb & Speden, 2000; Cluzel *et al.*, 2010). The Marlborough region similarly shows series of transitions from shallow- to deep-marine strata, consequently displaying affinities with rocks of the Eastern and Western Sub-belts in the North Island East Coast Basin. In the

Hawke's Bay-Wairarapa regions, there is minimal evidence for dextral displacement between the Sub-belts, implying little disruption of paleogeographic or depositional relationships from west to east (Crampton *et al.*, 2006). Irrespective of this, a working chronostratigraphic framework (Figures 2.39, 2.40, & 2.41) and sequence stratigraphy can be developed and applied without the strict application of Sub-belt divisions (see Chapter Seven; sequence stratigraphy).

Page intentionally left blank for formatting purposes

Chapter Three

OCEAN REDOX CONDITIONS OF THE SOUTHWEST PACIFIC DURING THE LATE PALEOCENE

"Today I resolved to discuss with the neighbour the subject of the boundary fence. Result: fisticuffs!"

–Taylor White, Christmas Day, 1912. Paraphrased excerpt from Taylor White's diary, after whom the Taylor White section is named. Quotation courtesy of Hugh Morgans.

Sample transect through the Waipawa Formation at Taylor White, Angora Road, Wimbledon.

PREFACE TO CHAPTER THREE

The Waipawa Formation forms an important, isochronous surface across the East Coast Basin, and the wider Southwest Pacific, allowing direct correlation of the sequences across the various facies associations of the East Coast Basin, as well as forming a distinctly recognisable, pre-Neogene timeplane across the basin, which has utility in tectonic reconstructions.

Despite significant interest as a petroleum source rock, the depositional conditions of the formation have been widely debated. In particular, the application of a chemostratigraphic and sequence stratigraphic interpretation across the Waipawa interval has required a multi-disciplinary study to assess the deposition conditions of the Waipawa Formation and correlatives within, and beyond, the East Coast Basin, presented here. Chapter Three acts as a detailed case study through the Whangai, Waipawa Formations in six specific sections. This chapter expands beyond these sections, focussing primarily on changes in the Waipawa Formation across the various facies associations in the East Coast Basin.

This chapter has been prepared in manuscript format for submission to the journal *Chemical Geology*, and as such, follows formatting and structural conventions in line with the submission requirements of this journal. The development of this manuscript has been a collaborative process, with the contribution of the co-authors outlined below:

- *Ben Hines* – Measured sections, sample collection and preparation, bulk rock portable XRF analyses, data interpretation manuscript preparation.
- *Michael Gazley* – Provision of portable XRF instrumentation and standards.
- *Todd Ventura* – Source Rock Analyses.
- *Katie Collins* – Editorial process, statistical analyses.
- *Kyle Bland* – Project supervision, editorial process, funding for analyses.
- *James Crampton* – Project supervision, editorial process.

Chapter Three

OCEAN REDOX CONDITIONS OF THE SOUTHWEST PACIFIC DURING THE LATE PALEOCENE

Submitted to:

Chemical Geology

Corresponding author:
Benjamin R. Hines
Victoria University of Wellington, PO Box 600, Wellington, New Zealand
Email: ben.hines@vuw.ac.nz
Phone: +64 27 3056576

Co-authors:
Michael F. Gazley
CSIRO Mineral Resources, ARRC, PO Box 1130, Bentley 6102, Western Australia, Australia, and
Victoria University of Wellington, PO Box 600, Wellington, New Zealand
Email: michael.gazley@csiro.au

G. Todd Ventura
GNS Science, PO Box 30-368, Lower Hutt, New Zealand, and
St. Mary's University, B3H3C3, Halifax, Nova Scotia
Email: todd.ventura@smu.ca

Katie S. Collins
Victoria University of Wellington, PO Box 600, Wellington, New Zealand, and
Department of Geophysical Sciences, 5734 South Ellis Avenue University of Chicago, Chicago, Illinois 60637
Email: katiesusannacollins@gmail.com

Kyle J. Bland
GNS Science, PO Box 30-368, Lower Hutt, New Zealand
Email: k.bland@gns.cri.nz

James S. Crampton
GNS Science, PO Box 30-368, Lower Hutt, New Zealand, and
Victoria University of Wellington, PO Box 600, Wellington, New Zealand
Email: j.crampton@gns.cri.nz

Abstract

The depositional mechanism for late Paleocene, organic-rich, $\delta^{13}C_{org}$-enriched shales across the Southwest Pacific is poorly understood. Using a multi-proxy and high resolution chemostratigraphic approach, we assess paleoceanographic conditions, including paleo-redox states and productivity during the Late Cretaceous to Paleocene in the East Coast Basin, eastern North Island, New Zealand. Our new data provide insights into the depositional conditions and the petroleum potential of prospective source rocks in this basin.

Paleogene strata in the basin are dominated by a thick, largely homogenous succession of siliceous to moderately calcareous mudstone (Whangai and Wanstead formations). These formations are separated stratigraphically by the organic-rich Waipawa Formation, which was deposited under dysoxic to anoxic conditions during a period of sea level regression. Six key sections have been sampled, and a large number of hand samples were analysed by portable X-ray fluorescence for multi-element geochemistry (n = 372) and bulk pyrolysis (n = 220). These data enable correlation across the basin, and principal components analysis (PCA) and Bayesian mixture-modelling cluster analysis reveal vertical and lateral variations in chemical compositions. Redox-susceptible trace metals (e.g. U, Mo, V) and indices based on elemental ratios (e.g., Th/U, V/Sc, Ni/Co) are also measured to assess paleo-redox conditions.

Elemental indices show no significant change in detrital source from the Whangai to Wanstead formations, and an increase in sedimentation rate during deposition of the Waipawa Formation. We show that the organic-rich Waipawa Formation, of late Paleocene age, was deposited under dysoxic to anoxic conditions, likely associated with sea-level fall and regression. We infer that regression in the late Paleocene resulted in erosion on the shelf and/or sediment bypassing into deeper water, and increased delivery of nutrients and terrestrial organic matter to the site of Waipawa Formation deposition. This in turn caused a modest increase in marine productivity, which resulted in an expansion of an oxygen minimum zone, enhanced preservation and delivery of organic matter to the sea floor, and subsequent burial and preservation of organic matter within anoxic sediments.

Keywords: East Coast Basin; paleo-redox; Waipawa Formation; portable X-ray fluorescence (pXRF); principal components analysis (PCA); chemostratigraphy

3.1 Introduction

The Late Paleocene Southwest Pacific oceanographic-climate system is not well understood. During this time, a relatively short-lived event (*ca.* 0.7 Myr) resulted in the widespread deposition of organic-rich mudstones across many sedimentary basins around New Zealand, and reaching as far west as the Tasmanian shelf (Figure 3.1; Hollis *et al.*, 2014). The drawdown of organic carbon over such a broad area must have resulted from a notable perturbation of the ocean-climate system that has not left any known definitive imprint in global carbon isotope records. Integrated organic and inorganic geochemical approaches have the ability to refine our knowledge of the depositional environment and paleoceanographic changes that resulted in the abrupt, widespread preservation of organic carbon across the Southwest Pacific.

The Late Cretaceous to Paleogene succession of the East Coast Basin, North Island, New Zealand (Figure 3.1), contains the most extensive, and richest onshore outcrops of organic-rich mudstones in the Southwest Pacific. This provides a unique opportunity to study the depositional conditions in detail. Thick, siliceous to slightly-calcareous hemipelagic mudstones of Late Cretaceous–Paleogene age (Whangai Formation, ~600 m thick (~82 – 59 Ma), and Wanstead Formation ~500–600 m thick (57 – 37 Ma)) are separated stratigraphically by the relatively thin (~1.5 – 70 m thick; typically <30 m), organic-rich mudstone of the Waipawa Formation (59.4 – 58.7 Ma; Moore, 1988a, 1989a; Field & Uruski *et al.*, 1997; Hollis *et al.*, 2014).

The Waipawa Formation has been studied extensively, particularly in regard to its petroleum source rock potential (e.g. Moore, 1988a, 1989a; Field & Uruski *et al.*, 1997; Killops *et al.*, 1997, 2000; Hollis & Manzano-Kareah, 2005; Schiøler *et al.*, 2010), and also due to its significance for understanding global drivers for ancient environmental and climatic changes (e.g. Leckie *et al.*, 1995; Hollis *et al.*, 2005a, 2014). Although the Waipawa Formation is thermally immature in outcrop, over 300 oil and gas seeps have been recorded within the East Coast Basin (Field & Uruski *et al.*, 1997; Hollis & Manzano-Kareah, 2005; and references therein). Oil – source rock correlation studies based on organic $\delta^{13}C$ and $\delta^{34}S$ isotopic systems, as well as biomarker abundances, indicate that the formation, at least in part, is the likely source of some of these petroleum seeps, especially in the Southern Hawke's Bay-Wairarapa regions (Moore *et al.*, 1987; Moore 1988a; Rogers *et al.*, 1999, 2001; Schiøler *et al.*, 2010; Sykes *et al.*, 2012).

It has been argued that the Waipawa Formation represents dysoxic to anoxic seafloor conditions, on the basis of increased total organic carbon (TOC) preservation (0.5 – 13 % TOC), in comparison to the immediately-underlying Whangai Formation (<1.5 % TOC), as well as poor-to-absent foraminiferal and macrofaunas, and outcrop appearance (Moore, 1988a; Killops *et al.*,

2000; Rogers *et al.*, 2001; Hollis & Manzno-Kareah, 2005; Hollis *et al.*, 2014). The organic geochemistry of the Waipawa Formation and its correlative units have been addressed by Moore *et al.* (1987), Moore (1988a), Leckie *et al.* (1992, 1995), Killops *et al.* (1996, 1997, 2000), Rogers *et al.* (1999, 2001), Hollis and Manzano-Kareah (2005), Schiøler *et al.* (2010), and Hollis *et al.* (2005a, 2005b, 2014). However, despite this body of literature, bulk rock and trace element geochemical analyses and the application of widely applied paleo-redox proxies to our knowledge have not been reported and, as such, previous interpretations of the Waipawa Formation have not incorporated these important sources of information. These proxies are studied here across six stratigraphic sections (Figure 3.2) in order to provide a rigorous assessment of paleoenvironmental and paleoceanographic conditions.

The high sample throughput potential of portable X-ray fluorescence (pXRF) technology allows for high spatial and stratigraphic resolution sampling and, thus, detailed examination of geochemical and associated paleoenvironmental changes within depositional systems. The development of pXRF technology allows for the rapid collection of large datasets, and has become a widely accepted tool for data collection in diverse geological settings (e.g. Gazley *et al.*, 2011, 2015; Rowe *et al.*, 2012; Dahl *et al.*, 2013; Durance *et al.*, 2014; Piercey & Devine, 2014; Ross *et al.*, 2014; Simandl *et al.*, 2014). The application of rigorous quality assurance and quality control (QA/QC) protocols to pXRF workflows to produce reliable and robust datasets for quantitative applications means that data collected via pXRF analyses compare favourably with conventional laboratory analyses (Fisher *et al.*, 2014; Gazley & Fisher, 2014). By integrating organic and inorganic geochemical approaches we present a refined depositional model and report how Late Paleocene paleoceanographic changes resulted in the abrupt, widespread preservation of organic carbon across the Southwest Pacific.

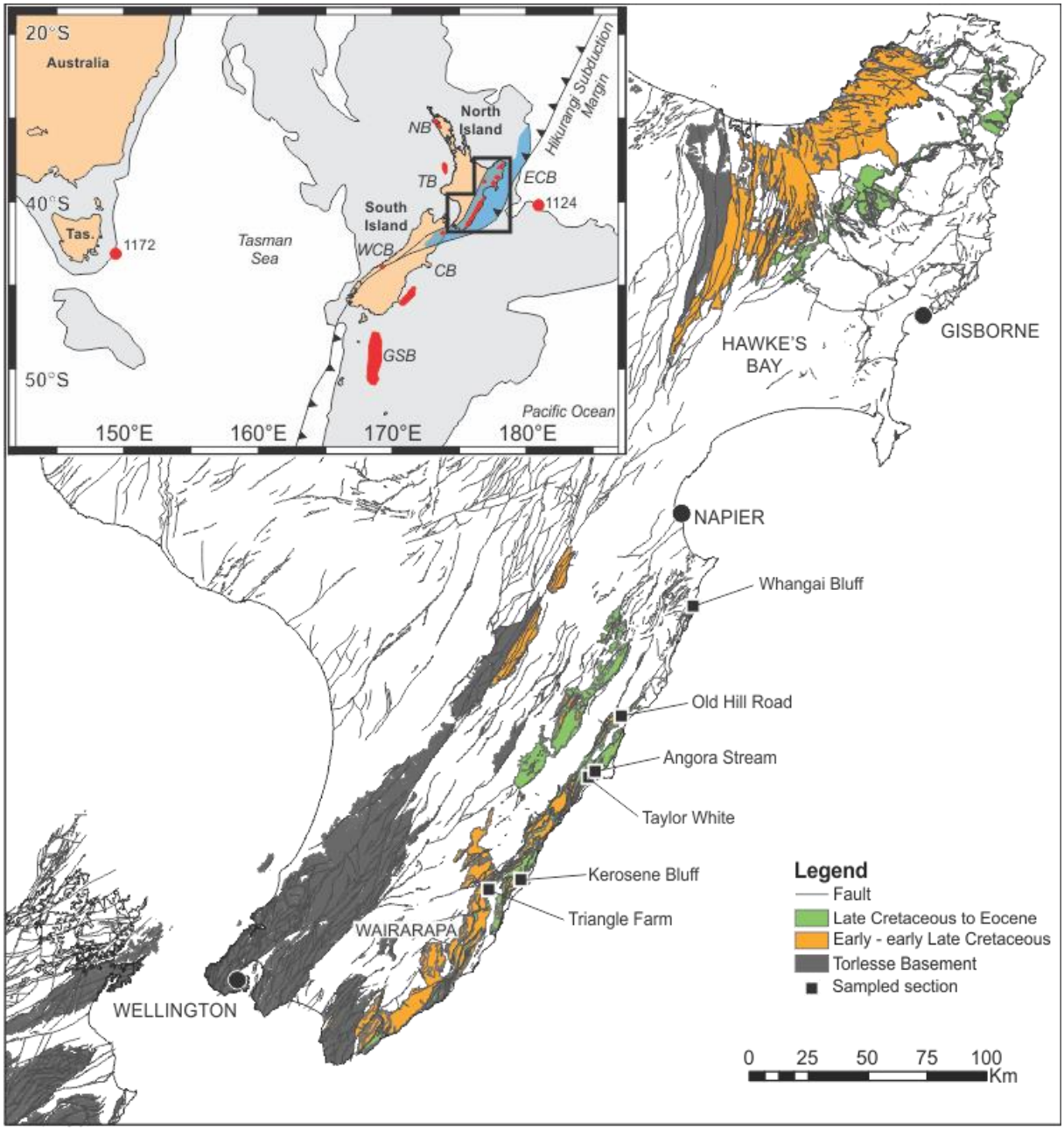

Figure 3.1: Location of sections sampled for this study within the East Coast Basin, North Island, New Zealand. Inset: East Coast Basin shown in blue, with the distribution of the Waipawa Formation and correlatives in the Southwest Pacific depicted red shaded areas. Guide to abbreviations; Tas. – Tasmania; ECB - East Coast Basin; CB - Canterbury Basin; GSB – Great South Basin; WCB – West Coast Basin; TB – Taranaki Basin; NB – Northland Basin. 1172 – ODP Site 1172; 1124 – ODP Site 1124. Geological map data are derived from the QMap 1:250 000 seamless dataset (Heron, 2014).

3.2 Geological Setting

3.2.1 Regional Stratigraphy

There is a general fining-upward trend within the Late Cretaceous-Paleogene stratigraphic succession of the East Coast Basin. This represents infilling of one, or more, trench-slope basins following the cessation of Mesozoic subduction, which was followed by thermal subsidence and passive margin sedimentation through the Late Cretaceous and Paleogene (Moore, 1988b; Field & Uruski *et al.*, 1997). This first-order depositional sequence was interrupted by the inception of the modern Hikurangi subduction margin in the Late Oligocene to Early Miocene. The western edge of the basin has since been uplifted and exposed as a forearc basin-accretionary wedge complex during Neogene deformation, providing exposures of the Late Cretaceous to Paleocene strata examined in this study.

The Late Cretaceous–Paleocene succession of eastern North Island is represented, in order of decreasing age, by the Whangai, Waipawa and Wanstead formations, which share the same broad spatial distributions (Moore, 1988a; 1989a; Field & Uruski *et al.*, 1997; Lee & Begg, 2002, Lee *et al.*, 2011). The Late Cretaceous to Paleocene Whangai Formation forms a widespread, thick (~600 m), fine-grained, siliciclastic unit, with correlatives identified in New Caledonia, DSDP Site 207 and DSDP Site 275, Northland, Marlborough (as the Herring and Woolshed Formations), and the Canterbury Basin (as the Conway Formation) (Crampton, 1988; Moore, 1988a; Laird, 1992; Field & Uruski *et al.*, 1997; Maurizot, 2011). Although it is rather homogeneous, the Whangai Formation is divided into several members across its lateral and vertical extent in the East Coast Basin; the Rakauroa, Upper Calcareous, Porangahau and Te Uri members (Figure 3.2; Moore *et al.*, 1986; Moore 1988b; Field & Uruski *et al.*, 1997). Likewise, the Waipawa Formation is an extensive unit, identified in Marlborough, as well as the Northland and Taranaki basins, with the correlative Tartan Formation in the Canterbury and Great South basins (Killops *et al.*, 1997; 2000; Schiøler *et al.*, 2010; Hollis *et al.*, 2014). In the East Coast Basin the Waipawa Formation is laterally equivalent to the Te Uri Member of the Whangai Formation (Figure 3.2; Rogers *et al.*, 2001), and both are typically underlain by either the Upper Calcareous or the Porangahau members of the Whangai Formation, and each, in turn, is overlain by calcareous and smectitic mudstones of the Wanstead Formation (Figure 3.2).

The Waipawa Formation has been defined from onshore outcrops in eastern North Island, where it typically comprises poorly-bedded, dark-brown to grey to brownish-black carbonaceous mudstone with moderate to high TOC (0.5–13%), (Moore, 1988a; 1989a). However, the definition

of the Waipawa Formation has been extended to include dark-grey, siliceous, organic-rich mudstones in Marlborough (Hollis *et al.*, 2005a, 2005b), and Northland, New Zealand (Isaac *et al.*, 1994; Hollis *et al.*, 2006), and dark-coloured mudstones of Paleocene age encountered in offshore petroleum wells in the Northland, northern Taranaki, and Canterbury-Great South basins, as well as beneath the East Tasman Rise (ODP site 1172; Figure 3.1). All of these occurrences of Waipawa Formation-like rocks have been recently referred to collectively as the "Waipawa Organofacies" (Figure 3.1; Schiøler *et al.*, 2010; Hollis *et al.*, 2014). Existing biostratigraphic data suggest that deposition of the Waipawa Organofacies in the East Coast Basin occurred in the upper part of NZP5 Dinoflagellate Zone and calcareous nannofossil zones NP5–NP7, indicating a Selandian to Thanetian age (late Paleocene; Crouch, 2001; Kulhanek *et al.*, 2015), and likely restricted to 59.4 – 58.7 Ma (Hollis *et al.*, 2014).

The Upper Calcareous and Porangahau members of the Whangai Formation were deposited at upper to middle bathyal depths (400–1000 m) (Wilson *et al.*, 1989; Leckie *et al.,* 1995), and is interpreted as being deposited during a transgression (Hollis *et al.*, 2014). Paleodepth indicators for the Waipawa Formation are sparse and poorly constrained, but generally indicate an upper bathyal depositional setting. Pervious workers have described a 'double pulse' of organic matter in the Waipawa Formation, where two noticeable peaks in TOC enrichment are apparent in the formation (Leckie *et al.*, 1995; Killops *et al.*, 2000; Hollis *et al.*, 2014). Increased concentrations of TOC (Moore, 1989a; Leckie *et al.*, 1995; Killops *et al.*, 2000), S, and trace metals (in particular Mo and U) in the Waipawa Formation has previously been suggested to indicate reducing conditions during deposition (Hollis *et al.*, 2014). Killops *et al.* (2000) suggested the Waipawa Formation represented prolonged upwelling of a warm, saline, nutrient-rich but oxygen-depleted bottom-water mass during the Late Paleocene. However, this interpretation is difficult to reconcile with the coeval deposition of the Waipawa Organofacies in multiple sedimentary basins in the Southwest Pacific Ocean and western Tasman Sea. Leckie *et al.* (1995) interpreted the Waipawa Formation as being deposited during a marine transgression, although more recently, Hollis *et al.* (2014) proposed that the deposition of the Waipawa Formation occurred in response to a two-phase regression in eustatic sea level, associated with an influx of terrestrial organic matter, and high marine productivity.

The Wanstead Formation is considered to be the deepest depositional environment in the Late Cretaceous-Paleogene East Coast Basin, with foraminiferal paleodepth indicators suggesting mid-bathyal depths (Moore & Morgans, 1987; Field & Uruski *et al.*, 1997). The typically clay-rich, and

pervasively bioturbated fabric suggest that the formation was deposited at low sedimentation rates at the peak of a marine transgression (Field & Uruski *et al.*, 1997).

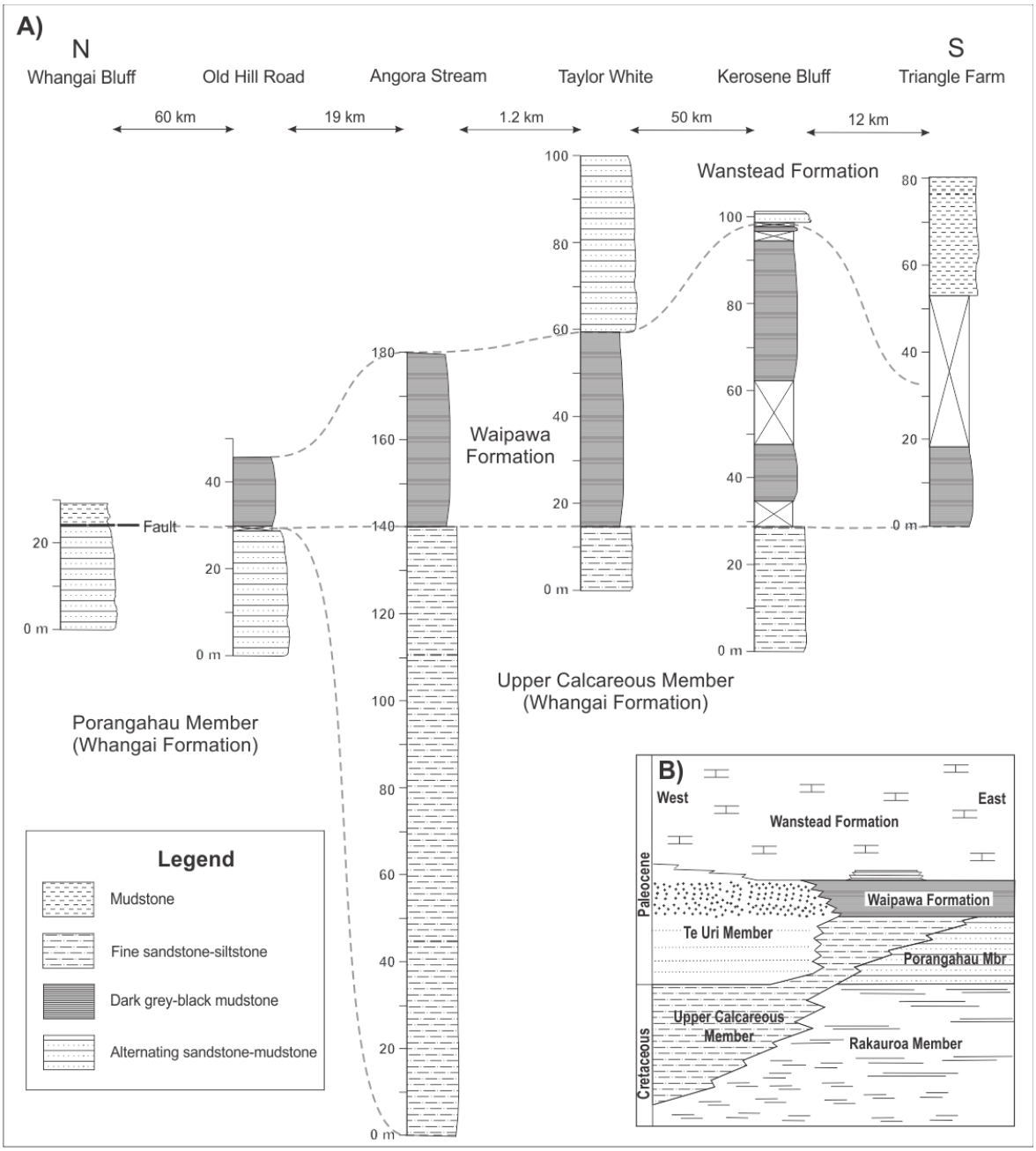

Figure 3.2: A) Stratigraphic relationships between the sections examined in this study (see Figure 3.1 for location of studied sections). Dashed lines indicate formation boundaries. B) Late Cretaceous to Paleocene chronostratigraphic relationships between members of the Whangai Formation and the Waipawa and Wanstead Formations in the East Coast Basin.

3.3 Paleo-redox Conditions

The accumulation of organic-rich sediments such as the Waipawa Formation requires either elevated reducing conditions (Demaison & Moore, 1980), high primary productivity (Pedersen & Calvert, 1990; Caplan & Bustin, 1999), high sedimentation rates (allowing burial and preservation of organic matter before it is oxidised in surface sediments or reworked by bioturbation), or a combination of these factors (Tyson & Pearson, 1991; Ingall *et al.*, 1993; Arthur & Sageman, 1994; Ingall & Jahnke, 1994; Murphy *et al.*, 2000; Katz, 2005).

The redox state of marine sediments is controlled by the availability of dissolved oxygen, and may be subdivided into the following divisions; oxic (>2.0 ml/L O_2), dysoxic (2.0 – 0.2 ml/L O_2), suboxic (0.2 > 0.0 ml/L O_2), anoxic (0.0 ml/L O_2), and euxinic (0.0 ml/L O_2 and free H_2S in the water column) (Tyson & Pearson, 1991; Arthur & Sageman, 1994).

The concentration and ratios of redox-sensitive trace elements provide insight into paleo-redox conditions and associated paleoenvironmental variability. Various elements are enriched by organic carbon drawdown (e.g. Ni, Cr), and elements precipitated in association with authigenic mineral complexes in reducing environments (e.g. V, U, Mo) can be used to determine an index for the oxygenation state of the water column and seafloor sediments at the time of deposition. Redox-sensitive trace elements are more soluble under oxidising conditions, therefore authigenic enrichment of these elements generally occurs in oxygen-depleted sedimentary facies.

Commonly used trace element proxies for paleo-redox conditions include Ni/Co, V/Cr, V/(V+Ni) and Th/U (Jones & Manning, 1994; Zhou *et al.*, 2012). Concentrations of many of the transition metals are influenced by Mn-Fe cycling, and given that beneath an anoxic water column several trace elements display an enrichment factor relative to the average shale, it is useful to normalise data and consider enrichment factors relative to average shale values (Wedepohl, 1971; Morford *et al.*, 2001). Enrichment factors for trace elements were determined by normalising to Al to remove the influence of detrital input, then divided by values determined for the average shale of Wedepohl (1971):

$$X_{EF} = (X_{sample}/Al_{sample})/(X_{avg.\ shale}/Al_{avg.\ shale})$$

An enrichment factor of 1 indicates values in proportion to the average shale, whereas $X_{EF} > 1$ is enriched, and $X_{EF} < 1$ is depleted relative to average shale values. The authigenic uranium (δU) component of sediments is estimated following Jones and Manning (1994), whereby the total Th is divided by three and subtracted from the total U, providing an index for paleo-redox conditions. However, whereas authigenic enrichments of Mo require sulphide concentrations exceeding ~10

μM (Helz *et al.*, 1996; Erickson & Helz, 2000), authigenic enrichments of U are decoupled from ambient sulphide concentrations (e.g., Klinkhammer & Plamer, 1991; McManus *et al.*, 2005; Tribovillard *et al.,* 2006). Similarly, V can be enriched under anoxic sulphide-poor conditions but strong enrichments require high dissolved sulphide concentrations, i.e. euxinic conditions (Breit & Wanty, 1991). Vanadium is preferentially enriched under reducing conditions and V/Sc can be used to differentiate between oxic and anoxic conditions (Gallego-Torres *et al.*, 2007).

In marine environments, U and Th typically exhibit similar geochemical behaviour, except under oxidising conditions (Chang *et al.*, 2009). This is because Th has a single oxidation state, Th^{4+}, whereas uranium may exist as either insoluble U^{4+} under reducing conditions, or soluble U^{6+} under oxidising conditions, resulting in the enrichment of U relative to Th under reducing conditions (Tribovillard *et al.*, 2006; Chang *et al.*, 2012). As such, Th/U is a widely applied proxy for differentiating between oxic and anoxic marine environments.

Both Mo and U form authigenic precipitates under reducing conditions. However, U is retained and sequestered directly into sediments, whereas Mo requires export from the surface ocean via adherence to Mn-thiomolybdates ($MoO_xS_{4-x}^{2-}$ where x= 0–3), before being subsequently released for secondary reactions by reducing conditions in sediments (the 'particulate shuttle' of Algeo and Tribovillard (2009) and Tribovillard *et al.* (2012)). Formation of Mn-thiomolybdates requires the availability of free hydrogen sulphide (i.e. anoxic to euxinic conditions), thereby U enrichment may occur independently and irrespectively of Mo enrichment (Tribovillard *et al.*, 2012). A dominant U enrichment typically characterises suboxic to anoxic conditions, whereas Mo enrichment is characteristic of anoxic to euxinic conditions (Tribovillard *et al.*, 2012).

The enrichment of S in mudstones is common under low oxygen conditions, and can be attributed to seafloor microbial reduction, which produces two moles of S for every mole of C consumed (Luckge *et al.*, 1999). Because of this, partial digestion of organic matter during or immediately following deposition results in an enhanced proportion of S. On this basis, the proportion of organic matter flux at the time of deposition can be derived by;

$$TOC_{OR} = TOC_{M} + TOC_{SR}$$

where TOC_{OR} is the original TOC deposited, TOC_{M} is the measured TOC value, and TOC_{SR} is the amount of organic carbon mineralised through sulphate reduction, which is determined by multiplying the measured S value by 0.75 to account for the molar ratio of C to S. This is multiplied again by 1.33 to account for a ~ 25% diffusion of S into porewater or the water column following the method of Veto *et al.* (1997, 2000, 2007) and Luckge *et al.*, (1999).

$$TOC_{SR} = S \times 0.75 \times 1.33$$

Productivity proxies include Zn, Ba, Cu, Ni, P and Cd. Phosphorous and Ba may be remineralised under reducing conditions, making them poor proxies, and Ni and Cd concentrations are typically below the detection limit of the pXRF instrumentation used in this study. However, trace metals (e.g. Ni, Cu, Zn, Pb, Cd and Co) are almost entirely delivered to the sediment in association with organic matter and are retained in association with sulphides (Brumsack, 2006; Tribovillard *et al.*, 2006), providing a proxy for organic matter flux, and therefore surface productivity. In marine systems, Ni, Cu and Zn are micronutrients, and their removal from the water column is associated biological productivity. The formation of organo-metallic complexes between Ni, Cu, Zn and organic matter can increase scavenging in the water column and the subsequent accumulation of these trace elements in sediments (Calvert & Pederson, 1993; Piper & Perkins, 2004). On this basis, these form good proxies for organic carbon sinking flux (i.e. paleo-productivity) as they are dominantly deposited in association with organic matter; therefore, enrichment occurs from passive accumulation in proportion to TOC regardless of the oxygenation state of seawater. Additionally, these elements are retained in solid solution in seafloor sediments by sulphides, while organic matter may be remineralised by bacterial activity under oxic conditions (Tribovillard *et al.*, 2005).

Normalising these elements to Al accounts for detrital flux; Cu/Al, Zn/Al and Ni/Al can be used as a proxy for autochthonous (e.g., surface marine) productivity and TOC drawdown and preservation (Calvert *et al.*, 1996; Beckmann *et al.*, 2005; 2008). Changes in sediment provenance and sedimentation rate can enhance primary productivity, particularly if there is a shift to a more mafic source, whereby more nutrients (e.g. P, Mn, Fe) are delivered to the ocean (Cox *et al.*, 2016). Silicon, Ti, K and Al are primary major element constituents of sediments and are independent of TOC complexes, and can therefore inform of changes in sediment supply, provenance and mineralogy. Titanium/Al informs of changes in provenance and sediment accumulation rate (e.g. Sageman *et al.*, 2003a; Turgeon & Brumsack, 2006), as both elements are biogeochemically inactive and only controlled by the detrital flux. However, mafic rocks have higher Ti contents and a shift in provenance to more mafic will be manifested in increasing Ti/Al. Similarly, changes in K/Al can be used to determine shifts in the bulk clay mineralogy, between illite and smectite + kaolinite (Hofmann *et al.*, 2003; Turgeon & Brumsack, 2006). Variation in Si/Al is indicative of changes in sediment accumulation rates (Hofmann *et al.*, 2003; Sageman *et al.*, 2003a; Beckmann *et al.*, 2005).

3.4 Methods

Six sections in the East Coast Basin were sampled, located between Hawkes's Bay in the north, and Wairarapa in the south (Figure 3.1 & 3.2). Five sections were measured in detail (Whangai Bluff, Old Hill Road, Taylor White, Kerosene Bluff and Triangle Farm; Figure 3.2) with a stratigraphic sampling resolution typically of 0.2 – 0.7 m. Archived samples from the Angora Stream dataset of Leckie *et al.* (1992, 1995) held at GNS Science, Lower Hutt, New Zealand were also included. In the measured sections, ~1 kg of fresh bulk rock was collected at each sample interval throughout the stratigraphic thickness. In some instances, a duplicate sample of weathered material was collected from the same sample horizon.

3.4.1 Portable X-Ray Fluorescence

All of the pXRF data presented here were obtained by whole rock XRF of 372 samples using a Olympus Innov-X™ Delta pXRF unit with a 10–40 kV (10–50 μA) Rh X-ray tube and a high-count rate detector. Portable XRF methods are consistent with the approaches outlined in Fisher *et al.* (2014) and Gazley and Fisher (2014). Samples were washed in distilled water to remove any adhering detritus and oven dried for 72 hours at 50 °C. They were then crushed using a Boyd Crusher with the plate gap set to 2 mm. The <1 mm sieved fraction was presented to the pXRF unit covered with polyethylene-free Glad Wrap™. Analyses of Glad Wrap™ placed over a SiO_2 blank showed that no contamination resulted from this medium. The pXRF unit was calibrated at the start of each sample run (20 samples per run) to a variety of research-grade, matrix-matched standards using the same analytical procedures for the standard as for the samples. Standards used were: BCS 267, BIR-1, G-2, GSP-1, JG-1 and PCC-1. The standards were selected to be matrix matched across the expected broad compositional space of the samples. The analytical uncertainty on each analysis is a function of run-time. To limit this uncertainty, but still maximise throughput, the total analysis time was set to 60 seconds (30 seconds per beam). Analytical uncertainties were typically ≤ 3% as reported by the pXRF unit. To check for contamination, SiO_2 blanks were analysed periodically (every 20 analyses).

Repeat analyses of the six standards were routinely collected during the analytical run, and show that the pXRF unit was very stable throughout. The median value for these standards was used to calculate a correction factor for each element. For most elements this took the form of $y = mx + c$; however, for some trace elements that have values that converge on 0, a $y = mx$ correction is often more appropriate (Fisher *et al.*, 2014). These standards were also used to calculate a lower limit of quantification (LOQ) following the approach of MacDougall and Crummett (1980), utilising repeated standard analyses. The majority of elements analysed return values above the lower limit

for quantification (LOQ). These values are presented in Appendix 3 along with summary statistics for each element in the dataset.

3.4.2 Inductively Coupled Plasma Mass Spectrometry and Atomic Emission Spectrometry

Throughout the sections sampled, U, Cr, Ni, Mo and S in the Whangai Formation, and particularly the Wanstead Formation, were below the detection limit of the pXRF methodology employed in this study for many samples. These are particularly important redox-sensitive elements, so whereas these elements can still be used to assess intra-formational variability in paleo-redox systems, their inter-formational variability was assessed using laboratory (ICP-MS and fusion XRF) analyses on sample splits from the Taylor White section.

A subset of nineteen samples from the Taylor White section were analysed by ALS Laboratories, Perth, Australia, for comparison to the pXRF data generated in this study (Appendix 3). Base metals (Ag, Cd, Co, Cu, Li, Mo, Ni, Pb, Sc, Zn) were determined using a by four-acid digestion method, where the sample was dissolved in a solution of perchloric, nitric, hydrofluoric and hydrochloric acids (ALS method ME-4ACD81), then analysed by inductively coupled plasma – atomic emission spectrometry (ICP-AES). Arsenic, Bi, Hg, Sb, Se, Te, and Tl were determined by a 45 minute digestion in aqua regia, dilution to 12.5 ml with deionised water and analysed by inductively coupled plasma-mass spectrometry (ICP-MS; ALS method ME-MS42). Whole rock analysis was performed by sample addition to a lithium metaborate/lithium tetraborate flux, fused in a furnace at 1025°C then major element abundances (Al_2O_3, BaO, CaO, Cr_2O_3, Fe_2O_3, K_2O, MgO, MnO, Na_2O, P_2O_5, SiO_2, SrO, TiO_2) determined by borate fusion XRF (ALS method ME-XRF26), and Ba, Ce, Cr, Cs, Dy, Er, Eu, Ga, Gd, Hf, Ho, La, Lu, Nb, Nd, Pr, Rb, Sm, Sn, Sr, Ta, Th, Tm, U, V, W, Y, Yb, and Zr, determined by ICP-MS after dissolution in a nitric, hydrochloric and hydrofluoric acid mixture (ALS method ME-MS81). Total carbon values were determined by sample combustion in a LECO induction furnace and quantitative detection of emitted CO_2 by infrared spectrometry (ALS method C-IR07). Total sulphur values were measured by a LECO gravimetric sulphur analyser, where SO_2 measured by an infrared detection system (ALS method C-IR08).

3.4.3 Comparison between pXRF and laboratory-based instrumentation

Many of the major elements (Al, Fe, Mn, Ti), and some trace elements (Zn, Sr, Rb), analysed by pXRF provide strong coefficients of determination (R^2) >0.8 with corresponding sample splits

analysed by ICP-MS and fusion XRF (Appendix 3). Other elements (Si, K, As, S, Pb, Cu) produced reasonably comparable results (R^2 values >0.6), despite low absolute concentrations (<10 ppm) for some elements (e.g., As, Pb).

Zirconium, Cr, Mo and U measured by pXRF correspond poorly with laboratory based fusion XRF and ICP-MS measurements, giving R^2 values between 0.3–0.6 (Appendix 3). For Mo and U, values are typically below 10 ppm, approaching the detection limit of the pXRF unit. Despite this, when U is normalised to Th, the ratios obtained are comparable to ratios derived from laboratory-based instruments. This may be due to matrix effects in the measurement of a sediment sample by pXRF and by solution ICP-MS.

Nickel performs poorly by pXRF, giving an R^2 value of <0.06 with lab data, and therefore pXRF analyses of Ni are excluded from geochemical indices in this study. Despite poor slopes, Th and V reproduce well (Appendix 3). Vanadium by pXRF corresponds moderately well with laboratory data (R^2 = 0.54), although it applied with the caveat that there is spectral overlap with Ti and Ba. When normalised against Cr and Ni, V values compare well to laboratory derived data for redox studies.

3.4.4 Bulk pyrolysis

Pyrolysis measurements were made using a Source Rock Analyzer (SRA) from Weatherford Laboratories housed at GNS Science, Lower Hutt, New Zealand. Approximately 100 mg of powdered rock were used for each bulk pyrolysis sample measurement. The pyrolysis program was set with the sample crucible entering the pyrolysis oven where it was held isothermal at 300°C for 3 minutes under a continuous stream of He carrier gas using a 100 ml/minute flow rate. This was followed by a 25°C/minute ramp to 650°C. The S1 and S2 signal intensities were recorded with a Flame Ionization Detector (FID) operated under a 65 ml/minute stream of H_2 gas and 300 ml/minute air. The pyrolysis cycle was then followed by an oxidation cycle performed at 630°C for 20 minute during which time the oven and crucible were flushed with dry air at 250 ml/minute. The generated carbon monoxide and carbon dioxide gases were measured by the instrument's IR cells. All sample sequences were run with three IFP 160000 analytical standard replicates (from Vinci Technologies, Institut Français du Pétrole) placed at the beginning, middle and end of each sample sequence.

3.4.5 Multivariate data exploration

High-dimensional data are challenging to interpret and visualise. Element-element pairwise plots are not always useful for identifying correlations in data. Ordinations using principal components analysis (PCA) allow linear combinations of variables that summarise the highest amount of dataset variance in the fewest dimensions and show correlations that are easier to interpret. Twenty-two elements were analysed by pXRF, of which thirteen elements had continuous representation throughout the dataset, necessary for PCA. A value of 0.22 *x* LOQ was substituted for samples that recorded less than the limit of detection (LOD) for elements that had less than 5.5% of their samples with data below LOD, assuming LOQ ≈ 3LOD. This substitution for <LOD is consistent with the recommendations of Martín-Fernández *et al.* (2012). The geochemical data are compositional and thus were log-ratio transformed prior to multivariate analysis to solve the closure issue (Aitchison, 1982, 1986; Aitchison *et al.*, 2000; Grunsky *et al.*, 2014; Mueller & Grunsky, 2016). Aitchison's centered log-ratio transformation was applied using the 'clr' function in the R package 'Hotelling' (Curran, 2013; R Development Core Team, 2017).

Sparse robust PCA is less sensitive to outliers and was designed for chemometric applications (Croux *et al.*, 2007; Filzmoser *et al.*, 2014). Sparse robust PCA was performed on the log-ratio transformed data using the 'PCAgrid' function in the R package 'pcaPP' (Croux *et al.*, 2007; Filzmoser *et al.*, 2014; R Development Core Team, 2017). Principal component analysis summarises variation in a multivariate dataset in terms of linear combinations of covarying input variables. This reduces data dimensionality, and clarifies intrinsic dataset structure. Principal component (PC) axes can be interpreted in terms of the original variables, are mutually orthogonal (assumed to be statistically independent), and are suitable for subsequent statistical analyses.

Scores from the first two PCs were input to Bayesian mixture-modelling cluster analysis using the 'Mclust' function from the R package Mclust (Fraley *et al.*, 2012; R Development Core Team, 2017) to identify objective subgroups of geochemically similar samples. Each sample was plotted along stratigraphic height within its section, coloured by subgroup, to recover a geochemical stratigraphy.

3.5 Results

3.5.1 Principal component analysis

There is a marked variability in major element composition up-section across formation boundaries, particularly in the measured values of K, Ca, Mn, Ti and Si. Principal Components Analysis of Al, Ti, Si, K, Fe, Pb, As, Zn, Sr, Mn, Zr and Rb has one statistically significant component identified using a broken-stick distribution (Figure 3.3a; Jackson, 1993); this

component explains 42% of the variance in the dataset. Positive values on PC1 are associated with covariance between K, Al and Ti, and negative values with a covariance between Mn and Sr (Figure 3.3). This is likely driven by the bulk mineralogy. The second principal component (PC2) explains 16% of the variance in the dataset. Positive values on PC2 are associated with covariance between Zn and As, and negative values with covariance between Si and Zr.

We chose to use both of the first two PCs (which explain ~60% of the variance in the dataset) in the cluster analysis in order to improve resolution and allow clearer visualisation of the data structure using an *x-y* scatterplot, rather than a univariate distribution. Cluster analysis on the first two PC axes found three clusters (Figure 3.3b). Clusters 1 (red) and 3 (blue) show negative and positive relationships to As and Pb, respectively, and Cluster 2 (green) occupies an intermediate position. Other notable patterns include Cluster 1 (red) showing a strong positive relationship with Mn and Zr, and a strong negative relationship with Zn. Cluster 2 (green) shows a positive relationship with Mn, Sr and Zn, whereas Cluster 3 (blue) displays positive correlation with As, Fe, Al, Rb, Ti and K.

Plotting geochemical groups by stratigraphic height within each section (Figure 3.3c), Clusters 1 and 2 comprise the Whangai and Wanstead Formations. Samples from the Upper Calcareous Member of the Whangai Formation fall dominantly within Cluster 2 (green; Figure 3.3b) and the Waipawa Formation is covered by Cluster 3 (blue; Figure 3.3b). The Porangahau Member of the Whangai Formation, and the Wanstead Formation, are described by a mix of Clusters 1 and 2 (red and green) and are dominated by Cluster 1 (red). Relationships between samples in the dataset that are not apparent in element vs element plots are revealed by the multivariate ordination. Significantly, spatially coherent clusters (Figure 3.3b, c) are identified. Although at this broad scale the Waipawa Formation is geochemically distinct from the Whangai and Wanstead formations, both which are shown to share geochemical affiliations, and furthermore, the members of the Whangai Formation can also be differentiated by PCA.

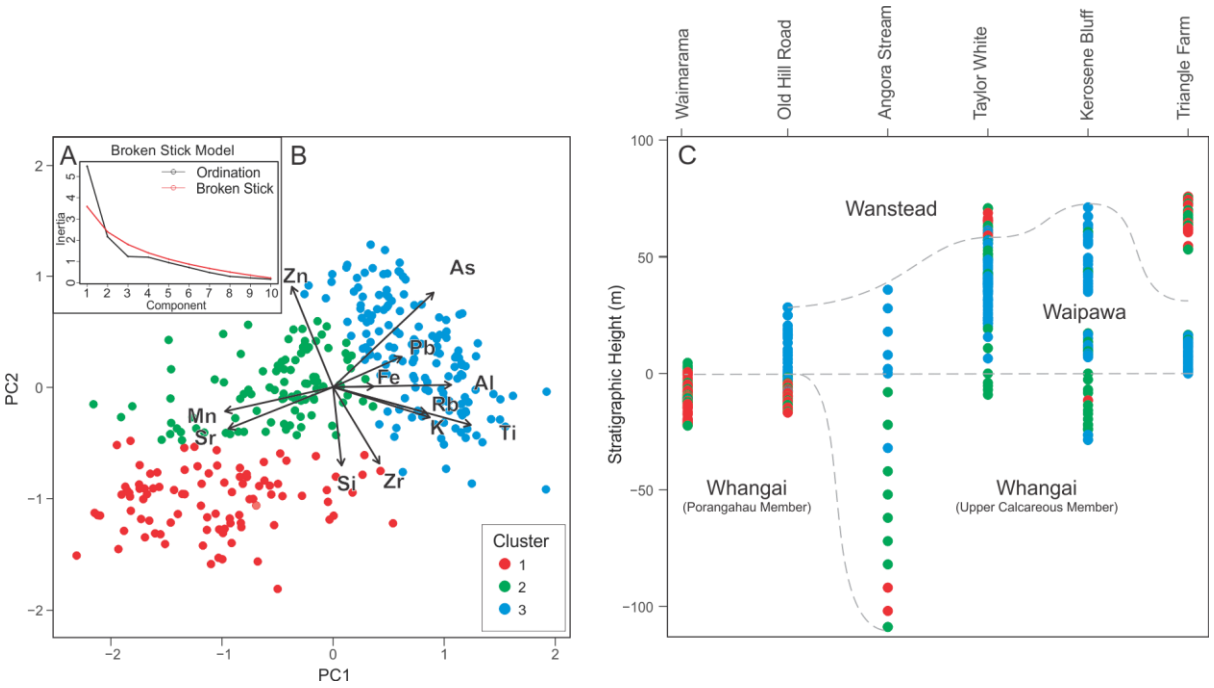

Figure 3.3: Principal Component analysis of pXRF data across the Whangai, Waipawa, and Wanstead formations, in sections sampled for this study. A) Broken stick model showing one significant component. B) Loadings plot of principal components 1 and 2, which together explain ~60 % of variance within the dataset (42% on PC1, 16% on PC2). Eigenvectors show the CLR-transformed variables relative to the PC axes. C) Samples coloured by cluster and plotted against stratigraphic height (normalised to base-Waipawa Formation). Dashed lines indicate formation boundaries.

3.5.2 Bulk pyrolysis

Within the studied sections, the Waipawa Formation has a variable TOC content, ranging from 1.0–6.0 wt. % (Figure 3.4), with the majority of samples forming a distinct organic-rich group (2–6 wt. %). The underlying Whangai Formation displays lower organic matter contents (0.2–1.5 wt. % TOC). The Whangai and Waipawa formations are thermally immature (T_{max} values ~410–435 °C; Figure 3.4a), suggesting that these rocks have not yet generated and expulsed hydrocarbons. A negative relationship between T_{max} and TOC in the Upper Calcareous Member, Waipawa Formation and Wanstead Formation (Figure 3.4a) is organofacies controlled as the thicknesses of these sections is not sufficient enough to cause elevated maturation. The low T_{max} values (<380°C) are likely to be inaccurate measurements caused by very low S2 peak heights. Total organic carbon values for the Porangahau Member at Old Hill Road are low (<0.5 wt. % TOC). The recorded hydrocarbon concentrations are positively correlated to the organic matter content of the strata sampled; as such, the S1 and S2 parameters are positively correlated with TOC for the Whangai and Waipawa formations in all sections (Figure 3.4b, c).

A cross plot of the oxygen index (OI) and the hydrogen index (HI) provides an approximation of the kerogen source of organic matter. The Waipawa Formation typically falls within the Type II to Type III kerogen fields (Figure 3.4), indicating a mixed marine-terrestrial, respectively, organic matter kerogen source. The Upper Calcareous Member of the Whangai Formation, as sampled at Taylor White and Kerosene Bluff, falls almost exclusively within the Type III kerogen field, indicating a terrestrial source. The Porangahau Member of the Whangai Formation, as sampled at Old Hill Road, and the Wanstead Formation sampled at Triangle Farm, have exceptionally low HI values (<20 mg HC/g TOC), indicating a Type IV, inert kerogen source.

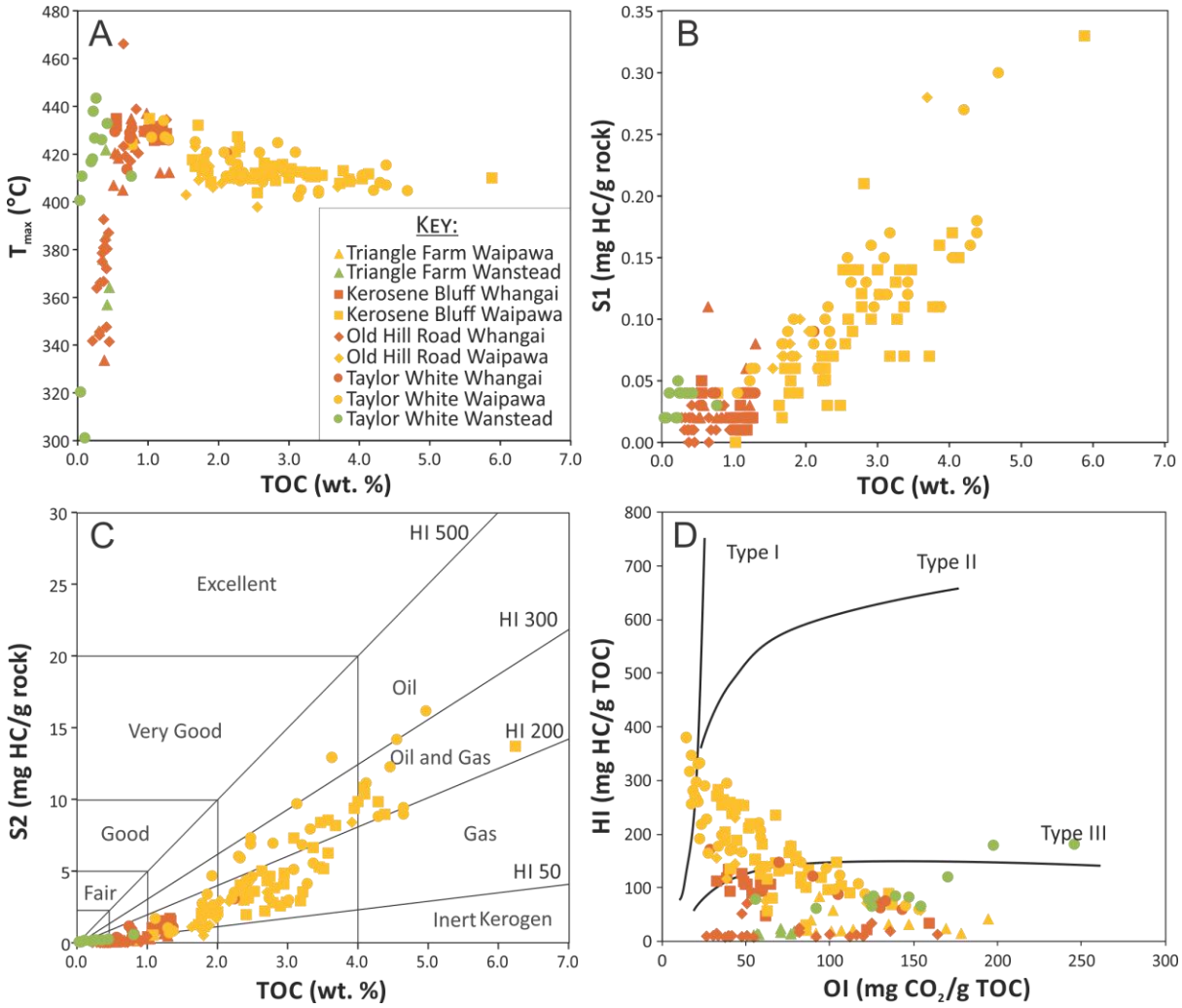

Figure 3.4: Bulk pyrolysis data for the Whangai, Waipawa, and Wanstead formations as sampled in this study. TOC vs. A) T_{max}, B) S1, C) S2, with generative potential indicated, D) Pseudo-van Krevelen diagram indicating kerogen classification by hydrogen index (HI) and oxygen index (OI) values.

3.5.3 Redox-sensitive trace element enrichments

Several trace elements are enriched in the Waipawa Formation with respect to the Whangai and Wanstead Formations. Strong enrichment factors are shown for TOC, S, and Mo. There are mild enrichments in Cd, Bi, U, Cr, As, Zn, and Ba (Figure 3.5). Enrichment factors for V, Pb and Fe are proportional to the average shale values of Wedepohl (1971), whilst Cu, Ni, P, Mn, Co, Sb and Tl are depleted (Figure 3.5). The Upper Calcareous Member of the Whangai Formation shows similar trace element enrichments and depletions with respect to the average shale as the Waipawa Formation, although with notably lower enrichments in TOC, S, Mo, and Cd (Figure 3.5). The majority of elements in the Wanstead Formation are in relative proportion to average shale values (Mo, As, Cu, Pb, Fe, Mn) or only weakly enriched (TOC, Bi, U, Cr, Zn, V, Ba) or depleted relative to the average shale (S, Ni, P, Co, Sb, Tl; Figure 3.5).

Trace metals that act as proxies for primary productivity, organic carbon drawdown and preservation (Ni, Zn, and Pb) have average enrichment factors (EFs) of 0.6, 1.4, 1.0 respectively, and average enrichment factors vary minimally (±0.2), showing little, to no, enrichment or depletion between the Whangai, Waipawa, and Wanstead formations. The largest offsets in enrichment factor across formation boundaries is demonstrated by TOC, S, Mo, U and Mn (±17, 6, 4, 2, 0.8 respectively; Figure 3.5). Strong enrichment factors for TOC and S indicate that these two components are integral in deciphering trace metal affiliations and redox conditions during the deposition of the Waipawa Formation. Manganese depletion in the Waipawa Formation (typical EF ~0.2; Figure 3.5; Table 3.1) in relation to both the average shale and the Whangai and Wanstead formations implies the removal of reduced Mn^{2+}, consistent with anoxia. Below the chemocline, reducing conditions produce soluble Mn^{2+} which diffuses away from the site of reduction, resulting in Mn depleted sediments. Because of the difference in the solubility of its different oxidation states (Mn^{2+} and Mn^{4+}), Mn is actively cycled across redox boundaries, with the greatest concentration occurring in suboxic sediments, near the suboxic-anoxic interface (Tribovillard *et al.*, 2006; Chang *et al.*, 2009).

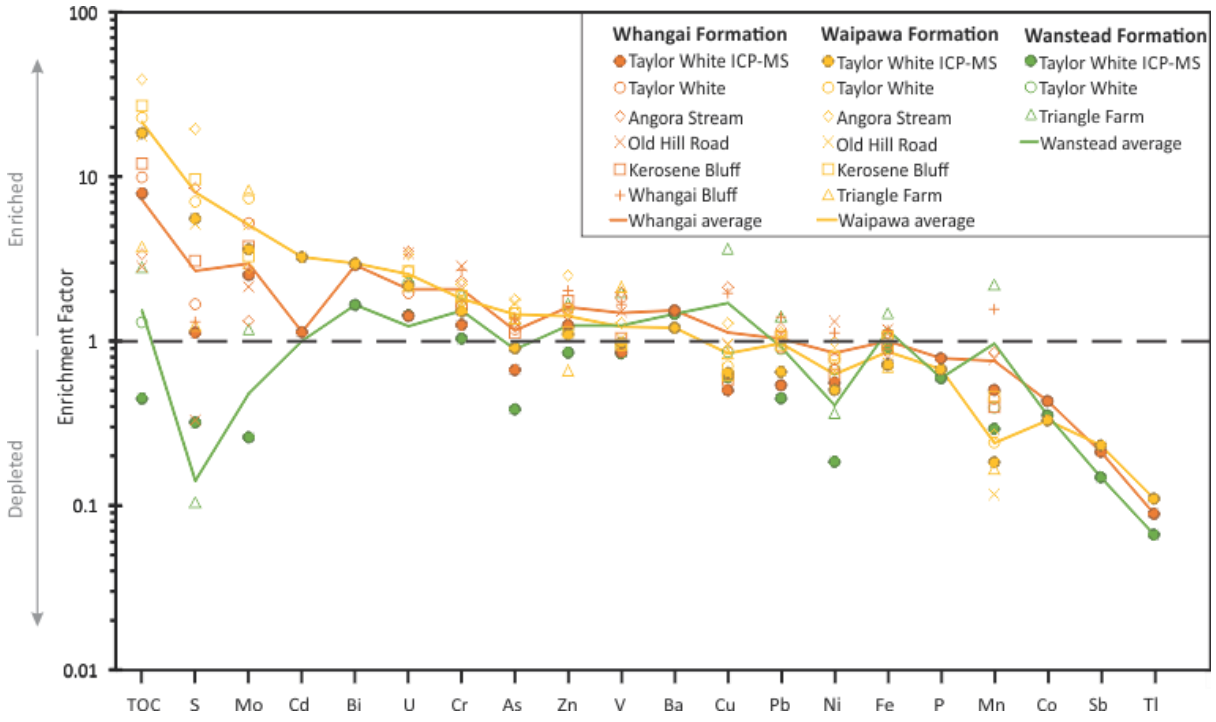

Figure 3.5: Mean enrichment factors normalised to average shale values from Wedepohl (1971), for TOC, sulphur, and selected redox-sensitive trace metals in the Whangai, Waipawa, and Wanstead formations across the sections sampled in this study. Lines indicate overall mean values for each formation. Data measured by ICP-MS are plotted in bolder colours than corresponding pXRF values. Several elements measured by ICP-MS were not detected by pXRF (Cd, Bi, Ba, P, Co, Sb, and Tl).

3.5.4 Organic carbon – sulphur relationships

Decreased oxygenation and the associated increased reducing conditions in either the water column or sediment pore waters result in increased organic carbon burial and preservation in marine basins, with concomitant microbial sulphate reduction leading to syngenetic and diagenetic pyrite formation (Rimmer, 2004; Brumsack, 2006). These processes facilitate the export and sequestration of trace metals in sediments and are responsible for the majority of trace metal enrichments under dysoxic to anoxic conditions.

In this context, the chemical composition of bulk sediment, particularly trace element distributions and S–Fe–TOC relationships, can be employed to distinguish past depositional environments and paleo-redox conditions (Rimmer, 2004; Brumsack, 2006; Rowe *et al.*, 2008, 2012). Paleoredox conditions can be assessed by the proportion of S relative to Fe (Raiswell *et al.*, 1988; Lyons & Severmann, 2006; Georgiev *et al.*, 2012). The ratio of S to Fe for the Waipawa Formation suggest the degree of pyritisation lies within the oxic to anoxic fields of Raiswell *et al.* (1988) (Figure 3.6a).

Values for the Whangai and Wanstead formations suggest a very low degree of pyritisation, sitting well within the oxic field (<0.52; Figure 3.6a). Increased terrigenous sediment supply, however, may limit the availability of reactive Fe, resulting in lower degrees of pyritisation and lower S/Fe for anoxic and euxinic settings. In addition, diagenetic effects, particularly outcrop weathering can also lower the elemental concentrations of S and Fe, with Fe being leached more rapidly than S, which could yield artificially elevated redox conditions. Because of these caveats, S/Fe alone cannot provide a clear insight into paleo-redox conditions, requiring the application of additional proxies.

Despite high enrichment factors, S and TOC in the Waipawa Formation are only weakly correlated ($R^2 = 0.3$), and S/TOC relationships for the Waipawa Formation are variable. A substantial proportion of samples analysed lie within the range of normal marine S/TOC, although a significant number also plot above normal marine conditions (Figure 3.6b). This discrepancy in the S/TOC ratio is attributed to sulphate reduction through bacterial decomposition of organic matter. The broad variability in S/TOC values is attributed to the two-phase increase of S/TOC ratios in the Waipawa Formation. Redox proxies show that the formation was deposited under oxygen deficient conditions, and higher TOC in the unit result in a greater TOC/S ratio.

The TOC_{OR} estimated for the Waipawa Formation is approximately 1.4–2.0 wt. % higher than the preserved (measured) TOC values (Table 3.1), implying that there was substantial syndepositional or early diagenetic degradation of organic matter by bacterial sulphate reduction. Microbial degradation within the water column preferentially removes marine organic carbon (predominantly comprised of simple lipids and carbohydrates), resulting in preferential preservation and the relative enrichment of terrestrial organic matter (e.g. Veto *et al.*, 1997; Luckge *et al.*, 1999). This explains, in part, the observation by various authors of an enhanced terrestrial signature in the Waipawa Formation and correlatives, recorded as higher proportions of terrestrial kerogen, and elevated $\delta^{13}C_{org}$ (Killops *et al.*, 2000; Rogers *et al.*, 2001; Schiøler *et al.*, 2010; Hollis *et al.*, 2014; Clowes, *in prep.*).

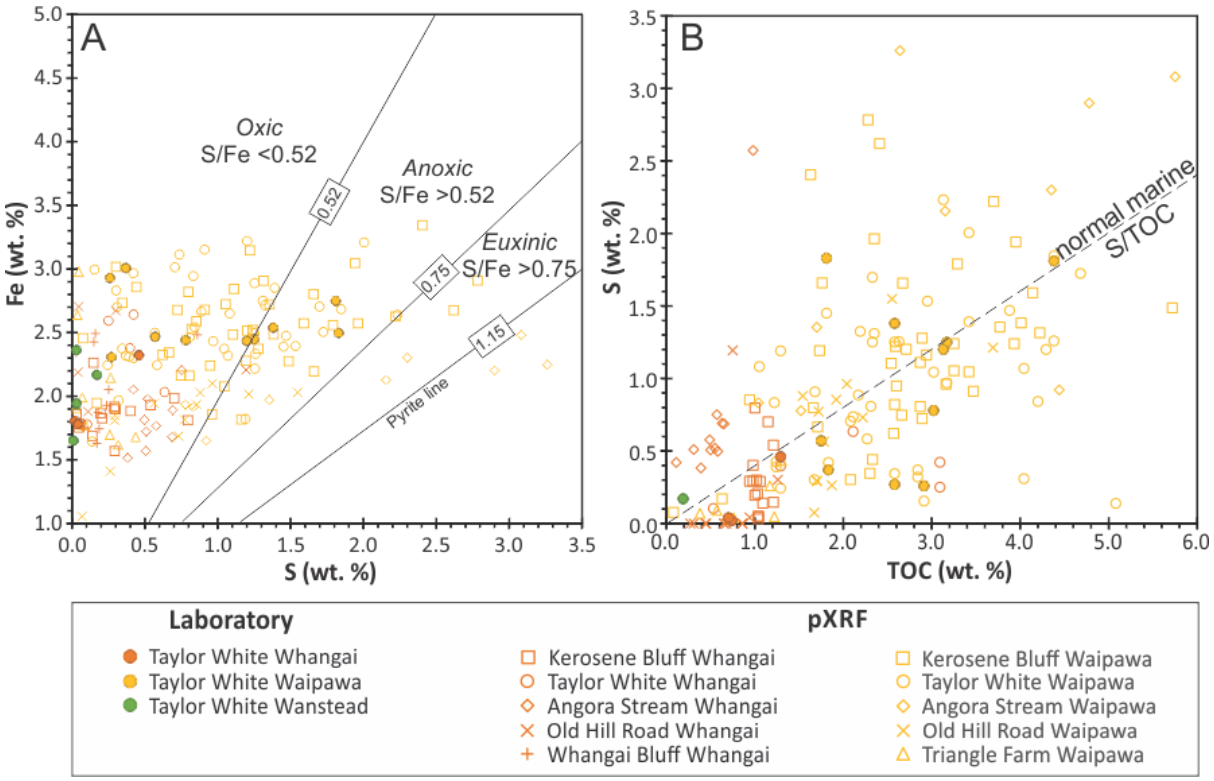

Figure 3.6: A) Fe/S relationships for the Whangai, Waipawa, and Wanstead formations sampled in this study. Oxic, anoxic and euxinic fields from Georgiev *et al.* (2012), after Raiswell *et al.* (1988). B) S/TOC relationships for the Whangai, Waipawa, and Wanstead formations sampled in this study. Iron is measured by laboratory-based XRF and pXRF. Sulphur values are from LECO and pXRF analyses. Normal marine S/TOC line from Berner and Raiswell (1983).

3.5.5 Paleo-redox proxies

In order to provide a direct indication of paleo-oxygenation, the trace metal proxies Ni/Co, V/Cr, V/(V+Ni), Th/U, U_{auth}, V/Sc, Mo/TOC, and Mo/U were used as indices of redox potential of the water column and sediments during deposition. Thorium/U is a widely applied proxy for differentiating redox conditions, with values from 0–2 representing anoxic environments, and values from 2–8 representing oxidising environments (e.g. Gallego-Torres *et al.*, 2007; Chang *et al.*, 2009; 2012). Thorium/U values in the Waipawa Formation range from 1.3–2.5 (average 2.0), whereas the Whangai and Wanstead formations range between 2.5–3.2 (average 2.9), indicating that anoxic to weakly oxic conditions prevailed during deposition of the Waipawa Formation, and fully oxic conditions during deposition of the Whangai and Wanstead formations (Figure 3.7a).

Authigenic U values derived from ICP-MS measurements for the Waipawa Formation average 1.4 ppm, which is above the threshold of 1.0 ppm for dysoxic conditions (Zhou *et al.*, 2012), and

substantially elevated relative to average values for the Whangai and Wanstead formations (0.12 and 0.08 ppm, respectively; Figure 3.7a).

Vanadium is preferentially enriched under reducing conditions and a V/Sc value greater than 9.1 can also be used to differentiate between oxic and anoxic conditions (Gallego-Torres *et al.*, 2007). The Waipawa Formation gives V/Sc ratios ranging from 8.6–10.7 (average 9.8), whereas the Whangai and Wanstead formations range from 7.5–9.25, with average values of 8.6 and 8.4, respectively (Figure 3.7b). V/Cr values in the range of 0–2 represent oxic conditions, whereas values in the range from 2–4 indicate dysoxic conditions. V/Cr values in the range of 4–10 are representative of suboxic to anoxic environments (Jones & Manning, 1994). There is generally very little differentiation in V/Cr between the Whangai, Waipawa and Wanstead Formations, with values of 0.95–1.06 (average 0.99) for the Whangai Formation, 0.74–1.66 (average 0.98) for the Waipawa Formation and 0.90–1.23 (average 1.2) for the Wanstead Formation. Another commonly used redox proxy is V/(V+Ni), where values >0.84 are indicative of euxinia, values in the range of 0.54–0.72 indicate anoxic water column conditions, 0.46–0.60 indicate water column dysoxia, and values <0.46 represent oxic conditions (Hatch & Leventhal, 1992). Vanadium/(V+Ni) has patchy spatial coverage, due to the poor Ni resolution and low counts by pXRF, although lab data for Taylor White gives values for the Whangai Formation of 0.67–0.87 (average 0.76), a range of 0.63–0.95 (average 0.80) for the Waipawa Formation, and a range of 0.86–0.91 (average 0.85) for the Wanstead Formation. The efficiency of V based proxies (V/Cr, V/(V+Ni)) is reduced under high sedimentation rates, as the rate of V diffusion is reduced and trace metal concentrations are diluted (Arthur & Sageman, 1994).

Mudstones deposited beneath an oxic water column typically have a Ni/Co ratio <5, with values from 5–7 reflecting dysoxic conditions and values >7 indicating anoxic conditions (Jones & Manning, 1994; Gallego-Torres *et al.*, 2007). Nickel/Co ratios for the Waipawa Formation range between 2.0 and 8.4, with an average of 4.0, suggesting a range of oxic and dysoxic conditions (Figure 3.7b). The Whangai Formation ranges from 2.7–5.6 an average ratio of 4.3, whereas the Wanstead Formation is substantially lower with a range of 1.7–3, and an average Ni/Co of 1.6 (Figure 3.7b).

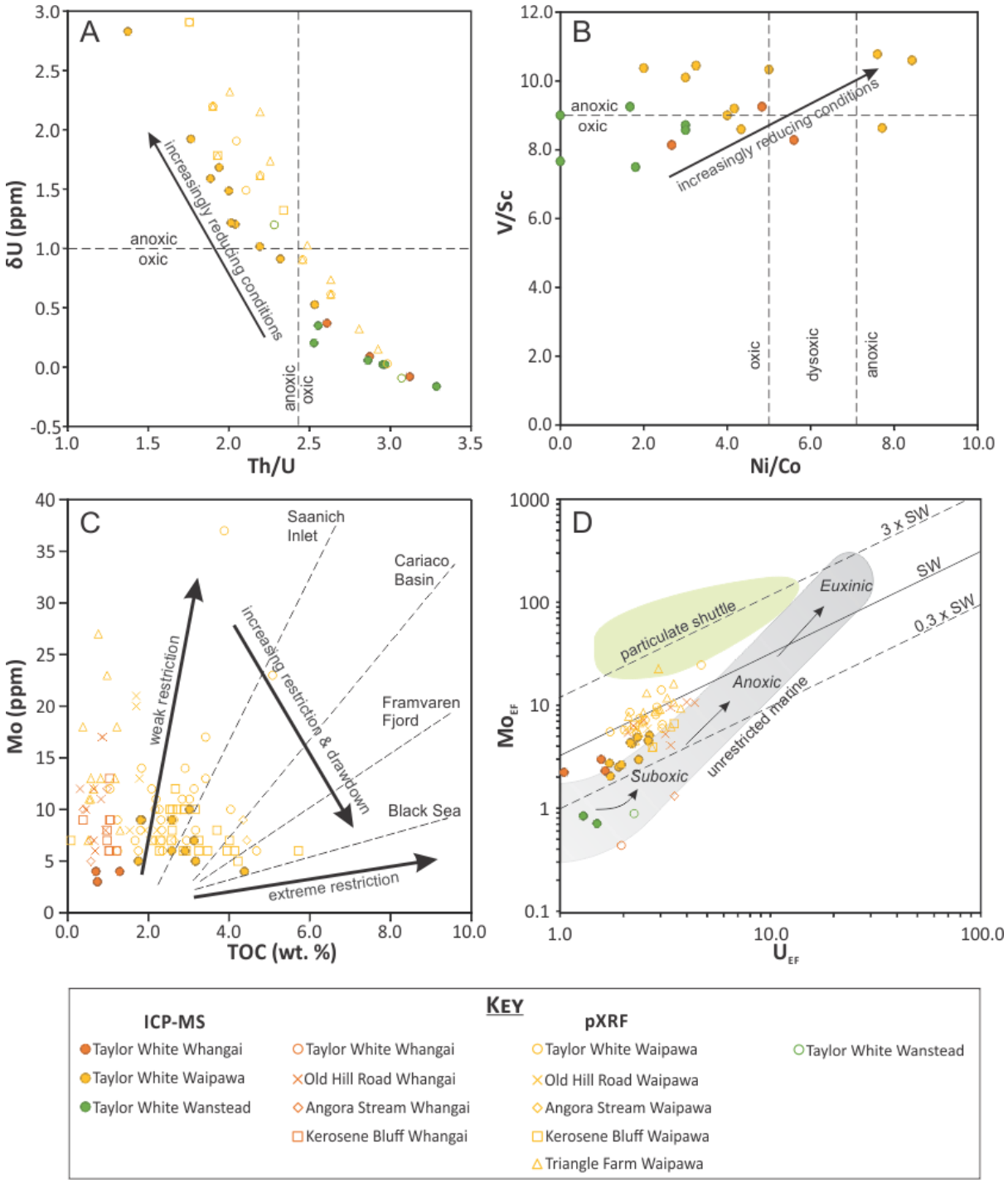

Figure 3.7: Trace element proxies for paleo-redox conditions from ICP-MS measurements of a subset of Taylor White samples, with additional data from pXRF analyses. A) Authigenic uranium vs Th/U. B) V/Sc vs Ni/Co. C) Mo vs TOC with trend lines of modern reducing sedimentary basins plotted from Tribovillard *et al.* (2012). D) Uranium enrichment factor plotted against Mo enrichment factors, with fields from Tribovillard *et al.* (2012).

Molybdenum-TOC relationships for the Whangai and Waipawa formations largely plot within the range of values given for modern anoxic sediments deposited in weakly restricted basins (Figure 3.7c), which is consistent with the deep, open marine depositional setting of the East Coast Basin during the Paleogene (e.g. Field & Uruski *et al.*, 1997; King *et al.*, 1999; Hines *et al.*, 2013). The relative enrichment of Mo with respect to U in the Waipawa Formation is interpreted as being indicative of water column anoxia (Mo:U approximately 5:2; Figure 3.7d). Based on patterns of trace element enrichment in modern reduced oxygen marine settings (Algeo & Tribovillard, 2009; Tribovillard *et al.*, 2012), anoxic conditions prevailed during deposition of the Waipawa Formation, as the Mo enrichment factor is disproportionately higher than the U enrichment factor than would otherwise be anticipated under unrestricted marine settings (Figure 3.7d).

Table 3.1: Average values for source rock analyses, trace element enrichments, redox proxies and additional proxies for depositional conditions for each unit and locality sampled in this study. POM = Porangahau Member, UCM = Upper Calcareous Member.

Section	**Whangai Bluff**	**Old Hill Road**		**Angora Stream**			**Taylor White**			**Kerosene Bluff**		**Triangle Farm**	
Unit	**Whangai (POM)**	**Whangai (POM)**	**Waipawa**	**Whangai (POM)**	**Whangai (UCM)**	**Waipawa**	**Whangai (UCM)**	**Waipawa**	**Wanstead**	**Whangai (UCM)**	**Waipawa**	**Waipawa**	**Wanstead**
Source Rock Analysis													
TOC (wt. %)	-	1	**2**	0	1	**4**	1	**3**	*0*	1	**3**	**1**	*0*
Tmax (°C)	-	388	**410**	403	423	**410**	425	**415**	*408*	429	**411**	**414**	*376*
HI	-	14	**111**	111	229	**300**	105	**207**	*103*	103	**179**	**30**	*13*
OI	-	75	**78**	18	34	**10**	102	**57**	*165*	75	**56**	**124**	*67*
Enrichment Factor													
U	4.5	3.4	**2.3**	-	-	**3.4**	0.2	**2.5**	*0.3*	-	**2.7**	**2.2**	*1.8*
Mo	2.8	2.1	**5.1**	-	2.7	**6.2**	0.4	**7.3**	*2.1*	3.8	**5.4**	**8.2**	*1.2*
S	0.9	0.3	**5.1**	4.1	7.8	**23.9**	1.1	**7.0**	*0.0*	2.6	**1.5**	**1.2**	*1.4*
TOC	-	2.8	**17.7**	0.5	10.2	**49.4**	9.9	**22.8**	*1.6*	12.0	**26.9**	**3.7**	*2.8*
V	1.4	1.3	**1.0**	1.8	1.7	**1.3**	1.1	**0.9**	*0.2*	1.0	**0.9**	**2.1**	*2.0*
Cu	1.6	0.9	**1.0**	1.2	0.8	**1.1**	0.6	**0.7**	*0.4*	0.6	**0.6**	**0.8**	*3.6*
Ni	1.0	1.3	**0.7**	0.7	0.7	**1.1**	0.8	**0.8**	*0.2*	0.6	**0.8**	-	*1.1*
As	1.1	1.3	**1.7**	0.9	1.4	**2.0**	1.2	**1.5**	*0.3*	0.6	**1.5**	**1.4**	*1.4*
Cr	2.7	2.7	**1.8**	-	2.2	**2.2**	1.6	**1.7**	*0.5*	1.6	**1.9**	**1.6**	*1.9*
Fe	1.2	1.2	**0.7**	1.0	1.1	**1.1**	0.9	**0.9**	*0.2*	1.0	**1.1**	**0.7**	*1.5*
Mn	1.6	0.8	**0.1**	0.9	0.5	**0.2**	0.4	**0.2**	*0.2*	0.4	**0.5**	**0.2**	*2.2*
Zn	2.0	1.6	**1.5**	1.5	1.7	**2.6**	1.6	**1.6**	*0.3*	1.8	**1.1**	**0.7**	*1.7*
Pb	1.4	1.1	**1.0**	1.1	1.1	**1.1**	0.9	**1.0**	*0.2*	1.1	**1.1**	**0.9**	*1.4*
Redox Proxies													
V/Sc	-	-	**-**	-	-	**-**	8.6	**9.8**	*8.5*	-	**-**	**-**	-
Ni/Co	-	-	**-**	-	-	**-**	4.4	**5.0**	*1.6*	-	**-**	**-**	-
V/Cr	0.8	0.7	**0.9**	-	0.8	**1.0**	0.8	**0.8**	*0.9*	0.9	**0.7**	**1.8**	*1.0*
V/(V+Ni)	-	0.7	**0.7**	0.8	0.7	**0.7**	0.8	**0.7**	*0.7*	0.7	**0.7**	**1.0**	*0.9*
Th/U	2.1	2.0	**3.1**	-	-	**2.1**	-	**2.2**	*2.7*	-	**2.0**	**2.5**	-
U_{auth}	1.5	2.9	**2.1**	-	-	**3.1**	1.8	**2.3**	*2.1*	-	**2.3**	**2.5**	*2.7*
Mo/TOC	-	3.9	**4.5**	-	4.2	**2.0**	-	**4.6**	*2.5*	3.9	**2.5**	**20.8**	*4.4*
S/TOC	-	0.1	**0.4**	1.0	1.0	**0.6**	0.1	**0.4**	-	0.3	**0.5**	**0.2**	*0.0*
Fe/S	18.4	28.5	**2.6**	0.2	0.4	**1.1**	17.3	**3.8**	-	0.1	**0.5**	**2.0**	*1.9*
Depositional Conditions													
Ti/Al	0.1	0.1	**0.1**	0.1	0.1	**0.1**	0.1	**0.1**	*0.1*	0.1	**0.1**	**0.1**	*0.1*
Si/Al	8.9	7.5	**5.2**	5.9	8.2	**5.5**	6.9	**4.5**	*7.6*	7.7	**4.8**	**5.4**	*7.6*
K/Al	0.3	0.3	**0.2**	0.3	0.2	**0.2**	0.2	**0.2**	*0.2*	0.2	**0.2**	**0.2**	*0.2*
Cu/Al	9.9	4.9	**5.2**	6.0	4.3	**7.4**	3.2	**3.6**	*4.4*	2.9	**3.1**	**4.3**	*18.3*
Ni/Al	7.9	10.6	**5.9**	5.7	5.6	**8.1**	7.6	**6.4**	*5.2*	4.4	**6.2**	-	*8.4*
Pb/Al	3.2	2.6	**2.3**	2.5	2.5	**2.5**	2.1	**2.3**	*2.0*	2.4	**2.4**	**2.1**	*3.2*
Zn/Al	21.8	17.3	**22.5**	16.2	18.1	**27.5**	17.8	**17.5**	*12.8*	19.0	**12.1**	**7.1**	*18.1*

3.5.6 Inorganic proxies

Various trace element indices and ratios are used to inform interpretations of paleoenvironmental and redox conditions during deposition. Titanium/Al values are constant throughout the Whangai, Waipawa and Wanstead formations. The lack of any discernible trend in in the distribution of Ti/Al values, suggests that there is no change in detrital source across the spatial and temporal extent of the sections studied (Figure 3.8a).

Potassium/Al provides an index for the bulk clay composition. The Waipawa Formation shows a slight increase in illite over smectite + kaolinite relative to the Whangai and Wanstead formation, with the exclusion of samples from the Porangahau Member at Angora Stream and Old Hill Road, and the flysch facies of the Wanstead Formation at Taylor White (Figure 3.8a), which are attributed to grain-size variability.

The Si/Al ratio can inform changes in terrigenous sedimentation rate, with a decrease in Si/Al demonstrating an increase in the sedimentation rate. Across the sections studied, the Whangai and Wanstead formations have a similar range of Si/Al (typically 6 – 10), whereas the Waipawa Formation has notably lower Si/Al (typically 3.7 – 5.5), indicating an increased sedimentation rate relative to the Whangai and Wanstead formations (Figure 3.8b). There is a broad range of variability in Ti/Al and Si/Al from the Porangahau Member at Old Hill Road, which is attributed to grain size variation (and associated changes in mineralogy) in the turbidite sequence sampled (Figure 3.8). The highest TOC preservation typically occurs in association with the lowest Si/Al values, suggesting that preservation of organic matter is associated with increased sediment accumulation rates (Figure 3.8b). Proxies for productivity and organic carbon drawdown and preservation (Ni/Al, Cu/Al, Zn/Al) are highly variable, and show similar proportions through the Whangai Formation and into the Waipawa Formation. However, they display a weak up-section co-variation with TOC (e.g. Figure 3.9).

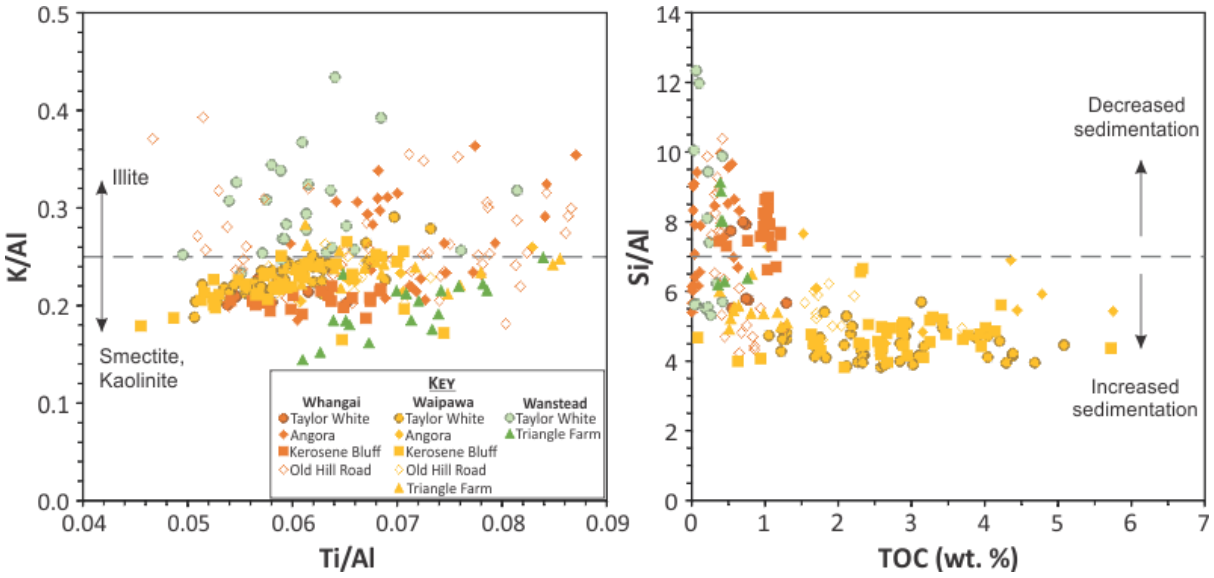

Figure 3.8: A) Potassium and Ti normalised to Al as provenance indicators. B) Sediment accumulation rates represented by Si/Al, relative to TOC values.

3.5.7 Stratigraphic variability – Taylor White case study

Complete stratigraphic exposure through the Waipawa Formation, where both upper and lower contacts are exposed is rare. At the Taylor White section, both are well exposed, and therefore, we use this section as a representative example of changes in geochemical relationships across formation boundaries (Figure 3.9). The sampling resolution across all sections in this study is considerably higher than previous studies, with 77 samples collected for pXRF analysis across the 80 m of outcrop measured at the Taylor White section. These are supplemented by a further 20 ICP-MS and fusion XRF analyses evenly distributed across the sample suite from this locality.

Titanium/Al values measured by pXRF lie within the same range of values across the Whangai, Waipawa and Wanstead formation at Taylor White. Lower resolution fusion XRF values also demonstrate no change in Ti/Al up-section (Figure 3.9). K/Al ratios show no change across the Whangai and Waipawa formations, but considerable variability across the Wanstead Formation (Figure 3.9). This is attributed to the alternating sandstone-mudstone of the Wanstead Formation sampled at this locality, and is attributed to mineralogical changes associated with grain size changes. Notably, mudstones samples from the Wanstead Formation have similar K/Al to the Whangai and Waipawa formations, showing that there is no noticeable change in clay mineralogy, and therefore provenance across these formation boundaries. This is consistent with the Ti/Al measured.

There is a decrease in Si/Al through the Whangai Formation, reaching a prolonged low in the Waipawa Formation (Figure 3.9), indicating increasing sediment supply/terrigenous influx leading

up to deposition of the Waipawa Formation. Changes in sediment accumulation, as measured by Si/Al, increases through the Waipawa Formation, before decreasing notably in the Wanstead Formation. The systematic variation in Si/Al through the Wanstead Formation arises from alternating sandstone-mudstones at Taylor White. Silicon/Al and the alternating sandstone-mudstone of the Wanstead Formation at Taylor White are indicative of higher sedimentation rates at this locality, associated with locally restricted turbidite deposition.

Nickel/Al, Cu/Al and Zn/Al demonstrate a small degree of covariance with TOC, however there are no substantial changes across formation boundaries. Nickel/Al and Zn/Al appear to demonstrate a stronger association with TOC than Cu/Al, suggesting that they are more responsive to changes in productivity. Changes in productivity proxies occur independently of changes in provenance and mineralogy. Iron values are relatively stable across all formations, although the Whangai and Wanstead formations generally have low S values, producing low S/Fe and S/TOC.

There is a distinctive broad double peak evident in the U_{auth}, Th/U, U_{EF}, HI and S/TOC trends, which fits the description of a 'double pulse' of organic carbon preservation across the Waipawa Formation described by previous authors (Leckie *et al.*, 1995; Hollis *et al.*, 2014). The top of the Waipawa Formation has a pronounced peak in Mo_{EF}, as measured by pXRF (EF = 15–18), however the ICP-MS measurements are somewhat lower (EF = 6), and demonstrate a double peak, consistent with other redox proxies. Calculation of TOC_{OR} suggest that as much as 40–50% of TOC has been remineralised, producing the elevated S concentrations within the Waipawa Formation.

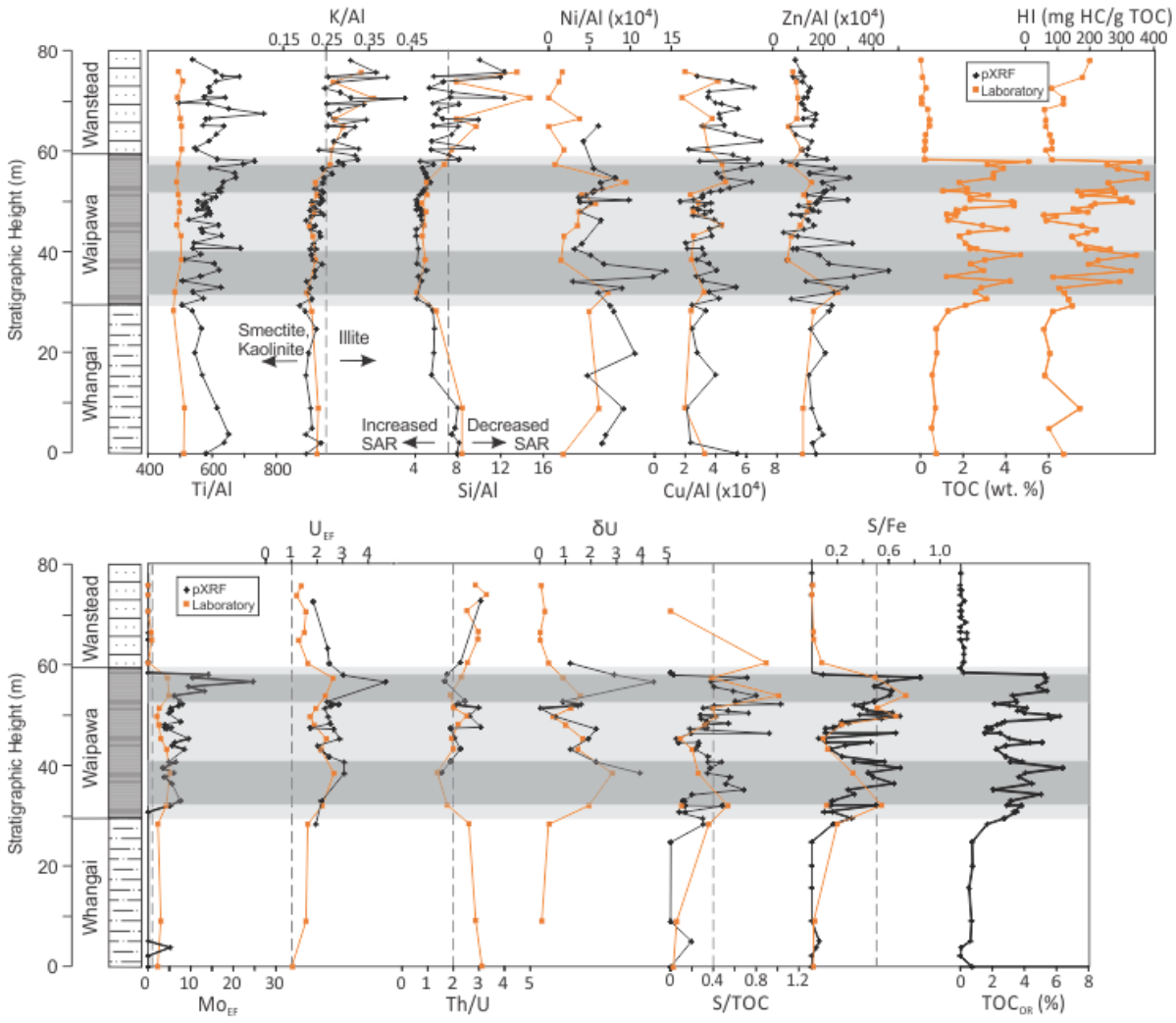

Figure 3.9: Selected elemental, and bulk pyrolysis data, enrichment factors and paleo-redox proxies against stratigraphic height in the Taylor White section, Southern Hawke's Bay. Shaded area indicates the Waipawa Formation, which here is underlain by the Upper Calcareous Member of the Whangai Formation and overlain by the Wanstead Formation. SAR = sediment accumulation rate.

3.6 Discussion

3.6.1 Chemostratigraphic framework

High-resolution sampling and multi-element geochemical analyses across the six sections studied here enable the correlation of geochemical trends. Principal component analysis reduces data dimensionality, summarises geochemical relationships as linear combinations of elemental data, and greatly facilitates interpretation, especially within lithologies. Cluster analysis successfully differentiates units at the formation and member levels and demonstrates that, despite small scale geochemical variability within and between sections, the lithostratigraphic units identified in this

study also represent chemostratigraphic divisions, with no significant intra-unit geochemical changes identified.

Cluster analysis differentiates three groups within the 372 samples analysed by pXRF. Cluster 1 (red; Figure 3.3) almost exclusively reflect samples from the turbidite sandstones in the Porangahau Member and the Wanstead Formation, and is differentiated on an increased Si and Zr content, consistent with the preferential partitioning of quartz and zircon in the coarse-grained (sand and silt) sediment fraction (Garcia *et al.*, 1994).

The Upper Calcareous Member is dominated by Cluster 2 (green, Figure 3.3), and to a lesser extent, the Porangahau Member and the Wanstead Formation. Cluster 2 is pulling out on the Mn, Sr and Zn eigenvectors, and as these all form cations that substitute into the carbonate matrix, we suggest that this cluster is differentiating (mildly) calcareous samples within these units.

Cluster 3 (blue; Figure 3.3) is almost entirely represented by samples from the Waipawa Formation, with the Fe, As and Pb eigenvectors likely associated with the strong sulphide component of the formation. Likewise, we suggest that the Ti and Al eigenvectors in Cluster 3 are representative of the increased sedimentation rate relative to other units (as shown by Si/Al), and the Rb and K eigenvectors responding to a shift in clay mineralogy across the formation (as shown by K/Al as proxy for bulk clay mineralogy). This chemostratigraphic framework demonstrates that the depositional conditions of the Waipawa Formation represent a broad deviation from the background depositional trends of both the underlying and overlying Whangai and Wanstead formations.

3.6.2 Redox Conditions

The deposition of black shale events represents a change in oceanographic conditions or depositional setting, creating a deviation from the background sedimentary signal (Algeo, 2004). This may be controlled by local upwelling, shifts in bottom water circulation, increased marine productivity, changes in sedimentation rate and burial, or a combination of these factors (Arthur & Sageman, 1994; Katz, 2005; Brumsack, 2006; Algeo & Maynard, 2008). Increased productivity during the time of deposition of the Waipawa Formation has been suggested by some authors as the cause for increased TOC (e.g. Killops *et al.*, 2000; Hollis *et al.*, 2014). Increased marine productivity requires an influx of bioavailable nutrients (e.g., Fe, Mn), requiring either upwelling to provide nutrient-rich waters or, alternatively, increased terrestrial discharge (Katz, 2005; Brumsack, 2006). This is difficult to reconcile with the inferred paleogeography of the region

during the Paleocene: a low-lying landmass with low erosion rates (Field & Uruski *et al.,* 1997; King *et al.*, 1999). In addition, paleo-productivity proxies (Ni/Al, Zn/Al, Cu/Al) considered in this study suggest a minor increase in marine productivity and preservation (Figure 3.9). Proxies for marine productivity and organic matter accumulation (Ni, Cu, Co, and Pb) show little relative enrichment or depletion between the Whangai, Waipawa and Wanstead formations (Figure 3.5; Table 3.1), yet there is significantly lower preservation of TOC in the Whangai and Wanstead formations. This indicates that a similar degree of marine productivity was present throughout the deposition of the Whangai, Waipawa and Wanstead formations. However, sediment accumulation rates (shown by Si/Al) show an increase during deposition of the Waipawa Formation, consistent with the changes in sedimentation rates across the Waipawa Formation determined by Hollis *et al.* (2014). Increased sedimentation rates in the Waipawa Formation (shown by decreased Si/Al), suggest that the elevated terrigenous flux was associated with increased supply of terrestrial organic matter shown by palynomorph studies of the Waipawa Formation (Clowes*,* in review). Therefore, the increased terrigenous sedimentation was accompanied by high terrestrial organic matter export, burial and preservation in slope-basin sediments. As Si/Al track an increase in sedimentation rate through the Waipawa Formation, enhanced organic matter preservation can be attributed to reduced oxygenation, as well as increased settling velocities and rapid burial preventing organic matter degradation.

3.6.3 Paleo-depositional setting

The broad distribution of the Waipawa Organofacies around the proto-New Zealand subcontinent suggests a regional influence for the deposition of organic-rich mudstone in shelf-slope sediments during the late Paleocene. Therefore a change in oceanographic conditions is the most plausible scenario for a regional change in depositional conditions that resulted in the deposition of the Waipawa Organofacies. Recently, two authors have suggested that a regression in eustatic sea level (e.g., Schiøler *et al.*, 2010; Hollis *et al.*, 2014) at this time may have been the causal mechanism. This would be consistent with increased sedimentation rates across the Waipawa Formation, whereby terrigenous sediments largely bypass exposed shelf areas, resulting in increased sediment deposition at bathyal depths.

The Upper Calcareous Member of the Whangai Formation is interpreted as being deposited during a transgression (Hollis *et al.*, 2014). Trace metal indices in the Whangai Formation indicate an oxic water mass during deposition, suggesting that anaerobic respiration was restricted to pore fluids below the sediment-water interface (Figure 3.10).

Some authors have described the Waipawa Formation as a two-phase depositional event, with a double pulse in TOC values (Killops *et al.*, 2000; Hollis *et al.*, 2014). Total organic carbon values measured through the sections sampled in this study are variable, and the 'double pulse' trend is not always apparent in the TOC data. However, there are two broad peaks present within HI, S/TOC and U_{auth} data from this study (Figure 3.9), supporting a two phase shift in paleoceanographic conditions during deposition of the Waipawa Formation, superimposed with variable preservation of organic carbon. In other coeval sections (for instance, Mead Stream) there is a very conspicuous double occurrence of black mudstone (Strong *et al.*, 1995; Hollis *et al.*, 2005a, b; Hines *et al.*, 2013).

A fall in eustatic sea level during the Late Paleocene is recorded in the Cenozoic sea level records of Haq *et al.* (1987), Hardenbol (1998) and Schmitz *et al.* (2011), with decreases in eustatic sea level across the known age range of the Waipawa Formation (59.4–58.7 Ma; Hollis *et al.*, 2014) corresponding to the Sel2/Th1 and Th2 sequence boundaries in the European succession (Hollis *et al.*, 2014). Estimates of the magnitude of this sea-level fall vary between ~12 and >50 m (Hollis *et al.*, 2014 and refs therein). This relative fall in sea level that coincided with the deposition of the Waipawa Formation, may have resulted in the exposure of large portions of the shelf. Consequently, terrigenous sediment largely bypassed shelf areas, increasing the delivery of terrestrial organic matter and increased nutrient flux to distal margins of the basin (Figure 3.10). The increased nutrient flux amplified marine productivity, increasing aerobic respiration in surface waters and creating an enhanced oxygen minimum zone, thereby facilitating the increased export of organic carbon and trace elements to the seafloor. The lithological contact between the Whangai and Waipawa formations is typically abrupt (over several centimetres); however, a gradual increase is apparent in TOC, S and trace metals concentrations across 1–2 metres between the Whangai and Waipawa formations, suggesting that this was a gradational transition.

The short-term sea-level record of Haq (2014) suggests a regression occurred c. 59.5 Ma, which may correspond to or immediately precede the first 'pulse' of TOC in the Waipawa Formation. This was subsequently followed by peak regression at c. 59.1 Ma, which assuming a linear sedimentation rate through the Waipawa Formation (as per Hollis *et al.*, 2014), would correspond with the middle of the Waipawa Formation where there is a notable decrease in reducing conditions and TOC preservation. Redox conditions fluctuated between anoxic to oxic/dysoxic during deposition of the Waipawa Formation. Full anoxia was only achieved within the Waipawa Formation for two brief periods (demonstrated by the double pulse in HI, U_{auth}, Th/U, S/TOC), and separated by a period of oxic to dysoxic conditions. Multiple records demonstrate that this is

a widespread signal across the basin, supporting the concept of two regressive cycles through the deposition of the Waipawa Formation.

There is a substantial increase in the HI of the Waipawa Formation relative to the enclosing Whangai and Wanstead formations, indicating a significant increase in organic matter richness in the Waipawa Formation. Surface water productivity may have been enhanced during deposition of the Waipawa Formation due to increased rate of nutrient supply, indicated by HI values increasing from ~100 mg HC/g TOC in the Whangai and Wanstead formations to ~350 mg HC/g TOC in the Waipawa Formation (e.g., Röhl & Schmid-Röhl, 2005). This is supported by a degree of covariance between paleoproductivity proxies (Ni/Al, Zn/Al and Cu/Al) and TOC (e.g. Figure 3.9). Oxygen supply may have been further depleted by biochemical demand for respiration and decomposition (Katz, 2005), meaning that the rate of organic matter supply exceeded oxygen supply in the basin, further exacerbating reducing conditions during deposition of the Waipawa Formation. The high HI and high TOC of the Waipawa Formation is consistent with shales deposited in a dysoxic to anoxic setting, resulting in increased preservation of Type-II kerogen (Tyson, 2005). The mixed Type-II and Type-III kerogen in the Waipawa Formation indicate a mixed marine algal- terrestrial plant organic matter source. Strongly enriched S concentrations, S/TOC relationships and calculated TOC_{OR} values imply that as much as 40–50% of the original organic matter was reduced on the seafloor. Increased organic carbon export to the seafloor under reducing conditions promotes microbial anaerobic reduction, resulting in the formation of free hydrogen sulphide, which is sequestered into the formation of authigenic sulphide phases in association with Cu, Fe, Pb, Ni, Cr and Mo (Figure 3.10). This in turn remineralises trace metals exported in association with organic complexes.

The abrupt transition from the Waipawa Formation into the Wanstead Formation marks marine transgression and a return to fully oxic conditions within the basin and sediments. Sedimentation rates during deposition of the Wanstead Formation were substantially lower than during deposition of the Waipawa Formation, and, as such, pervasive bioturbation of sea floor sediments resulted in the depletion, and cycling back into the water column of many trace element species, along with the near-complete degradation of organic matter, with preservation of only residual inert Type-IV kerogen (Figure 3.10).

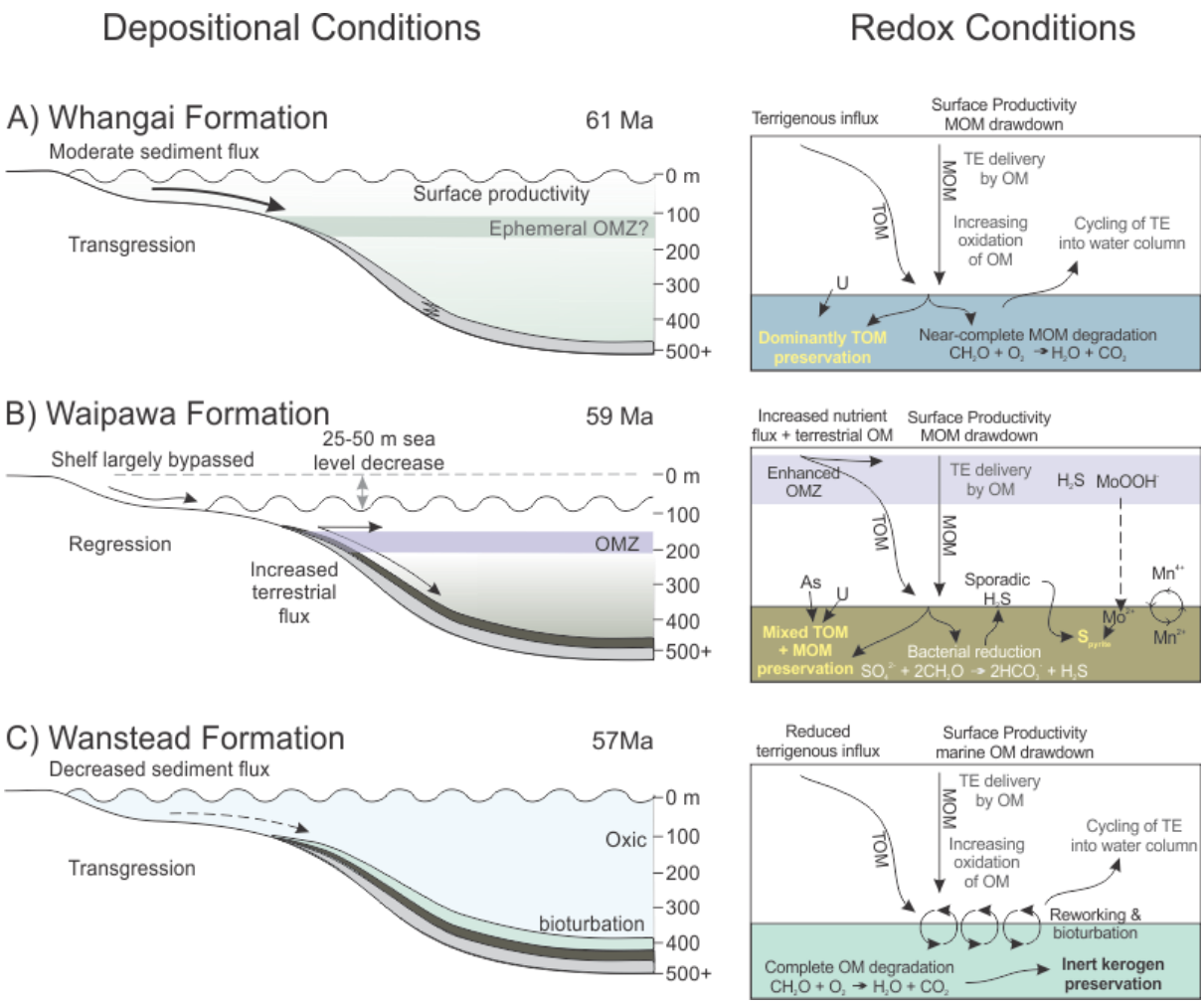

Figure 3.10: Depositional model for the Whangai, Waipawa, and Wanstead formations and the corresponding redox conditions during sediment deposition. OMZ = oxygen minimum zone, OM = organic matter, TOM = terrestrial organic matter, MOM = marine organic matter, TE = trace elements. A). Increasing oxidation of marine organic matter with depth and further reduction at or below the sediment water interface results in the cycling of most trace elements back into the water column. B). Increased nutrient flux causes increased marine organic matter production in tandem with terrestrial organic matter influx, resulting in an enhanced oxygen minimum zone. This promotes the preservation and delivery of organic matter to the seafloor, and anoxia at or below the sediment-water interface, C). Drawdown of marine organic matter through fully oxic conditions results in near-complete oxidation degradation of Type II and III kerogen. Any remaining organic matter is further degraded by pervasive bioturbation in conjunction with slow sedimentation rates.

3.7 Conclusions

The application of pXRF instrumentation to multiple sample suites through the latest Cretaceous–Paleocene succession of the East Coast Basin has generated a substantial amount of major and trace element data to assess the redox conditions during deposition. When compared to laboratory-based instrumentation, pXRF typically produces accurate measurements of many major elements

and trace elements, even at low concentrations, and proves to be a useful tool in the geochemical assessment of mudrocks. Across the six sections sampled and analysed in this study, PCA based on elemental data yields a consistent chemostratigraphic subdivision that differentiates the Waipawa Formation from the Whangai and Wanstead formations.

Redox proxies for the Whangai Formation show that it was deposited beneath an oxic water column, with a low to moderate sedimentation rate and terrigenous influx that included terrestrial organic matter.

Decreased Si/Al values show that sediment accumulation rates increased during deposition of the Waipawa Formation. Redox proxies (Th/U, U_{auth}, S/TOC) show two pulses of reducing conditions in the Waipawa Formation, which fluctuated between states of anoxic to dysoxic conditions in tandem with short-term changes in sea-level, with peak anoxia and organic carbon preservation coinciding with sea-level fall and regression. We infer that during regression, increased exposure of the shelf and sediment bypassing resulted in increased sediment and nutrient flux to the sites of Waipawa Formation accumulation, thereby increasing surface water productivity, and expansion of the oxygen minimum zone, as well as increasing both the burial rate and the volume of terrestrial organic carbon exported to the sea floor.

The overlying Wanstead Formation accumulated under slow sedimentation rates, with pervasive bioturbation and fully oxic conditions resulting in low TOC values comprised of Type-IV (inert) kerogen and trace element enrichment factors that deviate little from average shale values.

Changes in sea level explains the broad distribution of the Waipawa Formation, both within the basin and throughout the Southwest Pacific. Sea level regression accounts for the influx of increased terrestrial organic matter and increased sedimentation rates, particularly during a period of passive margin sedimentation in the New Zealand sector of the Southwest Pacific.

Acknowledgements

Funding for this research comes from the Sarah Beanland Memorial Scholarship, awarded to BRH by GNS Science. We are grateful for the support of Richard Sykes (GNS Science) and the GNS Science - Petroleum Source Rocks & Fluids programme (MBIE contract C05X0302), and also to Direct Crown Funding provided to GNS Science as part of the Petroleum Basins Research programme. The authors would like to thank Annette Rodgers for assistance with the pXRF unit housed at Waikato University. We are grateful for the in-depth comments from Marcus Kunzmann and Susanne Schmid on an early draft of this paper.

Chapter Four

DEPOSITIONAL FRAMEWORK FOR THE WAIPAWA FORMATION, EAST COAST BASIN, NEW ZEALAND:

'The information available in the case of Gisborne [and the East Coast region] is practically limited to the classification of strata in a few areas and some general speculations in geology… Compared with Taranaki and the Kotuku and Lake Brunner districts, Gisborne is exceedingly difficult country in which to conduct survey works. My summary of the survey results is, consequently, not quite satisfactory.

– J. D. Henry of the Colonial Oil Authority in: Oil Fields of New Zealand (1911).

View overlooking the Mead Stream gorge from Mead Hill. The range crest marks the approximate position of the Waipawa Formation.

PREFACE TO CHAPTER FOUR

The Waipawa Formation forms an important, isochronous surface across the East Coast Basin, and the wider Southwest Pacific, allowing direct correlation of the sequences across the various facies associations of the East Coast Basin, as well as forming a distinctly recognisable, pre-Neogene timeplane across the basin, which has utility in tectonic reconstructions.

Despite significant interest as a petroleum source rock, the depositional conditions of the formation have been widely debated. In particular, the application of a sequence stratigraphic interpretation across the Waipawa interval has required a multi-disciplinary study to assess the deposition conditions of the Waipawa Formation and correlatives within, and beyond, the East Coast Basin, presented here. Chapter Three acts as a detailed case study through the Whangai, Waipawa Formations in six specific sections. This chapter expands beyond these sections, focussing primarily on changes in the Waipawa Formation across the various facies association sin the East Coast Basin.

This chapter has been prepared in manuscript format for submission to the journal *Marine and Petroleum Geology*, and as such, follows formatting and structural conventions in line with the submission requirements of this journal. The development of this manuscript has been a collaborative process, with the contribution of the co-authors outlined below:

- *Ben Hines* – Measured sections, sample collection and preparation, bulk rock portable XRF analyses, data interpretation manuscript preparation.
- *James Crampton* – Project supervision, editorial process.
- *Kyle Bland* – Project supervision, editorial process.
- *Michael Gazley* – Provision of portable XRF instrumentation and standards, XRD analyses.
- *Katie Collins* – Editorial process, portable XRF analyses.
- *Yulia Uvarova* – XRD analyses.
- *Todd Ventura* – Source Rock Analyses.

Chapter Four

DEPOSITIONAL FRAMEWORK FOR THE WAIPAWA FORMATION, EAST COAST BASIN, NEW ZEALAND: *controls on Paleocene black shale deposition in the southwest Pacific*

In Preparation for:

Marine and Petroleum Geology

Corresponding author:
Benjamin R. Hines
Victoria University of Wellington, PO Box 600, Wellington, New Zealand
Email: ben.hines@vuw.ac.nz
Phone: +64 27 3056576

Co-authors:
James S. Crampton
GNS Science, PO Box 30-368, Lower Hutt, New Zealand, and
Victoria University of Wellington, PO Box 600, Wellington, New Zealand
Email: j.crampton@gns.cri.nz

Michael F. Gazley
CSIRO Mineral Resources, ARRC, PO Box 1130, Bentley 6102, Western Australia, Australia, and
Victoria University of Wellington, PO Box 600, Wellington, New Zealand
Email: michael.gazley@csiro.au

Yulia Uvarova
CSIRO Mineral Resources, ARRC, PO Box 1130, Bentley 6102, Western Australia, Australia,
Email: yulia.uvarova@csiro.au

G. Todd Ventura
GNS Science, PO Box 30-368, Lower Hutt, New Zealand, and
Email: todd.ventura@smu.ca

Katie S. Collins
Victoria University of Wellington, PO Box 600, Wellington, New Zealand
Email: katiesusannacollins@gmail.com

Kyle J. Bland
GNS Science, PO Box 30-368, Lower Hutt, New Zealand
Email: k.bland@gns.cri.nz

4.1 Introduction

The East Coast Basin is situated along the eastern margin of New Zealand's North Island, from East Cape, through to the Kaikoura Peninsula in the South Island (Figure 4.1). It covers approximately 75,000 km^2, half of which lies offshore. It is bounded to the west by the NE–SW-trending axial ranges of North Island, and extends eastwards offshore to the Hikurangi Subduction Margin. The basin itself has been partially uplifted by modern convergent tectonics; present-day elevations area are up to 2880 m above sea level, and water depths of offshore parts are in places more than ~1000 m. Sedimentary fill within the basin ranges from Early-mid-Cretaceous through to the Quaternary, and is on the order of 10,000 m-thick in the thickest and most complete sections of the basin (Grindley, 1960; Field & Uruski *et al.*, 1997).

Oil and gas seeps are common across the East Coast Basin, with more than 300 seeps documented within the onshore portion of the basin (e.g., McLernon, 1978; Francis, 1992, 1994, 1995; Francis & Murray, 1997; Francis *et al.*, 2004; Ventura *et al.*, 2014). Sixty-two wells have been drilled onshore, and only three offshore. Despite the large number of seeps across the basin, none of these wells have proven to be productive, although oil and gas shows have been encountered in several wells. Analysis of outcropping potential source rocks of late Paleocene age suggest their thermal maturities are just below the oil window in most places, although in the subsurface, burial depths indicate that source rocks may be in the oil window, or have passed through it (Leckie *et al.*, 1992). However, most wells are too shallow to encounter this interval, with only a handful wells reaching strata older than Neogene.

These late Paleocene source rocks termed the Waipawa Formation (Hollis *et al.*, 2014), have been extensively studied in terms of source rock potential and organic geochemistry (e.g. Moore, 1988a, Moore, 1989a; Field & Uruski *et al.*, 1997; Killops *et al.*, 1997, 2000; Rogers *et al.*, 2001; Schiøler *et al.*, 2010; Hollis *et al.*, 2014; Ventura *et al.*, 2014). However, depositional conditions and environments are poorly characterised, with a wide range of paleoenvironmental interpretations and varied paleoredox conditions ascribed to the formation. Deeper marine, distal facies associations of these source rocks in the southern Wairarapa and Marlborough regions form important analogues for understanding the source potential and petroleum systems of the adjoining Pegasus Basin (Uruski & Bland, 2010; Hines *et al.*, 2013; Bland *et al.*, 2015).

In the East Coast Basin (Figure 4.1), thick siliceous to slightly calcareous hemipelagic mudstones of the Late Cretaceous to Paleogene sequence are divided by the relatively thin (~1.5–70 m thick), but distinctive Waipawa Formation. This is underlain by the Whangai Formation and its various members, and overlain by the Wanstead Formation. The Waipawa Formation forms a distinctive,

approximately isochronous stratigraphic plane across the East Coast Basin, making it particularly useful for identification of facies associations, as a marker horizon in sequence stratigraphic interpretations, and for identifying potential piercing points in tectonic reconstructions.

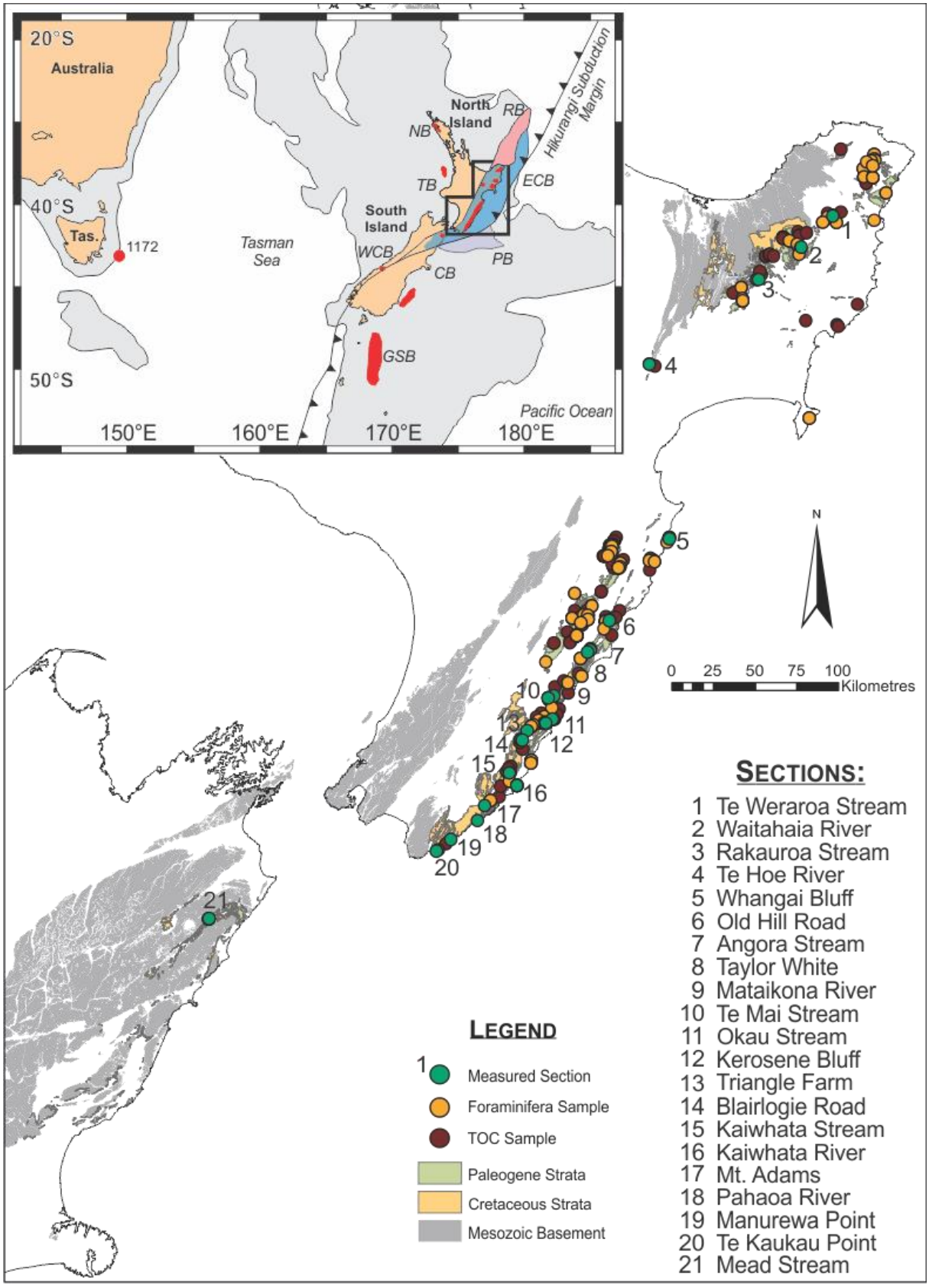

Figure 4.1: Location of outcropping Cretaceous and Paleogene strata in the East Coast Basin, and the location of source rock analyses, foraminiferal samples and measured sections referred to in text. Inset: Map of the Southwest Pacific showing the distribution of the Waipawa Organofacies (modified from Killops *et al.* 2000; Hollis *et al.* 2014). Base map data sourced from Heron (2014). Key to abbreviations;

ECB = East Coast Basin, RB = Raukumara Basin (pink), PB Pegasus Basin (purple), TB = Taranaki Basin, NB = Northland Basin, GSB = Great South Basin, CB = Canterbury Basin, WCB = West Coast Basin; 1172 = ODP Site 1172

4.1.1 Geological Setting

The Late Cretaceous-Paleogene stratigraphic succession of the East Coast Basin has a general fining-upwards trend, and records the cessation of Mesozoic subduction, followed by thermal subsidence and the onset of passive margin sedimentation (Moore, 1988b; Field & Uruski *et al.*, 1997; King *et al.*, 1999; King, 2000b). This first-order depositional sequence was interrupted by the inception of the modern Hikurangi subduction margin in the Late Oligocene to Early Miocene (King, 2000b; Nicol *et al.*, 2007). The western edge of the basin has been uplifted and exposed as a fore-arc basin-accretionary wedge complex during subsequent Neogene deformation, providing exposures of the Late Cretaceous to Paleocene strata examined in this study (Pettinga, 1982; Berryman, 1988; Ballance, 1993a; Lewis & Pettinga, 1993; Field & Uruski *et al.*, 1997; Nicol *et al.*, 2007).

The basement of the East Coast Basin primarily consists of Triassic to latest Early Cretaceous metasedimentary rocks of the Torlesse Supergroup, which were deposited along with associated volcanics in probable deep marine basins adjacent to the eastern Gondwana subduction margin (Moore & Speden, 1979, 1984; Field & Uruski *et al.*, 1997; Mortimer *et al.*, 2014). Subsequently, sedimentation in the basin during the Late Cretaceous was dominantly marine sandstones and mudstones in environments ranging from shelfal to lowermost slope settings, with sediments in the eastern portion of the basin likely representing infilling of one or more trench-slope basins in the stalled eastern Gondwana subduction system (Crampton, 1997).

The Upper Cretaceous to Oligocene sedimentary succession consist of variably siliceous and calcareous mudstone with localised occurrences of glauconitic sandstone and turbidite sequences (Moore, 1988b, 1989). This period is believed to have been tectonically stable, representing a time of quiescence and passive margin sedimentation, although there may have been instances of localised tectonic activity (e.g. Moore, 1980, 1989b; Isaac & Mazengarb, 1994; Crampton & Laird, 1997; Hines *et al.*, 2013). The late Piripauan to Teurian Whangai Formation is 100 to 500 m thick and occurs throughout the east coast (Moore, 1988a), with the Herring, Woolshed and Conway formations identified as correlative units in the Marlborough region (Crampton *et al.*, 2003, 2006). Further afield, lithologically similar correlatives have been identified in New Caledonia, DSDP sites 207 and 275, Northland, and the Canterbury and Great South Basins (Crampton, 1988; Moore,

1988a; Laird, 1992; Isaac *et al.*, 1994; Isaac *et al.*, 1996; Field *et al.*, 1997; Maurizot, 2011). Despite being largely homogeneous in appearance, the Whangai Formation has been subdivided into several lithofacies-based members across its lateral and vertical extent in the East Coast Basin: the Kirk's Breccia, Rakauroa, Upper Calcareous, Porangahau and Te Uri members (Figure 4.2; Moore *et al.*, 1986; Moore, 1988a; Field & Uruski *et al.*, 1997).

Whangai Formation is overlain by 10–50 m of brown-black, micaceous Waipawa Formation, of late Paleocene age. The Waipawa Formation is a regionally-extensive unit, and has been identified in Northland, offshore Taranaki Basin, and Marlborough, with the correlative Tartan Formation in the offshore Canterbury and Great South Basins (Isaac *et al.*, 1994; Isaac *et al.*, 1996; King & Thrasher, 1996; Killops *et al.*, 1997, 2000; Schiøler *et al.*, 2010; Hollis *et al.*, 2014). Waipawa Formation was originally defined from onshore outcrops in eastern North Island, where it typically comprises poorly-bedded, dark-brown to grey to brownish-black carbonaceous mudstone with moderate to high total organic carbon (TOC = 0.5–13%), and a positive shift in $\delta^{13}C$ (Moore, 1988a, 1989; Rogers *et al.*, 2001; Hollis *et al.*, 2014). However, the definition of the Waipawa Formation has been extended to include dark-grey, siliceous, organic-rich mudstones in Marlborough (Hollis *et al.*, 2005a, b), and Northland, New Zealand (Isaac *et al.*, 1994; Hollis *et al.*, 2006), and dark-coloured mudstones of Paleocene age encountered in offshore petroleum wells in the Northland, northern Taranaki, and Canterbury-Great South basins, as well as beneath the East Tasman Rise (Figure 4.1). All of these occurrences of Waipawa Formation-like rocks have been recently referred to collectively as the "Waipawa Organofacies" (Figure 4.1; Schiøler *et al.*, 2010; Hollis *et al.*, 2014). Organic carbon isotopes and TOC enrichments across the Waipawa Organofacies display a distinctive 'double pulse' of what is inferred to represent enhanced organic carbon preservation (Leckie *et al.*, 1995; Hollis *et al.*, 2014). Existing biostratigraphic data suggest that deposition of the Waipawa Organofacies in the East Coast Basin occurred in the upper part of NZP5 Dinoflagellate Zone and calcareous nannofossil zones NP5–NP7, indicating a Selandian to Thanetian age (late Paleocene), and likely restricted to 59.4–58.7 Ma (Crouch *et al.*, 2001; Hollis *et al.*, 2014; Kulhanek *et al.*, 2015). In some parts of the East Coast Basin, correlative facies of the Waipawa Formation have been identified in the upper Te Uri Member in the Western Sub-belt (Rogers *et al.*, 2001), within the Kaiwhata Limestone at Pahaoa River mouth (Tayler, 2011; Kulhanek *et al.*, 2015), and within the Mead Hill Formation in Marlborough (Strong *et al.*, 1995; Hollis *et al.*, 2005). Correlatives of the Waipawa Formation have also been identified in sections along the southeastern Wairarapa coast (Hines *et al.*, 2013) in association with Paleocene limestones. The infaulted Paleogene sedimentary succession cropping out on the Wairarapa coast has been interpreted as an allochthonous block that likely provides the closest analogue of the

sedimentary succession in the offshore Pegasus Basin (Moore, 1988a; Uruski & Bland, 2010; Adams *et al.*, 2013a; Hines *et al.*, 2013; Bland *et al.*, 2015). The offshore extent of the Waipawa Formation in the East Coast Basin is unknown, as exploration wells have yet to penetrate the Paleogene succession (Schiøler *et al.*, 2010). No evidence of the Waipawa Formation has been identified offshore in the East Coast Basin, although this interval is likely removed by a sedimentary hiatus or unconformity in ODP Site 1124 on the Hikurangi Plateau (Davy *et al.*, 2008).

In much of the northern part of the East Coast Basin, the Waipawa Formation is overlain by Upper Paleocene to Upper Eocene Wanstead Formation, a smectitic, micaceous, calcareous, often highly bioturbated mudstone with isolated occurrences of micritic limestone and glauconitic sandstones. Although Wanstead Formation slumps readily in outcrop, and as such, is poorly exposed, its stratigraphic thickness is estimated to be between 100 and 500 m (Cole *et al.*, 1992). Wanstead Formation is truncated locally by Oligocene and Miocene unconformities. The Whangai-Waipawa-Wanstead succession grades laterally southward into the Awhea Formation and the Kaiwhata and Mungaroa Limestones in Wairarapa, and then into the Mead Hill Formation and Amuri Limestone in Marlborough.

From the Late Oligocene to Recent, the East Coast Basin has been tectonically active, and consequently has been deformed extensively and re-oriented following the inception of the Hikurangi Subduction Margin through the basin in the Late Oligocene to Early Miocene. Miocene strata in the East Coast Basin vary in thickness from 2000 m to 8000 m, and consist of mudstones and turbiditic sandstones (Grindley, 1960; Field & Uruski *et al.*, 1997; Begg & Johnston, 2000; Lee & Begg, 2002). There are several Miocene and Pliocene slope and forearc basins, which typically have dimensions of 30 km by 10 – 20 km, likely formed near the trench-slope break (Pettinga, 1982; Neef, 1992; Lewis & Pettinga, 1993). The Miocene-Pliocene boundary is typically represented by an unconformity, above which there is a general shallowing trend. In the Hawke's Bay-Wairarapa, the Pliocene to Pleistocene is represented by shelfal mudstones and shallow marine coquina limestones (Beu *et al.*, 1980; Beu, 1995; Field & Uruski *et al.*, 1997; Bland *et al.*, 2013).

Figure 4.2: Lithostratigraphic and chronostratigraphic framework for the late Cretaceous to early Eocene East Coast Basin. Measured sections from this study and Moore (1988a). Inset shows key measured sections from Figure 4.1 and Figure 4.4, and the location of the section line. ATF = Adams-Tinui Fault, UCM = Upper Calcareous Member, TUM = Te Uri Member. Base map data sourced from Heron (2014). New Zealand stage abbreviations: Mp = Piripauan, Dw = Waipawan, Dm = Mangaroapan, Dh = Heretaungan. International Stages: San. = Santonian, Maast. = Maastrichtian, Sel. = Selandian, Than. = Thanetian.

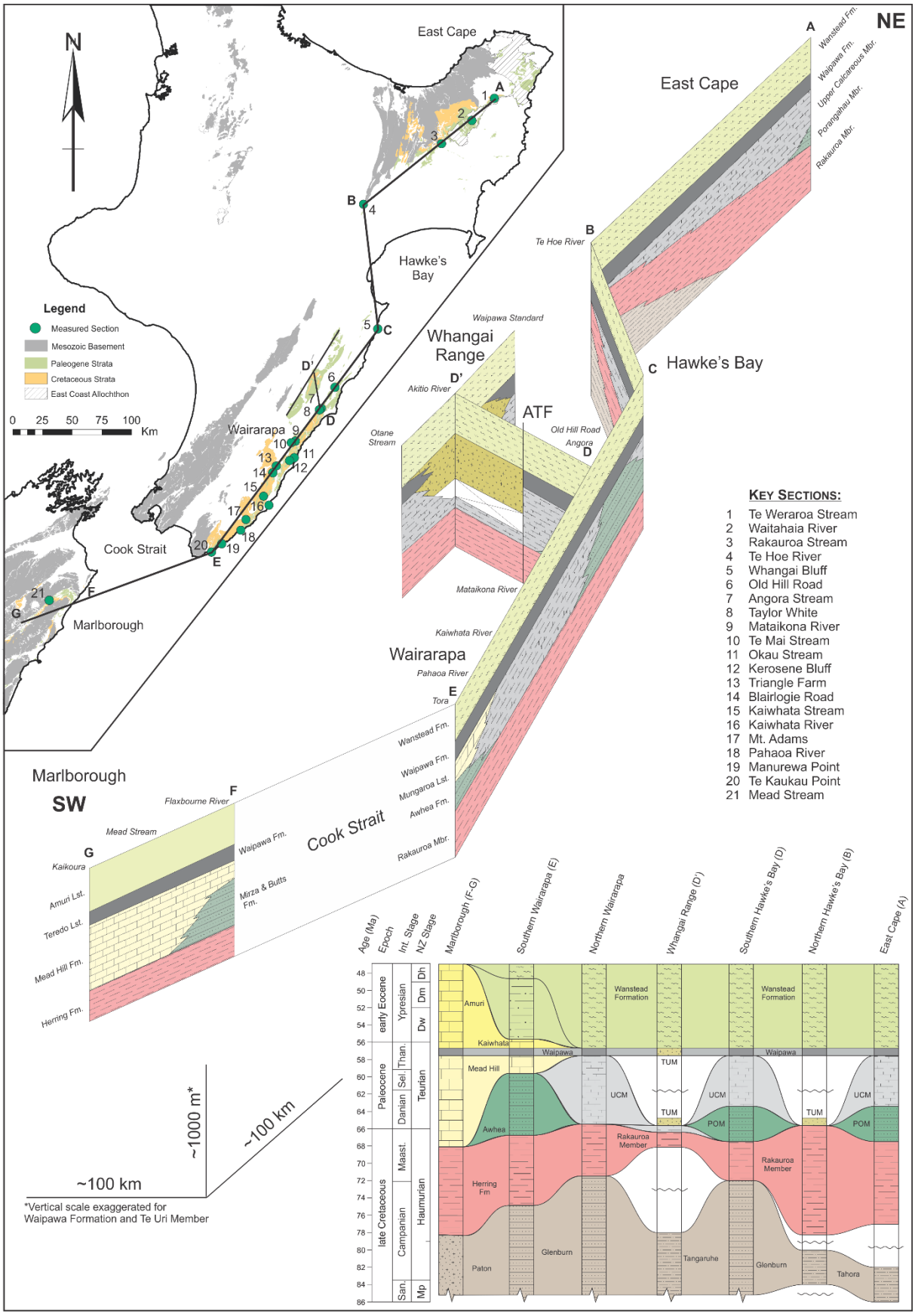

KEY SECTIONS:

1 Te Weraroa Stream
2 Waitahaia River
3 Rakauroa Stream
4 Te Hoe River
5 Whangai Bluff
6 Old Hill Road
7 Angora Stream
8 Taylor White
9 Mataikona River
10 Te Mai Stream
11 Okau Stream
12 Kerosene Bluff
13 Triangle Farm
14 Blairlogie Road
15 Kaiwhata Stream
16 Kaiwhata River
17 Mt. Adams
18 Pahaoa River
19 Manurewa Point
20 Te Kaukau Point
21 Mead Stream

4.2 Methods

The mechanism for carbon drawdown and enrichment in the Waipawa organofacies has not been satisfactorily explained, and models are variable, or focused on disparate aspects of the depositional system. Likewise, the type and quality of kerogen has not been satisfactorily explained by previous models, particularly with regard to the depositional environment of the Waipawa organofacies in the East Coast Basin. To address variability in previous interpretations, we apply a multidisciplinary approach to characterising source rock potential, paleo-redox conditions, environmental conditions, including depth and depositional environment, to provide an integrated model of depositional mechanisms. Multiple methods were applied to several measured sections to determine these characteristics, including foraminifera and ichnofacies assemblage characterisation to determine paleobathymetry, bulk rock inorganic geochemistry (portable X-ray florescence, pXRF; X-Ray diffraction, XRD) and organic chemistry (source rock analyses; SRA) to characterise paleo-redox states, sediment composition and relative accumulation rates, sediment provenance and source rock characteristics. This allows the characterisation of facies and depositional architecture for the Waipawa Formation and associated lithofacies (and organofacies), in a rigorous and consistent framework.

Five sections of typical Waipawa Formation (Old Hill Road, Taylor White, Angora Stream, Kerosene Bluff and Triangle Farm) from Hines *et al.* (Chapter 3) have been used as a starting dataset for the present study. The Hines *et al.* (Chapter 3) dataset comprises 372 pXRF analyses and 100 SRA analyses. To these data, here we add a further 461 pXRF, 162 SRA and 66 XRD analyses, from the five sections mentioned above and a further eight localities across the southern Hawke's Bay–Marlborough region (Table 4.1). An additional ten sections (Table 4.1) are included in the dataset in order to geochemically characterise and encompass the various depositional facies bracketing the Waipawa Organofacies within the East Coast Basin.

Table 4.1: List of measured sections and number of analyses run. Section numbers refer to Figure 4.2. Key to abbreviations: RAK = Rakauroa Member, POM = Porangahau Member, UCM = Upper Calcareous Member, TUM = Te Uri Member.

Locality	Locality No. (Fig. 4.2)	NZMS 260 Grid Ref.	Formation	pXRF	SRA	XRD
Waimarama	5	W22/526439	Whangai (POM)	51	-	-
Ongaonga Road		V22/131337	Whangai (UCM)	15	-	-
Old Hill Road	6	V24/162954	Whangai (POM)	55	24	-
			Waipawa	16	11	-
Taylor White	8	U24/044767	Whangai (UCM)	9	8	10
			Waipawa	44	36	20
			Wanstead	25	12	10
Angora Stream	7	U24/051785	Whangai (RAK)	10	2	-
			Whangai (POM)	8	3	-
			Whangai (UCM)	12	15	-
			Waipawa	6	6	-
Tawanui		U24/969863	Whangai (TUM)	17	-	-
			Wanstead	1	-	-
Big Saddle		U26 760342	Whangai (UCM)	17	-	-
Kerosene Bluff	12	U26/784331	Whangai (UCM)	19	17	1
			Waipawa	40	40	1
			Wanstead	1	1	1
Triangle Farm	13	T26/670291	Waipawa	25	13	3
			Wanstead	21	7	5
Bull Gully		U26/786326	Whangai (UCM)	26	-	-
Blairlogie Road	14	T26/647232	Waipawa	4	-	-
			Wanstead	5	-	-
Pahaoa River	18	T28/373751	Kaiwhata Limestone	1	-	-
			Waipawa	8	-	-
			Wanstead	7	-	-
Manurewa Point	19	S28/213638	Mungaroa Limestone	45	-	1
			Waipawa	6	6	1
Pukemuri Stream		S28/178615	Whangai (RAK)	96	-	1
			Manurewa	10	-	1
			Pukemuri Siltstone	-	-	1
			Wanstead	-	-	1
Cleft Section		S28/125566	Mungaroa Limestone	14	8	1
			Waipawa	8	8	1
Te Kaukau Point	20	S28/126 565	Mungaroa Limestone	25	-	-
			Waipawa	10	10	-
Opouwae River		S28/124570	Mungaroa Limestone	19	19	-
			Waipawa	9	9	1
Woodside Creek		P30/996192	Mead Hill	-	-	1
Benmore Stream		P30 932164	Herring	8	-	1
Swale Stream		P30/800189	Amuri Limestone	-	-	1
Mead Stream	21	P30/758160	Mead Hill	37	2	1
			Waipawa	7	5	1
			Amuri Limestone	8	-	-
Branch Stream		O30/685086	Amuri Limestone	85	-	-
Kaikoura		O31/668642	Herring	3	-	1
Total				**833**	**262**	**66**

4.2.1 Measured Sections and Sampling

Twenty-three sections in the East Coast Basin were sampled, located between Hawkes's Bay, Wairarapa, and Marlborough (Figure 4.1 & 4.2). Sections were measured using the tape and compass method, with sampling resolution accurate to 0.05 m; bed thicknesses were restored to true thickness trigonometrically. Twelve sections across the Waipawa Formation were measured in detail with a typical stratigraphic sampling resolution of 0.2–0.7 m, including six sections in Hawke's Bay and Wairarapa across the Whangai-Waipawa-Wanstead transition, and described in detail in Hines *et al.* (Chapter 3). In the measured sections, ~1 kg of fresh bulk rock was collected at each sample interval by removing ~20 cm of outcrop surface. In some instances, a duplicate sample of weathered material was collected from the same sample horizon.

4.2.2 Paleontology

Paleo-water depth estimates are based on selected benthic foraminifera species with calibrated minimum upper depth ranges (Figure 4.3; Appendix 5). These calibrations are derived from several sources, including the depth distribution of New Zealand Recent benthic foraminifera (Hayward, *et al.*, 2010), calibrated depth limits from New Zealand petroleum exploration wells (Hayward, 1986), and Deep Sea Drilling Project (DSDP) and Ocean Drilling Program (ODP) sites (Tjalsma & Lohmann, 1983; Van Morkhoven *et al.*, 1986). Benthic foraminifera typically occupy a range of depths, although the upper depth limit of a species can be a particularly useful paleoenvironmental and paleobathymetric tool (Van Morkhoven *et al.*, 1986). In addition, benthic foraminifera can also provide an indication of bottom water oxygenation (epifaunal species) and the oxygenation state of seafloor sediments (infaunal species) (Kaiho, 1994).

Foraminiferal census data were recovered from 947 samples from the New Zealand Fossil Record File (www.fred.org.nz), spanning the Whangai, Waipawa, Wanstead, Kaiwhata Limestone, Mungaroa Limestone, Manurewa, Pukemuri Siltstone, Awhea, Huatokitoki, Amuri Limestone, Teredo Limestone and Mead Hill formations. In reviewing the foraminiferal data from the late Cretaceous to Paleocene East Coast Basin, foraminiferal faunas of various workers and vintages were encountered, and careful vetting and editing of data was required in order to identify taxonomic synonyms and obsolete names (H. E. G. Morgans, pers. Comms. 2016).

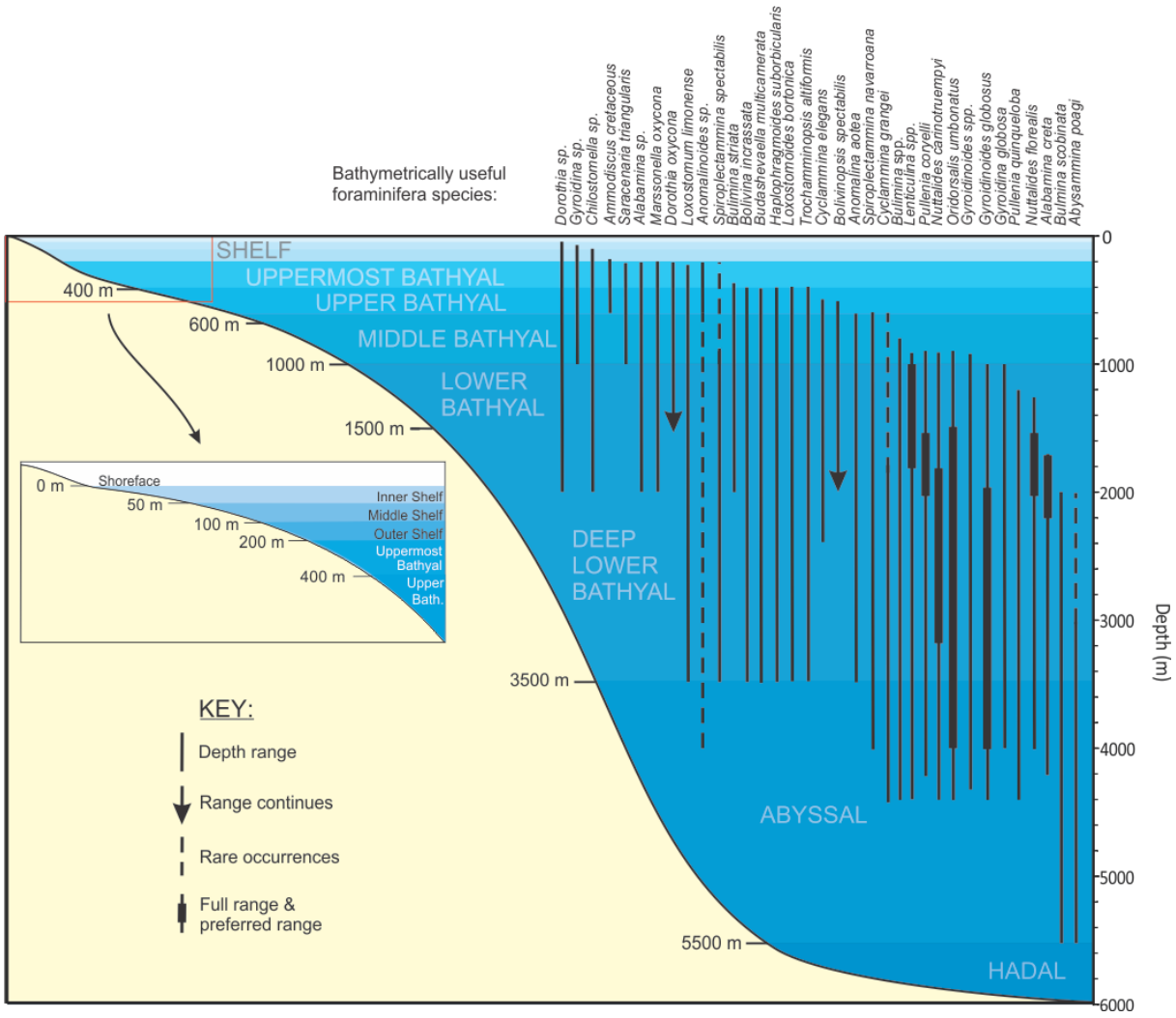

Figure 4.3: Paleoenvironmental classifications used in text, along with calibrated bathymetric ranges of benthic foraminifera species identified in the Cretaceous – Paleogene sediments of the East Coast Basin. Paleodepth ranges from Tjalsma & Lohmann (1983), Hayward (1986), and Van Morkhoven et al. (1986). Common foraminifera species from the Cretaceous – Paleogene East Coast Basin, with broad environmental preferences are included in Appendix 5. Paleodepth divisions from Morgans (2009) and Hayward *et al.* (2010).

4.2.3 Portable X-Ray Fluorescence

The pXRF data presented here were obtained by XRF analysis of 595 samples using an Olympus Innov-X™ Delta pXRF unit with a 10–40 kV (10–50 μA) Rh X-ray tube and a high-count rate detector. Portable XRF methods follow those of Hines *et al.* (Chapter 3), and are consistent with the approaches applied in Fisher *et al.* (2014) and Gazley and Fisher (2014). Samples were washed in distilled water to remove any adhering detritus and oven dried for 72 hours at 50 °C. They were then crushed using a Boyd Crusher with a 2 mm plate gap. The <1 mm sieved fraction was

presented to the pXRF unit covered with polyethylene-free Glad Wrap™. Analyses of Glad Wrap™ placed over a SiO_2 blank showed that no contamination resulted from this medium. Standards were run every 20 samples to allow the pXRF unit to be re-calibrated; they were a variety of research-grade, matrix-matched standards processed using the same analytical procedures as for the samples. Standards used were: BCS 267, BIR-1, G-2, GSP-1, JG-1 and PCC-1 (these are the same as utilised by Hines *et al.* (Chapter 3), which resulted in good correlations between laboratory and corrected pXRF data). The analytical uncertainty on each analysis is a function of run-time. To limit this uncertainty, but still maximise throughput, the total analysis time was set to 60 seconds (30 seconds per beam). Analytical uncertainties were typically ≤ 3% as reported by the pXRF unit. To check for contamination, SiO_2 blanks were analysed periodically.

Repeat analyses of the six standards were systematically collected during the analytical run, and show that the pXRF unit was very stable throughout. The median value for these standards was used to calculate a correction factor for each element. For most elements this took the form of $y = mx + c$ (where m is the slope and c is the offset); however, for some trace elements that have values that converge on 0, a $y = mx$ correction is often more appropriate (Fisher *et al.*, 2014). These standards were also used to calculate a lower limit of quantification (LOQ) following the approach of MacDougall and Crummett (1980), utilising repeated standard analyses. The majority of elements analysed return values above the lower limit for quantification (LOQ). These values are presented in Appendix 5, along with summary statistics for each element in the dataset (Appendix 5).

4.2.4 X-Ray Diffraction

A total of 66 samples were analysed by XRD in order to determine bulk rock modal mineralogy. This included a combination of detailed sampling in the Taylor White section, and spot samples from various localities (Table 4.1). X-ray diffraction (XRD) spectra of powdered samples for modal mineralogy were collected with a Bruker D4 Endeavor instrument fitted with a Co tube, Fe filter, and a Lynxeye position-sensitive detector, situated at the Australian Resources Research Centre, CSIRO, Perth, Australia. The measured 2-θ range was 5–90°, with a step size of 0.02° and a divergence slit of 1°.

4.2.5 Source Rock Analysis

Prior to this study, source rock analyses of the potential source rocks of the Whangai and Waipawa formations was limited to 172 analyses (Ventura *et al.*, 2014), largely from Moore (1988a) and

Leckie *et al.* (1992). With the exception of a few studies (e.g., Leckie *et al.*, 1992; 1995; Hollis *et al.*, 2014), these source rock analyses have been limited to reconnaissance-scale spot sampling across the basin. Sampling and analyses conducted for the present study has resulted in 226 new, stratigraphically constrained source rock analyses from eleven measured sections.

Pyrolysis measurements were made using a Source Rock Analyzer (SRA) from Weatherford Laboratories housed at GNS Science, Lower Hutt, New Zealand. Approximately 100 mg of powdered rock were used for each bulk pyrolysis sample measurement. The pyrolysis program was set with the sample crucible entering the pyrolysis oven, where it was held at 300°C for 3 minutes under a continuous stream of He carrier gas at a flow rate of 100 ml/minute. This was followed by a 25°C/minute ramp to 650°C. The S1 and S2 signal intensities were recorded with a Flame Ionization Detector operated under a 65 ml/minute stream of H_2 gas and 300 ml/minute air. The pyrolysis cycle was then followed by an oxidation cycle performed at 630°C for 20 minutes, during which time the oven and crucible were flushed with dry air at 250 ml/minute. The generated carbon monoxide and carbon dioxide gases were measured by the instrument's infrared cells. All sample sequences were run with three IFP 160000 analytical standard replicates (from Vinci Technologies, Institut Français du Pétrole) placed at the beginning, middle, and end of each sample sequence. Each sample sequence comprised 25 samples.

Important parameters derived from the source rock analyser include the S1 peak, which shows the volatile portion of geologically generated bitumen, the S2 peak, which shows the bitumen that would be generated if burial and maturation continued, T_{max}, which provides an estimate of thermal maturity of the rock, hydrogen index (HI) which allows the type of organic matter to be estimated, and the oxygen index (OI), which allows the thermal degradation of the kerogen to be estimated (Carroll & Bohacs, 2001).

Immature kerogen types can be determined using HI values, whilst in samples that have entered the oil window, kerogen type can be distinguished using a cross-plot of HI and OI, referred to as a pseudo-van Krevelen diagram, or using a cross-plot of HI vs T_{max} (Carroll & Bohacs, 2001). There are four kerogen types, which reflect the organic matter type and the generative potential of the kerogen (Carroll & Bohacs, 2001). Type I kerogen is characterised as being derived from lacustrine algal matter. Type II kerogen is a derived from marine organic matter, primarily algae. Type III kerogen has a terrestrial source, and is dominantly plant derived. An additional kerogen type, Type IV refers to inert, oxidised organic matter that has little to no volatile matter remaining.

4.3 Results

4.3.1 Stratigraphy and Sedimentology

The Waipawa Formation is typically a dark-brown to grey-black, micaceous, siliceous, non-calcareous, massive to weakly-bedded siltstone. The formation varies from 5 to 70 m-thick across the basin (Figure 4.4). Framboidal pyrite is common in thin-sections of the Waipawa Formation, and jarosite and gypsum are commonly observed on weathered outcrop surfaces (Appendix 5). Greensands are commonly associated with the Waipawa Formation, either as discrete beds within the formation (e.g. Okau Stream), or immediately underlying or overlying the formation (e.g. Otane Stream, Taurekaitai Stream, Mangatarata Valley; Mangawarawara Stream; see discussion). The base of the formation is typically gradational with the Upper Calcareous Member of the Whangai Formation, although in some localities it unconformably overlies Rakauroa Member (e.g. Rakauroa Stream, Taurekaitai Stream, Mangawarawara Stream) or disconformably overlies the Porangahau Member (e.g. Old Hill Road, Waimarama; Figure 4.4). In many outcrops the top of the formation is marked by an unconformable surface. Deformed beds, presumably formed by syn-depositional slumping, have been observed within the Waipawa Formation or sedimentary rocks immediately underlying the Waipawa Formation, in multiple localities (e.g. Old Hill Road, Kaiwhata Stream, Te Mai; Moore, 1989a; this study). *Bathysiphon* sp. foraminifera are common in the Waipawa Formation, and rare, largely decalcified and fragmentary bivalves and gastropods have been recovered (e.g. Moore, 1988a; Clowes *et al.*, 2016). Bioturbation is common and often pervasive in the formation, although it is often indistinct meaning individual traces are rarely identifiable.

The southeast Wairarapa coast between Glenburn and Te Kaukau Point contains outcrops of dark-coloured mudstones and shales within mid- to late Paleocene micritic limestones of the Kaiwhata and Mungaroa Limestones. Along with dark mudstones at Mead Stream Marlborough, these dark-coloured rocks have been correlated with the Waipawa Formation on the basis of age and organic carbon content (Hollis *et al.*, 2005a, 2014; Hines *et al.*, 2013; Kulhanek *et al.*, 2015). These sections include Pahaoa River Mouth, Manurewa Point, Opouwae River mouth and Te Kaukau Point, and are typically only 1-3 m-thick (Browne, 1987; Hollis & Manzano-Kareah, 2005; Hollis *et al.* 1998 [unpub], Tayler, 2011; Uruski & Bland, 2010; Hines, 2012, 2015; Hines *et al.*, 2013; Hollis *et al.*, 2014; Kulhanek *et al.*, 2015). Centimetre to dm-bedding and lamination are present at Pahoa River mouth, Manurewa and Te Kaukau points, and Mead Stream. Large (<8 cm) pyrite nodules and pyrite infilled *Ophiomorpha* burrows are reasonably common the Waipawa Formation at Te Kaukau Point (Appendix 5).

The uppermost beds of the Te Uri Member of the Whangai Formation have been geochemically correlated with the Waipawa Formation based on increased TOC and a positive $\delta^{13}C_{org}$ excursion relative to underlying sedimentary strata (Rogers *et al.*, 2001; Hollis *et al.*, 2014). The Te Uri Member is typically comprised of poorly-bedded glauconitic sandstone and mudstone, and varies from 5 to 40 m thick. Sedimentary structures include tool marks, cross-bedding and bioturbation (Leckie *et al.* 1992; this study).

4.3.2 Paleo-water depth Determinations

Foraminifera

Foraminiferal assemblages in the Whangai and Waipawa Formations are dominated by low-diversity, dominantly agglutinated faunas. Paleo-depositional depths of the Whangai Formation vary across the lateral extent of the basin. At Te Hoe River, a locality interpreted to mark the paleoshoreline in the Late Cretaceous (Piripauan; Isaac *et al.*, 1991), foraminifera from the latest Cretaceous to Paleocene Rakauroa and Te Uri members (e.g., *Ammodiscus cretaceous, Bolivinopsis spectabilis*) favour depositional depths between 200 and 500 m. Further north in the East Cape area, these depositional depths are better constrained to between 500–600 m in the Rakauroa and Upper Calcareous members, likely representing a deepening trend to the northeast. South of Te Hoe River, in the southern Hawke's Bay to northern Wairarapa regions, upper depositional depths for the Whangai and Waipawa formations are constrained to between 400 and 600 m, largely based on assemblages containing *Dorothia oxycona*, *Alabamina* sp. and *Ammodiscus cretaceous*. The Upper Calcareous Member in the Whangai Range produces foraminifera-based paleo-water depth estimates of ~200 m, shallower than the ~500 m paleo-water depths recorded for the Whangai Formation elsewhere in the surrounding area (Figure 4.4b). Although foraminiferal faunas from the Te Uri Member are poor, there is a notable reduction in inferred paleo-water depth from 500–600 m to 100–200 m between the Upper Calcareous Member and the Te Uri Member. Ichnofacies-based paleo-water depth estimates from the Te Uri Member at Tawanui imply an outer shelf (200–300 m) paleo-water depth (Leckie *et al.*, 1992; see below), consistent with foraminifera-based depth estimates, and notably shallower than strata of the same age outside of the Whangai Range. In southern Wairarapa, paleo-water depth estimates for the Whangai Formation, Waipawa Formation and the correlative Paleocene strata range between 600 and 1000 m, constrained to 800–1000 m paleo-water depth in the Tora Block, based on assemblages containing *Stensioina beccariiformis, Nuttallinella florealis, Rzehakina epigona* and *Kalamopsis grzybowskii*. Paleocene paleo-water depths from the Mead Hill Formation and Amuri Limestone are estimated to be between 800 and 1200 m, based on assemblages that include *Stensioina beccariiformis, Nuttallinella florealis,* and *Rzehakina*.

Almost all of the foraminiferal taxa recovered from the Waipawa Formation are comprised entirely of agglutinated forms, and are generally interpreted as opportunistic browsers or scavengers that quickly occupy a niche when it becomes unfavourable for cosmopolitan, calcareous species (Jones & Charnonk, 1985; Leckie *et al.*, 1992). Across a north–south transect of 30 foraminiferal faunas sampled from the Waipawa Formation, the minimum upper depth limit for foraminifera notably decreases southwards. Despite the broad paleo-water depth ranges inhabited by many species within these faunal assemblages, this provides some indication of changing paleo-water depth, as bottom water anoxia and environmental stressors likely suppress the maximum depth limit of these species. The poor faunas recovered from the Waipawa Formation likely resulted from syn-depositional poor bottom-water oxygenation. Species that are found in Waipawa Formation faunal assemblages are typically colonising species, the most obvious being *Bathysiphon* sp. The occurrence of clusters of *Bathysiphon* tests in the Waipawa Formation is commonly noted (e.g. Moore, 1980, 1987b, 1988a, 1989a; Leckie *et al.*, 1992, 1995; Appendix 5), although elsewhere they characteristically occur in association with turbidite/flysh deposits (e.g. Hines *et al.*, 2013; Miller, 1995, 2005). The large *Bathysiphon* individuals observed in the Waipawa Formation (*cf. B. boucoti*) preferred a seafloor environment receiving high-sedimentation and nutrients and are believed to have been able to exploit a pulsed delivery of organic material in a lower bathyal setting (Miller, 2005).

There is a substantial deepening trend observed across the transition into the Wanstead Formation (e.g. Hines *et al.*, 2013). Eocene sections of the Wanstead Formation often yield well-preserved, diverse deep-marine foraminiferal faunas (H. E. G. Morgans, pers. comms). Middle to Late Eocene faunas from the Wanstead Formation and Amuri Limestone have been ignored in this study, as they produce substantially deeper paleo-water depths than Teurian to Mangaorapan (Paleocene to Early Eocene) faunas and are not relevant to understanding of the Waipawa Formation and correlatives.

Bioturbation fabrics and Ichnofacies

An independent indication of paleo-water depth can be provided by trace fossil assemblages. The Waipawa Formation, in places, demonstrates evidence of bioturbation, although typically traces are indistinct and unidentifiable. However, the underlying units provide good indications of paleo-water depth, particularly in the Porangahau Member at Old Hill Road and Waimarama, the Mungaroa Limestone at Manurewa and Te Kaukau points, and the Te Uri Member at Tawanui.

Ichnofaunas of the Whangai Formation commonly include *Planolites*, *Chondrites* and *Zoophycos*, particularly the Porangahau Member and the Upper Calcareous Member directly underlying

Waipawa Formation, indicative of the *Zoophycos* ichnofacies (e.g. Ekdale, 1988). Trace fossils in the Mungaroa Limestone at Te Kaukau Point and Manurewa Point are well characterised as belonging to the deep marine *Zoophycos* to *Nerites* ichnofacies, indicating a mid-bathyal depositional setting (Hines, 2012; Hines *et al.*, 2013), and these ichnofacies are generally characteristic of the Cretaceous to Paleogene succession of the East Coast Basin. The depth ranges inferred for these ichnofacies support the paleo-water depth interpretations provided by benthic foraminiferal assemblages. The *Zoophycos* ichnofacies is typically developed in fine-grained sediments deposited in bathyal, oxygen-depleted environments (Ekdale, 1985; Ekdale & Mason, 1988; Leckie *et al.*, 1992; Bromley, 1996; Savrda *et al.*, 2001; Algeo & Maynard, 2004).

The uppermost Te Uri Member is, in places, intensely bioturbated with *Planolites*, *Thallasinoides, Teichichus* and *Skolithos* (Moore, 1987a; Leckie *et al.*, 1992; Rogers *et al.*, 2001), taxa that characterise the *Cruziana* ichnofacies. The occurrence of *Zoophycos* and *Teichichnus* bioturbation in the Te Uri Member indicates an assemblage of opportunists that colonise inhospitable zones on the limit of habitability (Bromley, 1990; Leckie *et al.*, 1992), and the *Cruziana* ichnofacies is inferred to be indicative of outer shelf depths (Ekdale, 1985).

Depositional Model Development

Few outcrops of the Waipawa Formation expose both the upper and lower contacts. Because Waipawa Formation is situated between the soft rocks of the overlying Wanstead Formation and comparatively competent rocks of the underlying Whangai Formation, it tends to accommodate deformation, in particular shearing and brittle deformation, between the two units. However, where complete sections are observed (e.g. Taylor White, Old Hill Road), they appear to define a distinct clinoform-like trend in stratigraphic thickness along an approximately north-south transect (Figure 4.4). It is important to remember that this transect is likely to be orientated obliquely to the paleo-slope, and that this trend may reflect the fact that the modern-day outcrop extent is arrayed somewhat obliquely to original depositional strike. At Te Hoe River, there is 10 m of Waipawa Formation overlying 10 m of Te Uri Member. Foraminiferal fauna here suggest that depositional depths may have been as shallow as 200 m, which is consistent with the shallow- to marginal-marine strata immediately underlying the 40 m of Whangai Formation at this locality. At Kerosene Bluff, one of the easternmost Waipawa Formation localities, there is 70 m of Waipawa Formation, with a depositional depth of 500–800 m. Further south, at Tora, the Waipawa Formation is only 1.8 m thick and has a minimum depositional depth of 800 m. At the southernmost outcrop of Waipawa Formation in the East Coast Basin, there is a 3 m-thick interval in Mead Stream, with a depositional depth of 900–1500 m (Strong *et al.*, 1995). Based on paleo-

water depth and lithofacies associations, Waipawa organofacies in the East Coast Basin can be divided into three distinct depositional facies:

1. Proximal Waipawa: Proximal Waipawa has a restricted outcrop distribution, identified only at Te Hoe River and the Whangai Range. It is defined here as the uppermost beds of the Te Uri Member cropping out in the Whangai Range that demonstrate a characteristic positive $\delta^{13}C_{org}$ excursion, and Waipawa Formation that was deposited in association with the Te Uri Member (Te Hoe River) that has a comparatively shallow depositional depth (200–400 m; likely outer shelf, Hollis *et al.*, 2014). The shallow-marine, clastic-starved Te Uri Member, the 'proximal' Waipawa, which is characterised by thick (>5 m) sections, with comparatively low-sedimentation rates, paleo-water depths of typically 200–600 m, and which are underlain directly by Whangai Formation and overlain by Wanstead Formation. Although the Te Uri Member in the Whangai Range is not strictly proximal, it shares a characteristically shallower depositional setting with the Te Hoe River section (see discussion).
2. Typical Waipawa: characterised by the 'typical' dark-coloured mudstones of the Waipawa Formation deposited in association with the Whangai and Wanstead formations (e.g. as at Taylor White, Angora Stream, Old Hill Road, Triangle Farm, Kerosene Bluff, Blairlogie Road). Typical Waipawa Formation is characterised by a stratigraphic thickness of 10–50 m in the Western Sub-belt, and depositional depths of 400–500 m. In the Coastal Block of the Eastern Sub-belt, thicknesses range up to 70 m, although typically 50 m or less, and have foraminiferal faunas that indicate depositional depths of 500–600 m, although perhaps as much as 800 m in southern areas, such as Tora.
3. Distal Waipawa: characterised by thicknesses typically <5 m, paleo-water depths of >800 m, and deposition in association with deep marine micritic limestones (e.g. Pahaoa River, Manurewa Point, Te Kaukau Point, Opouwae River and Mead Stream). Across the Adams-Tinui Fault, in the Tora Block of the Eastern Sub-belt, there is an abrupt change in facies association from typical Waipawa to distal Waipawa, and depositional paleo-water depths shift to 600–1000 m. Depositional depths at Tora, constrained by foraminiferal faunas, indicate depths >800 m, whereas further south, at Mead Stream, the depositional depth of the Waipawa Formation is between 900–1500 m, likely in the range of 1000–1200 m.

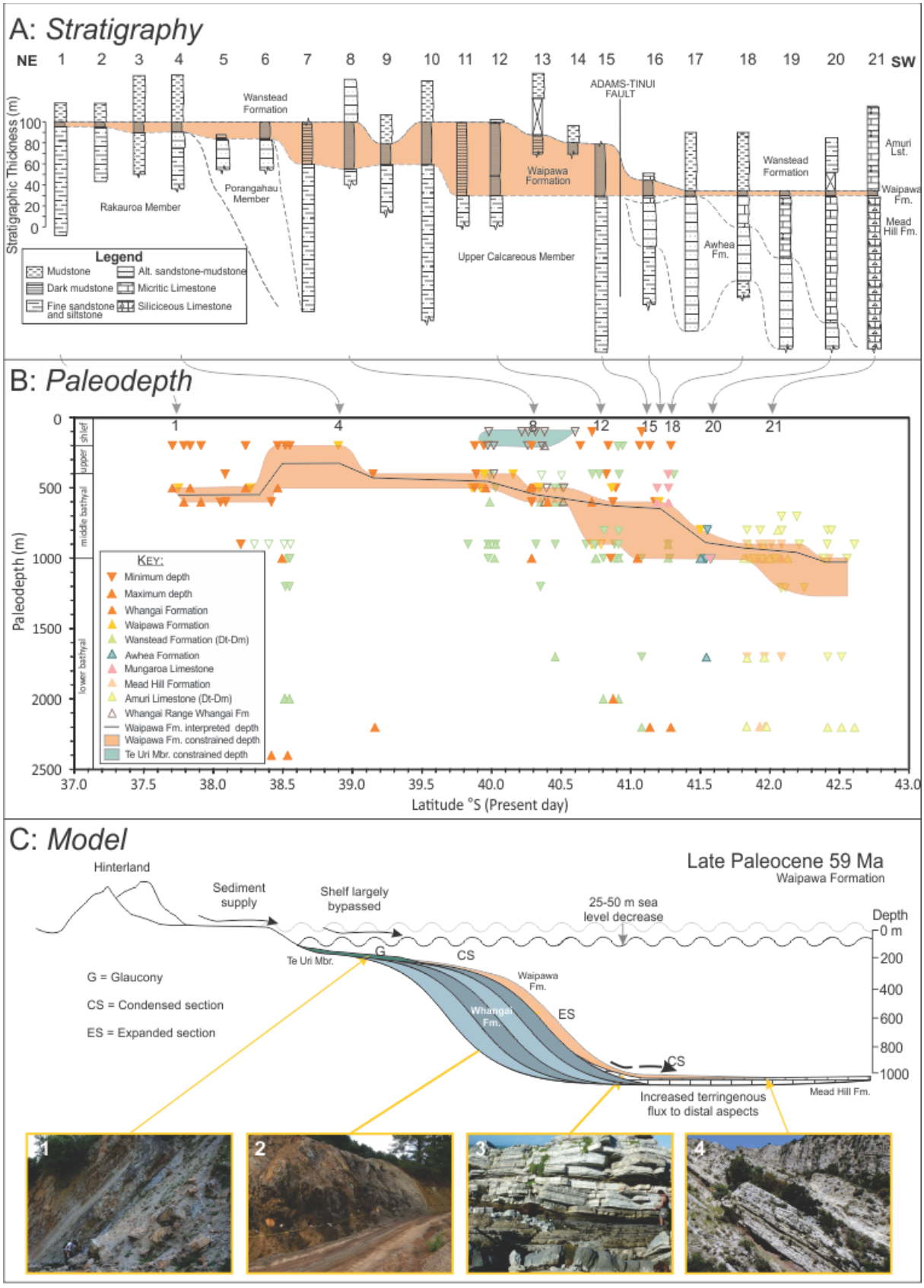
A: Stratigraphy
NE
SW
Stratigraphic Thickness (m)
Wanstead Formation
ADAMS-TINUI FAULT
Waipawa Formation
Amuri Lst.
Waipawa Fm.
Mead Hill Fm.
Porangahau Member
Rakauroa Member
Upper Calcareous Member
Awhea Fm.
Legend
Mudstone
Alt. sandstone-mudstone
Dark mudstone
Micritic Limestone
Fine sandstone and siltstone
Siliciceous Limestone
B: Paleodepth
Paleodepth (m)
shelf
upper bathyal
middle bathyal
lower bathyal
KEY:
Minimum depth
Maximum depth
Whangai Formation
Waipawa Formation
Wanstead Formation (Dt-Dm)
Awhea Formation
Mungaroa Limestone
Mead Hill Formation
Amuri Limestone (Dt-Dm)
Whangai Range Whangai Fm
Waipawa Fm. interpreted depth
Waipawa Fm. constrained depth
Te Uri Mbr. constrained depth
Latitude °S (Present day)
C: Model
Late Paleocene 59 Ma
Waipawa Formation
Hinterland
Sediment supply
Shelf largely bypassed
25-50 m sea level decrease
Depth
Te Uri Mbr.
G
CS
Waipawa Fm.
Whangai Fm.
ES
Mead Hill Fm.
G = Glaucony
CS = Condensed section
ES = Expanded section
Increased terrigenous flux to distal aspects

Figure 4.4: Development of a depositional model for the Waipawa organofacies across the East Coast Basin, produced through the compilation of thickness and paleo-water depth data. A) When arranged by geospatial position, stratigraphic thickness and paleo-water depth, a distinct clinoform profile emerges for the Waipawa Formation in a northeast–southwest transect of the East Coast Basin, as highlighted by the orange polygon. Section numbers refer to locality numbers in Figure 4.2. Note that there has been substantial early Neogene shortening across the Adams-Tinui Fault. B) Maximum and minimum paleo-water depth constraints on the Whangai and Waipawa Formation across the East Coast Basin. The orange polygon highlights maximum and minimum paleo-water depth constraints for the Waipawa Formation determined from benthic foraminiferal faunas. C) Schematic depositional model for the Waipawa Formation (shown in orange) in the East Coast Basin, showing the transition from shallow, shelfal depositional facies, through to slope and basin-floor depositional settings. Representative outcrops of the Waipawa Formation in the East Coast Basin are shown in relation to their proposed depositional setting. C1) Te Uri Member of the Whangai Formation at Tawanui, representing a correlative of the Waipawa Formation in condensed, shallow marine sections. C2) Waipawa Formation at Taylor White, showing a thick section of massive, dark-coloured mudstone characteristic of 'typical' Waipawa. C3) Waipawa Formation at Manurewa Point, where dark-coloured mudstones are associated with turbiditic sandstones and micritic limestones, interpreted as a base-of-slope setting. C4) Waipawa Formation at Mead Stream, interpreted to represent a bathyal, basin-floor setting. Note the double layer of dark mudstone in photos C3 and C4 separated by micritic limestone.

4.3.3 Organic Chemistry

Proximal Waipawa, represented in outcrop by the uppermost Te Uri Member at Tawanui and the Waipawa Formation at Te Hoe River, has TOC values of <0.5 wt % and 1.16–3.1 wt %, respectively (Rogers *et al.*, 2000; Killops *et al.*, 2001; Hollis *et al.*, 2014). Typical Waipawa has variable TOC content, usually in the range of 1.0–6.0 wt %, although sometimes as low as 0.5 wt. % (Figure 4.5), with the majority of samples analysed from the unit forming a distinct organic-rich group (2–6 wt %). There is a negative relationship between T_{max} and TOC in the Waipawa organofacies (Figure 4.5a). T_{max} values for the Waipawa organofacies generally range from ~410–435°C (Figure 4.5a), with typical Waipawa producing lower T_{max} values (generally 400–435°C), than distal Waipawa (generally 420–435 °C).

The recorded hydrocarbon concentrations are positively correlated with the organic matter content; as such, the S1 and S2 (mg HC/g rock) parameters are positively correlated with TOC in all sections (Figure 4.5B, 4.5C). The S2 peak can be used to assess the generative quality of a prospective source rock. Proximal Waipawa has poor source rock characteristics, with an inert kerogen source determined by bulk pyrolysis (Figure 4.5c). Typical Waipawa produces a good to

excellent, primarily gas and wet gas source rock, whereas distal Waipawa produces poor to fair, dry gas-prone source rocks or an inert kerogen source (Figure 4.5c).

Samples from the Waipawa organofacies typically fall within the Type II to Type III kerogen fields (Figure 4.5), indicating a mixed terrestrial-marine organic matter kerogen source. Proximal Waipawa from the Tawanui produces low HI (73–89 HC/g TOC) and OI (33–200 mg CO_2/g TOC) values indicative of a Type IV, inert kerogen source. Typical Waipawa produces a broad range in HI (5–370 HC/g TOC) and OI (5–195 mg CO_2/g TOC) values, indicating a range from Type I to Type IV kerogen, though dominantly falling between the Type II and Type III fields (Figure 4.5d). Distal Waipawa generally has similar HI and OI values (2–100 HC/g TOC; 10–125 mg CO_2/g TOC, respectively) to proximal Waipawa, indicating a Type IV kerogen.

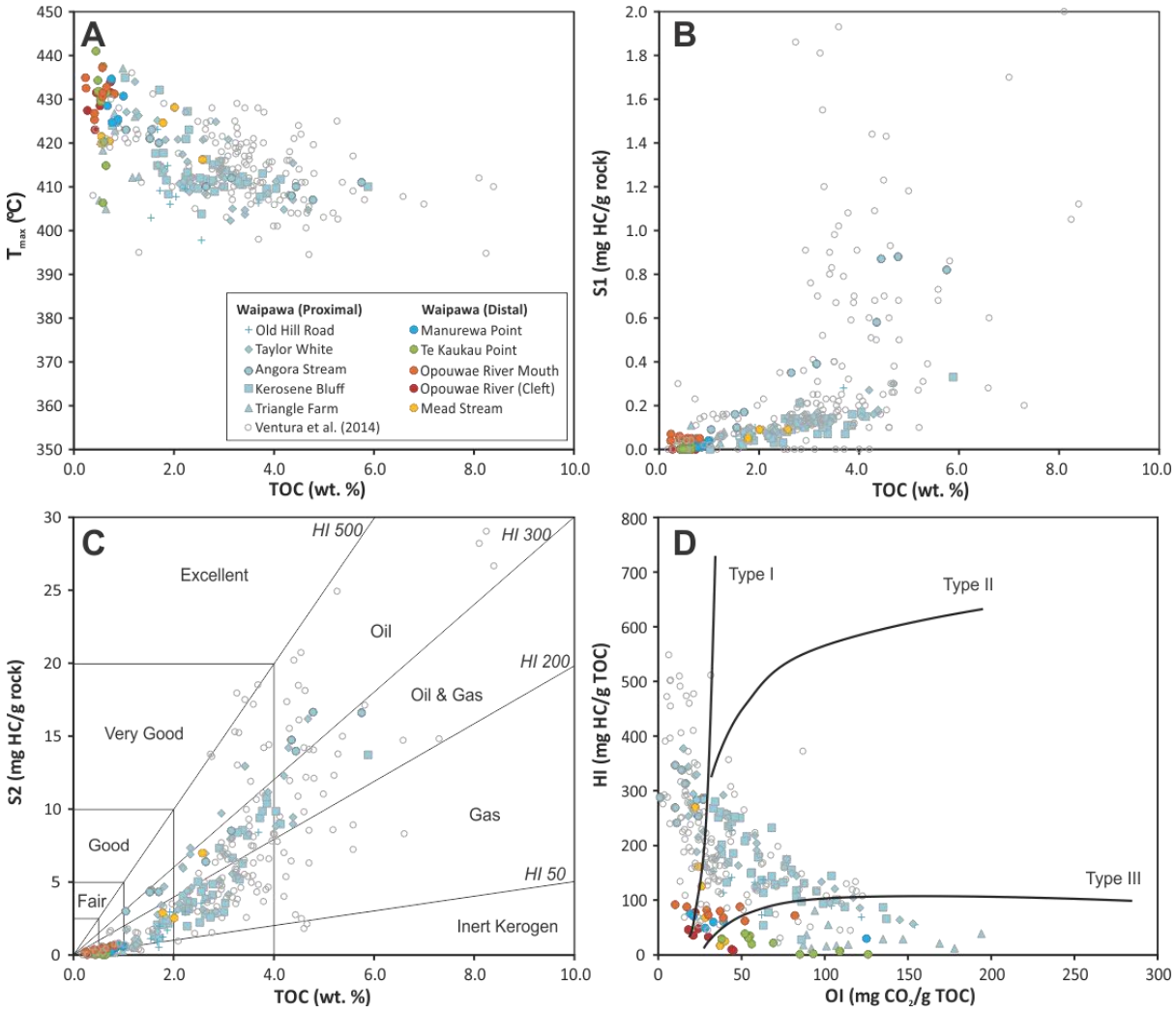

Figure 4.5: Source rock analyses of typical Waipawa (pale blue samples are from Hines *et al.*, Chapter 3), distal Waipawa (coloured circles) and all values measured for the Waipawa Formation as compiled in Ventura *et al.* (2014; open circles).

4.3.4 Inorganic Chemistry

In paleo-redox studies, the chemical composition of bulk sediment, particularly trace element enrichments, S–Fe–TOC relationships, and elemental indices, can be employed to distinguish past depositional environments and paleo-redox conditions (Jones & Manning, 1994; Rimmer, 2004; Brumsack, 2006; Rowe *et al.*, 2008, 2012).

Sulphur – Iron – Carbon Relationships

Reduction of organic matter under reducing conditions leads to the formation and preservation of iron pyrite, making S–Fe–TOC relationships particularly informative of paleo-redox conditions and early stage sedimentary diagenesis. A number of trace elements that typically occur in enhanced concentration in organic-rich shales are commonly hosted by pyrite, or other sulphide mineral phases, as well as organic matter (Schoepfer *et al.*, 2017). On this basis, paleo-redox conditions can be assessed by the proportion of S relative to Fe (Raiswell *et al.*, 1988; Lyons & Severmann, 2006; Georgiev *et al.*, 2012). Therefore, in order to understand trace element enrichments across the highly variable lateral extent of the Waipawa Formation, it is important to consider S-TOC-Fe relationships to assess the source and chemical association of trace element enrichments.

The degree of pyritization, estimated from Fe-S relationships, can be used to interpret paleo-redox conditions. Proximal Waipawa sampled at Tawanui produces exceptionally high Fe with respect to S, indicating a high proportion of an Fe-bearing mineral phase (other than pyrite), and consequently all samples plot well within the oxic field with a degree of pyritization (DOP) of <0.52 (Figure 4.6a). Proximal Waipawa Formation samples dominantly plot in the oxic field, but also extend into the anoxic (DOP 0.52–0.75), and to a lesser extent, the euxinic fields (DOP >0.75) of Raiswell (1988). Samples from the distal Waipawa facies all plot within the oxic field (DOP <0.52) (Figure 4.6a).

Sulphur–TOC relationships provide information about reduction of organic matter in a marine setting and the source of pyrite sulphur. Samples from proximal Waipawa at Tawanui plot above the normal marine S/TOC line (Figure 4.6b). Samples from typical Waipawa are fairly evenly distributed across the normal marine S/TOC line, and samples from distal Waipawa facies have low (typically <1%) TOC, and proportionally high S values, plotting above the normal S/TOC line (Figure 4.6b). Because only a minor portion of Fe is present in the form of pyrite (demonstrated by weak Fe-S relationships; Figure 4.6a), and the organic carbon compounds are likely to be refractory, the accumulation of sulphide compounds can be shown on a ternary diagram (Figure

4.6c; Rowe *et al.*, 2008; Schoepfer *et al.*, 2017). A ternary diagram of S-TOC-Fe broadly demonstrates an increasing proportion in S, corresponding to a comparative reduction in Fe/TOC.

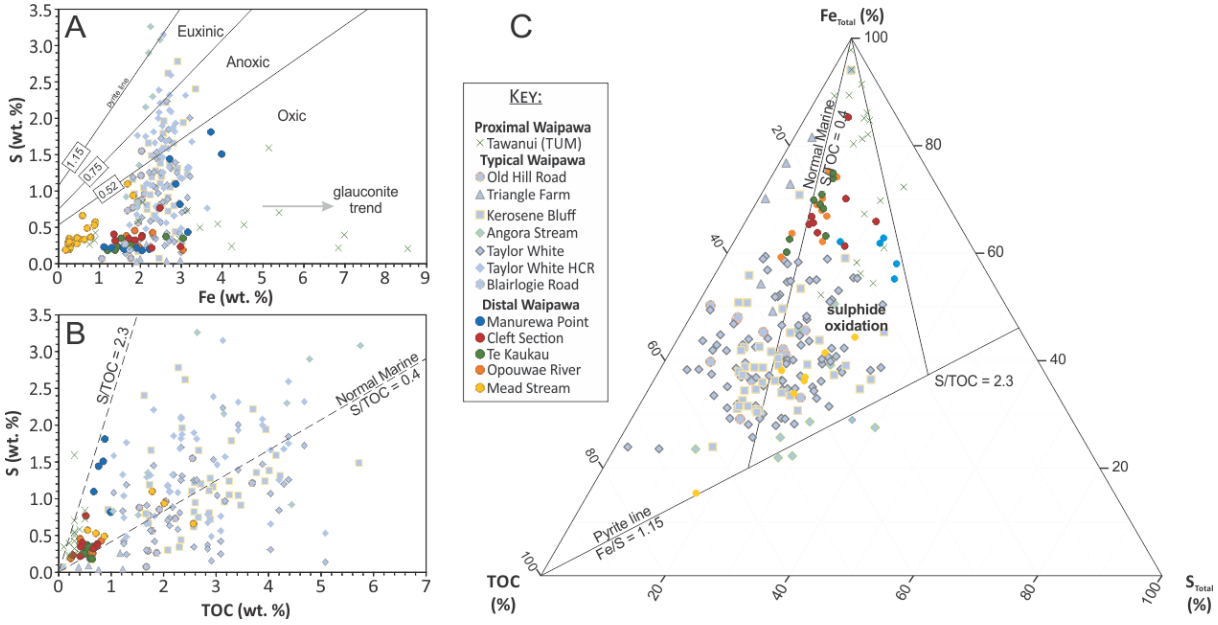

Figure 4.6: A) Sulphur and Fe relationships for the Waipawa Formation in proximal settings (pale blue) and distal settings (coloured circles). Lines represent the degree of pyritization (DOP) values for paleo-redox states. Redox divisions after Georgiev *et al.* (2012). B) Sulphur and TOC relationships for proximal and distal Waipawa Formation. The modern, normal marine S/TOC line is plotted, showing the oxic-dysoxic trend of Berner & Raiswell (1983) and Algeo & Maynard (2004). C) Ternary diagram showing the normalised relative proportions of S, TOC, and Fe. The normal marine line trend of Berner & Raiswell (1983) and Algeo & Maynard (2004) is plotted, along with the stoichiometric pyrite line (Fe/S = 1.15) and the S/TOC line of Schoepfer *et al.* (2017) oxidative and sulphide oxidation zones.

Enrichment factors

The Waipawa organofacies displays a distinctive pattern of trace-element enrichment that holds true even in atypical (proximal and distal) facies associations of the Waipawa Formation, whereby the most enriched trace elements are Mo and U, and the most depleted element is Mn. Element enrichment factors follow the characteristic pattern of Mo>U>Cr≥As≥Zn≥V>Cu≥Pb≥Ni≥Fe>Mn, although absolute values for enrichment factors vary (Figure 4.7). Proximal Waipawa displays similar enrichment factors to typical Waipawa, with the exception of a relative depletion in Cu_{EF} and enrichment in Fe_{EF} and Cr_{EF}. Distal Waipawa Formation sampled at Pahaoa River, Manurewa Point, Opouwae River and Te Kaukau Point, form a spectrum of trace element enrichment factors between the typical Waipawa Formation

enrichments of Hines *et al.* (Chapter 3) and those measured at Mead Stream, the paleo-deepest and most distal site.

Total organic carbon and S enrichment factors across the Waipawa organofacies behave differently in different settings. Enrichment factors (EF) for TOC in proximal Waipawa at Tawanui (EF=4.8) are lower than typical Waipawa (EF=21), although are substantially elevated relative to average shale values of Wedepohl (1971). Distal Waipawa generally has lower TOC_{EF} relative to typical Waipawa, although Mead Stream has an average TOC_{EF} of 26 (Figure 4.7). Sulphur enrichment factors in proximal Waipawa at Tawanui (EF=6.6) are comparable to average S_{EF} in typical Waipawa (EF=6.7). Distal Waipawa S_{EF} is lower than the average value for typical Waipawa, except for Mead Stream, which has an S_{EF} of 14 (Figure 4.7). Weathered samples of typical Waipawa from Triangle Farm and Blairlogie Road give low S_{EF} of 1.2 and 2.5, respectively (Figure 4.7).

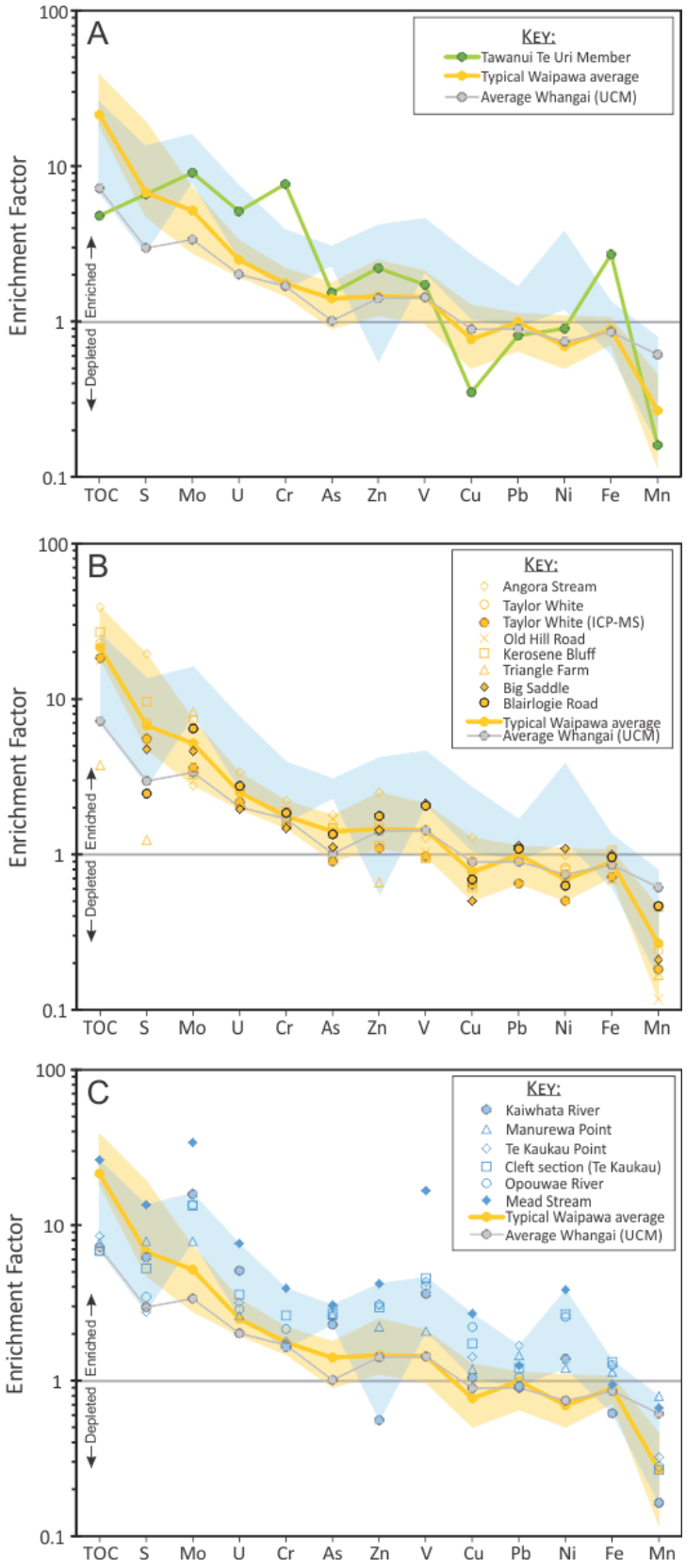

Figure 4.7: Element enrichment factors for A) proximal Waipawa (Te Uri Member at Tawanui), B) typical Waipawa (data from Hines *et al.*, Chapter 3, with new data from Blairlogie Road and Big Saddle), and C) distal Waipawa. The range of typical Waipawa and distal Waipawa (excluding outliers) are shown as shaded yellow and blue areas, respectively.

Trace Element Paleo-redox Proxies

Compared to the proximal Waipawa Formation, enrichment factors are considerably lower for TOC and S in the distal Waipawa facies, suggesting that organic carbon preservation was lower, and reducing conditions were not as prevalent. However, the distal Waipawa Formation typically exhibits greater enrichments in other redox-sensitive elements assessed in this study. The application of additional redox proxies is required to disentangle paleo-redox conditions from paleo-productivity and preservation signals. Widely applied paleo-redox proxies are assessed here to supplement interpretations drawn for S-TOC-Fe relationships, and provide a direct indication of paleo-oxygenation. The trace metal proxies V/Cr, V/(V+Ni), U/Th, U_{auth}, and Mo/U were used as indices of redox potential of the water column and sediments during deposition, and enable direct comparison to proxies used in Chapter 3.

The enrichment of Mo with respect to U in the Waipawa Formation can be indicative of water column anoxia (Mo:U; Chapter 3; Figure 4.8a). Comparison of Mo and U enrichment factors show that Mo_{EF} is disproportionately higher with respect to U_{EF} in all settings of the Waipawa organofacies in the East Coast Basin, than would be expected in unrestricted marine settings, suggesting anoxic conditions were prevalent across the basin.

Uranium is removed from seawater and precipitated under reducing conditions, whereby U^{6+} is reduced to U^{4+} which is precipitated or adsorbed into solid sediments, producing an authigenic enrichment of U with respect to Th, which occurs in a single oxidation state (Th^{4+}) under both oxidising and reducing conditions (Zheng *et al.*, 2002). Uranium/Th is a widely applied proxy for differentiating redox conditions, with values from 0.75–1.25 representing dysoxic environments, and values >1.25 representing anoxic environments (e.g. Gallego-Torres *et al.*, 2007; Chang *et al.*, 2009; 2012). Proximal Waipawa has U/Th values from 1.44–5.6 (average 2.69) indicating anoxic conditions. Uranium/Th values in typical Waipawa range from 0.24–1.4 (average 0.57), and in distal Waipawa range from 0.33–0.89 (average 0.58; Figure 4.8c), indicating that oxic to anoxic conditions prevailed during deposition of the Waipawa Formation. Authigenic U was calculated following the method of McManus *et al.* (2005), where the authigenic fraction is estimated using lithogenic U/Al and the Al of the sediment, with any excess U taken to represent authigenic U (i.e. $U_{auth}=U_{sample}–(U_{ave.\ shale}/Al_{ave.\ shale})\times Al_{sample}$). Authigenic U values of 5–12 are indicative of dysoxic conditions, whereas values >12 indicate anoxic conditions (Jones & Manning, 1994; Gallego-Torres *et al.*, 2007). Proximal Waipawa at Tawanui gives U_{auth} values of 5.6–10.8 (average 9.0) indicating deposition under dysoxic conditions. Authigenic U values for distal Waipawa lie within the range of values determined for typical Waipawa in Chapter 3. A number of the values derived

are above the threshold of 5 for dysoxic conditions, although typical Waipawa tends to have slightly higher U_{auth} values (3.2–11.6; average 5.3) relative to distal Waipawa (3.2–8.8, average 4.6; Figure 4.8c), although given the range of values no significance is ascribed to this interpretation.

Vanadium is preferentially enriched under reducing conditions and can also be used to differentiate between oxic and anoxic conditions (Jones & Manning, 1994; Gallego-Torres *et al.*, 2007). Vanadium/Cr values in the range of 0–2.0 represent oxic conditions, values in the range from 2.0–4.25 indicate dysoxic conditions, and V/Cr values >4.25 are representative of suboxic to anoxic environments (Jones & Manning, 1994). The Waipawa organofacies has V/Cr values that cover the oxic to anoxic fields (Figure 4.8d). Proximal Waipawa from Tawanui plots within the oxic field. Typical Waipawa primarily lies in the oxic field, whereas distal Waipawa typically falls in the dysoxic field, although some samples from Mead Stream lie in the anoxic field (Figure 4.8d).

There is generally very little differentiation in V/(V+Ni) between proximal and distal Waipawa Formation. The V/(V+Ni) proxy characterises euxinia at values >0.84, whereas, values in the range of 0.54–0.72 indicate anoxic water column conditions, 0.46–0.60 indicate water column dysoxia, and values <0.46 represent oxic conditions (Hatch & Leventhal, 1992). For V/(V+Ni), all values plot within the dysoxic to anoxic fields, with almost all values in the anoxic field (Figure 4.8d). With V/(V+Ni) there appears to be no substantial separation in redox state between the proximal, typical, and distal Waipawa Formation.

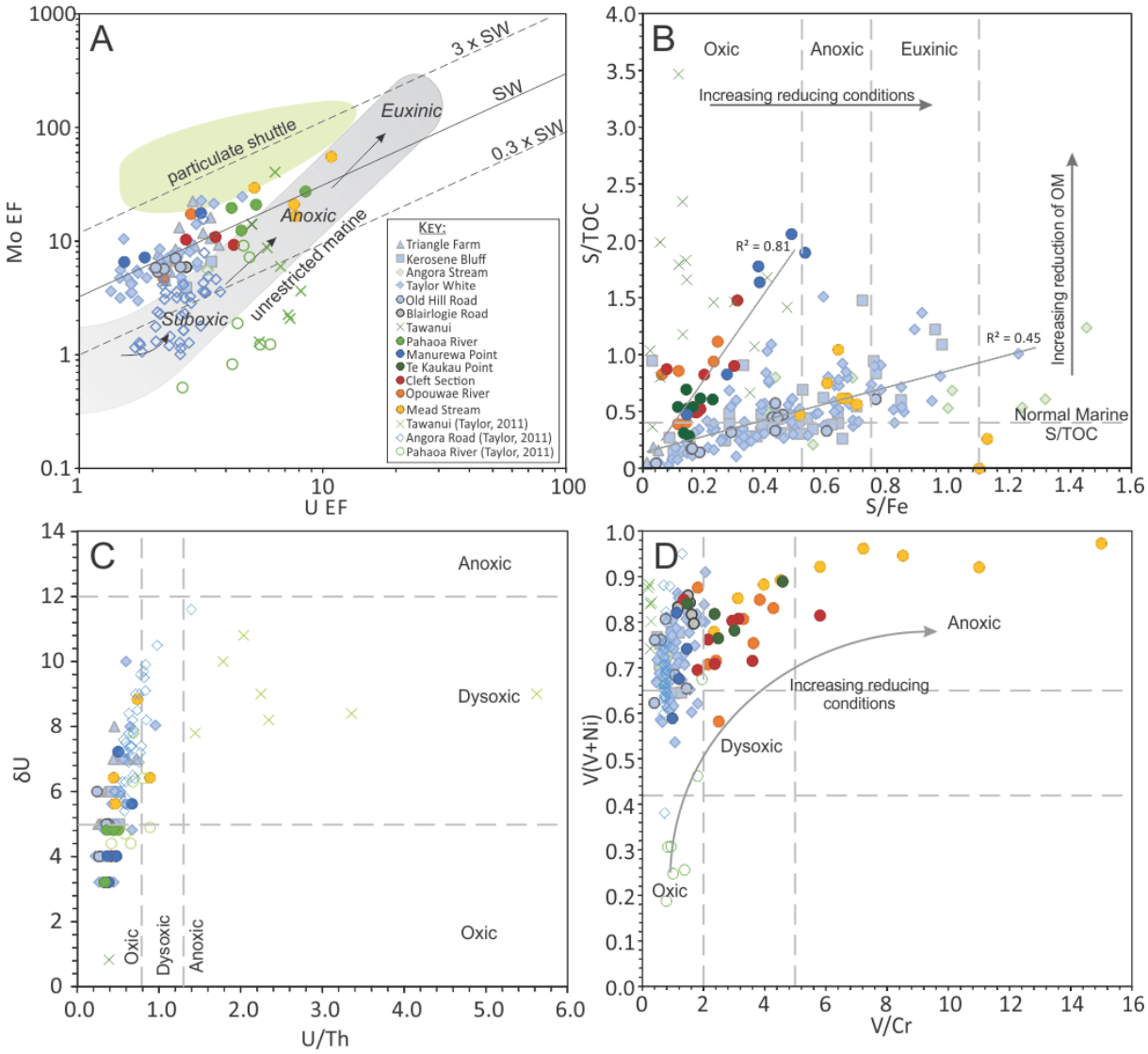

Figure 4.8: Trace element proxies for paleo-redox conditions from pXRF analyses of the Waipawa Formation, subdivided into proximal and distal Waipawa Formation. A) Uranium enrichment factor plotted against Mo enrichment factors, with fields from Tribovillard *et al.* (2012). B) S/TOC plotted against S/Fe, providing an index of degree of pyritization, S-TOC-Fe relationships, and paleo-redox conditions. C) Authigenic U vs U/Th. D) V(V/Ni) vs V/Cr.

Major element ratios

Various elemental indices and ratios are used to inform interpretations of paleoenvironmental and redox conditions during deposition. Of particular interest are K/Al, Zr/Al, Ti/Al, and K/Al. Potassium/Al provides an index for the bulk clay composition, particularly illite, smectite and kaolinite clays. An increase in Ti/Al and Zr/Al represent an increase in material derived from a mafic source, whereas a decrease in Si/Al is interpreted to demonstrate an increase in the sedimentation rate (Sageman *et al.*, 2003a).

Proximal Waipawa from Tawanui give high K/Al ratios, between 0.3 and 1.5, whereas both typical and distal Waipawa fall within the range of generally 0.15–0.30, which is the same range of values of the underlying Whangai Formation (Figure 4.9a). There is no strong differentiation in Zr/Al values between proximal, typical and distal Waipawa (Figure 4.9a), and values from the Waipawa organofacies sampled are within the range of Whangai Formation sampled (Figure 4.9a). There is substantial variation in Zr/Al values from the Mungaroa Limestone, Porangahau Member, and some outcrops of the Wanstead Formation, all associated with flysch-type sediments, and such variability is attributed to changes in grain size and therefore mineralogy (Figure 4.9a). Micritic limestones from the Mead Hill Formation, Mungaroa Limestone, Kaiwhata Limestone and Amuri Limestone generally give low Zr/Al and K/Al values indicative of carbonate dilution (Figure 4.9a).

Proximal Waipawa from Tawanui produces high Si/Al values (10.5–13), in comparison to typical Waipawa (Si/Al = 3.5–6; Figure 4.9b). Distal Waipawa gives a broad range in Si/Al values (5–28), with the majority giving higher values than typical Waipawa (Figure 4.9b). There is no significant shift in Ti/Al values between the proximal, typical and distal Waipawa, or the Whangai Formation (Figure 4.9b), consistent with Zr/Al values.

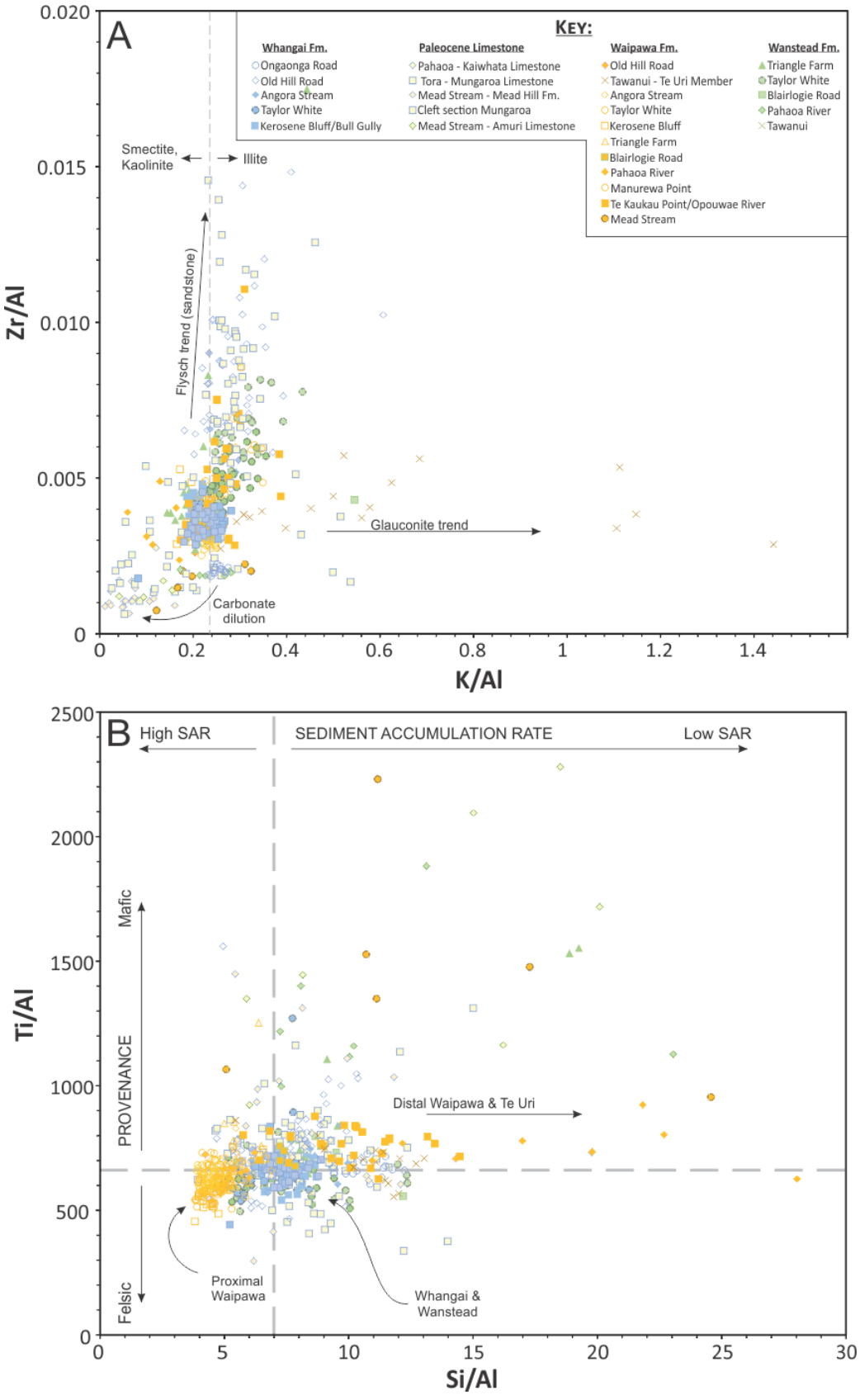

Figure 4.9: A) Plot of K/Al against Zr/Al as bulk sediment provenance indicators and mineralogical trends for the formations covered in this study. B) Plot of Si/Al as a proxy for sediment accumulation rate and Ti/Al as a bulk rock provenance indicator.

Bulk Mineralogy

The Waipawa Formation displays a distinctive dark-grey/brown-black colouration in outcrop, regardless of whether it has an organic carbon content of 0.5 % or 5 %, whereas the underlying Whangai Formation may have TOC contents of 2 % and remain a pale-grey colour. This suggest that a mineralogical control, rather than carbon content, controls the distinct colouration of the Waipawa Formation. Bulk modal mineralogy, determined by XRD, was applied to 67 samples from the Waipawa Formation and surrounding units to assess changes in mineralogy, both across formation boundaries and across the geographic extent of the formation.

Forty samples from the Taylor White section were analysed across the Whangai (10), Waipawa (20), and Wanstead (10) formations. The modal mineralogy is dominated by quartz, albite and illite/muscovite (illite and muscovite are largely indistinguishable by XRD). Albite shows a general increasing trend up-section, and illite/muscovite and chlorite display a corresponding decrease up-section (Figure 4.10A). There is a notable absence of orthoclase in samples from the Upper Calcareous Member of the Whangai Formation. Montmorillonite is entirely absent from the Waipawa Formation, although low abundances are present in the Upper Calcareous Member and the Wanstead Formation. Montmorillonite, as determined by XRD, could be a number of different clay minerals, although there is a distinct spectrum present, and montmorillonite has previously identified as a major constituent of the Whangai Formation clay mineral content by Moore (1988a).

Eight samples were analysed across the Waipawa to Wanstead formations at Triangle Farm. Three samples from the Waipawa Formation at Triangle Farm show similar proportions of quartz, illite, albite, orthoclase and montmorillonite to Taylor White, but a lower proportion of chlorite, and no detectable jarosite or gypsum (Figure 4.10B), despite the increased weathering apparent in outcrop at this locality. The Wanstead Formation at Triangle Farm has a similar proportion of quartz, illite, chlorite and montmorillonite to Taylor White, despite the distinct differences in lithology between the two locations (non-calcareous alternating sandstone-mudstone with minor greensand beds at Taylor White, and calcareous, clay-rich mudstone at Triangle Farm). The differences in mineralogical composition between Taylor White and Triangle Farm are apparent in the high (20–40%) carbonate content of the Wanstead Formation at Triangle Farm, with a corresponding decrease in albite, and an absence of orthoclase.

Across a north-south transect, the Upper Calcareous and Rakauroa members of the Whangai Formation and the correlative Herring Formation display comparable proportions of albite and chlorite (Figure 4.10C). The proportion of illite/muscovite is similar in the Upper Calcareous Member at Taylor White and Kerosene Bluff and the Herring Formation at Benmore Stream,

though notably lower than the values measured for the Rakauroa Member at Pukemuri Stream and the Herring Formation at Kaikoura (Figure 4.10C). Montmorillonite was only observed in samples from the Upper Calcareous Member (Figure 4.10A, C), suggesting either a spatial or temporal restriction as these are also the youngest samples from the Whangai Formation analysed by XRD.

Compared to proximal facies, distal Waipawa Formation becomes increasingly dominated by quartz and contains a smaller total number of mineral species identified by XRD (Te Kaukau Point, Opouwae River and Mead Stream; Figure 4.10D). The increasing proportion of quartz relative to clay minerals is consistent with increased Si/Al trend across the more distal sections of the Waipawa Formation (Figure 4.9).

Figure 4.10: Changes in the bulk modal mineralogy determined by XRD through the Taylor White (A) and Triangle Farm (B) sections. C–F, North to south transects through the Whangai Formation, Waipawa Formation, Wanstead Formation and Paleocene–Eocene limestones in the East Coast Basin, showing changes in the bulk modal mineralogy determined by XRD. Values for the Whangai, Waipawa and Wanstead formations at Taylor White and Triangle Farm represent averaged values for the data presented in Figure 4.10a and 4.10b. Members of the Whangai Formation are represented by: RAK = Rakauroa Member, UCM = Upper Calcareous Member, HF = Herring Formation. PS = Pukemuri Siltstone. For Paleocene–Eocene limestone, ML = Mungaroa Limestone, MH = Mead Hill Formation, AL = Amuri Limestone.

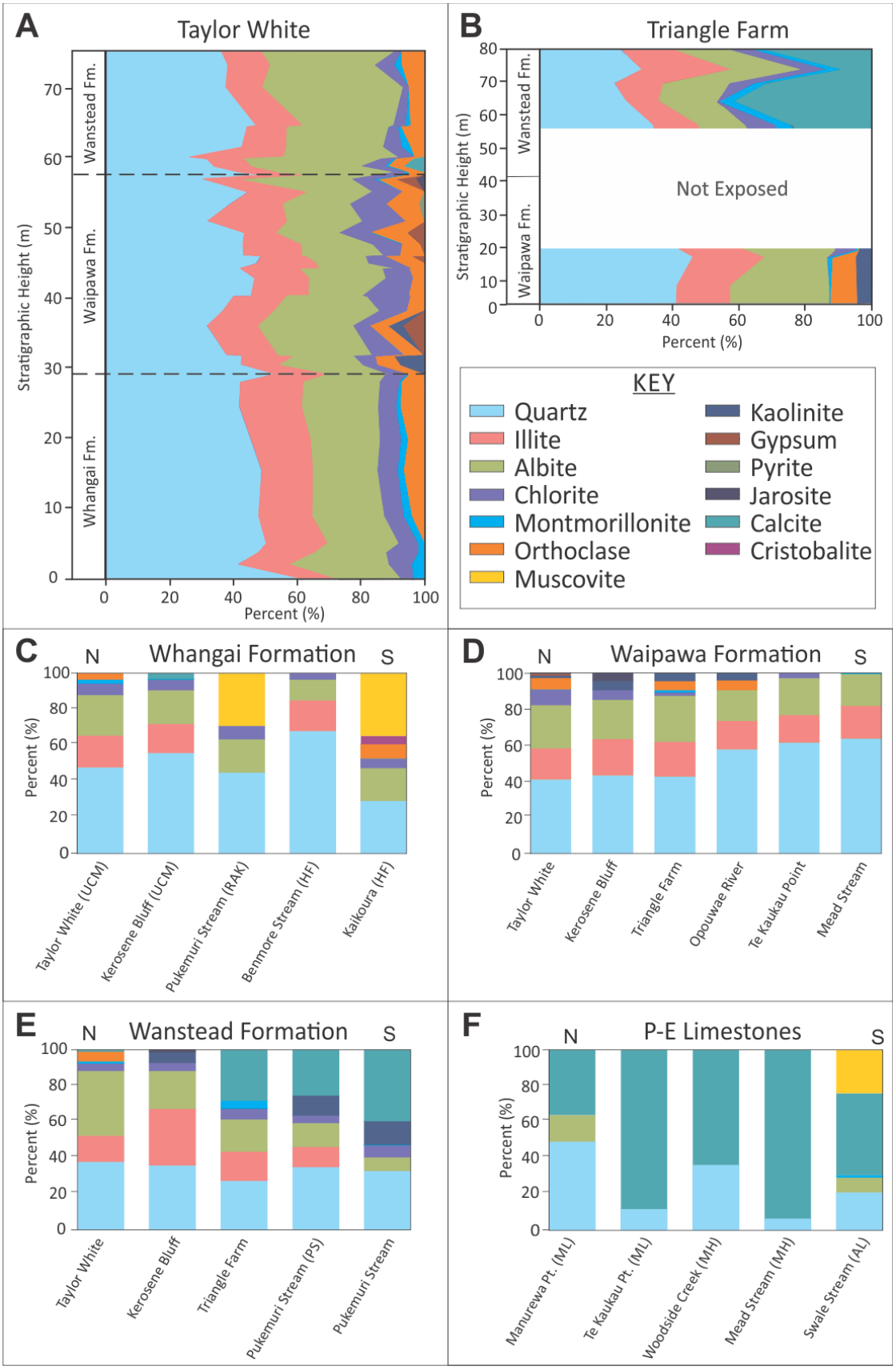
A
Taylor White
Stratigraphic Height (m)
Wanstead Fm.
Waipawa Fm.
Whangai Fm.
Percent (%)
B
Triangle Farm
Stratigraphic Height (m)
Wanstead Fm.
Not Exposed
Waipawa Fm.
Percent (%)
KEY
Quartz
Illite
Albite
Chlorite
Montmorillonite
Orthoclase
Muscovite
Kaolinite
Gypsum
Pyrite
Jarosite
Calcite
Cristobalite
C
N
Whangai Formation
S
Percent (%)
Taylor White (UCM)
Kerosene Bluff (UCM)
Pukemuri Stream (RAK)
Benmore Stream (HF)
Kaikoura (HF)
D
N
Waipawa Formation
S
Percent (%)
Taylor White
Kerosene Bluff
Triangle Farm
Opouwae River
Te Kaukau Point
Mead Stream
E
N
Wanstead Formation
S
Percent (%)
Taylor White
Kerosene Bluff
Triangle Farm
Pukemuri Stream (PS)
Pukemuri Stream
F
N
P-E Limestones
S
Percent (%)
Manurewa Pt. (ML)
Te Kaukau Pt. (ML)
Woodside Creek (MH)
Mead Stream (MH)
Swale Stream (AL)

4.4 Discussion

4.4.1 Paleoenvironment and Depositional Setting

Paleo-water depth assessments based on foraminiferal faunal assemblages demonstratably change across the geographical extent of the Waipawa Formation, and across bounding units. The shallowest depositional environment for the Waipawa Formation in the East Coast Basin lies around the Te Hoe River area, and progressively deepens both north-eastwards towards East Cape, and southwards towards Marlborough where it reaches its greatest paleo-water depths. Paleo-water depths determined from foraminiferal assemblages from the Whangai Formation, support the southward-deepening trend of the Waipawa Formation assemblages, albeit with better constraints on the maximum paleo-water depths. This trend is discernable despite the often large range of paleo-water depth values attributed to any given foraminiferal fauna assemblage; depth interpretations are also consistent with observed ichnofaunas at scattered localities. Similarly, changes in facies associations related to the Waipawa Formation conform with interpretations of depositional depth. The Waipawa Formation is thin in comparatively shallow settings, ranging from 5–10 m-thick, increasing to 50-70 m thick in inferred slope settings, before becoming notably thinner (3-5 m thick) in deeper, more distal settings. The two layers, or "pulses" of the Waipawa Formation in distal portions of the basin (e.g. Manurewa Point, Mead Stream) is an exaggeration of the double pulse of organic matter and clastic sediments observed in the proximal Waipawa Formation (Chapter 3).

Applying this assessment of spatial and stratigraphic trends, the Waipawa Formation in comparatively shallow settings (e.g. Te Hoe River) and deeper marine, distal settings (e.g. Pahaoa River, Te Kaukau Point, Mead Stream) represent condensed sections. Condensed sections are typically characterised as thin, arealy extensive units, comprised of pelagic to hemipelagic sediments with high organic carbon content and authigenic minerals (e.g. glauconite, phosphorite, and siderite) and, in many instances may be associated with high degrees of bioturbation and hardground formation, and located at the base of prograding clinoforms (Leckie *et al.*, 1992).

In individual sections, K/Al through the Waipawa Formation demonstrates a slight increase in illite over smectite and kaolinite relative to the Whangai and Wanstead formations (e.g. Chapter 3). However, when all data from across the transect is plotted, there is no significant change in K/Al, suggesting no notable deviation in the supply of either illite or smectite and kaolinite (Figure 4.9a). Similarly, the limited variability in K/Al, Zr/Al and Ti/Al values across the Whangai, Waipawa and Wanstead formations suggests that there is no change in the provenance of the terrigenous sediment supply (Figure 4.9a). Samples from the Te Uri Member have high K/Al values, along

with high Fe and Cr enrichment factors, attributed to the increased proportion of glauconite in these samples (Figure 4.9a). Potassium/Al values in the Te Uri Member suggest that glauconite was moderately evolved (K/Al = 4–6) indicative of suboxic pore waters (Amorosi *et al.*, 2007; Essa *et al.*, 2016). The development of glauconite is often a reliable indicator of low sedimentation rates, typically associated with condensed sections (Amorosi, 1995). Proximal Waipawa at Tawanui has high Si/Al values, interpreted here to be indicative of decreased sedimentation rates with respect to the underlying Whangai Formation (Figure 4.9b). In comparison, Si/Al values in typical Waipawa are low, indicating higher sediment accumulation rates, and in distal areas Si/Al values are substantially higher, indicative of decreased terrigenous sedimentation rates.

Applying the age model for the Waipawa Formation based on biostratigraphic and paleomagnetic evidence presented in Hollis *et al.* (2014) and Kulhanek *et al.* (2015), linear sedimentation rates for the Waipawa Formation are estimated, with the thickest sections returning sedimentation rates approaching 10 cm/kyr. The most proximal sections of the Waipawa Formation (and the Te Uri Member) typically give sedimentation rates of 0.6–1.4 cm/kyr. The more distal sites (Pahaoa River mouth, Te Kaukau Point and Mead Stream) give linear sedimentation rates of 0.2–0.5 cm/kyr.

The Te Uri Member underlies the Waipawa Formation in the most inboard shelfal areas (e.g. Te Hoe River). Elsewhere, the uppermost beds of the Te Uri Member are laterally equivalent to the Waipawa Formation in topographic and structural highs that are isolated from terrigenous sedimentation. The Te Uri Member is diachronous, in some places underlying isochronous Waipawa Formation (e.g. Te Hoe River), but in the Whangai Range deposition of the Te Uri Member persisted and interfingered with the Waipawa Formation (e.g. Otane Stream, Tauekaitai Stream). The Te Uri Member is 5 to 40 m-thick, but spans from 66 Ma to 58.7 Ma. If the age and thickness of the entire Te Uri Member are considered, it yields exceptionally low linear sedimentation rates of 0.06–0.43 cm/kyr, consistent with evidence that the Te Uri Member represents a Paleocene condensed section, and likely includes an unconformity or sedimentary hiatus at the base of the upper Te Uri Member. In nearby sections, the correlative interval is comprised of 100–600 m of sediment (Figure 4.11a). Hardground development within the Te Uri Member (Leckie *et al.*, 1992; Taylor, 2011), indicates that a sedimentary hiatus or paraconformity separates the lower and upper (=Waipawa equivalent) Te Uri Member. With the exception of the Te Hoe River section and the Hukarere-1 well, Te Uri Member is restricted in outcrop to the Whangai Range area in the southern Hawke's Bay (Figure 4.11a, b). The uppermost portion of the Te Uri Member has been correlated geochemically to the Waipawa Formation on the basis of TOC enrichment and a positive $\delta^{13}C_{org}$ excursion (Rogers *et al.*, 2001; Hollis *et al.*, 2014).

The Tangaruhe and Mangawhero anticlines in the Whangai Range area were both active structures in the late Cretaceous (Crampton, 1997), and may have still been active in the Paleocene, or at the least were apparently structural highs (Smiley, 2014). Rapid vertical and lateral facies changes in the Tangaruhe Formation underlying the Whangai Formation, and the juxtaposition of two facies of the Tangaruhe Formation across the axis of the Tangaruhe Anticline (Crampton, 1997), imply further folding and shortening post-deposition of the Tangaruhe Formation. Deposition of the Te Uri Member across structural highs would result in clastic sedimentation bypassing the area, explaining the restricted outcrop distribution of the glauconitic Te Uri Member in this area, and account for lateral facies relationships between the Waipawa Formation and Te Uri Member (Figure 4.11c). These facies relationships have been further reinforced by compression and structural shortening in the Neogene.

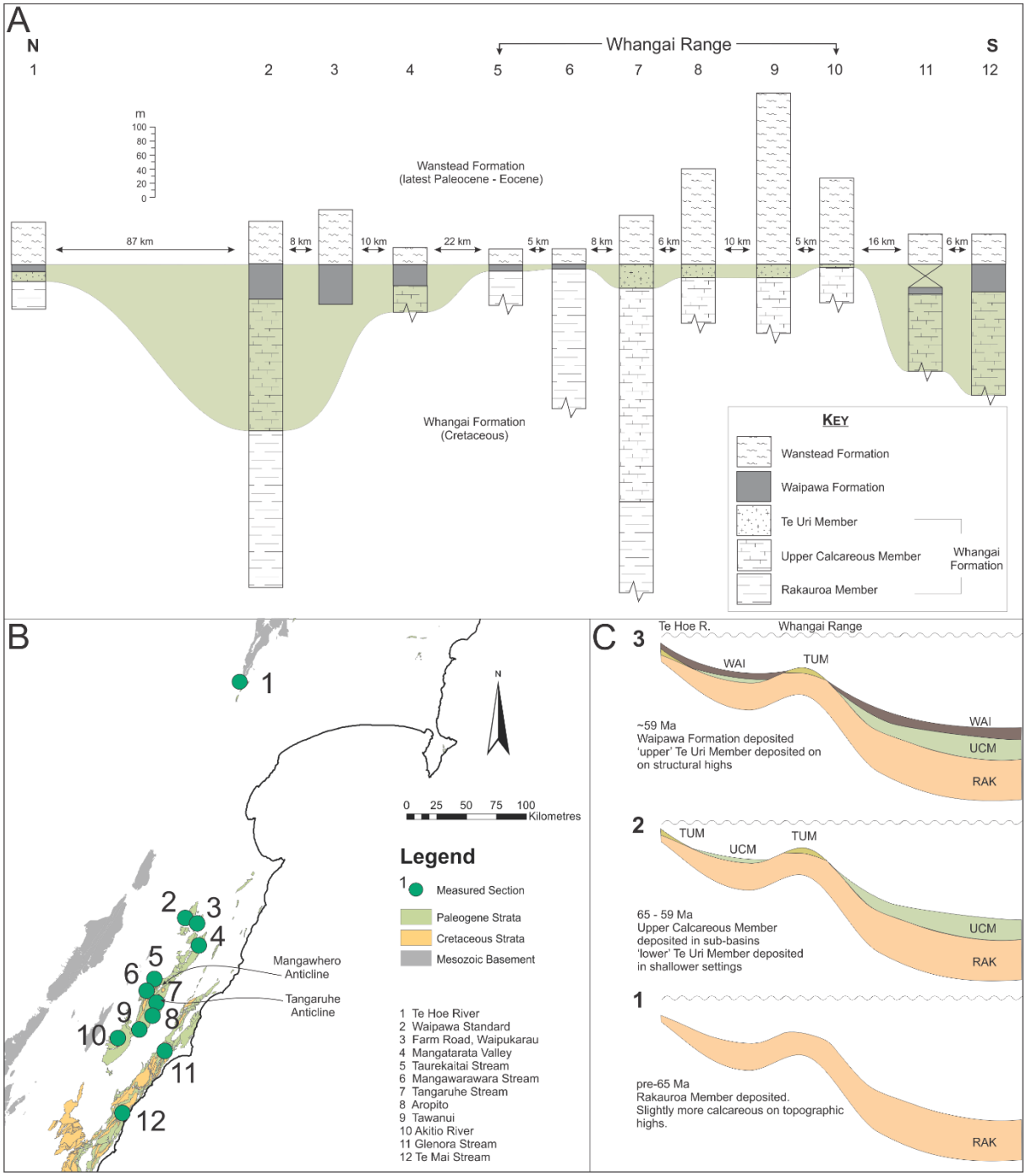

Figure 4.11: A) Northwest to southeast transect across the Whangai Range, showing the condensed early to early-late Paleocene succession across the Whangai Range, and the thinning of the Waipawa Formation on the western side of the range. B) Map showing the location of sections shown. C) Model for the coeval deposition of the Te Uri Member and Waipawa Formation in different parts of the basin. RAK = Rakauroa Member, UCM = Upper Calcareous Member, TUM = Te Uri Member, WAI = Waipawa Formation.

4.4.2 Kerogen Source

Despite the bathyal setting (>200 m paleo-water depth) for the Whangai and Waipawa Formations, there is a strong terrestrial kerogen source indicated by multiple proxies, including source rock analyses, organic biomarkers, thin-section analyses, and palynomorph studies (Killops *et al.*, 2000; Schiøler *et al.*, 2010; Gehlen, 2012; Hollis *et al.*, 2014; Clowes, 2016).

Bulk-rock pyrolysis parameters indicative of kerogen type measured in this study are quite low (HI = <300; OI <200), suggesting a mixed terrestrial-marine to dominantly terrestrial kerogen source. The data from the distal Waipawa Formation (except some samples from Mead Stream) plot close to the origin of the Type III and Type IV maturation pathways, indicating a dominantly terrestrial to inert kerogen source (Figure 4.5). Indication of a dominantly terrestrial kerogen source in distal settings is consistent with typical Waipawa Formation (e.g. Hines *et al.*, Chapter 3), although given the likely deep-marine setting it is surprising that a stronger marine kerogen component is not present. Concordant up-section variability in TOC and $\delta^{13}C_{org}$ in multiple sections suggest that the Waipawa organofacies contains at least two discrete terrestrial organic carbon preservation events (Hollis *et al.*, 2014).

Changes in the organic matter source result in variations in the bulk organic $\delta^{13}C$ composition, or in individual compounds. Compound-specific $\delta^{13}C$ analyses of the aromatic and saturate source rock kerogen fractions for late Cretaceous and Paleocene strata in the East Coast Basin demonstrate a dominantly terrestrial, to mixed terrestrial-marine source (Killops *et al.*, 2000). $\delta^{13}C_{org}$ and C/N values from the Waipawa Formation at Te Hoe River (Hollis *et al.,* 2014), represent an intermediate value between values derived for modern marine and lacustrine algae and C3 plants (Meyers, 1994), suggesting a mixed kerogen signal, consistent with bulk pyrolysis analyses.

The Waipawa Formation and correlative late Paleocene sedimentary rocks of the Waipawa Organofacies (e.g. uppermost Te Uri Member, Waipara Greensand, Tartan Formation) demonstrate a distinctive positive shift in $\delta^{13}C_{org}$ relative to units above and below, indicative of increased terrestrial organic matter flux into the basin during this time. Carbon isotope analyses through the Waipawa organofacies and bracketing units demonstrate a correlation with TOC, with isotopically lighter $\delta^{13}C_{org}$ values associated with higher TOC values (Figure 4.12). This is the inverse of the trend typically exhibited by marine shales, suggesting that isotopically lighter $\delta^{13}C_{org}$ values in the Waipawa Formation are associated with an influx of terrestrial organic carbon (e.g., Hollis *et al.*, 2014). Alternatively, a positive shift in $\delta^{13}C_{org}$ has previously been shown to represent an increase in burial flux of organic matter (Arthur *et al.*, 1987, 1988; Sageman *et al.,* 2003b), which is consistent with increased sedimentation rates across the Waipawa Organofacies, and avoids

assumptions about the isotopic composition of Paleocene organic matter. The elevated terrestrial organic matter loading observed in the Waipawa Formation likely occurs in tandem with the increased terrigenous sedimentation rates across the formation.

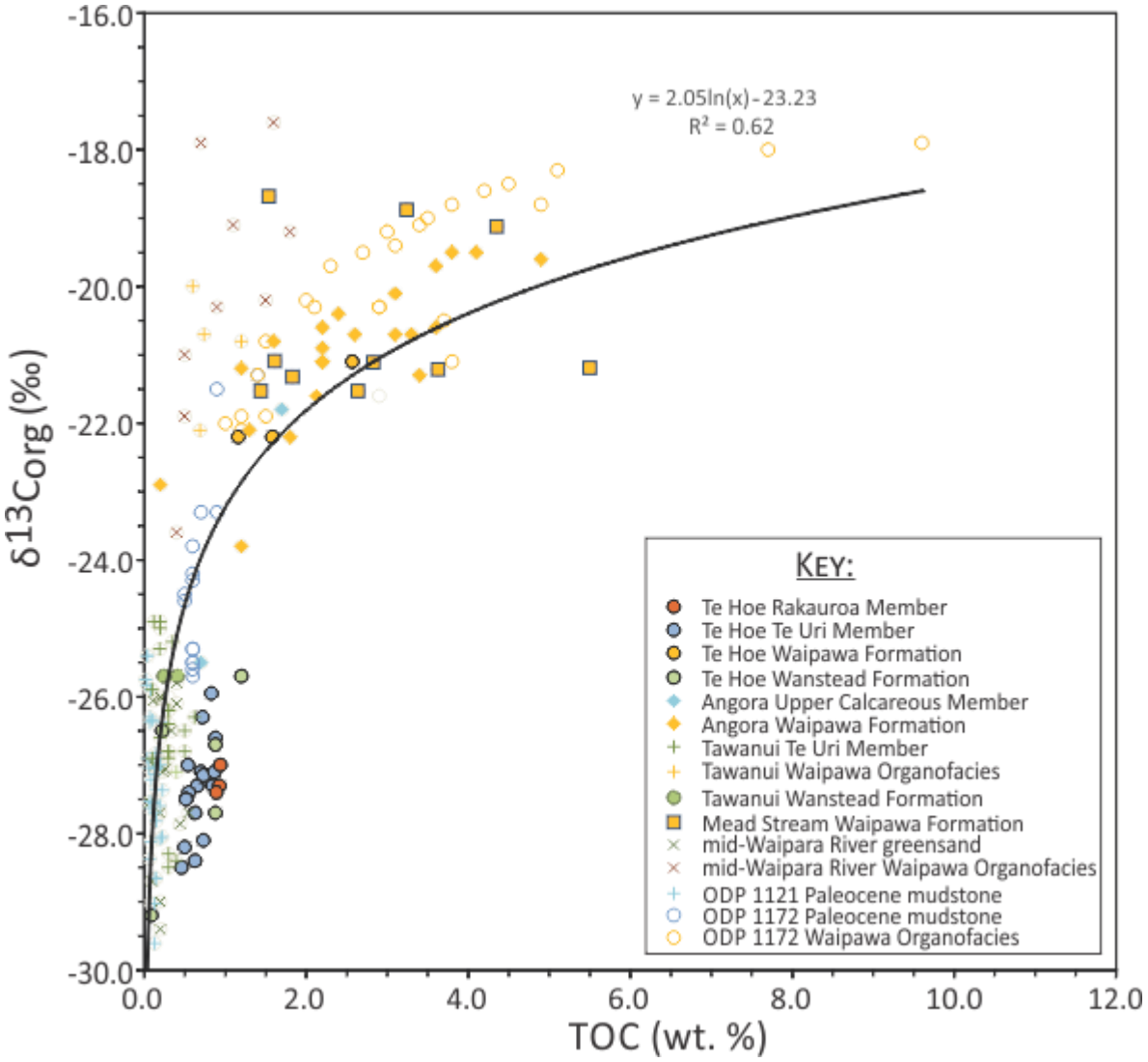

Figure 4.12: Cross-plot of TOC against $\delta^{13}C_{org}$ for the Waipawa Formation and associated sediments. Data sourced from Hollis *et al.* (2014). Waipawa organofacies identifies lateral correlatives of the Waipawa Formation.

Palynofacies analysis of the Waipawa Formation also demonstrates a strong terrestrial component, however, typically shows little or no evidence of amorphous organic matter (AOM), which is an indication marine organic matter (Gehlen, 2012; Clowes, 2016). Herein lies one of the great paradoxes of the Waipawa Formation. Source rock, organic carbon isotopes, and biomarker analyses of the Waipawa Formation tend to indicate a mixed kerogen source, however, palynological analyses consistently fail to show any amorphous organic matter (AOM) indicative

of marine kerogen, instead being dominated by terrestrial plant fragments. One possible answer to this paradox is that AOM, already low in the underlying Whangai Formation is swamped and diluted by the increased terrestrial flux, and therefore does not register in point counts. One possible reason for this is that microbial sulphate reduction in the water column has largely removed the simpler marine carbohydrates, resulting in a relative increase in terrestrial kerogen (as per Hines *et al.*, Chapter 3). Although sulphate-reducing bacteria prefer marine-sourced carbohydrate, they do not exclusively use it as a substrate, and source-rock kerogen classification systems do not consider diagenetic losses from pre-lithified sediments. Alternatively, low sedimentation rates in distal settings allow for a higher degree of bioturbation, which may suggest that biological reduction of organic matter has occurred, resulting in largely inert kerogen.

Assessment of paleo-water depths and proximal–distal relationships in the Waipawa Formation has allowed the $\delta^{13}C_{org}$ data from Schiøler *et al.* (2010) and Hollis *et al.* (2014) to be reviewed in new light. The Waipawa Formation has been characterised across multiple basins and lithofacies on the basis of a notable positive $\delta^{13}C_{org}$ excursion (Rogers *et al.*, 2001; Hollis *et al.*, 2014). Looking at the magnitude of this excursion with respect to underlying strata and the paleo-water depths determined from this study (East Coast Basin) and previous works (Tartan Formation, Canterbury and Great South basins; Schiøler *et al.*, 2010; ODP Site 1172, East Tasman Rise; Hollis *et al.*, 2014), a strong trend emerges (Figure 4.13). The magnitude of the $\delta^{13}C_{org}$ excursion across the Waipawa Formation is up to 4.5 ‰ less in deeper sections (Figure 4.13). The $\delta^{13}C_{org}$ excursion is much more pronounced in shallow settings, suggesting a greater contribution of heavier $\delta^{13}C$ organic matter compared to deeper settings.

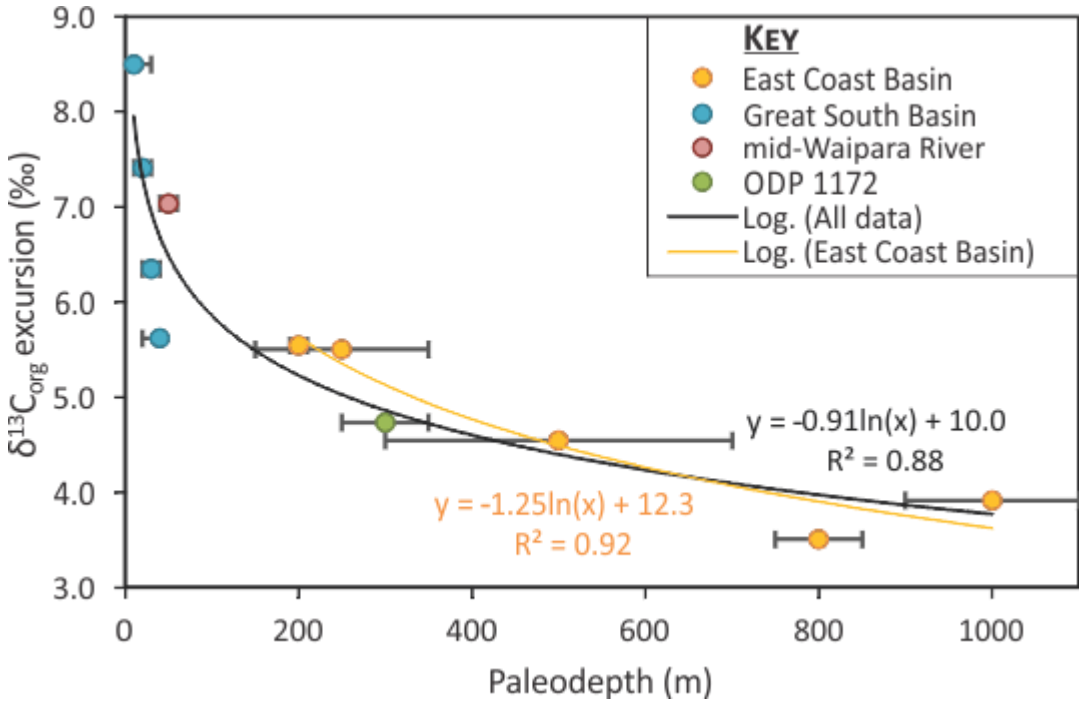

Figure 4.13: Plot of paleo-water depth against the magnitude of the $\delta^{13}C_{org}$ excursion across the transition into the Waipawa Organofacies. Carbon isotope data sourced from Schiøler *et al.* (2010), Tayler (2011) and Hollis *et al.* (2014). Paleo-water depths are derived from benthic foraminiferal assemblages recorded in FRED.

4.4.3 Paleoredox Conditions

The Waipawa Formation has been variously described as forming under either dysoxic, suboxic. or fully anoxic conditions (e.g. Moore, 1988a; Leckie *et al.*, 1995; Killops *et al.*, 2000; Rogers *et al.*, 2001; Hollis *et al.* 2014). Paleo-redox proxies presented here indicate that the Waipawa Formation varied from oxic to anoxic conditions. These mixed results are attributed to changes in sea-water oxygenation, pore fluid concentration and composition, and variable early stage diagenesis across the depositional settings of the Waipawa Formation, and also in part attributed to changes in the prevailing redox conditions during deposition. Therefore, paleo-redox conditions in the Waipawa Formation vary both up-section and laterally, making the development of a source rock and depositional model complicated.

Reducing conditions in sediments are often microbially mediated and range from oxic reducing, to denitrification (dysoxic conditions) to sulphate reducing (suboxic to euxinic conditions). Importantly, the heterotrophic activity of nitrate- and sulphate-reducing organisms is much lower than aerobic hydrocarbon oxidation. Decreased oxygenation and the accompanying reducing conditions in either the water column, or pore waters beneath the sediment water interface, result

in increased organic carbon accumulation and preservation in marine settings. During this process, concomitant microbial sulphate reduction results in syngenetic and early diagenetic pyrite formation (Rimmer, 2004; Brumsack, 2006). Authigenic precipitation of sulphide complexes facilitates the export and sequestration of trace metals in sediments and are responsible for the majority of trace metal enrichments associated with dysoxic to anoxic conditions (Tribovillard *et al.*, 2006; Algeo & Maynard, 2009). Pyrite framboids are common in proximal, typical and distal Waipawa, and along with pyrite nodules and the pyritization of burrows in distal Waipawa are evidence of early stage diagenesis (Appendix 5). Almost all outcrops of the Waipawa Formation show traces of Fe-oxides, jarosite and gypsum (Figure 4.10) which are secondary weathering products of pyrite.

Caveats of redox proxies

Some discrepancies are evident between various proxies and the implied level of anoxia in each setting. Across the Waipawa organofacies in the East Coast Basin, V/(V+Ni) indicates anoxia, whereas V/Cr indicates oxic conditions in all settings. Similarly S/Fe as a proxy for DOP suggests dominantly oxic conditions across all settings. These discrepancies make validation of individual proxies important, necessitating and assessment of both the syn-sedimentary and diagenetic processes that affect the distribution of redox-sensitive trace elements (McManus et al., 2005). In addition to being precipitated in sediments underlying bottom waters with low dissolved oxygen, U is enriched in sediments with high fluxes of particulate carbon (Zheng *et al.*, 2002). This is particularly relevant for the Waipawa Formation, where sedimentation rates are high, and the organic carbon content is proportional to sediment supply (Figure 4.14). Similarly, V is associated with organic matter, although a fraction may be deposited in association with silicate minerals, particularly clays (Jones & Manning, 1994; Tribovillard *et al.*, 2006). This means that the reliability of V-based proxies (V/Cr, V/(V+Ni)) is reduced in settings with elevated clastic sedimentation, as the rate of V diffusion is reduced and trace metal concentrations are diluted (Arthur & Sageman, 1994). Increased terrigenous sediment supply may dilute the proportion of freely available reactive Fe, resulting in a lower degree of pyritization and lower S/Fe for anoxic and euxinic settings.

V/Cr suggests that the distal Waipawa was deposited under greater reducing conditions than those in the typical Waipawa (Figure 4.8d). However, Cr is typically bound to organo-metallic complexes; therefore typical Waipawa, with the highest TOC, will have a disproportionate amount of Cr with respect to V, resulting in low V/Cr. In addition, in distal areas there will be a greater proportion of V bound in the clays with respect to Cr, resulting in higher V/Cr indicating reducing conditions.

Evidence for nitrate reduction

Vanadium is commonly used to reconstruct redox conditions in the nitrate reduction zone (Piper, 1994; Piper & Perkins, 2004), which characterises dysoxic conditions (Schröder & Grotzinger, 2007). Denitrifying bacteria are an important consideration in the reduction of organic matter in marine systems. Denitrification occurs where deoxygenated water masses are present, such as areas of increased upwelling, where an increased sinking flux of phytoplankton generates high oxygen demand in the water column, and high TOC drawdown in underlying sediments (Brumsack, 2006). Dissolved nitrogen replaces oxygen as the primary electron receptor during bacterially mediated oxidation of organic matter (Demaison & Moore, 1980; Jenkyns *et al.*, 2007), creating a stepwise reduction pathway of nitrate to nitrite, to nitric oxide, to nitrous oxide, to nitrogen, resulting in the loss of isotopically light N_2 to the atmosphere (Naqvi *et al.*, 1998). In such circumstances, increases of TOC are accompanied by comparatively high $\delta^{15}N$ values, providing a means of assessing denitrification of organic matter. Similarly, an increase in preserved C/N values may relate to compositional losses of N during microbial reduction (Ingall & Jahnke, 1997; Sageman *et al.*, 2003b). A concomitant increase in C/N, $\delta^{15}N$ and TOC across the Waipawa Formation at Te Hoe River (data from Hollis *et al.*, 2014; Appendix 5), suggests that denitrification and nitrate reduction were occurring in proximal settings during deposition of the Waipawa Formation.

Sulphur/TOC values in proximal Waipawa at Tawanui are elevated with respect to the normal marine S/TOC, suggesting that the reduction of organic matter resulted in an increase of S with respect to TOC. The Te Uri Member at Tawanui produces high Fe with respect to S, indicating a high proportion of an Fe-bearing mineral phase (other than pyrite), attributed to glauconite, resulting in low S/Fe values (Figure 4.6a). The development of glauconite is associated with suboxic conditions (Essa *et al.*, 2016), consistent with S-TOC-Fe trace element enrichments and redox indices in this setting.

Evidence for sulphate reduction

Up-section trends in multiple sections of the Waipawa Formation show that there was temporal variability and alternation of the redox state during deposition. Sections of typical Waipawa that have been sampled in greater detail (Kerosene Bluff, Old Hill Road and Taylor White) produce a range of S-TOC-Fe values that are spread across the oxic and sulphide oxidation zones. This is attributed to the 'double pulse' of the Waipawa Formation, whereby there were two pulses of enhanced reducing conditions and TOC preservation within the Waipawa Formation, separated by a brief period where more oxic conditions prevailed. This variation within the formation

produces a range of TOC, Fe and S values, producing the variation between oxic and sulphate reduction.

The Mo enrichment factor is disproportionately higher than the U enrichment factor than would otherwise be anticipated under unrestricted marine settings (Figure 4.8a), suggesting suboxic to anoxic conditions prevailed during deposition of the Waipawa Formation (Algeo & Tribovillard, 2009; Tribovillard *et al.*, 2012). This is consistent with Mn depletion across all settings (Figure 4.7), indicative of suboxic to anoxic reducing conditions during deposition (Brumsack, 2006; Tribovillard, 2006).

Existing sulphur isotopic analyses provide insight into redox conditions that can be compared to the inorganic trace element proxies examined in this study and Hines *et al.* (Chapter 3). A sample from the Waipawa Formation at the Waipawa standard section, and a sample from the correlative uppermost Te Uri Member at Tawanui, yielded $\delta^{34}S$ values of -25.5‰ and -26.9‰ (V-CDT scale), respectively (Rogers *et al.*, 2001). These values are consistent with those of anoxic and sulphate-replete conditions, in which the fractionation of sulphur isotopes is restricted to the range of kinetic isotope effects of sulphate reduction by anaerobic bacteria (-25 ± 10‰; Canfield, 2001; Chambers *et al.*, 1975; Kaiho *et al.*, 1996). In comparison, $\delta^{34}S$ values obtained by Kaiho *et al.* (1996) for the Wanstead Formation at Tawanui give background values of -20 to -42‰. Taking into account the $\delta^{34}S$ seawater value for the Paleocene (+16.5‰ to +18‰; Claypool *et al.*, 1980; Kurtz *et al.*, 2003; Turchyn & Schrag, 2006), this translates to an offset of -36.5‰ to -60‰, which is within the range of values for sulphur fractionation in modern oxic oceanic basins (-50 ±10 ‰), due to reoxidation of sulphides by aerobic bacteria or by other oxidants subsequent to being incorporated in redox cycling (Kaiho *et al.*, 1996). This assessment comes with the caveat that recent studies have demonstrated that microbial sulphate reducers can fractionate as much as 70‰ (Canfield *et al.*, 2010; Sim *et al.*, 2011; Wing & Halevy, 2014). This means that a re-oxidative S cycle is not required to create a large isotopic difference between sulphate and sulphite, and a re-oxidative S cycle can only be identified using multiple S isotopes (including ^{33}S). However, to a first-order approximation, $\delta^{34}S$ suggest that anaerobic bacterial respiration was occurring in both the uppermost Te Uri Member and the Waipawa Formation. This may explain enriched S relative to TOC values (Figure 4.6 & 4.8b), with the contribution of S present under low oxygen conditions being attributed to sea-floor microbial reduction, which produces two moles of S for every mole of C consumed (Luckge *et al.*, 1999). Because of this, partial digestion of organic matter during or immediately following deposition has resulted in the increased proportion of inorganic sulphur observed.

There is a strong correlation between S/TOC and S/Fe in distal Waipawa ($R^2 = 0.81$; Figure 4.8b), suggesting that there was significantly greater reduction of organic matter, providing the source of pyrite sulphur and resulting in the increased proportion of S relative to TOC. The strong correlation between S/Fe and S/TOC indicates S is retained and preferentially remineralised as sulphides during early stage diagenesis. Samples of the Waipawa Formation from Mead Stream, Manurewa Point, Te Kaukau Point, and Opouwae River, all plot within the sulphide oxidation zone (Figure 4.6), suggesting that despite low TOC and S, sulphide oxidation was occurring in deeper, more distal settings, although sediment and organic matter supply was lower (compared to more proximal sections), resulting in lower TOC accumulation and preservation. This observation would support the low TOC and HI values determined by SRA if sulphate reduction had reduced the proportion of TOC and increased the proportion of inert, Type IV kerogen in these distal settings.

More oxic conditions in distal Waipawa, as indicated by paleo-redox proxies, are consistent with lower preserved-TOC values and lowered sedimentation rates. Trace element concentrations are progressively enriched in the deep-water distal Waipawa from Pahaoa River mouth to Mead Stream. Trace metal enrichments indicative of increased marine productivity (e.g. Ni, Cu, Cr, Zn; Figure 4.7) follow a similar pattern, but kerogen and organic biomarkers for the presence of marine organic matter are low at these localities. This may indicate that marine organic matter was exported to the sea floor and subsequently oxidised or, alternatively, these trace metals may be delivered to deeper portions of the basin as organo-metallic complexes in association with terrestrial organic matter, which appears to the be the dominant kerogen type in these settings.

Redox-sensitive trace metals and elemental indices display variable evidence for anoxia and sulphate reduction in the Waipawa Formation. This is in part because the Waipawa Formation has been demonstrated to contain multiple pulses of reducing conditions (Hines *et al.*, Chapter 3). Despite this, anoxicity was not sufficient to completely remove infaunal or epifaunal biotas and produce a typical, laminated black shale (e.g. Leckie *et al.*, 1992). This would suggest that sedimentation rates were high enough to promote anoxicity below the sediment-water interface, but anoxia did not rise into the water column, and likewise, sedimentation rates were not sufficiently high enough to smother bioturbators. Bioturbators were likely able to cope with a pulsed delivery of sediment, as suggested by the common *Bathysiphon* sp. in the formation.

The increasing oxygenation of bottom waters indicated by redox proxies and organic carbon preservation fits the upwelling model in the slope setting of the East Coast Basin, whereby an enhanced oxygen minimum zone in shelf and slope settings (proximal and typical Waipawa)

produces bottom water anoxia, whilst deeper settings show indications of oxic bottom water conditions and oxic reduction of organic matter (Figure 4.15).

4.4.4 Depositional Model

One of the major complications in characterising the paleo-redox conditions for the Waipawa Formation is that although being deposited in a marine environment, the source rock kerogen is predominantly terrestrial in origin, and most paleo-redox proxies and models assume TOC content to be exclusively marine in origin (Tyson, 2001). This presents a problem in understanding the depositional mechanisms of units such as the Waipawa Formation, where the majority of the kerogen is terrestrial, or mixed terrestrial-marine in origin.

In models for the formation of organic-rich shales in marine settings there exists an interplay between marine productivity (i.e. nutrient supply), and organic matter preservation (i.e. reducing conditions and/or sedimentation rate). In applying established models to the Waipawa organofacies, marine productivity is no longer an issue as TOC content is dominantly terrestrial in origin and likely in proportion with terrigenous sediment delivery to the basin. The quality of organic matter preservation is determined by time spent in the oxic zone, both suspended in the water column and in the oxic zone of sea-floor sediments. Areas with increased sedimentation rates are likely to have the greatest organic carbon preservation potential, as the increased sediment load in these areas is likely to be associated with an increased sinking flux. Increased sedimentation rates mean that organic matter spends less time in oxic surface sediments before being preserved by early stage diagenesis and anoxic pore waters, as well as decreasing the density and volume of bioturbation.

Uranium uptake in sediments is influenced by both bottom-water oxygen concentration, and the organic carbon oxidation rate, indicating a relationship between the rate of U uptake and the depth of oxygen penetration, with the depth of oxygen penetration influenced by the combination of carbon degradation, bottom water oxygen content, and sedimentation rate (McManus et al., 2005). Rapid burial also means that there was little to no opportunity for the redox boundary to fluctuate above or penetrate far below the sediment water interface. This means that U and Mo are not remobilised into the water column, explaining the notable enrichment of these elements across the Waipawa Formation, and the depletion in Mn. Pyrite, Fe and Mo accumulate under sulphate-reducing conditions, but are also influenced by changes in sedimentation rate (Raiswell, 1988; Piper, 1994). This implies that elevated sea-floor reducing conditions apparent in typical Waipawa

Formation is associated with higher sediment accumulation and burial rates. Therefore, increased organic matter preservation in the Waipawa Formation is correlated with sedimentation rate. When the average TOC value is plotted against formation thickness for each of the measured sections sampled in detail for this study, a distinct trend becomes apparent, with thicker sections (and therefore higher sedimentation rates) having higher average TOC values (Figure 4.14). In the more distal portions of the basin, sedimentation rates were lower, and consequently organic matter remained in surface sediments and within the oxidation zone for longer, resulting in lower TOC values and a greater proportion of inert kerogen. The oxidation process may vary, from increased bioturbation and reworking of sediments, to respiration and oxygen diffusion across the sediment-water interface, or even sulphide oxidation in pore waters.

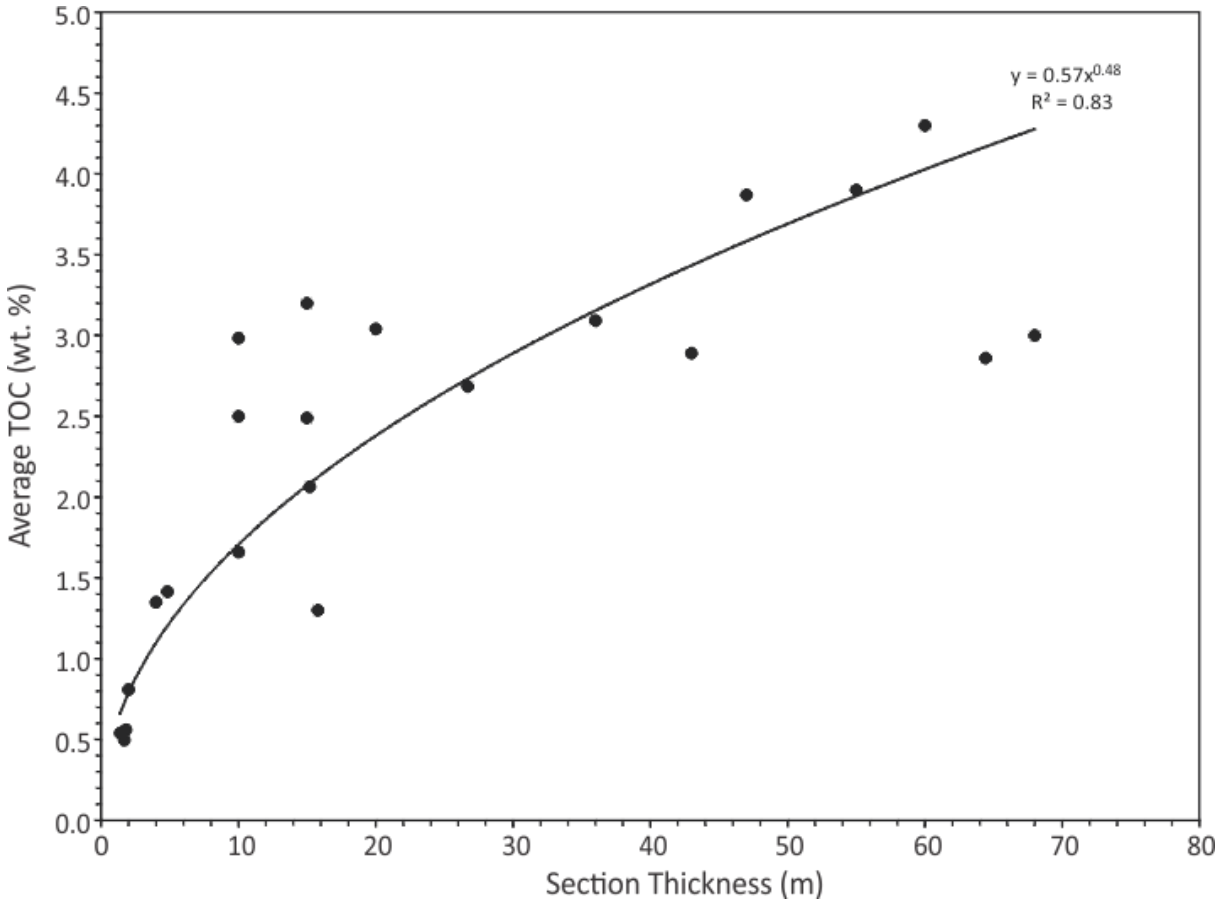

Figure 4.14: Section thickness plotted against average TOC value for the Waipawa Formation in the East Coast Basin, demonstrating a strong correlation between thickness and average TOC. Plotted regression is for measured sections only.

The identification of the Waipawa Organofacies in multiple sedimentary basins around the southwest Pacific suggests a broad-scale, regional event resulting in the deposition of organic-rich

mudstone in shelf-slope sediments during the late Paleocene. Recent work has proposed that a regression resulting from eustatic sea-level fall at this time (e.g., Schiøler *et al.*, 2010; Hollis *et al.*, 2014) may have been the causal mechanism, which resulted in the bypassing of shelf environments and increased sedimentation at shelf depths (Hines *et al.*, Chapter 3). The identification of the Waipawa Organofacies on the East Tasman Rise, offshore Reinga-Northland Basin, and offshore Taranaki Basin, implies that this was a widespread event not restricted to the eastern margin of the proto-New Zealand subcontinent.

A eustatic sea-level fall during the late Paleocene is observed in the Cenozoic sea-level records of Haq *et al.* (1987), Hardenbol (1998) and Schmitz *et al.* (2011), and occurs across the known age range of the Waipawa Formation (59.4–58.7 Ma; Hollis *et al.*, 2014). This corresponds to the Sel2/Th1 and Th2 sequence boundaries in the European succession (Hollis *et al.*, 2014). The magnitude of this sea-level fall is estimated to vary between ~12 and >50 m (Hollis *et al.*, 2014, and references therein). The two layers ("pulses") of the Waipawa Formation in distal portions of the basin (e.g. Manurewa Point, Mead Stream) is an exaggeration of the double pulse of organic matter and clastic sediments observed in the typical Waipawa Formation (Leckie *et al.*, 1995; Hollis *et al.*, 2014; Hines *et al.*, Chapter 3), and may represent a fourth-order sequence stratigraphic response to sea-level variability.

A fall in relative sea level during the deposition of the Waipawa Formation may have exposed large portions of the continental shelf. Consequently, terrigenous sediment supply largely bypassed shelf areas, resulting in the increased delivery of terrestrial organic matter, and increased sediment accumulation rates and nutrient flux to distal margins of the basin (Figure 4.15). Syn-sedimentary slumping of the Waipawa Formation or sediments immediately underlying the Waipawa Formation is observed in multiple localities (e.g. Old Hill Road, Kaiwhata Stream, Te Mai; Moore, 1989; this study). In Neogene sediments of the Taranki Basin, the incidence of slump folding and disturbed sediments most likely occurs during late highstand–early lowstand time, induced by a fall in relative base level (King *et al.*, 1994; King & Browne, 2001). Such slumping is interpreted to be triggered by oversteepening or sediment loading of the shelf margin, or by overpressure of pore fluids, which would have been exacerbated by a fall in relative base level (King *et al.*, 2011). This line of evidence would support sea-level regression during deposition of the Waipawa Organofacies suggested by Schiøler *et al.* (2010) and Hollis *et al.* (2014).

The shallowest depositional setting preserved from the late Paleocene East Coast Basin is inferred to be represented by Te Uri Member, with estimated paleo-water depths of 200–300 m. As previously mentioned, Te Uri Member is characterised by exceptionally low sedimentation rates

(0.6–1.4 cm/kyr), and the development of glaucony. Source rock analyses show that the Te Uri Member is dominated by terrestrial and inert organic matter (Type III and Type IV kerogen), suggesting oxidation of organic matter occurred either in the water column or post deposition below the sediment-water interface (Figure 4.15).

In slope settings, sedimentation rates were substantially higher (≤10 cm/kyr), which is reflected by the low Si/Al values (4–6). Increased terrigenous sedimentation resulted in an associated flood of terrestrial organic matter, demonstrated by palynofacies analysis. An associated increase in terrigenous flux could also induce a notable increase in nutrient supply in the water column, resulting in increased biological respiration and the development of an enhanced oxygen minimum zone (Figure 4.15). This would help promote the preservation and drawdown of organic matter and Mo to seafloor sediments. A portion of this organic matter is reduced by microbially mediated processes resulting in the formation of H_2S in pore fluids, which precipitates as sulphide complexes, resulting in increased enrichment factors for siderophile and chalcophile elements (e.g. Cu, Pb, Cr, Ni, As and Mo). Uranium becomes enriched through authigenic precipitation from seawater beneath suboxic to anoxic conditions. Carbon/N values from the Waipawa Formation at Te Hoe River suggest denitrification was an important process in shallow (~300 m paleo-water depth) sections of the Waipawa Formation. Foraminiferal index species for bottom water oxygenation show that typical Waipawa deposited under dominantly aerobic conditions, although there were some anoxic and intermediate index species present (Kaiho, 1991).

In more distal settings of the Waipawa Formation (800–1000 m paleo-water depth), although sedimentation rates were much lower (0.2–0.5 cm/kyr) they reflect a notable increase in terrigenous sediment flux against a background of otherwise bioclastic-dominated sedimentation. Despite the low preservation of TOC in these settings (typically 0.5–1.0%), trace element enrichments indicate increased reducing conditions in these settings. Trace metals associated with sulphide phases and strong S-TOC-Fe relationships indicate strongly reducing conditions. Visual assessment of pyrite framboids (>20 μm diameter) and large diagenetic pyrite nodules (Appendix 5), suggest that this may have been restricted to below the sediment-water interface. The low TOC values measured, and the strong relationship between S-TOC-Fe, may suggest that TOC may have been remineralised to provide the sulphide source. Another consideration is that the relatively greater uptake of redox-sensitive elements by sediment in distal settings may be due to the much longer residence time of particles on the sea floor than in the water column, or possibly due to the higher sulphide concentrations encountered below the sediment-water interface (e.g. Meyers *et al.*, 2005; Algeo & Maynard, 2009). Elemental ratios and bulk rock XRD show no apparent shift in sediment

provenance across the Waipawa Formation that may explain a change in sediment source areas, or may have promoted marine productivity; this, therefore, implies a change in relative sea level is the most like driver and explanation for the differential preservation of organic carbon across the Waipawa Formation.

Source rock analyses suggest a mixed marine and terrestrial kerogen source across the Waipawa Formation, despite palynofacies analyses showing an almost exclusively terrestrial kerogen. A potential explanation is that there is a minor component of marine organic matter-derived lipids preserved in the Waipawa Formation, which can subsequently be identified by SRA but not with palynological processing methods. Organic carbon isotope excursions across the Waipawa Formation are consistent with a terrestrially derived kerogen source (Hollis *et al.*, 2014), and the strong relationship between the magnitude of the excursion and water depth would support this (Figure 4.13). The strong correlation between section thickness (as a proxy for sedimentation rate) and average TOC suggests that organic matter flux occurs in association with sediment supply, and supports the $\delta^{13}C_{org}$ to depth correlation. This relationship would suggest that during the Paleocene in the East Coast Basin, sedimentation rate is the primary control on organic matter burial and preservation, with oxygen availability being a secondary consideration during the deposition of the Waipawa Formation. This would explain the notable variability of redox proxies within sections and across the lateral extent of the formation.

During the late Paleocene–Eocene, after Waipawa Formation deposition, a general trend of Cenozoic marine transgression in the East Coast Basin continued. The paleo-shoreline moved landward, resulting in a notable reduction in sedimentation rates across the Wanstead Formation. These lower sedimentation rates result in increased bioturbation, which in turn resulted in the oxidation and depletion of organic carbon. Consequently, these actions resulted in the low TOC values and low HI and OI values indicating a Type IV inert kerogen through the majority of samples analysed from the formation.

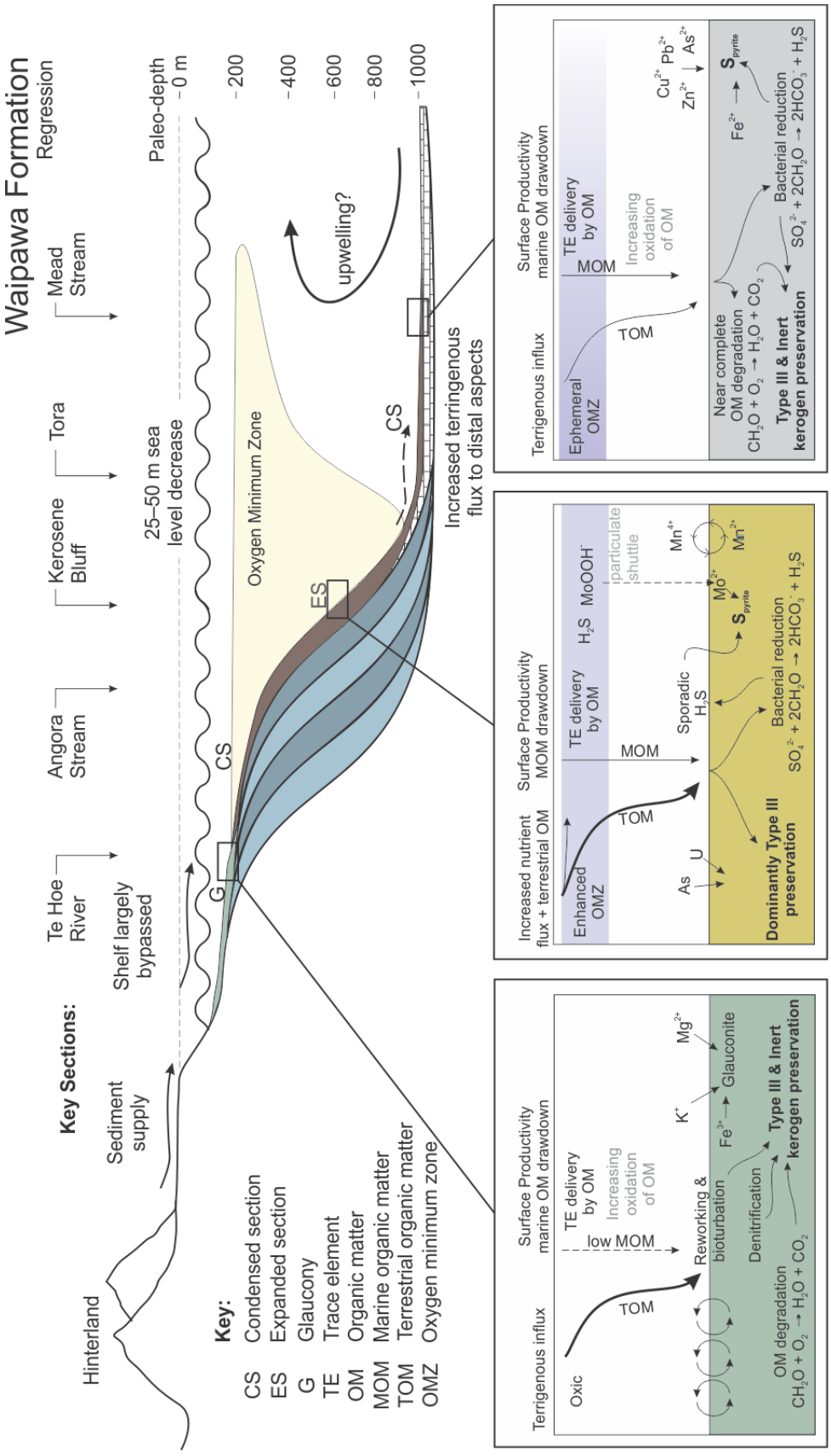

Figure 4.15: Integrated redox and depositional model for the Waipawa Formation across the East Coast Basin, explaining variations in formation thickness, paleo-water depth, dissolved oxygen availability and redox reactions, and organic carbon preservation and type.

4.5 Conclusions

In applying a multidisciplinary approach to over twenty-one outcrops in the East Coast Basin, the vertical and lateral facies relationships of the Waipawa Organofacies can be disentangled, and some of the issues regarding its depositional history and petroleum potential answered. The Waipawa Formation is thin in shelf settings (<10 m), and thickens across slope environments, before thinning in distal areas of the basin. Proximal sediment-starved areas are characterised by the deposition of the Te Uri Member, a condensed section dominated by glaucony, and a reduced TOC enrichment (relative to the Waipawa Formation), but with a positive shift in the $\delta^{13}C_{org}$ signal present in uppermost beds that is characteristic of the Waipawa Formation elsewhere. Assessment of foraminiferal faunas from the Waipawa Formation and the immediately underlying units has demonstrated a progressive basinward deepening trend across the formation, and has also highlighted lateral relationships with shallow-marine strata. The Waipawa Formation is thickest and has the richest source rock potential in slope settings between ~400–600 m paleo-water depth, with sedimentation rates lowest in both proximal and distal settings.

Source rock analysis, palynofacies assessment and carbon isotopes are indicative of a dominantly terrestrial kerogen source, in keeping with the depositional model presented herein. Organic carbon preservation is strongly associated with sediment supply and accumulation rates, and is the primary control of organic carbon burial and preservation. Paleo-redox conditions are variable vertically and laterally across basin, forming a secondary consideration in assessing organic carbon preservation. In proximal settings, denitrification appears to be a key redox process in the Waipawa Formation, with microbial-mediated sulphate reduction becoming increasingly important with increasing paleo-water depth. Bulk modal mineralogy and elemental ratios show no change in sediment provenance, ruling out changes in sediment source or productivity as a factor in increased TOC across the Waipawa Formation.

Acknowledgments

We acknowledge use of data contained in the New Zealand Fossil Record File (www.fred.org). Funding for this research comes from the Sarah Beanland Memorial Scholarship, awarded to BRH by GNS Science. We are grateful for the support of Richard Sykes (GNS Science) and the GNS Science - Petroleum Source Rocks & Fluids programme (MBIE contract C05X0302), and also to Direct Crown Funding provided to GNS Science as part of the Petroleum Basins Research programme. This work has benefited from discussion with Hugh Morgans (GNS Science).

Page intentionally left blank for formatting purposes

Chapter Five

TECTONIC RECONSTRUCTION OF THE EAST COAST BASIN AND WIDER ZEALANDIA

"Essentially, all models are wrong, but some are useful."

- George Box (1987) Empirical model building and response surfaces.

Surface expression of the Clarence Fault, tributary or Mead Stream. Photo: James Crampton.

PREFACE TO CHAPTER FIVE

Statement of Authorship

This chapter represents entirely my own writing, and all figures — unless otherwise credited — are my own. Model development has been an iterative process and I have been involved in that process from inception, although this generation of the model is the intellectual property of Hannu Seebeck.

The contributions from external sources are as follows:

- Hannu Seebeck – The base model output from GPlates for the 0–40 Ma reconstruction, lengthy discussion on plate kinematics, geophysical modelling for key parameters that govern model kinematics (not shown or discussed herein). Hannu has built the wider Gplates model for the entire SW Pacific-Antarctic region, which provides the context and boundary conditions in which the detailed model sits.

My contributions are as follows:

- The application and testing of the geological model are my own work, except where outlined or otherwise explained
- The basic East coast structural division was substantially my own, although it has been simplified in this rendition of the model.
- The concept, data preparation, application and interpretation are my own intellectual property.
- The testing and application of the model demonstrated is entirely my own work, incorporating the development of paleomagnetism-model rotation comparisons, detrital zircon clusters, heavy mineral groupings, and crustal volume calculations.

Chapter Outline/Overview

This chapter explains the initial assumptions in the development of the model, followed by testing and application of the model against geological, geochemical and geophysical datasets. The ultimate purpose of the model is to develop a palinspastic framework upon which the stratigraphic and paleoenvironmental development of the Late Cretaceous–Eocene East Coast Basin can be assessed.

Chapter Five

TECTONIC RECONSTRUCTION OF THE EAST COAST BASIN AND WIDER ZEALANDIA

5.1 Introduction

The propagation of the Australian-Pacific plate boundary through the New Zealand region in the late Eocene to early Miocene resulted in the development of a number of major physiographic features in the southwest Pacific region (Figure 5.1). The position and geometry of the East Coast Basin prior to the inception of the modern plate boundary between the Australian and Pacific plates continues to be a contentious issue in paleogeographic reconstructions of the proto-New Zealand subcontinent (Zealandia; Mortimer *et al.*, 2017) and the Southwest Pacific region (Figure 1.2). The ultimate purpose of the structural model developed herein is to derive a palinspastic framework upon which the stratigraphic and paleoenvironmental development of the Late Cretaceous–Eocene East Coast Basin can be assessed. In order to produce a pre-Neogene model base, varied Neogene deformations must be sequentially backstripped. Placing the East Coast Basin within a palinspastic model framework requires consideration of the structural trends of the wider New Zealand region. To do this, multiple geological and geophysical datasets are integrated to provide a holistic overview of regional and basin structural evolution during Neogene plate boundary propagation.

The East Coast Basin is a Cretaceous-Cenozoic sedimentary basin that initiated in a dominantly passive margin setting, but has evolved within a convergent plate boundary setting during the Neogene (Field & Uruski *et al.*, 1997). In many previous reconstructions of New Zealand, the East Coast Basin is either omitted, or depicted as a broad triangular zone of unconstrained and unspecified deformation (e.g., Walcott, 1987; Rait *et al.*, 1991; Bradshaw *et al.*, 1996; Sutherland *et al.*, 2001; Collot *et al.*, 2009; Reyners, 2013; Mortimer, 2014). Previous reconstructions of the East Coast Basin tend to treat the region as a single, simple block (e.g., Ballance, 1976; King, 2000a), or a small series of blocks (Wallace & Beavan, 2004; Lamb, 2011) or deformation zones (Nicol *et al.*, 2007). Due to the largely unquantified internal deformation and uncertainties in the estimates of timing and the magnitude of vertical and lateral movement in the Neogene, the East Coast Basin is often used to accommodate uncertainties in the volume of shortening associated with the development of the Hikurangi subduction margin in paleogeographic reconstructions.

There is considerable variability in the location of the East Coast Basin in paleogeographic reconstructions of the southwest Pacific (Figure 1.2; King, 2000a). These reconstructions can be divided into two general schools of thought: one requiring considerable strike-slip movement and

a minor rotational component (e.g., Cole, 1986; Ballance, 1976; Carter & Norris, 1976; Cooper & Tulloch, 1992; Beu, 1995); and the alternative, requiring substantial rotation of the region with a minor component of strike-slip displacement (e.g., Lamb, 1988; Gray & Norton, 1988; Uruski & Wood, 1993; Lewis & Pettinga, 1993; King, 2000a; Nicol *et al.*, 2007; Wood & Stagpoole, 2007; Seebeck *et al.*, 2014). Considering that paleomagnetic studies have demonstrated that there has been 60–110° of Neogene vertical-axis rotation in the East Coast Basin (excluding the East Coast Allochthon; Walcott & Mumme, 1985; Mumme *et al.*, 1989; Rowan & Roberts, 2008; Lamb, 2011), this would favour a reconstruction approach with a large rotational component and a comparatively minor strike-slip contribution. Such an interpretation is also supported by estimates of offset across major crustal-scale faults in North Island (e.g., Beanland *et al.*, 1998; Nicol *et al.*, 2007).

The basin can be divided, from west to east, into four major tectonic divisions that reflect the modern subduction zone. These are the frontal ridge (axial ranges), the inner forearc basin, outer forearc basin (coastal ranges), and the accretionary wedge (Figure 1.2). The axial ranges mark the primary boundary from compressional deformation in the east into strike-slip deformation to the west, whereas the coastal ranges mark the onshore expression of the accretionary wedge, with the intervening area forming the forearc. In addition, late Neogene to Recent strike-slip faults (the Carterton, Kamingi and Alfredton faults) are obliquely cutting the NNE-oriented structural trend of the forearc (Figure 5.2).

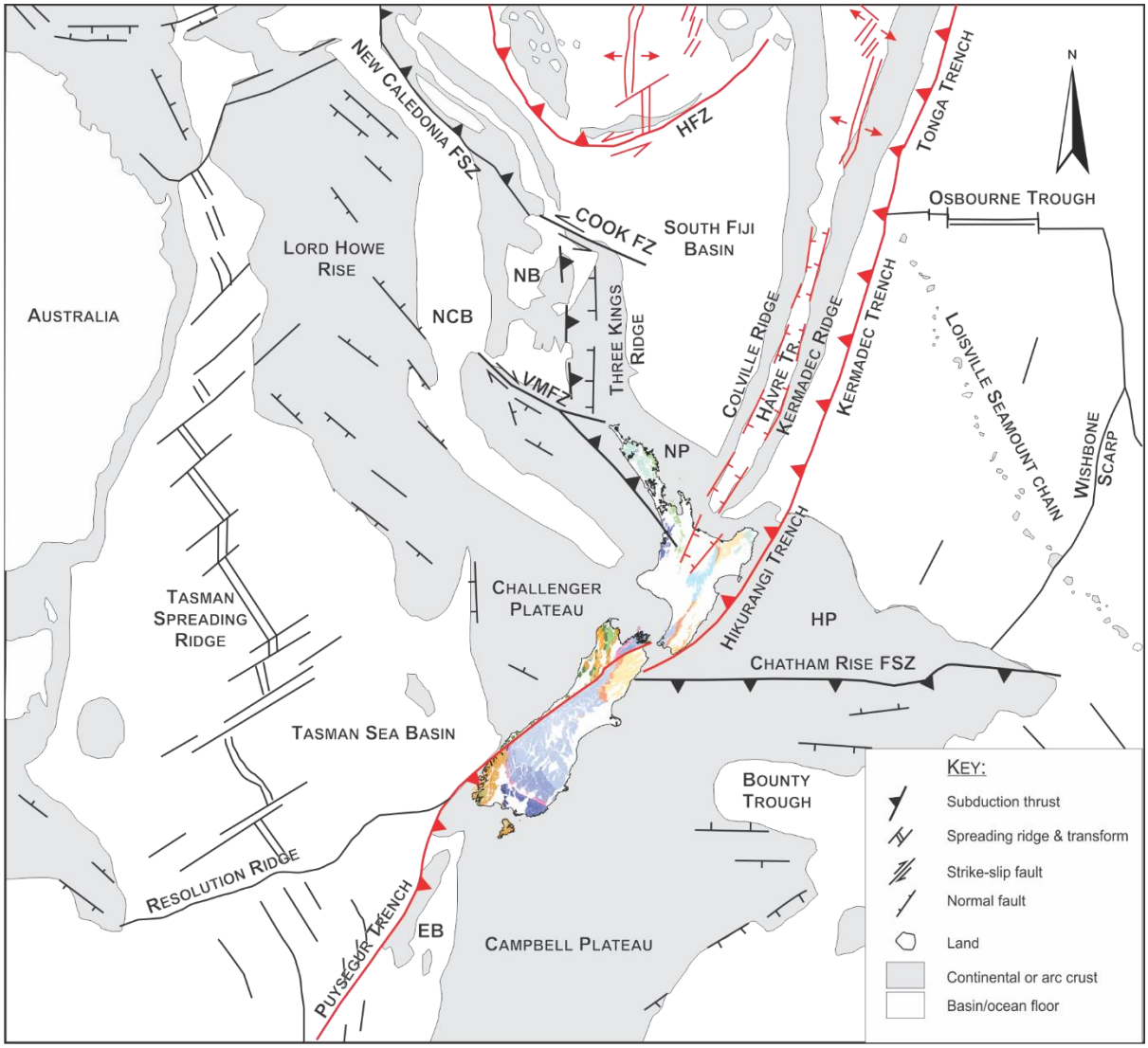

Figure 5.1: Structural and physiographic features in the New Zealand region of the southwest Pacific. Key to abbreviations: HP – Hikurangi Plateau, EB - Emerald Basin, NP – Northland Plateau, NB – Norfolk Basin, NCB – New Caledonia Basin, VMFZ – Vening Meinesz fracture zone, HFZ – Hunter Fracture Zone, FSZ – Fossil Subduction Zone, FZ – fracture zone. Black denotes fossil and relict structures, red indicates active structures. Basement geology superimposed on New Zealand – see Figure 5.2 for key. Onshore geology from Heron (2014), submarine physiographic and tectonic features from Schellart *et al.* (2006).

Despite well-developed understandings of relative plate motions between the Pacific and Australian plates, it remains difficult to reconcile the ≥90° of rotation in the East Coast Basin with deformation trends across the New Zealand region. Substantial Neogene rotation should result in substantial crustal shortening in the southern Hikurangi margin, yet seismic interpretation and balanced cross-sections indicate only ~30 km of Neogene shortening in southern Wairarapa (Nicol & Bevan, 2003; Nicol *et al.*, 2007). In addition, the low metamorphic grade of basement strata

exposed in the central North Island and the axial ranges is inconsistent with a high amount of crustal shortening.

The East Coast Basin has been deformed extensively, dissected, dislocated and re-oriented following the inception of the Hikurangi subduction margin through the basin. The post-Oligocene structural style is primarily compressional, as evidenced by early Miocene emplacement of thrust sheets in the Raukumara Peninsula and possible thrust sheet emplacement in southern Hawke's Bay-northern Wairarapa (Delteil *et al.*, 2006). In the northern East Coast Basin, early Miocene NE–SW shortening in Raukumara is associated with obduction of the East Coast Allochthon from the subducting Pacific Plate (Rait, 2000). The Northland and East Coast allochthons were emplaced along with a number of structural assemblages that formed during a brief, vigorous, early Miocene deformation event during the onset of subduction beneath the North Island and Marlborough (Rait *et al.*, 1991; Isaac *et al.*, 1994; Rait, 2000). The East Coast and Northland allochthons are estimated to have been emplaced at 21–24 Ma, in a southwest direction (Rait *et al.*, 1991; Isaac *et al.*, 1994; Kamp, 1999; Rait, 2000; Mortimer *et al.*, 2003; Furlong & Kamp, 2009).

Post-early Miocene shortening has been interrupted by at least two tectonic reorganisations since the Late Miocene. Neogene subduction and dextral strike-slip has continued to the present day, with the largest proportion of dextral faulting occurring since the late Miocene (Cashman *et al.*, 1992; Beanland *et al.*, 1998; Barnes *et al.*, 2002; Kamp, 1987; Nicol & Wallace, 2007). The Australian-Pacific Euler pole shifted abruptly south-westward at 6.5–5 Ma, resulting in increased convergence across the plate boundary, consequently causing the development of the Marlborough fault zone and the uplift and subaerial exposure of parts of the inner forearc in the Hawke's Bay-Wairarapa (Cande *et al.*, 1995; Kelsey *et al.*, 1995; Sutherland, 1995; Little & Roberts, 1997). The onset of extension of the Taupo Volcanic Zone at ~2 Ma (Wilson *et al.* 1995; Wallace *et al.*, 2004) and the initiation of dextral strike-slip displacements on the North Island fault system (Beanland, 1995; Beanland *et al.*, 1998) resulted in the current tectonic style observed along the margin at the present day. Many geological and geophysical constraints associated with this varied tectonic evolution of the Hikurangi Margin should be taken into account when developing an integrated reconstruction for the region, and are discussed in the following section.

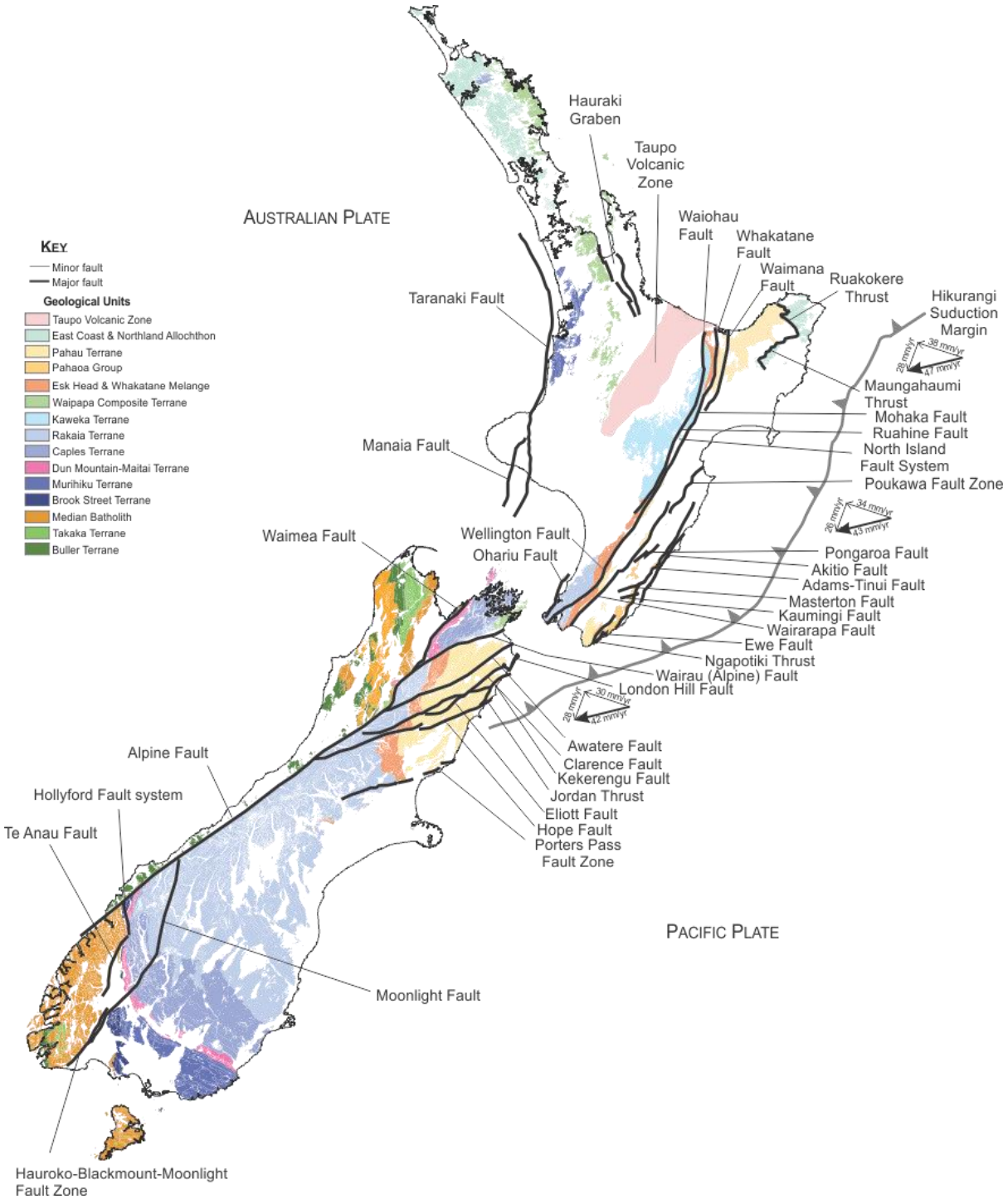

Figure 5.2: Major faults and structures discussed in text. Greater detail of the Marlborough fault system is depicted in Figure 5. Outcrop distributions of New Zealand's basement terranes, the Northland and East Coast allochthons, and the Taupo Volcanic Zone, are plotted for reference (see map legend). Map data sourced from Heron (2014). Relative plate motion vectors from Nicol *et al.* (2007).

5.2 Model Constraints, Initial Assumptions & Method

The model presented here is synthesised from new and published geological and geophysical datasets, including sedimentological, mineralogical, structural, plate tectonic, paleomagnetic, and stratigraphic data. Actual model development is achieved using GPlates open-source plate tectonic reconstruction software (www.gplates.com; Boyden *et al.*, 2011; Qin *et al.*, 2012). GPlates interacts with widely available geographic information systems software, and provides a consistent framework within which block models can be developed to estimate deformation within the plate boundary zone. One of the key benefits of applying the GPlates software is that the model is easily adaptable as new data and ideas develop.

The East Coast region is widely considered to have been within a tectonically passive setting from latest Cretaceous to late Eocene (e.g., Ballance, 1993b; Field & Uruski *et al.*, 1997; King, 2000a; Uruski, 2010). Therefore, the Cretaceous to Eocene geometry of the reconstructed Zealandia model is assumed to be largely fixed by the Recent to Eocene reconstruction, which in turn, is derived by retroactively removing Neogene deformation across the plate boundary. The kinematics of deformation on the contemporary plate margin are best described in terms of spatially continuous strain (e.g., Beanland & Haines, 1998; Wallace *et al.*, 2004; Nicol *et al.*, 2007). On the other hand, paleomagnetic data and GPS block models define large regions of consistent vertical-axis rotations (e.g. Wallace *et al.*, 2004, 2007; Lamb, 2011). Similarly, structural data also provides evidence for block faulting on scales of 10's to 100's of km along strike.

The GPlates software used in the development of this model is limited to a largely rigid-block model output that does not readily allow for the degree of plastic deformation that is common in a convergent plate boundary zone. As such, most deformation is implicitly accommodated on faults bounding rigid crustal blocks (e.g. King, 2000a). A number of assumptions were required in the initial development of the model. These include: identifying and defining continental blocks, determining the initial configuration of blocks, establishing finite plate rotations, and assessing internal rotation of structural blocks within the plate boundary deformation zone. These considerations are outlined below.

5.2.1 *Block Assignment & Definition*

Of the assumptions required in order to establish the baseline for the model, arguably the most important is the definition of continental blocks, and determining the precursor relationships between these continental blocks (King, 2000a). Block boundaries applied herein are defined

primarily on the basis of geological and structural considerations, and also changes in gravity and magnetic data. Preference for structural division was given to faults that demonstrated evidence of early Miocene or pre-Neogene existence, and structures that form distinctive features within the geological, structural and physiographical division of the New Zealand region. In most cases, block divisions are well-defined by discrete structures, although in a few places block boundaries are considered a diffuse zone of faulting and deformation. The division of structural blocks along basement-penetrating faults of Early or pre-Miocene age, with consideration of pre-Neogene geology, has resulted in a similar structural subdivision of the North Island East Coast to that of Moore (1988b; Figure 5.3A). Although the model presented here draws on previous GPS-based models (e.g. Wallace *et al.*, 2004, 2012; Figure 5.3B) and paleomagnetism-based reconstructions (e.g. Lamb, 2011; Figure 5.3C), block geometries applied here in this study differ substantially from previous reconstructions (Figure 5.3D). These structural subdivisions have been simplified for expression within the model, with often moderately complex geometries reduced to simple block structures and straight boundaries for clarity of presentation. In the present-day offshore region, the blocks are limited by the 2000 m isobath. In establishing the base model, the wider Zealandia region is divided into five major crustal blocks, following King (2000a), but with further subdivision in the Taranaki, Marlborough and East Coast areas. In this model, the East Coast Basin is represented by a number of separate crustal blocks that move independently within a basin-scale envelope.

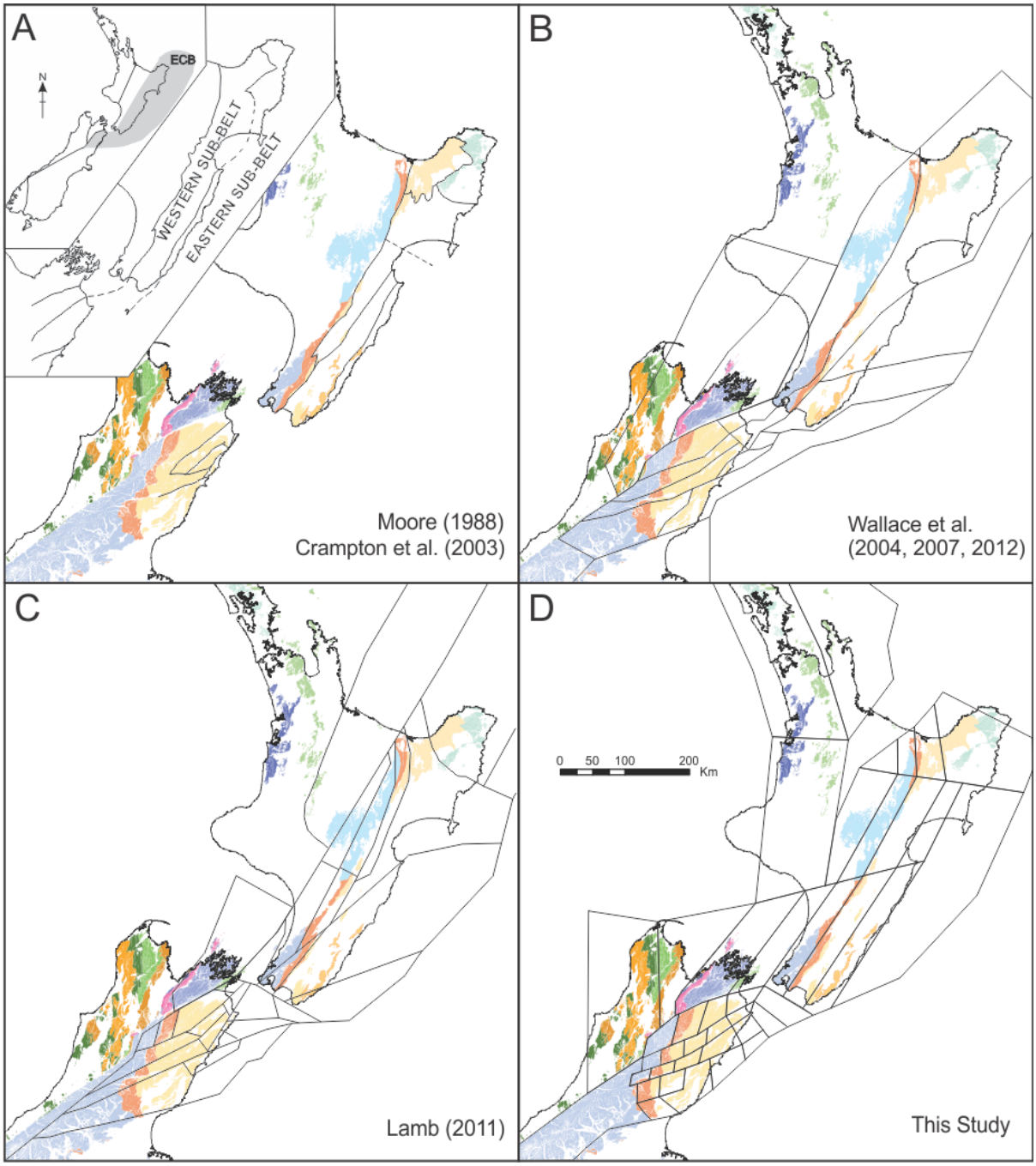

Figure 5.3: Block models for the East Coast Basin from previous studies, and this study. A) North Island structural divisions from Moore (1988b), and South Island block divisions from Crampton *et al.* (2003). Sub-belts shown for reference from Moore (1988b, modified after Crampton, 1997). New Zealand broad-scale block divisions of King (2000a) shown in inset map. B) Block model from Wallace *et al.* (2004, 2007, 2012) for Pliocene movements of the East Coast Basin. C) Neogene model from Lamb (2011). D) The structural block divisions adopted in this study.

The Neogene structural division of the New Zealand region (excluding the TVZ) appears to be largely governed by existing, mostly Cretaceous-aged structures. The Alpine Fault formed through the growth and interconnection of smaller faults as displacement of the boundary increased, until reaching the present-day length of 600 km; i.e. a zone of faults that became progressively interconnected during Miocene times (Sutherland, 1999a). So it follows that the Alpine Fault as a continuous structure may be much younger than the Oligocene to early Miocene age generally accepted for its inception (Sutherland, 1999a). An alternative hypothesis is that the Alpine Fault was an existing Cretaceous structure that already had hundreds of kilometres of sinistral offset prior to the Neogene (Lamb *et al.*, 2016).

Several major faults in North Island were active structures in the Late Cretaceous (Nicol *et al.*, 2007; Stagpoole & Nicol, 2008; Reilly *et al.*, 2015; Crampton, unpublished data). These include the Mohaka Fault, for which there must have been an earlier, Cretaceous structure prior to the Piripauan-Haumurian, as Pahau Terrane is juxtaposed against late Cretaceous Karekare Formation, both of which are demonstrably overlain by Piripauan-Haumurian Tahora Formation (Crampton & Moore, 1990; Isaac *et al.*, 1991). The Adams-Tinui Fault was interpreted as an active structure in the latest Cretaceous by Moore (1980). In addition to the North Island Fault System, the Waimea-Flaxmore Fault zone, and the Taranaki Fault run sub-parallel to Mesozoic basement fabrics, suggesting that many post-Oligocene faults occupy pre-existing planes of weaknesses (e.g. terrane boundaries, stratigraphic contacts and faults; Barnes & Audru, 1999; Nicol *et al.*, 2007). The Clarence Fault is an example of Neogene reactivation of a Cretaceous structure, as it can clearly be demonstrated that late Cretaceous dikes have intruded a pre-existing shear zone, before being sheared and deformed during Neogene movements (Figure 5.4). Within the Torlesse basement, the Clarence Fault forms the southwestern boundary of a ~400 m-wide zone of intense shearing and brittle deformation that formed prior to a period of mid-Cretaceous dike intrusion at 100 Ma, before being reactivated in the late Cenozoic with an oblique slip sense (Crampton *et al.*, 1998; Nicol & Van Dissen, 2002). While many faults in the North Island were active structures during the Cretaceous, it is rarely demonstrable at the outcrop scale.

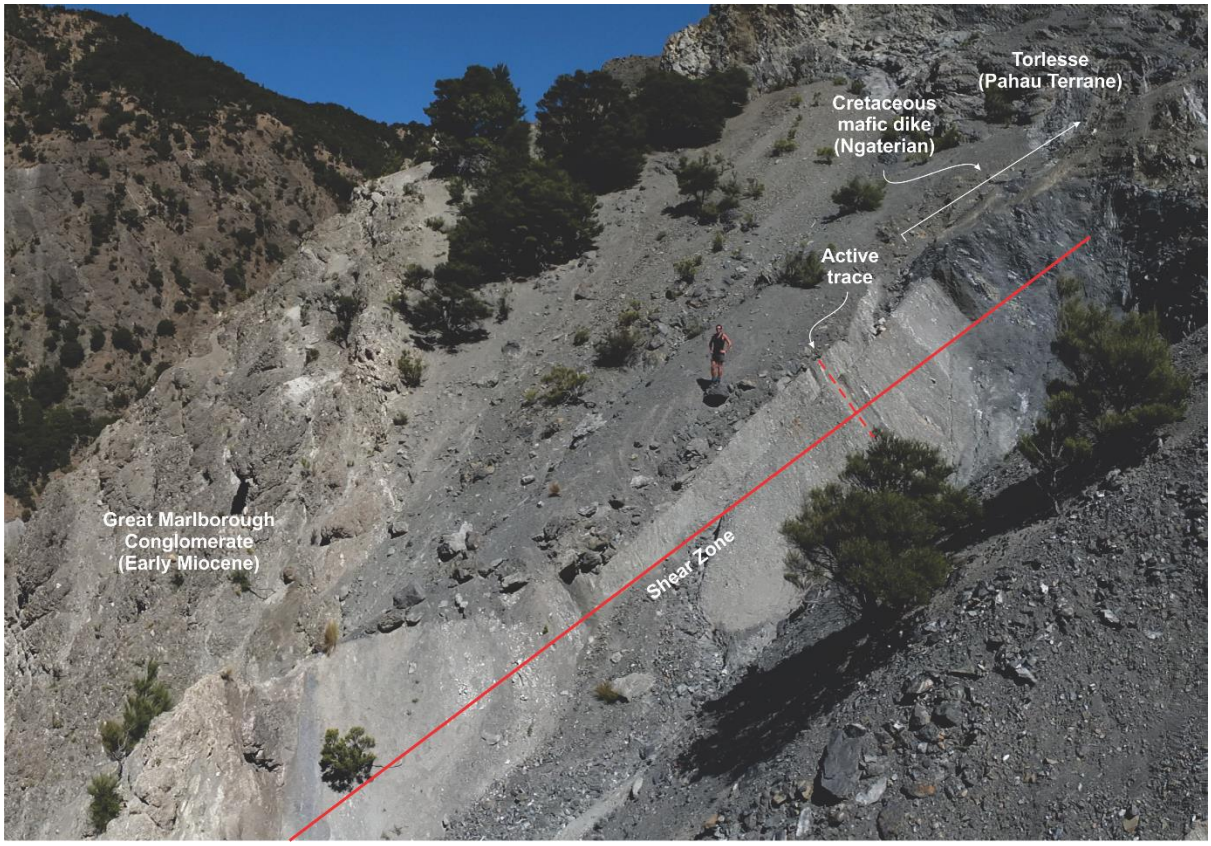

Figure 5.4: Exposure of the Clarence Fault in a tributary of Mead Stream, showing broad shear zone, and late Cretaceous dike intrusion within the shear zone, suggesting the Clarence Fault is a Cretaceous structure that has been reactivated in the Neogene. Figure for scale. Photo: James Crampton.

5.2.2 Regional Base Model

Major offsets of basement markers across the Alpine, Wairau, Hollyford, and Hauroko faults support the division of the South Island into four crustal blocks (as per King, 2000a; Wood & Stagpoole, 2007; Mortimer, 2014). In this reconstruction, the northwestern South Island is considered a single stable block, fixed to the Australian Plate (Turner *et al.*, 2012). The east Nelson Block is bounded by the Waimea-Flaxmore and Wairau faults. Areas south of the currently developing Porters Pass Fault Zone in central-eastern South Island are considered to be largely undeformed and continuous with the Chatham Rise, and therefore regarded as a single block. The Fiordland area, comprised of Western Province basement units and rocks of the Median Batholith, is separated as a separate crustal block along the Te Anau-Livingston, Hauroko, and Alpine faults.

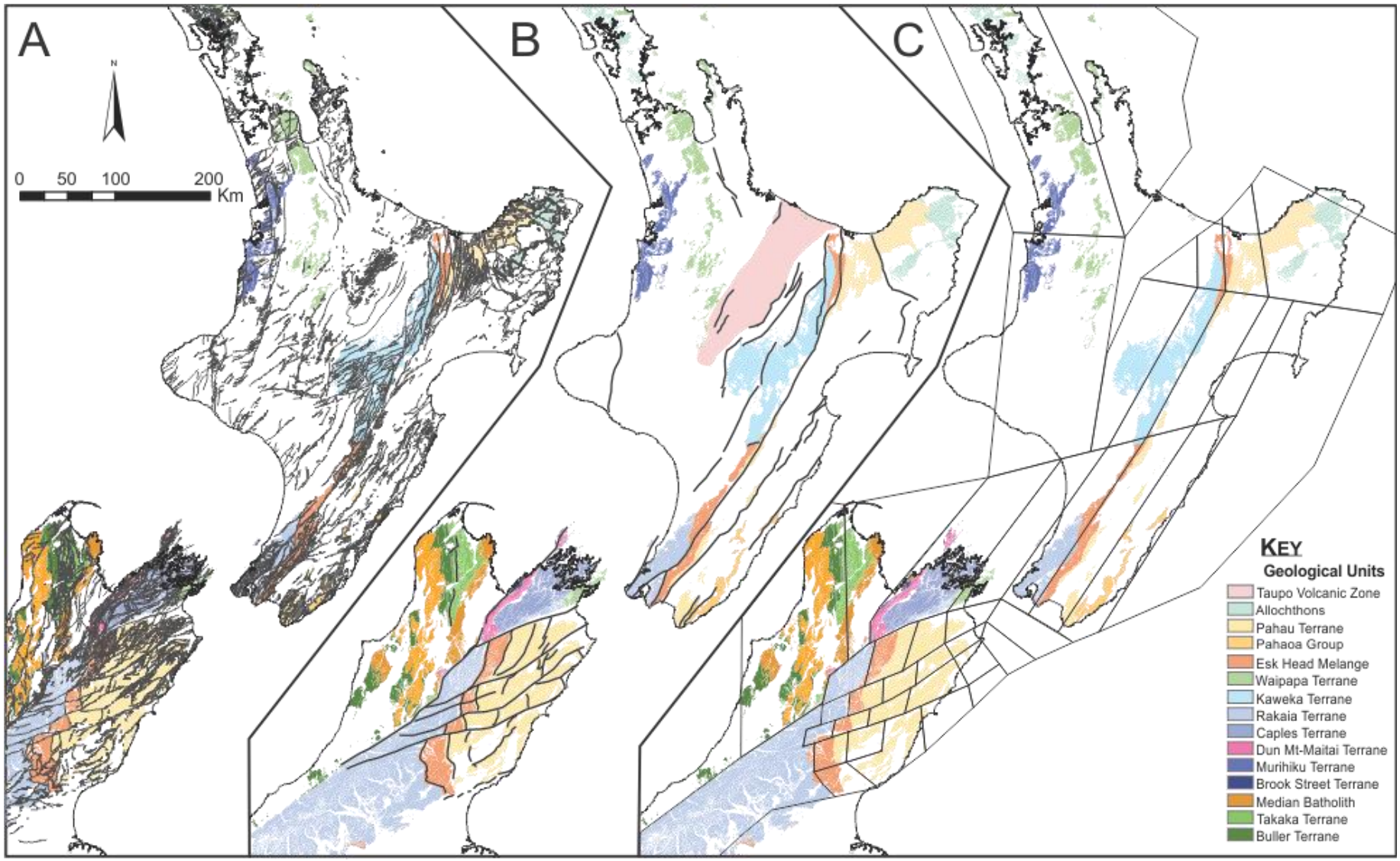
A
B
C
N
0 50 100 200
Km
KEY
Geological Units
Taupo Volcanic Zone
Allochthons
Pahau Terrane
Pahaoa Group
Esk Head Melange
Waipapa Terrane
Kaweka Terrane
Rakaia Terrane
Caples Terrane
Dun Mt-Maitai Terrane
Murihiku Terrane
Brook Street Terrane
Median Batholith
Takaka Terrane
Buller Terrane

Figure 5.5: A) All mapped faults in the central New Zealand region. B) Important, block-bounding structures identified and used in this study. C) Simplified structural block divisions applied in the GPlates model of this study. Map data sourced from Heron (2014). Panel C enlarged in Figure 5.6. Bounding structures included in Table 5.1.

5.2.3 *East Coast Structural Division*

In the model developed and presented herein, the North Island East Coast Basin has been simplified along major structural trends and tectono-geomorphic features, with a block configuration that is similar to the structural division of Moore (1988b; Figure 5.3A). Subdividing the basin along major, crustal-scale and basement-penetrating structures essentially produces a micro-plate model for the East Coast region that is detailed enough so that aspects of brittle deformation, particularly strike-slip motions, are not obscured, but without getting lost in minute and largely unresolved variability across the basin (Figure 5.5). Similarly, such a division allows the paleomagnetic histories of individual fault-bounded blocks to be incorporated into the reconstructions.

Major block-bounding structures are summarised in Table 5.1. The North Island axial ranges are divided into three separate blocks, namely the Urewera Range (2), Ruahine Range (6), and the Rimutaka-Tararua ranges (12; Figure 5.6). West of the axial ranges, the Kaimanawa Range (5) and Kapiti Island (13) have been differentiated from the axial ranges into two separate structural blocks on the basis of higher metamorphic grade. The Kaimanawa block (5) is delineated by the Ngamatea Fault in the east, and the Taupo Volcanic Zone to the west, and basement strata are comprised, in part, of Kaimanawa Schist (Mortimer, 1993). The Kapiti block (13) is differentiated by a change in basement strata composition (Waipapa Terrane) and metamorphic zonation across the Ohariu Fault that can be correlated with low grade schist in the Marlborough Sounds (Figure 5.6; Mortimer, 1993; Adams & Graham, 1996; Adams *et al.*, 2009). East of the axial ranges, the Raukumara Ranges (2) and northern Urewera Ranges (3) have been differentiated along the Whakatane Fault. South of this, the modern forearc basin is subdivided into a Hawke's Bay block (7) and a Wairarapa block (11), separated from the axial ranges by the Wellington-Ruahine-Mohaka fault system (Figure 5.6; Table 5.1). The outer forearc-coastal ranges are again separated into separate Hawke's Bay (8) and Wairarapa (10) structural blocks, delineated as continuous linear feature by splays and relay structures between the Wairarapa, Alfredton, Matuki, Tukituki and Poukawa fault zones (Figure 5.6; Table 5.1). There are limited offshore data available across Hawke Bay, although the trend of the Napier Fault, Pania Reef and the Cretaceous stratigraphy of the Opoutama-1 well on Mahia

Peninsula provide a guide for the placement of this boundary (Mazengarb & Speden, 2000; Lee *et al.*, 2011). Offshore, the accretionary prism is treated as a single structural block (9), following Wallace *et al.* (2004) and Nicol and Wallace (2004). The East Coast Allochthon/Raukumara structural block (1) is delineated by the Ruakokere and Maungahaumi thrusts in following Mazengarb and Harris (1994) and Leonard *et al.* (2010). The southern boundary of this block is largely inferred, due to the absence of pre-Neogene outcrop or notable structures, and late Neogene sedimentary strata obscuring structural boundaries (Moore, 1988b; Mazengarb & Harris, 1994).

The Cook Strait area is divided into a complex series of *en-echelon*-style fault blocks (Pondard & Barnes, 2010; Holdgate & Grapes, 2015), which have been simplified within the broader context of our model. Marlborough has been divided across the major structures of the Marlborough Fault System (Wairau, Awatere, Clarence, London Hill, Fidget, Jordan Thrust, Kekerengu, and Porters Pass faults), and further divided across smaller, obliquely oriented shear zones within the larger structures. Particularly for northern Marlborough, the division and reorganisation of the crust into smaller, equidimensional blocks is more representative of vertical-axis rotation and late Neogene deformation (Hall *et al.*, 2004). The approximately equidistant subdivision of structural blocks in Marlborough allows correlation of key piercing points, in particular the Esk Head Melange, allowing rotation and correlation of Marlborough structural blocks with their North Island counterparts, without creating an unrealistic, splayed fan-like continental margin in reconstructions.

Table 5.1: Major structures used to delineate structural divisions of the GPlates model used in this study.

Block Name	Block Number	West Bounding Structure	East Bounding Structure
East Coast Allochthon	1	Motutohora Fault	Hikurangi subduction margin
Raukumara 1	2	Whakatane Fault	Motutohora Fault
Axial Range 1	3	Waiohau-Awakeri faults, Edgecumbe Fault	Whakatane Fault
Axial Range 2	6	Ngamatea Fault	Mohaka Fault
Kaimanawa 1	4	Kaimanawa Fault/TVZ	Waiohau-Awakeri faults
Kaimanawa 2	5	TVZ	Ngamatea Fault
Axial Range 3	12	Ohariu Fault	Wellington Fault
Hawke's Bay 1	8	Arbitrary placement; no major mapped faults, dominantly Pliocene geology)	Lachlan Fault
Hawke's Bay 2	7	Mohaka Fault	Arbitrary placement; no major mapped faults, dominantly Pliocene geology)
Accretionary Wedge	9	Akitio Fault	Hikurangi subduction margin
Wairarapa 1	10	Wairarapa, Alfredton, Pongaroa, Tukituki, Poukawa fault zones	Akitio Fault
Wairarapa 2	11	Wellington-Mohaka Fault	Wairarapa, Alfredton, Pongaroa, Tukituki, Poukawa fault zones
Taranaki-Whanganui	41	Mania and Takanaki faults	TVZ
Northland	43	Taranaki Fault	Kerepehi Fault
Coromandel	42	Kerepehi Fault	2000 m isobath
Kapiti	13	Picton Fault	Ohariu Fault
East Nelson	40	Waimea-Flaxmore Fault	Picton Fault
Cook Strait	14, 15	Arbitrary placement	Hikurangi subduction margin
North Awatere Valley	20	Awatere Fault, rotation boundary	Clarence Fault
North Clarence Valley	25	Clarence Fault, rotation boundary	Hope Fault
Wairau valley	16-19	Wairau Fault	Awatere Fault
Awatere valley	21-24	Awatere Fault	Clarence Fault
Clarence valley	26-29	Clarence Fault	Hope Fault
Kaikoura	31	Hope Fault	offshore fault system, southern Hikurangi subduction margin
North Canterbury 1	32	Hope & Hurunui Bluff faults	Porters Pass Fault zone
North Canterbury 2,3	33, 34	Hope Fault	Hurunui Bluff Fault
North Canterbury 4	35	Hurunui Bluff Fault	Porters Pass Fault zone
South Island (PAC)	36	Axis of oroclinal bending	2000 m isobath
Southern Alps	37	Alpine Fault	Axis of oroclinal bending
Northwest Nelson (AUS)	38, 39	2000 m isobath	Waimea-Flaxmore Fault

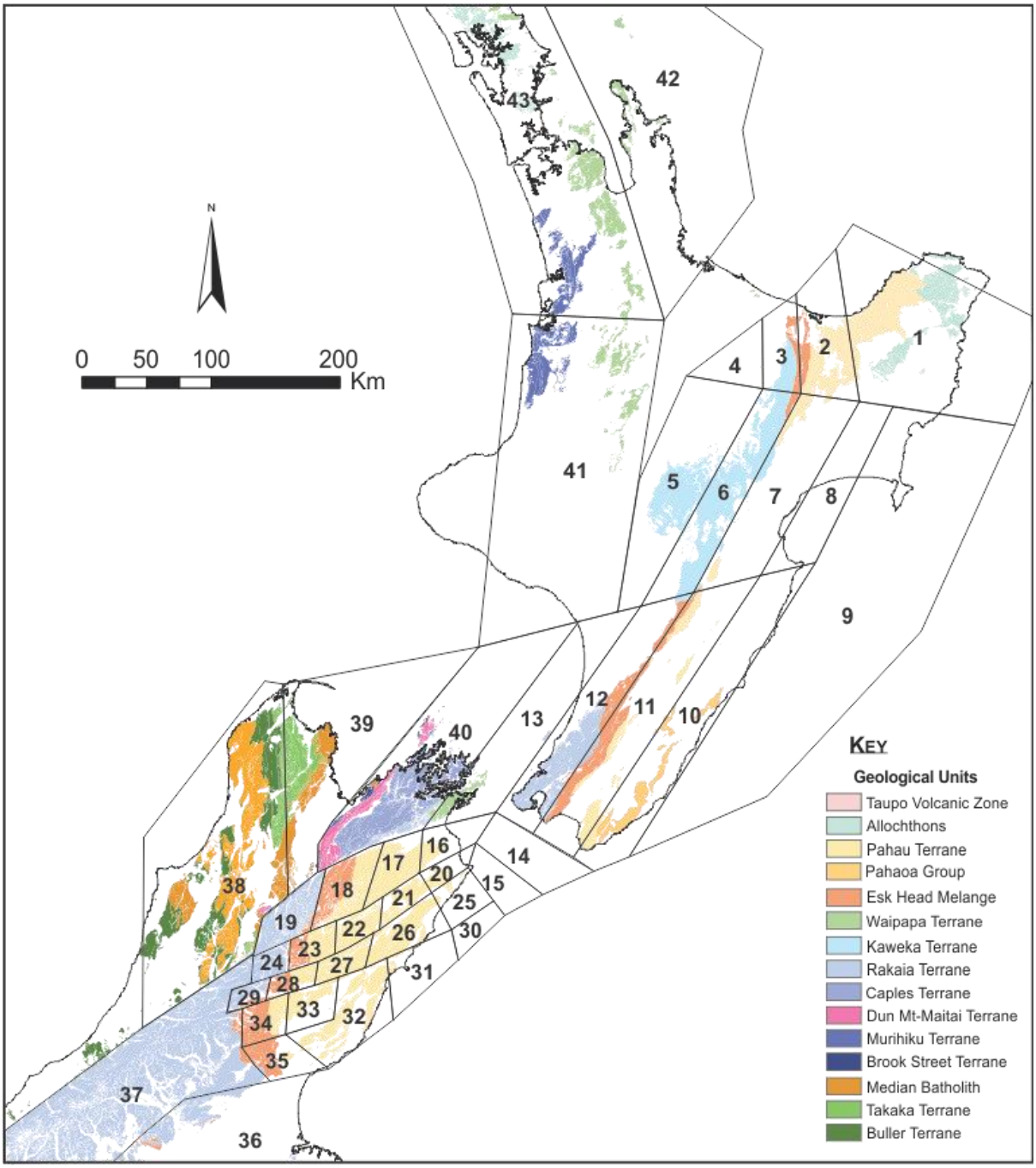

Figure 5.6: Numbered structural blocks discussed in text. Numbers correspond to the bounding structures presented in Table 5.1.

5.2.4 Mesozoic versus Cenozoic Bending of Basement Terranes

Since the analysis of the Alpine Fault movement history by Harold Wellman in 1949 (in Benson, 1952), the timing and amount of bending of New Zealand basement terranes have been amongst the most debated topics in New Zealand geological literature (Kingma, 1959; Suggate, 1963; Wellman, 1971; Molnar *et al.*, 1975; Carter & Norris, 1976; Walcott *et al.*, 1981; Walcott, 1984; 1998; Kamp, 1987; Gray & Norton, 1988; Lamb & Bibby, 1989; Vickery & Lamb, 1995; Bradshaw *et al.*, 1996; Little & Roberts, 1997; Sutherland, 1999a; King, 2000a; Hall *et al.*, 2004; Nicol *et al.*, 2007; Lamb, 2011; Mortimer, 2014; Lamb *et al.*, 2016).

Identification of basement piercing points is an important factor in resolving this debate. These include: the Dun-Mountain-Maitai Terrane, the Esk Head Belt, the axis of Haast Schist metamorphism, Mesozoic continental-ocean margin, the Median Batholith, Darran Suite intrusives, regional syncline axes, Eocene rift margin (e.g. Sutherland *et al.*, 2000), form-lines from steeply dipping-sub-vertical basement strata, and regional-scale Mesozoic faults in South Island (Mortimer, 2014). On both sides of the Alpine Fault the trends of regional strike of basement rocks bend towards subparallel alignment with the Alpine Fault, defining an oroclinal bend (Wellman, 1956; King, 2000a; Mortimer, 2014).

The Maitai Terrane includes the Dun Mountain ophiolite assemblage, which is associated closely with the Junction Magnetic Anomaly and gravity anomalies (Sutherland, 1999a, 1999b). The distinctive rock types and geophysical characteristics allow it to be mapped in detail across the country, providing a continental strain marker for deformation across Zealandia. Most models agree that the Junction Magnetic Anomaly-Dun Mountain-Maitai Terrane was bent during the Mesozoic Rangitata Orogeny (Kamp, 1987; Bradshaw *et al.*, 1996; Sutherland, 1999a). The debate has recently centred on whether the other major basement-derived structural lineation and piercing point, the Esk Head Belt, was bent in the Mesozoic or the Neogene (e.g., Mortimer, 2014; Lamb *et al.*, 2016; van der Meer, 2016). Four possibilities for the pre-plate boundary development positions of the Dun Mountain-Maitai Terrane are considered (following Sutherland, 1999a):

1a) Prior to 45 Ma, the Alpine Fault was a pre-existing structure that had already accumulated 350 km of sinistral offset (e.g. Lamb *et al.*, 2016). This assumes a rigid plate motion model, with all relative displacement between the two plates being accommodated by slip on the Alpine Fault (Figure 5.7).

1b) The Alpine Fault existed prior to 45 Ma, but with <350 km of sinistral displacement, requiring most of the post-45 Ma displacement to be on the Alpine Fault, with a limited amount of distributed deformation (Figure 5.7).

2) The Alpine Fault formed after 45 Ma, with 480 km of dextral displacement, and 350 km of distributed shear across a zone adjacent to the Alpine Fault (e.g., Sutherland, 1999a; Cox & Sutherland, 2007; Figure 5.7).
3) Prior to 45 Ma, the Alpine Fault existed with <480 km of dextral offset, requiring a substantial proportion of plate boundary offset since 45 Ma to be distributed as crustal deformation west of the Alpine Fault (e.g., van der Meer, 2016; Figure 5.7).

Contemporary strain measurements and paleomagnetic data demonstrate that there has been a component of distributed dextral shear across the Cenozoic plate boundary (Walcott, 1984; Lamb, 2011; Little & Roberts, 1997; Sutherland, 1999a), including high Cenozoic brittle strain within 100 km of the Alpine Fault that has resulted in the Murihiku Terrane being dispersed as fault slivers (Mortimer, 2014). If there was dextral strike-slip prior to 45 Ma, then a complex S-shaped geometry must be required (Figure 4), with a large proportion of plate motion since 45 Ma distributed as continental deformation, rather than being focused on the Alpine Fault, as the total plate motion is well-constrained (Sutherland, 1999a). This leaves two primary hypotheses for the development of the oroclinal bend through New Zealand, which have largely divided models and reconstructions into two camps, with much debate.

Kamp (1987) and Sutherland (1999a) suggest that the Dun Mountain-Maitai Terrane was modestly deformed to create a smooth, continuously curved geometry during the late Triassic accretion of the Rakaia Terrane, implying that most deformation occurred during the late Oligocene–Neogene (Figure 5.7B). This suggests that of the approximately 780 km of post-Eocene relative movement between the Australian and Pacific plates, >50 % (480 km) has been partitioned into the Alpine Fault, and the remainder accommodated by distributed shear, mainly within the Southern Alps (Sutherland, 1999a; Sutherland *et al.*, 2000; Cox & Sutherland, 2007). Subsequently, the Dun Mountain-Maitai Terrane was additionally deformed, and the Esk Head Belt primarily deformed during Neogene deformation. The alternative model implies pre-Eocene, likely Cretaceous sinistral movement of the Alpine Fault, which is then reactivated in the Neogene with a substantial dextral displacement (e.g. Lamb *et al.*, 2016). There are compelling arguments for mid-Cretaceous bending of the Gondwana continental margin at c. 105 Ma, associated with the collision of the Hikurangi Plateau with the Cretaceous subduction system (e.g. Davy *et al.*, 2008; Reyners *et al.*, 2011, 2017; Figure 5.7C).

A largely Neogene origin for the development of oroclinal bending is adopted in the model presented in this thesis (Figure 5.7B). The Esk Head Belt (170 Ma; Adams *et al.*, 2011) is a substantially younger feature than Dun Mountain-Maitai Terrane (280 Ma; Kimborough *et al.*, 1992), providing 110 Myr to deform the Dun Mountain-Maitai Terrane before the accretion of the Esk Head Belt. This aside, orogenic belts do not have to be linear features over large distances (e.g., the orogenic belt associated with the Talaud Orogeny, North Moluccas, Indonesia; Simandjuntak & Barber, 1996), and the Esk Head Belt may have originated with some degree of bending. Rigid plate reconstruction of this strain marker across the Alpine-Wairau Fault can be achieved in ~4.5 Myrs at full relative plate rates which suggests the ~150 km offset presently observed was accrued since the middle Miocene.

The rotation and translation of a number of the basement markers and piercing points can be explained by simple post-Eocene rigid rotation and translation of the Australian Plate relative to the Pacific Plate as the Emerald Basin opened (Sutherland, 1995; Mortimer, 2014). There is evidence of large-scale, Neogene deformation in the Emerald Basin that would support Neogene bending of the orocline (Hayes *et al.*, 2009). Additionally, there is evidence of tightening of the Southland syncline concurrent with post-Oligocene oroclinal bending (Little & Mortimer, 2001).

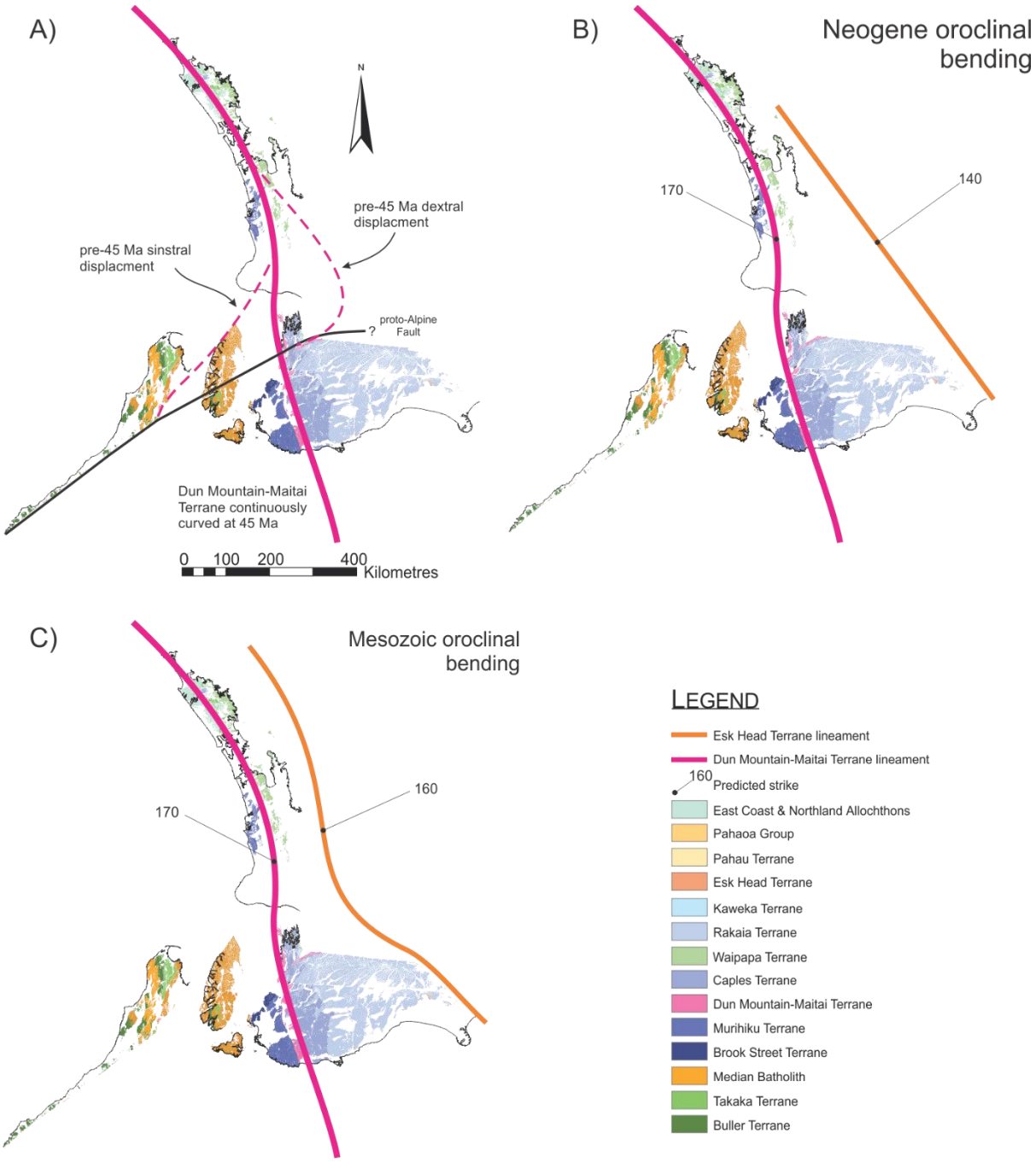

Figure 5.7: Various assumptions about the orientation of the Dun Mountain-Maitai Terrane (and Junction Magnetic Anomaly) and the Esk Head Belt during the late Eocene (45 Ma), along with predicted strikes for this time. A) Geometry for a continuously curved, dextrally displaced and sinistrally displaced Dun Mountain-Maitai Terrane at 45 Ma (modified after Sutherland, 1999a). B) Geometry of the Esk Head Belt assuming dominantly Neogene oroclinal bending. This model is adopted in this study. C) Geometry for Esk Head Belt adopting Mesozoic oroclinal bending. The East Coast and Marlborough outcrop geology has been removed for clarity. Block divisions displayed here are representative of the structural divisions of King (2000a).

5.3 Model Development

Retro-deformation of the palinspastic tectonic model developed in this study was done in two parts. The wider New Zealand region was retro-deformed as a series of large, simple structures, while the East Coast Basin was treated as a series of smaller complex structures within a large zone of deformation that was then incorporated within the regional reconstruction.

Paleomagnetic vertical rotation data from Lamb (2011) and Lamb *et al.* (2016) have been used here alongside additional paleomagnetic datasets from around New Zealand (Grindley *et al.*, 1977, 1994; Oliver *et al.*, 1979; Hunt & Smith, 1980; Sherwood, 1988; Haston *et al.*, 1989; Haston & Luyendyk, 1991; Cassidy, 1993; Briggs *et al.*, 1994; Fujii *et al.*, 1994; Tanaka *et al.*, 1996; Ohneiser *et al.*, 2008; Dallanave *et al.*, 2014, 2016). Declination anomalies have been determined from these data by plotting site mean directions of normal and reversed polarity data in the same hemisphere to determine mean declinations, with the deviations from north providing declination anomalies (e.g. Ohneiser *et al.*, 2008).

Detailed studies have demonstrated that the magnetic signal in Neogene marine sedimentary rocks from many New Zealand basins is dominated by authigenic greigite, formed after deposition of the sediments in a process that often results in the dissolution of detrital magnetite (Turner, 2001; Rowan & Roberts, 2006). Consequently, there is substantial potential for secondary magnetic overprints as authigenic greigite develops, and the development of a dominantly chemical remnant magnetisation, often at the cost of the primary remnant magnetisation. This means that there are substantial errors inherent in many paleomagnetic datasets, and care must be taken with the interpretation and application of these datasets. Because much of the Torlesse basement terranes are oriented vertically to sub-vertical, kilometre-scale basement strike orientations can also be applied as proxy for vertical-axis rotations (e.g. Little & Roberts, 1997; Mortimer & Little, 2001; Hall *et al.*, 2004).

Ever since Harold Wellman demonstrated ~480 km of dextral strike-slip displacement across the Alpine Fault, various workers have presented models proposing the extension of this large displacement through the East Coast Basin (e.g. Kingma, 1958; Ballance, 1976; Cole, 1986; Lamb, 1988; Cutten & Delteil, 1993; Beu, 1995; Mortimer, 1995; Delteil *et al.*, 1996). However, because the strike of major faults in the North Island are oriented subparallel to the basement fabrics, there are few piercing points for absolute, unequivocal strike-slip displacement markers, and models with large (>50 km) strike-slip displacements remain controversial (Nicol *et al.*, 2007). Thus, some authors have proposed that deformation is accommodated by large amounts of strike-slip motion (e.g., Cutten & Delteil, 1993; Beu, 1995), whereas others suggested that there has been minimal

strike-slip and deformation is accommodated by a higher degree of rotation in the basin, and vertical offsets (i.e. shortening; e.g. Nicol *et al.*, 2007). During the early to middle Miocene the Hikurangi subduction margin was approximately orthogonal to the Alpine Fault and the relative plate motion vector of the Pacific Plate in relation to the Australian Plate (King, 2000a; Nicol *et al.*, 2007). With such fault geometries and kinematics, there is no requirement for strike-slip in the East Coast Basin, with strike-slip on the Alpine Fault transferred onto the subduction thrust as dip-slip, or into the overriding plate as compression (Nicol *et al.*, 2007). Furthermore, if the relative boundary of continental crust is taken into account (approximated by the 2000 m isobath), many reconstructions with large strike-slip displacements become entirely infeasible (e.g., Kear, 1993, 2004; Cole & Lewis, 1991; Figure 1.2). The amount of slip displacement through the North Island East Coast Basin is the primary distinguishing feature between most structural models of the New Zealand region. In the interests of developing a conservative model, strike-slip displacements are based on quantified amounts from published datasets. Neogene shortening, in the context of the model presented herein, is dominantly within the East Coast Basin.

5.3.1 Regional Model Development

Retro-deforming plate rotations, the Northland, Fiordland, South Island and Northwest Nelson blocks are oriented to honour the alignment of basement terranes and terrane-boundary piercing points. Key terrane markers establish the first-order geometry of blocks (discussed above, e.g., Esk Head Melange, Dun Mountain-Maitai Terrane – Junction Magnetic Anomaly; Mortimer, 2014), that were once contiguous between North and South Islands. Alignment of basement terranes and their boundaries, which may have been approximately co-linear and laterally continuous in the Late Cretaceous (although this inference is subject to some debate, see Sutherland, 1999a; Mortimer, 2014; Lamb *et al.*, 2016), provides constraints on pre-Neogene basin configuration. The placement of the Fiordland Block is somewhat problematic and speculative, and as such, the model follows previous reconstructions by aligning it with northwest Nelson (e.g. King, 2000a), based on correlations between the Median Batholith and Darran Suite volcanics.

Vertical-axis Rotations

Finite rotations of the Australia-Pacific plate circuit are well-constrained from 26–0 Ma, with the Australian plate having rotated 27° with respect to the Pacific Plate during the past 26 Ma, as well as progressively moving northwards (Musgrave, 1989). The Australian Plate can be demonstrated

to have rotated quite consistently at ~1°/Myr with respect to the Pacific Plate throughout the Cenozoic, whilst moving steadily towards lower latitudes (Cande & Stock, 2004; Schellart *et al.*, 2006; Lamb, 2011). The components of the Pacific Plate within the model are progressively rotated anticlockwise with respect to a fixed Australian Plate. The northwest Nelson, West Coast and Northland regions have been treated as fixed blocks with respect to the Australian Plate.

Rotation of structural blocks are based on the vertical-axis rotations derived from paleomagnetic declination anomaly data (detailed below) and by the boundary conditions imposed by far-field plate motions (e.g., Lamb, 2011). The resulting rotation of blocks and motion paths are compared here against existing geological and geophysical constraints. The primary timing of Neogene block rotations is governed by constraints in the far-field plate motions of the Australian-Pacific-Antarctic plate system (e.g., Sutherland, 1995; 1999b; Cande & Stock, 2004; Seton *et al.*, 2012). Secondary timing of block rotation is determined by well-constrained geological events (e.g., vertical-axis rotations within northern Marlborough region from ca. 4 Ma; Little & Roberts, 1997). Along with paleomagnetic vertical-axis rotations, the blocks within the model move relative to Northland and Northwest Nelson, as these regions are considered to be attached to the Australian Plate and have not rotated significantly during Neogene plate boundary deformation. The eastern South Island crustal block is regarded as fixed to the Pacific Plate. The Chatham Rise is considered to have been locked in approximately the same relative position since the Late Cretaceous, with paleomagnetic data from the Chatham Islands suggesting <4° of rotation during the Cenozoic (Figure 5.8; Grindley *et al.*, 1977). Vertical-axis block rotations are based on the key assumption that the majority of deformation of significant basement terrane trends occurred during the Neogene as discussed previously (see King (2000a) for discussion).

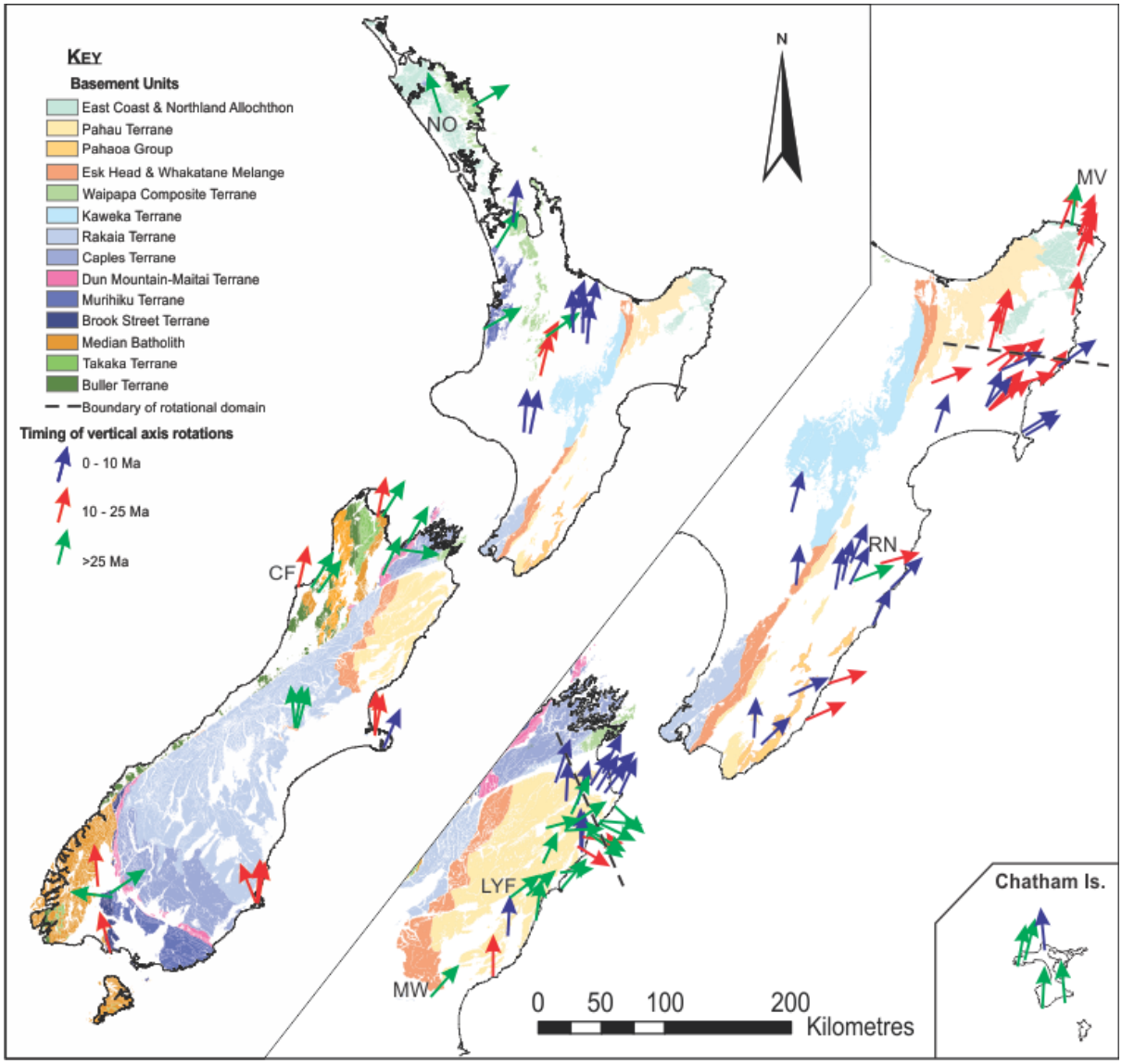

Figure 5.8: Outcropping basement strata in onshore New Zealand with declination anomalies plotted for various paleomagnetism study sites. Paleomagnetism data sourced from Lamb (2011), Lamb *et al.* (2016), Sherwood (1988), Hunt and Smith (1980), Dallanave *et al.* (2014, 2016), Briggs *et al.* (1994), Grindley *et al.* (1994), Tanaka *et al.* (1996), Grindley *et al.* (1977), Oliver *et al.* (1979), Haston and Luyendyk (1991), Cassidy (1993), Haston *et al.*, 1989, Fujii *et al.* (1994), Ohneiser *et al.* (2008).

Basement Structural Grain

Stable areas of the model (King Country and Northwest Nelson) have a basement fabric mean strike orientation of 176°. The Dun Mountain-Maitai Terrane in the East Nelson Block has a mean strike orientation of 211–224°, indicating 35–48° degrees of clockwise rotation with respect to fixed crustal blocks (Northwest Nelson, Northland; Figure 5.9). In support of a Cenozoic age for vertical-axis rotation of the East Nelson Block, there has been 32 ± 15° of vertical-axis rotation

between the Taieri-Wakatipu Synform in west Otago and Goulter Syncline in Marlborough, interpreted as pre-Neogene contiguous structures (Mortimer, 2014). Most of the regional strike changes that define the oroclinal bend are contained in eastern South Island, and maximum clockwise rotations of 100° occur adjacent to the Alpine Fault. Across the various Marlborough fault blocks, the Esk Head Belt demonstrates a basement fabric trend of 209° to 110°–131°, indicating bending of 78–99°. The amount of bending of the Esk Head Belt in Marlborough is comparable with the 85° of bending across the oroclinal bend in Southland (Figure 5.9). Therefore, an oroclinal fold axis can be drawn approximately 100 km east of the Alpine Fault, linking the ~85° bending of the Esk Head Belt with a similar amount of bending of the Dun Mountain-Maitai Terrane (Figure 5.9). The Median Batholith also changes strike orientation, but is offset across structures between Fiordland and Stewart Island.

The internal basement structural lineation of the Fiordland block is important for paleogeographic reconstructions. The Jurassic-Cretaceous volcano-plutonic belt (Darran Suite) provides a more precise strain marker than the Median Batholith as a whole (Mortimer, 2014; Lamb *et al.*, 2016). Importantly, the lineation of the Darran Suite within the Median Batholith in Fiordland, which strikes 010°, has been rotated 55° with respect to the 315° strike of the Darran suite in Stewart Island.

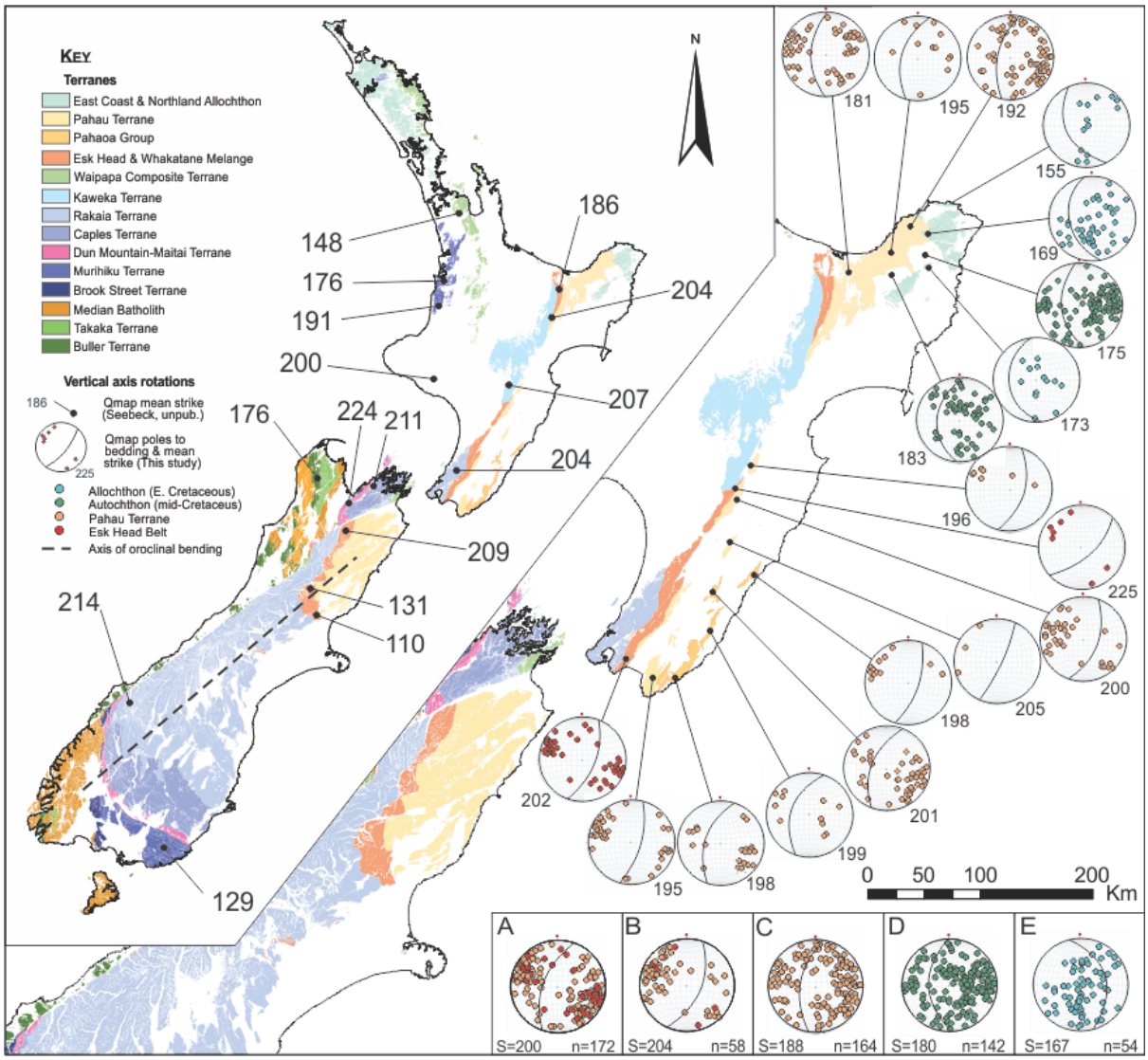

Figure 5.9: Mean basement strike measurements extracted from the QMAP GIS. New Zealand-wide data compiled from 50 km gridded analysis by Seebeck (unpublished). North Island East Coast basement data derived herein from 20 km grids from QMAP sheets, with all measurements shown as lower-hemisphere, equal-area projections. Points plotted on stereonets are coloured by basement units. Inset: Poles to bedding and mean bedding planes for all strike and dip data by region. A) Wairarapa, B) Hawke's Bay, C) Raukumara basement (autochthon), D) Raukumara basal cover (autochthon), E) East Coast Allochthon basal cover. S = mean strike, n = number of observations.

Strike-slip Movements

Significant strike-slip displacements associated with Neogene deformation of the New Zealand region are largely restricted to the East Coast region (discussed below), and the Alpine Fault. Within the wider regional model, the 780 km of relative motion between the Australian and Pacific plates is accommodated on the Alpine Fault.

Shortening

The New Zealand plate boundary began to evolve in the mid-late Eocene as the southwest South Island began to actively subside in an extensional zone that propagated northwards in response to seafloor spreading in the Emerald Basin (King, 2000a). Spreading of the Emerald Basin began around 40 Ma, with associated rifting propagating into central and western New Zealand at 30 Ma (King, 2000a). During this period the East Coast Basin is interpreted to have been more-or-less contiguous with the eastern South Island, and both were rotating anticlockwise in response to spreading in the Emerald Basin (King, 2000a).

There has been ~90 km of east-west shortening in the South Island since 6.4 Ma, 70% of which is accommodated on the Alpine Fault (Walcott, 1998; Sutherland *et al.*, 2000). In addition to this, balanced cross-sections through the NW Nelson region indicate as much as 30 km of Neogene shortening, associated with movement on the Alpine Fault (Ghisetti *et al.*, 2016a).

The Taranaki Fault Zone is one of the longest and highest displacement contractional structures (>10 km) in the New Zealand region (King & Thrasher, 1996; Stagpoole & Nicol, 2008). The Taranaki Fault Zone is contained entirely within the Australian Plate and includes the Waimea-Flaxmore Fault, the Manaia Fault, and the Tarata Thrust. The Taranaki Fault has accommodated displacement prior to the Oligocene, with the northern tip of the fault stepping southward over the past 30 Ma (Stagpoole & Nicol, 2008). Nicol *et al.* (2007) estimate 75 ± 35 km of Miocene shortening across the Taranaki and Whanganui Basins (including the Taranaki Fault system), comparable to the 70 ± 30 km shortening estimated by Stern *et al.* (2006).

Extension

Neogene extension in the New Zealand region is largely restricted to the Hauraki Gulf, TVZ, Havre Trough, and parts of the Taranaki Basin. During the late Neogene, the Hauraki Rift developed in the back arc of the Hikurangi subduction margin, parallel to the now-extinct Coromandel volcanic arc (Hochstein & Nixon, 1979; Davidge, 1982; Hochstein & Balance, 1993; Wilson & Rowland, 2016). Subsequently, extension shifted from the Hauraki Rift to the Taupo Rift at 2–3 Ma (Wilson & Rowland, 2016). Extensional faulting is predominant in the Taupo Volcanic Zone, continuing in backarc basins north of New Zealand as the Lau-Havre Trough (Nicol *et al.*, 2007). Seismic, gravity and magnetic profiles across the offshore Taupo Volcanic Zone suggest as much as 80% crustal thinning, consequently resulting in 32 km of extension since 1.6 Ma (Davey *et al.*, 1995). There has been an estimated 35 km of extension across the Taupo Volcanic Zone (Nicol *et al.*,

2007). There has been 80–100 km of back-arc extension in the southern Havre Trough since ~4 Ma (Stern, 1987; Wright, 1993, 1994).

5.3.2 East Coast Model Development

Vertical-axis Rotations

Vertical-axis rotation data in the New Zealand region have identified two hinge zones within the broader East Coast region, the first north of Wairoa (Mumme *et al.*, 1989; Walcott, 1989; Rowan & Roberts, 2005; Lamb, 2011), and the second in Marlborough, where there has been notable increases in the internal rotation of structures during the past 4 Ma (Figure 5.8; Little & Roberts, 1997). Differential rotations are indicated by paleomagnetic and structural data across Cook Strait. Changes in structure and a distinct boundary between paleomagnetically defined domains in the largely unrotated Raukumara Peninsula and the rotated Wairoa domain, also appears to suggest a change in the intra-plate coupling that may have allowed differential rotation (Figure 5.8; Reyners, 1998).

The model developed herein applies a differential rotation to Marlborough structural blocks, as opposed to the bulk rotation applied by Crampton *et al.* (2003) in their palinspastic reconstruction of the Marlborough region. Application of a bulk rotation works well at a local scale and provides a reasonable approximation of rotation but, in the context of reconstructing the pre-Neogene continental margin of eastern New Zealand, it results in an unrealistically splayed continental boundary. To realistically apply a differential rotation to the Marlborough region without resulting in a splayed distribution of blocks, a finer, equidistant block division, such as that suggested by Little and Roberts (1997) and Hall *et al.* (2004), has been applied here.

Ben More Anticline

Folding on the Ben More Anticline affects the orientation of paleomagnetic declinations, requiring careful selection of the paleomagnetic data points selected for inclusion within the retro-deformed model for the northern Marlborough region (Figure 5.10). Paleomagnetic declination anomalies from the belt of Paleogene limestones east of the Clarence Fault and on the west limb of the Ben More Anticline are in the range of 21–88° (mean = 55°), whereas values from the northeastern Ben More Anticline are oriented 97–128° (mean = 117°), indicating ~60° rotation of Paleogene limestones around the axis of the anticline (Figure 5.10). Structural data from Little & Roberts (1997) indicate 70° clockwise rotation of basement strata in the vicinity of the anticline, broadly consistent with the ~60° rotation from paleomagnetic declination anomalies (Figure 5.8 & 5.10).

There is evidence that Paleogene strata in the Marlborough area were consistently tilted ~45° to the northwest within each structural block, prior to subsequent deformation (Crampton *et al.*, 2003). The interpretation of tilting followed by progressive clockwise rotation of the northeastern end of the Clarence Block is consistent with rotational domains observed by Little and Roberts (1997) in northeastern Marlborough, whereby paleomagnetic declination anomalies and basement structural grain show a 3–50° rotation across northeastern Marlborough with respect to southern Marlborough.

Vertical-axis rotation data from northern Marlborough show that the bending of the Ben More Anticline is a late Miocene feature. Oligocene and early Miocene paleomagnetic samples from the Kekerengu and Cape Campbell areas have similar vertical-axis rotations to the northeastern Ben More Anticline. Vertical-axis rotation from Pliocene samples near the Clarence River mouth and a single late Miocene sample from Cape Campbell are largely unrotated, likely constraining the timing of bending on the Ben More Anticline. Browne (1992) shows a consistent swing of strike in early to middle Miocene strata around the nose of the Ben More Anticline, suggesting that deformation occurred in the middle to late Miocene. This explains almost all of the exceptionally high paleomagnetic vertical-axis rotations in eastern Marlborough (Figure 5.8).

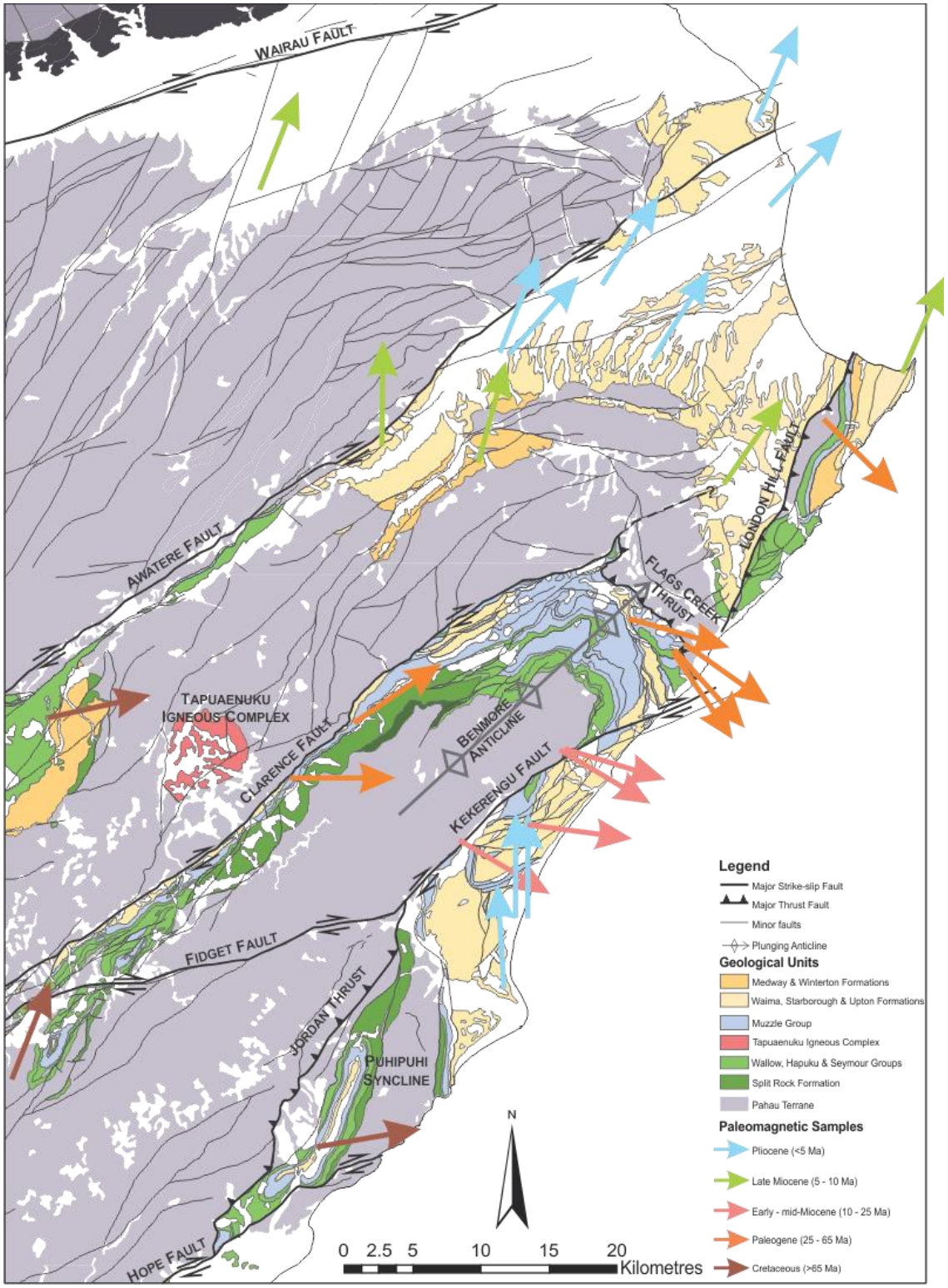

Figure 5.10: Map of northeastern Marlborough showing major structures in relation to the Ben More Anticline. Pre-Neogene vertical-axis rotations indicate probable middle to late Miocene bending of the Ben More Anticline and regions further to the northeast. Paleomagnetic data from Lamb (2011), Dallanave *et al.* (2015). Map data from Heron (2014).

Basement Structural Grain

This study extends the use of bedding formlines from basement strata from the Marlborough region (Little & Roberts, 1997; Hall *et al.*, 2004), Canterbury-Otago, Westland, and Northwest Nelson areas (Mortimer, 2014), and eastern North Island (extracting data from the QMAP GIS, after Begg and Johnston (2000), Mazengarb and Speden (2000) Lee and Begg (2002), Leonard *et al.* (2010) and Lee *et al.* (2011)).

In the North Island axial ranges, the Esk Head Belt has a basement fabric striking 186° in the Whakatane area, but between Waikaremoana and Wellington, this increases to 204–207° (Figure 5.9; Seebeck, unpublished data), coincident with a rotation boundary in the Gisborne area suggested by paleomagnetic vertical-axis rotation data (Mumme *et al.*, 1989; Rowan *et al.*, 2005; Lamb, 2011).,

Basement strike trends across the North Island East Coast are remarkably consistent, and support the ~70° of bulk Neogene vertical-axis rotation consistently applied across the East Coast structural blocks within the model (Figure 5.9, Appendix 7 [Supplementary Tables 5.2 & 5.3]). Across the East Coast Allochthon, there is 20–30° less clockwise rotation than that expressed within the rest of the East Coast Basin, consistent with paleomagnetic measurements (Figures 5.8 & 5.9). Comparison of vertical-axis rotation of basement structural grain between the Waipapa Terrane in the Auckland region and the East Coast suggests ~60–70° of relative clockwise rotation (Figure 5.9). Across Cook Strait and the Wairau Fault, the structural trend of the Esk Head Belt remains markedly constant (204 and 209°, respectively; Figure 5.9). This suggests that despite the 150 km of dextral displacement, there has been almost no differential rotation across this boundary, as basement fabrics associated with this strain marker are sub-parallel in the Wellington and southern Marlborough regions. Basement strike and declination anomaly data in Marlborough demonstrate a 1:1 relationship (Little & Robert, 1997; Hall *et al.*, 2004). This relationship would suggest that Neogene rotation accounts for all vertical-axis rotation of the Marlborough region with respect to the rest of New Zealand since the Mesozoic (e.g., Lamb, 2011).

Strike-slip Movements

Faults in the North Island do not appear to have exceeded ~20 km of total strike-slip displacement individually, and strike-slip displacements of more than a few kilometres cannot be reliably demonstrated on any faults in the North Island Fault System (Nicol *et al.*, 2007). During the late Neogene, there has been minimal strike-slip motion on NE–SW-oriented fault systems, with most displacement occurring during the Plio-Pleistocene (Cashman *et al.*, 1992; Erdman & Kelsey 1992; Beanland *et al.*, 1998; Nicol *et al.*, 2007; Nicol & Wallace, 2007).

The Mohaka and Ruahine Faults lack appropriate markers for the determination of net horizontal displacement (Erdman & Kelsey, 1992). However, estimates derived from late Neogene sedimentary rocks suggest that dextral strike-slip across the Ruahine Fault since the early Pliocene is likely to be less than 10 km, and the Mohaka Fault has had <2 km of strike-slip displacement since 2 Ma (Beanland *et al.*, 1998; Bland & Kamp, 2006). Nicol *et al.* (2007) suggest maximum displacement across the Wellington-Mohaka fault system of ~20 km in the last 2.4–3.7 Myr.

A displacement of 16 to 22 km of dextral displacement is estimated across the Poukawa Fault Zone since the Late Pliocene, based on a re-alignment of outcropping ridges of mid-Pliocene Awapapa Limestone (Cashman *et al.*, 1992). In the retro-deformation along the Poukawa Fault Zone presented by Cashman *et al.* (1992), alignment of the fault displaced positions of the Awapapa Limestone also require ~25° of anticlockwise rotation since c. 3.5 Ma, consistent with the vertical-axis rotation trends demonstrated in paleomagnetic data at this time (Figure 5.8).

The Pongaroa-Waihoki fault zone has been active since the Otaian, with ~13 km of dextral strike-slip displacement on the Pongaroa Fault during the early to middle Miocene (Ridd, 1967). Northeast-trending faults along the coastal ranges (e.g. the Adams-Tinui Fault) have been suggested to have accommodated ~300 km of Neogene transcurrent movement (e.g., Delteil *et al.*, 1996). This implied displacement is unreasonable in the context of geological constraints, especially given the narrow, 3 Myr window that this strike-slip displacement is inferred to have occurred. Minimal lateral movement along the Adams-Tinui Fault is interpreted in this model, consistent with Moore (1988b).

The distribution of the Te Aute lithofacies limestones (Figure 5.11A) have been revised herein to demonstrate that late Neogene strike-slip motion on the Wairarapa, Alfredton, Mangatarata, Tukituki and Poukawa fault zones is on the order of <15 km of dextral strike-slip since 2.5 Ma (Figure 5.11B). Previously, Beu (1995) had estimated 100 km of dextral strike-slip within the East Coast Basin, with ~60 km of slip on this fault system (Figure 5.11C). Revision of the outcrop

distribution of these fault systems shows that this estimate can be significantly reduced. The linear distribution of the Te Aute lithofacies is much more geologically reasonable (Figure 5.11B), consistent with a long seaway through the region at this time (e.g., Trewick & Bland, 2012), and produces strike-slip estimates comparable to other indicators of strike-slip in the basin. The Wellington Fault at Te Marua shows 8 km of dextral strike separation and distributed shear across the Esk Head Belt, comparable with 7 ± 1 km displacements of major rivers across the Wellington Fault (Berryman *et al.*, 2002; Nicol *et al.*, 2007). The total strike-slip on the Wellington Fault is comparable with the estimated lateral displacement on the Ruahine and Mohaka Fault systems (Nicol *et al.*, 2007).

The Esk Head Belt demonstrates dextral displacement across the Wairau, Awatere, Clarence, and Hope Faults (Silberling *et al.*, 1988; Hall *et al.*, 2004; Lamb, 2011; Mortimer, 2014). Within the Marlborough Fault System, the Esk Head Belt has an aggregated dextral offset of 55 km, and across the Wairau-Alpine Fault and Cook Strait, the Esk Head Melange is offset by 150 km (Begg & Johnston, 2000; Rattenbury *et al.*, 2006; Forsyth *et al.*, 2008; Mortimer, 2014).

Within the Marlborough Fault System, Little and Jones (1998) demonstrate that the Awatere Fault system has only been active since c. 7 Ma, during which time it has accrued 34 km of dextral strike-slip motion. Crampton *et al.* (2003) estimate 25 ± 10 km of strike-slip across the Clarence Fault based on the present-day distribution of the Warder Coal Measures. Similarly, strike-slip displacement of 16–35 km on the Clarence Fault would bring the thickest sections of the Gridiron Volcanics to a point adjacent to the Tapuae-O-Ueneku Igneous Complex (Crampton *et al.*, 2003). Strike-slip displacement on the Jordan Thrust and the Kekerengu Fault is estimated to be approximately 5 km (Van Dissen, 1989; Van Dissen & Yates, 1991; Crampton *et al.*, 2003), although Quaternary fault slip data suggests that as much as 15 km of strike-slip movement may have been transferred from the Hope Fault onto the Kekerengu Fault and Jordan Thrust (Crampton *et al.*, 2003). Dextral displacement on the Hope Fault is estimated to be 20 km based on the offset of conglomerate beds within the Torlesse (Freund, 1971; Crampton *et al.*, 2003). Evidence, including syn-sedimentary deformation within the Great Marlborough Conglomerate, suggest that during the early Miocene, a proto-Marlborough fault system linked the early Hikurangi subduction system with the proto-Alpine Fault across the newly-formed plate boundary (Lamb & Bibby, 1989; Little & Jones, 1998). Through most of the Miocene, plate motion through South Island and across the Marlborough Fault System was slightly divergent or pure strike-slip, becoming slightly convergent after ~12 Ma, with increased convergence after 6.4 Ma following a southwest shift in Euler pole position (Walcott, 1998; Sutherland, 1995; Little & Jones, 1998). Initiation of significant strike-slip

movement on the Marlborough fault system is well-constrained between 6.4–7.4 Ma (Little & Jones, 1998).

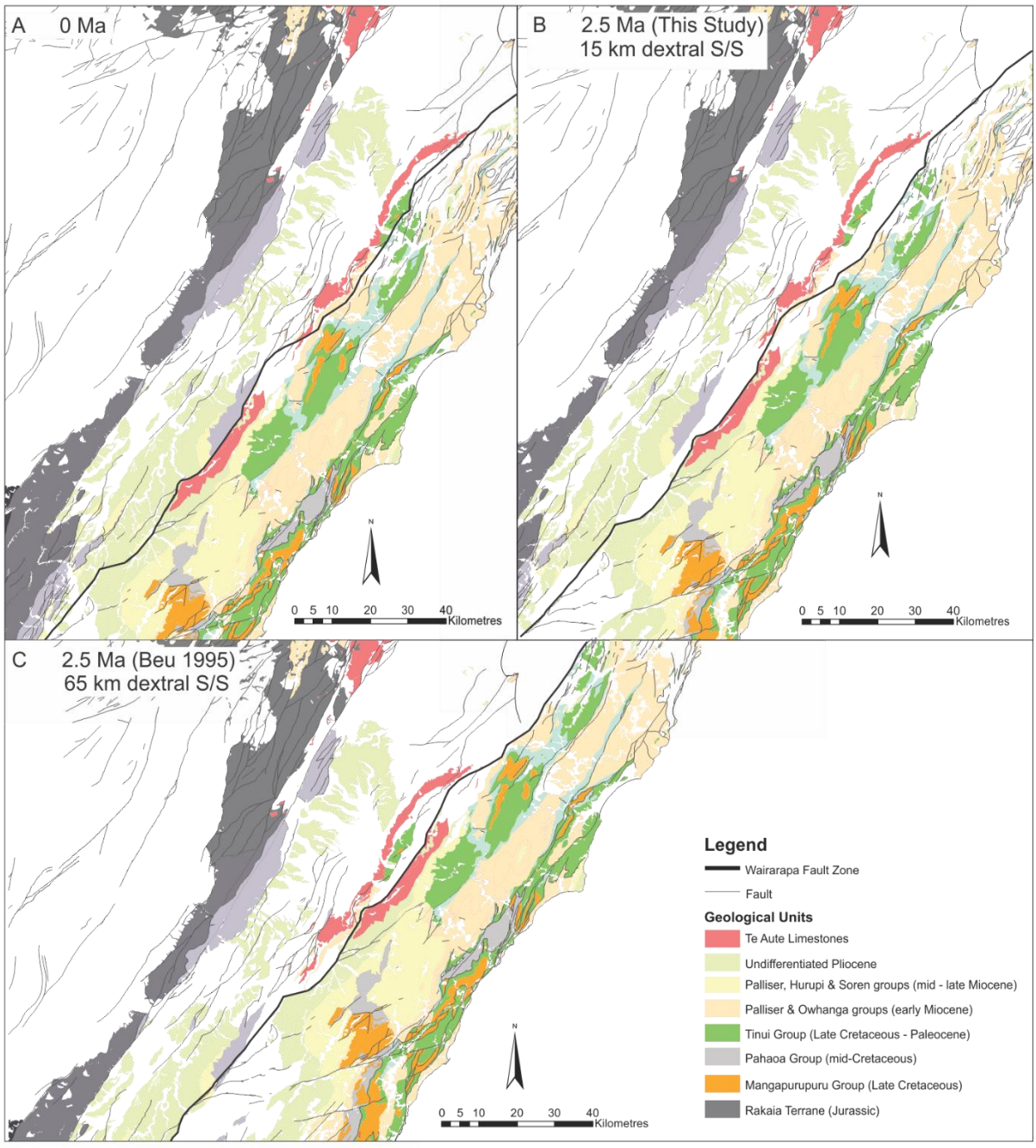

Figure 5.11: Different interpretations of late Neogene distribution of Te Aute Limestone lithofacies. A) Present-day distribution of the Te Aute lithofacies limestones. B) Retro-deformation for the Mangapanian Stage adopted by this study, resulting in ~15 km of strike-slip displacement distributed across the Wairarapa, Alfredton, Mangatarata, Tukituki and Poukawa fault zones. Map data sourced from Heron (2014). C) Reconstruction of the Mangapanian Stage from Beu (1995), with 65 km of strike-slip movement distributed across the same fault systems, resulting in a very different outcrop distribution of Te Aute lithofacies limestones.

Table 5.2: Summary of adopted strike-slip estimates for major faults in the East Coast Basin (see text for discussion)

Fault	Dextral Strike-Slip	Reference
Pongaroa Fault	13 km	Ridd (1967)
Wellington Fault	8 km	Berryman *et al.*, 2002; Nicol *et al.*, 2007
Mohaka Fault	10 km	Bland & Kamp (2006)
Wellington-Mohaka	20 km	Nicol *et al.* (2007)
Ruahine Fault	10 km	Bland & Kamp (2006)
Adams-Tinui Fault	<10 km	Moore (1988)
Poukawa Fault	16–22 km	Cashman *et al.* (1992)
Wairarapa Fault	100 km	Beu (1995)
	<40 km	This study; Revised from Beu (1995)
Wairau Fault	150 km	Begg & Johnston (2000); Rattenbury *et al.* (2006); Forsyth *et al.* (2008)
Awatere Fault	13-16 km	McLean (1986); Siberling *et al.* (1988)
	34+10 km	Little & Jones (1998)
Clarence Fault	25± 8 km	Crampton *et al.* (2003)
Clarence-Fidget-Kekerengu Faults	18 km	Siberling *et al.* (1988); Reay (1993); Vickery (1994)
Jordan Thrust-Kekerengu Fault	10±5 km	Van Dissen (1989); Van Dissen & Yates (1991); Crampton *et al.* (2003)
Hope Fault	20 km	Freund (1971); Crampton *et al.* (2003)
Porters Pass Fault	2 km	Cowan *et al.* (1996)

Shortening

Neogene shortening, in the context of the model presented herein, is dominantly within the East Coast Basin. To reconstruct spatial relationships of structural blocks through time, it is necessary to estimate the amount, timing, location and orientation of shortening in the East Coast Basin. Results of this analysis are summarised in Table 5. The tectonic regime has been dominated by shortening since the initiation of subduction in the Early Miocene (Field & Uruski *et al.*, 1997), interrupted by at least two tectonic reorganisations since the Late Miocene. Most of the Neogene convergent plate motion in eastern North Island has been accommodated on the subduction interface (Nicol *et al.*, 2007). Average shortening rates of 3–8 mm/yr in the upper plate are much lower than the average of 34 mm/yr rate of plate convergence since the Oligocene, making the subduction interface the most important contractional structure in the North Island (Nicol *et al.* 2007).

Development of the Hikurangi Margin included early Miocene shortening of ~90 km (50 km across the East Coast Basin, and 40 km across the axial ranges), and not in excess of 150 km (Nicol *et al.*, 2007). Section construction and restoration results in an estimated ~56 km of cumulative

shortening across northern Marlborough, with estimates decreasing southwards (Crampton *et al.*, 2003). The location and magnitude of shortening vary spatially across the Marlborough region and estimates are summarised in Table 5.3.

Early Miocene thrusting is interpreted to have occurred along the length of the Hikurangi Margin, suggesting that subduction reached its southernmost extent at or prior to 18 Ma (Chanier & Ferriere, 1989; Rait *et al.*, 1991; Delteil *et al.*, 1996; Nicol *et al.*, 2007). The early Miocene thrusting episode responsible for the stacking of thrust sheets in the Raukumara Peninsula and Wairarapa had a 6–7 Myr duration (Chanier & Ferriere, 1991). Periods of accelerated deformation occurred during the middle and late Miocene (11–14 Ma and 5–7 Ma) (Field & Uruski *et al.*, 1997; Chanier *et al.*, 1999; Kamp, 1999; Nicol *et al.*, 2002). Shortening occurred dominantly adjacent to the axial ranges, in a 20–50 km wide zone immediately east of the ranges, and in the ~50 km immediately adjacent to the subduction margin (Nicol *et al.*, 2007). The upper flanks of the Ruahine and Kaweka ranges have in places marine rocks c. 2.4 Ma in age, although uplift of the ranges is interpreted to both predate and postdate deposition of these strata (Nicol *et al.*, 2007). This is in line with two phases of uplift proposed for the axial ranges since 5 Ma; after ~1.5 Ma and 2.5–3.7 Ma (Melhuish, 1990; Beanland *et al.*, 1998; Nicol *et al.*, 2007).

Table 5.3: Compiled shortening estimates across the East Coast Basin.

Model Block	Location	Pliocene Shortening (km)	Miocene Shortening (km)	Reference
Raukumara	Raukumara Peninsula	>2.0	>25 >45	Mazengarb & Speden (2000) Rait *et al.* (1991)
Accretionary Prism	Hawke Bay	26±4	35±7	Nicol & Uruski (2005); Nicol *et al.* (2007); Uruski & Funnell (1995)
	Offshore Wairarapa	10.4±1	>16±5	Morgans *et al.*, 1995; Nicol *et al.* (2007); Uruski & Funnell (1995); Barnes & Mercier de Lepinay, 1997; Nicol & Beavan, 2003
Hawkes Bay	Wairoa	1±0.5	7±2	Barnes *et al.* (2002); Mazengarb & Speden (2000)
	Tukituki River		>3±1.5	van der Lingen & Pettinga (1980)
Inland Hawkes Bay	Ongaonga	7±1.5		Melhuish (1990)
	Kereru	3.7±1.2		Beanland *et al.* (1998) Cashman *et al.* (1992)
	Pohokura		14	Cutten & Delteil (1994)
Inland Wairarapa	Martinborough	2.5±1		Begg & Johnston (2000); Nicol *et al.* (2002)
	Carterton	2.3±0.7	8.5±3	Cape *et al.* (1990)
	Eketahuna	4±1		Beanland *et al.*, 1998; Nicol *et al.* (2007)
	Norsewood	6±2		Nicol *et al.* (2007)
	Dannevirke	7±2		Nicol *et al.* (2007)
East Wairarapa	Akitio		9±3	Nicol & Beavan (2003)
	Flat Point		>10	Chanier (1991)
	Adams-Tinui Fault		10	Rait *et al.* (1991)
	Mataikona		>10	Lee & Begg (2002)
	Tora		>12	Alexander (1990)
Total Wairarapa	Woodville	10±2		Nicol & Beavan (2003)
Tararuas	South Eketahuna		12±3	Nicol *et al.* (2007)
Kawekas	Mohaka River	0.6 ±0.3		Beanland (1995)
Awatere Valley	Hodder River		4±2	Crampton *et al.* (2003)
Clarence Valley	Mead Stream		17	Crampton *et al.* (2003)
	Clarence Fault		2.5±0.5	Crampton *et al.* (2003)
	Seymour Stream		10	Crampton *et al.* (2003)
Kekerengu Block	Kekerengu		7	Crampton *et al.* (2003)
Kaikoura Block	Kaikoura Penisula		2	Crampton *et al.* (2003)
	Haumuri Bluff		4	Crampton *et al.* (2003)
	Waiau River		5	Crampton *et al.* (2003)
Cape Campbell	Flags Creek Thrust		5	Crampton *et al.* (2003)
	Flags Creek Thrust		10-25	Rait *et al.* (1991)
	London Hill Fault		1.3	Crampton *et al.* (2003)
Whanganui	Whanganui	3.8±1		Nicol & Beavan (2003)
Taupo	Bay of Plenty	30±10		Davey *et al.* (1995)
Whanganui	Whanganui Basin-Kapiti Island	2.3±1		Nicol *et al.* (2007)
East Nelson Block	Queen Charlotte Sound		7±4.5	Nicol & Campbell (1990)
	Waimea-Flaxbourne Fault		3±1.5	Thrasher *et al.* (1995)
Taranaki-Kapiti Island	Taranaki-Whanganui basins		75±35	Stern *et al.* (2006); Nicol *et al.*, 2007; Nicol & Stagpoole (2008)

Extension

There is very little evidence for Neogene extension in the East Coast Basin, although extension associated with thrust complexes within the accretionary prism in Hawke Bay during the middle to late Miocene (c. 14–4 Ma) has been noted by Barnes and Nicol (2004), Nicol and Uruski (2005) and Burgreen-Chan *et al.* (2016). These formed through polyphase deformation on an opposed-dipping thrust duplex under a compressional regime (Barnes & Nicol, 2004). Uruski (1992) identified a number of basins in Cook Strait that initially developed as half-grabens resulting from Late Cretaceous to Paleocene rifting, before developing into pull-apart basins in the Neogene due to transcurrent faulting in Marlborough and the North Island.

5.4 Incorporation of Structural and Tectonic Constraints in GPlates Model

The foundations for the model lie within a plate motion circuit describing the relative motions of the Australian, Antarctic (East and West), and Pacific plates (e.g., Cande & Stock, 2004). The timing of these movements are governed by seafloor spreading rates, and as such the time planes for the model are tied to chrons of the geomagnetic polarity timescale for which total reconstruction poles governing the relative motions of the plates within the Australia-Antarctica-Pacific plate circuit have been calculated. Total reconstruction poles used in this study include those from Cande & Stock, (2004), Croon *et al.* (2008) and Granot *et al.* (2013). The New Zealand subcontinent was reconstructed for the ages 2.58 (C2Ay), 4.0, 6.04 (C3Ay), 10.95 (C5o), 20.13 (C6o), 26.55 (C8o) and 40.13 Ma (C15o), as there is good control on the seafloor spreading ages in the Australia–Antarctic-Plate plate circuit for these times (e.g., Cande & Stock, 2004). The selection of instantaneous stage poles for the time steps outlined above are interpolated from the Australia-Antarctica-Pacific plate circuit by the GPlates software. Primary considerations in the adopted retro-deformations applied to this model include substantial vertical-axis rotations in northern Marlborough from 4 Ma to present (e.g., Little & Roberts, 1997; Lamb, 2011; Randall *et al.*, 2011), opening of the Havre Trough (<4 Ma; Malahoff *et al.*, 1982; Stern, 1985), development of the Taupo Volcanic Zone (<4 Ma; Wilson & Rowland, 2016), translation of the East Coast Allochthon on Raukumara Peninsula (21–25 Ma; Rait *et al.*, 1991), and the general correlation between rates of convergence or rifting, and rotation (e.g., Wallace *et al.*, 2009).

The model preserves the areal extent and line length of the present-day block configurations, and as such, retro-deformed models will show areas of future extension as overlapping structures, and areas of future convergence as void space between blocks. Similarly, future dextral movements

appear as retroactive sinistral displacements. Clockwise vertical-axis rotations are retroactively shown as anticlockwise movements of structural blocks. Because of the rigid constraints on the model, most plate-boundary related deformation is accommodated in the areas between structural blocks.

5.4.1 Regional Reconstruction

In the palinspastic model presented (Figure 5.12), vertical-axis translation and vertical-axis rotation of microblocks within the Neogene deformation zone move relative to a fixed Australian plate (e.g., Northland and NW Nelson blocks). Many previous models (e.g., King, 2000a) adopt this relative frame of reference while others (e.g., Lamb, 2011) have adopted a Pacific plate frame of reference. Herein, the 1°/Myr clockwise rotation of the Australian Plate with respect to the Pacific Plate, is applied as a 1°/Myr retroactive anticlockwise rotation to the Pacific Plate (represented by the South Island block) going forward in time through the model (Figure 5.12).

A Neogene origin for the development of oroclinal bending is adopted in this model after King (2000a). Although depicted in our reconstruction as a rigid block reconstruction, the likely tectonic solution that preserves the continuity of basement trends involves substantial, non-rigid intracontinental deformation, whereby line lengths do not remain constant (e.g., Mortimer, 2014). Much of the regional model development required aligning basement terrane piercing points to a pre-Neogene position determined by the plate rotation circuits, under the assumption of a largely linear Esk Head Terrane (e.g., Kamp, 1986; King, 2000a; Nicol *et al.*, 2007; Furlong & Kamp, 2009) and only mildly bent Dun Mountain-Maitai Terrane (e.g., Sutherland, 1999a). Development of the East Coast Basin model component required a much more iterative approach to determine the model path for each individual micro-plate.

The Taranaki-Whanganui Block is rotated 30° at 26.55 Ma to maintain contiguous basement trends in the Dun Mountain-Maitai Terrane, and is in line with paleomagnetic vertical-axis rotation trends from the region, with a linear rotation rate extrapolated to 0 Ma (Figure 5.12). The East Nelson block is rotated 35° at 26.55 Ma to retain contiguous structural trends with the Dun Mountain-Maitai Terrane in Northland, and alignment of the Goulter Sycline in Marlborough with the Taieri-Whakatu Synform in Otago. A linear extrapolation of 35° clockwise rotation is retroactively applied to the model. A 55° anticlockwise rotation is applied to the Fiordland block to retain linear basement trends within the Darran Suite intrusives, which is retroactively extrapolated to 0 Ma as linear clockwise rotation. The relative position of the Fiordland block with respect to the South

Island is poorly constrained. Opening of the Emerald Trough between 40.13 and 26.55 Ma results in 8° of anticlockwise rotation of the South Island with respect to the Australian Plate, controlled by the plate circuit.

Shortening of 90 km across the South Island since 6.04 Ma is represented by a 90 km space between the South Island and East Nelson block, as most of the shortening occurs on the Alpine Fault, and due to the rigid nature of the GPlates model. The 90 km between blocks is apparent in the 10.95 Ma timeplane (Figure 5.12), and shortening is linearly and retroactively induced in the model from 6.04 Ma onwards.

The TVZ is closed by 34 km at 2.55 Ma in the model, based on modelled crustal extension across the northern TVZ (Nicol *et al.*, 2007) and the age of the oldest extrusive volcanics identified (Wilson *et al.*, 1995). North of the TVZ, ~80 km of extension and incipient back-arc spreading within the Havre Trough is restored at 6.04 Ma (Figure 5.12).

5.4.2 East Coast Basin Reconstruction

A bulk rotation of 70° anticlockwise was applied to structural blocks in the North Island East Coast Basin (excluding the East Coast Allochthon) at 26.55 Ma, based on consistent trends within vertical-axis rotations derived from both basement structural trends and paleomagnetic data (Figure 5.12). A linear, clockwise rotation was applied to these blocks and extrapolated towards 0 Ma. A conservative estimate of 50 km of Neogene shortening is considered across the North Island East Coast Basin in the model, demonstrated as a 50 km-wide void between the accretionary prism block and the Hawke's Bay to Wairarapa blocks at 26.55 Ma, due to the rigid nature of the GPlates reconstruction. The placement of the accretionary wedge in the 26.55 Ma reconstruction is governed by the edge of continental crust (approximated by the 2000 m isobath), placed so as to produce a smoothly defined continental margin.

Dextral strike-slip between structural blocks within the East Coast Basin is modelled to initiate at 6.04 Ma. A total of 40 km dextral strike-slip displacements on the Wellington to Mohaka faults, and 25 km on the Pongaroa Fault and associated structures are incorporated in the North Island East Coast Basin from 26.55 Ma. These relative offsets are largely governed by spatial issues and total line length of blocks at this time, and are as conservative as possible within the wider geographic setting of the model in the 26.55 Ma reconstruction. Progressive rotation of structural blocks between 26.55 Ma and 6.04 Ma, mean that the total dextral strike-slip displacement across the Wellington-Mohaka and Pongaroa structures is 20 km, which is in line with geological evidence

for displacements during this period. Note that in the reconstructions presented in Figure 5.12, small displacements, generally on the order of less than 1–5 km, are not resolved at the scale of reconstruction.

The Marlborough structural blocks are fixed to, and rotate with the Pacific Plate at 1°/Myr clockwise from 40 Ma until 10.95 Ma (Figure 5.12). Throughout this period, the Esk Head Terrane forms a contiguous, linear basement trend across the North Island and Marlborough, accounting for the similar orientation of basement fabrics between Wellington and Marlborough.

Dextral strike-slip on the Marlborough Fault System is initiated on the Wairau Fault between 10.95 and 6.04 Ma in the GPlates model, with the most displacement on the Marlborough Fault System occurring from 4 Ma (Figure 5.12). This is based on geological evidence presented by Little & Jones (1998), who demonstrate that no significant strike-slip displacements occurred across the Marlborough Fault System prior to 6.4–7 Ma. This is also consistent with the model presented in Reyners *et al.* (2017), who interpret the Rakaia Terrane and Esk Head Belt to be contiguous through New Zealand until c. 10 Ma, after which time they propose that 80 km of margin-normal displacement occurred in association with the Hikurangi Plateau entering the Neogene Hikurangi subduction system.

Propagation of the proto-Wairau/Alpine Fault through the Cook Strait region with a dextral displacement begins at 10.95 Ma in the model, with significant movements on the Marlborough fault system beginning at 6.4 Ma. Individual structural blocks in the Marlborough region are extrapolated in a linear fashion along fixed paths from 10.95 to 0 Ma, based on average slip-rates the interpreted timing of major movements on the Marlborough Fault system (e.g., Little & Jones, 1998).

Incorporation of the regional model with the East Coast Basin model results in a substantial, triangular void area between the axial ranges, the Taranaki-Whanganui block and the South Island block. Development of this model has aimed to keep the size of this void space as conservative as possible, and subsequently it is substantially smaller than presented in previous models (a third of the size), but remains unavoidable with the spatial area of structural blocks, and the respective rotations that must be applied to the various components of the model in order to stay true to the geological evidence.

Between 26.55 to 40 Ma, the East Coast Basin blocks were considered tectonically inactive, and are fixed to the passively rotating Pacific Plate (moving at 1°/Myr anticlockwise forward in time). Effectively the palinspastic configuration at 26.55 Ma is the same as at 40 Ma, albeit with a lesser

displacement of the South Island block (with respect to NW Nelson) that arose from up to 350 km of crustal spreading in the Emerald Basin between 40 Ma and 26.55 Ma (Furlong & Kamp, 2009).

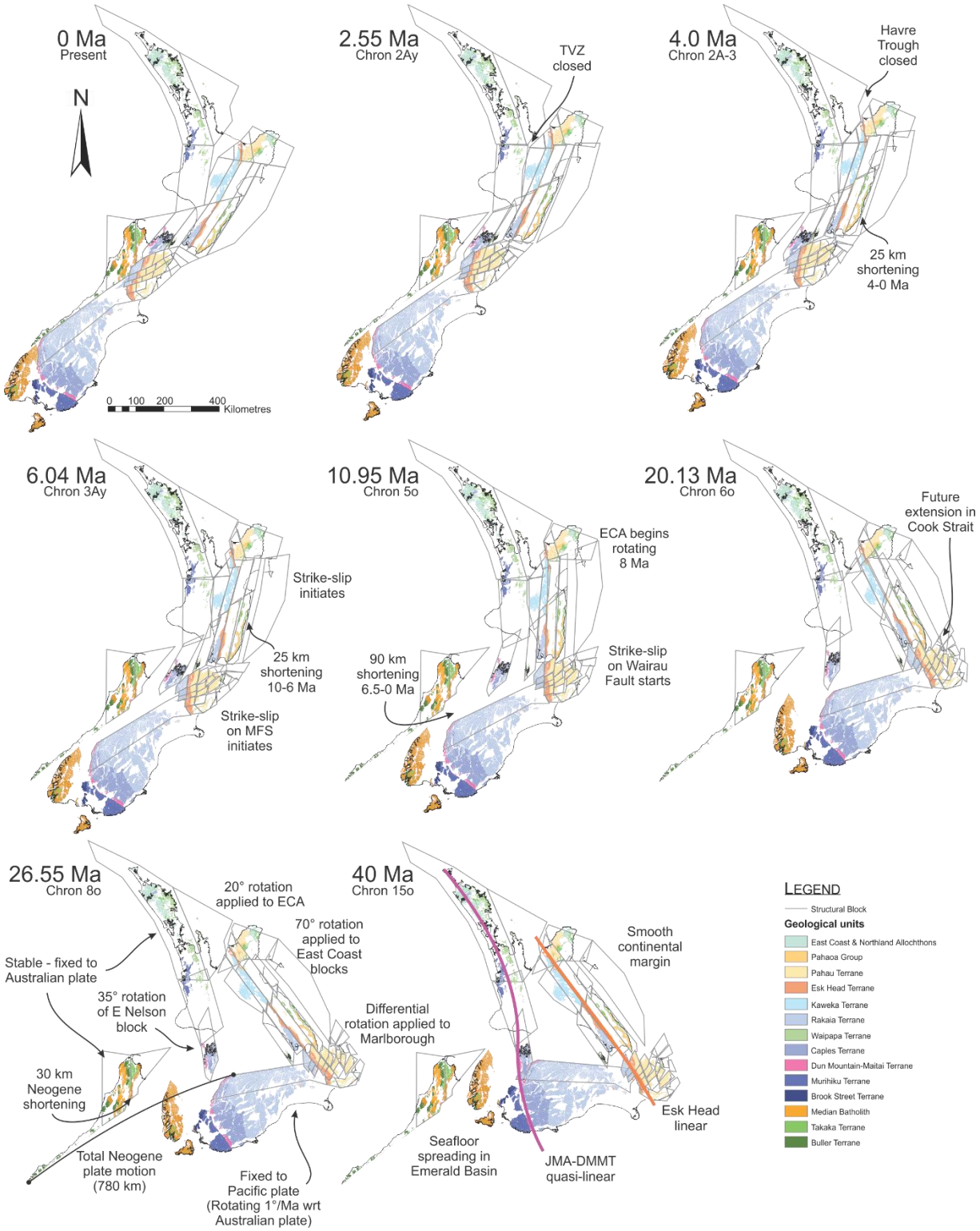

Figure 5.12: Palinspastic maps for selected time-planes with geology superimposed, displaying the progressive reconstruction of Neogene deformation across Zealandia. Maps produced by GPlates software (see text). QMAP geological data from Heron (2014).

5.5 Model Results and Discussion

At a broad scale, the reconstruction of the wider New Zealand region produces a reconstruction that is comparable to that derived by a number of previous reconstructions (e.g. King, 2000a; Wood & Stagpoole, 2007; Nicol *et al.*, 2007; Lamb, 2011). This is unsurprising as the fixed components of the model (Northland and NW Nelson fixed to Australian Plate; South Island fixed to Pacific Plate) are constrained by well-established, finite relative plate motion kinematics (e.g. Cande & Stock, 2004). The real distinction between models lies within the adopted retro-deformation of the East Coast Basin. The 26.55 Ma reconstruction produces an East Coast Basin orientation that is broadly similar to the King (2000a) reconstruction, however, the reconstruction presented here has a substantially smaller eroded mass in the central New Zealand region, and the internal configuration of the basin is resolved. In terms of areal extent, the 6.04 and 26.55 Ma models presented in this study are remarkably similar to the 5 Ma and 24 Ma reconstructions of Nicol *et al.* (2007) despite the different approaches (rigid versus plastic deformation) undertaken. The key difference to these previous models is the well-constrained and repeatable tectonic framework that the model presented here is based within.

5.5.1 Declination Anomaly – Model Rotation Relationship

Paleomagnetic data from the Australian Plate fit the model path well, with the exception of two outliers, Cape Foulwind (CF) and samples from the Northland Ophiolite (NO; Figure 5.13A). Paleomagnetic declination anomaly data from the Pacific Plate (Figure 5.13B) also fit the model well. The two most notable outliers are Leslie Hills (LYF) and mid-Waipara River (MW) samples. These sample localities are within the Porters Pass Fault Zone, and could possibly be explained by localised rotation and deformation on small-scale local structures (e.g., Little & Roberts, 1997). Samples from the Matakaoa Volcanics (MV) and early Miocene sedimentary rocks show that the East Coast Allochthon did not rotate prior to ~8 Ma (Figure 5.13C). The model rotation path may overestimate the amount of rotation in the North Island East Coast Basin by 10–15° on the basis of late Miocene samples, although this is only constrained by a single pre-Miocene data point from Rangitato, central Hawke's Bay (RN; Figure 5.13C). In the Marlborough region, exceptionally high rotations within the model for the Cook Strait region are in line with the northernmost Marlborough samples (e.g. Cape Campbell), although are higher than would be expected, and may indicate a need for future interrogation and refinement of the model (Figure 5.13D). The various structural blocks of the central Marlborough region (Wairau, Awatere, Clarence, and Kaikoura) have been displayed for clarity as a single highlighted zone, as these blocks behave in a similar and

consistent manner within the model (Figure 5.13D). Notable exceptions are the northernmost fault blocks for the northern Wairau Valley (NWV) and the northern Awatere Valley (NAV), which show an additional, modelled ~30° of clockwise rotation, consistent with measured vertical-axis rotations in these regions (Figure 5.13D; Little & Roberts, 1997; Hall *et al.*, 2004; Lamb, 2011). Across the Marlborough structural blocks there is a southward-decreasing trend in the amount of clockwise rotation from Cape Campbell to northern Canterbury (Figure 5.13D), consistent with a progressive transition from the amount and rate of rotation in the North Island East Coast (Figure 5.13C) to the lower relative rate of rotation across the Pacific Plate (Figure 5.13B).

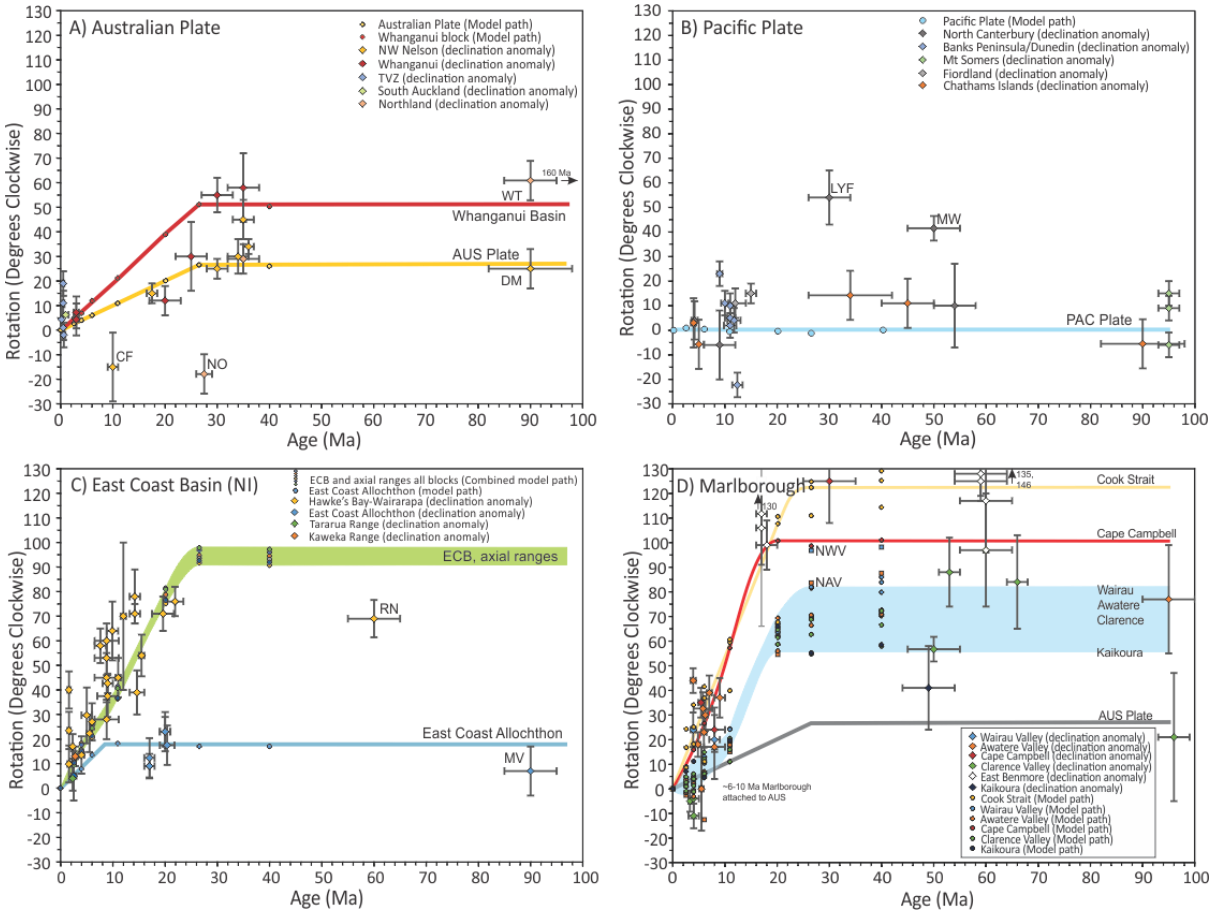

Figure 5.13: Vertical-axis rotations of blocks derived from the paleogeographic model used here, for selected timeframes, in comparision to paleomagnetic declination anomaly data. A) Declination and model values from the Whanganui Basin and the fixed Australian Plate (AUS), showing ~1°/Ma rotation with respect to the Pacific Plate (PAC). B) Declination and model values from the Pacific Plate and north Canterbury. C) Declination and model values from the East Coast Basin, East Coast Allocthon and the axial ranges. D) Declination and model values from across Marlborough. Coloured lines indicate the model rotation paths (labelled) for individual blocks or regions. In panel D, paleomagnetic declinations from the east limb of the Ben More Anticline, Marlborough, are shown as white diamonds – refer to discussion. DM = Dun Mountain, NO = Northland Opiolite, CF = Cape Foulwind, WT = Waipapa Terrane, Northland, LYF = Leslie Hills, MW = mid-Waipara River, RN = Rangitato, MV = Matakaoa Volcanics, NWV = North Wairau Valley, NAV = North Awatere Valley, AUS = Australian Plate, PAC = Pacific Plate, ECB = East Coast Basin, TVZ = Taupo Volcanic Zone.

5.5.2 East Coast Basin Deformation Trends

The translated retro-deformations for the rigid-body reconstruction of the East Coast microplate model are presented here (Figure 5.14), with arrow azimuth used to indicate the retro-deformed vertical-axis rotation, and motion vector paths indicating the retroactive movements of the microplates through time (corresponding to the colouring of arrows). These translation paths are normalised to a common datum at 0 Ma in Figure 5.15 for comparison between blocks and basin subdivisions (Raukumara Peninsula, Hawke's Bay, Wellington-Wairarapa, and Marlborough). The angle of the relative plate convergence vector of the Pacific Plate with respect to the Australian Plate through the Neogene is derived from Euler pole positions from Sutherland (1995) and King (2000a), and included to aid interpretation of broad-scale deformation trends (Figure 5.15B, D). The broad-scale temporal interpretation of plate boundary strain orientations is based on the respective orientation of the plate convergence vector and the directionality of the translated model path (Figure 5.15).

Raukumara Peninsula

The model path for the Raukumara Peninsula does not start rotating until between 10.95 and 6.04 Ma, which aligns with paleomagnetic evidence that rotation began at ~8 Ma (Rowan *et al.*, 2005; Figure 5.13), demonstrating that the rotational moments of this block are consistent with geologically derived kinematic data. The consistency of the GPlates model is illustrated by the highest rotation rates of ~2.8°/Myr for the allochthon block between 6.04 and 4.0 Ma, decreasing to around 2°/Myr between 2.58 and 4.0 Ma, in comparison to 2.88°/Myr in the present-day Raukumara region (Nicol & Wallace, 2007).

The orientation of allochthon emplacement was not included in the GPlates model, but rather, the reconstructed location of the East Coast Allochthon block in this reconstruction was estimated by the location of unrifted continental crust in the western Bay of Plenty, and considerations of the along-strike length of the East Coast blocks in relation to the South Island. The East Coast Allochthon comprises only a small overall thickness of the crust, and in the context of the large-scale motion of the crustal blocks considered here, the East Coast Allochthon can be considered as a 'rafted' sediment mass upon a crustal block. Notably, the vector orientation of the structural block changes substantially following the emplacement of the allochthon between 26.55 and 20.13 Ma, coincident with the timing of allochthon emplacement (Figure 5.15A). The positioning of the East Coast Allochthon block during the early Miocene would be consistent with a southwest

emplacement direction for the East Coast Allochthon (e.g., Stoneley, 1968; Kenny, 1984; Rait *et al.*, 1991), and consistent with the timing and emplacement direction of the Northland Allochthon (e.g., Rait, 2000).

Hawke's Bay

The pre-Neogene model rotation path for the North Island East Coast corresponds well with existing paleomagnetic data (Figure 5.13), for example, the middle Miocene model rotations show a rate of rotation (4°/Myr) consistent with paleomagnetic declination anomaly data (4–4.5°/Myr) vertical-axis. The good fit of the structural kinematic model to paleomagnetic declination anomaly data (Figure 5.13) demonstrates that the model is internally consistent. The Hawke's Bay, Wairarapa, accretionary prism and the axial range blocks, have an average rotation rate of ~4°/Myr through the duration of the model, which is broadly consistent with the modern-day measured rotation rates of 3.71°/Myr in the Wairarapa, although higher than the present-day rotation rates measured in the accretionary wedge (3.0°/Myr), and the axial ranges (2.85°/Myr; Nicol & Wallace, 2007).

The translated vector motion paths of the Hawke's Bay blocks are comparable to that of the accretionary prism. Vector motion of structural blocks in the Hawke's Bay appears to be controlled by convergence/compression from 26.55 to 10.95 Ma, when it changes to oblique slip during the development of the plate boundary through to the Hikurangi margin (Figure 5.15B).

Wellington–Wairarapa

The alignment of model vector paths from the Wellington-Wairarapa region along a great circle suggests that at 20.13 Ma, there was no relative offset between the various fault blocks of the Wellington-Wairarapa region (Figure 5.15C). By 10.95 Ma, the vector nodes have become offset by <10 km between each respective block, indicating that strike-slip faulting initiated between 20.13 and 10.95 Ma, at a rate of approximately 1mm/yr. This is consistent with interpretations of geological evidence that suggest strike-slip faulting in the Wairarapa region during the Altonian to Otaian (21.7–15.9 Ma; e.g., Ridd, 1967; Cutten & Delteil, 1993; Delteil *et al.*, 1996).

Translated vector paths for the Wellington-Wairarapa model domains fall into alignment from 4.0 Ma (Figure 5.15C) along an orientation of 033–034°E, congruent with the mean strike orientation of major strike-slip faults in the southeastern North Island (Nicol *et al.*, 2007). The alignment and

orientation vector paths from 4.0 Ma indicate that strike-slip (and oblique-slip with a strong horizontal component) have been the dominant mode of deformation in the model from 4.0–0 Ma. This is consistent with geological evidence that indicates that notable strike-slip displacements on the Wellington-Mokaha faults are a Pliocene to Recent feature (Erdman & Kelsey, 1992; Beanland, 1995; Beanland *et al.*, 1998; Bland & Kamp, 2006; Nicol *et al.*, 2007). Mean Pliocene slip rates in the Hawke's Bay and Wellington-Wairarapa domains (across all blocks) determined from the model are comparable to the Plio-Pleistocene averaged margin-parallel strike-slip rate estimates from Nicol *et al.* (2007) and the cumulative present-day slip rates of the major Hawke's Bay-Wairarapa fault systems (Table 5.4).

Table 5.4: Mean slip rates for the present day faults in the Hawke's Bay-Wairarapa in comparison to average Plio-Pleistocene slip rates, and mean Pliocene slip rate determined from the GPlates model presented here.

Fault	Slip Rate (mm/yr)	Source
Ohariu Fault	5.3	Nicol & Wallace (2007)
Wellington -Ruahine-Whakatane faults	3.5-3.6	Nicol & Wallace (2007)
Wairarapa Fault	2.9	Nicol & Wallace (2007)
Poukawa Fault zone	4.7	Nicol & Wallace (2007)
Mohaka Fault	5.4	Nicol & Wallace (2007)
Total (Present day):	21.9	
Plio-Pleistocene margin parallel average	26	Nicol *et al.* (2007)
Hawke's Bay-Wairarapa Pliocene mean slip rate	23.3	This Study

Marlborough

The translated model paths in Marlborough (Figure 5.15D) need to be filtered to remove the dominant influence of the Alpine Fault and the relative plate motion between the Australian and Pacific plates, which masks the relative and respective movements of the Marlborough fault blocks. The substantial displacement exhibited in Figure 5.15D reflects motion of the Pacific Plate throughout the Neogene, and is therefore recording the displacement on the Alpine Fault. If the amount of movement on the Alpine Fault is subtracted (480 km) from the translated paths, the remaining amount of motion on the Marlborough Fault System is approximately equal to that of the Neogene translation of the accretionary prism (~250 km), cumulatively totalling 730 km in the model (compared to 780 km suggested by plate closure models). If the cumulative 55 km of relative

internal displacement across the Esk Head Belt within the Marlborough fault system is included, this demonstrates that the model kinematics are internally consistent with the amount and distribution of finite plate motion.

Of particular note in the reconstruction is that the Rakaia-Esk Head-Pahau terranes were contiguous across the Wairau Fault and Cook Strait until 10.95 Ma, but are displaced by ~100 km by 6.0 Ma, implying average slip rates on the Wairau Fault of ~20 mm/yr through this 4.95 Myr interval. Although seemingly high, this is not too dissimilar to the present day intraplate-parallel slip vector of 27 mm/yr on the Alpine Fault (Ghisetti *et al.*, 2016a). Therefore, in this reconstruction, all intraplate motion is placed on the Wairau Fault for the period between 10.95 and 6.0 Ma, rather than being distributed across the Marlborough Fault Zone, as it is from 6.0 Ma to the present.

Structural blocks within the Cook Strait region accommodate a number of volumetric and line length issues in placing East Coast structural blocks within the restrictions of the wider tectonic model. Somewhat serendipitously, running the model path from a pre-set position at 26.55 Ma to 0 Ma results in early to middle Miocene extension in Cook Strait. Extension in this region is broadly consistent with the development of *en-echelon*-style pull-apart basins in Cook Strait (e.g. Lewis *et al.*, 1994), and pre-Tongaporutuan extension in central Palliser Bay (Barnes & Audru, 1999), and early Miocene to Pleistocene extension in the Wairau and Flaxbourne basins (Barnes & Audru, 1999; Holdgate & Grapes, 2015).

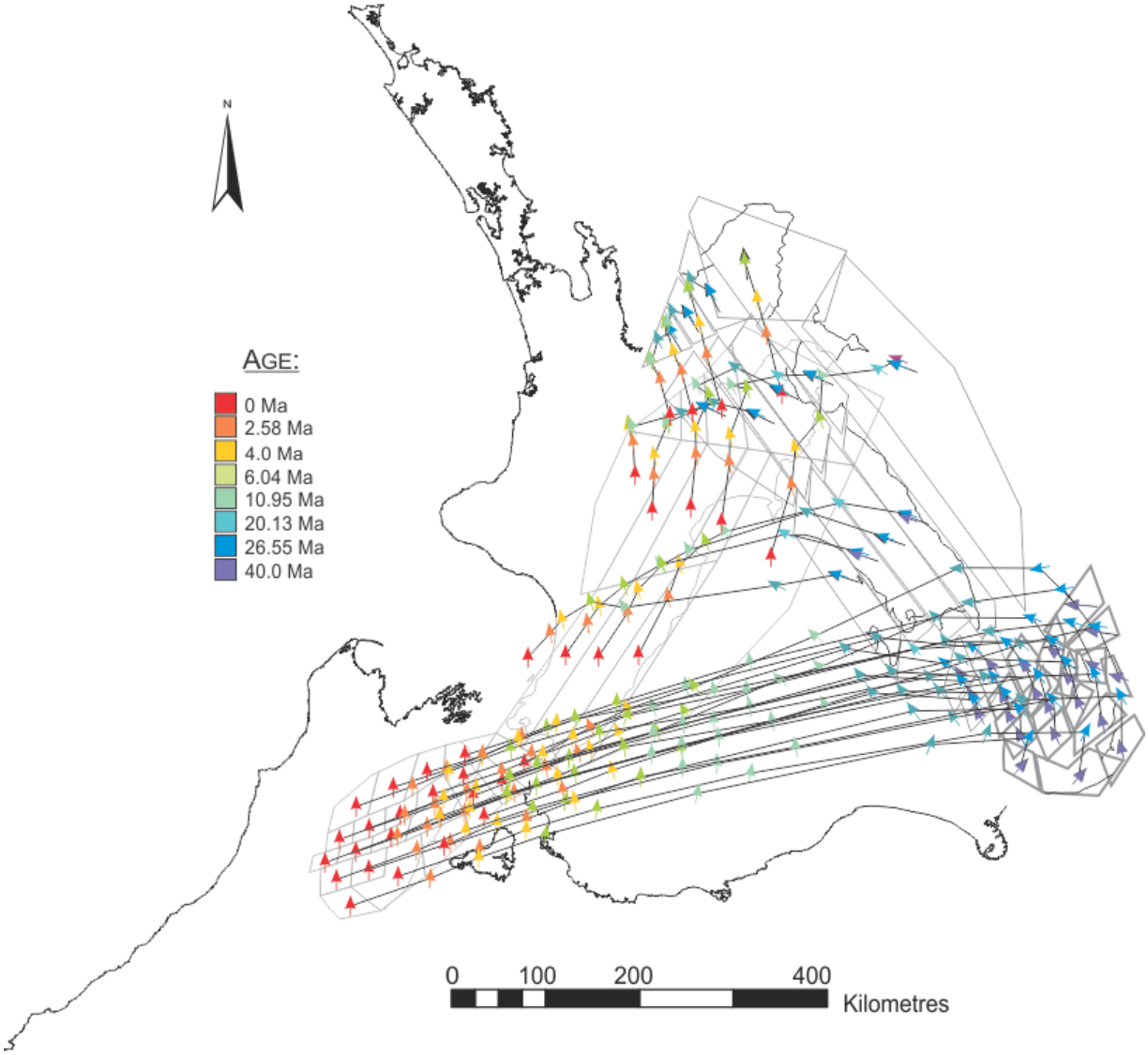

Figure 5.14: Microplate vector paths for the rigid body reconstruction of the East Coast-Marlborough region. Arrow colours indicate age, and arrow azimuth indicates the retro-deformed vertical-axis rotation adopted in the model (i.e. the inverse of Neogene vertical-axis rotations).

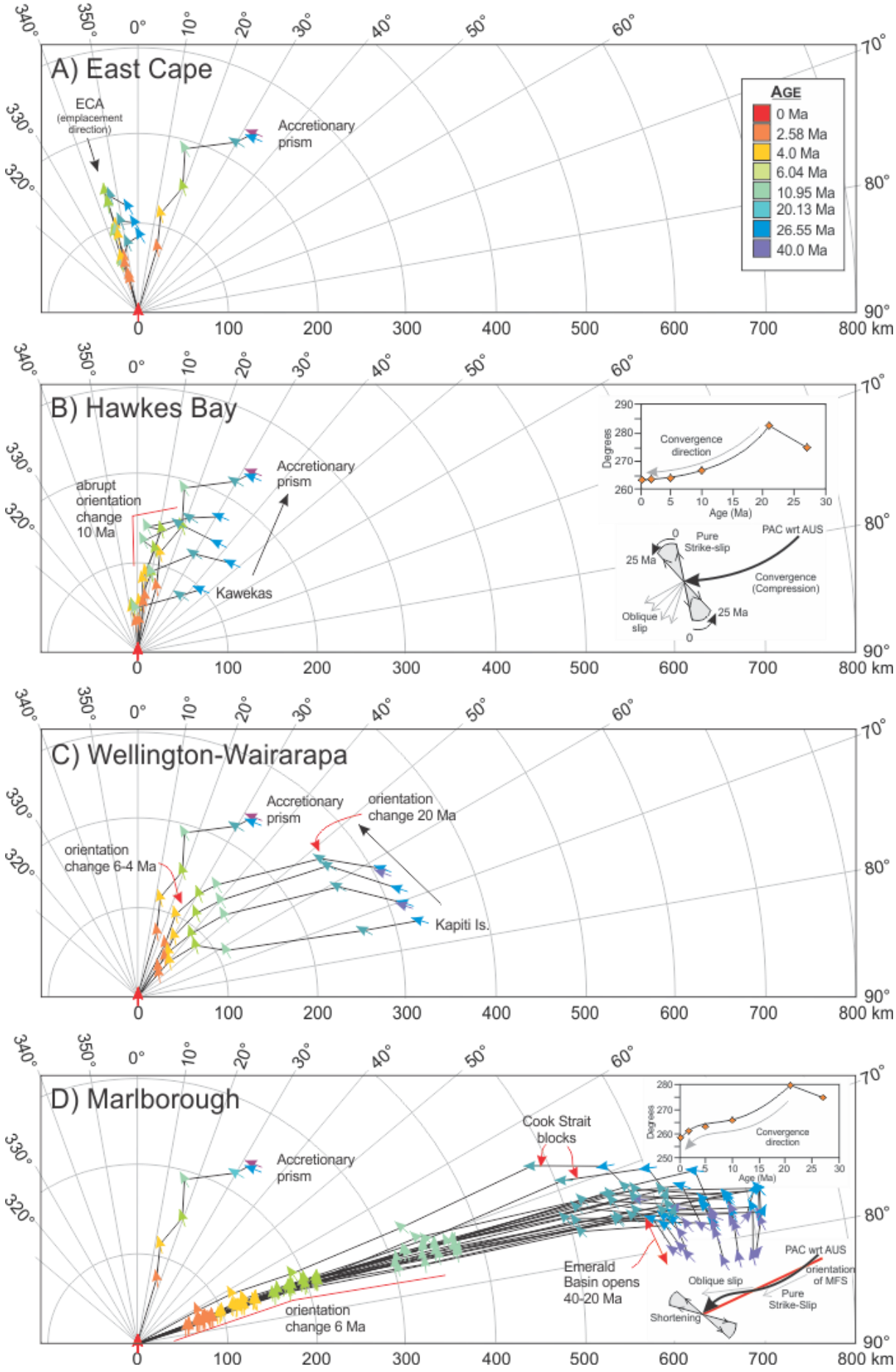
A) East Cape
ECA
(emplacement direction)
Accretionary prism
AGE
0 Ma
2.58 Ma
4.0 Ma
6.04 Ma
10.95 Ma
20.13 Ma
26.55 Ma
40.0 Ma
B) Hawkes Bay
abrupt orientation change 10 Ma
Accretionary prism
Kawekas
Convergence direction
Degrees
Age (Ma)
PAC wrt AUS
Pure Strike-slip
25 Ma
Convergence (Compression)
Oblique slip
C) Wellington-Wairarapa
Accretionary prism
orientation change 20 Ma
orientation change 6-4 Ma
Kapiti Is.
D) Marlborough
Accretionary prism
Cook Strait blocks
Emerald Basin opens 40-20 Ma
orientation change 6 Ma
Oblique slip
Pure Strike-Slip
Shortening
orientation of MFS
0
100
200
300
400
500
600
700
800 km

Figure 5.15: Vector translation with respect to a fixed Australian Plate. Microplate vector paths from Figure 5.14 normalised to 0 Ma for subdivisions of the eastern margin. A) Raukumara Peninsula, B) Hawke's Bay, C) Wellington-Wairarapa, D) Marlborough. The vector path of the accretionary wedge is plotted on each panel for reference. Arrow colours indicate age, and arrow azimuth indicates the retro-deformed vertical-axis rotation adopted in the model (i.e. the inverse of Neogene vertical-axis rotations). Inset: Angle of convergence vector of the Pacific Plate with respect to the Australian Plate through the Neogene. Angle derived from Euler pole positions from Sutherland (1995) and King (2000a). Broad-scale temporal interpretation of plate boundary strain orientations based on convergence vector. MFS = Marlborough Fault System. Shortening orientation for Marlborough region from Nicol & Dissen (2002).

5.5.4 Shortening

The timing, amount and location of shortening within the New Zealand region is a contentious issue that varies between most reconstructions. Most publications agree that shortening dominantly occurred within the East Coast Basin during a phase of early Miocene shortening associated with the emplacement of thrust sheets (e.g., Delteil *et al.*, 1996), and a renewed phase of shortening in the Pliocene, resulting in the subaerial emergence of the forearc (Cashman *et al.*, 1992; Bland *et al.*, 2008; Trewick & Bland, 2012).

The distribution of structural blocks within the timeplanes of the reconstructed model indicate shortening in the East Coast Basin during three intervals; 26.55 Ma, ~10 Ma and 6 Ma to present, within the temporal resolution of the model presented (Figure 5.12). The corresponding change in translated vector motion paths between 10-6 Ma is consistent with the onset and southward progression of oblique-slip in the basin. The orientation of translated vector paths between 26.55 and 20.13 Ma implies that shortening that occurs during this interval is normal to, and governed by relative plate convergence. Shortening between 4.0 and 2.55 Ma is consistent with a renewed phase of oblique-slip during the Pliocene.

Early Miocene Shortening (26.55 – 20.13 Ma)

Thermochronological studies in the Waikaremoana area and Kaimanawa Ranges indicate an early Miocene cooling event (24–20 Ma and 27–20 Ma, respectively) indicative of an early Miocene thrusting event and accelerated denudation (Kamp, 1999; Jiao *et al.*, 2015). Thermal history modelling of Jiao *et al.* (2015), demonstrate that the uplift/unroofing on the Kaimanawa Mountains, west of the Ngamatea Fault and the westernmost block of the axial ranges, occurred at 27 Ma. In

addition, thermochronological data from the axial ranges suggest that the Ngamatea Fault bounding the Kaimanawa Schist demonstrated substantial thrusting before c. 20–17 Ma, with accelerated exhumation and cooling at ~20 Ma between the Ngamatea and Wellington-Mohaka Fault system (Jiao *et al.*, 2015).

Early Miocene compression in the Wairarapa is indicated by imbricate thrust sheets east of the Adams-Tinui Fault, with 10 km of shortening interpreted by Rait *et al.* (1991), although the distribution of Paleogene strata would suggest that the actual displacement is higher (Moore, 1988a, 1988b; Lee, 1996; Chapter Four). Stratigraphic evidence for early Miocene shortening in the vicinity of the Adams-Tinui Fault includes the late Altonian Takiritini Formation in eastern Wairarapa. The Takiritini Formation comprises sandstone, siltstone, and algal limestone lithofacies, the latter suggesting at least some deposition within the photic zone in a setting with low sedimentation (Kamp & Nelson, 1988; Nalin *et al.*, 2008). However, the Takiritini limestone overlies bathyal flysch sediments of the Whakataki Formation of Waitakian to early Altonian age, implying rapid uplift rates at this time (Johnston, 1980; Field, 2005; Nalin *et al.*, 2008; Bailleul *et al.*, 2013). The Takiritini Formation is up to 1000 m-thick in places (Lee & Begg, 2002), requiring rapid creation of accommodation space during deposition. Likewise, the formation is overlain by a substantial thickness of Neogene sedimentary rocks (Lee & Begg, 2002), implying significant subsequent subsidence. A series of similar limestones of similar age and with similarly restricted distributions occur across the eastern Wairarapa and Hawke's Bay, suggesting a chain of bathymetric highs associated with thrust-related folding. This is indicative of rapid uplift and burial across the East Coast Basin, consistent with substantial crustal shortening at this time.

The transition from purely compressional to transpressional displacements in the East Coast occurred during the Otaian to Altonian (mid- to late-early Miocene; Delteil *et al.*, 1996) and corresponds with a notable deviation in the vector translation paths at ~20.13 Ma (Figure 5.15B, 5.15C; at the resolution of the model time-slices presented here). This indicates the model is in broad agreement with geological observations.

Late Middle Miocene Shortening (10.95 – 6.0 Ma)

A widely noted change in relative plate motion between the Australian and Pacific plates resulted in pronounced kinematic changes at 6.04 Ma (Chron 3Ay), most notably an increase in the convergence rate perpendicular to the Alpine Fault (Walcott, 1998; Cande & Stock, 2004). In the Marlborough region, this interval marks the transition from near-pure strike-slip (26–6 Ma) to

transpression at 6 Ma on the Marlborough Fault Zone and Alpine Fault (Kamp, 1986; Little & Jones, 1998; Walcott, 1998; King, 2000a; Ghisetti *et al.*, 2016a).

In the North Island, thermochronological data from Jiao *et al.* (2015) show that the Wellington-Mohaka Fault demonstrated significant thrusting before ~10–7 Ma, and east of the fault, exhumation and cooling of basement rocks occurred at 10–7 Ma (Jiao et al., 2015). The timing of this event is consistent with an earlier thermochronological study in the Wellington and Wairarapa regions, indicating rapid unroofing and denudation at 8.5 Ma (Kamp, 2000). The timing and location of this unroofing event implies a southwards propagation in shortening between 20 Ma and 10–5 Ma between the Kaweka Ranges and the southern Tararua Ranges. Likewise, the exhumation rate of the North Island axial ranges has varied along the strike of the North Island Fault System since the late Miocene, with lower rates in the central parts of the axial ranges, and significantly higher rates at the southern end (Jiao *et al.*, 2015). The stratigraphic record within the middle to late Miocene (10–7 Ma; Tongaporutuan Stage) preserves a series of terrestrial deposits within a dominantly marine succession (e.g. Putangirua Conglomerate, Sunnyside Conglomerate, Mangaoranga Formation, Blowhard Formation; Neef, 1984; Field & Uruski *et al.*, 1997; Vella & Collen, 1998; Browne, 2004). Uplift at 10 Ma is also indicated by the complete denudation of the Eketahuna area (Kelsey *et al.*, 1995). Within the model presented here, oblique strike-slip in the North Island East Coast initiates between 10.95 and 6.04 Ma, and continues to the present (Figure 5.15B). The Hawke's Bay transitions to oblique slip at 10 Ma, and blocks within the Wellington region transition to oblique slip between 6.04 and 4.0 Ma (Figure 5.15 B, 5.15C).

Progression of the model path also indicates a shortening event between 10–6 Ma that largely falls out of spatial restriction between individually rotating blocks within the wider regional tectonic framework. The timing of this shorting is congruent with geological evidence for shortening and compression in the basin at this time indicated by Nicol and Uruski (2005), although in contrast to an extensiton period interpreted by Ghisetti *et al.* (2016b; Figure 5.16A).

Pliocene-Recent Shortening (4.0 – 0 Ma)

There has been significant Pliocene shortening on the accretionary complex, with as much as 22 km of shortening in the area immediately west of the subduction thrust during the past 2 Myr (Ghisetti *et al.*, 2016B). Pliocene shortening of ~25 km is demonstrated in the model with the translation of the accretionary wedge block towards the Hawke's Bay – Wairarapa from 4.0 Ma (Figure 5.12). The amount of both early and late Neogene shortening in the upper plate generally

increases southwards in the forearc (Figure 5.16B; Beanland *et al.*, 1998; Nicol *et al.*, 2007), represented in the translated model paths by the significant increase in length of the Wellington-Wairarapa vector paths (Figure 5.15).

Total Neogene shortening across the East Coast Basin and axial ranges was estimated to be 90 km by Nicol *et al.* (2007), with a maximum shortening estimate of 150 km. Most of this shortening is interpreted to have been transferred to the plate interface in the Hawke's Bay region (e.g. Nicol *et al.*, 2007). However, some of this shortening must have occurred in the forearc and axial ranges to see the demonstrable uplift and unroofing trends in stratigraphic and thermochronological data. This is consistent with the translated model vector paths (Figure 5.15 B, C, & 5.16A), and the interpretation of Jiao *et al.* (2015) that exhumation associated with shortening is located within the fore-arc and the overriding Australian Plate. The vector motion path of the model indicates a total spatial translation of ~150 km for structural blocks in the Hawke's Bay (Figure 5.15B), consistent with the maximum estimate of shortening associated with relative plate motion through the Neogene by Nicol *et al.* (2007).

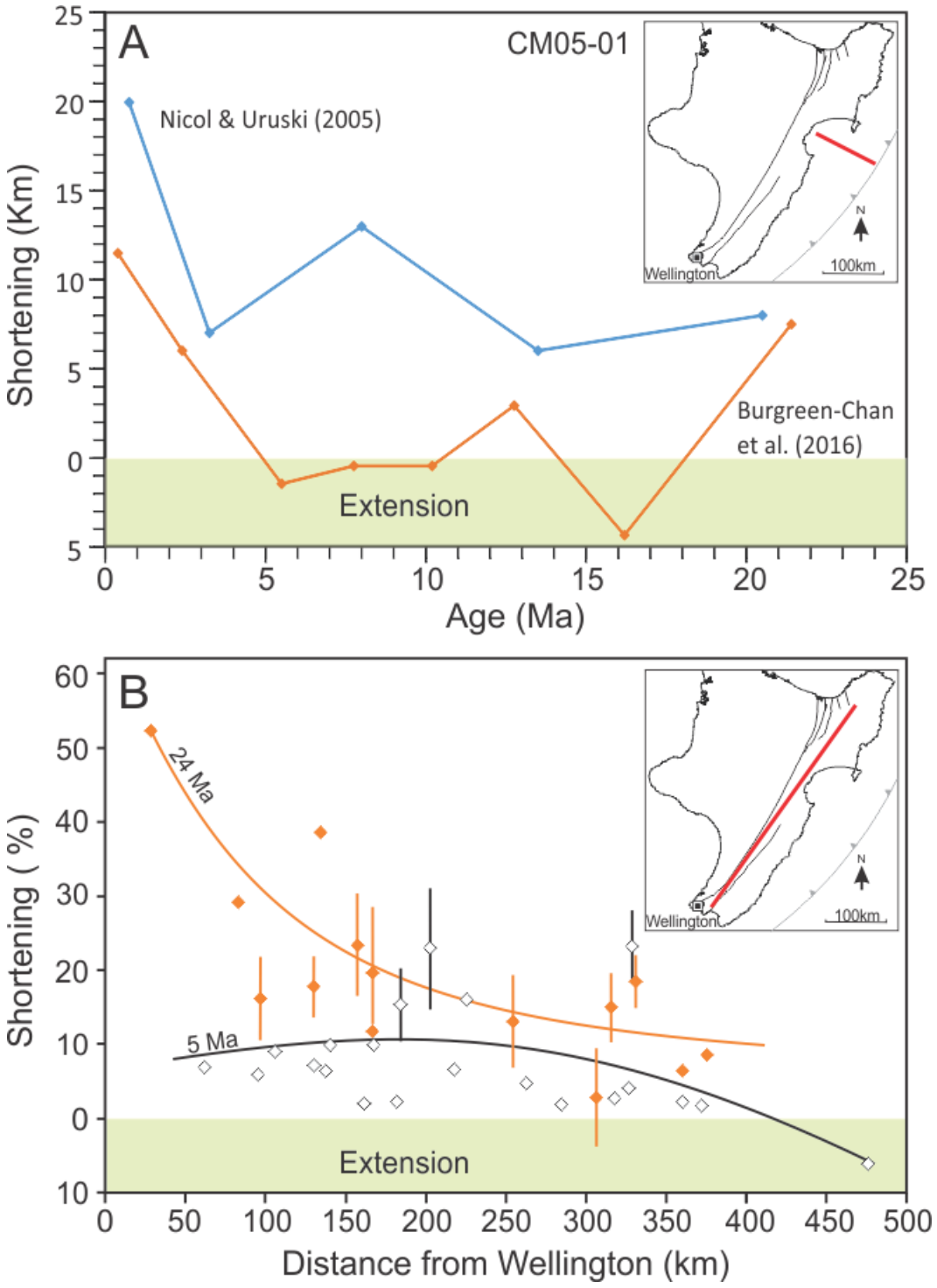

Figure 5.16: Neogene shortening estimates from the East Coast Basin. A) Calculated margin-orthogonal shortening estimates (kilometres of line length and percentage shortening) for various intervals interpreted from two different balanced cross-section interpretations of a seismic line through Hawke Bay (CM05-01), devolved from Nicol & Uruski (2005) and Burgreen-Chan *et al.* (2016). B) Percentage shortening for two time periods across a margin-parallel transect extending northeast of Wellington based on 5 Ma and 24 Ma margin-perpendicular shortening datasets from Nicol *et al.* (2007). Error bars are shown where available.

5.5.5 Crustal Volume Calculations

Reconstruction of crustal volume mass-balance in the New Zealand region during the Cenozoic has demonstrated that the pre-Neogene (65–25 Ma) rock distribution can be accounted for by erosion and sedimentation (Wood & Stagpoole, 2007). However, at c. 25 Ma, there is a significant increase in the non-rigid deformation of a large region in the centre of New Zealand, and erosion/sedimentation fails to account for the loss in crustal mass at this time. This led Wood and Stagpoole (2007) to invoke crustal underplating.

Gravity and seismic anomalies have identified an over-thickened crustal root beneath present-day New Zealand with a volume of 2,200,000 km^3 (±200,000 km^3; Wood & Stagpoole, 2007). In order to reconcile the volume of this crustal root inferred to have developed during Oligocene-Neogene compression along the Australian-Pacific margin, along with sedimentary fill in basins surrounding Zealandia since this time, Wood and Stagpoole (2007) use the large volume of missing crust from the King (2000a) Zealandia reconstruction. There are two issues with this approach; primarily, such a large volume of missing crust in central Zealandia is inconsistent with the present-day expression of basement rocks – the removal of a 110,000 km^2 area to a thickness of 28 km depth would result in the exposure of lower crustal rocks at the surface, yet metamorphic gradients in exposed basement strata are weak. Secondly, assuming the crustal root is sourced internally from Zealandia fails to account for the subducted portion of the Hikurangi Plateau. Seismic tomography has identified an area of very high P-wave velocities at 30–100 km depths beneath New Zealand, interpreted as subducted oceanic crust of the Hikurangi Plateau (Figure 5.17; Reyners *et al.*, 2011; Love *et al.*, 2015). This area of high P-wave velocities covers an area of ~200,000 km^2, and assuming an average thickness of 12 km for the subducted Hikurangi Plateau (Davy *et al.*, 2008) produces a volume of 2,400,000 km^3 that is not accounted for in the crustal balance equations of Wood and Stagpoole (2007), and is consistent with the estimated volume of the crustal root beneath New Zealand. This external source of material for the crustal root beneath New Zealand means that such a large volume of material is not required to be sourced from central Zealandia.

Following the estimates for clastic input into sedimentary basins around New Zealand from Wood and Stagpoole (2007), this leaves 465,800 km^3 (±50,000 km^3) of clastic material to be accounted for between 25 Ma and the present. The void in the centre of our reconstruction, located between the Taranaki and East Coast basins is 29,282 km^2. When combined with an area of 10,164 km^2 between Fiordland and the Nelson Block, there is a total 39,446 km^2 of missing crust between 25 Ma and the present day. This represents a substantial reduction from previous crustal volume balance efforts, almost a third of the 110,000 km^2 calculated by Wood and Stagpoole (2007) for the

void resulting from the King (2000a) reconstruction at 25 Ma, and consistent with the Nicol *et al.* (2007) reconstruction. Assuming that the clastic component within sedimentary basins around New Zealand is predominantly derived from sediment eroded from central Zealandia, the area of the missing clastic wedge from the model present herein would require stripping of cover and basement to a depth of 11.8 km.

Table 5.5: total solid basin volume (at 0% porosity) of clastic sediment deposited in basins around NZ through the Neogene from Wood and Stagpoole (2007).

Age (Ma)	**Clastic sediment volume in western basins (km^3)**	**Clastic sediment volume in eastern basins (km^3)**	**Clastic sediment volume in southern basins (km^3)**	**Clastic sediment volume in all basins (km^3)**	**Clastic uncertainty (km^3)**
0–5	123,300	85,400	33,400	242,100	66,600
5–10	59,500	31,700	20,200	111,400	34,700
10–15	63,000	33,400	18,200	114,600	37,500
15–20	53,700	35,700	17,100	106,500	35,000
20–25	41,400	37,000	16,000	94,400	35,100
Total	**340,900**	**223,200**	**104,900**	**669,000**	**208,900**

Pressure-temperature estimates from thermocalc pseudosection modelling of low-grade metasediments at Terawhiti, western Wellington, are 5.3 ± 2 kbar at 265 ± 50°C with lawsonite absent (Gazley *et al.*, *in submission*). These values indicate burial depths in the range of 15 to 21 km, with a low geothermal gradient, potentially explaining the low metamorphic grade of exposed basement strata. Apatite and zircon analyses of the Kaimanawa Schist along the western margin of the central North Island's Kaimanawa Mountains can provide an approximate burial constraint. Apatite and zircon fission track analyses from Jiao *et al.* (2014) give Cretaceous ages for zircon populations and late Oligocene-early Miocene ages for apatite populations, indicating that apatite fission tracks were reset in the Cenozoic, whereas zircon fission tracks were not. This implies Cenozoic burial temperatures between 60–270°C (based on the partial annealing zones of apatite and zircon; Naeser, 1979; Green *et al.*, 1989; Yamada *et al.*, 1995; Tagami *et al.*, 1996; Bernet, 2009). Modelling of apatite fission tracks provide better-constrained estimates, indicating Oligocene to early Miocene burial temperatures of 80–120°C (Jiao *et al.*, 2014). Applying a conventional thermal gradient of 25°C/km (e.g., Jiao *et al.*, 2014) equates to burial depths of 3.2–4.8 km, whereas a lower geothermal gradient of 16°C/km (e.g. Cape Terawhiti; Gazley *et al.*, *submitted*) suggests a maximum of 8 km of uplift and erosion.

Taking into account geological evidence and metamorphic grade of the remaining basement strata, the smaller volume of unaccounted void space within the tectonic model presented here produces an estimate of crustal volume balance that is arguably more reasonable than assuming erosion and underplating of the entire 28 km thickness of crust within this area (as per Wood and Stagpoole, 2007). These estimates do not take into account margin parallel shortening that may be accommodated within the wedge of missing crust.

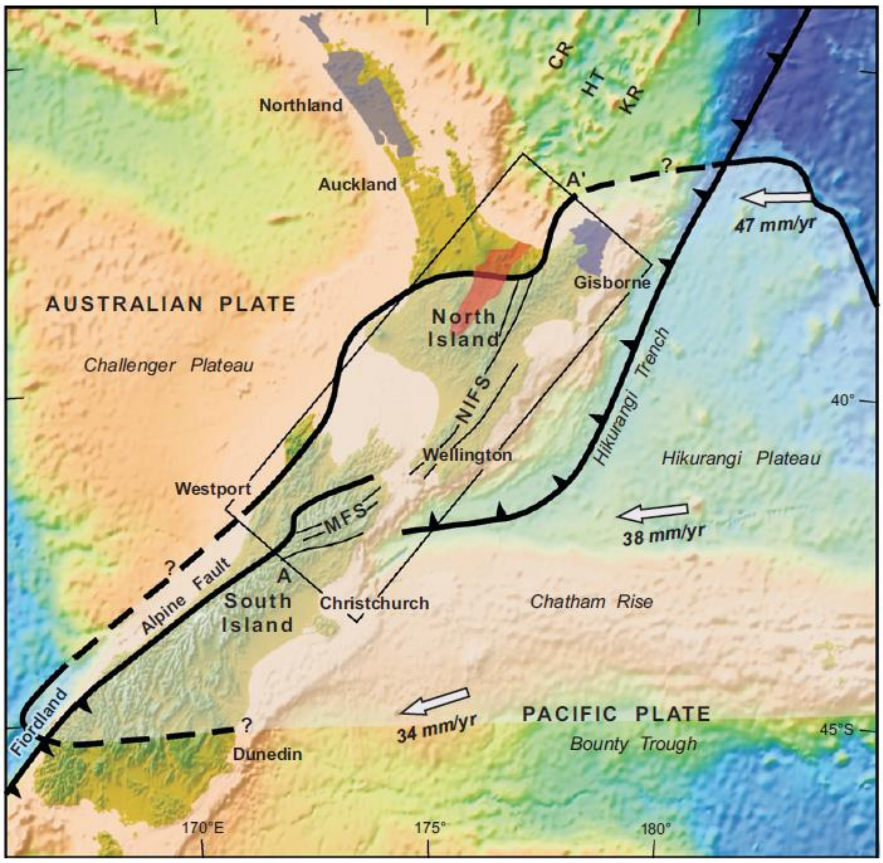

Figure 5.17: Distribution of the high P-wave velocity anomaly beneath New Zealand, interpreted by Reyners *et al.* (2011) to represent the subducted parts of the Hikurangi Plateau. The subducted extent of the Hikurangi Plateau represented by solid line, and inferred subducted extent indicated by dashed line. CR – Coromandel Ridge, HT – Havre Trough, KR – Kermadec Ridge. Figure sourced from Reyners *et al.* (2011).

5.6 Wider Implications of the Model & Future Work

Retaining a contiguous, linear basement trend of the Dun Mountain-Maitai Terrane through the Northland, Taranaki, East Nelson and South Island structural blocks, with respect to fixed plate reconstruction results in issues with line lengths. Consequently, there are areas of overlap in the model in the present-day King Country and Whanganui areas, where structural blocks overlap in

palinspastic reconstructions. However, in progressive development and application of retroactive vertical-axis rotations to the structural blocks, this results in southwards progressing, extensional trend, primarily between 20.13 Ma and 4.0 Ma. The timing and location of this trend approximates the trend exhibited by the development and southward propagation of the Waitemata, Otunui and Whanganui basins through the Neogene (e.g. Furlong & Kamp, 2009). Although serendipitous, this may provide an avenue for future research and refinement of the model. Between 20.13 and 10.95 Ma, the Taranaki-Whanganui block moves southwards (Figure 5.12), possibly driving extension in the Waitemata Basin (21–16 Ma) and Otunui Basin (14–6 Ma; Furlong & Kamp, 2009). The further southward movement of the east Nelson Block with respect to the Taranaki-Whanganui block possibly drives extension and development of the Whanganui Basin from ~6 Ma and the subsequent southward migration of the depocentre (Kamp *et al.*, 2004; Furlong & Kamp, 2009; Nicol, 2011).

The clockwise rotation of the Taranaki-Whanganui block with respect to the fixed Australian Plate, particularly the western stable platform, likely accounts for late Neogene structural inversion of the southern Taranaki Basin and the development of the northern and central grabens. Although these were not considered in the development of the model, a finer subdivision of the Taranaki Basin could be readily incorporated into the wider Zealandia model presented here. There remains considerable insight into the structural development of the wider Zealandia region to be determined from incorporating structural and geological data from the western basins of New Zealand in to the palinspastic tectonic model presented here. In addition, future iterations of model development should consider the incorporation of Neogene geology in the East Coast Basin, and an assessment of the distribution of the Neogene geological units through the various timeplanes of the model presented here.

In summary, the palinspastic paleogeographic model for the East Coast Basin developed here provides a platform for paleoenvironmental reconstructions, in a format that is adaptable and editable as new ideas develop or data become available. Future adjustments to the model could include minor refinement in the positon of block boundaries between the accretionary wedge and the Hawke's Bay-Wairarapa blocks to more closely approximate the Adams-Tinui fault system. The incorporation of shortening estimates, particularly the inclusion of plastic deformation at a temporal resolution that corresponds with reconstructed timeplanes would provide greater control on the relative placement of structural blocks through model stages. The most significant improvement to the model would be the incorporation of Neogene geological data, in particular structural and lithofacies trends, to both constrain and test the model.

Page intentionally left blank for formatting purposes

Chapter Six

SEDIMENT PROVENANCE: *In Search of a Hinterland*

"To see a World in a Grain of Sand.
And a Heaven in a Wild Flower,
Hold Infinity in the palm of your hand.
And Eternity in an hour."
- William Blake, Auguries of Innocence. (1803).

A summer storm front edging down Dee Stream, Clarence valley

PREFACE TO CHAPTER SIX

Overview

This chapter represents a multi-disciplinary approach to assessing provenance sources in the East Coast Basin, particularly in light of the palinspastic tectonic reconstruction for the East Coast Basin and wider New Zealand region presented in Chapter Five. Sediment provenance is an important consideration in paleogeographic reconstructions.

In addition to the large amount of bulk-rock geochemical data gathered during this thesis, detrital zircon and heavy mineral datasets from the literature are analysed to produce a holistic overview and interpretation of sediment provenance. Integration of these datasets within the context of the new tectonic reconstruction means that provenance characteristics and sediment pathways can be considered and assessed.

Contributions from External Collaborators

Katie Collins – Hierarchical cluster analysis of detrital zircon data and PCA of heavy minerals.

Michael Gazley – Provision of portable XRF instrumentation and standards used, in addition to data normalisation and XRD analysis and spectra interpretation

Yulia Uvarova – XRD analysis and spectra interpretation.

Chapter Six

SEDIMENT PROVENANCE: *In Search of the Hinterland*

6.1 Introduction

Assessment of provenance indicators within sedimentary basins provides an indication of hinterland tectonics, sediment transport paths and basement uplift and unroofing, all of which contribute to the development of geodynamic model of basin evolution. In the case of the East Coast Basin, and the wider Zealandian tectonic reconstruction, much of the Cretaceous continental source area has been eroded and/or displaced by Neogene tectonism. Here, published detrital zircon age-frequency distributions and heavy mineral assemblage studies from across the eastern Gondwana sedimentary basins (Northland, East Coast and Canterbury basins) are reassessed through the application of rigorous ordination and clustering methods, and applied in tandem with new bulk-rock compositional data to provide indications of sediment provenance and transport pathways.

Because of the differing styles of datasets, analysis of detrital zircons and heavy mineral assemblage data required the application of two different types of cluster analysis. To differentiate the different clusters and datasets being discussed, clusters derived from a hierarchical cluster analysis of detrital zircon data are denoted by a capital 'Z' (e.g., Cluster Z1), and clusters identified using a principal components analysis of heavy mineral assemblage data are differentiated using a capital 'H' (e.g., Cluster H1).

Basement Geology

The New Zealand basement strata are divided into multiple terranes and subterranes, which are broadly categorised as Western and Eastern provinces, separated by the Median Batholith granitoids (Tuhua Intrusives; Figures 6.1, 6.2; Mortimer *et al.*, 2014). The Paleozoic to Mesozoic basement terranes of the New Zealand subcontinent evolved through successive phases of accretion during subduction along the eastern margin of Gondwana, providing an inherited structural lineation of basement fabrics, with terranes being from a few kilometres to tens of kilometres wide and extending for hundreds to thousands of kilometres (Mortimer, 2014).

Western Province terranes are comprised of the Buller and Takaka Terranes. The Eastern Province terranes comprise Brook Street, Dun Mountain-Maitai, Murihiku, Rakaia and Pahau terranes. The Buller Terrane is the western-most terrane recognised in the New Zealand region, comprised of

variably metamorphosed siliciclastic sandstones and mudstones of Ordovician age (Mortimer, 2004). The tectono-stratigraphic setting of the Buller Terrane is poorly resolved, and may have been either an active or passive continental margin (Mortimer, 2004). The Takaka Terrane is comprised of siliciclastic, carbonate and volcanic rocks of Cambrian to early Devonian age (Mortimer, 2004). The tectonic setting of the Takaka Terrane is interpreted to include both a Cambrian intra-ocean island arc, succeeded by an Ordovician-Devonian continental passive margin (Mortimer, 2004). The Median Batholith is composed dominantly of felsic plutons of primarily Jurassic to mid-Cretaceous age that intrude the bounding Takaka and Brook Street terranes (Mortimer *et al.*, 1999; Allibone *et al.*, 2009).

Paleozoic to Mesozoic indurated metasedimentary rocks of the Eastern Province terranes crop out extensively across New Zealand (e.g., Mortimer, 2004). Most of these terranes have distinctive quartz-feldspar-lithic modes and bulk-rock geochemical compositions that range from rhyolitic to basaltic and reflect various tectonic settings with respect to the Gondwana subduction margin (Roser & Korsch, 1986, 1999; Mortimer, 2004). From west to east, these terranes are the Brook Street, Murihiku, Dun Mountain-Maitai, Caples, Waipapa, Rakaia, Esk Head, and Pahau Terranes. The Brook Street Terrane is dominantly comprised of subduction-related, basaltic volcanics and volcaniclastic detritus of Permian age (Kimborough *et al.*, 1992; Mortimer, 2004). The Murihiku Terrane is dominated by a 9–13 kilometre-thick stratigraphic succession of Late Permian to Late Jurassic volcaniclastic marine sandstone. Internal structure of the Murihiku Terrane is simple, and the tectono-stratigraphic setting is interpreted as a prolonged forearc or backarc basin (Mortimer, 2004). The Dun Mountain-Maitai Terrane is a narrow, remnant belt of obducted Permian oceanic crust and mantle, and associated volcaniclastic sediments (Kimborough *et al.*, 1992; Turnbull, 2000; Mortimer, 2004). Where the Dun Mountain-Maitai Terrane is not expressed at the surface, it can be delineated by the Junction Magnetic Anomaly (Hunt, 1978; Mortimer, 2014). The Dun Mountain-Maitai Terrane, whilst originally a linear or quasi-linear feature, now records a distinctive S-shaped curve through onshore New Zealand, known as the New Zealand orocline.

To the east of the Dun Mountain-Maitai Terrane, Caples Terrane is a weakly metamorphosed, Permian to Triassic marine volcaniclastic sequence. The petrofacies of the Caples Terrane has an average andesitic composition (Mortimer & Roser, 1992; Mortimer, 2004). The boundary between the Caples Terrane and the quartzofeldspathic Rakaia Terrane to the east has been overprinted by metamorphism associated with formation of the Haast Schist (Mortimer, 2004, 2014). The Waipapa Terrane (Bay of Islands and Waipa terranes; Mortimer, 2004) is interpreted as a late Jurassic-early Cretaceous, volcaniclastic suite derived from the Median Batholith, and deposited across the all Eastern Province terranes older than the Pahau Terrane (Mortimer, 2004; Adams *et*

al., 2009). The internal structure of the Waipapa Terrane is complex and imbricated, associated with trench-slope basin and trench fill deposits (Mortimer, 2004). Petrofacies of the Waipapa Terrane are nearly-identical to those of the Rakaia Terrane (Mortimer, 2004).

The Rakaia and Pahau terranes are the most areally extensive of any basement terranes. Both are turbidite-dominated, but differ in age and petrography (Roser & Korsch, 1999; Mortimer, 2004; Smale, 2007). The Rakaia Terrane is structurally complex, characterised by eastward-younging strata, with metamorphic grade increasing westwards into the Haast Schist (Mortimer, 2004, 2014). These characteristics are consistent with formation within an eastward facing accretionary wedge of the Torlesse composite terrane on the Gondwana margin (Beggs, 1993; Mortimer, 2004). The Rakaia Terrane is dominated by turbiditic quartzofeldspathic sandstone-mudstones (>95%) of Permian to Late Triassic age (Roser & Korsch, 1999; Mortimer, 2004). Sandstones of the Rakaia Terrane have an average rhyodacitic composition and are, therefore, compositionally distinct from other basement terranes (Mortimer, 2004).

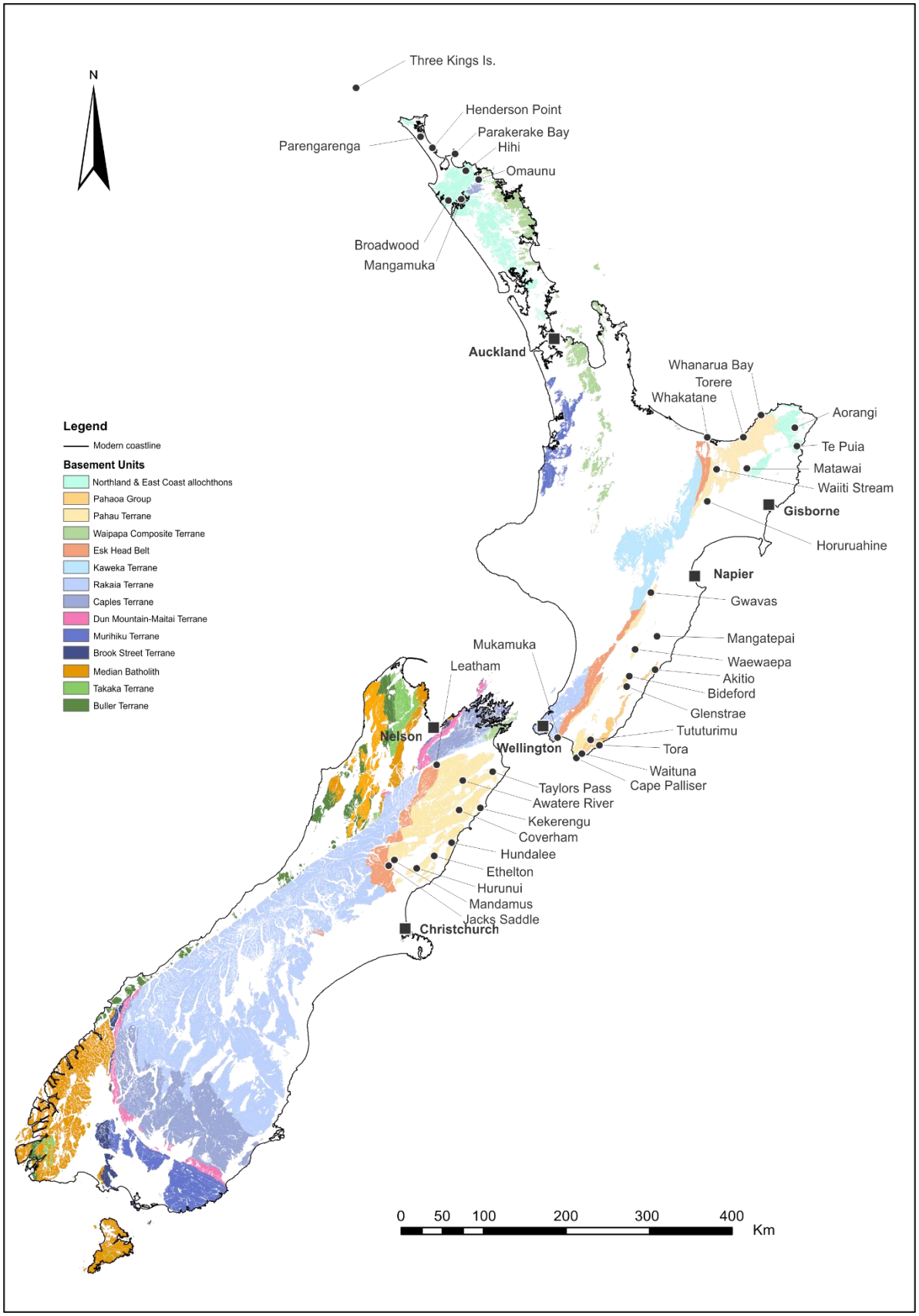

Figure 6.1: Present-day outcrop distribution of basement terranes in mainland New Zealand and zircon sample localities from Adams *et al.* (2008, 2013a, 2013b) referred to in text. Base map data from Heron (2014).

The Esk Head Mélange is a tectonostratigraphic unit that separates the petrographically, paleontologically and geochronologically distinct Rakaia (or Kaweka in central North Island) and Pahau Terranes (Silberling *et al.*, 1988; Mortimer *et al.*, 2004; Leonard *et al.*, 2010). The mélange incorporates materials from both neighbouring terranes, including rafts and blocks of coherent strata, as well as exotic clasts (Leonard *et al.*, 2010). The Esk Head Mélange is considered to be latest Jurassic to middle Early Cretaceous in age, approximately 160–130 Ma, likely 135–130 Ma (Stevens, 1963; Speden, 1972; Wilson *et al.*, 1988; Adams *et al.*, 2011). The Esk Head Terrane approximates the western limit of the East Coast Basin.

The Pahau Terrane has a broadly similar lithologic composition to the Rakaia Terrane, dominantly comprised of alternating sandstone-mudstone of Late Jurassic–early Cretaceous age, with common tuffs (Mortimer, 2004; Adams *et al.*, 2013a). The Pahau Terrane was deposited in a series of depositional basins along a section of the accretionary wedge on the convergent margin of eastern Gondwana (Bassett & Orlowski, 2004; Adams *et al.*, 2013), and is partly coeval with metamorphism and exhumation of the Rakaia Terrane at ~135 Ma (Kamp, 2000; Mortimer, 2004). Much of the Pahau Terrane is likely recycled from Rakaia Terrane rocks, although additional volcanic input is required to produce young (100 Ma) zircon $^{238}U/^{206}Pb$ age modes (Mortimer, 2004; Adams *et al.*, 2013a, 2013b). The Pahau Terrane is generally quartzofeldspathic, although it can be subdivided into an older volcanoclastic suite, the Waioeka Petrofacies, and a younger quartzofeldspathic suite, the Omaio Petrofacies (Mortimer, 1995; Kamp, 1999; Adams *et al.*, 2013). The Waioeka Petrofacies was deposited between 125–116 Ma based on detrital zircon $^{238}U/^{206}Pb$ and zircon fission track analyses (Kamp, 1999; Adams *et al.*, 2009; 2013a). The Omaio Petrofacies forms the youngest, uppermost, and outboard part of the Gondwana accretionary prism, deposited between 116–108 Ma based on zircon fission track (Kamp, 1999). The Pahaoa Group sediments of the Hawke's Bay and Wairarapa regions are included within the Omaio Petrofacies (Kamp, 2000).

Subduction at the Gondwana margin continued until the Early Cretaceous (110–100 Ma; Davy *et al.*, 2008), with the East Coast Basin developing subsequently as one of several near-continuous basin depocentres oriented margin-parallel at this time (the other basins being the Raukumara and Pegasus basins). Terranes of the Eastern Province outcrop in the East Coast Basin, though Western Province terranes provide important markers and piercing points in regional structural reconstructions, as well as being potential sediment sources for the Cretaceous-Cenozoic cover succession in the East Coast Basin.

Immediately prior to the separation of Zealandia from the Australian continental margin, the Zealandia segment underwent a profound change during the mid-Cretaceous, resulting in the

cessation of long-lived Permian-Cretaceous subduction (Torlesse–Haast Schist accretionary wedge, and the associated Median Batholith magmatic arc), which was replaced with widespread intracontinental crustal extension (Adams *et al.*, 2017). Consequently, this resulted in the rapid unroofing of granulites and granitoid complexes in Fiordland and Westland (Tulloch & Kimborough, 1989; Ireland & Gibson, 1998; Adams *et al.*, 2017).

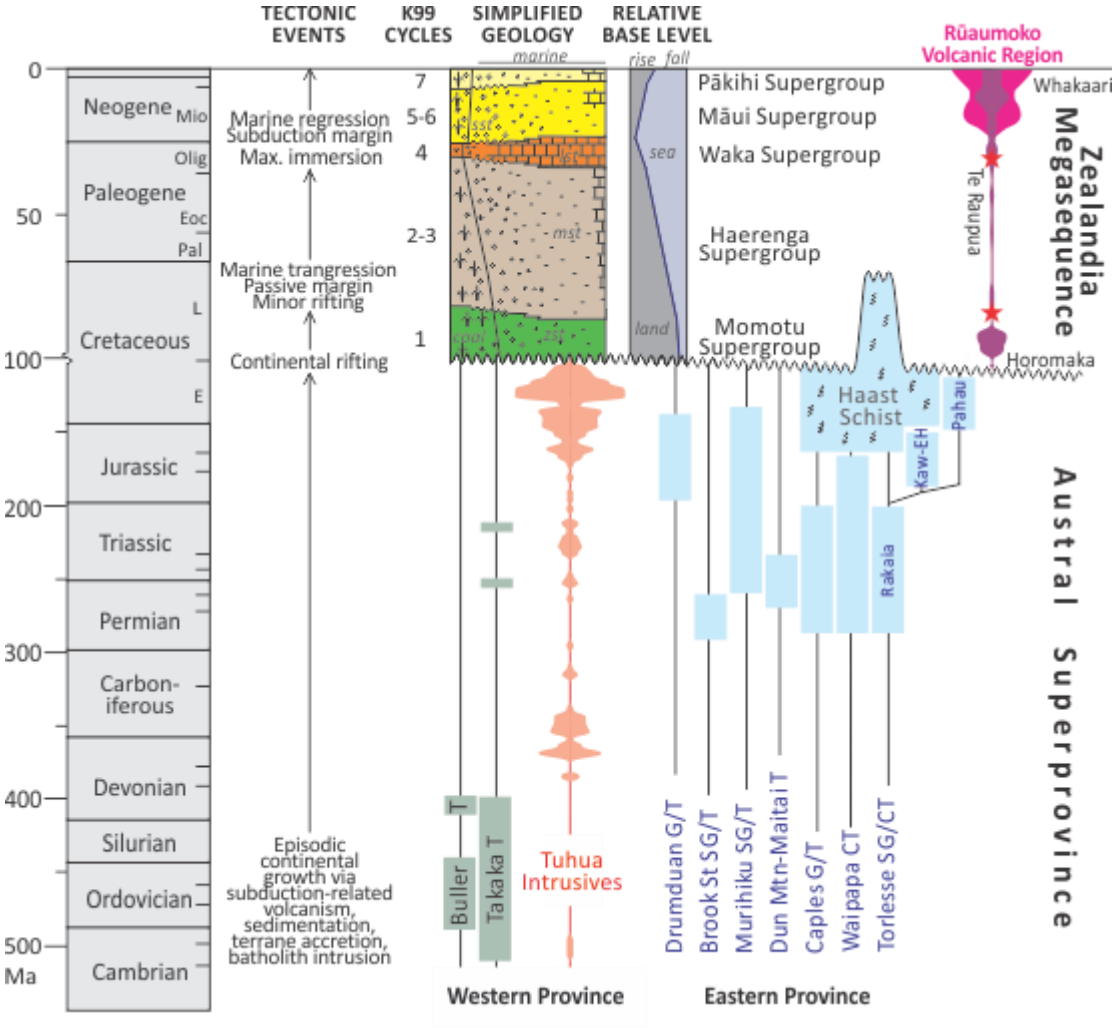

Figure 6.2: Age and stratigraphic associations of basement terranes in New Zealand, and the overlying supergroups of the cover succession. Granitoids of the Median Batholith are grouped with the Tuhua Intrusives. Modified from Mortimer *et al.* (2014). Key to abbreviations: SG =Supergroup, G = Group, T = Terrane, CT = Composite Terrane. K99 refers to second-order cycles identified by King *et al.* (1999).

6.2 Detrital Zircon Age Populations

6.2.1 Introduction to Detrital Zircons

Assessment of detrital zircon $^{238}U/^{206}Pb$ age populations is a commonly applied tool that is used to identify the age and provenance of sedimentary rocks (Adams *et al.*, 2013a, 2013b, 2017). Typically, populations of ages from a sample reveal distinct age modes, which indicate the ages of particular source components, either primary or reworked. In the case of the New Zealand basement terranes, the youngest detrital grain ages within basement terranes have been used to indicate the minimum depositional or formation age. This has had particular application in the case of the Pahau Terrane and associated metasediments, in constraining the cessation of Mesozoic subduction on the eastern margin of New Zealand (e.g., Mortimer *et al.*, 2016; Adams *et al.*, 2017). Thus there are a large number of published detrital zircon ages along the eastern margin of New Zealand, in particular from the East Coast Basin.

6.2.2 Methods

Binned detrital zircon $^{238}U/^{206}Pb$ age populations from 42 samples (typically 60–90 $^{238}U/^{206}Pb$ ages per sample) across the East Coast Basin, Northland Allochthon and Chatham Islands (Adams *et al.*, 2008, 2013a, 2013b), were examined. Age-frequency data from $^{238}U/^{206}Pb$ analyses from Adams *et al.* (2008, 2013a, 2013b) were binned by geological epoch, with ages represented by percent frequency. Two samples from the Mokoiwi Formation East Coast Allochthon were included in the cluster analysis on the basis of their Urutawan-Motuan age, which is comparable to the age of samples considered to be basement from the Omaio Petrofacies and the Pahaoa Group.

In order to assess provenance characteristics of basement terranes in eastern New Zealand, hierarchical cluster analysis was performed in the programming software 'R' (R Core development team, 2017), in the 'fastcluster' package, using function *hclust* and the method 'average' (an unweighted pair-group method with arithmetic averages [UPGMA]; Borcard *et al.*, 2011). The hierarchical cluster analysis used a Mahalanobis distance metric (function *vegdist*) for its dissimilarity index, enabling variable count data across various samples to be standardised, effectively z-transforming the data (Oksanen *et al.*, 2013). A trimming line was applied to the resulting dendrogram to subdivide the dataset into four clusters (Figure 6.3). Preliminary data exploration indicated that including age-frequency data from both basement and cover sedimentary rocks strongly biased clusters, apparently -based largely on geography, resulting in no resolvable trend

across the dataset. Age-frequency distributions from the basement terrane clusters were then used to characterise the limited dataset of detrital zircon data available for cover sediments in the East Coast and Northland.

Table 6.1: Sources of detrital zircon age frequency data used herein.

Region	Unit	No. Samples	Data Source
East Cape	Esk Head Melange	5	Adams *et al.* (2013a)
East Cape	Undifferentiated Pahau	1	Adams *et al.* (2013a)
East Cape	Waioeka Petrofacies	2	Adams *et al.* (2013a)
East Cape	Omaio Petrofacies	3	Adams *et al.* (2013a)
East Cape	East Coast Allochthon	2	Adams *et al.* (2013a)
East Cape	Late Cretaceous cover	3	Adams *et al.* (2013a)
Hawkes Bay-Wairarapa	Undifferentiated Pahau	4	Adams *et al.* (2013a)
Hawkes Bay-Wairarapa	Pahaoa Group	6	Adams *et al.* (2013a)
Hawkes Bay-Wairarapa	Late Cretaceous cover	3	Adams *et al.* (2013a)
Marlborough-North Canterbury	Undifferentiated Pahau	8	Adams *et al.* (2013a)
Marlborough-North Canterbury	Late Cretaceous cover	4	Adams *et al.* (2013a)
Northland	Houhora Complex	3	Adams *et al.* (2013b)
Northland	Northland Allochthon	5	Adams *et al.* (2013b)
Northland	Mangakahia Complex	1	Adams *et al.* (2013b)
Northland	Punakitere Sandstone	4	Adams *et al.* (2013b)
Chatham Islands	Chatham Schist	3	Adams *et al.* (2008)
Chatham Islands	Late Cretaceous cover	1	Adams *et al.* (2013a)

6.2.3 Results

Cluster Z1 is dominated by a bimodal distribution of zircons of Precambrian and Triassic age (Figure 6.3). All of the samples from the Esk Head Belt and the Whakatane Melange fall within this group, both of which mark the tectonic suture between the Rakaia and Pahau Terranes (Rattenbury & Isaac, 2012). Both of the samples from the Chatham Schist (Adams *et al.*, 2008) also fit the binned age distribution of cluster one. The remaining five samples in cluster Z1 are sourced from the Pahau Terrane, four of which are from the North Island. Cluster Z2 contains a mixed zircon age population, with an increasing proportion of younger zircons (Figure 6.3). Five of the seven samples within cluster Z2 are from North Island Pahau Terrane, three of these from the correlative Omaio Petrofacies and Pahoa Group, the youngest components of the Pahau Terrane.

The two exceptions are a single sample each from the Pahau Terrane in the South Island and the Houhora Complex in Northland (Figure 6.3). Cluster Z3 is characterised by a detrital zircon population that contains little to no Jurassic and Devonian-Silurian zircons, with a moderately-high proportion of Cretaceous, Triassic-Carboniferous, and Precambrian zircons (Figure 6.3). These samples are primarily sourced from undifferentiated Pahau Terrane in the South Island, although one sample is from Tora in the far southeast of the North Island, which reinforces inferred stratigraphic similarities and linkages between Tora and Marlborough (Hines *et al.*, 2013). Cluster Z4 is dominated by Cretaceous zircons, with little to minor input from older sources (Figure 6.3). The samples within cluster Z4 are among the youngest considered in the dataset, including two samples each from the Houhora Complex, the East Coast Allochthon, the Omaio Petrofacies, and the Pahaoa Group. The remaining two samples are both from the older Waioeka Petrofacies of the Pahau Terrane.

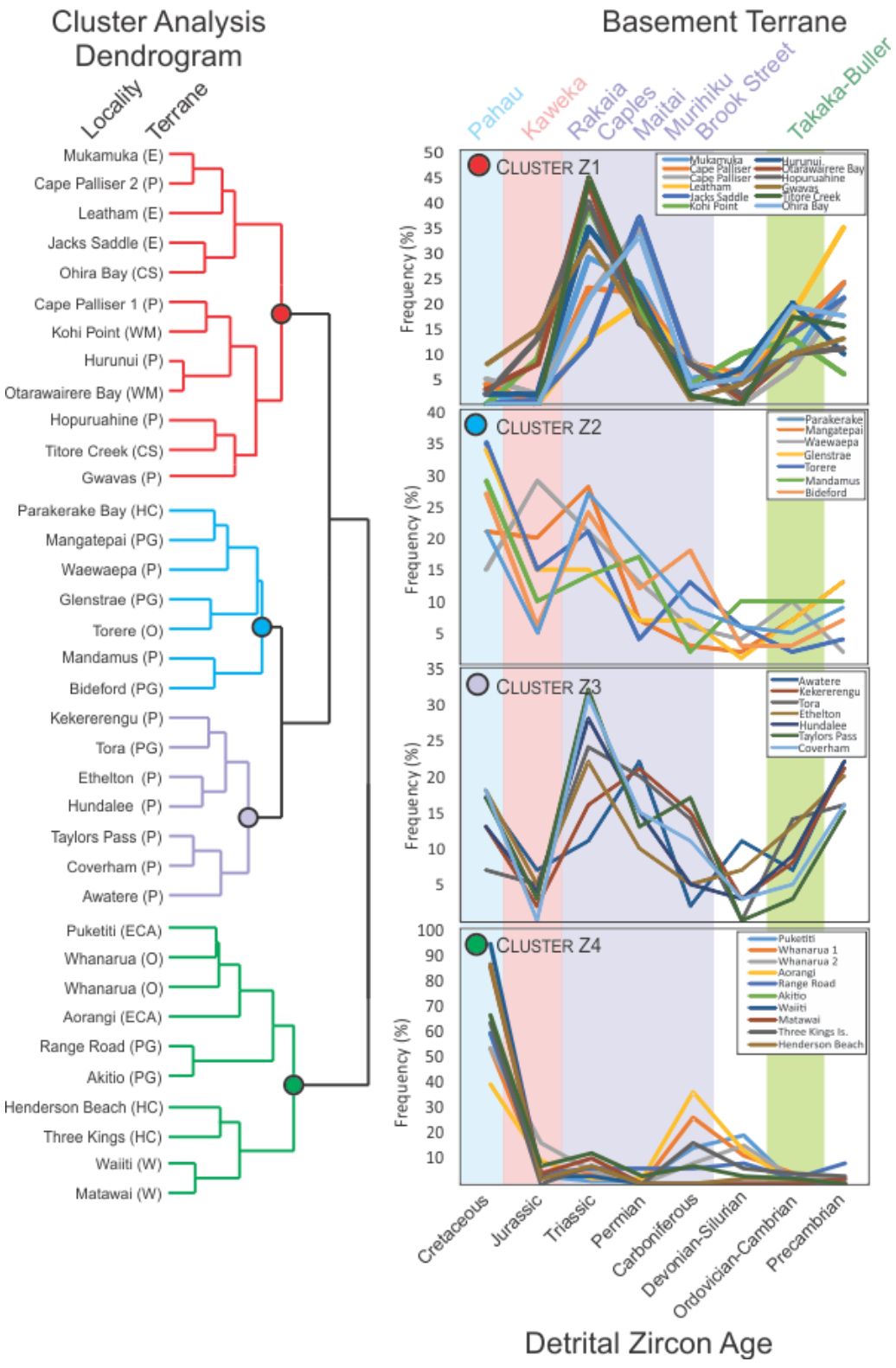

Figure 6.3: Hierarchical cluster analysis of detrital zircon age populations from basement strata in the East Coast and Northland basins, Chatham Islands, and two samples from the East Coast allochthon, plotted alongside age-frequency distributions for groups identified by cluster analysis. Raw data from Adams *et al.* (2008, 2013a, b). Key to terrane abbreviations: W – Waioeka petrofacies, O – Omaio petrofacies, PG – Pahaoa Group, P – Pahau Terrane, HC – Houhora Complex, ECA – East Coast Allochthon, E – Esk Head Belt, CS – Chatham Schist.

Age-frequency distribution data for detrital zircon studies of cover strata of the East Coast Basin, Northland and Chatham Islands exhibit a strong correlation to patterns identified within basement age-frequency distributions (Figure 6.4). Ngaterian to Teratan aged samples from the Wairarapa, Hawke's Bay and East Cape, and a single Haumurian sample from the Mangakahia Complex (Northland) all have little to no Cretaceous zircons and a broad peak in Triassic-Permian zircons, with a subsidiary Ordovician to Precambrian peak (Figure 6.4). This age-frequency distribution correlates well with cluster Z1, which is dominantly comprised of samples from the Esk Head Mélange and Pahau Terrane.

All the cover sediments from the Marlborough area for which zircon age-frequency data were available (with the exception of Ward), contain moderately-high proportions of Cretaceous, Triassic-Permian and Precambrian zircons, with low Jurassic, and Carboniferous to Ordovician-Cambrian age modes (Figure 6.4). This distribution correlates well with cluster Z3, which is comprised almost entirely of Marlborough Pahau Terrane. Latest Cretaceous (Haumurian) cover from Ward correlates better with cluster Z1, based on dominant Permian and Precambrian age modes, with low proportions of Cretaceous, Jurassic, and Carboniferous to Devonian-Silurian zircons.

The remaining zircon age frequency data that were available had a very high Cretaceous age mode, with low proportions of other age modes (Figure 6.4). This included a single sample each from East Cape (Matawai) and the Chatham Islands (Pitt Island), and four samples from the Punakitere Sandstone in Northland (Figure 6.4). This distinctive age distribution is characteristic of cluster Z4, which is comprised of the youngest components of the basement terranes studied herein (Omaio Petrofacies, and samples from the East Coast and Northland allochthons, and the Houhora Complex).

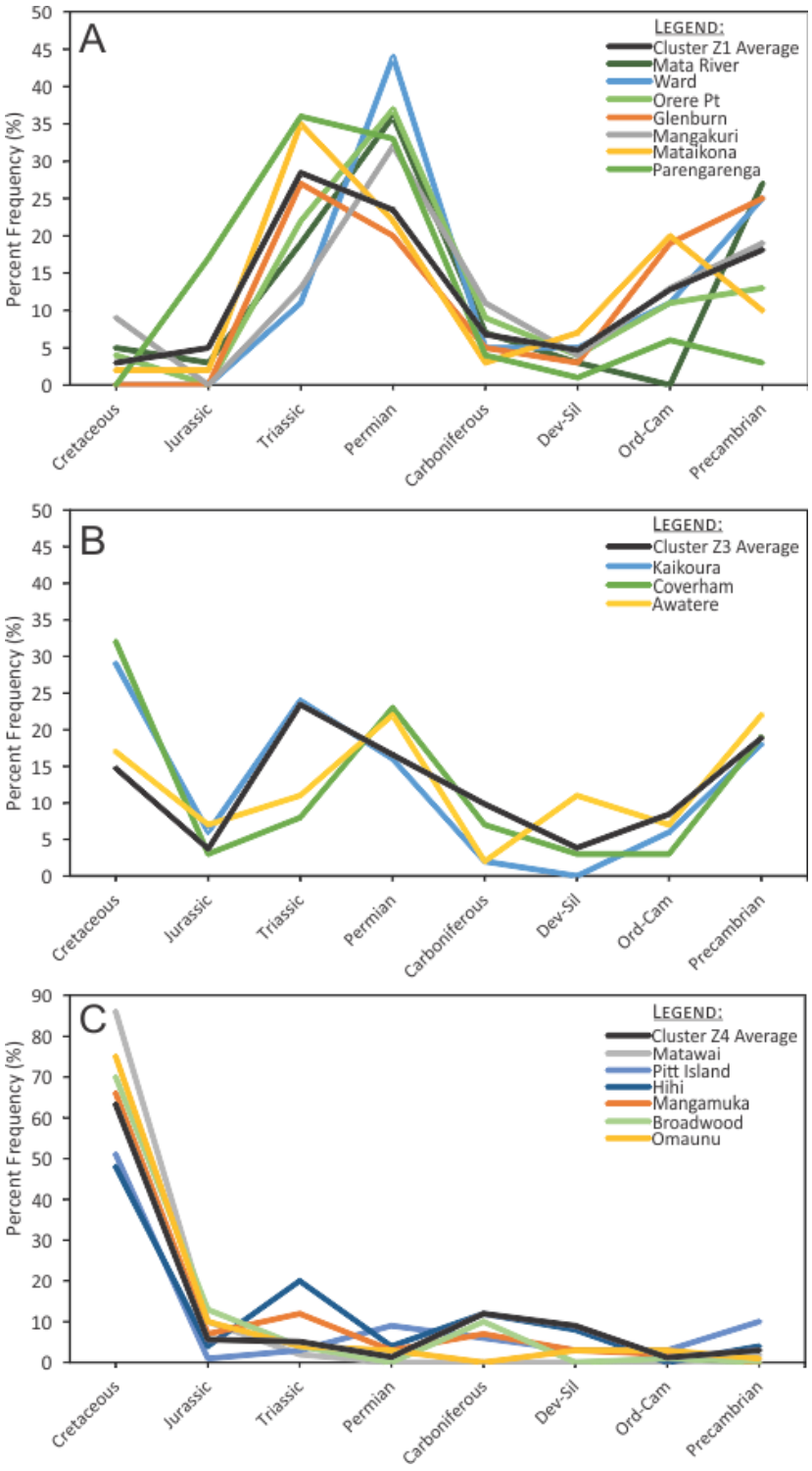

Figure 6.4: Binned detrital zircon age models from cover sediments of the East Coast Basin, Chatham Island and Northland in comparison to clusters identified by hierarchical cluster analysis of basement binned age distributions. A) Cover sediments displaying an affinity with cluster Z1. B) Cover sediment displaying an affinity with sediments from cluster Z3. C) Cover sediment samples showing a comparable distribution to cluster Z4. Zircon age-frequency data from Adams *et al.* (2013a, 2013b).

6.2.4 Interpretation of Detrital Zircon Age Modes

Samples from the Northland Allochthon share the same detrital-zircon age-distribution as the samples from the East Coast Allochthon, suggesting that these two obducted masses shared a common sediment source and potentially that they were once contiguous. Apatite fission track ages across the top of the Coromandel Peninsula are depressed with respect to corresponding zircon ages (Jiao *et al.*, 2017), suggesting there may have been allochthonous strata up to <3 kilometres thick across this region, which is also consistent with the Furlong and Kamp (2009) interpretation of the allochthon distribution.

Based on the detrital zircon age populations, cluster Z1 is primarily sourced from Eastern Provence terranes, with a notable proportion of Precambrian zircons also included (Figure 6.3). Cluster Z2 incorporates increasing proportions of zircons from various terranes progressing from the Western to Eastern provinces, with the large majority sourced from the Esk Head Belt and Pahau Terrane. Cluster Z3 has a very similar age-frequency distribution to cluster Z1, except with a notable proportion of Cretaceous zircons (Figure 6.3). Finally, Cluster Z4 is dominated by young, Cretaceous-aged zircons that largely obscure any provenance signals from older sources (Figure 6.3).

When plotted on the reconstructed pre-Neogene paleogeographic model developed in this study (Chapter Five), the four clusters form a distinctive linear geographic arrangement (Figure 6.5). This arrangement, and the inferred age interpretations, are consistent with progressive accretion from the east and the associated development of sub-basins on the Gondwana subduction margin.

The dominant Eastern Province-derived provenance of clusters Z1 and Z3 indicate that sediment was primarily sourced from local re-sedimentation of basement within a restricted region (Figure 6.5). The proportion of Cretaceous zircons in cluster Z3 indicates input from coeval volcanism, supported by the occurrence of long, needle-like zircon grains and euhedral apatite in heavy mineral separates (Hines, unpublished data; Appendix 8). The trend of progressively increasing frequency of younger zircons in cluster Z2 indicates a large catchment area, sourcing sediment from much of the Zealandian hinterland, from the Western towards the Eastern Province (Figures 6.3, 6.5). The dominant proportion of Cretaceous zircons in cluster Z4 suggests that the Northland, East Cape, and Wairarapa regions had a substantial volume of zircons approximately synchronous with the depositional age of the sediment, potentially sourced from contemporaneous volcanism (Figures 6.3, 6.5; Adams *et al.*, 2013a, 2017).

Ngaterian to Teratan aged cover sediments from the Wairarapa, Hawke's Bay and East Cape are almost certainly from the Glenburn Formation and the correlative Tikihore Formation, based on location and age assignment in Adams *et al.* (2013a). These samples all correlate well with cluster Z1, which suggests that there was a source of sediment derived from Eastern Province (likely Rakaia) terranes supplying much of the North Island East Coast at this time (Figure 6.4). The strong correspondence between Cretaceous cover sediments from Marlborough with Pahau Terrane from Marlborough (cluster Z3) indicates a locally derived source (Figure 6.4). The sample from Matawai was sourced from Korangan-aged strata in East Cape, which may be coeval with the Omaio Petrofacies, suggesting that the same sediment source was likely supplying these strata. The similar age modes of the Houhora Complex samples and the oldest sedimentary rocks in the Northland Allochthon, the Punakitere Sandstone, either implies cannibalism of the local Houhora Complex during the late Cretaceous supplying sediment to the Punakitere Sandstone, or a sediment pathway from early Late Cretaceous rhyolitic volcanism (c. 101 Ma; Tulloch *et al.*, 2009) persisted from deposition of the Houhora Complex (100–108 Ma; Adams *et al.*, 2013b) to deposition of the Punakitere Sandstone (80–90 Ma; Adams *et al.*, 2013b).

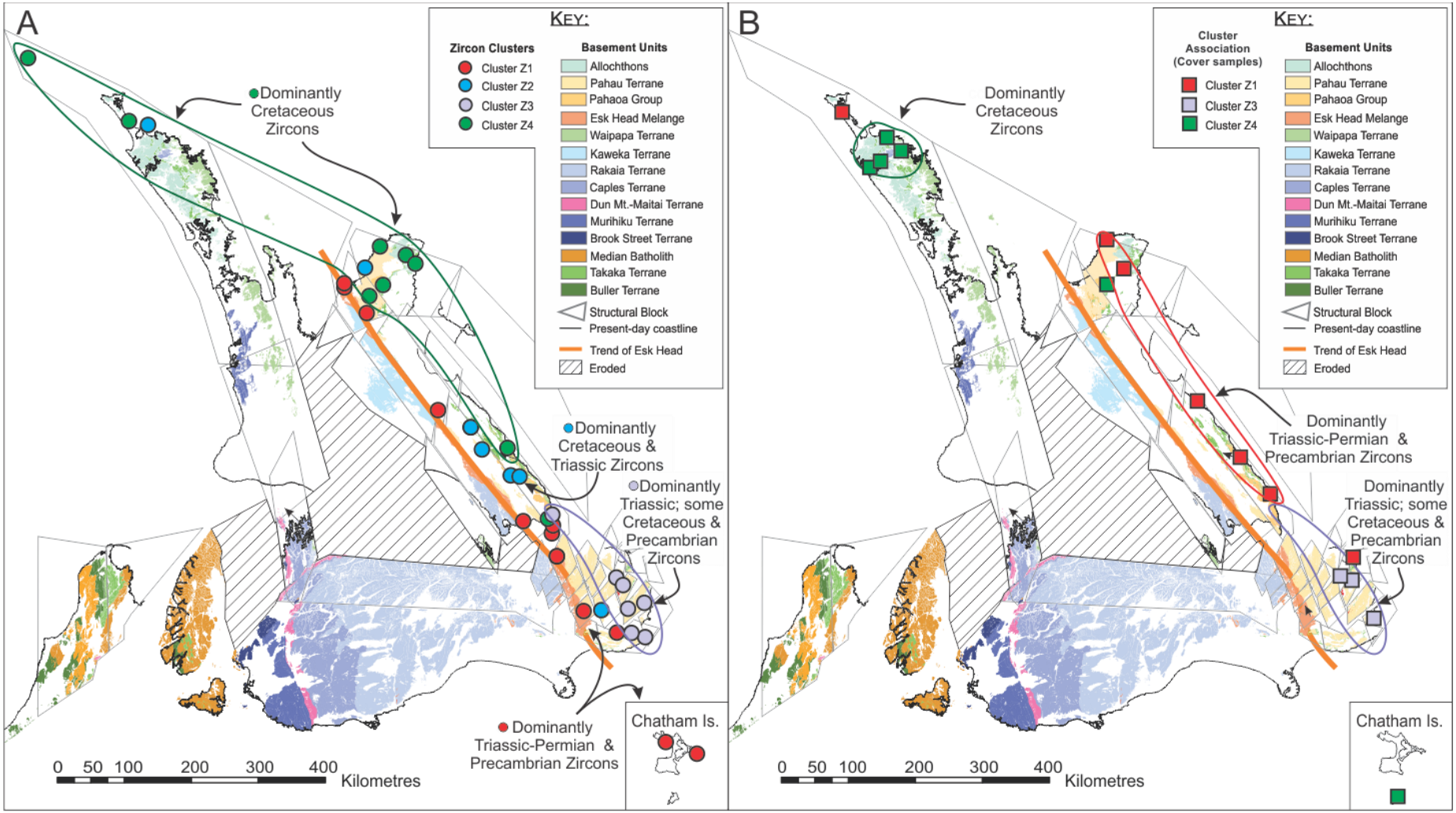
A
KEY:
Zircon Clusters
Cluster Z1
Cluster Z2
Cluster Z3
Cluster Z4
Basement Units
Allochthons
Pahau Terrane
Pahaoa Group
Esk Head Melange
Waipapa Terrane
Kaweka Terrane
Rakaia Terrane
Caples Terrane
Dun Mt.-Maitai Terrane
Murihiku Terrane
Brook Street Terrane
Median Batholith
Takaka Terrane
Buller Terrane
Structural Block
Present-day coastline
Trend of Esk Head
Eroded
Dominantly Cretaceous Zircons
Dominantly Cretaceous & Triassic Zircons
Dominantly Triassic; some Cretaceous & Precambrian Zircons
Dominantly Triassic-Permian & Precambrian Zircons
Chatham Is.
0 50 100 200 300 400
Kilometres
B
KEY:
Cluster Association (Cover samples)
Cluster Z1
Cluster Z3
Cluster Z4
Basement Units
Allochthons
Pahau Terrane
Pahaoa Group
Esk Head Melange
Waipapa Terrane
Kaweka Terrane
Rakaia Terrane
Caples Terrane
Dun Mt.-Maitai Terrane
Murihiku Terrane
Brook Street Terrane
Median Batholith
Takaka Terrane
Buller Terrane
Structural Block
Present-day coastline
Trend of Esk Head
Eroded
Dominantly Cretaceous Zircons
Dominantly Triassic-Permian & Precambrian Zircons
Dominantly Triassic; some Cretaceous & Precambrian Zircons
Chatham Is.
0 50 100 200 300 400
Kilometres

Figure 6.5: A) Spatial distribution and allocation of clusters identified by hierarchical cluster analysis of basement detrital zircon assemblages, plotted on a retro-deformed reconstruction of the New Zealand region during the Cretaceous-Paleogene. Chatham Island sample sites inset (to scale). B) Distribution of cluster associations of detrital zircon age-frequency relationships for samples of cover sediments in the East Coast and Northland basins.

6.3 Heavy Mineral Cluster Analysis

6.3.1 Introduction to Heavy Minerals

The analysis of heavy mineral suites is one of the most important and widely-applied techniques in determining the provenance of sedimentary strata (Morton & Hallsworth, 1994). Basement terranes around New Zealand are characterised by distinctive heavy mineral suites, associated with their tectono-stratigraphic setting (Smale, 1989, 1990, 2007). Samples from Western Province terranes (Buller Terrane, Median Batholith and Karamea Batholith) are from restricted areas, and their heavy mineral distributions display distinctive, useful characteristics (Smale, 2007). In the Median Batholith, Fiordland, granitiod samples are dominated by prominent peaks in biotite and hornblende. However, in the Karamea Batholith, biotite is even more abundant, but hornblende is only a minor component (Smale, 2007). The Buller Terrane is characterised by approximately equal proportions of semi-opaque debris (dominantly altered epidote group minerals), biotite and chlorite, and only trace amounts of other heavy minerals.

Eastern Province terranes contain distinctive heavy mineral populations (Smale, 2007). Samples from the Murihiku Terrane comprise low-grade metasedimentary rocks, and heavy mineral suites comprise zircon, epidote, hornblende and apatite. These mineral suites are indicative of residual mineral species that have survived intrastratal dissolution, or authigenic minerals formed during diagenesis and/or low-grade metamorphism (Brothers, 1959; Smale, 2007). The Rakaia and Pahau Terrane heavy mineral suites are separated from other basement terranes by an abundance of low-grade metamorphic epidote (including semi-opaque debris; SODeb) and detrital biotite (Smale, 1990, 2007). Garnet, biotite and sphene are prominent constituents, indicating a dominantly granitic source, and indicators of contemporaneous volcanism (e.g., magnetite, pyroxene and hornblende) are typically sparse (Smale, 2007).

Although there is considerable overlap in the heavy mineral suites from the Rakaia and Pahau terranes, they do show some distinctive features. In the Rakaia Terrane, biotite, apatite and hornblende are more prevalent than in the Pahau Terrane, although hornblende may be irregularly distributed, and is possibly restricted to older, Permian-aged Rakaia Terrane sediments (Smale,

1990, 2007). Garnet is more abundant in the Pahau Terrane and, in locally restricted areas, magnetite is prominent, perhaps reflecting a higher frequency of coeval volcanism during deposition of the Pahau Terrane (Smale, 1990, 2007; Smale & Laird, 1995). Heavy mineral assemblages from Esk Head Melange demonstrate equal affinity with both Rakaia and Pahau terranes, showing that samples from the Esk Head have retained the compositional characteristics of the original Rakaia and Pahau sources of the melange (Smale, 1997, 2007).

6.3.2 Methods

High-dimensional data, such as the heavy mineral assemblages presented here (268 samples, comprised of 25 mineral species), are difficult to interpret and visualise in large sample databases. Ordination approaches such as principal components analysis (PCA) can be applied to simplify high-dimensional datasets by identifying linear combinations of variables that summarise the highest amount of dataset variance in the fewest dimensions, and show correlations that are readily interpreted in terms of the original variables. In addition, principal component (PC) axes are mutually orthogonal (assumed to be statistically independent) and are suitable for subsequent statistical analyses. The compiled heavy mineral dataset (Table 6.2) is based entirely on samples prepared and counted by David Smale, and is therefore considered internally consistent. The assemblage data are compositional, and therefore were log-ratio transformed prior to multivariate analysis to solve the closure issue (Aitchison, 1982, 1986; Aitchison *et al.*, 2000; Grunsky *et al.*, 2014; Mueller & Grunsky, 2016). Aitchison's centred log-ratio transformation was applied using the 'clr' function in the R package 'Hotelling' (Curran, 2013; R Development Core Team, 2016). Sparse robust PCA was performed on the log-ratio transformed data using the 'PCAgrid' function in the R package 'pcaPP' (Croux *et al.*, 2007; Filzmoser *et al.*, 2014). Sparse robust methods are less sensitive to outliers than standard PCA and this sparse robust PCA was designed specifically for chemometric applications (Croux *et al.*, 2007; Filzmoser *et al.*, 2014). Two of the resulting 25 PCs (explaining a total of 38% of the variance in the dataset) were identified as significant (explaining more variance than would be expected by chance) by use of a broken stick screeplot (Appendix 8; Jackson, 1993). The low proportion of variance explained by the first two PCs is because the total variance is partitioned out amongst all of the 25 PCs. To identify chemical subgroups within the dataset, cluster analysis was applied. The method used was mixture model cluster analysis using the expectation-maximisation (EM) algorithm, in which the number of clusters is not set *a priori*, but determined from the data – in finite mixture models, each component probability distribution is a cluster, and determining the number of clusters that best explains the data becomes a statistical

model-choice problem (Fraley & Raftery, 2002). The cluster analysis used here was performed on the two significant PCs using Bayesian mixture-modelling clustering (function 'mclust') from the Mclust R package (Fraley *et al.*, 2012) which uses the Bayesian Information Criterion (BIC) to determine the number of groups present in the dataset. Mclust fits Gaussian mixture models of varying complexity to identify natural clusters in multi-dimensional data. The 'best' model is selected by minimizing the BIC, which uses the model likelihood and a penalty term for the number of parameters. For the heavy mineral data, three clusters are preferred, although a model with two clusters is also plausible; models with more than three clusters are not considered to be likely. Cluster assignment probabilities are shown in Appendix 8.

Table 6.2: Data sources for heavy mineral datasets used here.

Location	Stratigraphic Unit/Age	Number of Samples	Reference
Northland	Torlesse	3	Smale (1988b)
Raukumara	Pahau Terrane, Cretaceous-Eocene cover	18	Field & Uruski *et al.* (1997)
Te Hoe River	late Cretaceous cover	5	Crampton & Moore (1990)
Whangai Range	mid-late Cretaceous cover	15	Crampton (1997)
Wellington	Rakaia, Esk Head Terranes	27	Smale (1997)
Marlborough	Pahau Terrane, Cretaceous cover	95	Smale & Laird (1995)
Haumuri Bluff	Cretaceous cover	10	Smale (1987)
Ethelton	Rakaia Terrane	4	Smale (1978)
Waipara, Oxford, Mt Somers	Rakaia, Pahau Terrane, Cretaceous-Eocene cover	63	Smale (1983, 1987; 1989)
Oamaru, Kakahau, Waitaki	Torlesse, Cretaceous-Eocene cover	28	Smale (1988a, 1990)

6.3.3 Results

Bayesian mixture-modelling cluster analysis identified three groups within the heavy mineral dataset (Figure 6.6). Most samples contain a high proportion of ilmenite (~30–40%), along with some proportion of white, fine-grained aggregates of either epidote or pumpellyite with quartz, referred to as semi-opaque debris (SODeb; Smale, 1988; Smale, 2007). Heavy mineral assemblage data, cluster assignment, and cluster assignment probability values for the statistical analyses presented are included in Appendices 8 and 10.

Cluster H1 demonstrates an antithetic relationship with pyrite, chlorite, and allanite, and a broad discrimination on PCs 1 and 2, apparent in the eigenvectors for epidote, zircon, ilmenite, epidote and hornblende (Figure 6.6). Cluster H1 is dominated by samples from Rakaia Terrane from

Canterbury and Wellington (n =45), and a minor contribution from Pahau Terrane (n = 8) and Cretaceous-Cenozoic cover sediments (n= 11). Cluster H1 is characterised by samples with high biotite and epidote with minor pumpellyite, and low clinozoisite, apatite and chlorite, with minor garnet and clinopyroxene (Figure 6.7A), corresponding well with the average values for Canterbury and Wellington Rakaia Terrane (Figure 6.7B).

Cluster H2 is discriminated on PC1 by the orientation of the eigenvectors for chlorite, apatite, biotite, clinozoisite, pumpellyite and sphene. Cluster H2 is almost entirely comprised of Pahau Terrane (n =42) and Cretaceous-Cenozoic cover samples (n=52), with a small component of Rakaia Terrane samples (n=10). Cluster H2 correlates with the average Pahau Terrane values exceptionally well (Figure 6.7), although with notably lower pyrite. Cluster H2 is represented by high proportions of SODeb and epidote, low zircon, with minor pumpellyite and apatite (Figure 6.7A).

Cluster H3 is comprised almost exclusively of Cretaceous cover sedimentary rocks (n = 73), with a small proportion of Rakaia Terrane (n=11) and Pahau Terrane (n=9). The mineral frequency distribution of cluster H3 fits the Pahau Terrane distribution well, although with substantially higher ilmenite and zircon, and significantly lower epidote group minerals, attributed to leaching (Figure 6.7). Additionally, cluster H3 is also characterised by high pyrite, and low biotite (Figure 6.7A).

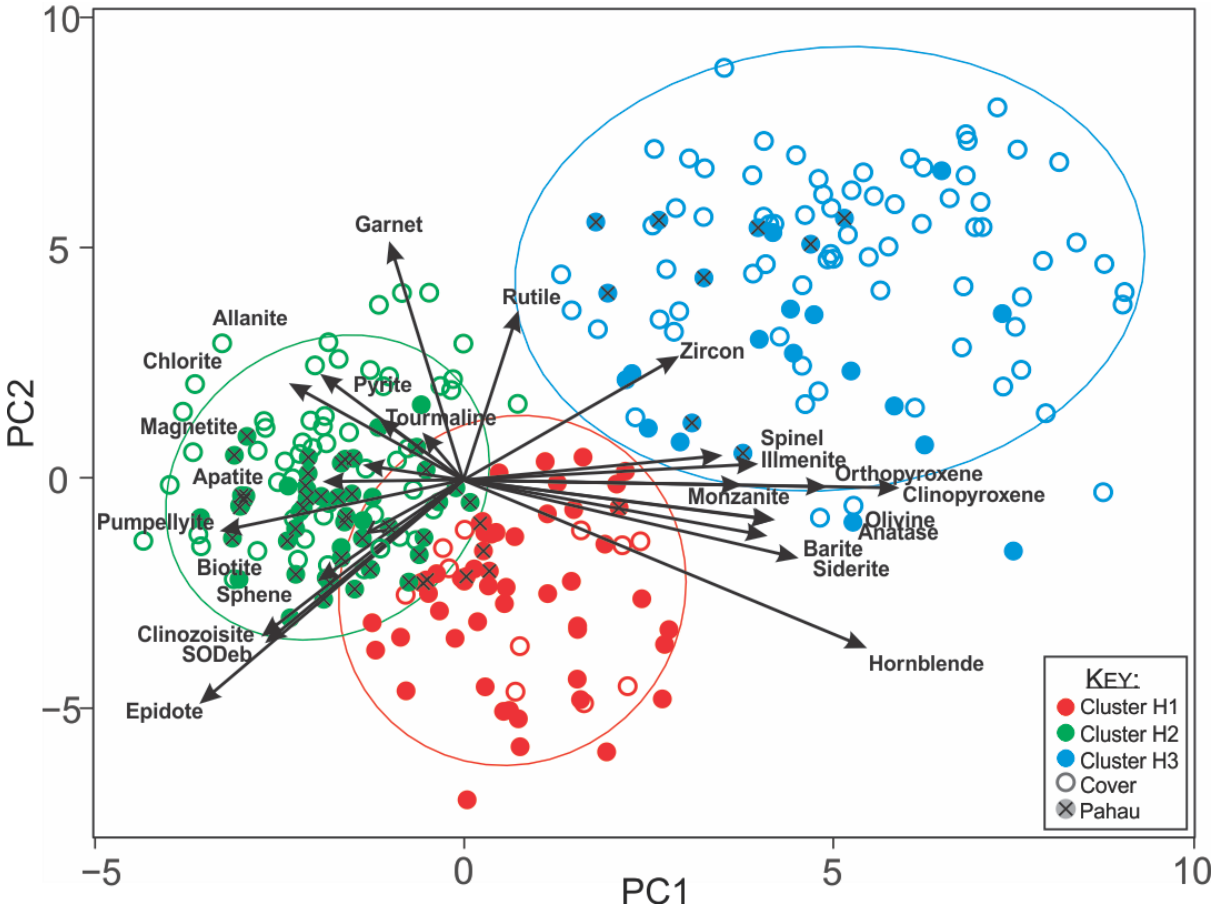

Figure 6.6: Principle components 1 and 2 from PCA of Mesozoic to Paleogene heavy mineral populations across eastern New Zealand. Together these components explain 38% of the variance. The 95% equal probability ellipses are shown for each cluster. Solid circles represent samples from the Rakaia and Pahau basement terranes, with the Pahau Terrane indicated by crossed circles. All other basement samples are from the Rakaia Terrane and Esk Head Belt. Open circles depict samples from cover sedimentary rocks. SODeb = solid opaque debris. Vectors indicate relative loadings of each heavy mineral class on each axis.

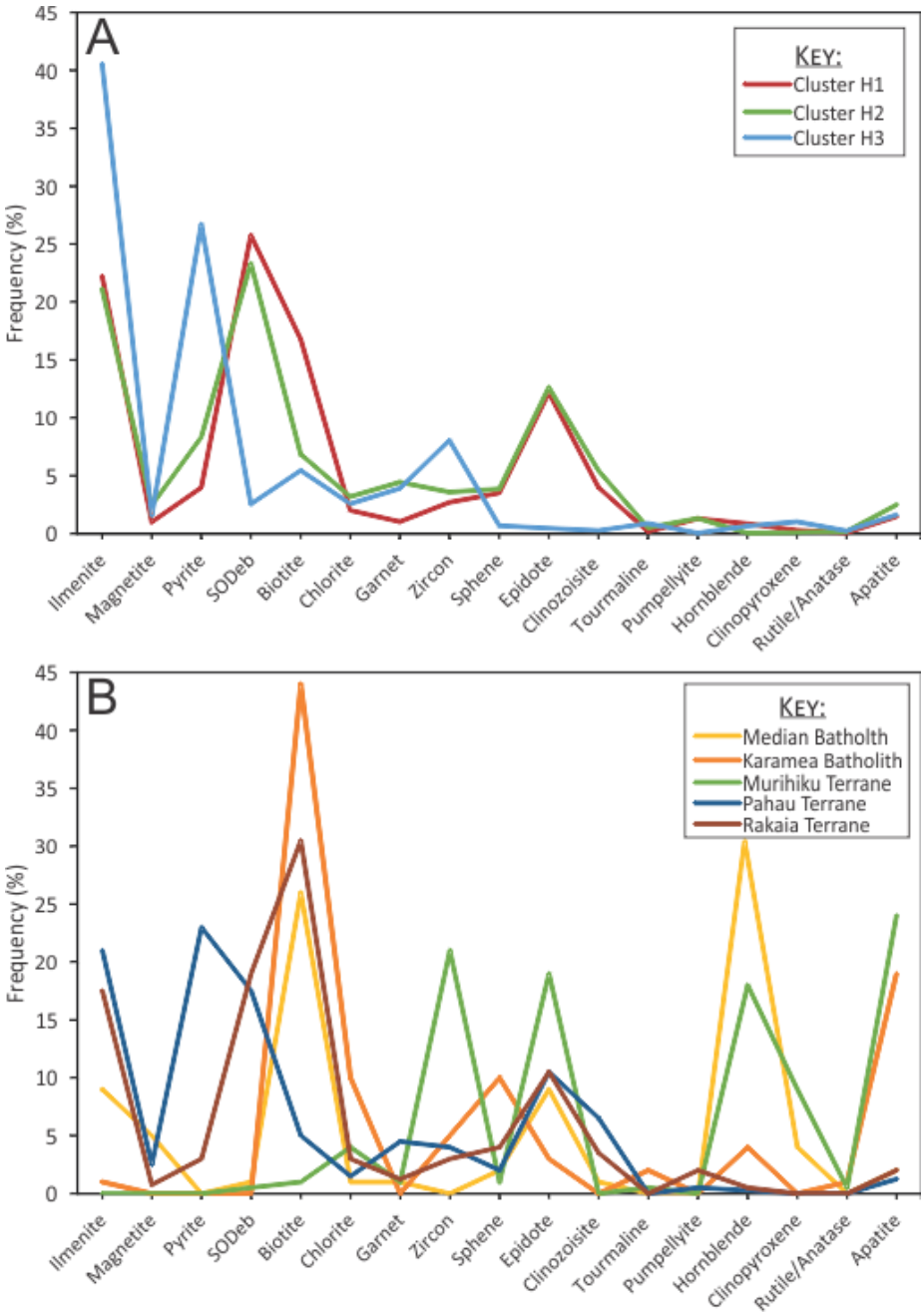

Figure 6.7: A) Average heavy mineral assemblage values for clusters identified using PCA (Figure 6.6). B) Average values for the terranes for which significant heavy mineral datasets exist. Data sourced from Smale (2007).

Table 6.3: Average heavy mineral percent frequency composition of important mineral species for regional divisions of basement terranes and cover sediments.

		Ilmenite	Magnetite	Pyrite	Sodeb	Biotite	Chlorite	Garnet	Zircon	Sphene	Epidote	Clinozoisite	Allanite	Tourmaline	Pumpelyite	Hornblende	Pyroxene	Rutile	Apatite
Rakaia Terrane	**Wellington**	14.4	0.9	9.2	12.8	38.8	2.3	0.8	3.3	2.5	6.0	4.7	0.2	0.5	1.2	0.1	0.2	0.0	1.4
	Canterbury	19.7	0.4	14.2	28.0	10.9	1.7	2.3	1.9	2.7	11.1	2.2	0.2	0.2	1.2	0.2	1.9	0.0	0.5
	Otago	20.1	0.3	0.4	23.8	16.5	2.8	0.7	2.0	4.7	14.5	3.3	0.0	0.2	1.1	1.7	0.1	0.0	2.4
Pahau Terrane	**Wellington**	16.0	0.0	36.5	9.1	5.5	2.0	4.5	5.0	2.0	11.0	8.0	0.1	0.0	0.0	0.0	0.0	0.0	0.5
	Canterbury	30.6	0.8	9.1	26.3	5.4	2.0	3.9	3.9	2.1	8.9	2.9	0.2	0.3	1.6	0.4	0.3	0.0	1.6
	Marlborough	25.3	5.4	3.9	23.9	7.5	3.1	3.7	1.8	3.3	13.8	3.7	0.3	0.4	1.0	0.0	0.1	0.1	2.6
Cover Sediments	**East Coast**	29.1	1.4	34.9	5.2	2.0	4.0	2.8	7.2	2.6	5.6	2.0	0.1	0.4	0.4	0.2	0.2	0.1	1.8
	Marlborough	27.6	2.2	17.8	14.5	4.5	3.3	4.9	5.9	2.8	7.1	3.8	0.3	0.8	0.6	0.2	0.3	0.3	2.9
	Canterbury	57.4	0.9	3.8	9.9	1.5	0.8	5.7	9.7	0.3	1.9	1.8	0.0	0.8	0.5	0.2	0.7	0.3	0.5
	Otago	63.5	0.4	0.0	12.0	0.0	0.0	0.1	10.3	0.3	3.8	4.0	0.0	4.0	1.0	0.6	0.3	0.0	0.3

6.3.4 Interpretation of Heavy Mineral Assemblages

Smale and Laird (1995), and Smale (1997) used hierarchical cluster analysis to identify commonalities within heavy mineral assemblages in the Marlborough and Wellington regions respectively. These clusters show little similarity with the clusters identified in this study, likely because of the different method of cluster analysis used, and the larger dataset incorporated here, and therefore the higher degree of internal variability. Rakaia Terrane samples from the Wellington region were interpreted as being largely derived from a granitic source, although garnet composition from some samples suggest that a subset of samples have a mixed high-grade metamorphic and granitic source (Smale, 1997). Heavy mineral assemblages from the Pahau Terrane in the Marlborough region were interpreted by Smale and Laird (1995) as being derived from recycled granitic material, which had been affected in the first cycle by low grade regional metamorphism. Likewise, Pahau Terrane samples from Wellington were interpreted by Smale (1997) as being derived from the Rakaia Terrane.

Cluster H1 is interpreted as recycled granitic material (high ilmenite, biotite, and epidote), on the basis of heavy mineral distributions that correlate with the Karamea and Median batholiths (Figure 6.7A, B), consistent with the interpretation of Smale and Laird (1995). The geographic distribution of basement samples from cluster H1 broadly follows the trend of the Haast and Alpine schists, and high textural zones within the Rakaia Terrane (e.g. Kapiti Island, Cape Terawhiti).

Cluster H2 is indicative of a higher proportion of metamorphic minerals, shown by the eigenvectors for allanite, pumpellyite, clinozoite and chlorite, despite being largely comprised of cover samples. This cluster assignment suggests a source containing granitic material (based on sphene, apatite, biotite, tourmaline) that has undergone low grade metamorphism (adding pumpellyite and clinozoisite). Therefore, cluster H2 is interpreted as largely reworked Rakaia Terrane that was incorporated into either Pahau Terrane or into cover sediments based on the strong similarity in mineral distributions with the Pahau Terrane (Figure 6.7).

Cluster H3 discriminates strongly on the PCs due to leaching and weathering of sediments, apparent in the direction of the eigenvectors for the resistate phases ilmenite, rutile and zircon (retained during leaching, and therefore proportionally increased) and the antithetic relationship with biotite, epidote, SODeb and clinozoisite (first minerals lost to leaching during diagenetic alteration; Smale & Laird, 1995). This cluster is also characterised by very high pyrite (Figure 6.7B), which likely reflects secondary precipitation given the degree of leaching, rather than primary sedimentary cycling. Consequently, samples in these clusters are not particularly useful for determining provenance characteristics. Leaching is common in Cenozoic cover sedimentary units, with samples from Cretaceous–Paleogene cover sediments all leached to varying degrees, in contrast to the Torlesse-derived samples, which show little to no evidence of leaching (Smale, 1987b, 2007; Smale & Laird, 1995). The abundance and diversity of heavy mineral assemblages in Eastern Province basement rocks (Rakaia and Pahau terranes) suggests that they became indurated soon after deposition, and therefore the effects of intrastratal dissolution are significantly less than Cretaceous–Paleogene cover sedimentary rocks (Smale, 1989, 2007; Smale & Laird, 1995).

Interpretation of basement trends and groupings within the cluster analysis to samples from cover sediments enable an estimate of sediment provenance in the cover succession to be determined. Cover sediments in cluster H1 are attributed to the reworking of Rakaia Terrane and/or a granitic source (Figures 6.6, 6.7 & 6.8). Cover sediments that lie within cluster H2 are interpreted as having a dominantly Pahau Terrane provenance (Figures 6.6, 6.7 & 6.8). Cover sediment samples in cluster H3 are considered too leached or diagenetically altered to provide any clear indication of provenance (Figures 6.6 & 6.8).

The cluster analysis differentiates between subtle changes in heavy mineral compositions, picking up compositional changes in Rakaia Terrane that has been eroded locally, recycled and deposited as Pahau Terrane nearby (Figure 6.8). Similarly, Pahau Terrane or a combination of Pahau and Rakaia terranes have been eroded locally and recycled into mid-Cretaceous sedimentary cover rocks in the Marlborough region, with very little transport and reworking (Figure 6.8; Smale & Laird, 1995). The relative abundance of biotite is a key distinction between cluster H1 and H2, with cluster H1 containing a substantially higher proportion of biotite than either clusters H2 or H3. As biotite does not survive sediment recycling and transport particularly well (Smale & Laird, 1995; Smale, 1990, 2007), this supports the interpretation that the Rakaia Terrane was derived from a granitic source. Additionally, the low proportion of biotite in clusters H2 and H3 can be attributed to the losses during first- or second-order sediment cycling of Rakaia Terrane into Pahau Terrane or Cretaceous-Cenozoic cover sediments.

Cover samples from Marlborough contain a high proportion of biotite compared to cover samples from elsewhere (Table 6.3), indicating proximity to a coeval volcanogenic or metamorphic source, interpreted by Smale and Laird (1995) as the intrusives associated with Tapuae-o-Uenuku and its various extrusive products (Lookout and Gridiron volcanics), and/or the associated contact metamorphic aureole. Alternatively, the high proportion of biotite could be retained from Pahau Terrane (Table 6.3), with a short transport pathway.

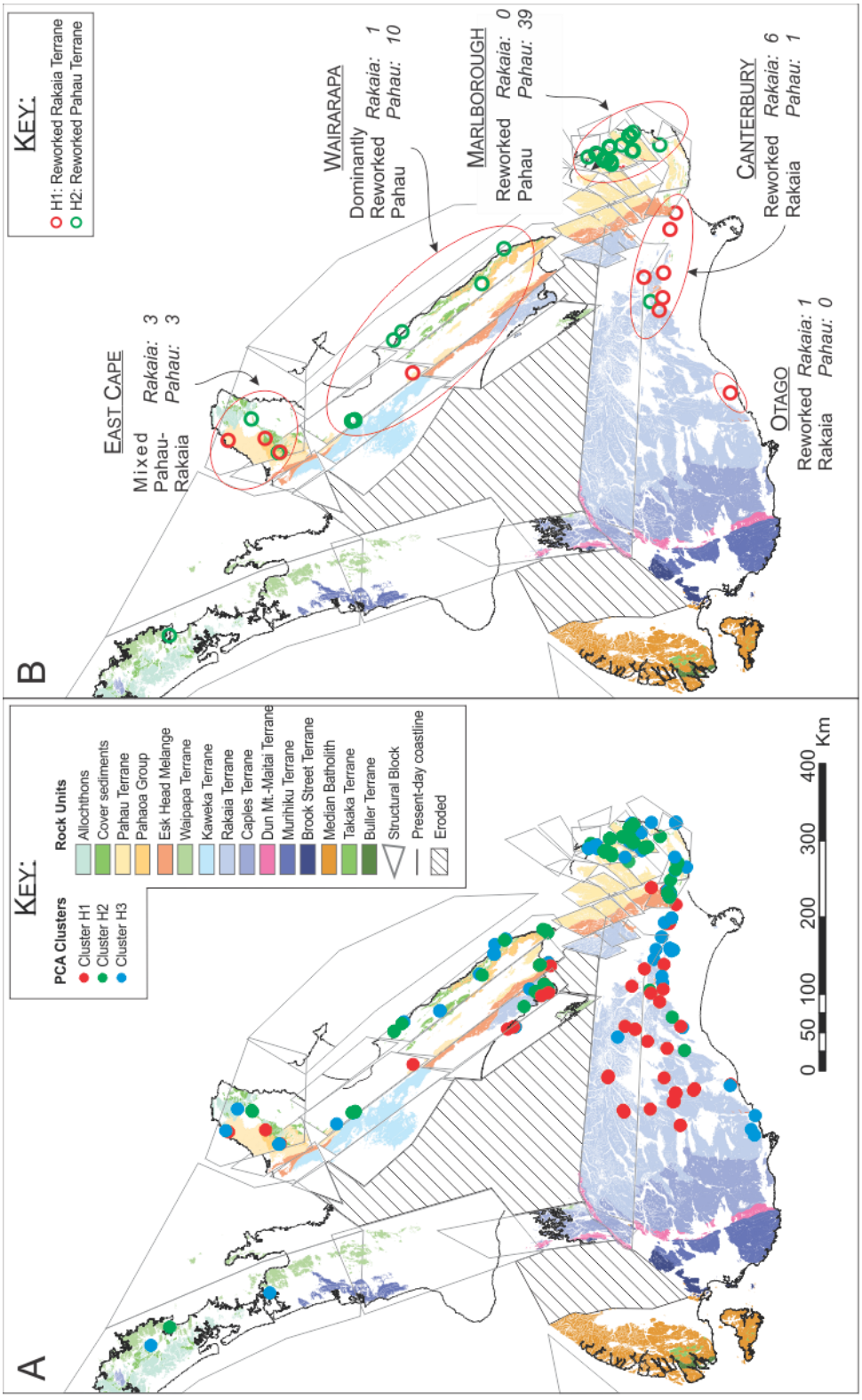

Figure 6.8: Spatial distribution of clusters identified through principal component and Bayesian cluster analyses of basement and cover heavy mineral assemblages, plotted on retro-deformed reconstruction of the New Zealand region during the Cretaceous-Paleogene (Chapter Five). A) Allocation and distribution of all clusters. B) Distribution, interpretation and regional proportions for clusters from Cretaceous-early Paleogene cover sediments. Samples localities in B shown as hollow circles due to the proximity and overlap of points at this scale. Cover samples interpreted as leached have been omitted.

6.4 Bulk-Rock Composition

6.4.1 Introduction to Bulk-Rock Geochemistry

Silicon, Ti, K and Al are the primary major element constituents of the sediments analysed, and can yield information on changes in sediment supply, provenance and mineralogy. Aluminium is dominantly restricted to the fine-grained aluminosilicate fraction in marine sediments, and therefore normalising major element composition to Al forms a reliable index of accounting for detrital flux (Clavert *et al.*, 1996; Beckmann *et al.*, 2005).

Titanium/Al gives information on changes in provenance and sediment accumulation rate (e.g., Sageman *et al.*, 2003; Turgeon & Brumsack, 2006), as both elements are biogeochemically inactive and their concentrations are only controlled by the detrital flux. However, mafic rocks have higher Ti contents and a shift in provenance to a more mafic source will be manifested as increasing Ti/Al. Titanium is hosted in heavy mineral species (e.g., rutile, sphene), so increased Ti/Al values may indicate a stronger volcaniclastic or metamorphic sediment source (e.g., Beckmann *et al.*, 2005). Similarly, a concordant increase in Ti/Al and decrease in Zr/Al represent an increase in material derived from a mafic source.

The primary source of K in marine sediments is from K-feldspar (e.g., orthoclase) and illite, and as such, the proportion of K in marine sediments is associated with the supply of continental siliciclastics (Calvert *et al.*, 1996; Beckmann *et al.*, 2005). Changes in K/Al can therefore be used to determine shifts in the bulk clay mineralogy, between illite and smectite and kaolinite clays (Hofmann *et al.*, 2003; Beckmann *et al.*, 2005; Turgeon & Brumsack, 2006). Variation in Si/Al is indicative of changes in sediment accumulation rates, with a decrease in Si/Al is interpreted to represent an increase in the sedimentation rate (Hofmann *et al.*, 2003; Sageman *et al.*, 2003a; Beckmann *et al.*, 2005).

Bulk modal mineralogy determined by X-Ray Diffraction (XRD) is used to provide additional insight into compositional and mineralogical end-members, complimenting a comprehensive bulk-rock XRF dataset.

6.4.2 Methods

Bulk-rock geochemistry analytical methods used herein are identical to the detailed pXRF and XRD methodology presented in Chapters Three and Four. Portable-XRF analyses were conducted on 992 samples from 23 localities, across various stratigraphic units (Appendix 4). Bulk modal

mineralogy, determined by XRD, was applied to sixty-seven samples from the Whangai, Waipawa, Wanstead and correlative formations to assess changes in mineralogy, both across formation boundaries and across the geographic extent of formations (Appendix 4). Bulk modal mineralogy determined by XRD also aids in the identification of the major mineral constituents of sediments for interpretation of elemental trends.

6.4.3 Bulk Mineralogy Results

Illite/muscovite (largely indistinguishable by XRD) form a substantial proportion of the modal mineralogy of the Herring lithofacies, Waipawa and Wanstead formations and the Rakauroa and Upper Calcareous member of the Whangai Formation (Figure 4.10). Similarly, the Herring lithofacies, Rakauroa and Upper Calcareous members have a significant proportion of albite and chlorite (Figure 4.10C). Forty samples at a moderately-high sampling resolution were analysed by XRD through a succession of Whangai, Waipawa, and Wanstead formations to assess temporal change in modal mineralogical contribution (Chapter Four). The modal mineralogy is dominated by quartz, albite and illite, with albite demonstrating a general increasing trend up-section, whereas illite and chlorite display a corresponding decrease up-section (Chapter 4; Figure 4.10A). Samples analysed by XRD across the Waipawa and Wanstead formations at Triangle Farm correspond well with bulk modal mineralogy from Taylor White (Figure 4.10B).

Across a north-south transect, the Waipawa Formation becomes increasingly dominated by quartz, and the total number of mineral species identified by XRD decreases southwards (Figure 4.10D). The increasing proportion of quartz with respect to clay minerals is consistent with increased Si/Al values in the southern Wairarapa and Mead Stream Waipawa Formation samples (Figure 4.9). X-Ray diffraction analysis of the clay fraction of the Wanstead Formation indicates that montmorillonite is the dominant clay mineral, with a notable proportion of illite (Morgans, 2016). Unsurprisingly, the Paleocene-Eocene limestones (Mungaroa, Mead Hill and Amuri Limestone formations) are dominated by carbonates and a moderately large proportion of quartz (10–50%), although the Mungaroa and Amuri limestones have a notable presence of clastic minerals (albite, and albite and muscovite respectively; Figure 4.10F).

6.4.4 Major Element Compositional Results

Major element plots generally show a tightly constrained clustering amongst Piripauan to Eocene sedimentary rocks sampled here, with sub-trends apparent within the dataset. There is a distinctive

difference in the major element composition of the Gentle Annie Formation with respect to the other units sampled. A detailed analysis of elemental trends (K/Al, Zr/Al, Ti/Al, and Si/Al) through the Whangai, Waipawa and Wanstead Formations is discussed in Chapters Three and Four, and are summarised here. The Upper Calcareous Member and the Waipawa Formation from all locations display well-constrained clustering, along with both the siliceous flysch and calcareous mudstone facies of the Wanstead Formation. The distinct variability in the major element components of the Porangahau Member is attributed to grain-size variation within the decimetre-bedded, alternating sandstone and mudstones of the unit (sandstone = high SiO_2, low K_2O, TiO_2; mudstone = low SiO_2, high TiO_2, K_2O).

The SiO_2 associations across the units sampled show three end members within the lithologies sampled; carbonate sediments (low SiO_2, low Al_2O_3), organic-rich sediments (high SiO_2, high Al_2O_3), and organic-rich sediment associated with carbonates (high SiO_2, low Al_2O_3; Figure 6.9A). The trend from the 'typical' Waipawa Formation (Hawke's Bay-Wairarapa; Chapter Four), towards the more siliceous Waipawa Formation (distal Waipawa; outcrops in southern Wairarapa-Marlborough), outline a distinct trend from high terrigenous flux towards a silica excess, either from biogenic silica or detrital quartz (Figure 6.9A). The silica-rich Rakauroa Member, and the Upper Calcareous Member, and Wanstead Formation also plot on this trend.

The trend extending from the carbonate samples (Mead Hill Formation, Mungaroa Limestone, Amuri Limestone) towards the Waipawa end-member is marked by a linear boundary, likely proportional to a compositional trend of a mix of illite, biotite, plagioclase and/or orthoclase, identifying background sedimentation (i.e. clay line). The intervening area outlined by these end members is dominantly comprised of flysch sediments included within the Glenburn Formation, Porangahau Member, Manurewa Formation, Wanstead Formation (Taylor White), and the Mungaroa Limestone (Manurewa Point; Figure 6.9A). Samples from the Gentle Annie Formation fall along a similar compositional trend as the latest Cretaceous-Paleogene samples, but with exceptionally high SiO_2 and Al_2O_3. This is in contrast to samples from the approximately coeval Champagne Formation and Ouse Siltstone that show a compositional trend that is intermediate between the Waipawa and carbonate end members.

A silica excess is observed above the clay line, interpreted as an increase in either biogenic or detrital quartz (Figure 6.9A). Particularly in the case of flysch sediments, it is likely to represent an increased proportion of detrital quartz deposited in association with sandstone beds. A proportional decrease in the Si-Al trend is interpreted to represent increasing dilution by carbonate (Figure 6.9A).

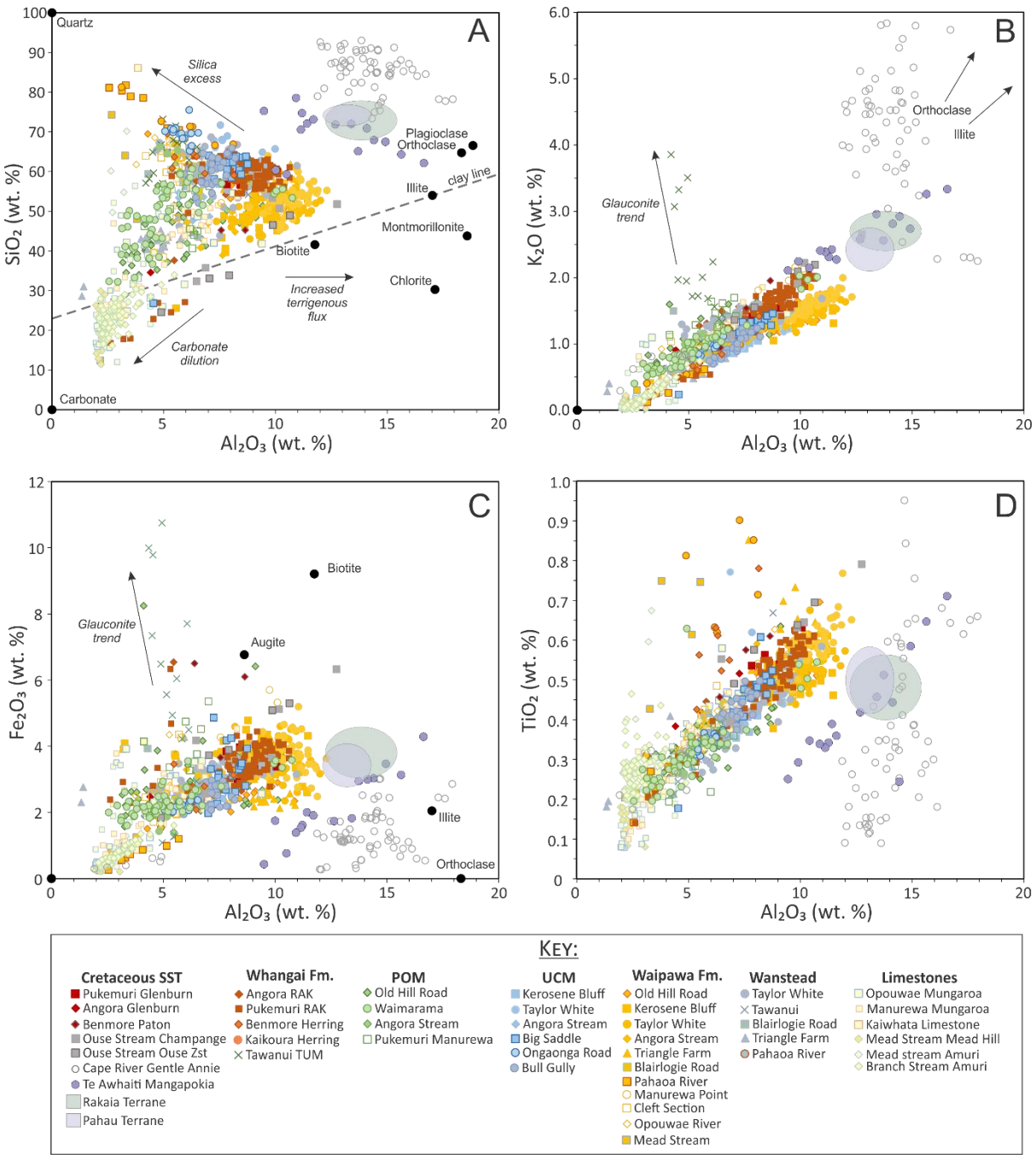

Figure 6.9: Summary diagram of major element distribution across various stratigraphic units of the East Coast Basin determined by pXRF analysis. A) SiO_2 plotted against Al_2O_3. B) K_2O plotted against Al_2O_3. C) Fe_2O_3 plotted against Al_2O_3. D) TiO_2 plotted against Al_2O_3. Te Awaiti Mangapokia Formation data from Barnes (1990). Rakaia and Pahau terrane fields from Roser and Korsch (1999). Key to abbreviations: RAK = Rakauroa Member, TUM = Te Uri Member, POM = Porangahau Member, UCM = Upper Calcareous Member.

Samples from the Gentle Annie Formation show high K_2O, likely indicative of either high proportions of orthoclase and/or illite (Figure 6.9B). Samples from the Glenburn and Paton Formations generally exhibit similar elemental compositions (SiO_2 and K_2O) as the Rakauroa Member and Herring lithofacies, but with proportionally higher Fe_2O_3 and lower Al_2O_3, and in the Paton Formation, slightly higher TiO_2 (Figure 6.9C, D). The K_2O-Al_2O_3 relationship exhibits a linear trend across all samples (except Gentle Annie Formation), indicating little change in the source of bulk-rock constituents. A sub-trend is evident, where samples from the Upper Calcareous Member and Waipawa Formation have lower K_2O values than the Rakauroa and Porangahau Members and the Wanstead Formation. Samples from glauconitic sandstones, particularly the Te Uri Member, give high K/Al and Fe/Al, indicative of the high proportion of K and Fe associated with glauconite (Figure 6.9B, C). Notably samples from the Paton Formation do not fall on this trend. Micritic limestone from the Mead Hill, Mungaroa and Amuri Limestone formations generally give low K/Al values in response to low terrigenous flux and dilution by bioclastic carbonate (Figure 6.9B).

Analyses of Fe_2O_3 plotted against Al_2O_3 form a linear trend, directed towards carbonate dilution, as exhibited by the other major elements assessed here (Figure 6.9C). Samples from the Ouse Siltstone, Champagne, and Paton formations have proportionally higher values than average trend of the rest of the dataset. Analyses from the Gentle Annie Formation lie away from this trend, with proportionally low Fe_2O_3 values, although within the range of values of other sediment analysed (Figure 6.9C). With the exception of the Gentle Annie Formation, all samples form a linear relationship between TiO_2 and Al_2O_3 (Figure 6.9D). Analyses from the Gentle Annie Formation fall within the same range of TiO_2 values as the rest of the data set, but lie outside of the trend. Samples from the Ouse Siltstone, Champagne and Paton formations show slightly higher proportions of TiO_2 than the other units sampled (Figure 6.9D).

A cross-plot of Si/Al and Ti/Al provides an indication of sedimentation rate and a broad assessment of provenance, respectively (Figure 6.10). Unsurprisingly, Si/Al indicate low sediment accumulation rates (SARs) through the Amuri, Mead Hill, and Mungaroa Limestone formations (Figure 6.10). In contrast, Si/Al ratios from the Rakauroa Member and Waipawa Formation (in Hawke's Bay-Wairarapa; see Chapter Four for a discussion in Whangai-Waipawa-Wanstead SARs) indicate high sedimentation rates (Figure 6.10). The Gentle Annie, Ouse Siltstone and Champagne Formations also have low Si/Al values indicative of high SARs.

The ratio of Ti/Al provides an indication of volcanigenic source. Titanium/Al values for the majority of the sediments sampled have transitional values, indicating either a mixed source, or an

intermediate volcanogenic source (Figure 6.10). Analyses of the Gentle Annie Formation indicate a felsic provenance for the unit. Analyses of the Late Cretaceous to Eocene formations in the northern Clarence Valley area (Ben More Stream – Paton and Whangai formations; Mead Stream – Mead Hill, Waipawa, and Amuri Limestone formations; Branch Stream – Amuri Limestone), indicate a mafic sediment source, not recorded in samples from the Whangai Formation at Kaikoura, or in the North Island East Coast.

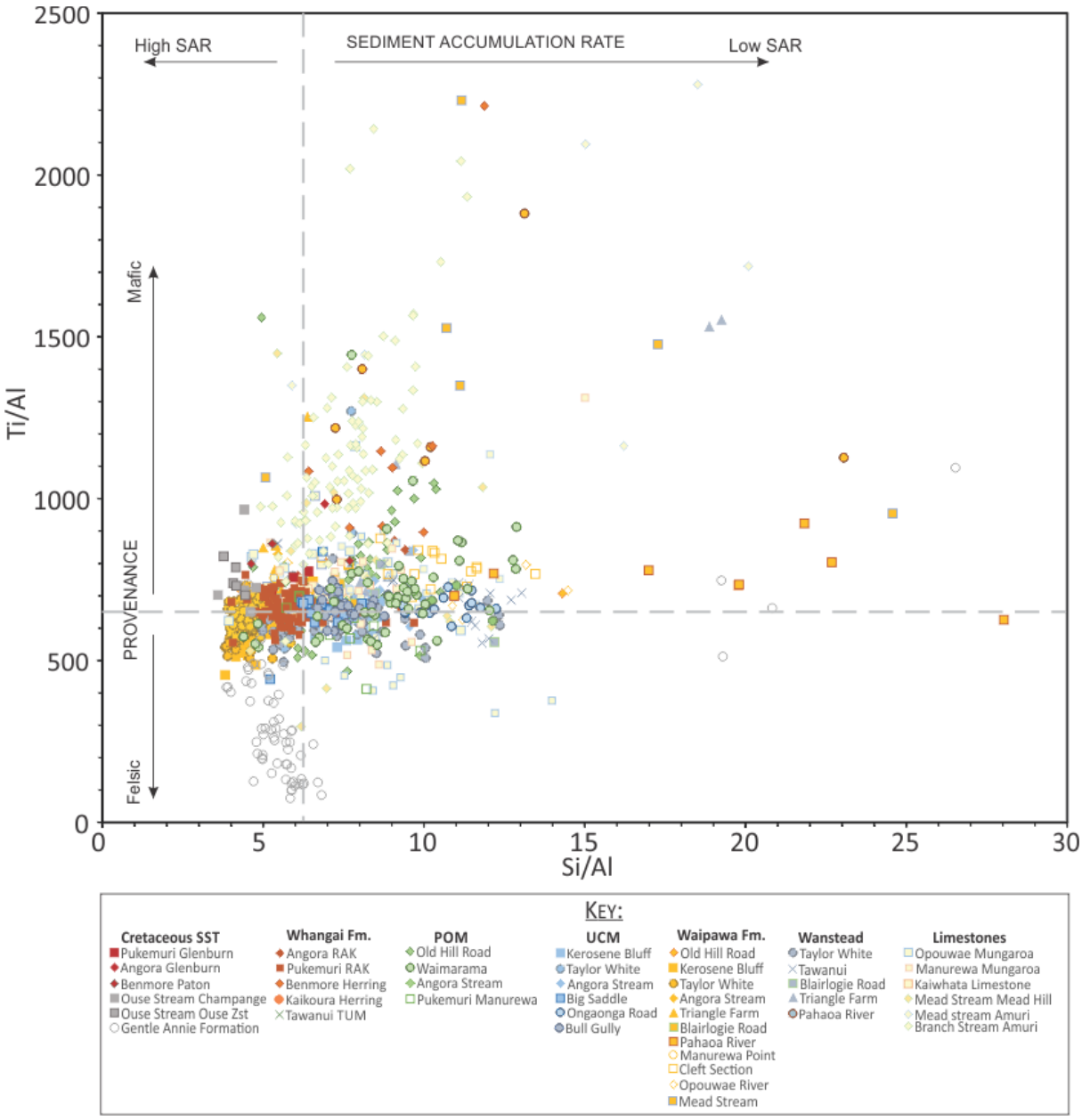

Figure 6.10: Plot of Si/Al vs Ti/Al as proxies for changes in sediment accumulation rates and sediment provenance. Key to abbreviations: RAK = Rakauroa Member, TUM = Te Uri Member, POM = Porangahau Member, UCM = Upper Calcareous Member, SAR = Sediment accumulation rate.

6.4.5 Interpretation of Bulk-Rock Geochemistry

Titanium/Al, Zr/Al, K/Al values are consistent throughout the Glenburn, Whangai, Waipawa and Wanstead formations (and correlative units), suggesting the sediment supply had a consistent composition for a long period of time (Piripauan to Mangaorapan), across the basin. Furthermore, values determined by XRD for albite, plagioclase and orthoclase in the Paleogene samples analysed (Chapter Four) are comparable to percentages derived by Barnes (1990) for the Early Cretaceous Mangapokia Formation. The major element data from the various formations presented here suggests that there may have been comparatively little change in detrital source from the mid-Cretaceous to the early Eocene. However, the slightly higher proportion of TiO_2 and Fe_2O_3 with respect to Al_2O_3 in samples from the Ouse Siltstone, Champagne and Paton formations, in addition to moderately-high Ti/Al in the Whangai Formation in Ben More Stream and the Amuri Limestone, may imply a component of the bulk sediment was derived from a mafic source area (Figure 6.9). This is supported by the presence of magnetite throughout the Amuri Limestone, which hosts the primary paleomagnetic signal in these sediments, rather than the autochthonous mineral greigite, as occurs during this interval elsewhere (Dallanave *et al.*, 2014, 2015). The samples of the Whangai Formation analysed from Kaikoura show no index minerals in XRD or bulk-rock geochemical indicators for mafic volcanism, indicating that the supply of mafic, volcanically derived sediment may have been restricted to the northern Clarence Valley area (Figure 6.11).

The Mangapokia Formation forms the uppermost part of the Pahau Terrane in the Wairarapa area. Mangapokia Formation samples from Barnes (1990) show consistently higher Al_2O_3, SiO_2 and K_2O, and proportionally lower Fe_2O_3 and TiO_2 (with respect to Al_2O_3) compared to the Cretaceous-Paleogene samples analysed here, indicating derivation from a more felsic source. Barnes (1990) interprets the Mangapokia Formation as having a similar geochemical composition to the Pahau Terrane elsewhere, consistent with the average Pahau and Rakaia terrane values from Roser and Korsch (1999; Figure 6.9).

A highly felsic composition is indicated by very high SiO_2 and Al_2O_3, and low Fe_2O_3 in the Gentle Annie Formation. The broadly similar compositional trend of the latest Cretaceous-Paleogene sediments (Whangai, Waipawa and Wanstead formations) and the Gentle Annie Formation, suggest that these sediments shared a common source, with the strong felsic signal becoming diluted in latest Cretaceous-Paleogene sediments by an increased proportion of clay and/or mafic mineral modes (Figure 6.11). Conglomeratic clasts comprised of granite and diorite are common in the Cape River section sampled here.

Bulk-rock geochemistry indicates that the Gentle Annie Formation is more felsic than the Mangapokia Formation, indicating that the Gentle Annie Formation represents a brief period where a felsic source had a significant influence on the geochemical character of the sediment. Tulloch *et al.* (2009) identify a cluster of rhyolitic tuffs across the New Zealand region at 101 and 97 Ma. The 101 Ma tuffs are approximately coeval with the deposition of the Gentle Annie Formation, and could indicate a pulse of rhyolitic volcanism that is expressed in the Gentle Annie Formation. The identification of granitic clasts, in association with schist, marble, dacite and metabasalt clasts within the Gentle Annie Formation would suggest that the source of the felsic signature is the Median Batholith, although more detailed geochemistry of clast composition is required to determine this. The indication of high sediment accumulation rates through the Gentle Annie, Ouse Siltstone and Champagne formations from geochemical proxies (Figure 6.10) compares well with their sedimentology and interpreted depositional conditions.

The strong K_2O and Fe_2O_3 trend indicative of glauconitic sediments is not apparent in the Paton Formation samples from Ben More Stream (Figure 6.9B, C). In conjunction with the increased proportion of TiO_2, this implies that the distinctive green colour in the Paton Formation likely originates from chlorite, rather than glauconite, as suggested by Crampton (1988). This may also explain the difficulty in differentiating fresh Paton Formation from Hapuku Group, with weathered Paton Formation presenting the clear, distinctive green colouration (Crampton & Laird, 1997). A chlorite-rich Paton Formation is consistent with indicators of mafic sediment sources within the formation, and the abundance of epidote identified in heavy mineral separates (Appendix 8).

The Whangai Formation, particularly the Rakauroa Member, has an unusually high silica content (Figure 6.9A; Moore, 1988a). The high SiO_2 content of the Rakauroa Member is likely attributed to diagenetic alteration and remobilisation of biogenic silica from radiolaria and diatoms. It may represent the end member of multiple cycles of erosion and re-deposition, although this seems unlikely as deposition corresponds with the accumulation of the siliceous limestones of the Mead Hill Formation in Marlborough.

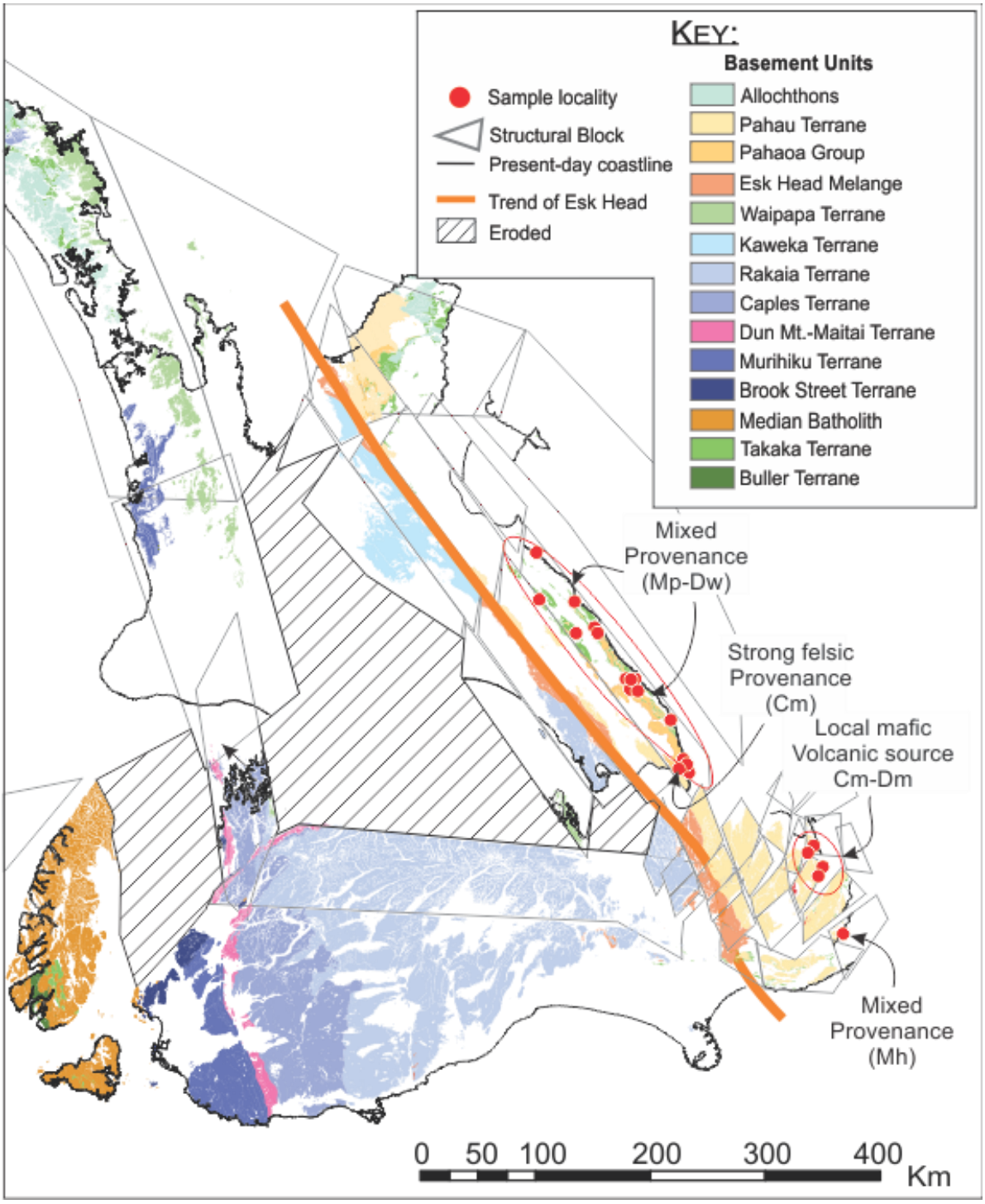

Figure 6.11: Locations of sections sampled for bulk-rock geochemical analyses plotted on retro-deformed reconstruction of the New Zealand region during the Cretaceous-Paleogene, along with interpretations based on major element compositions.

6.5 Discussion of Provenance Characteristics

The application of robust statistical analytical approaches allows the identification of rigorously defined groups in a transparent and repeatable manner. On their own, each dataset and methodology (detrital zircon ages, heavy mineral assemblages, and bulk-rock geochemistry) provides insights into aspects of sediment provenance. However, combining multiple methods provides a holistic view of sediment provenance and cycling. An understanding of sediment provenance provides insight into sediment pathways, hinterland tectonics and upland source regions. Detrital zircon studies are likely the best tool for resolving the absolute sediment sources, although it is not particularly sensitive to sediment cycling. Heavy mineral suites, on the other hand, appear to be dominantly controlled by sediment cycling and are more useful for identifying local sediment sources. When applied in tandem, these techniques are particularly robust, and can be used to identify multiple cycling of sediments. Placing these datasets within the context of a rigorously-tested, retro-deformed palinspastic tectonic model is particularly beneficial for identifying trends within, and between, the very different methods applied to sediment provenance identification (Figures 6.5, 6.8, 6.11 & 6.12).

Detrital grain studies (Adams *et al.*, 2013a, 2013b) have shown that easternmost basins of the Cretaceous Zealandia landmass have inputs dominantly from the then and presently far-field Western Province terranes. Detrital zircon patterns indicate that during the syn-rift phase of Gondwana breakup (110–83 Ma), the Median Batholith was a significant upland source contributing to all the fluvial, marginal marine and marine basins of the Taranaki, Northland and East Coast basins, with a west to east drainage pattern (present-day orientation) (Adams *et al.*, 2017). However, analysis of detrital zircon patterns in this study suggest that the Median Batholith only formed a significant source in the northern part of the East Coast Basin, although bulk-rock geochemistry and clast petrology suggests that the Gentle Annie and Mangapokia formations in the southern Wairarapa may have been derived from the Median Batholith, with some contribution of Western Province terranes. The felsic nature of the Gentle Annie Formation indicates that these sediments were either dominantly sourced from the Median Batholith (and/or the respective extrusive products), or from a pulse of unrelated rhyolitic volcanism at c. 101 Ma (e.g. Tulloch *et al.*, 2009). Notably, however, samples of comparable age in Marlborough (Champagne Formation and Ouse Siltstone) do not show such a strong felsic signature, and instead have a mixed composition, similar to the late Cretaceous to Eocene (Piripauan-Mangaorapan) sediments sampled in this study. This observation is consistent with heavy mineral assemblages from the basal cover succession in Marlborough, which suggest local derivation of sediments.

In the southern North Island at Tora, clasts of marble, schist, granite, dacite and metabasalt have been identified in Mangapurupuru Group strata (Barnes *et al.*, 1988; observed during the present study). Similar lithologies within Cretaceous conglomerates of the East Coast Basin are also noted in the East Cape, Hawkes Bay and Tinui areas (Kingma, 1971; Johnston & Browne, 1973; Black, 1980; Lillie, 1980). This collection of lithologies is indicative of cycling of clasts from the Median Batholith and Western Province terranes into the East Coast region, giving a strong indication of sediment transport pathways. The collection of lithologies within the Mangapokia and Gentle Annie formations in the southern Wairarapa (Barnes, 1990; observed in this study), suggests that a Median Batholith source is a reasonable assumption for the felsic signature recorded in major element ratios from the Gentle Annie Formation. In the present-day geological setting, this collection of lithologies crops out in the Northwest Nelson area, and when considered in the context of the structural reconstruction (Chapter Five), represents a long (>500 km) transport pathway (Figure 6.12).

Detrital zircon age populations from the East Coast and Northland basins are characterised by a substantially diminished proportion of Western Province (Devonian-Carboniferous) zircons in comparison to other basins in New Zealand (Adams *et al.*, 2017). Subsequently, Adams *et al.* (2017) interpreted local basement sources (Rakaia, Pahau and Waipapa terranes), as the major sources for detrital zircon contributions in the East Coast and Northland basins. The analysis of detrital zircon ages presented here can be used to produce a finer division than the Adams *et al.* (2017) interpretation. Zircon age-frequency data from Northland and Raukumara are dominated by Cretaceous ages, indicating a large proportion of zircons are derived from the approximately coeval Median Batholith. Age-frequency relationships in zircon assemblages from the Wairarapa and Hawke's Bay are dominated by a mixed signal from the Median Batholith and the Rakaia Terrane, with a diminishing proportion of progressively older zircons. These zircon age-frequency distributions in the North Island East Coast Basin are resolving variations between the Waioeka Petrofacies (Cluster Z1) and the Omaio Petrofacies (Clusters Z2 and Z4) of the Pahau Terrane. This pattern is consistent with interpretations of these petrofacies, whereby the Waioeka Petrofacies is comprised of an older, volcaniclastic source, and the Omaio Petrofacies was sourced from a comparatively young, quartzose-feldspathic source.

Assemblages from the Marlborough regions are dominated by Rakaia and older Eastern Province zircon age modes, although notably the subordinate Median Batholith and Western Province age modes provide approximately equal components. Cretaceous sedimentary fill in the Marlborough region is dominated by a heavy mineral signal that indicates that Cretaceous cover is predominantly derived from the nearby Pahau Terrane (Figure 6.12C). This is consistent with the stratigraphic

record at this time, governed by the deposition of mass-transport deposits in locally restricted basins (e.g., Laird, 1992; Crampton & Laird, 1997; Field & Uruski *et al.*, 1997; Crampton *et al.*, 2003). Detrital zircon patterns from the basal Cretaceous cover succession of the Marlborough area indicate a far-field source for sediments. This apparent disparity between the heavy mineral and detrital zircon systems can be explained by deposition of cover sediments from the local erosion and re-sedimentation of Pahau Terrane, which in Marlborough is partially recycled from Rakaia Terrane, comprised of inherited Western Province zircons. Therefore, multiple cycling through basement terranes explains the varied, inherited zircon age distributions.

The chloritic composition of the Paton Formation (e.g., Crampton, 1988; this study), high proportion of epidote minerals and the presence of magnetite, high Ti/Al values, and high proportion of biotite in heavy mineral samples (Smale & Laird, 1995), all provide strong indications of a mafic source in the northern Clarence Valley area during the late Cretaceous to Paleogene (Figure 6.12). This may be attributed to the local erosion and re-sedimentation of the extrusive products of the nearby Tapuae-o-Uenuku or Blue Mountain igneous complexes.

The Canterbury Basin has a notable absence of early Cretaceous zircons from the Median Batholith (Adams *et al.*, 2017), suggesting that the local basement, particularly the Rakaia Terrane was a substantial upland area eroding and supplying the Canterbury Basin during the Cretaceous-Eocene, with a regional paleo-north-south drainage gradient (Figure 6.12). This is consistent with heavy mineral associations identified in PCA that suggest a Rakaia Terrane source for cover sediments in the Canterbury Basin (Figures 6.7 & 6.8).

Integration of the various provenance datasets considered here provides firm indications of upland source areas, sediment pathways and hinterland tectonics. During the initial stages of Pahau Terrane deposition and accretion (~116–130 Ma), sediment supply was from a mixed Rakaia Terrane and Median Batholith source (Figure 6.12A). During the later stages of Pahau Terrane deposition (~108–116 Ma), the Median Batholith or its extrusive products were providing a considerable source of sediment to the Omaio Petrofacies and Pahaoa Group shelf-slope basins on the outboard margin of the Gondwana accretionary prism in the present-day Northland, East Cape, Hawke's Bay and Wairarapa regions (Figure 6.12A). In the Marlborough region, sediment supply through deposition of the Pahau Terrane appears to have been sourced entirely from cannibalism of the Rakaia Terrane (Figure 6.12A), as indicated by heavy mineral assemblages and detrital zircon age modes.

Sediment sourced from the Median Batholith indicates that a long (>500 km), substantial, continental sediment transport pathway existed at this time. The increased prevalence of a Median

Batholith source in the later stages of Pahau accretion suggests the active uplift and unroofing of granitoids. The widespread deposition of mixed Rakaia-Median Batholith to dominantly Median Batholith derived sediments across what was a broad continental margin, from Northland to the Wairarapa (~800 km), and the absence of this signal in the Marlborough region indicates the presence of a structural or physiographic divide between the present-day southern Wairarapa and northern Marlborough. This interpretation may be consistent with the interpretation of Marlborough as a separate sub-basin at this time, or alternatively that it may have been supplied by a smaller, independent drainage system.

By the mid-Cretaceous (~100 Ma), either the contribution of the Median Batholith to sediment load was subsiding, or the Rakaia Terrane was supplying a greater proportion of sediment to the East Cape, Hawke's Bay and Wairarapa areas (Figure 6.12B). Heavy mineral assemblages indicate that in the Wairarapa-Hawke's Bay, the Pahau Terrane was also providing a subordinate proportion of the sediment load. The southern Wairarapa appears to have had localised deposition of possibly Median Batholith-derived felsic sediments at this time. Heavy mineral assemblages, detrital zircon and bulk-rock geochemical provenance indicators for the basal cover sediments in Marlborough indicate the local Pahau Terrane was the dominant sediment source, indicating short, locally restricted sediment transport pathways (Figure 6.12B). The transition towards sediment derived from locally-adjacent basement terranes may indicate either subdued relief in hinterland topography, the termination of continental-scale sediment transport systems, or tectonic truncation of supply routes from Western Province and Median Batholith sediment sources. Deposition of the Houhora Complex in Northland at this time is dominated by young Cretaceous detrital zircon age modes, showing that early Late Cretaceous rhyolitic volcanism (Tulloch *et al.*, 2009), was still providing the dominant sediment source to this region (Figure 6.12B). Similarly, the Median Batholith (or c. 101 Ma volcanism associated with the Houhora Complex) was also primary component of the sediment source to the East Cape area, although present in a mixed Rakaia-Cretaceous volcanism signal. The potential sediment pathway from the Median Batholith (or Houhora Complex) and the East Cape areas is shorter than would be required to deposit these sediments in the Hawke's Bay-Wairarapa and Marlborough areas (Figure 6.12B). The mid-Cretaceous basal cover sediments in the Chatham Island area show evidence of coeval volcanism in detrital zircon ages, consistent with active mafic and felsic volcanism in this area at around this time (Takahe Volcanics; Tulloch *et al.*, 2009).

By the Late Cretaceous (~86 Ma), all regions along the eastern Zealandia margin record local sediment sources. Zircons from the Punakitere Sandstone in Northland have a dominant Cretaceous age mode, possibly indicating a Median Batholith source, although they are just as likely

to be locally derived from the erosion and redeposition of the Houhora Complex, which shares the same zircon age-frequency distribution (Figure 6.12C). Heavy mineral assemblages from Cretaceous cover sediments of the East Cape region have a mixed Rakaia-Pahau source, consistent with detrital zircon age populations (Figure 6.12C). Cretaceous-Paleogene sediments in the Hawke's Bay-Wairarapa regions are characterised by heavy mineral assemblages that indicate a predominantly Pahau source, with a subsidiary contribution from the Rakaia Terrane (Figure 6.12C). The Marlborough region continues to be dominated by local, Pahau derived sediment sources, although in a restricted area around the northern Clarence Valley, the Tapuae-o-Uenuku Igneous complex and/or the extrusive products, the Lookout and Gridiron volcanics, add a mafic contribution to locally-deposited sediment (Figure 6.12C), apparent in bulk-rock geochemistry and heavy mineral suites from this area. Heavy mineral assemblages indicate that Cretaceous to Paleogene cover sediments in the Canterbury Basin were wholly derived from recycled Rakaia Terrane (Figure 6.12C). Provenance characteristics during deposition of the Pahau Terrane and mid-Cretaceous cover sediments indicate long sediment transport pathways (Figure 6.12). The widespread reduction in sediment transport pathways across the eastern margin of Zealandia by the late Cretaceous suggests a shift in the drainage divide. In the Early Cretaceous (~125–100 Ma) the drainage divide was far inland, around the crest of the Median Batholith, whereas by the late Cretaceous (~86 Ma), the divide had moved eastwards in response to stretching and crustal thinning in the west associated with opening of the Tasman (van der Meer *et al.*, 2016), and thermal subsidence associated with abandonment of the Median Batholith arc system following cessation of subduction on the Gondwana margin. Bulk-rock geochemistry indicates a consistent composition across the Hawke's Bay-Wairarapa and Marlborough regions throughout the Cretaceous-Paleogene, indicating no significant change in sediment provenance between ~82–56 Ma, supporting the interpretation of locally derived sediment pathways, which are less likely to demonstrate provenance changes in long-term stratigraphic records.

Index minerals and elemental proxies for mafic volcanism in the northern Marlborough area are inferred to be derived from the erosion of the Tapuae-o-Uenuku volcanic edifice. The restricted distribution of indicators for mafic volcanism in the northern Marlborough area indicate that sediment transport in this area was such that the erosional products from Tapuae-o-Uenuku did not spread far. From a paleogeographic view point, this suggests that there were no other volcanos in the now-eroded hinterland mass that were contributing sediment to the North Island East Coast Basin. Similarly, other volcanic complexes in the Canterbury region (e.g., Mt Somers, Mandamus) do not appear to be contributing to basin sediments during the late Cretaceous-Paleogene.

Crampton *et al.* (2003) argued that during the late Cretaceous there was a significant boundary between Marlborough and the remainder of the East Coast Basin. This boundary corresponds, more-or-less, to the position of the modern plate boundary, hinting at a long-term structural control on this region. The distinct differences in sediment sources and the implied sediment pathways identified in this study suggest that this boundary may have been in existence for much longer. Reyners *et al.* (2011, 2017) interpret the edge of the Hikurangi Plateau that was subducted beneath the eastern margin of Gondwana between 110–100 Ma as a major structural control on the location of the modern plate boundary and the location of intra-plate volcanism since 110 Ma. The position of the boundary identified by Reyners *et al.* (2011, 2017) corresponds with the position identified by Crampton *et al.* (2003) and this study.

In summary, the integration of detrital zircon, heavy mineral assemblages and bulk-rock geochemistry datasets results in a demonstrable transition in sediment provenance through the Cretaceous, from a dominantly reworked granitic source during deposition of the Pahau Terrane, transitioning to dominantly locally derived sediment sources by the mid-Cretaceous (~100 Ma) with localised felsic and mafic sources. By the late Cretaceous (`86 Ma), sediments were almost entirely sourced from locally reworded basement strata.

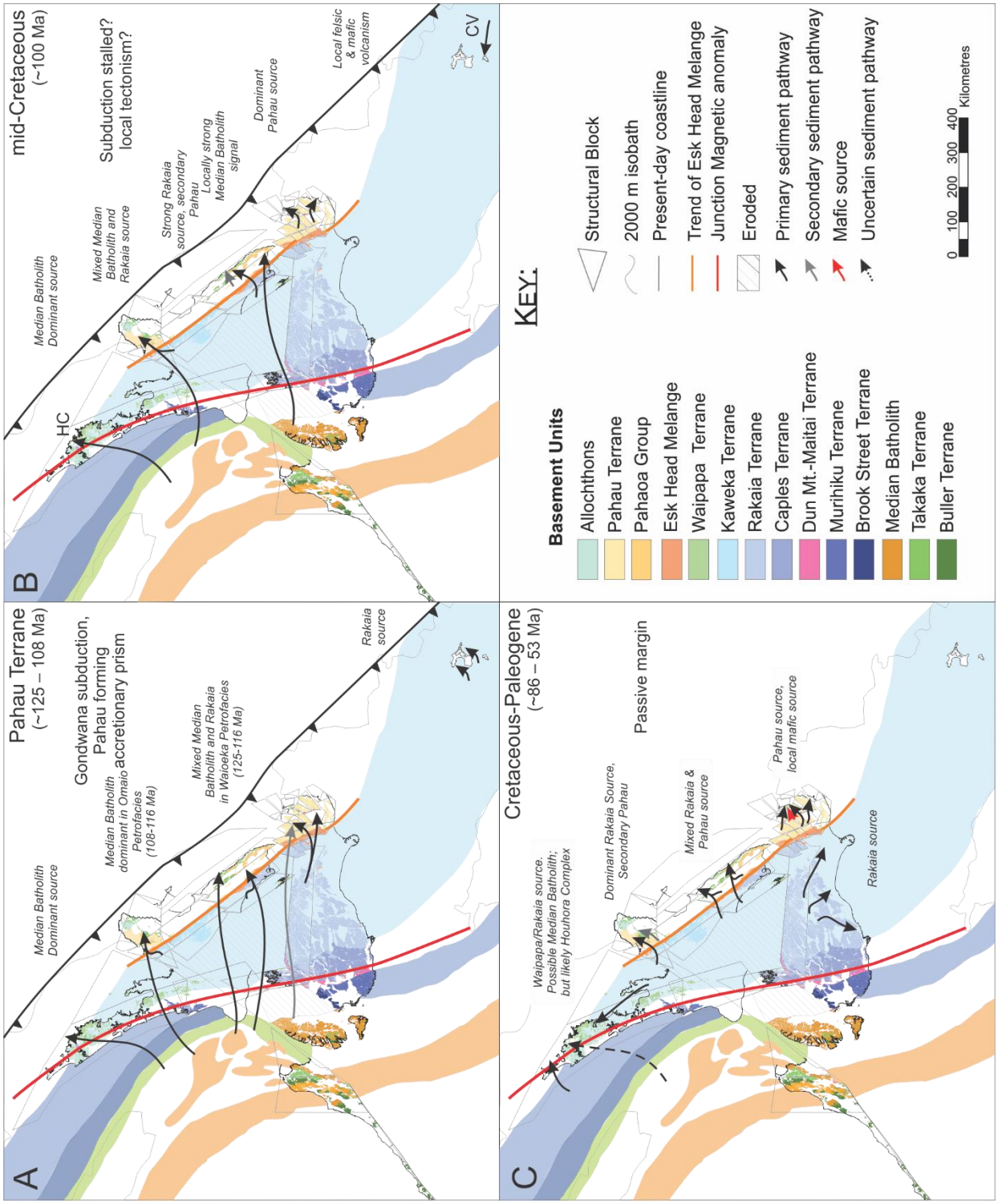

Figure 6.12: Inferred sediment transport pathways plotted on retro-deformed reconstruction of the New Zealand region during the Cretaceous-Paleogene. Interpretation of sediment transport direction and provenance for three time intervals based on provenance indicators from detrital zircon and heavy mineral assemblages, and bulk-rock geochemistry. A) 125–108 Ma during deposition of the Pahau Terrane. B) Approximately 100 Ma, during deposition of the basal cover sequence in the East Coast Basin. C) Late Cretaceous to Early Eocene deposition of basin fill and cover sequences. HC = Houhora Complex, CV = Coeval Volcanism.

Page intentionally left blank for formatting purposes

Chapter Seven

SEQUENCE STRATIGRAPHIC FRAMEWORK FOR THE LATE CRETACEOUS – PALEOGENE EAST COAST BASIN, NEW ZEALAND

Here are three distinct successive periods of existence, and each of these is, in our measurement of time, a thing of infinite duration... The result, therefore, of this physical inquiry is, that we find no vestige of a beginning, no prospect of an end.

- James Hutton, identifying the famous unconformity at Siccar Point, Scotland.
In: Theory of the Earth (1795).

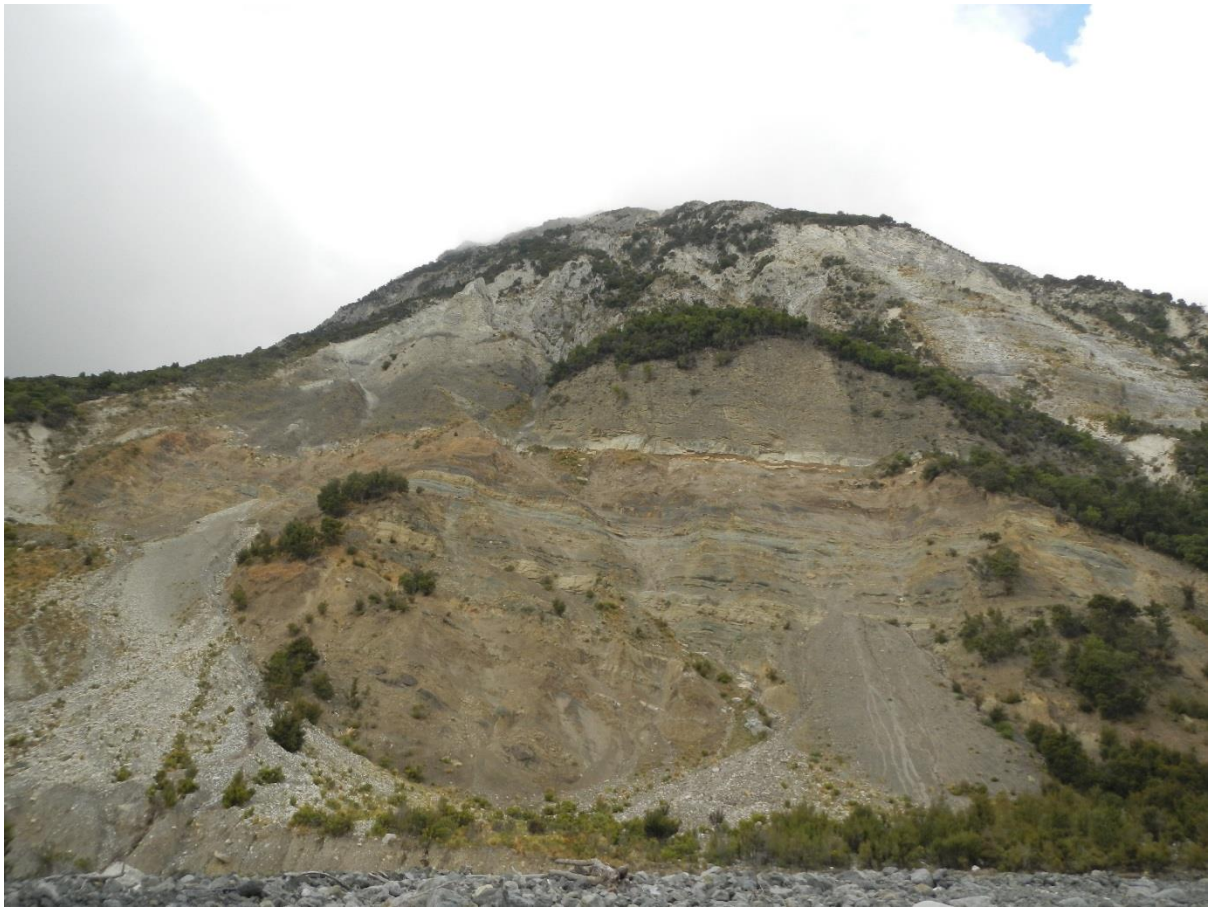

Outcrop in Wharekiri Stream, demonstrating a condensed mid-Cretaceous succession (Split Rock Formation–Branch Sandstone; Ngaterian–Haumurian), overlain by the latest Cretaceous–middle Eocene Mead Hill and Amuri Limestone formations (latest Haumurian–Bortonian). Photo taken prior to the Kaikoura earthquake of 14th November, 2016.

PREFACE TO CHAPTER SEVEN

Overview

This chapter builds upon field observations, revised age control, and published literature, most of which is discussed and reviewed in Chapters Two, Three, and Four.

The chapter introduces broad-scale (first-order) sedimentary cycles identified in the East Coast Basin by previous workers, and then discusses the sequence stratigraphic concepts used in the development of subsequent second- and third-order sequence stratigraphic frameworks. The development of a second-order sequence stratigraphic framework highlights important surfaces, intervals, and time planes for relevant palinspastic reconstructions of the basin (Chapter Eight).

A third-order sequence stratigraphic framework for the latest Cretaceous–Eocene succession in the study area is then presented, the development of which is underpinned by analysis of 52 stratigraphic sections across the East Coast Basin. This has allowed for the identification of multiple sequence boundaries, systems tracts, and other stratigraphic surfaces.

The derived sequence stratigraphic framework is then considered in the context of sequence stratigraphic records within the New Zealand region, as well as established global eustatic sea-level records.

Fission track sample preparation, counting and modelling results were supervised by Diane Seward (Victoria University of Wellington).

Chapter Seven

SEQUENCE STRATIGRAPHIC FRAMEWORK FOR THE LATE CRETACEOUS–PALEOGENE EAST COAST BASIN, NEW ZEALAND

7.1 Introduction

The first- and second-order sequence stratigraphic framework for the wider New Zealand region and the East Coast Basin are reasonably well-understood, underpinning the New Zealand mega-sequence proposed by King *et al.* (1999), and utilised by Mortimer *et al.* (2014). The 100 Myr-long transgressive-regressive mega-sequence from the Late Cretaceous to Recent (the "Zealandia Megasequence" of Mortimer *et al.*, 2014) can be further divided into largely tectonically-controlled, second-order depositional cycles of 5 to 25 Myr duration. These second-order cycles can be correlated between sedimentary basins as major, unconformity-bound packages (King, 2000b).

Such broad cycles were previously identified in the East Coast Basin by Pettinga (1982) and Moore *et al.* (1986) as an overall fining-upwards succession from Late Cretaceous sandstone to Paleocene–Eocene mudstone and muddy limestone that can be further sub-divided into four broad sedimentation phases:

1. Early- to mid-Cretaceous – Deposition of dominantly shallow-marine sediments in small, locally restricted, tectonically controlled basins.
2. Mid- to Late Cretaceous to Paleocene – Deposition of a fining-upwards siliciclastic sequence during thermal subsidence in a passive margin setting.
3. Late Eocene to Oligocene – Deposition of a fine-grained, calcareous sequence, representing peak inundation of the basin.
4. Late Oligocene – Deposition of mass-flow deposits and increased sedimentation rates in response to the southward propagation of the modern (Hikurangi) plate boundary.

The Late Cretaceous and Paleocene passive-margin succession within the East Coast Basin has previously proven difficult to extend beyond a first- or second-order sequence stratigraphic interpretation. This is primarily due to the extent of overprinted Neogene deformation and inherent difficulties in recognising <100 m sea-level variations in fine-grained, deep-marine lithologies associated with long-term deposition on quiescent margins. Through integrating widespread and detailed outcrop and facies analysis in conjunction with geochemical

characterisation of lithologic units, biostratigraphy and reinterpretation of the depositional environments and correlation between units, a multi-order sequence stratigraphic framework is herein proposed for Late Cretaceous to Eocene strata. The development and application of a regional, high-resolution dinocyst zonation scheme for the Late Cretaceous (Roncaglia *et al.*, 1999; Crampton *et al.*, 2001; Schiøler *et al.*, 2002; Schiøler & Crampton, 2014) and Paleogene (Crouch *et al.*, 2014) successions in the New Zealand region, along with Paleogene microfossil studies (Hines *et al.*, 2013; Kulhanek *et al.*, 2015), have been particularly beneficial in producing a detailed assessment of time-transgressive relationships in units across the East Coast Basin. Construction of the composite stratigraphic section for the East Coast Basin developed by and presented in this thesis has been possible through the application of revised age control across a number of key sections across the basin, and calibration of the New Zealand Geological Timescale (Raine *et al.*, 2015) to the International Geological Timescale (Gradstein *et al.*, 2012). This latter point has enabled correlation of the East Coast Basin's stratigraphy with various global stratigraphic records.

7.2 Sequence Stratigraphic Concepts

Sequence stratigraphy is a stratigraphic approach that subdivides a stratigraphic record into mappable rock bodies based on their bounding discontinuities and correlative conformities. Because of this, it can highlight cyclical patterns in depositional sequences and allows for easier correlation of lithostratigraphically variable sedimentary successions. Sequence stratigraphy was originally designed for the interpretation of seismic sections, though sequence stratigraphic principles can be readily applied to outcrop studies (Van Wagoner *et al.*, 1988; Naish *et al.*, 1996).

At least seven orders of cyclical deposition are known from sedimentary basins worldwide, resulting from tectonic and eustatically-driven changes in relative sea level and accommodation space. First order cycles are inferred to result from changes in ocean basin volume over timescales of ~100 Myr (Allen & Allen, 2013). Second order cycles, with periods of 5–100 Myr, are thought to reflect thermo-tectonic subsidence, and other large basin-scale tectonic processes (King *et al.*, 1999; King, 2000b). The origin of third-order cycles is unclear, but they may result from tectonically or eustatically-driven processes, or combinations of both (Allen & Allen, 2013). They typically occur over five to ten million years, and are governed by the interplay of local, basin-scale tectonics and climatic variables (Mitchum & Van Wagoner, 1991; Allen & Allen, 2013). Fourth- to seventh-order cycles have durations of between c. 500–19 kyrs, and are generally controlled by eustatic oscillations of sea level forced by cyclical variations in Earth's orbit (e.g. Naish & Kamp, 1997; Kondo *et al.*, 1998).

Development of a sequence stratigraphic framework requires the identification of important surfaces and unconformities. The interpretation of systems tracts used in this thesis (see below) follows the depositional sequence (II) nomenclature outlined by Haq *et al.* (1987) and Van Wagoner *et al.* (1988), as modified by Catuneanu (2006). Particular importance is attached to the identification of sequence boundaries, which are the significant, defining surfaces for any given cycle. Sequence boundaries are defined as either unconformities or their correlative conformities, the formation of which typically occurs during falling sea level. Whether a sequence boundary or correlative conformity develops is dependent upon an interplay between the depositional environment, water depth, accommodation space, and sediment supply during deposition of a given sedimentary sequence. Once a sequence has been identified, it can be subdivided into systems tracts, defined by bounding surfaces, the formation of which is a response to changes in relative sea level (Van Wagoner *et al.*, 1988; Hunt & Tucker, 1993; Naish & Kamp, 1997). These surfaces are used to identify and distinguish the individual systems tracts of a cyclic sequence, and include the regressive surface of marine erosion (RSE), transgressive surface of erosion (TSE), the maximum flooding surface (MFS), and the sequence boundary (Figure 7.1).

Lowstand Systems Tract

The sequence boundary marks the surface between the regressive systems tract (RST) and the lowstand systems tract (LST; Figure 7.1). Sequence boundaries are generated by a fall in relative sea level, resulting in a loss of accommodation space. Typically, due to low sedimentation rates and/or erosion, the RSE and sequence boundary often form a compound surface, represented as a subaerial unconformity in shallow-marine settings, and a correlative conformity in deeper marine environments (Catuneanu, 2006; Catuneanu *et al.*, 2009, 2011). The correlative conformity is often marked by an abrupt basin-ward shift in facies. In distal settings, the correlative conformity may display no distinct features, and the position can only be approximated. Often, not all components of the systems tracts within a single sequence stratigraphic cycle can be identified in the sedimentary record, particularly when assessing either deep-marine or very shallow-marine systems.

The LST forms when the rate of sedimentation outpaces relative sea level during the late-fall and early-rise stages of the sea level curve. The LST is bounded by a sequence boundary or correlative conformity at the base, and sometimes by a transgressive surface of erosion (TSE) at the top (Figure 7.1). During times of the lowest relative sea level, the incision of rivers into the exposed continental shelf allows sediment to be supplied directly into deeper-water settings, therefore LST

is sometimes accompanied by basin-floor submarine-fan deposits, and attendant delivery systems (such as canyons, channels, and levee systems).

Transgressive Systems Tract

A rise in base level may be marked by a TSE that caps the LST, and represents the first major flooding surface to follow a sequence boundary (Van Wagoner *et al.*, 1988; Figure 7.1). The TSE corresponds to the landward erosional transition of shoreface settings (Abbott, 1998). Consequently, this results in the extensive reworking of existing deposits by wave and storm currents. The TSE may be accompanied by stratigraphic condensation or erosion, particularly in shallow-marine settings, where sediments become trapped in newly formed accommodation space at the landward end of a depositional system. This can result in the formation of hardgrounds and lag deposits (Savrda, 1991; Naish & Kamp, 1997; Savrda *et al.*, 2001).

The TST forms when the rate of sedimentation is outpaced by the rate of relative sea level rise. It may be bounded by a TSE at the base and a maximum flooding surface (MFS) at the top (Catuneanu, 2006; Figure 7.1), and is marked by an upwards deepening trend. In situations where no LST deposits are preserved, the TSE may be superimposed on the sequence boundary.

Highstand Systems Tract

A MFS marks the boundary between the TST and the HST, and corresponds with the highest relative sea-level rise (Catuneanu *et al.*, 2009, 2011). The MFS is commonly represented by extensive stratigraphic condensation (Van Wagoner *et al.*, 1988; Figure 7.1). Condensation may be represented by a variety of features, including the formation of glauconite, phosphate, pyrite, and siderite (Amorosi, 1995; Catuneanu, 2006). Hardgrounds may form, and these may be subsequently mineralised with iron, manganese and phosphorite crusts (e.g. Wignall, 1991; Gale, 1996). Slow sediment accumulation rates also result in the accumulation of more skeletal material, creating unusually fossiliferous horizons or shell beds. Similarly, slow sedimentation rates allow bioturbators more time to rework sediment, resulting in an increased degree of bioturbation (Catuneanu, 2006). The MFS marks the point within a sequence that the focus of sedimentation begins to prograde basinward. At the seismic-scale, this is represented as a downlap surface that records a transition from a retrogradational stacking pattern to a progradational stacking geometry (Van Wagoner *et al.*, 1988). In outcrop, changes in dip across the downlap surface are typically too

shallow to be resolved, although the downlap surface will typically be marked by a sharp transition from bioclastic TST deposits to siliciclastic siltstone, coinciding with the MFS (Abbott, 1998).

The HST occurs during the late-rise and early-fall stages of a sea-level-rise phase, where the rate of sea-level rise falls below the sedimentation rate (Catuneanu, 2006). The HST is often bounded by a MFS at the base, and the transition into the overlying RST (see below) may be gradational, or may be marked by an erosional regressive surface of erosion.

Regressive Systems Tract

The regressive surface of marine erosion (RSE) marks a fall in base level, and may be represented by an erosional unconformity in non- to shallow-marine environments, or a correlative conformity in deeper-marine settings (Carter & Naish, 1998; Catuneanu *et al.*, 2011). The RSE marks the base of the regressive systems tract (RST, Hunt & Tucker, 1992), and develops when the rate of sea-level fall exceeds the rate of basin subsidence, resulting in the formation of an erosional surface through wave-based sea-floor scour in shallow settings (Naish & Kamp, 1997). In shallow-marine settings, continued sea-level fall results in the seaward migration of the shoreline across the RSE, typically resulting in beach and nearshore sandstone facies overlying shelfal siltstones.

The RST forms during sea-level fall, and may be bounded at its base by an unconformity in shallow marine parts of the basin. It is bounded at its top by a sequence boundary (Catuneanu, 2006; Figure 7.1). As sea level begins to fall, the development of new sequence boundary will begin to erode into underlying sediment. Consequently, the RST is rarely preserved, and entire systems tracts or even sequences can be removed during extremely low or long-lived sea-level lowstands.

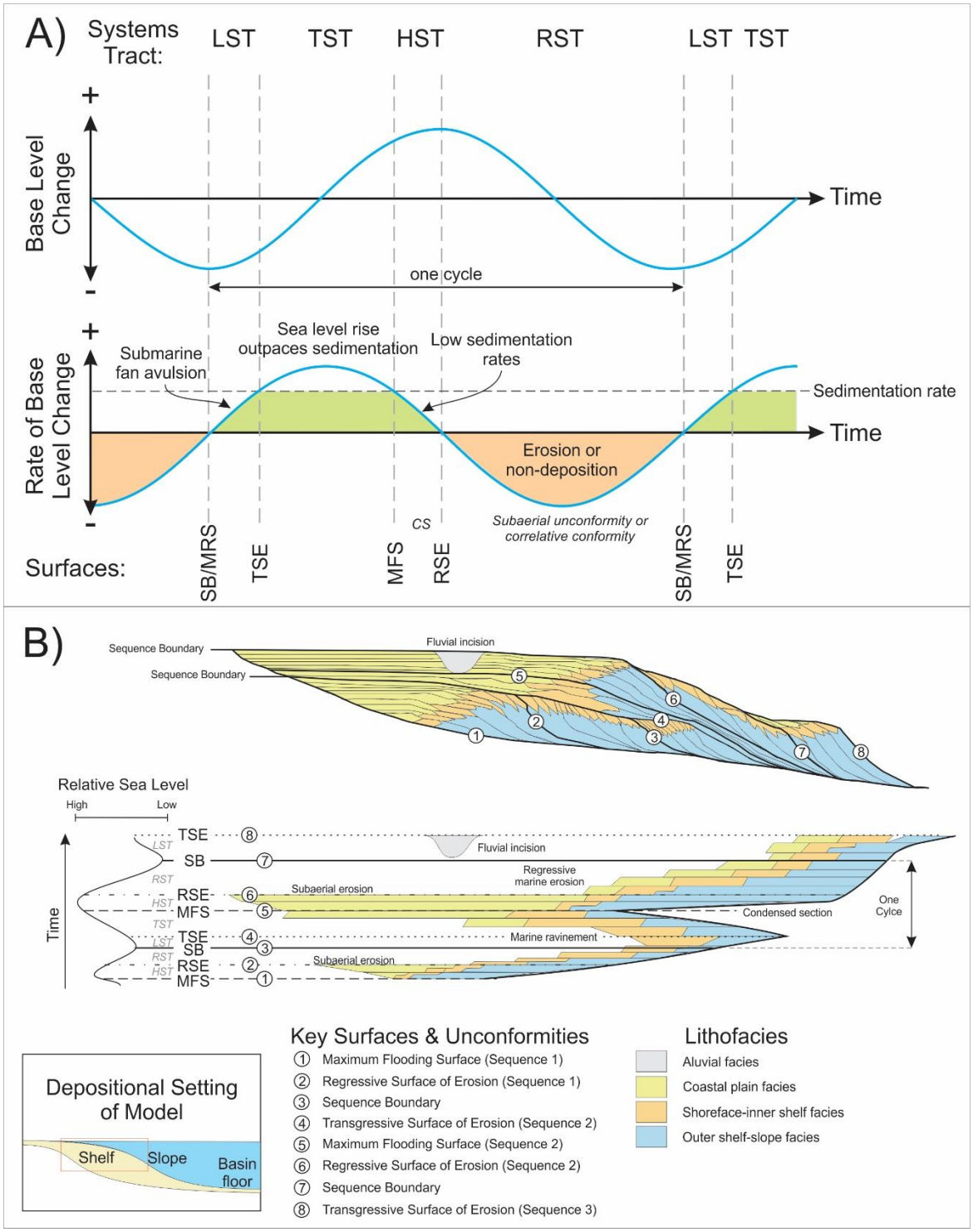

Figure 7.1: A) Relationship between base sea-level, rates of base level change and sediment supply with regard to systems tracts and surfaces, outlining basic sequence stratigraphic concepts. B) Conceptual model of stacking patterns within a sedimentary sequence, showing how sea-level change affects bathymetry, stratigraphic surfaces and facies relationships. Modified from Naish & Wilson (2009). Key to abbreviations: LST = lowstand systems tract, TST = transgressive systems tract, HST = highstand systems tract, RST = regressive systems tract, CS = condensed section, SB = sequence boundary, MRS = marine ravinement surface, TSE = transgressive surface of erosion, MFS = maximum flooding surface, RSE = regressive surface of erosion.

7.3 Second-Order Sequence Stratigraphic Division of the East Coast Basin

7.3.1 Overview

A second-order sequence stratigraphic framework for New Zealand's Cretaceous–Cenozoic succession was presented by King (2000b). Building upon this, Mortimer *et al.* (2014) presented a revised, New Zealand-wide stratigraphic hierarchal grouping of tectono-sedimentary successions. Because of the location of the East Coast Basin on the outboard edge of Zealandia as it rifted from Gondwana, and the generalisation required for a New Zealand-wide tectono- and sequence stratigraphic framework, the King (2000b) sequence boundaries do not exactly align with the significant unconformities observed in the East Coast Basin.

The Late Cretaceous to Oligocene strata of the East Coast Basin (Tinui and Mangatu groups) represent the transgressive and high-stand phases, respectively, of a first-order cycle (Zealandia Megasequence), that corresponds, in part, to the Haerenga and Waka supergroups of Mortimer *et al.* (2014). Superimposed on this are a series of successive second and possible third-order sequences. The Urutawan–Piripauan succession in the East Coast Basin essentially encompasses a period of varied but progressive basin fill, marked by complex depositional patterns in a series of disparate slope basins and variable topography that had persisted from the cessation of subduction along the Gondwana margin. This was interrupted by three significant, widespread tectonic events that outline tectonically-controlled second-order cycles in the Late Cretaceous succession.

This study has identified five second-order sequences in the East Coast Basin, each bounded by key unconformities, incorporating the Urutawan-Motuan coarse basal facies, the intra-Motuan unconformity, the intra-Ngaterian unconformity, the intra-Piripauan unconformity, the overlying transgressive trend of the Piripauan–late Teurian succession, and the Waipawan–Runangan deep-marine succession (Figure 7.2).

7.3.2 Marlborough Second-Order Sequences

Sequence One (S1)

The base of sequence S1 is marked by an angular, erosional unconformity with deposition of the coarse-grained basal facies of the Champagne Formation and correlatives over Pahau Terrane during the Urutawan (Crampton *et al.*, 2004b; Figure 7.2 & 3.3). Sequence S1 is tectonically influenced, and as such it is difficult to resolve internal systems tracts; however, the formation is tentatively identified as the LST. In Ouse Stream, a dense accumulation of *Mytiloides ipuanus* in the

lowermost Ouse Siltstone possibly marks a condensed section (Figure 2.24A), interpreted here as a transgressive surface (Figure 7.3). At Coverham (middle Clarence Valley), the upper Ouse Siltstone is marked by a coarsening-upwards trend, increasingly dominated by alternating sandstone and mudstone affected by syn-sedimentary slumping (Figure 2.24B), interpreted here as the development of a slope-fan system. The contact between the Wharf Sandstone and Swale Siltstone is marked by a thin concretionary and nodular horizon (Hollis *et al.*, 2013; J. Crampton Pers. Comms. 2018), interpreted as sediment starvation, thereby identifying a MFS and marking the base of the HST (Figure 7.3), which is characterised by deposition of laminated, bioturbated and concretionary mudstone of the Swale Siltstone. Elsewhere in Marlborough, this sequence is marked by the deposition of undifferentiated Split Rock Formation across an angular unconformity, below which lies Pahau Terrane rocks (Figure 7.2 & 7.3).

Sequence Two (S2)

The base of sequence S2 is marked by a significant unconformity, particularly in southern and southwestern Marlborough, with deposition of terrestrial lithofacies of the Warder Formation during the late Ngaterian (c. 97 Ma) over an erosional and angular unconformity with basement or Split Rock Formation (Reay, 1993; Beu *et al.*, 2014; Figures 7.2, 7.3 & 7.4). The immediately overlying shallow-marine lithofacies of the Bluff Sandstone are much more widespread and indicative of transgression during sequence S2 (Reay, 1993). Although obscured by the Gridiron Volcanics in many sections, the TSE is approximated by the contact between the Warder Formation and the Bluff Sandstone (Reay, 1993; Figure 7.3). The overlying Hapuku Group–Nidd Formation rocks represent a condensed section (Schiøler *et al.*, 2002), interpreted as the HST.

Sequence Three (S3)

Sequence S3 is represented by the Paton Formation, its base represented by an unconformable contact (Schiøler *et al.*, 2002; Figure 7.2 & 7.3). The deposition of the shallow-marine sandstones of the Paton Formation (Schiøler & Wilson, 1998; Crampton *et al.*, 2000) is interpreted as the LST, with the overlying Whangai Formation (Herring facies) interpreted as the TST (Figure 7.3). The contact between the Paton and Whangai formations is variably marked by either an unconformity, a sedimentary hiatus or a nodular horizon (Schiøler *et al.*, 2002), and to represent a transgressive surface.

Sequence Four (S4)

The base of sequence S4 is marked by the deposition of the shallow-marine (inner shelf) sandstones of the Branch Sandstone, which overlies outer shelf mudstones of the Whangai Formation (Reay & Strong, 1992). The base of the Branch Sandstone is variably marked by lag deposits, nodular horizons, and hardground development, marking the sequence boundary (Reay & Strong, 1992; Reay, 1993; This Study; Figure 7.3). The Branch Sandstone itself is interpreted as a LST, and the overlying Mead Hill Formation is interpreted as a TST, supported by rapid deepening in paleobathymetric indicators between ~68 Ma and 66 Ma (Strong *et al.*, 1995; Crampton *et al.*, 2003; Figure 7.3).

Sequence Five (S5)

Deposition of the Mead Hill Formation is interrupted by the deposition of the Waipawa Formation at Mead Stream (Strong *et al.*, 1995; Hollis *et al.*, 2005a), or elsewhere by a significant erosional unconformity at the base of the Teredo Limestone Member (Hollis *et al.*, 2005b), marking the sequence boundary for sequence S5 (Figure 7.2 & 7.3). Deposition of the Waipawa Formation around the Mead Stream area demonstrates an increased terrigenous sediment flux relative to the otherwise pelagic-dominated background sedimentation of the Mead Hill Formation, and interpreted as a LST (Chapter Four). Greensands within the Teredo Limestone Member indicate stratigraphic condensation south of Mead Stream at this time. The overlying micritic limestone and marls of the Amuri Limestone indicate a return to pelagic-hemipelagic sedimentation, with a pronounced deepening recorded through the Amuri Limestone between the Waipawan and Bortonian (Strong *et al.*, 1995). Deposition of the Fells Greensand during the Bortonian (Morris, 1987) is interpreted as reduced sedimentation rates associated with a sea-level highstand.

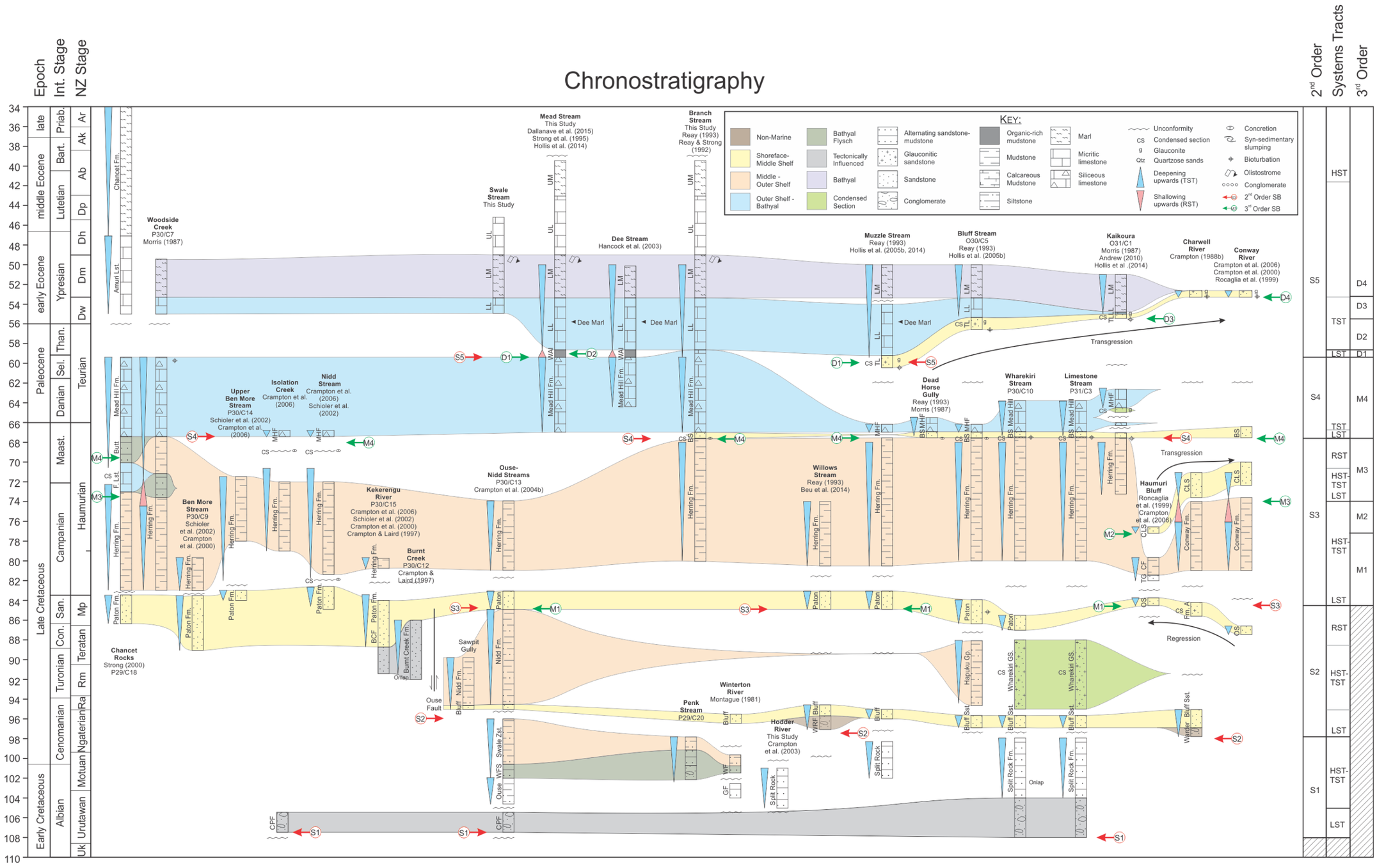

Figure 7.2: Chronostratigraphic panel for the Marlborough area, coloured by broad facies associations for the identification of second-order sequences. CPF = Champagne Formation, WF = Winterton Formation, GF = Gladstone Formation, WFS = Wharf Sandstone Member, WAI = Waipawa Formation, TG = Tarapuhi Grit, CF = Conway Formation, CLS = Claverley Sandstone, BS = Branch Sandstone, MHF = Mead Hill Formation, WF = Warder Formation, Bluff = Bluff Sandstone, F. Lst = Flaxbourne Limestone, TL = Teredo Limestone Member, LL = Lower Limestone Member, LM = Lower Marl Member, UL = Upper Limestone Member, UM = Upper Limestone Member.

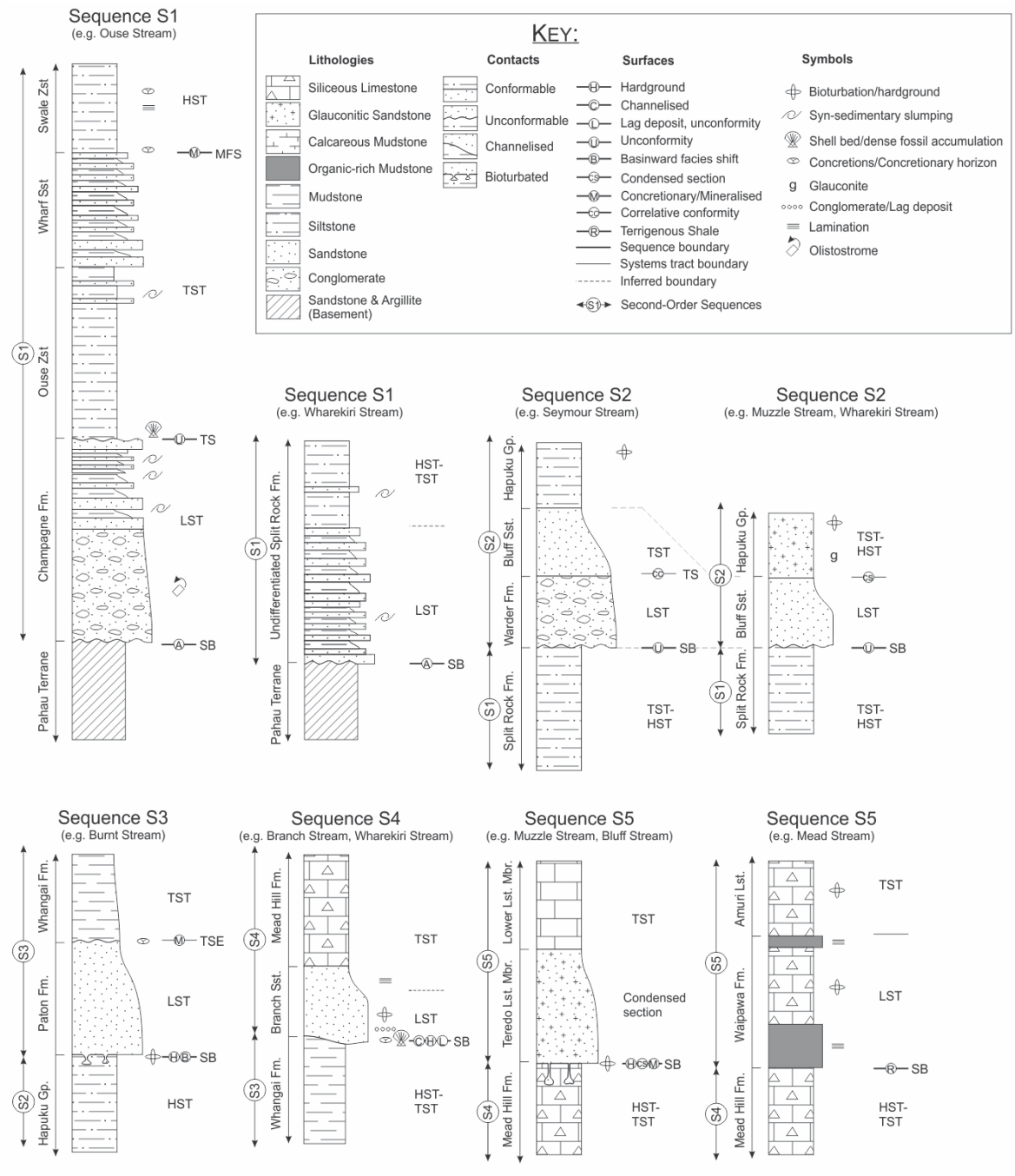

Figure 7.3: Stylised, generic stratigraphic motifs for second-order sequences in the Marlborough area. Sequences are based on those identified in Figure 7.2.

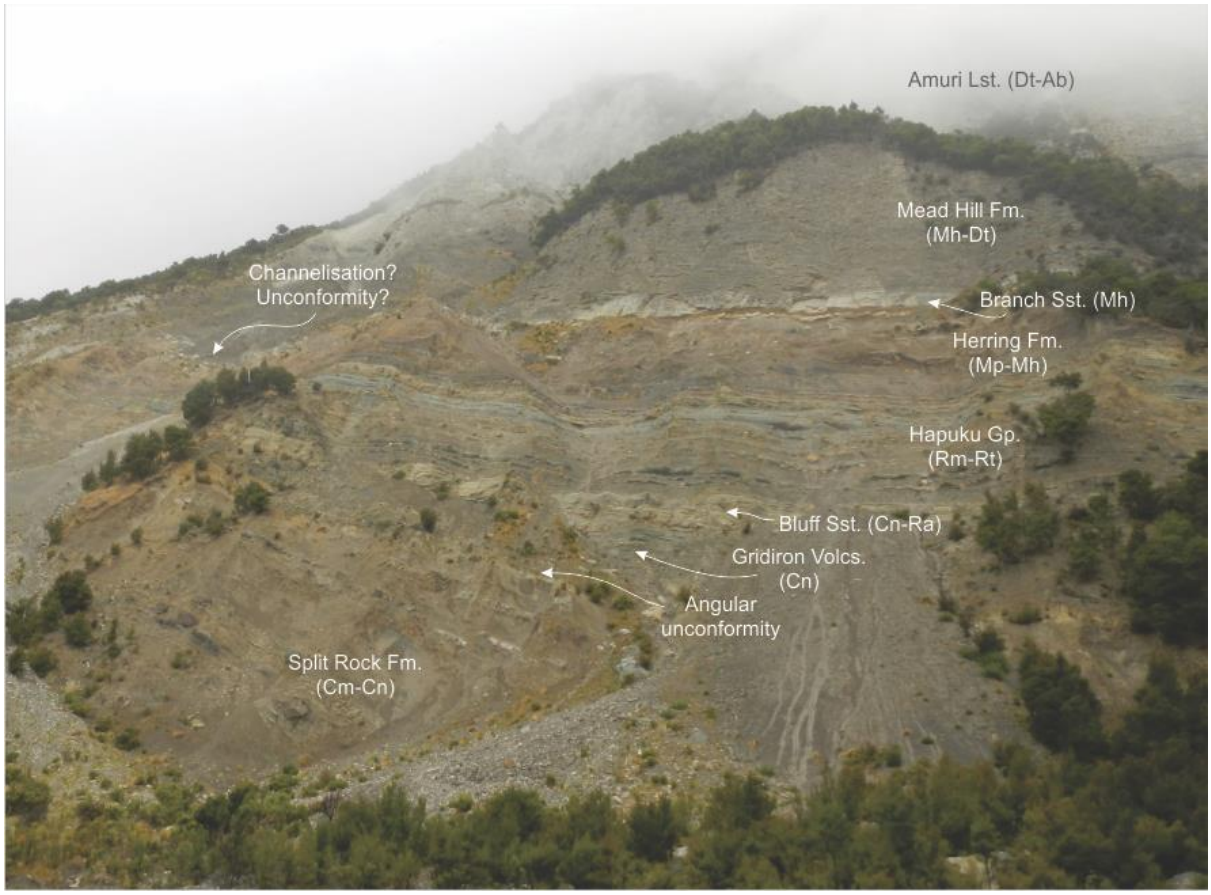

Figure 7.4: Exposure of a condensed stratigraphic section in Wharekiri Stream (BT28/652298) from Motuan–Ngaterian Split Rock Formation through to Teurian–Bortonian Amuri Limestone. There is a distinct angular unconformity separating Ngaterian Split Rock Formation and the Ngaterian Gridiron Volcanics. Notably, there is a condensed thickness of the Hapuku Group to Whangai Formation (Herring facies), collectively spanning ~24 Myr. Note the possible channel-fill or erosional unconformity at the base of the Mead Hill Formation.

7.3.3 Hawke's Bay-Wairarapa (Eastern Sub-belt) Second-Order Sequences

The stratigraphic succession and facies changes through Cretaceous to Paleogene strata of the eastern Hawke's Bay-Wairarapa demonstrate consistent, repeated, and reproducible facies transitions (Figure 7.5 & 7.6).

Sequence One & Two (S1 & S2)

In the eastern Hawke's Bay to Wairarapa regions, no sequences have yet been resolved in Clarence and Raukumara series sedimentary rocks, due to the nature of the facies associations within the deep-water, submarine-fan depositional setting of the representative Glenburn Formation. It is notoriously difficult to separate autocyclic components of deep-marine fan systems, and to then interpret within a sequence stratigraphic framework. The oldest sedimentary rocks identified

within the Eastern Sub-belt are Ngaterian in age. Therefore, within the second-order framework interpreted here, the first second-order sequence (S1) of the East Coast Basin (identified elsewhere) is absent from the Eastern Sub-belt.

The second depositional sequence identified in the Hawke's Bay-Wairarapa Eastern Sub-belt is entirely comprised of Glenburn Formation, deposited from the Ngaterian to Piripauan-lower Haumurian (Crampton, 1997; Field & Uruski *et al.*, 1997). The timing of the upper and lower sequence boundaries across this interval is consistent with the second-order cycles identified in Marlborough. Internal subdivision of this cycle is avoided here due to the complexities of the depositional setting of the Glenburn Formation.

Sequence Three (S3)

The base of sequence S3 is represented by an unconformity between the Glenburn Formation and the Rakauroa Member (Whangai Formation), a contact that is only exposed in a few locations in eastern Hawke's Bay-Wairarapa (Figure 7.5). Decimetre- to metre-bedded sandstones at the base of the Rakauroa Member are interpreted as a LST, and the overlying siliceous mudstone that forms the bulk of the Rakauroa Member is interpreted as a TST (Figure 7.6).

Sequence Four (S4)

Sequence S4 is common in the Eastern Sub-belt, and marked by deposition of the Porangahau Member, which is interpreted as a series of deep-water submarine-fan systems (Figure 7.5). These strata are coeval with deposition of shallow-marine sandstones in Marlborough (Figure 7.2), and are interpreted as a lowstand slope-fan system. The overlying Upper Calcareous Member is interpreted as a TST-HST (Figure 7.6).

Sequence Five (S5)

The base of sequence S5 is marked by the widespread deposition of the organic-rich mudstones of the Waipawa Formation, interpreted to represent increased terrigenous flux during a late Paleocene lowstand (Chapter Four; Figure 7.6). The geographically widespread expression of this event, in a range of depositional settings and sedimentary basins (Chapter Four; Figure 7.5) suggests that this was a regionally-significant event. In North Island, the Waipawa Formation marks the transition from the dominantly micaceous, poorly-calcareous mudstones of the Whangai Formation to the smectitic, highly-calcareous mudstones of the Wanstead Formation, with paleobathymetric indicators for significant deepening during this period (Chapter Two and Four). Deepening of deep-marine depositional settings through the Wanstead Formation between the Waipawan and Bortonian is indicative of the TST during sequence S5 (Figure 7.6).

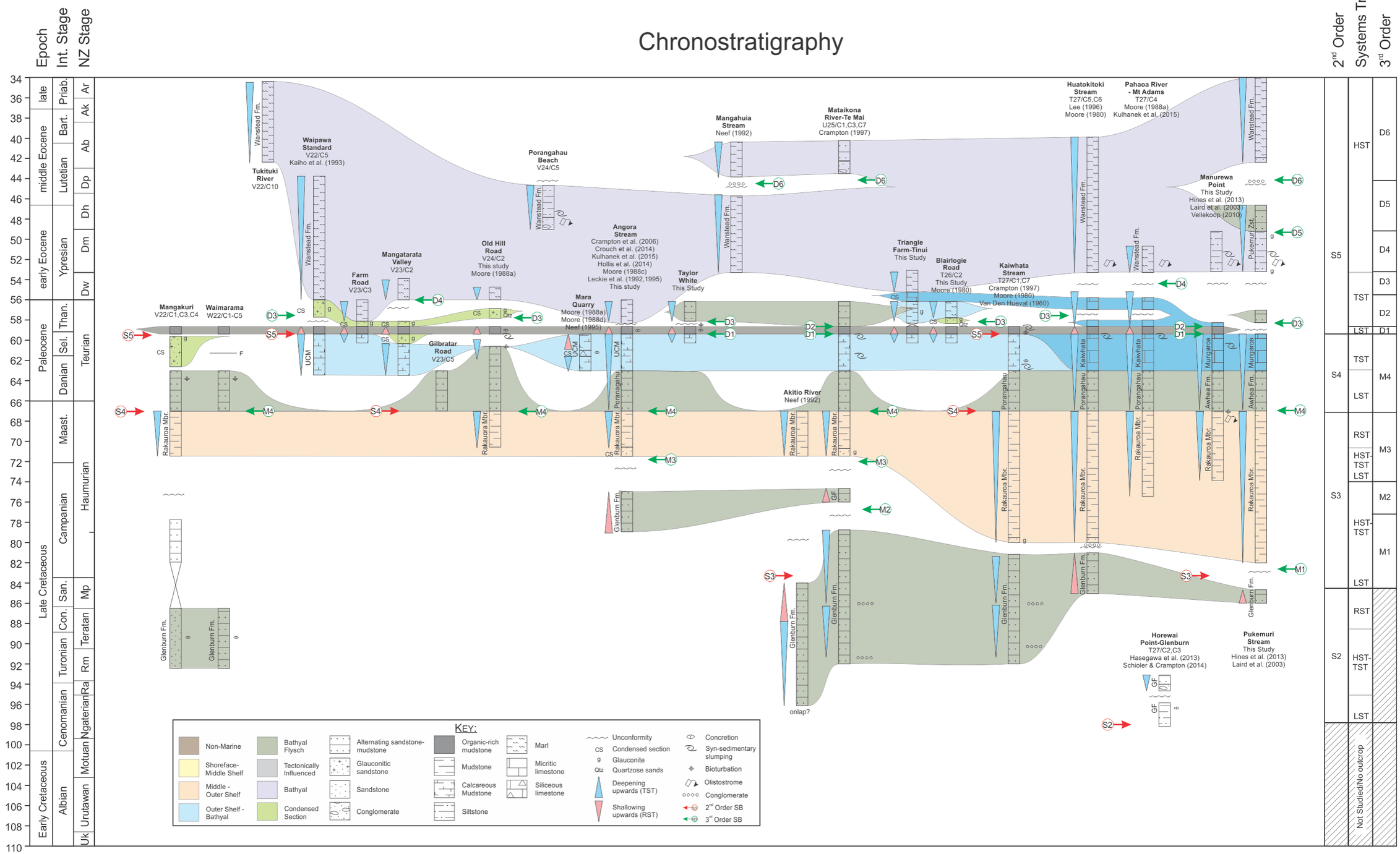

Figure 7.5: Chronostratigraphic panel, coloured by broad facies associations for the identification of second-order sequences in the eastern Hawke's Bay-Wairarapa regions. GF = Glenburn Formation, UCM = Upper Calcareous Member.

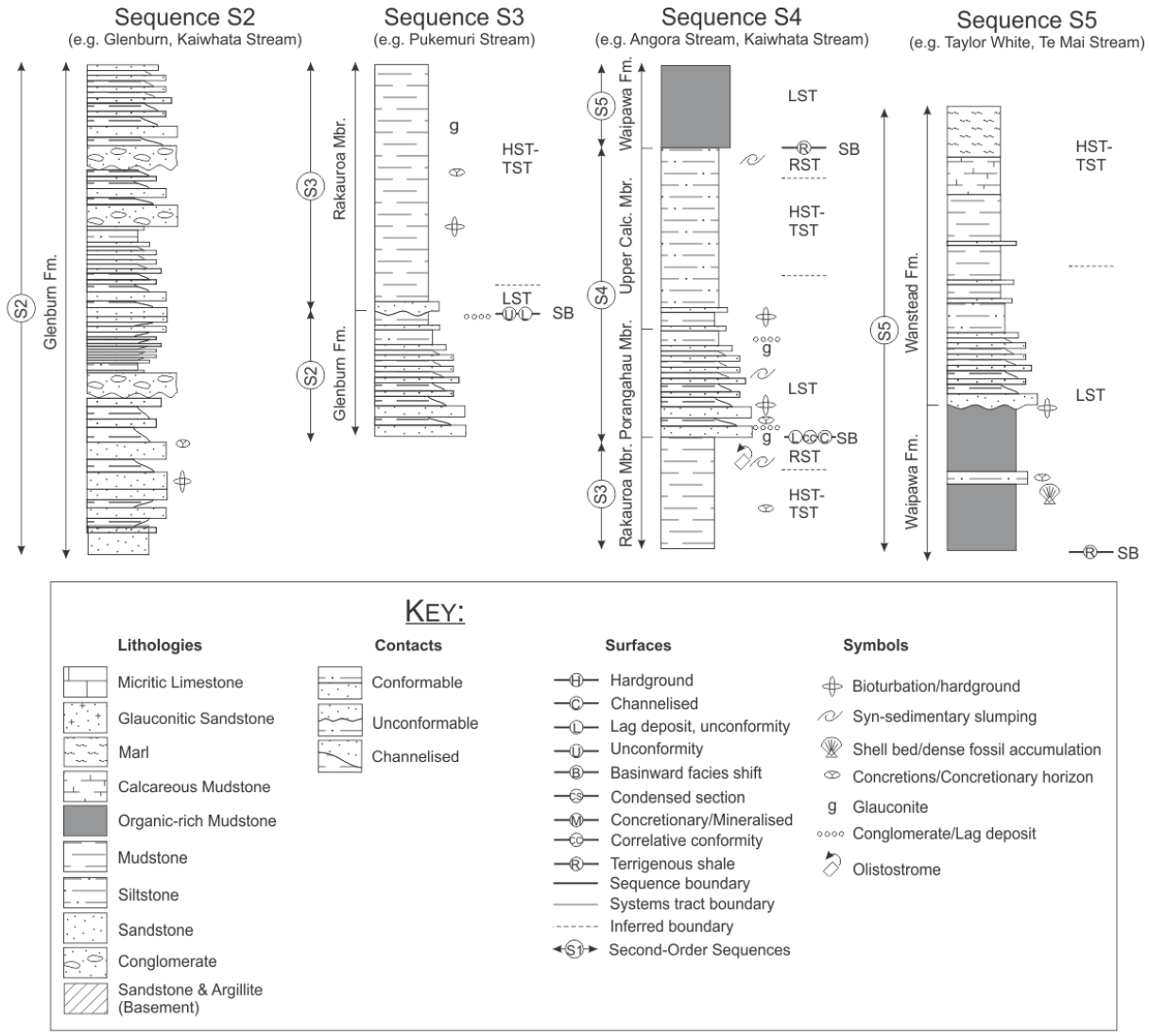

Figure 7.6: Stylised, generic stratigraphic motifs for second-order sequences in the eastern Hawke's Bay-Wairarapa area. Sequences are based on those identified in Figure 7.5.

7.3.4 Western Hawke's Bay-Wairarapa (Western Sub-belt) Second-Order Sequences

Second-order sequences in the Western Sub-belt are poorly preserved, often incomplete, and dominated by stratigraphic condensation (Figure 7.7). However, despite this, the stratigraphic succession provides some surfaces suitable for sequence stratigraphic correlation across the basin.

Sequence One & Two (S1 & S2)

The base of sequence S1 is marked in the Whangai Range by an erosional, angular unconformity, upon which the coarse-grained sedimentary melange of the Gentle Annie Formation lies (Crampton, 1989; Figure 7.7). This is broadly interpreted as a LST, although the formation is likely tectonically influenced (Crampton, 1989). The overlying Springhill Formation is interpreted as

shallowing-upwards during the sequence S2 succession with progressively decreasing sedimentation rates (Adams, 1985; Crampton, 1997), indicative of a TST and HST (Figure 7.8).

Sequence Three (S3)

In the Whangai Range, the base of sequence S3 is marked by a significant unconformity, where in most sections, all of the Raukumara series has been removed (Figure 7.7 & 7.8). Immediately above the unconformity, the coarse Piripauan-aged basal facies of the Tangaruhe Formation is interpreted as a LST (Figure 7.8). This grades upwards into highly bioturbated, glauconitic mudstone of Piripauan to early Haumurian age, indicative of reduced sedimentation rates during a TST and HST. The high glauconite content of the Tangaruhe Formation (Crampton, 1997), and abundant fish teeth in grain mounts (this study), suggest the upper part of the formation represents a condensed section, interpreted as a HST.

Sequence Four (S4)

A significant unconformity (~11 Myr; Crampton *et al.*, 2006; FRED) separates the Tangaruhe Formation and Rakauroa Member (Whangai Formation), marking the sequence boundary between sequences S3 and S4 (Figure 7.7 & 7.8). The base of the Rakauroa Member is marked by metre- to decimetre-bedded sandstone, interpreted as a LST, that grades upwards into siliceous, concretionary mudstone indicative of reduced sedimentation rates during a TST (Figure 7.8).

Most of the Paleocene (66–57 Ma) is represented by a condensed section in the Whangai Range area by the Te Uri Member (Whangai Formation), marked by a bioturbated glauconitic sandstone at the base, interpreted here as the S4 MFS (Figure 7.8). The basal glauconitic sandstone of the Te Uri Member sits above the K-Pg boundary, representing a condensed section during the HST (Figure 7.8). Elsewhere, the Teurian Stage is removed across a bioturbated unconformity between the Rakauroa Member and the Waipawa Formation, marking the S5 sequence boundary.

Sequence Five (S5)

The upper glauconitic sandstone of the Te Uri Member has been geochemically correlated with the Waipawa Formation (Rogers *et al.*, 2001), and is interpreted as a condensed section during the S5 LST (Figure 7.8). The timing of sequence five in eastern Hawke's Bay-Wairarapa is approximately coincident with the formation of a hardground at the base of the upper Te Uri Member at Tawanui (Leckie *et al.*, 1992; Taylor, 2011; Hollis *et al.*, 2014), suggesting this hardground represents the sequence boundary (Figure 7.8).

Condensed sections are apparent in the Wanstead Formation in the Whangai Range, although identification of sequence-bounding unconformities or correlative conformities are lacking, and age control is generally poorly resolved, and as such sequence stratigraphic interpretations are not resolved through sequence S5 (Figure 7.7). The MFS in sequence S5 is represented by a glauconitic sandstone unit marking the top of the Wanstead Formation during the Bortonian–Kaiatan in the Whangai Range area (Leckie *et al.*, 1992; Morgans, 2016), corresponding with the approximately coeval Te Waka Greensand lithofacies in Raukumara Peninsula (Phillips, 1985; Kenny, 1984, 1986), and the Bortonian-aged Fells Greensand Member of the Amuri Limestone in Marlborough (Morris, 1987; Reay, 1993).

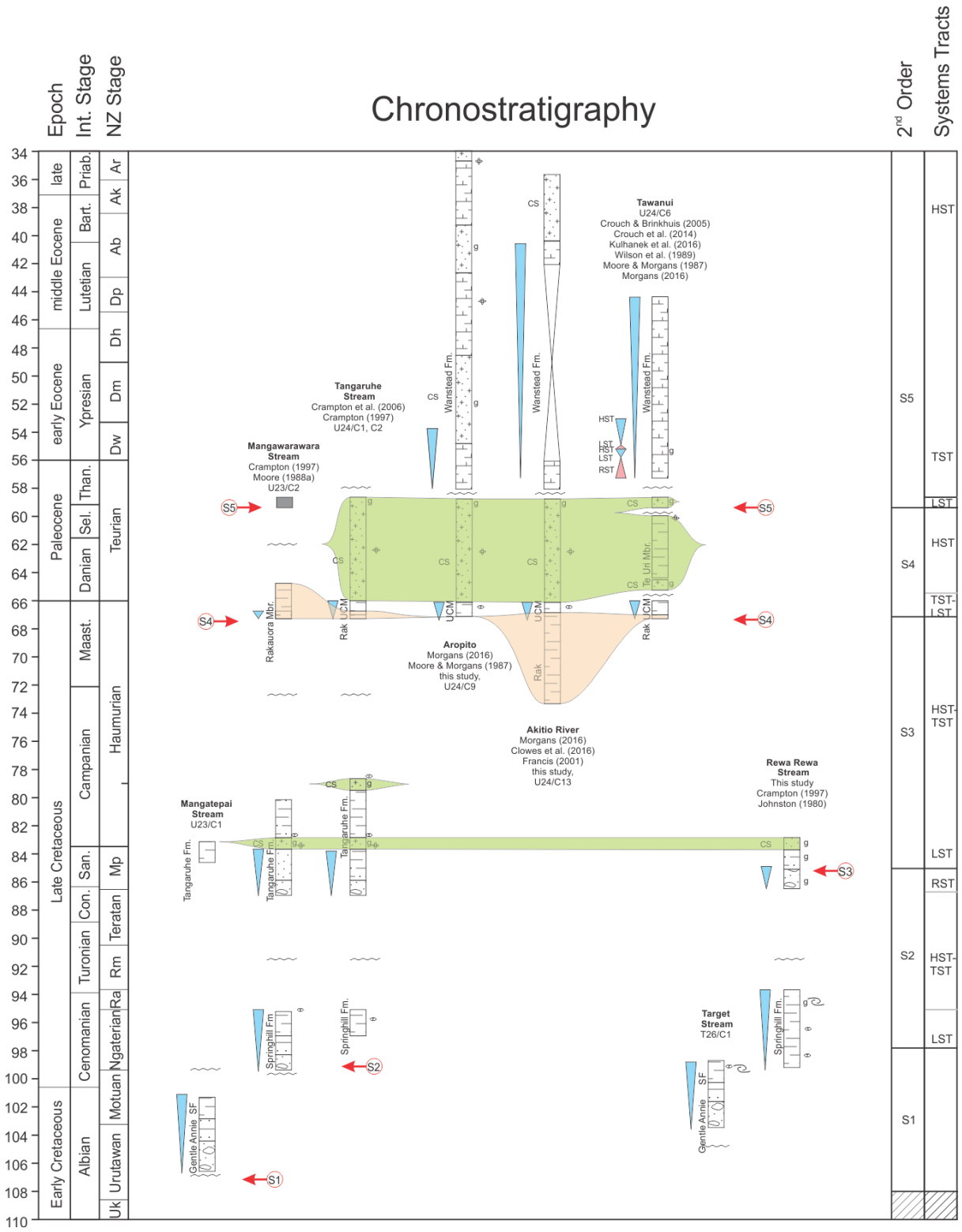

Figure 7.7: Chronostratigraphic panel, coloured by broad facies associations for the identification of second-order sequences, in the western Hawke's Bay-Wairarapa region. SF = Springhill Formation, Rak = Rakauroa Member, UCM = Upper Calcareous Member. Refer to Figure 7.5 for key.

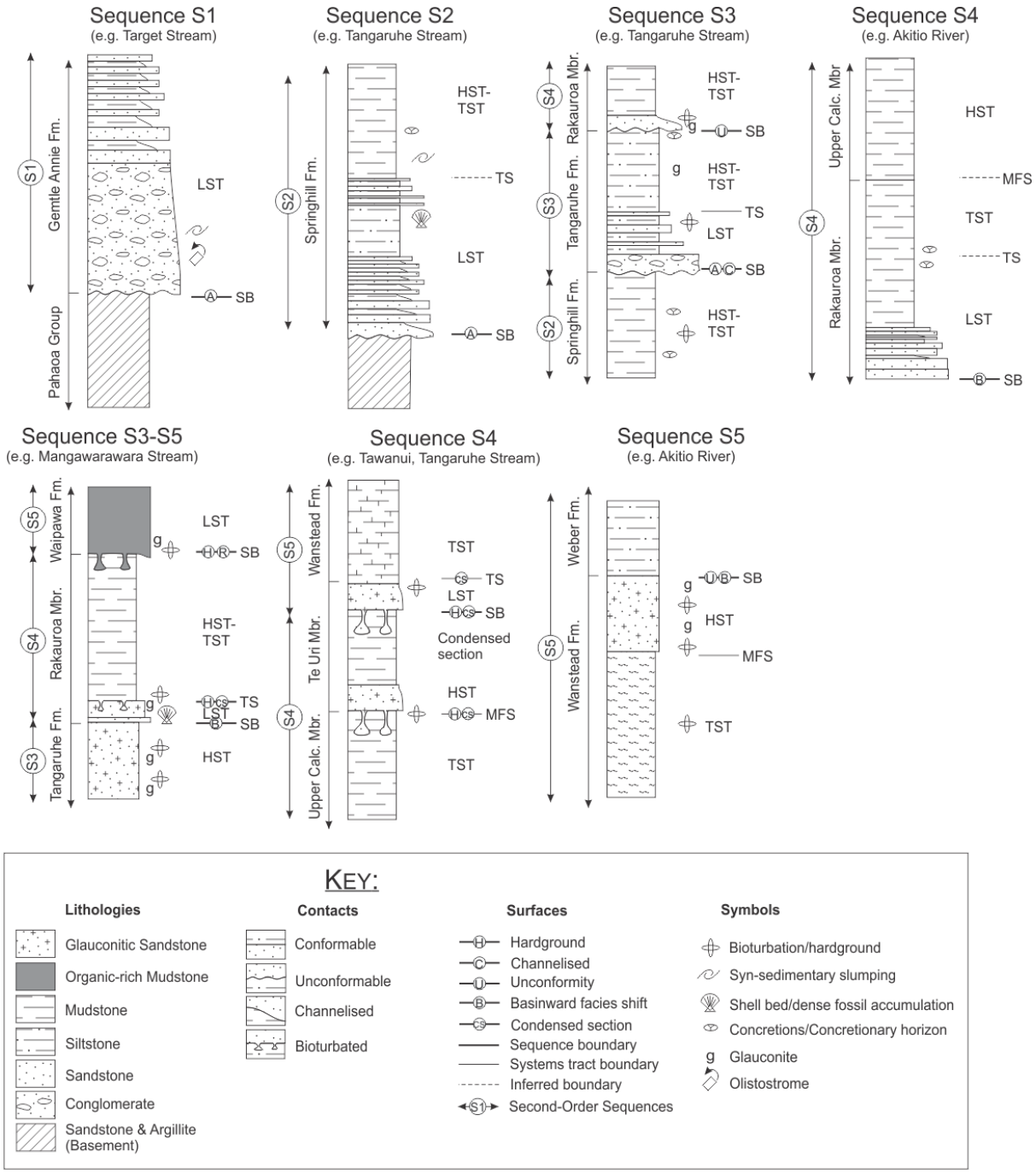

Figure 7.8: Stylised, generic stratigraphic motifs for second-order sequences in the western Hawke's Bay-Wairarapa area. Sequences are based on those identified in Figure 7.7.

7.3.5 Raukumara Peninsula-East Cape Second-Order Sequences

Stratigraphic relationships in the Raukumara Peninsula are complex and, for much of the Cretaceous–Paleogene succession, identifying and correlating full sequences across the region is difficult. In the East Coast Allochthon, Cretaceous sedimentary rocks are almost entirely comprised of the Glenburn (Tikihore) Formation, and identification and correlation of sequences

within the long-lived, widespread deep-marine fan system is difficult. However, the sequences that are identified correspond with those in the Hawke's Bay-Wairarapa and Marlborough areas. Here, the East Coast Allochthon and Western Sub-belt sedimentary successions are considered together.

Sequence One (S1)

The base of sequence S1, within the Urutawan Stage (c. 108 Ma), is marked by an erosional, angular and sometimes channelised unconformity into the underlying Pahau Terrane and/or Koranga Formation. The lowermost sedimentary strata in the sequence typically comprise sandstones and conglomerates of the basal Karekare Formation, and the Te Wera and Waimana sandstones, interpreted here as the LST (Figure 7.9 & 7.10). These coarse basal facies grade upwards into the siltstones and mudstones of the Karekare Formation, with the contact marking the transgressive surface (Figure 7.10). In the Waitahaia River area, the Karekare Formation records marine deepening between the Motuan to Ngaterian stages (Phillips, 1985), interpreted here as the TST.

Sequence Two (S2)

A coarsening trend from the late Ngaterian to the Arowhanan (Phillips, 1985), represents the LST of sequence S2 (Figure 7.10). Deposition and interfingering of the Waitahaia Formation with Karekare Formation during the Ngaterian is interpreted as development of a lowstand fan system, with the transition into the overlying concretionary mudstone typical of the Karekare Formation occurring during the Raukumara Series, and representative of the TST (Figure 7.9 & 7.10). In Mangaotane Stream, the mid-Teratan (c. 88 Ma) corresponds with a coarsening of sedimentary lithofacies (Crampton *et al.*, 2001), that possibly marks a RST of Sequence 2.

Sequence Three (S3)

The base of sequence S3 is generally marked by a significant unconformity between the Karekare and Tahora Formations, marking the sequence boundary at c. 86 Ma (Figure 7.9 & 7.10). Sequence S3 is well-represented in the Raukumara area, marked by the widespread deposition of the Tahora Formation (Figure 7.9). Alluvial sedimentary lithofacies at the base of the Tahora Formation (Moore *et al.*, 1988; Browne, 1991; Isaac *et al.*, 1991) represent the LST, with the transition into shallow-marine facies through the Piripauan marking the overlying TST (Figure 7.10). The alternating sandstone-mudstone package at the base of the Owhena Formation is interpreted as a correlative lowstand fan, which in turn grades up into mudstone-dominated, outer shelf facies representative of the TST-HST (Figure 7.10). The upper and lower contacts of the Owhena Formation are marked by nodular horizons and a sedimentary hiatus, indicating stratigraphic condensation. The lower contact with Teratan-aged Karekare Formation is interpreted here as the

sequence S3 boundary, whereas the upper contact with the Haumuriana-aged Rakauroa Member is interpreted as the transgressive surface of erosion (Figure 7.10).

In sections where the Tahora or Owhena Formations are not present, the base of the Rakauroa Member is marked by an unconformable surface overlain by a basal conglomeratic lag and sandstone that grades up into the siliceous mudstone (e.g. Mangaotane Stream). The Rakauroa Member is interpreted as the TST to HST, with the lower contact between the shallow-marine sandstones of the Tahora Formation and outer shelf mudstones of the Rakauroa Member interpreted as a TSE.

Sequence Four (S4)

Throughout much of the Raukumara area, the sequence boundary for sequence S4 is not identified, and age control on the Rakauroa and Upper Calcareous members is poor. At the very least, the Rakauroa Member is largely restricted to the Haumurian Stage (latest Cretaceous) and the Upper Calcareous Member is primarily Teurian (Paleocene) in age, and the transition between the two generally represents a fining upwards trend with progressively decreasing sedimentation rates up-section. Such lithofacies trends likely represent marine transgression. Sequence S4 is recognised in the East Coast Allochthon by an unconformity of a late Haumurian (c. 68 Ma) age that separates Glenburn Formation and Rakauroa Member, thereby marking the sequence boundary. In the Te Hoe River-Mangahouanga Stream area of northwest Hawke's Bay, deposition of the Te Uri Member marks an early to middle Teurian condensed section, interpreted as a HST (Figure 7.10). The bioturbated basal contact of the Te Uri Member (Moore, 1987a) is interpreted as the MFS (Figure 7.10).

Sequence Five (S5)

In Rakauroa Stream the Upper Calcareous and Te Uri Members are missing entirely, with a significant, bioturbated unconformity at the base of the Waipawa Formation. The bioturbated contact between either the Rakauroa or Te Uri members with the overlying Waipawa Formation marks the S5 sequence boundary, represented by the abrupt lithofacies transition into the Waipawa Formation (Figure 7.10). Above this interval, very few detailed stratigraphic logs for the Wanstead Formation are available, and only isolated, partial records are identified (Figure 7.9). The Bortonian-aged Te Waka Greensand lithofacies in the Mangatu area (Kenny, 1984, 1986; Field & Uruski *et al.*, 1997), is a condensed section, interpreted as the MFS within this sequence (Figure 7.9 & 7.10).

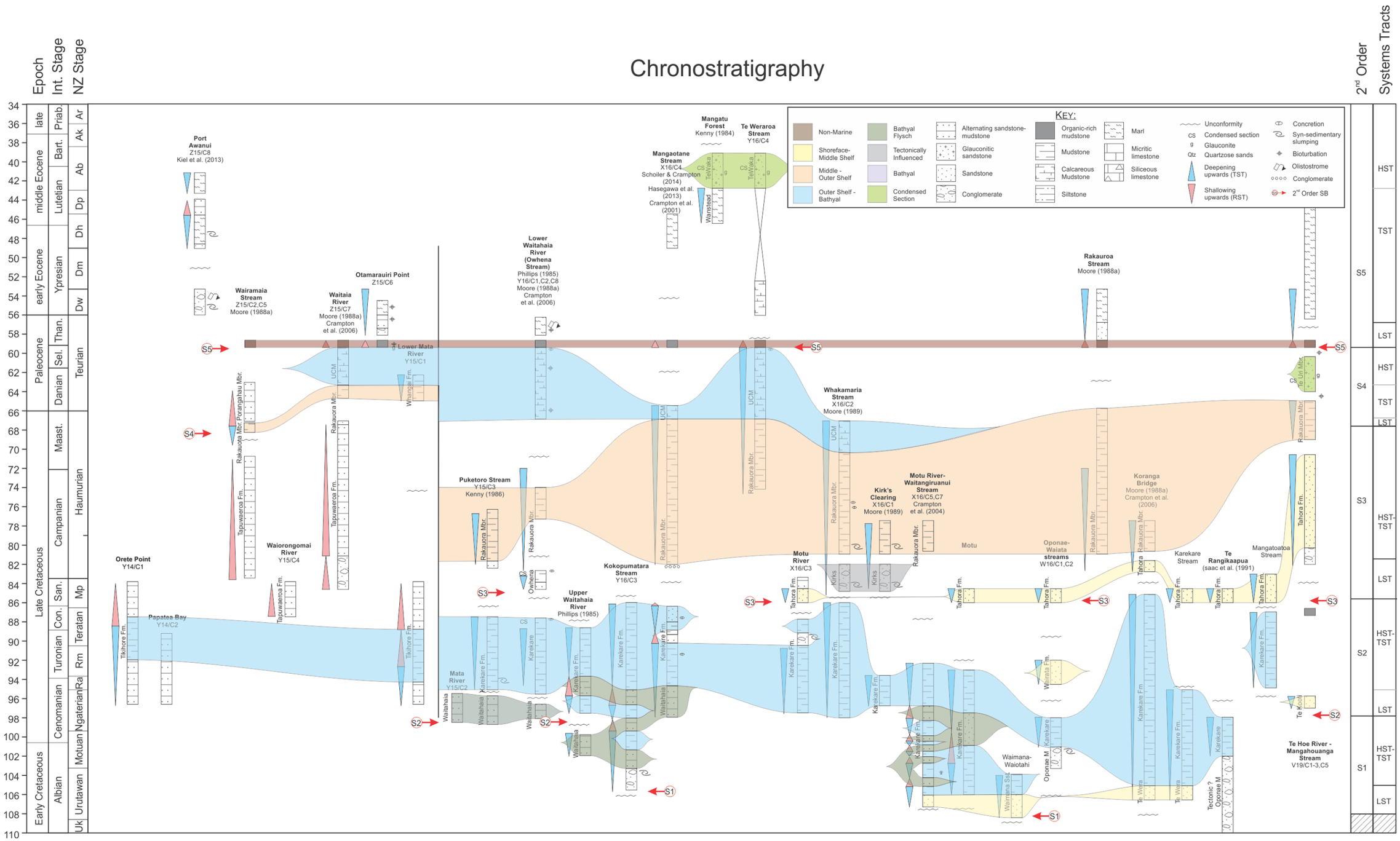

Figure 7.9: Chronostratigraphic panel for the Raukumara Peninsula-East Cape area, coloured by broad facies associations for the identification of second-order sequences. UCM = Upper Calcareous Member.

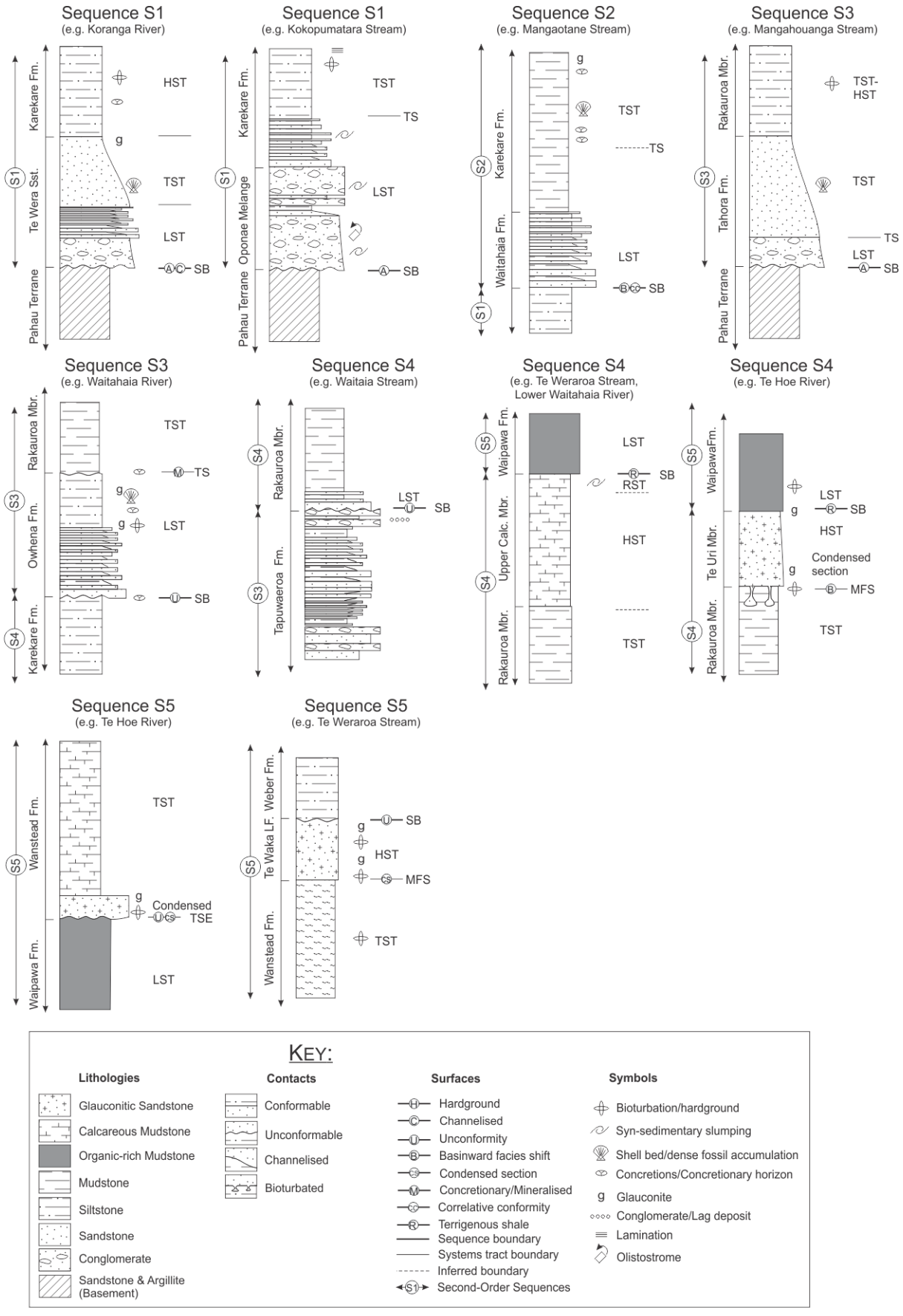

Figure 7.10: Stylised, generic stratigraphic motifs for second-order sequences in the Raukumara Peninsula-East Cape area. Sequences are based on those identified in Figure 7.9.

7.4 Correlation of Second-Order Sequences

Sequence S1

The oldest sequence recognised by King (2000b) comprises mid-Cretaceous non-marine and marine transgressive deposits overlying a Ngaterian unconformity. This unconformity is widely recognised across New Zealand sedimentary basins, where it generally separates "basement" from "cover" rocks. However, within the East Coast Basin, deposition of the cover succession had been occurring since the Korangan Stage in the Raukumara area (Koranga Formation), and since the Motuan Stage in Marlborough, whereas deposition of so-called basement rocks continued elsewhere (Mazengarb, 1993; Mazengarb & Harris, 1994; Crampton *et al.*, 2003; Laird & Bradshaw, 2004). These cover rocks are widely represented across the East Coast Basin by coarse-grained basal facies (e.g., Koranga, Oponae Melange, Gentle Annie, and Champagne formations; Figure 7.11 & 7.12), which are overlain by marine sandstones and mudstones, and typically truncated by a Ngaterian unconformity (e.g., Figure 7.4). In western parts of the East Coast Basin, particularly Marlborough (Crampton & Laird, 1997), the early depositional phases of this sedimentary sequence began between 108–103 Ma within fault-controlled grabens (King *et al.*, 1999; Davy *et al.*, 2008). Elsewhere in the East Coast Basin, infilling of extensional basins appears to have usually occurred around the base of the Motuan Stage (Moore & Speden, 1984; Crampton, 1989; Laird, 1992 Laird & Bradshaw, 2004). Therefore, the base of the stratigraphically lowest second-order sequence within the East Coast Basin ranges from Korangan to Ngaterian age. This interval has a duration of ~20 Myr, and as such, is unlikely to represent the true base of a single second-order sequence. Rather, this likely represents at least two sequences, but the lower sequence (of Korangan age) is only preserved in a few isolated pockets (e.g. Koranga Formation at Koranga). Taking this into account, the base of the lowermost sequence that can be correlated across the basin is Urutawan in age (Sequence S1; Figure 7.11), and the overlying second-order sequence is dominantly comprised of the Champagne, Split Rock, Gentle Annie, Springhill, and Karekare Formations (Figure 7.12).

Sequence S2

A widespread intra-Ngaterian unconformity marks the top of the lowermost widespread sequence in the East Coast Basin, marking the sequence boundary for sequence S2. In several sections, an angular unconformity marks the sequence boundary (e.g., Figure 7.4), and elsewhere, there is an abrupt basinward facies shift during the mid-Ngaterian. The overlying sequence is dominantly comprised of Hapuku and Wallow Group sedimentary rocks in Marlborough, and in North Island by the deposition of the Karekare and Glenburn formations (Figure 7.12). An approximately intra-

Piripauan unconformity has been recognised widely across the East Coast and Canterbury basins, thereby constraining the top of the S2 sequence within the East Coast Basin (King *et al.*, 1999; King, 2000b; Crampton *et al.*, 2006; Figure 7.11). This sequence is dominated by the widespread deposition of marine sedimentary rocks (e.g., Karekare Formation, Glenburn Formation).

Sequence S3

The late Piripauan to late Haumurian was characterised by regional marine transgression and the progressive burial of submarine topography, by an upwards-fining succession, and the onset of passive-margin subsidence throughout the East Coast region (Figure 7.11). Included within this sequence are the sandstone-dominated Tangaruhe and Tahora formations in western parts of the basin, and mass-flow conglomerate and flysch lithofacies of the upper Glenburn Formation in eastern parts of the basin. In Marlborough, the sequence comprises shallow-marine sandstones of the Paton Formation, and Tarapuhi Grit, and Okarahira Sandstone, which are overlain by the dominantly siliceous and micaceous lithofacies of the Haumurian-aged Whangai (Rakauroa Member and Herring facies) and Conway formations.

Sequence S4

A late Haumurian unconformity across the basin marks base of the S4 sequence. The sequence encompasses deposition of the Porangahau Member and Butt Formation fan systems, and the coeval, inferred, shallow-marine sandstones of the Branch Sandstone (Figures 2.39, 2.41 & 7.11). Deposition of these units imply a drop in relative sea level across the basin. This corresponds with Moore (1989c), who interpreted the deposition of the Porangahau Member as representing a sea-level regression of ~50 m across the K-Pg boundary, which in turn caused the progradation of submarine fans, and was in turn followed by rapid transgression and deposition of the Upper Calcareous Member (Moore, 1988b, 1989c). Sequence S4 becomes increasingly calcareous up-section, reflected by deposition of the Upper Calcareous Member-Mungaroa Limestone-Mead Hill Formation in the latest Haumurian and the early Teurian (latest Cretaceous–early Paleocene; Figure 7.12).

Sequence S5

The late Teurian Waipawa Formation marks distinctive lithological changes in the East Coast Basin, from siliceous, micaceous lithofacies to smectitic clay-rich calcareous lithofacies in North Island (Chapter Four), and from siliceous limestone to micritic limestone and marl in Marlborough. Therefore, this study suggests that the base of the Waipawa Formation, and age-equivalent strata, marks a late Teurian sequence boundary (Figure 7.11 & 7.12). In the largely slope

settings that this formation was deposited in (Chapter Four), this is expressed as a correlative conformity at the base of the Waipawa Formation. The timing of this event corresponds with a significant fall in eustatic sea level in both the Haq *et al.* (1987) and Kominz *et al.* (2008) sea-level curves (Figure 7.12). Rocks above this sequence boundary are characterised by the deposition of clay- and carbonate-rich sedimentary facies (Wanstead and Amuri Limestone formations), indicative of progressive transgression, reducing terrigenous sediment input, and notable deepening across the basin (Strong *et al.*, 1995; King, 2000b; Hollis *et al.*, 2005a; Hines *et al.*, 2013; Figure 7.12). The Wanstead Formation represents the deepest depositional environment of the Cretaceous–Paleogene East Coast Basin succession, with paleodepths ranging from mid-bathyal to abyssal (Field & Uruski *et al.* 1997; Hines *et al.*, 2013).

The late Eocene to early Oligocene is widely considered to represent peak marine transgression and passive-margin development around Zealandia (e.g. Landis *et al.,* 2008). In the East Coast Basin, this interval is represented by the boundary between the Wanstead and Weber formations, which is generally marked by a greensand facies (Leckie *et al.*, 1992; Clowes *et al.*, 2016; Figure 7.12). This greensand facies is interpreted to mark the regional MFS of the King (2000b) first-order cycle (Figure 7.12). In addition to this, the Oligocene saw the development of permanent Antarctic ice sheets and the associated deep-water formation (Kennett, 1977; Coxall *et al.*, 2005; Lyle *et al.*, 2007), resulting in the development of a deep western boundary current along the eastern margin of Zealandia and the widespread development of the Marshall Paraconformity in the East Coast and Canterbury basins between 29–32 Ma (Lewis, 1992; Fullthorpe *et al.*, 1996; Carter *et al.*, 2004; Morgans, 2016).

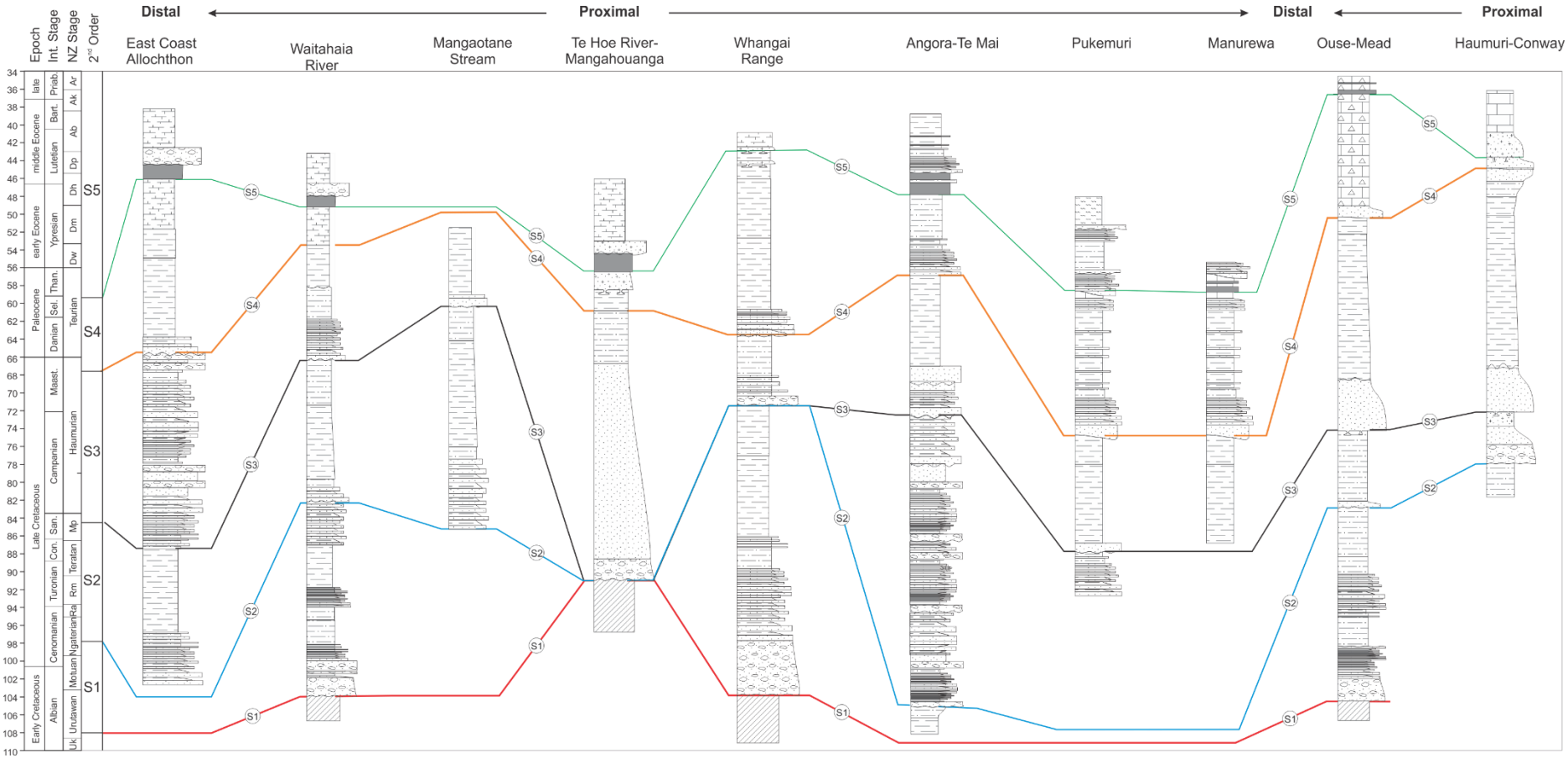

Figure 7.11: Correlation of second-order sequences across composite sections for the various sub-regions of the East Coast Basin with the New Zealand geological timescale (NZ GTS 15; Raine *et al.*, 2015).

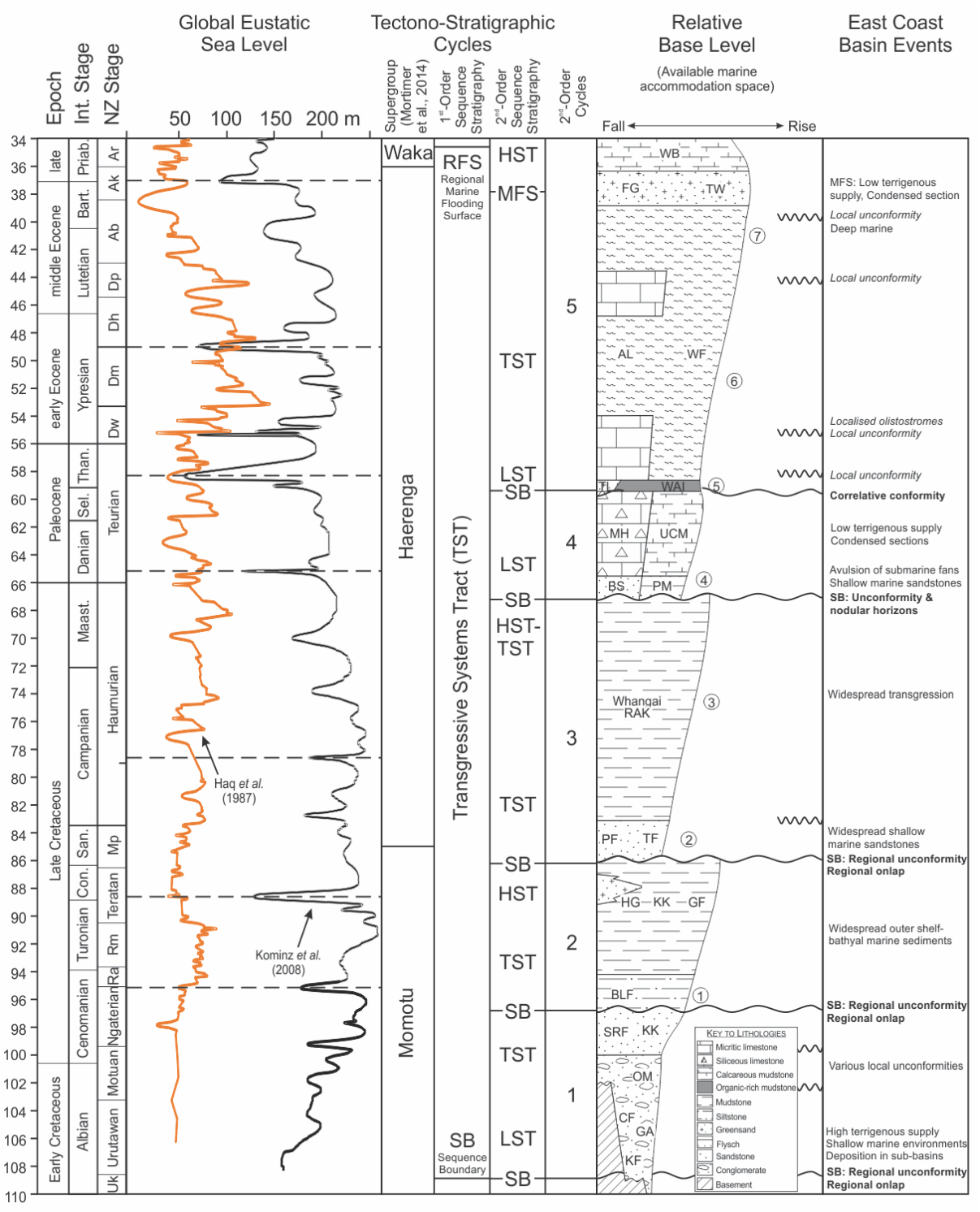

Figure 7.12: Generalisation and summary of the Cretaceous-Paleogene stratigraphic succession in the East Coast Basin, and the stratigraphic position of second-order cycles defined in this chapter. Geological timescale is from Raine *et al.* (2015). The global sea-level curve from Haq *et al.* (1987) and Kominz *et al.* (2008) are shown for reference. Second-order cycles from the Kominz *et al.* (2008) curve are bounded by dashed lines. Stratigraphic supergroups from Mortimer *et al.* (2014), and first-order sequence stratigraphic divisions from King (2000b). The graphic lithology summarises broad changes in relative sea level for the East Coast Basin (and therefore sediment accommodation space), providing

an indication of changing relative base level. Second-order sequence stratigraphic divisions are informed by regionally significant surfaces, basin-wide assessment of shoreline progradation or retrogradation, and changes in relative base level. Timeplanes identified for palinspastic reconstruction (Chapter Eight) are labelled circles 1–7. MFS= maximum flooding surface, SB = sequence bounding unconformity, LST = lowstand systems tract, TST = transgressive systems tract, HST = high stand systems tract. KF = Koranga Formation, GA = Gentle Annie Formation, CF = Champagne Formation, OM = Oponae Melange, SRF = Split Rock Formation, KK = Karekare Formation, BLF = Bluff Sandstone, HG = Hapuku Group, GF = Glenburn Formation, PF = Paton Formation, PM = Porangahau Member, UCM = Upper Calcareous Member, BS = Branch Sandstone, MH = Mead Hill Formation, RAK = Rakauroa Member, WAI= Waipawa Formation, TL = Teredo Limestone Member, AL = Amuri Limestone, WF = Wanstead Formation, TW = Te Waka Greensand, FG = Fells Greensand, WB = Weber Formation.

7.5 Cretaceous to Paleogene Third-Order Sequence Stratigraphy

7.5.1 Introduction

Within the second-order stratigraphic divisions of the East Coast Basin, a series of surfaces and coeval facies associations can be identified across the basin. Within the Mata and Dannevirke series, in particular, age control is sufficient such that approximately coeval facies transitions can be identified and correlated across substantial tracts of the basin. Such correlations reveal a potential series of third-order cycles. To better define these third-order cycles, significance needs to be attached to unconformable surfaces, in addition to interpretation of depositional environments of the strata between those surfaces. The application of a new and regionally consistent, integrated lithostratigraphic and chemostratigraphic framework for the deep-marine sedimentary rocks of the East Coast Basin, as developed and presented in this thesis (Chapters Two, Three, and Four), has allowed for the development of a robust third-order sequence stratigraphy, at least in some regions.

This thesis has identified approximately ten third-order sequences within the East Coast composite section, based on correlation of stratigraphic trends and facies between Marlborough and Hawke's Bay-Wairarapa (Figure 7.2 & 7.5). A simplistic labelling system has been devised for these sequences, based on their position within the various Series of the New Zealand Geological Timescale. For example, a sequence occurring within the Late Cretaceous Piripauan–Haumurian Stages of the lower Mata Series is labelled M1, whereas the next sequence, within the Haumurian Stage in the Mata Series, is identified as M2, and so on (Figure 7.2 & 7.5). Sequence boundaries as labelled refer to the boundary at the base of each sequence.

7.5.2 Marlborough Third-Order Sequences

Despite structural complexities, stratigraphic relationships in the Marlborough area are generally well-resolved and well-dated, and the area provides the most complete record of third-order sequences. Within the Marlborough stratigraphic succession, a range of paleoenvironments have been identified, from non-marine and near-shore shallow-marine settings to deep-marine environments, and the approximately isochronous transitions between depositional settings are reasonably well-resolved, or age control is such that correlations can be drawn between coeval units. Because of this, the Marlborough region effectively acts as the keystone to resolving many of the third-order sequences identified in the East Coast Basin.

Mata Series Third-Order Sequences

Sequence M1

The M1 sequence boundary is variably marked by either an erosional unconformity, a depositional hiatus/condensed section, or a bioturbated unconformity at the base of the Paton Formation during the late Teratan to early Piripauan (Schiøler *et al.*, 2002; Crampton *et al.*, 2006; Figure 7.2 & 7.13). Shallow-marine facies of the Paton Formation are regarded as a LST for the M1 sequence (Figure 7.13). The contact between the Paton Formation and the overlying Whangai Formation is marked by a sedimentary hiatus, and in some sections a concretionary horizon (Schiøler *et al.*, 2002), thereby marking the M1 transgressive surface. The Whangai Formation represents the TST (Figure 7.13). In the Conway River area, the Conway Formation is marked by highly bioturbated mudstones representing the M1 TST-HST, which coarsens upwards into a RST.

In the Conway area, the Whangai Formation records a transitional succession from outer shelf to upper slope conditions, coastal progradation, and shallowing up-section (Crampton, 1988; Roncaglia & Schiøler, 1997; Roncaglia *et al.*, 1999; Crampton *et al.*, 2000), interpreted as the M1 TST, HST, and RST, respectively (Figure 7.2).

Sequence M2

At Haumuri Bluff, the older middle Campanian age applied to the Claverley Sandstone by Roncaglia *et al.* (1999) is comparable to the M2 sequence identified in the Hawke's Bay-Wairarapa area, and may mark a sequence that is poorly resolved in the basin. Deposition of the shallow-marine Claverley Sandstone over the outer shelf depositional setting of the Conway Formation is indicative of regression during the mid-Haumurian (Figure 7.2).

Sequence M3

The conformable contact between the Conway and the Haumurian-aged (middle to late Campanian) Claverley Sandstone marks the M3 sequence boundary (Roncaglia *et al.*, 1999; Wilson *et al.*, 2005; Crampton *et al.*, 2006). Elsewhere in the Marlborough region, deposition of the Whangai Formation continued, although sequence boundaries have been identified within the Whangai Formation in the northern Clarence Valley (Schiøler *et al.*, 2002; Crampton *et al.*, 2006; Figure 7.2). Approximately coeval with the Claverley Sandstone, alternating sandstone and mudstone was deposited within the Whangai Formation in the Woodside Creek area (Morris, 1987; Laird, unpublished), interpreted as a lowstand fan during the M3 sequence in the deeper depositional setting in this part of the basin.

Sequence M4

The latest Haumurian (lower *M. druggii* zone; c. 68 Ma) Branch Sandstone variably overlies the Whangai Formation with either an erosional, bioturbated or channelised contact. In several sections, the contact is marked by hardground development (Figure 7.14A), or by mineralised lag deposits, informing the placement of the M4 sequence boundary at the base of the Branch Sandstone. In some sections (e.g. Nidd Stream, Isolation Creek) this interval is completely absent, and marked by a dolomitised horizon separating the Whangai and Mead Hill formations (Figure 7.14B). Alternating sandstone and mudstone of the Butt Formation was deposited in the Chancet Rocks-Flaxbourne River area (Strong, 2000), interpreted as a lowstand fan during the M4 sequence (Figure 7.13). The Mead Hill Formation is characterised by rapid transgression between 67–66 Ma (Strong *et al.*, 1995; Strong, 2000; Hollis *et al.*, 2003a, 2003b, 2005a; Crampton *et al.*, 2003). The fine-grained, pelagic sedimentary rocks of the Mead Hill Formation obscure further subdivision of systems tracts in the M4 sequence.

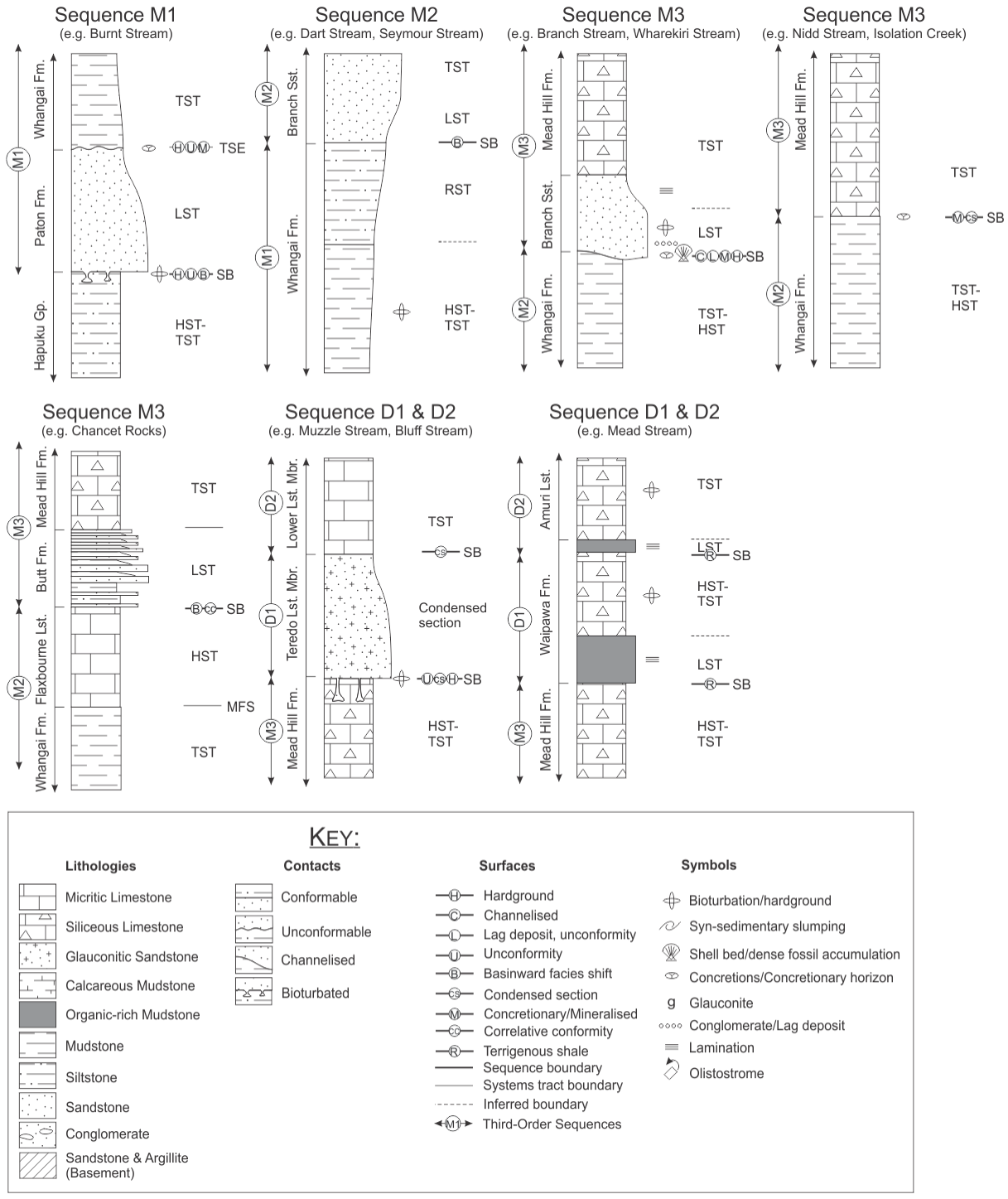

Figure 7.13: Third-order sequence stratigraphic motifs for the Mata and Dannevirke series in the Marlborough area.

Dannevirke Series Third-Order Sequences

Sequences D1 & D2

Deposition of the late Teurian (late Paleocene) Waipawa Formation was a two-phase event in the Mead Stream section, with two pulses of terrigenous strata separated by siliceous limestone. The base of the D1 sequence is marked by an influx of fine-grained terrigenous lithofacies in the lower Waipawa Formation in Mead Stream (Mudstone A of Strong *et al.*, 1995), interpreted as rapid sedimentation during a LST (Figure 7.13). The overlying interval of siliceous limestone is interpreted to represent low rates of terrigenous sedimentation during the subsequent TST-HST.

A second pulse of terrigenous sediment (Mudstone B of Strong *et al.*, 1995) is interpreted as the LST of the subsequent D2 sequence, with the overlying Lower Limestone of the Amuri Limestone representing a prolonged TST-HST (Figure 7.13). Further south in Muzzle Stream, the base of the D1 sequence is marked by a significant unconformity at the base of the Teredo Limestone Member, across which all Paleocene-aged Mead Hill Formation has been removed (Hollis *et al.*, 2005b; Figure 7.2). The Teredo Limestone Member is comprised of glauconitic sandstone, and represents a condensed section representing the time encompassed by the D1 and D2 sequences (Figure 7.13). Hardground development at the base of the Teredo Limestone Member, along with the presence of phosphatic nodules and abundant glauconite, suggests a significant period of non-deposition (Reay, 1993). The basal Teredo Limestone Member is comprised of cross-bedded sandstone, interpreted to represent the high-energy, shallow-marine facies deposited during the LST (Reay, 1993). The overlying highly glauconitic, strongly bioturbated upper Teredo Limestone Member (Reay, 1993), is interpreted as deposition during the HST and encompasses the MFS.

Sequence D3

The sub-Teredo Limestone Member unconformity youngs southwards: the member has a Waipawan age in Bluff Stream and at Kaikoura (Hollis *et al.*, 2005b; Figure 7.2), and a Waipawan to Mangaorapan age in Charwell-Conway River area (Crampton, 1988b). This is indicative of significant erosion during the late Teurian and stratigraphic condensation between the late Teurian and late Waipawan. The base of the Teredo Limestone Member in the Charwell-Conway River area approximates the D3 sequence boundary identified in the Hawke's Bay-Wairarapa (see below).

Sequences and systems tracts in the overlying Amuri Limestone are generally not resolvable due to the fine-grained, dominantly pelagic nature of the constituent lithofacies, and climatic overprinting of the eustatic sea-level signal. The marl members of the formation (Dee Marl, Lower Marl, and Upper Marl members) have been interpreted to represent periods of elevated terrigenous

sediment input associated with increased weathering as a result of the Paleocene–Eocene Thermal Maximum (Dee Marl Member), the Early Eocene Climatic Optimum (Lower Marl Member) and the Middle Eocene Climatic Optimum (Upper Marl Member) (Nicolo *et al.*, 2010; Slotnick *et al.*, 2012; Dallanave *et al.*, 2015). However, there may have been an additional influence on the lithologic changes exhibited by these members. Deformed beds characteristic of syn-sedimentary slumping are commonly observed at the contact between the Lower Marl and Upper Limestone members (late Mangaorapan-early Heretaungan; Figure 2.35F). Early Eocene syn-sedimentary slumping and olistostrome deposits have also been documented from many localities in eastern North Island within the Wanstead Formation of Mangaorapan to Porangan age (Moore, 1980; Hines *et al.*, 2013; C. Hollis & H. Morgans, Pers. comm. 2017).

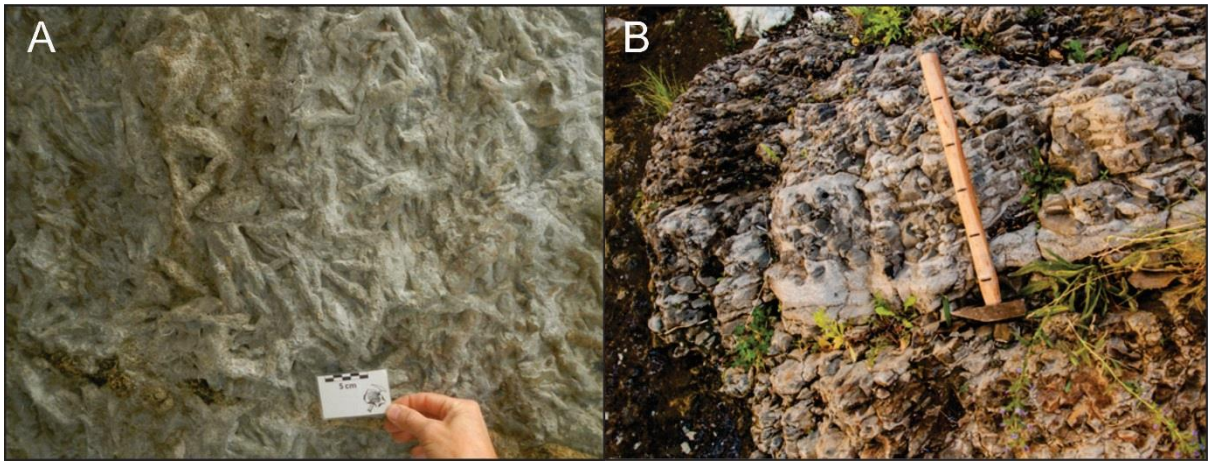

Figure 7.14: A) Extensive *Thalassinoides* bioturbation, marking a hardground at the base of the Branch Sandstone in Wharekiri Stream (BT28/647296). B) Dolomitised horizon (at hammer head) separating the Whangai (bottom) and Mead Hill formations (top) in the absence of Branch Sandstone at Isolation Creek (BS28/817613).

7.5.3 Eastern Hawke's Bay-Wairarapa Third-Order Sequences

Mata Series Sequences

Sequence M1 & M2

The stratigraphic contact between the Glenburn Formation and Rakauroa Member (Whangai Formation) is diachronous, becoming progressively younger from southern Wairarapa towards Te Hoe River in northwest Hawke's Bay (Figure 2.39 & 7.5; Crampton *et al.*, 2006). Similarly, there is a southward-thinning and younging trend at the base of the Whangai Formation in Marlborough (see Figure 2.41). At Tora, this contact is coeval with the M1 sequence boundary in Marlborough (Figure 7.2, 7.5, & 7.15). Further north, in the Glenburn-Kaiwhata River area this contact is

younger, and corresponds with the M2 sequence boundary, marked by an erosional unconformity at the base of the Rakauroa Member and a conglomeratic, mineralised lag deposit, overlain by sandstone grading into siliceous mudstone (Moore, 1980; Figure 7.5 & 7.15).

Sequence M3

At Angora Stream, the transition between the Glenburn Formation and Rakauroa Member is apparently conformable (Crampton *et al.*, 2006), although marked by a thick sandstone bed at the base of the Rakauroa Member, before grading upwards into siliceous mudstone. However, below the Glenburn-Rakauroa lithostratigraphic contact, a significant hiatus (c. 75–71.5 Ma; Crampton *et al.*, 2006) occurs within the Glenburn Formation at Angora Stream, corresponding with the M3 sequence boundary identified in Marlborough. At Manurewa Point, syn-sedimentary slumping and an olistostrome in the uppermost Rakauroa Member is interpreted as the M3 RST (Figure 7.15; Hines, 2015). Similar syn-sedimentary slumping in the upper Rakauroa Member also occurs in Makorokoro and Kaiwhata streams (Moore, 1988a).

Sequence M4

The sequence boundary at the base of the M4 sequence is marked in the Tora area by channelisation at the base of the Whangai Formation's Porangahau Member (Hines *et al.*, 2013; Figure 7.15) and hardground development (Vellekoop, 2010). Elsewhere, the sequence boundary is marked by a conformable shift to deposition of alternating sandstone and mudstone of the Porangahau Member, which is interpreted as deposition of a lowstand fan, the base of which marks a correlative conformity (Moore, 1988a, 1989c). The transition into the Upper Calcareous Member and Mungaroa Limestone is representative of the TST in the M4 sequence (Figure 7.15).

Siliceous-micritic limestone couplets within the Upper Calcareous Member at Mara Quarry (Moore, 1988a, 1988c), along with deposition of the glauconitic Te Uri Member and the micritic limestone member of the Mungaroa Limestone, are interpreted as a condensed section of middle Paleocene age, representing the M4 HST at c. 61 Ma (Hines *et al.*, 2013; Kulhanek *et al.*, 2015).

Slumping of the Waipawa Formation or rocks immediately underlying the Waipawa Formation occurs in multiple localities (e.g. Old Hill Road, Kaiwhata Stream, Te Mai; Moore, 1988a, 1989a; this study). This is interpreted to have occurred during the RST-LST phases of sequences M4-D1, induced by a fall in relative base level at the top of the M4 sequence (Chapter Four), and preceding the D1 LST represented by the basal Waipawa Formation.

Dannevirke Series Sequences

Sequences D1 & D2

The Waipawa Formation is a two-phase event (discussed in Chapters Three & Four). In a number of sections, a thin, grey siltstone occurs midway through the Waipawa Formation (Moore, 1989a; Figure 7.15), which is interpreted here as the sequence boundary for the second cycle within the Waipawa Formation. Elsewhere, this distinction is obvious, as at Manurewa and Te Kaukau points, and Mead Stream, where beds of organic-rich, siliceous mudstone are separated by micritic limestone (Chapter Four; Figure 7.13 & 7.15). Deposition of the micritic limestone indicates low terrigenous sedimentation, interpreted as TST-HST deposits within sequence D1. This lithofacies pattern was repeated subsequently in a second pulse of siliciclastic sedimentation in the Waipawa Formation, representing the D2 LST.

Sequence D3

The base of the late Teurian D3 sequence is marked by channelisation into the Mungaroa Limestone, followed by the deposition of alternating sandstone-mudstone of the Awheaiti Formation at Tora, and elsewhere in the eastern Wairarapa-Hawke's Bay by alternating sandstone-mudstone in the lower Wanstead Formation (Figure 7.15). In the absence of flysch-type lithofacies, the base of the Wanstead Formation is often marked by glauconitic sandstones and/or an unconformity above the Waipawa Formation (Figure 7.5). This unconformity and channelization is interpreted as a sequence boundary, with the overlying alternating sandstone-mudstone representative of the LST. A thin but laterally extensive, exceptionally glauconitic sandstone associated with siderite concretions is evident across the Tora area and is interpreted as a HST within sequence D3. This bed approximates the Mangaorapan-Heretaungan Stage boundary (Hines *et al.*, 2013).

Sequences D4 – D6

Heretaungan flysch in the upper Pukemuri Siltstone is interpreted as a LST within sequence D4 (Figure 7.15). This is truncated by an unconformity, across which the Porangan Stage has been removed. This surface is identified in a number of sections across the East Coast Basin, and is interpreted as the D5 sequence boundary. The Porangan unconformity in the East Coast Basin is variably marked by either a conglomeratic horizon (e.g. Tora), glauconitic sandstone, or a sedimentary hiatus, all of which mark the D6 sequence boundary.

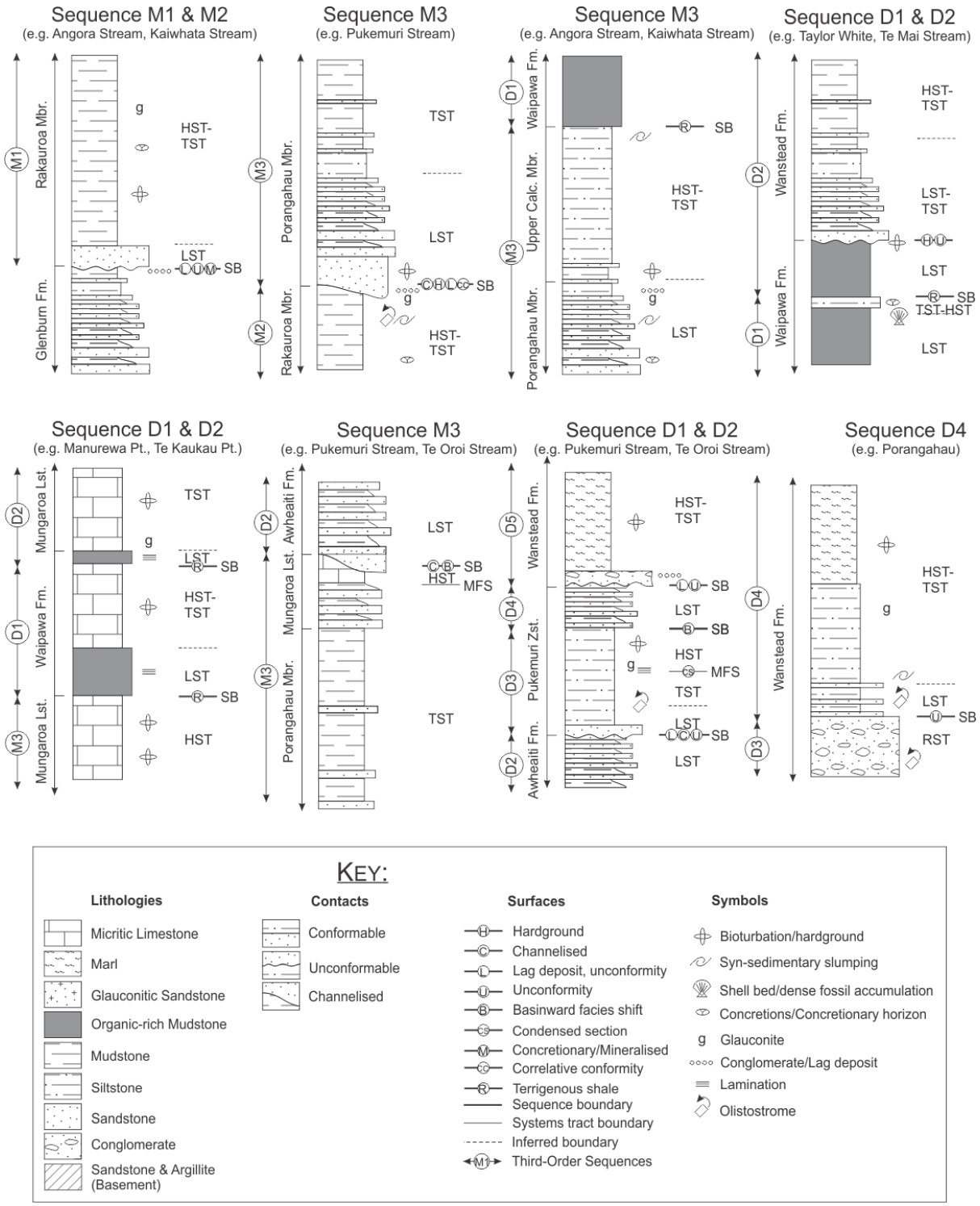

Figure 7.15: Third-order sequence stratigraphic motifs for the Mata and Dannevirke series in the eastern Hawke's Bay-Wairarapa area.

7.5.4 Supporting Evidence

Due to the generally patchy outcrop distribution and age control on Wanstead Formation outcrops in the Raukumara Peninsula and Whangai Range areas, it is difficult to readily define and map third-order sequences in these areas. However, sufficient observations from the Raukumara Peninsula and Whangai Range areas do exist to provide supporting the presence of Dannevirke series sequences otherwise identified in Marlborough and the eastern Hawke's Bay–Wairarapa regions. These observations include:

- In a number of sections in the Raukumara Peninsula area, the interval immediately above the Waipawa Formation is either marked by an erosional unconformity across which rocks of late Teurian age have been removed, or marked by glauconitic sandstones, indicating stratigraphic condensation (Figure 7.9). These correspond with surfaces identified in the upper D2 sequence.
- Where late Teurian to Waipawan-aged Wanstead Formation is present in Raukumara Peninsula, the formation is characterised by syn-sedimentary slumping and olistostrome deposits (Figure 7.9). This is interpreted as slumping associated with a RST with sequence D2. Associated unconformable surfaces and stratigraphic condensation mark the formation of the D3 sequence boundary during the early Waipawan.
- Crouch & Brinkhuis (2005) interpreted a RST through much of the Waipawan Stage at Tawanui (Whangai Range, southern Hawke's Bay). This interpretation is consistent with the paucity of the stratigraphic record through the Waipawan Stage in the Tora-Glenburn and Raukumara Peninsula areas, and can be correlated with the D3 RST.
- A Porangan unconformity at Port Awanui (northeast Raukumara Peninsula; Keil *et al.*, 2013; Morgans unpublished; Figure 7.9), corresponds with an unconformity of similar age identified in the eastern Hawke's Bay-Wairarapa, and an interval of stratigraphic condensation in the Whangai Range, interpreted here as the D6 sequence boundary.

7.6 Synthetic Sequence Stratigraphy: Case Study

Traditional stratigraphic approaches to sequence stratigraphy can be integrated with chemostratigraphic principles to produce a multi-disciplinary interpretive framework, in effect producing a synthetic sequence stratigraphy. Jarvis *et al.* (2001) demonstrated a strong correlation between sequence stratigraphic surfaces and systems tracts, and major-element chemical distribution within strata. Changes in sea level and sedimentation are invariably linked, and identification and interpretation of trends in both factors are important considerations in identifying systems tracts (Jarvis *et al.*, 2001). Likewise, changes in sedimentation rates result in differences in the proportion of sand to clay, and the ratio of authigenic to allochthonous sediment, which can have a distinct geochemical expression. Therefore, the presence of the Mata Series third-order sequences identified above can be tested by looking for a geochemical expression that can be correlated with surfaces and systems tracts.

In the East Coast Basin, dating of latest Cretaceous to Paleogene sedimentary strata has dominantly been reliant on age control based on microfossil biostratigraphy, although not at a resolution suitable for the determination of average sedimentation rates within individual systems tracts of the third-order sequence stratigraphic cycles identified in this chapter. However, bulk-rock major-element geochemistry can be used to provide an approximation of sediment accumulation rates (SARs). This can be achieved by determining a ratio of the terrigenous-derived sediment fraction (represented by SiO_2 in quartz and feldspar), which can then be normalised to the aluminosilicate flux (Al_2O_3 in deep-marine depositional settings), thereby removing the effects of autochthonous sediment sources (bioclastics and authigenic minerals; Chapters Three, Four, & Six). Although estimation of SARs using this method across the Upper Calcareous Member (Whangai Formation), Waipawa, and Wanstead formations is discussed in detail in Chapters Three and Four, it also has application in assessing the sequence stratigraphic boundaries identified through lithostratigraphic analysis as presented in this chapter.

Third-Order Surfaces & Sediment Supply

The use of high-resolution portable XRF analyses has resulted in the accumulation of a large geochemical database that have a variety of chemostratigraphic applications. A moderately high-resolution dataset was gathered through the uppermost Glenburn Formation and the thick, fine-grained homogenous succession of the Rakauroa Member in Pukemuri Stream, at an average

sample spacing of <3 m. This corresponds to temporal sampling resolution of c. 160 ka across the c. 18.6 Myrs represented by the stratigraphic record sampled (Figure 7.16).

Sequence stratigraphic event surfaces have a geological and lithological signature, which therefore should be accompanied by a geochemical expression, either due to changes in grain size or the proportion of authigenic vs allogenic minerals present. All the sequence boundaries that span the record represented here, except for sequence M2, demonstrate low K/Al, high Si/Al, and low Zr/Al values (Figure 7.16A, B. C). This is consistent with a reduced terrigenous flux at this time; low K/Al indicates a low proportion of clays (particularly low illite), and low Zr/Al indicates low volcaniclastic input (typically derived from continental sources; e.g., Hofmann *et al.*, 2003; Sageman *et al.*, 2003a; Turgeon & Brumsack, 2006). The temporal resolution of sampling through the Glenburn Formation is too low to identify any geochemical relationships across the M1 sequence boundary.

In a broad sense, the Si/Al ratios measured through the Rakauroa Member represent moderately high SARs, consistent with a second-order TST across the East Coast Basin at this time. Resolving below this scale, much finer variability becomes apparent (Figure 7.16B). Third-order sequence boundaries identified through lithostratigraphic analysis correspond with peaks in Si/Al (except M4), indicating low sedimentation rates. Silicon/Al values are particularly high at the M3 and M4 sequence boundaries (Figure 7.16B).

Wehausen & Brumsack (1999) interpret abrupt increases in Si/Al and corresponding decreases in Ti/Al, K/Al and Zr/Al, as the effect of sediment winnowing, resulting in the removal and/or decreased proportion of the clay-sized fraction, consequently creating an enrichment of elements that are associated with the remaining sand- and silt-sized fractions and heavy minerals. In the deep-marine setting into which the Rakauroa Member at Pukemuri Stream was deposited, this may also be the case, with reduced sediment loads during regressive and lowstand systems tracts resulting in winnowing of sediments, removal of the clay fraction, and therefore causing decreased K/Al and Zr/Al, and increased Si/Al associated with a reduced proportion of clays. The Pukemuri Stream dataset, at least partially, vindicates the third-order sequence boundaries identified through the Haumurian Stage (upper Mata Series) in this study through assessment of stratigraphic trends.

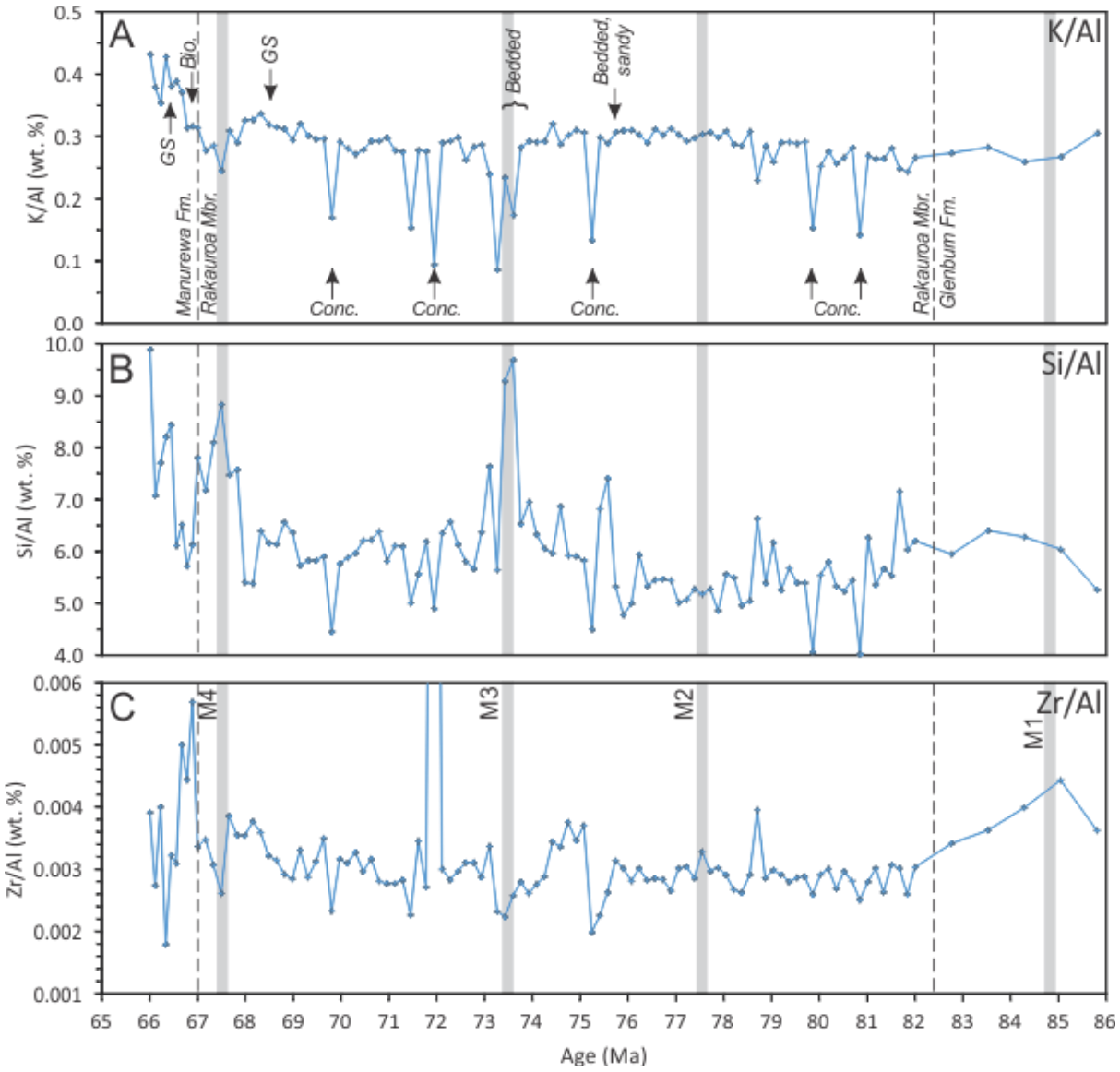

Figure 7.16: Portable XRF analyses of A) K/Al, B) Si/Al, and C) Zr/Al, from the Rakauroa Member (Whangai Formation) in Pukemuri Stream section (southeast Wairarapa) plotted against a simple, linear age model. Dashed lines indicate formation boundaries, grey bars indicate the sequence boundaries identified through lithostratigraphic analysis, and labelled according to Figure 7.6. Lithological characteristics noted during logging of the section are arrowed. GS = Greensand, Bio. = Bioturbated surface, Conc. = concretion.

7.7 Correlation of Third-Order Sequences

The application of the Kominz *et al.* (2008) relative sea-level curve to the East Coast third-order sequences identified in this study results in a remarkably good correlation (Figure 7.17), as does correlation with sequence boundaries in European (Haq, 2014) and the New Jersey coastal plain records (Miller *et al.*, 2003, 2004, 2005; Kominz *et al.*, 2008). However, it is uncertain how many of these correlations arise by chance alone. The correlations between sequences documented by Crampton *et al.* (2006) and the New Jersey sequence record have been statistically demonstrated to have only an 8% chance of coincidental correlation. Therefore, given the degree of correspondence between the Crampton *et al.* (2006) record and sequence boundaries identified in this study, this may suggest that the late Cretaceous boundaries identified in this study have some wider significance.

Despite the different approaches taken, there is strong agreement in the sequence-bounding surfaces identified by Schiøler *et al.* (2002), Crampton *et al.* (2006) and this study (palynofacies analysis, high-resolution quantitative biostratigraphy, and lithostratigraphic analysis, respectively). The placement of multiple event levels, which were identified by the application of the high-resolution constrained optimisation (CONOP) quantitative biostratigraphic method at a single composite level, was interpreted by Crampton *et al.* (2006) as representing sedimentary hiatuses, equivalent to sequence-bounding surfaces. That said, these hiatuses may also represent stratigraphic condensation associated with the HST/MFS and the RST/RSE. Of the fifteen sequence-bounding unconformities between the Teratan and late Haumurian (Coniacian–Maastrichtian, 86–67 Ma) identified by Crampton *et al.* (2006), only two (72.5 and 68.7 Ma) do not coincide with well-dated hiatuses in the New Jersey sea-level record (Miller *et al.*, 2003, 2004, 2005; Kominz *et al.*, 2008). The correlation between New Zealand stratigraphic sequences and Northern Hemisphere records suggests that sequence boundaries identified by Crampton *et al.* (2006) reflect a response to global eustatic sea-level variability.

Haq (2014) includes ten of the sequence boundaries identified by Crampton *et al.* (2006) in his comparison with the revised European eustatic sea-level record. However, Haq (2014) has not scaled ages of the events with respect to the revised international timescale of Gradstein *et al.* (2012), resulting in mismatched correlations. When scaled to GTS12, eight of the events identified by Crampton *et al.* (2006) correspond with sequence boundaries identified in the European record of Haq (2014) (Figure 7.17). Of the third-order sequences identified in Mata Series rocks here, all except the M4 sequence boundary correspond with the Haq (2014) sequences.

For the late Paleocene, Hollis *et al.* (2014) present the most recent and precise chronology for the Waipawa Organofacies and associated events, which is adopted herein (Figures 7.17). The interpretation of the sequence stratigraphic surfaces and events associated with the deposition of the Waipawa Formation by Hollis *et al.* (2014) are entirely consistent with the detailed lithostratigraphic, chemostratigraphic, and paleoenvironmental studies conducted during the course of this thesis (Chapters Three & Four).

Each of the sequence boundaries identified in the Eocene part of the East Coast Basin composite record, compiled in this study, can be correlated with a sequence-bounding hiatus in the New Jersey coastal plain record of Browning *et al.* (1996; rescaled to GTS12). Crouch & Brinkhuis (2005), through assessment of dinoflagellate assemblages, identified two third-order sequences across the late Paleocene to early Eocene (57–53 Ma) in the Tawanui section southern Hawke's Bay (Figure 7.17). The sequence boundaries of Crouch & Brinkhuis (2005), and SB 2 & 4 of Higgs *et al.*, (2012, 2017) correspond with sequence boundaries identified in this study at the base of D3 & D4 (Figure 7.17). Sequence boundaries identified in this study correspond well with sequence boundaries identified by Higgs *et al.* (2012, 2017) in the Taranaki Basin, which presently lies off North Island's western coast. The Eocene sequence boundaries identified herein in the East Coast Basin (D3–D6) also correspond with sequence-bounding hiatuses in the New Jersey record. Unconformities or condensed sections of Porangan age are notable in a number of sections across the East Coast, Canterbury, and Taranaki basins (Stoneley, 1968; Morgans, 2009; Higgs *et al.*, 2012; Hines *et al.*, 2013; Dallanave *et al.*, 2016). This implies a widespread event between 45.7-42.6 Ma across the New Zealand region. The timing of this event corresponds with a significant unconformity and a fall in sea level in the New Jersey record (Figure 7.17), suggesting that this event has a eustatic control.

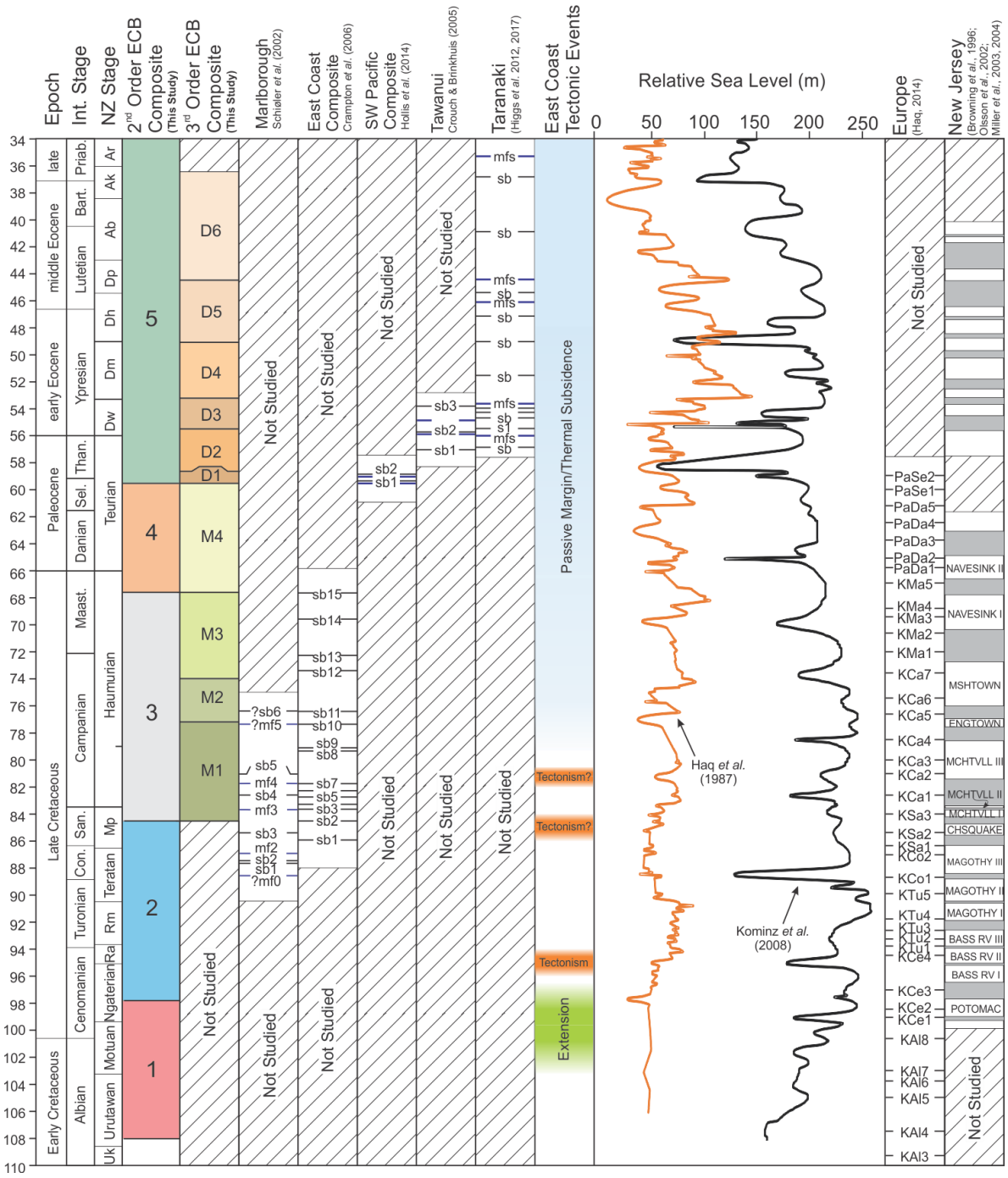

Figure 7.17: Summary of third-order sequence stratigraphic studies in the East Coast Basin (Schiøler *et al.*, 2002; Crouch & Brinkhuis, 2005; Crampton *et al.*, 2006), Taranaki Basin (Higgs *et al.*, 2012, 2017) and Southwest Pacific (Hollis *et al.*, 2014) alongside the composite East Coast Basin record produced in this study. Ages have been re-scaled to NZGTS15 (Raine *et al.*, 2015). Relative sea-level curves from Haq *et al.* (1987) and Kominz *et al.* (2008). Regional tectonic events from Strogen *et al.* (2017) and Crampton *et al.* (*in prep.*). Sequence boundaries (sb) are shown as black lines, and maximum flooding surfaces (mfs) are shown as blue lines where identified. Phases of active basin extension and rifting are shown in green, likely compressional phases are shown in orange, and passive-margin thermal subsidence are shown in pale blue. Sequence boundaries within the Crouch & Brinkhuis (2005), Crampton *et al.* (2006), Hollis *et al.* (2014), and Higgs *et al.* (2012, 2017) records are arbitrarily numbered

(oldest to youngest). Numbering of sequence boundaries and maximum flooding surfaces in the Marlborough record correspond with that applied in Schiøler *et al.* (2002). Labelling of sequence boundaries in the European succession follows Haq (2014). Hiatuses in the New Jersey succession are indicated by grey bars, and the sedimentary successions are labelled as per Miller *et al.* (2003, 2004). Mshtown = Marshalltown, Engtown = Englishtown, Mchtvll = Merchantville, Chsquake = Cheesequake, Bass Rv = Bass River. Third-order sequences identified in this study are labelled with respect to their position within the relevant Series associated with the New Zealand Geological Timescale (explained in text).

7.8 Stratigraphic Motifs

A series of generalised stratigraphic motifs have been identified from the second- and third-order sequences in the East Coast Basin. These motifs remain markedly similar regardless of the change in magnitude between orders, suggesting that these generalised motifs are dimensionless patterns, independent of duration and sequence thickness, and controlled by additional factors. The rate of sediment supply and the depositional setting are the two greatest controls on the sequence pattern exhibited in the East Coast Basin. Terrigenous sediment supply to the basin is largely derived from the shoreline and typically accumulates in shelf-slope sediment wedge (Figure 7.18). Differences in accommodation (subsidence plus eustatic sea-level change) and sediment supply control sequence architecture, including the nature and significance of surfaces (Miller *et al.*, 2004). The rate of change of accommodation space within this clastic wedge is largely controlled by the amount of space created by relative sea-level change, and the rate at which the basin is subsiding. Therefore, the primary controls on the development of different sequence stratigraphic motifs are:

- The position of the paleoshelf with respect to where sediment is accumulating, as this partly controls the available accommodation space, the maximum water depth, and distance from clastic sediment sources.

- The relationship between the rate of terrigenous sediment supply and the rate of change in sea level can vary in magnitude during a eustatic cycle, therefore controlling the thickness and nature of the transgressive and highstand systems tract (e.g. Saul *et al.*, 1999).

Therefore, sequence types for different locations across a paleoshelf-slope transect can be represented by simplified sequence stratigraphic models and motifs, which summarise the consequent stacking pattern and stratigraphic and facies associations that arise between particular rates of sea-level change and sediment supply.

The major sedimentary facies represented in the basin fill are deposited across a range of non-marine to abyssal depths, although the majority of the sedimentary succession is characterised by outer shelf to upper slope settings. The stratigraphic motifs identified across the East Coast Basin are dominated by submarine fan and outer shelf-slope facies. Of the stratigraphic motifs identified across the basin, the stratigraphic architecture of Cretaceous to Paleogene sequences can be represented by eight generalised stratigraphic motifs. The eight sequence stratigraphic motifs identified here represent successively distal aspects of the paleoshelf-slope transect.

1. The Tahora motif corresponds to fluvial, coastal plain and inner shelf facies. Named for the Piripauan Tahora Formation in southwestern Raukumara, this motif is also demonstrated during the Ngaterian Warder Formation and Bluff Sandstone in Marlborough. Non-marine terrestrial and alluvial sediments characterise the LST in this motif, followed by transgression into shallow marine sandstones, followed by an interval of stratigraphic condensation (HST).

2. The Branch motif is representative of inner to middle shelf settings, and is named for the Branch Sandstone in Marlborough. This motif is characterised by shallow marine sediments (LST) abruptly sandwiched between outer shelf, fine-grained facies.

3. The Rakauroa motif is named for the Rakauroa Member. Although the base of the Rakauroa Member is diachronous, regardless of age, the stratigraphic motif remains markedly similar, characterised by a sharp sequence boundary marked by a thin grit of conglomeratic layer, overlain by proportionally thin, metre to decimetre-bedded sandstone unit representing the LST, typically grading into massive siliceous mudstone (TST-HST).

4. The Te Uri motif represents periods of low sedimentation in shelf environments, resulting in the formation of a condensed section. This motif is named for the Te Uri Member, but also characterises the coeval Teredo Limestone Member in Marlborough. The Te Uri motif generally comprises a bioturbated lower contact corresponding to either the sequence boundary, or the transgressive surface (depending on location and sequence preservation), overlain by glauconitic sandstone marking a stratigraphic condensation throughout much of the sequence. Several variations of this motif are apparent, likely due to the differing states of sequence preservation.

5. The Champagne motif is named for the Champagne Formation in Marlborough, although it is also encompassed by the Gentle Annie Formation and Oponae Melange in the Hawke's Bay-Wairarapa and Raukumara Peninsula areas, respectively. The Champagne motif is characterised by rocks deposited in slope environments, where either tectonism and/or base level fall results

in syn-sedimentary slumping and olistostrome emplacement. Such lithofacies are often immediately overlain by flysch-type strata and levee deposits that are associated with slope- or basin-floor fan deposition as part of the LST. Jointly, these olistostrome deposits and flysch facies are interpreted as a LST. This succession fines upwards into mudstone-dominated sediments of the lowstand wedge, and condensed sections associated with the TST and HST.

6. The Porangahau motif is characterised by the avulsion of basin floor fan systems in bathyal settings. Named for the Porangahau Member (Whangai Formation), the sequence boundary at the base of this motif is characterised either by submarine channelization (e.g. at Pukemuri Stream) or by a correlative conformity, across which there is sharp transition to the deposition of flysch lithofacies that represents development of a lowstand fan system (e.g., Angora Stream). These facies typically grade upwards into siltstones and mudstones representative of a lowstand clastic wedge before grading into a poorly differentiated TST. This motif is pervasive throughout the sequences identified in the East Coast Basin, and characterises sequences from of Urutawan-Motuan (Early Cretaceous) to Teurian (late Paleocene) age.

7. The Mead motif is characterised by an abrupt 'pulse' of fine-grained terrigenous, siliciclastic sediment during the LST, contrasting sharply with the pelagic background sedimentary signal. This motif is named for the Mead Stream section in Marlborough, where this motif crops out characteristically. This motif is unique to the Waipawa Formation, but is included here because of the geographically widespread nature of the motif. Variations of the motif in shallower depositional settings includes the inclusion of a thin, grey siltstone separating the two pulses of organic-rich mudstone in eastern Hawke's Bay-Wairarapa (e.g. Figure 7.6).

8. The Isolation motif characterises distal settings where the lowstand systems tract shows no stratigraphic representation, and is instead represented by a sedimentary hiatus. This is only observed in a few specific instances within the East Coast Basin sequences, and is associated with a brief LST interval, and sea-level changes of notably short duration.

Interpretation of third-order cyclicity in the basin is dependent upon recognition of as many as four strata-bounding surfaces within each sequence. In stratigraphic order, these are: the lower sequence boundary, the transgressive surface, the downlap surface, and the upper sequence boundary. In many of the distal stratigraphic motifs identified in the East Coast Basin, the sequence boundary is marked by a correlative conformity, across which there is an abrupt shift to deposition of flysch facies.

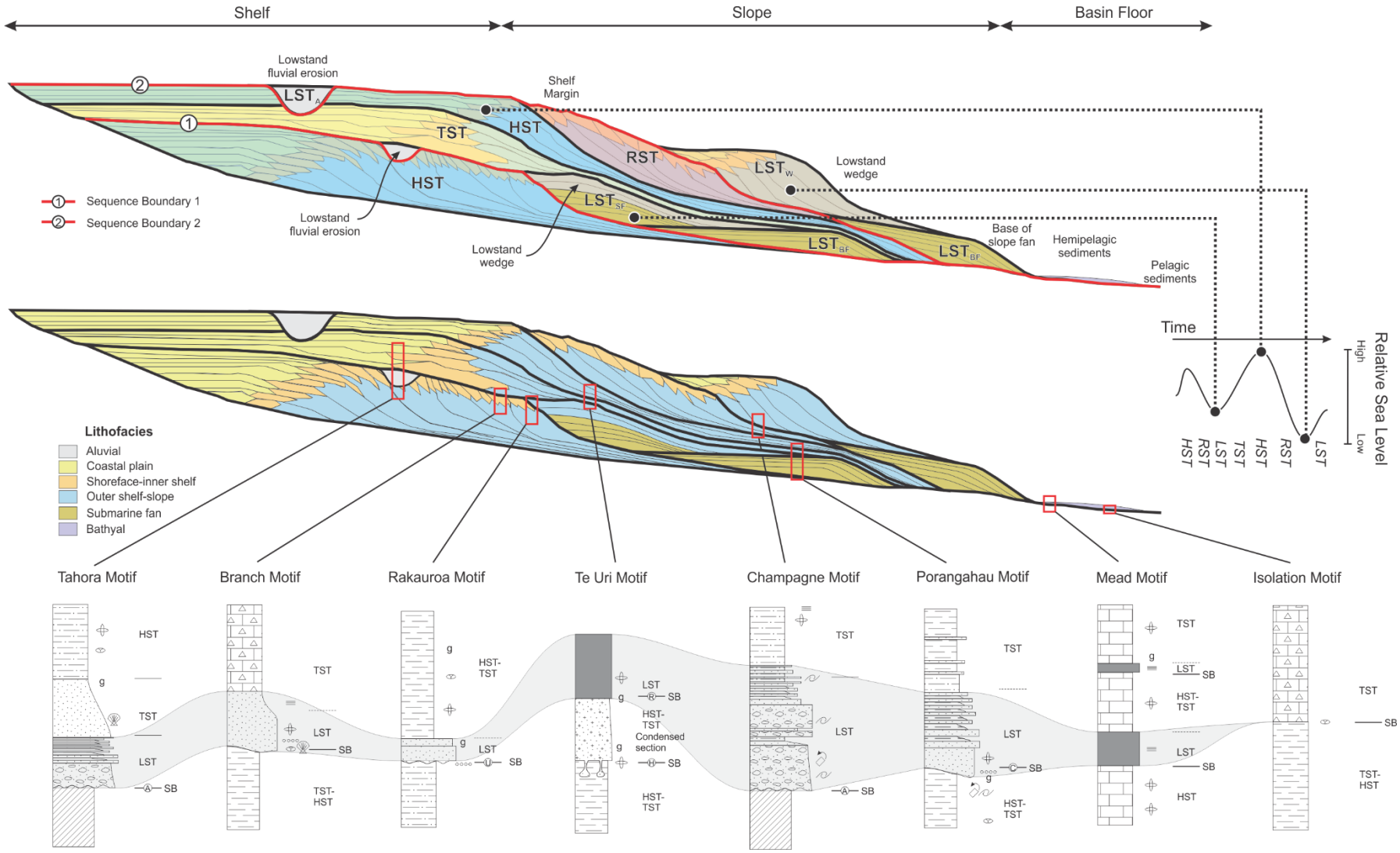

Figure 7.18: Sequence stratigraphic model framework for common, recurring, and significant stratigraphic motifs identified in this study. Model modified after Van Wagoner *et al.* (1988), Saul *et al.,* 1999, and Naish and Wilson (2009). Refer to Figure 7.15 for key to symbols.

Within the East Coast succession it is rare for all components of a cycle to be preserved (or distinctly recognisable). The East Coast succession is dominantly comprised of LST and TST packages. The LST is the most common systems tract in the stratigraphic motifs identified in this study, and two different expressions of the LST are depicted. Deposition of a lowstand basin-floor fan system is commonly associated with deep-water clastic sequences (Van Wagoner *et al.*, 1988) and, in the East Coast Basin, deposition of slope-fan systems is common during lowstand periods. Such rocks may or may-not be capped by a thin lowstand clastic wedge (Figure 7.18).

The architecture of third-order cycles identified in this study suggests that TST deposits in western parts of the basin are dominantly represented by shallow-marine strata. By contrast, in eastern, more distal parts of the basin, equivalent rocks often dominated by lithofacies deposited in the lowstand fan and clastic wedge (Figure 7.18; e.g. Porangahau Member/motif).

Non-preservation of the RST is common in many clastic shelf-slope settings globally, where the rate of sea-level fall generally outpaces the rate of sediment supply, which results in either a sedimentary hiatus or erosion (Hunt & Tucker, 1992; Naish & Kamp, 1997). The RST is rarely preserved in either western or eastern parts of the study area, even in the largely deep-marine-dominated lithofacies within the Eocene succession (Wanstead Formation and Amuri Limestone). Marine ravinement has in most instances removed RST and terrestrial deposits in the older, shallower-marine sequences, although these such strata are occasionally preserved around the margins of the basin. In deeper depositional settings, the surfaces that separate the HST and RST are rarely recognisable, and as such, are generally not illustrated in the stratigraphic motifs presented in Figure 7.18. Although a lack of biostratigraphic resolution may be one reason for this, the deep-water depositional setting of such formations means that is it difficult to resolve sea-level changes of <100 m within resolution of available paleoecological and paleobathymetric indicators.

7.9 Sequence Stacking Patterns

Due to the tectonically disrupted, dislocated, and localised nature of the East Coast Basin's present-day outcrop exposure (particularly in the early to mid-Cretaceous interval), a consequence of post-depositional Neogene active-margin tectonics, deconvolving lithofacies stacking patterns is difficult. In the latest Cretaceous to Paleogene parts of the East Coast Basin record, a composite of key sections across the basin can be used to demonstrate the relative movements of the paleoshoreline, therefore facilitating a reconstruction of stacking patterns (Figure 7.19; Enclosure 1). The mid-Cretaceous to Eocene units documented throughout this study demonstrate a broad retrogradational marine depositional succession, consistent with a first-order transgressive phase across Zealandia through this time. Superimposed on this are a series of inter- and intra-formational stacking patterns indicative of a second-order response to sea-level and tectonic variability. Interpretation at the third-order scale becomes much more difficult (as discussed above), largely due to the nature of fine-grained, pelagic to hemipelagic sedimentary lithofacies that dominate the basin fill. Resolution below the third-order scale is not possible with the current age control, regardless of the difficulties identifying parasequences within the largely deep-marine depositional settings of the basin fill.

7.9.1 Second-Order Stacking Patterns

From the mid-Teratan to the late Piripauan, the Glenburn Formation represented an aggradational to progradational fan system, congruent with a high sediment load and progressive filling of accommodation space that is inferred to be the abandoned eastern Gondwana subduction trench (Crampton, 1997). The notable thickness of shallow-marine Tahora Formation in the Mangahouanga Stream area (400 m), is interpreted to represent sustained sediment input during marine transgression, and infilling of available accommodation space. The overlying Rakauroa Member of the Whangai Formation, and the correlative "Herring facies" of Marlborough, represent a west-directed retrogradational stacking pattern of early to latest Haumurian age, from the deepest part of the basin (Woodside Creek–Tora area), towards the northwest (in North Island) and southwest (Marlborough). This is representative of the overall second-order transgressive phase through this interval. The base of the Porangahau Member and Butt Formation fan systems, along with the base of the shallow-marine Branch Sandstone, form a coeval surface across the basin (Figures 2.39 & 2.41). These units imply a reduction in relative sea level across the basin, informing the placement of a sequence boundary preceding the LST of sequence two, which is marked by deep-water submarine-fan avulsion and the deposition of shallow-marine sandstones elsewhere in the basin. This supports the interpretation of Moore (1989c), who suggested that

deposition of the Porangahau Member reflected a sea-level regression of ~50 m across the K-Pg boundary, followed by rapid marine transgression during sequence two (Moore, 1988a, 1989c). The Okarahira-Paton, Whangai, and Teredo Limestone Member formations each demonstrate retrogradational (i.e. landward) movement of the shoreline during transgressive systems. This is demonstrated by the base of the older portion of each of these formations being deposited in the deeper part of the Marlborough sub-basin, and progressively younging southwards, being unconformably deposited over underlying sediments and/or basement.

7.9.2 Third-Order Stacking Patterns

Stratigraphic relationships, lithofacies interpretations, and structural complications can be resolved with little ambiguity through the late Piripauan to Mangaorapan third-order sequences identified in this study (M1–D3; Enclosure 1). Resolving these relationships has allowed a detailed consideration of sedimentation in the basin to be undertaken, resulting in a new model for the stratigraphic relationships observed between various lithofacies across the basin (Figure 7.19).

The M1 sequence was selected as the base for this model, primarily because it overlies a major unconformity of Piripauan age, and marks the transition to a completely passive margin setting. Secondly, the widespread deposition of the shallow marine facies (Tahora and Paton formations) form a distinctive, age and environment boundary across the basin, that is readily recognised in facies changes (e.g. Figures 7.2 & 7.9). Overall transgression across cycles M1–M4 results in the retrogradational stacking of successive sequences inboard towards the Te Hoe River area in North Island, and the Haumuri Bluff-Conway River area in northeastern South Island (Figure 7.19). The basal LST of the M4 sequence is recorded by the deposition of the Porangahau Member in southeast North Island and the Chancet Rocks area of coastal Marlborough, and basinward progradation of shallow-marine Branch Sandstone in western Marlborough. During the succeeding TST and HST, the Upper Calcareous Member (Whangai Formation) was deposited in upper slope settings. In southern Wairarapa, the HST was marked by the deposition of pelagic, micritic limestones (Figure 7.19), whereas equivalent rocks in the Marlborough region were characterised by pelagic bioclastic sediment accumulation that became particularly thick in distal areas. The overlying D1 lowstand records high terrigenous sedimentation rates across the basin, resulting in enhanced terrestrial organic carbon supply and burial (Figure 7.19; Chapter Four). The thickest sections accumulated in upper slope settings during the D1 sequence. In the broad shallower shelfal setting of the Marlborough region this LST is marked by a significant unconformity across much of the region.

The characteristics of the D2 LST is either unresolved in the lithofacies succession, or had no distinctive sedimentary effect in the Raukumara region, where it is apparently marked by initial deposition of the Wanstead Formation. In the Wairarapa region, upper slope settings and some middle slope settings were marked by short-lived deposition of flysch (Figure 7.19). In Marlborough, there is no distinctive lithological expression through the bioclastic-dominated Lower Limestone Member of the Amuri Limestone, although the Dee Marl Member, its formation attributed to increased terrigenous influx associated with the PETM (Hancock *et al.*, 2003; Nicolo *et al.*, 2010), is approximately coeval with the D3 LST. The successive D3–D5 transgressions resulted in the accumulation of substantial volumes of fine-grained sediments at progressively increasing paleodepths. Overall, throughout the duration of the M2–D4 sequences, the basin was passively subsiding, with the rate of subsidence apparently increasing during the late Paleocene in order to account for the significant increases in Eocene paleodepths, consistent with thermal and 1D-modelling (next section).

Schiøler *et al.* (2002) identified sequence boundaries and maximum flooding surfaces in the Marlborough region based on dinoflagellate abundance and phytoclast ratios and their occurrence in relation to lithological changes. Schiøler *et al.* (2002) note that the sandy shallow-marine Paton Formation demonstrated a significantly stronger response to sea-level changes when compared to the finer-grained outer-shelf Whangai Formation (Herring facies). This observation implies that relative sea-level oscillations were probably <50 m, as the threshold between separate paleoenvironmental classifications was not crossed. A similar observation is made in the Tahora Formation of northern Hawke's Bay-western Raukumara Peninsula, whereby significant thicknesses of sediments accumulated (~450 m), yet the depositional environment remained within a nearshore to inner-shelf setting, suggesting enhanced subsidence at a rate that matches the rate of sediment accumulation.

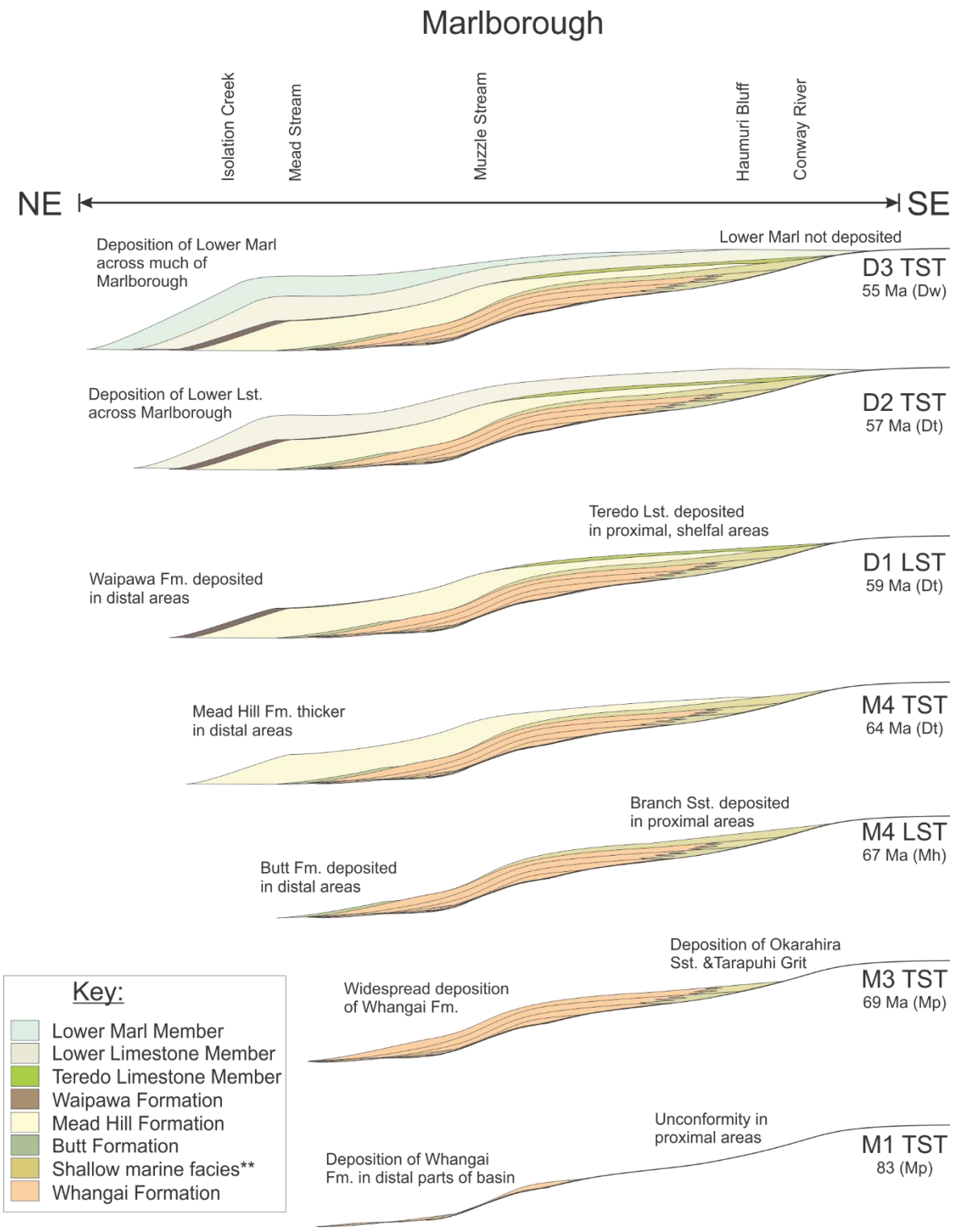

Figure 7.19A: Schematic stratigraphic model for stacking patterns of latest Cretaceous to Eocene sedimentary rocks within the third-order M1–D3 sequence succession in Marlborough, as documented in this study. No scale is implied (vertical or horizontal). ** Shallow marine facies include inner shelf and marginal marine sediments of the Paton Formation, Branch Sandstone, Claverley Sandstone, Okarahira Sandstone and Tarapuhi Grit.

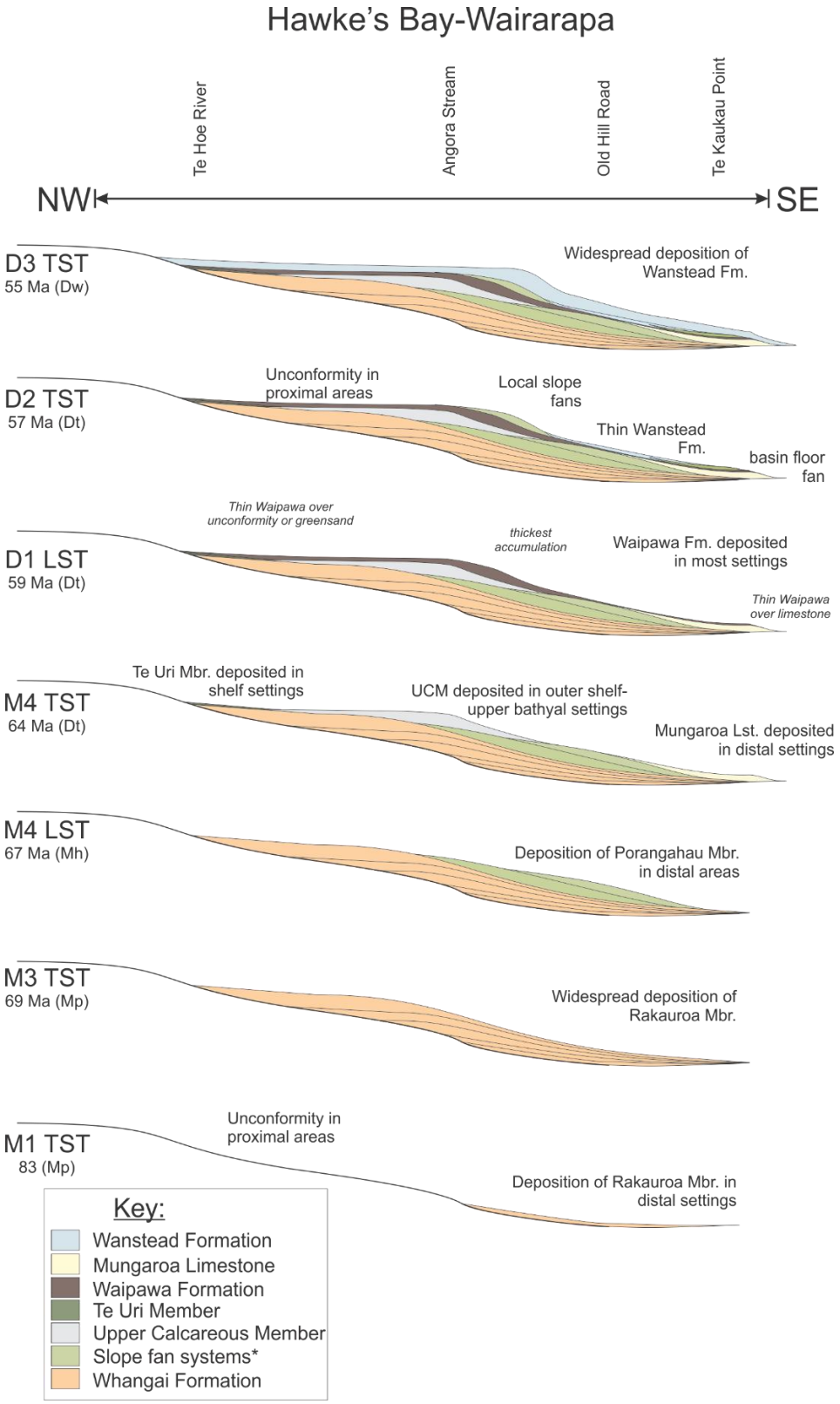

Figure 7.19B: Schematic stratigraphic model for stacking patterns of latest Cretaceous to Eocene sedimentary rocks within the third-order M1–D3 sequence succession in the Hawke's Bay-Wairarapa region, as documented in this study. No scale is implied (vertical or horizontal). * Slope fan systems includes the Porangahau Member, Awheaiti Formation, and lower flysch facies in the Wanstead Formation.

7.10 Basin Subsidence

Basin subsidence plays an important role in the creation and availability of sediment accommodation space, contributing to the interplay between sedimentation rate and sea-level variability, and ultimately impacts how these factors manifest in the stratigraphic record.

Broad-scale basin subsidence is apparent from the inferred paleodepth changes throughout the Cretaceous–Paleogene succession, with a pronounced deepening trend particularly evident in the latest Cretaceous to late Eocene. Such subsidence is consistent with the well-established concept of a late Cretaceous–Eocene thermally subsiding passive margin setting for the East Coast Basin (Ballance, 1993b; Davy *et al.*, 2008; Bland *et al.*, 2015). However, although there was significant variation in stratigraphic thickness and paleo-water depths across the basin, a generalised gradient existed with shallow and thin stratigraphic sequences in the west, and deep and thick sequences in the east. In particular, paleodepth indicators from the Wanstead Formation indicate rapid and significant deepening of the basin during the Eocene, particularly in the Eastern Sub-belt.

Estimates of the magnitude of basin subsidence can be derived from thermochronological modelling (e.g., Kamp, 1999; Jiao *et al.*, 2015) or from one dimensional modelling of the basin (e.g., Field & Uruski *et al.*, 1997). Thermochronological data for three samples from Kamp (1999), remodelled by Jiao *et al.* (2015; two from Te Urewera [Figure 7.20A], one from the Raukumara Range [Figure 7.20B]) are compared here to a preliminary thermochronological model from Glenburn (coastal Wairarapa; Figure 7.20C; this study; including track length frequency distribution used to create the model; Figure 7.20D), and 1D-models for the Te Hoe River and Pukemuri Stream stratigraphic successions (Figure 7.20E, F).

Apatite fission track thermochronological data from the Te Urewera (Waikaremoana) area (Kamp [1999] samples 9601-55, 57, remodelled by Jiao *et al.* [2015]), suggest that the samples have barely entered the partial annealing zone (PAZ) for apatite (60–120°), suggesting that throughout their thermal history these samples have stayed near the surface with minimal burial (Figure 7.20A). Apatite thermochronogical modelling of data from the Raukumara Range (Kamp [1999] sample 9601-37, remodelled by Jiao *et al.* [2015]), show burial temperatures of 120°C at c. 40 Ma, although there are significant uncertainties in the thermal history prior to 40 Ma (Figure 7.20B). Comparison of burial temperatures between the Te Urewera and Raukumara models show that there was significantly greater burial in the Raukumara area, with basement strata buried approximately 4.5–5 km (assuming 25°C/km thermal gradient) at 40 Ma. Due to the uncertainties in the thermal model prior to 40 Ma, it is difficult to estimate the rate or timing of this burial. However, the best-fit model path indicates 1 km of subsidence between 100–40 Ma (Figure 7.20B), although within

the errors of the model, this could be as much as 3 km subsidence. A preliminary apatite thermochronological model from a sample of the Glenburn Formation at Glenburn (this study), follows a very similar thermal history to the Raukumara basement sample, showing peak burial temperatures of 100°C at 40 Ma, with 1 km of burial/subsidence occurring between 70–40 Ma (Figure 7.20C). Assuming a regional thermal gradient of 25°/km (as per Jiao *et al.* 2015), these models indicate that burial has not exceeded ~2 km in the Te Hoe River area of northwest Hawke's Bay, entirely consistent with 1D-modelling of the stratigraphic thicknesses and interpreted paleodepths of the Cretaceous–Paleogene succession in this area (Figure 7.20E). One kilometre of burial/subsidence in the Glenburn area, as indicated by thermal history modelling in this study, is consistent with 1D-modelling from the nearby Pukemuri Stream, which also indicates 1 km of tectonic subsidence, and the accumulation of a ~1 km stratigraphic thickness of sediment between 70–40 Ma (Figure 7.20F).

Jointly, these models indicate that there was substantially less basin subsidence on the western margin of the East Coast Basin (Te Hoe River–Te Urewera area), compared to the further outboard regions such as the Raukumara Range and Glenburn-Tora areas. These model observations would imply that less sediment accommodation space was available in the Te Hoe River–Te Urewera areas, consistent with the reduced thickness of late Cretaceous–Paleogene succession in this area, and the shallower paleodepths evident from sedimentology, and macro-and microfaunas. The amount of subsidence in the deeper, more distal aspects of the basin is comparable to the thickness of accumulated latest Cretaceous–Paleogene strata in the Glenburn and Tora area.

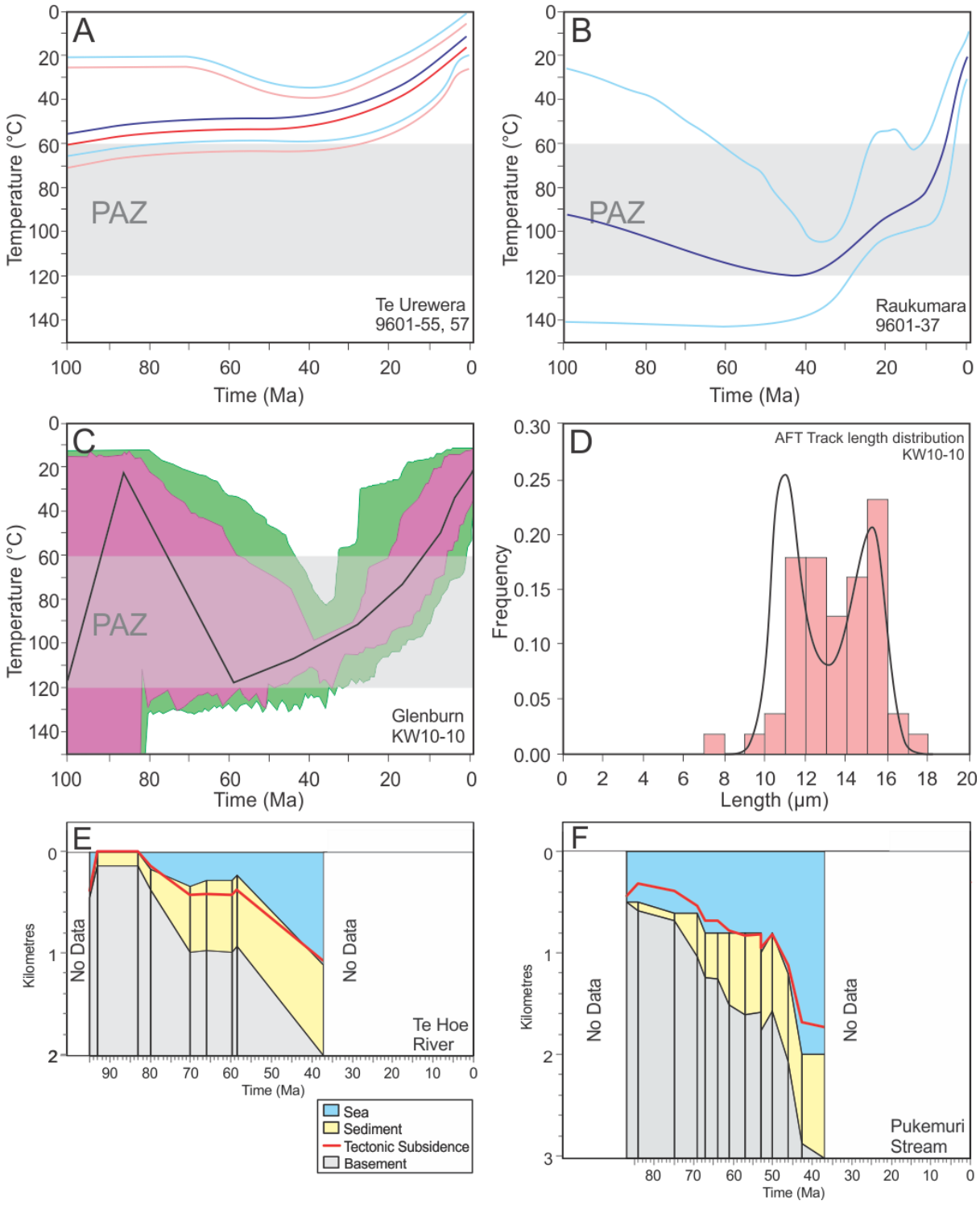

Figure 7.20: A) Exhumation/burial history for samples 9601-55 and 9601-57 from the Waikaremoana area of Te Urewera modelled in QTQt by Jiao *et al.* (2015). Blue line (sample 9601-57) indicates structurally higher position than sample 9601-55 (red line), with their respective 95% confidence intervals shown by pale blue and red lines respectively. B) Exhumation/burial history for sample 9601-37 the Raukumara Range, modelled in QTQt by Jiao *et al.* (2015). 95% confidence intervals shown by pale blue and red lines respectively. C) Thermal history model for the Glenburn area (sample KW10-10; this study) modelled in HeFTy. Black line show the mean model path. Purple envelope shows 68%

confidence interval, green envelope shows 98% confidence interval. D) Apatite fission track length distribution used in the construction of the KW10-10 HeFTy model. E) 1D-model for the stratigraphic succession at Te Hoe River. F) 1D-model for the stratigraphic succession at Pukemuri Stream. The burial history models shown in E) and F) were produced using the "geohistory.exe" tool, developed By Phil Scadden and GNS Science.

7.11 Summary

In the East Coast Basin, distinctive phases of tectonism at 105 Ma, 98 Ma, and 82 Ma, can be tied to significant basin-wide unconformities, as well as various phases of volcanism in the wider New Zealand region (Tulloch *et al.*, 2009; Crampton *et al., in prep.*). A major intra-Ngaterian event is recognised in the East Coast Basin resulting in a regionally extensive unconformity (Figure 7.4 & 7.17; Phillips, 1985; King, 2000b, Crampton *et al. in prep.*). The top of the Clarence-Raukumara sequences have been truncated by a Piripauan uplift, folding, and erosional event, resulting in a regional unconformity underlying the M1 sequence (Moore, 1978, 1989b; Phillips, 1985; Isaac *et al.*, 1991; Kamp, 1999; Crampton *et al.*, in prep.; Figure 7.17). Third- and second-order sequence boundaries identified here correspond with sequence boundaries in the European succession (Haq, 2014) and the New Jersey records (Browning *et al.*, 1996; Miller *et al.*, 2003, 2004, 2005; Kominz *et al.*, 2008), demonstrating that the East Coast Composite section is recording a eustatic signal. The exception to this is the S3 and M4 sequences, which appear to correspond with local subsidence.

The second-order cycles identified by King (2000b) in the New Zealand Cretaceous–Paleogene succession, and the third-order sea-level cycles of Schiøler *et al.* (2002), show a poor correlation with the European sequences identified by Haq *et al.* (1987; Figures 7.12 & 7.17). On this basis, both King (2000b) and Schiøler *et al.* (2002) attributed significant local unconformities to several phases of local tectonic activity. In Raukumara Peninsula, deposition had been ongoing since the Korangan, and since the Urutawan in Marlborough, with various local and regional unconformities of generally short duration (<1–2 Myr), a number of which can be attributed to tectonic events (Laird, 1992; Schiøler *et al.*, 2002; Laird & Bradshaw, 2004; Crampton *et al.*, 2003, 2006).

Distinguishing eustatic signals from tectonic signals within a sequence stratigraphic framework is both problematic and contentious (Miller *et al.*, 2004; Crampton *et al.*, 2006). This is particularly in regard to the variability and discontinuity between sea-level records (e.g., Haq *et al.*, 1987; Hardenbol *et al.*, 1998; Miller *et al.*, 2003; Kominz *et al.*, 2008). In addition, in the probable absence of extensive polar ice sheets during the Cretaceous, it remains uncertain whether there actually

were high-frequency, eustatic sea-level fluctuations, and if so, what the causal mechanism was (Miller *et al.*, 2004; Crampton *et al.*, 2006).

Recent revision of stratigraphic surfaces in the European succession incorporating morphological changes in response crustal warping by (Haq, 2014) has resulted in a high degree of correspondence between the European and New Jersey sea-level records. The correlation between sea-level events from the European succession (north-western Europe, Russian platform; Haq, 2014), the New Jersey coastal plain (Miller *et al.*, 2003, 3004, 2005; Kominz *et al.*, 2008), and the East Coast Basin (Crampton *et al.*, 2006; this study), demonstrates that Cretaceous sea-level undoubtedly had a third-order control.

High-resolution quantitative biostratigraphic analysis by Crampton *et al.* (2006) demonstrated that the stratigraphic record in shelf–slope marine strata of the East Coast Basin is substantially incomplete, with 50–75% of time missing from the geological record (at the 1–25 Myr scale). This observation expresses the importance in considering multiple, composite records, as has been achieved in this study. In addition, the amount of missing time from the stratigraphic record, and the complexities in resolving high-frequency records in sections within a substantially tectonically disrupted basin, suggests that resolving below a third-order cyclicity will not be a straightforward task.

Page intentionally left blank for formatting purposes

Chapter Eight

SYNTHESIS & CONCLUSIONS:

Palinspastic Reconstructions of the East Coast Basin

"Tomorrow, and tomorrow, and tomorrow,
Creeps in this petty pace from day to day,
To the last syllable of recorded time…"
-spoken by Macbeth, in Macbeth, William Shakespeare

Looking down the gorge in Branch Stream, Seaward Kaikoura Mountains in far distance. Photo from Kyle Bland.

Page intentionally left blank for formatting purposes

Chapter Eight

SYNTHESIS & CONCLUSIONS:

Palinspastic Reconstructions of the East Coast Basin

8.1 Introduction

The paleogeographic maps presented in this chapter provide the medium to summarise inferences derived from tectonic, sequence stratigraphic and paleoenvironmental data presented in previous chapters and appendices 1, 6, and 11. The maps are accompanied by the overarching summary and conclusions of this thesis.

8.2 Palinspastic Reconstructions

The tectonic reconstruction presented in Chapter Five has been stepwise retro-deformed to 40 Ma to provide a structural base for paleogeographic reconstructions. The structural base for the paleogeographic model was pinned at 40 Ma, as it pre-dates the propagation of the modern Australia-Pacific plate boundary through New Zealand, and also marks the youngest interval selected for paleogeographic reconstruction. Retro-deformation of the tectonic model was not extended beyond 40 Ma, due to general and widespread evidence for tectonic stability in the East Coast region between 85–40 Ma, and throughout much of the New Zealand region during this period (e.g., King, 2000a). In addition, uncertainties and errors associated with the Australian-Antarctic-Pacific plate system, which drives regional scale movements within the tectonic model, increase substantially beyond 40 Ma, resulting in little benefit from attempting to force the model beyond this point. There is evidence for tectonism in the East Coast Basin during the Ngaterian, the earliest interval selected for paleogeographic reconstruction. However, the timing, style and distribution of this tectonism are poorly resolved, and it is therefore difficult to quantify and include within the model.

Data from 331 stratigraphic sections were incorporated into the final reconstruction from across the East Coast Basin, including data from petroleum exploration wells (20 sections), the East Coast Cretaceous-Cenozoic programme (CCP; 158 sections), published literature (153 sections) and fieldwork conducted during the course of this thesis (88 sections; Figures 2.1 & 8.1). In addition, a large amount of paleontological data were accessed through the fossil record electronic database (FRED; www.fred.org.nz).

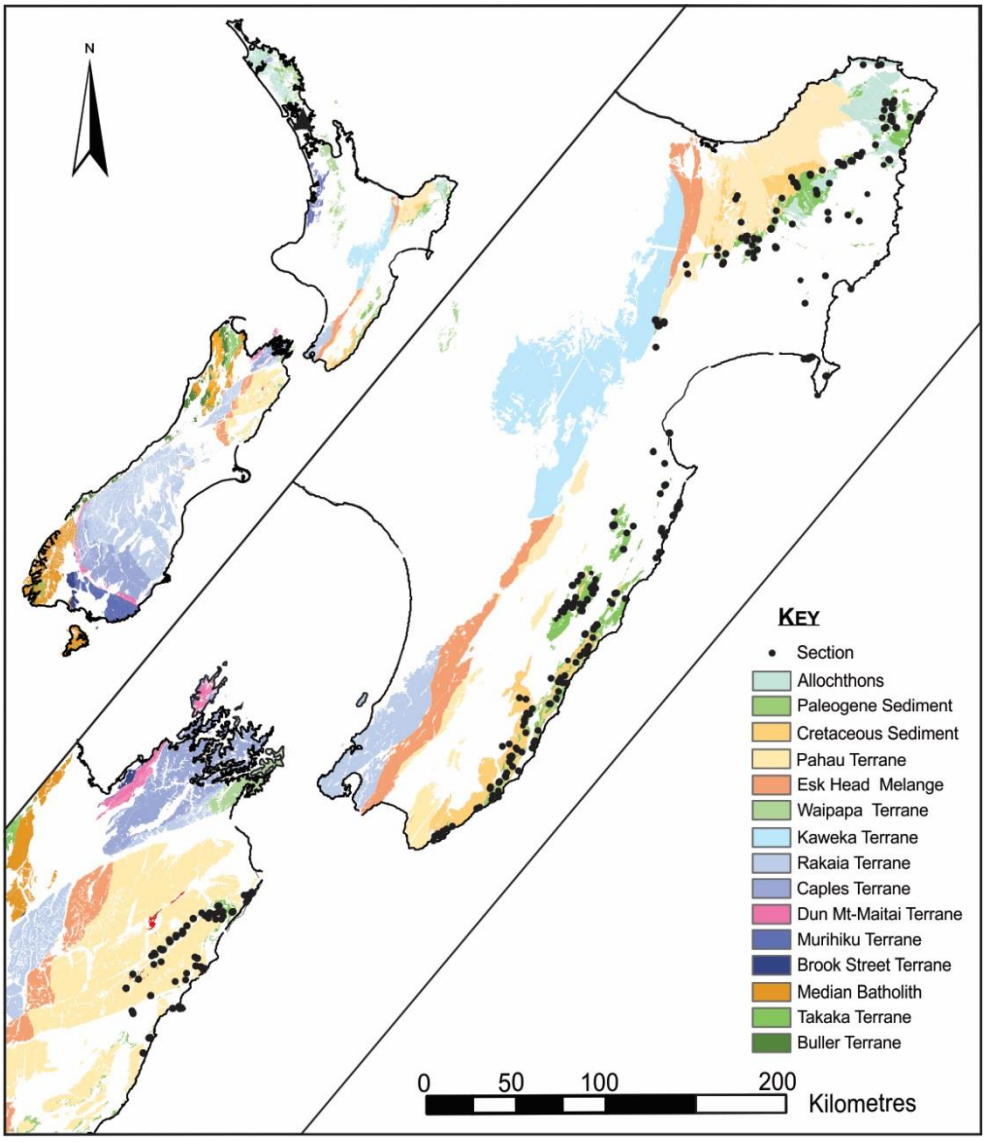

Figure 8.1: Location of sections compiled in this study to produce the paleogeographic maps presented in Figures 8.3–8.9.

Seven timeplanes were selected for palinspastic reconstructions. These are: the Ngaterian (~95 Ma), Piripauan (~85 Ma), early-Late (mid-) Haumurian (~75 Ma), Cretaceous-Paleogene (K/Pg) boundary (66 Ma), late Teurian (~59 Ma), Mangaorapan (~50 Ma), and the Bortonian (~40 Ma). These timeplanes have been selected based on two factors; 1) representation within the stratigraphic record, and 2) key surfaces within the first- to second-order depositional sequence (Chapter Seven), spaced at approximately 10 Ma intervals. These intervals correspond to reconstructed timeplanes in the Taranaki, Deepwater Taranaki, Northland, Aotea, Reinga, Canterbury, and Great South basins (Arnot & Bland *et al.*, 2016; Strogen *et al.*, 2017; Sahoo & Bland *et al.*, 2017). Jointly, these reconstructions provide Late Cretaceous and Cenozoic paleogeographies for the majority of the Zealandia continent.

Paleodepth determinations applied herein are dependent largely on benthic foraminiferal-based paleodepth assessments, outlined in Chapter Four (Figure 8.2). Paleodepth estimates are supplemented in some cases by paleo-bathymetric indicators within dinoflagellate assemblages (e.g., Roncaglia *et al.*, 1999; Crampton *et al.*, 2000; Schiøler *et al.*, 2002), macrofossil associations (e.g., Black, 1980; Phillips, 1985), and sedimentary structures (e.g., Black, 1980; Moore, 1988a; Leckie *et al.*, 1992; Wilson *et al.*, 2005). Paleodepth divisions used in palinspastic reconstructions follow conventional divisions used in paleo-bathymetric estimations and paleogeographic reconstruction for the Cretaceous-Cenozoic in the New Zealand (e.g., Hayward, 1986; Morgans, 2009; Hayward *et al.*, 2010; Arnot & Bland *et al.*, 2016; Strogen *et al.*, 2017; Sahoo & Bland *et al.*, 2017).

Paleocurrent direction presented in paleogeographic reconstructions in most instances, represent averaged values from a single locality. Where a range of directions are indicated in a dataset, the dominant direction(s) are plotted. Determination of paleocurrent directions is based on the long-axis orientation of flute casts, parting current lineations, ripple orientations, and channel structures (e.g., Crampton & Laird, 1997; Isaac *et al.*, 1991). Paleoslope directions are determined by the orientation of the axial plane of syn-sedimentary slump folds. Regional geographic trends and distributions are discussed relative to the reconstructed north, and as such orientations that are given with respect to the paleogeographic orientation are referred to with the prefix 'paleo-' (e.g. paleo-north).

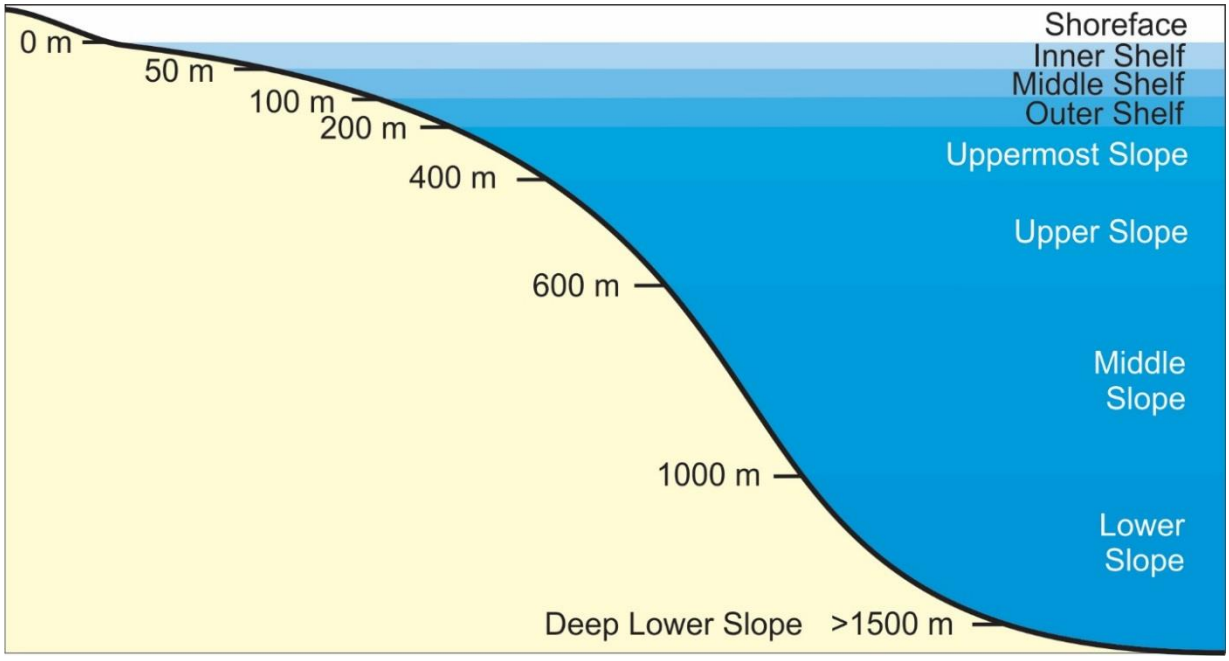

Figure 8.2: Adopted paleodepth classification scheme used in paleogeographic reconstructions. Modified from Morgans (2009) and Hayward *et al.* (2010).

8.3 Paleogeographic Reconstructions

8.3.1 Ngaterian

In paleo-northwestern areas, the late Ngaterian is marked by deposition of either slope-fan systems of the Waitahaia Formation, or shelfal mudstones of undifferentiated Karekare Formation. The paleo-west of the basin fill is characterised by deposition of the Springhill Formation at middle- to outer-shelf depths (Chapters Two & Seven; Crampton, 1997). Paleo-eastern parts of the basin are dominated by a coarsening-upwards succession of submarine fan and channel structures deposited at slope depths (Glenburn Formation) infilling the abandoned Mesozoic subduction trench on the relict eastern Gondwana subduction system (Crampton, 1997).

Relict sub-basins inherited from Early to mid-Cretaceous grabens and half-grabens in the paleo-southern part of the basin, in the Marlborough area (Laird & Bradshaw, 2004), were progressively infilled by the Split Rock Formation, eventually forming a shallow shelf that persisted throughout most of the Late Cretaceous. These sub-basins had been buried by the late Ngaterian, demonstrated by the widespread deposition of terrestrial, marginal- and shallow-marine strata associated with the Warder and Bluff Sandstone formations across much of Marlborough.

Sediment provenance in the paleo-northwestern parts of the basin are derived from a mixed Median Batholith (or other felsic source; see Chapter Six) and reworked Rakaia Terrane source (Figure 8.3). Sediment provenance changes southwards in the basin, with a dominantly reworked Rakaia Terrane and minor Pahau Terrane source in the paleo-central and eastern parts of the basin (Chapter Six; Figure 8.3), with an isolated occurrence that demonstrates a strong Median Batholith and Western Province provenance. Deposition within the paleo-southeastern regions of the basin are dominated by a locally-derived Pahau Terrane source (Chapter Six; Figure 8.3).

Paleocurrent orientations are varied across the basin, although paleo-north to northeast current orientations tend to prevail in paleo-northeastern and paleo-southeastern areas of the basin. Paleo-west-oriented currents in the paleo-western and paleo-northern areas of the basin might indicate relict topography in local sub-basins. Similarly, a single paleoslope direction indicates a paleo-southwest slope orientation, although little significance should be attached to a single measurement.

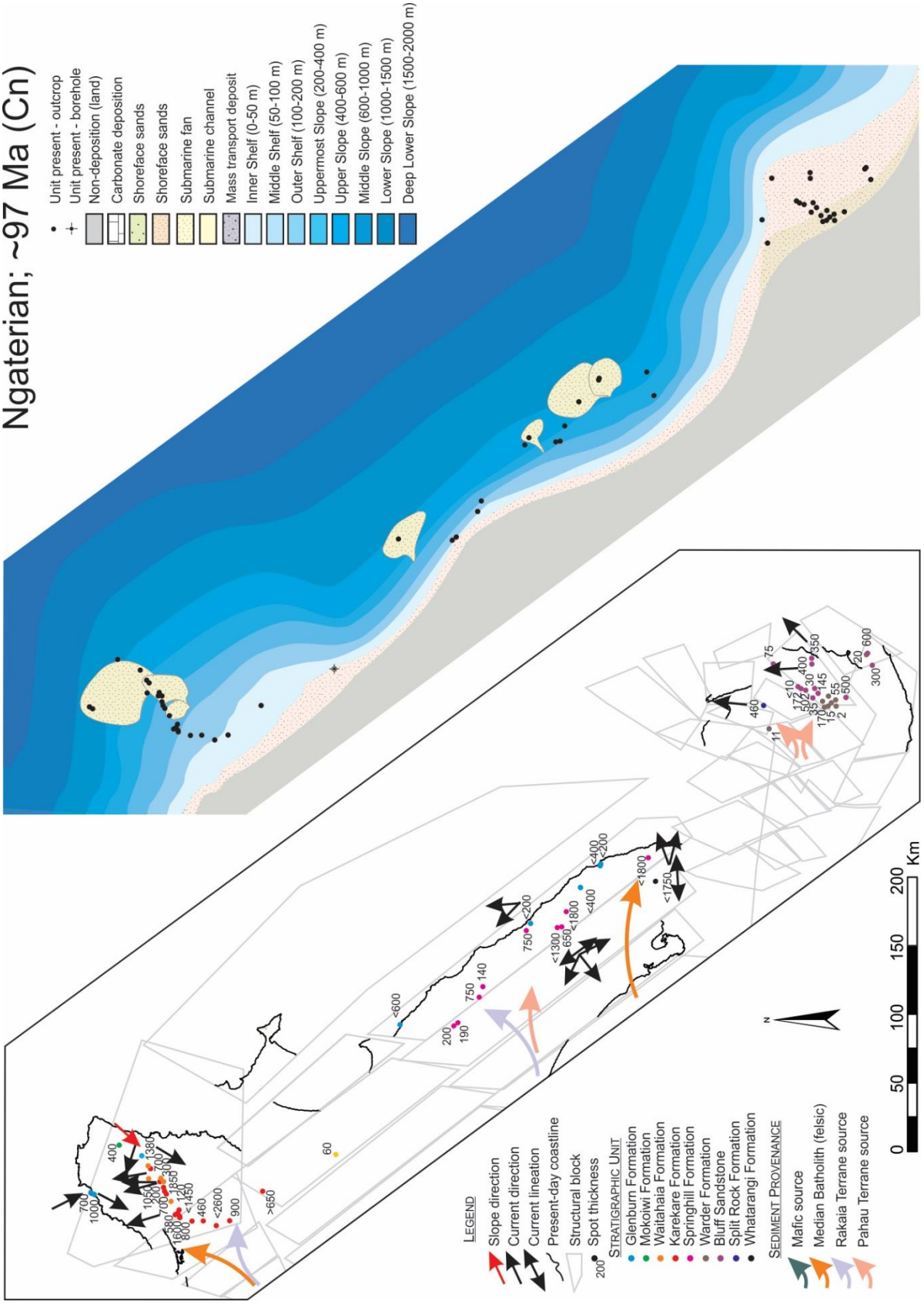

Figure 8.3: Distribution of formations and measured sections spanning the Ngaterian, and spot thicknesses, alongside interpreted paleobathymetry and paleodepositional settings.

8.3.2 Piripauan (85 Ma)

The paleo-northwest of the basin is characterised by the deposition of nearshore and inner-shelf sediments and linear sandbars and channel complexes of the Tahora Formation (Isaac *et al.*, 1991). The Tahora Formation deepens progressively paleo-eastwards to an outer-shelf environment, grading into the slope-fan lithofacies of the Owhena Formation (Phillips, 1985; Isaac *et al.*, 1991). Paleo-western, central areas of the basin record deposition in nearshore environments at Ngapaeruru-1 (Smiley, 2014), deepening paleo-eastwards to middle–outer shelf environments settings (Tangaruhe Formation; Crampton, 1997). Paleobathymetric highs were present within paleo-western and northwestern areas, evident in debris-flow deposits that indicate local sediment shedding on the margins of the highs (Mangawarawara Member and Kirk's Breccia Member). In the paleo-northwest, these deposits have been associated with localised, margin-parallel faulting and fold propagation at this time (Moore, 1989b; Moore *et al.*, 1989; Isaac *et al.*, 1991).

Between the Ngaterian and Piripauan, paleo-eastern parts of the basin are dominated by the deposition of a widespread, generally coarsening- and shallowing-upwards succession of flysch lithofacies, representing the long-lived submarine fan systems of the Glenburn Formation, infilling the relict topography associated with the extinct Mesozoic subduction complex.

Paleo-southeastern areas are characterised by the widespread deposition of shallow-marine sandstones in inner- to outer-shelf environments (Paton Formation), across a broad, shallow shelf. In the paleo-southernmost extent of the basin, deposition of the terrestrial to marginal-marine sediments (Okarahira Sandstone) indicates the location of the paleoshoreline.

Sediment provenance varies across the basin, and marks an evolution of sediment sources since the Ngaterian. The paleo-northwest had a dominantly Rakaia Terrane source, with a subordinate proportion derived from the Pahau Terrane (Chapter Six; Figure 8.4). Central and paleo-eastern areas of the basin are characterised by a mixed Rakaia and Pahau Terrane source (Chapter Six, Figure 8.4). Sediment in the paleo-southeastern areas is derived from locally-derived Pahau Terrane and, in a restricted area, from a locally-derived mafic source (Chapter Six; Figure 8.4).

Paleocurrents are predominantly from paleo-eastern parts of the basin, and commonly indicate paleo-northwest to paleo-northeast directed currents. A single paleoslope orientation indicates a paleo-northwards facing slope direction (Figure 8.4).

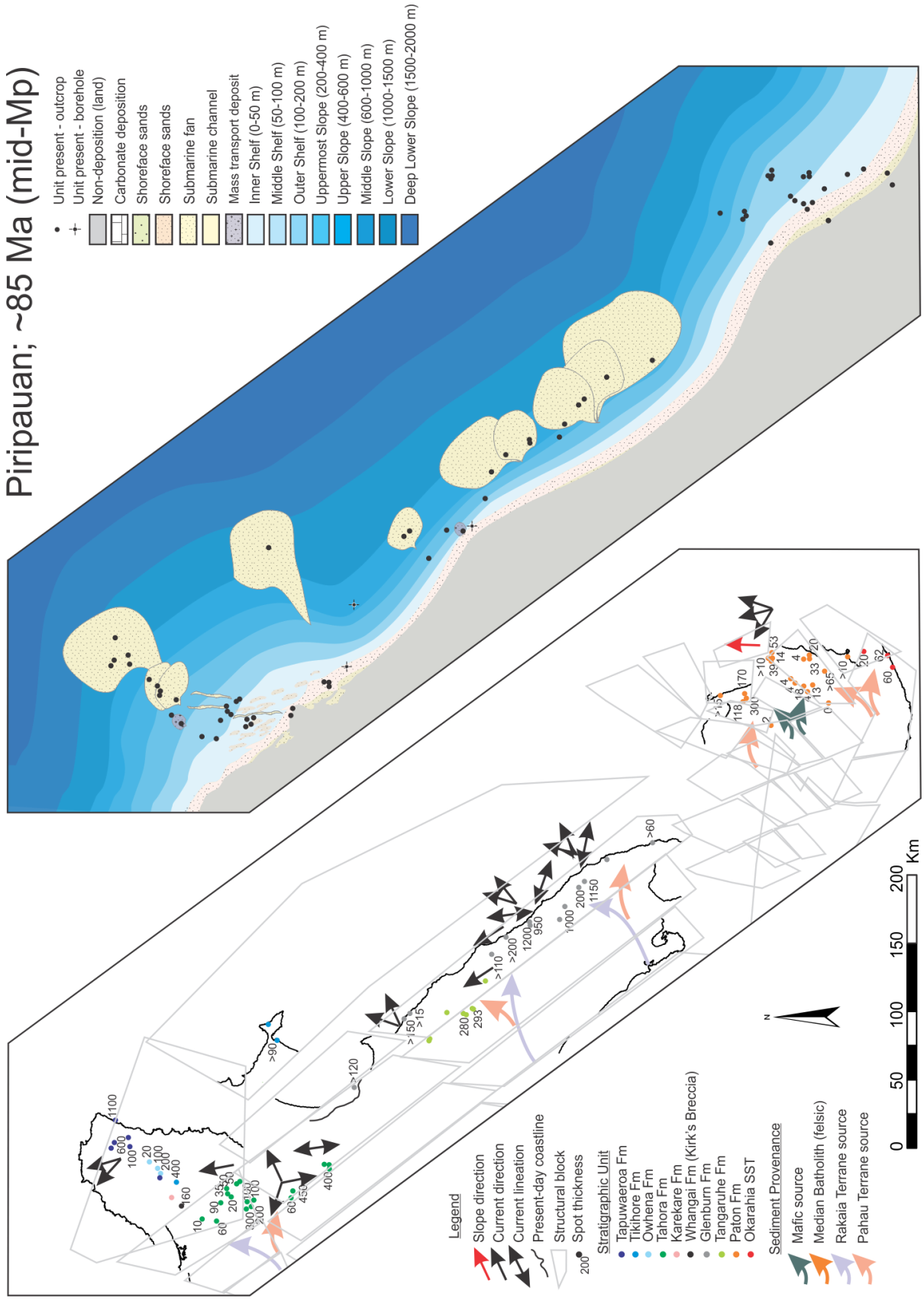

Figure 8.4: Distribution of formations and measured sections spanning the Piripauan, and spot thicknesses, alongside interpreted paleobathymetry and paleodepositional settings.

8.3.3 Haumurian (~75 Ma)

Marine transgression is apparent between the Piripauan and Haumurian paleogeographic reconstructions (Figures 8.4 & 8.5). The abrupt cessation of submarine fan deposition (Glenburn Formation) in paleo-eastern parts of the basin during the late Piripauan to early Haumurian, was followed by the widespread deposition of massive, siliceous mudstones of the Whangai Formation (Rakauroa Member and Herring facies). This is inferred to coincide with an abrupt reduction in hinterland topography during the late Piripauan to early Haumurian (Neef, 1995).

Paleo-northwestern areas deepen to middle- to outer-shelf depths (Tahora Formation), with paleo-northeastern and eastern areas reaching middle-slope depths (Rakauroa Member). Likewise, central, paleo-western areas deepen to upper-slope depths (Upper Calcareous Member). In the paleo-southeast, paleodepths are primarily between middle-shelf and uppermost-slope depths (Whangai [Herring] Formation), the paleo-southernmost sections indicating inner-shelf settings (Conway Siltstone). The younging and thinning of the Whangai Formation southwards across the paleo-southeast, with little change in depositional setting, is in agreement with the interpretation of a shallow shelf, with a low gradient, a feature inherited during the Ngaterian. Further towards the paleo-northwest, there are few constraints on the width of the shelf. The localised presence of carbonaceous siltstone and coal in the thickest, and paleo-westernmost section of the overlying Branch Sandstone suggests possible subaerial emergence (Reay, 1993), providing an indication of where the Haumurian shoreline lay.

Despite a widespread, distinctive change in bulk lithology towards siliceous, micaceous mudstone across the basin, no distinct changes in sediment provenance pathways are distinguishable between the Piripauan and the Haumurian.

Paleocurrent directions are variably oriented, but are commonly directed margin-parallel, towards the paleo-northwest, or are directed margin-perpendicular, in a paleo-northeast direction (Figure 8.5).

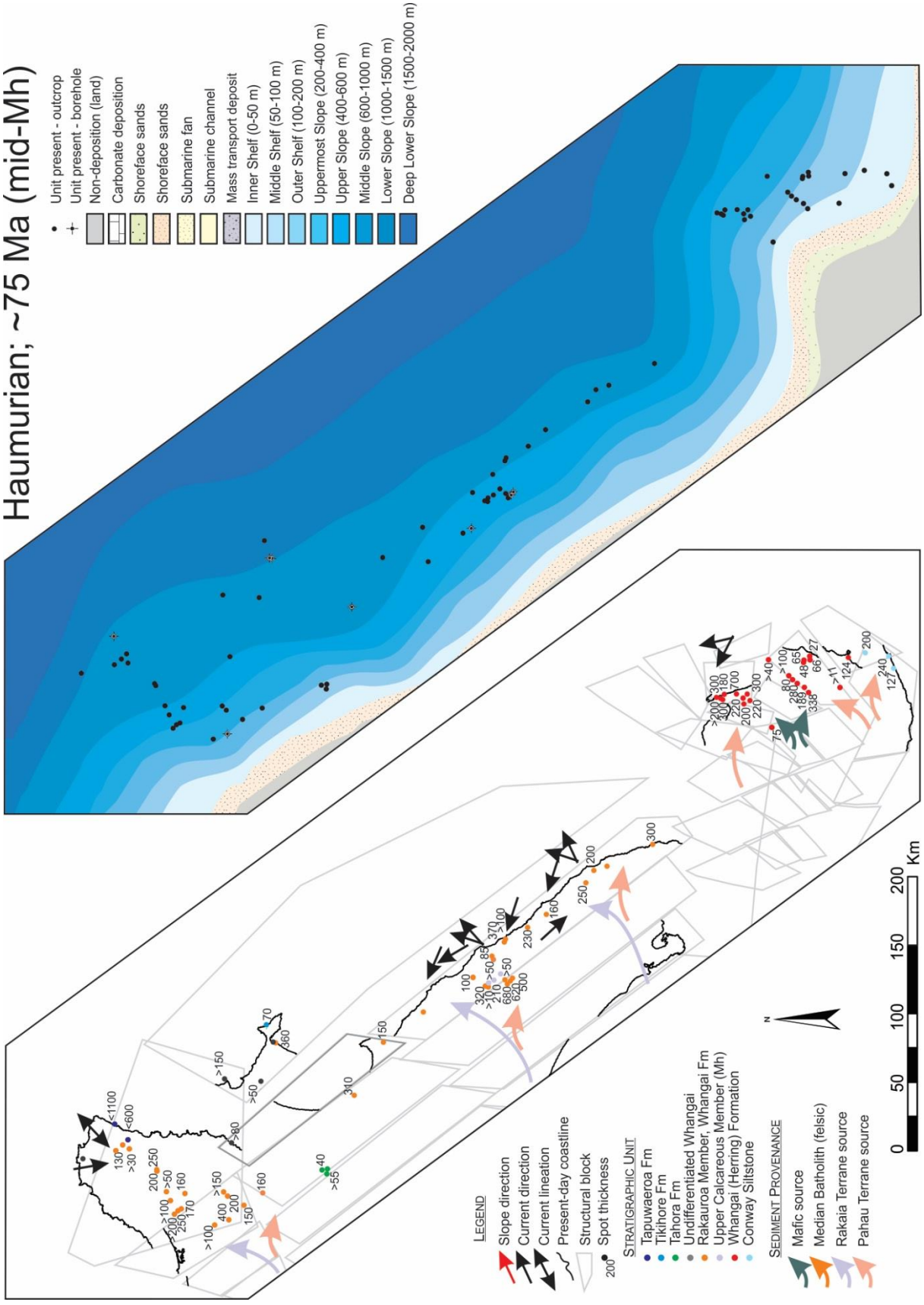

Figure 8.5: Distribution of formations and measured sections spanning the Haumurian, and spot thicknesses, alongside interpreted paleobathymetry and paleodepositional settings.

8.3.4 K/Pg Boundary (66 Ma)

The interval immediately preceding the K/Pg boundary (from ~67 Ma) is marked by a distinctive sea-level lowstand across the East Coast Basin (Chapter Seven). Paleo-western parts of the basin at this time are marked by either continued deposition of the Rakauroa Member or an unconformity at the top of the Rakauroa Member. In a very restricted area in the central part of the basin (Whangai Range), there was the development of an early Paleocene condensed section (Te Uri Member) which developed through reduced sedimentation rates, possibly on a bathymetric high (Chapter Four). The paleo-eastern parts of the basin are characterised by the development and progradation of geographically discrete submarine fan systems (Porangahau Member; eastern Raukumara and eastern Hawke's Bay-Wairarapa areas). In the paleo-southeastern region, there is no distinct stratigraphic change across the K/Pg boundary, with the widespread deposition of the Mead Hill Formation (some of which has been removed by the development of an unconformable surface in paleo-southern to southwestern areas). The preceding lowstand interval reached its maximum at ~67 Ma, as marked by the shallow-marine Branch Sandstone at the base of the Mead Hill Formation in Marlborough and, from 67–66 Ma, by rapid deepening characterised by deposition of the Mead Hill Formation (e.g., Crampton *et al.*, 2003).

Sediment pathways are stable through the latest Cretaceous and Paleogene, with paleo-northeastern areas characterised by a dominant Rakaia Terrane sediment source, with a minor component derived from the Pahau Terrane (Chapter Six; Figure 8.6). Central areas of the basin demonstrate a mixed Rakaia and Pahau Terrane source (Chapter Six; Figure 8.6). In paleo-southeastern areas, sediment is derived from locally sourced Pahau Terrane, and in a restricted region, from an eroding mafic igneous body (Chapter Six; Figure 8.6).

Paleocurrents are known from a single area, and indicate paleo-north to paleo-northeast directed flows in the central, paleo-eastern area of the basin.

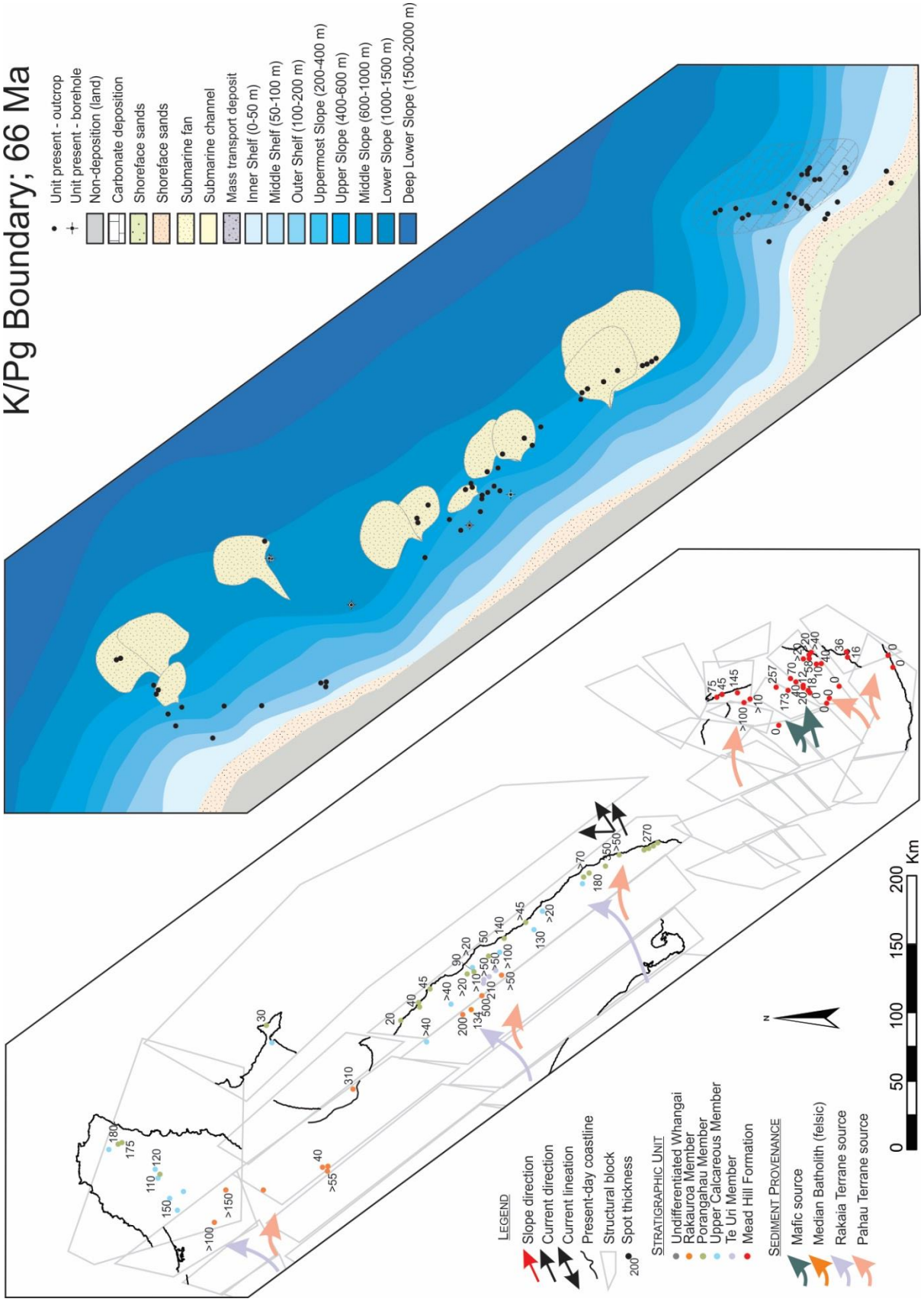

Figure 8.6: Distribution of formations and measured sections spanning the K/Pg boundary, and spot thicknesses, alongside interpreted paleobathymetry and paleodepositional settings.

8.3.5 Late Teurian (~59 Ma)

There is a wealth of data available for the late Teurian interval, in stark comparison to the preceding intervals (Piripauan, mid-Haumurian; K/Pg boundary), due to the considerable petroleum industry interest in this interval for prospective source rocks (particularly the Waipawa Formation). The Waipawa Formation is distributed across the full extent of early Paleogene succession in the basin, with the exception of Hukarere-1, the Whangai Range and southern Marlborough (Hurunui High) area, although correlative units and/or surfaces are present across these areas. The presence of the Waipawa Formation (and correlatives) in these sections is particularly useful from a paleogeography viewpoint, as it provides a distinctive, isochronous interval of narrow thickness and duration, perfectly suited for correlation across the >500 km length of the basin (Chapters Three, Four & Seven; Figures 8.7, 7.19 & 7.20).

Paleobathymetric data, derived from foraminiferal and ichnofaunal proxies across the Waipawa Formation and correlative strata, are considered in Chapter Four. These data indicate outer-shelf to uppermost-slope settings across the formation in the paleo-northwest of the basin, deepening paleo-eastwards to middle–lower-slope settings (Figure 8.7). Paleo-western parts of the basin are characterised by deposition of a glauconitic lithofacies within a restricted distribution, in outer-shelf to uppermost slope depths (Te Uri Member, Whangai Range; Chapter Four; Figure 8.7). The very restricted distribution of the Te Uri Member during this interval, along with stratigraphic and paleontological evidence (Chapter Two, Four), indicates that this area was a structural high, representing a shallower environment than coeval sections in adjacent northern Whangai Range and Eastern Sub-belt sections (Chapter Four). In the absence of paleobathymetric data from the Te Uri Member in Hukarere-1, this has been indicated as a structural high based on correlation with the environmental setting indicated by the Te Uri Member in the Whangai Range. If this is in fact a structural high, the Whangai Range and the Hukarere-1 structure could represent a margin parallel structure, perhaps consistent with the implication of inherited topography from the extinct Mesozoic subduction margin.

Provenance patterns from the K/Pg persist through to the late Teurian interval (Figure 8.7). Paleo-north and paleo-east of the Whangai Range is characterised by upper-slope depths, deepening towards middle-slope settings to the paleo-southeast (Tora). The paleo-southeastern area of the basin (Marlborough) is characterised by the deposition of the Teredo Limestone Member in middle-shelf to uppermost-slope settings. The Waipawa Formation has been identified in isolated sections in the northern Marlborough area, and was deposited at middle-slope depths (Figure 8.7).

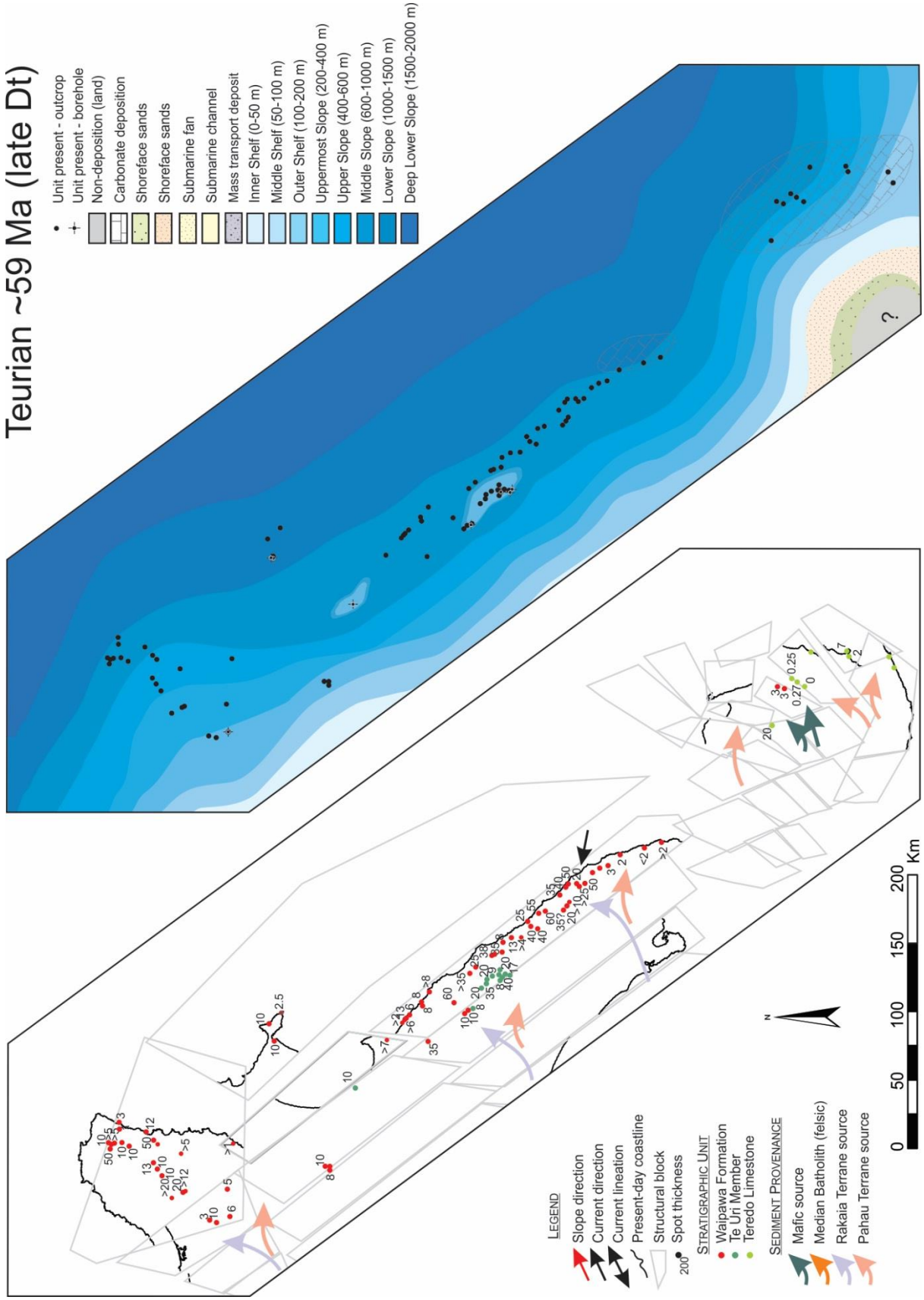

Figure 8.7: Distribution of formations and measured sections spanning the late Teurian, and spot thicknesses, alongside interpreted paleobathymetry and paleodepositional settings.

8.3.6 Mangaorapan (~50 Ma)

The period between the late Teurian and Mangaorapan is dominated by a marine transgression trend across the basin. The physiography of the basin at this time is characterised by deposition at slope depths, generally in the range of 200–1000 m paleodepth. No notable structural or bathymetric highs are evident at this time.

In central and paleo-northern areas of the basin, the sedimentary succession is dominated by fine-grained, smectitic mudstone and marl of the Wanstead Formation. In the paleo-southeast (Marlborough), the deposition of pure, micritic limestones during the late Paleocene to early Eocene is interrupted by widespread deposition of alternating marl and micritic limestone during the Mangaorapan to early Heretaungan. This marl is interpreted as a sedimentary response to increased terrestrial discharge associated with increased rates of weathering and terrigenous discharge during the Early Eocene Climatic Optimum (e.g., Slotnick *et al.*, 2012; Dallanave *et al.*, 2015). The distinction between the calcareous, smectitic mudstone in central and paleo-northern parts of the basin, and micritic limestone in paleo-southeastern areas, indicates that the Marlborough area was either more distal, or buffered from terrigenous influx.

Although sedimentation rates are notably reduced across this interval, and there is a distinctive shift to smectitic-clay dominated sediments in the central and paleo-northern parts of the basin at this time, geochemical indicators suggest that sediment provenance remained similar to that during the preceding K/Pg and Teurian reconstructions (Figure 8.8).

Despite lithological differences between the Wanstead Formation and the Lower Marl member of the Amuri Limestone, they can both be characterised by the deposition of fine-grained, carbonate-rich sediments, at paleodepths between 200–1000 m. Isolated occurrences of mass-transport deposits occur across the basin within the Wanstead Formation (Tora, Glenburn, Porangahau, and Port Awanui areas) during the Mangaorapan (Figure 8.8).

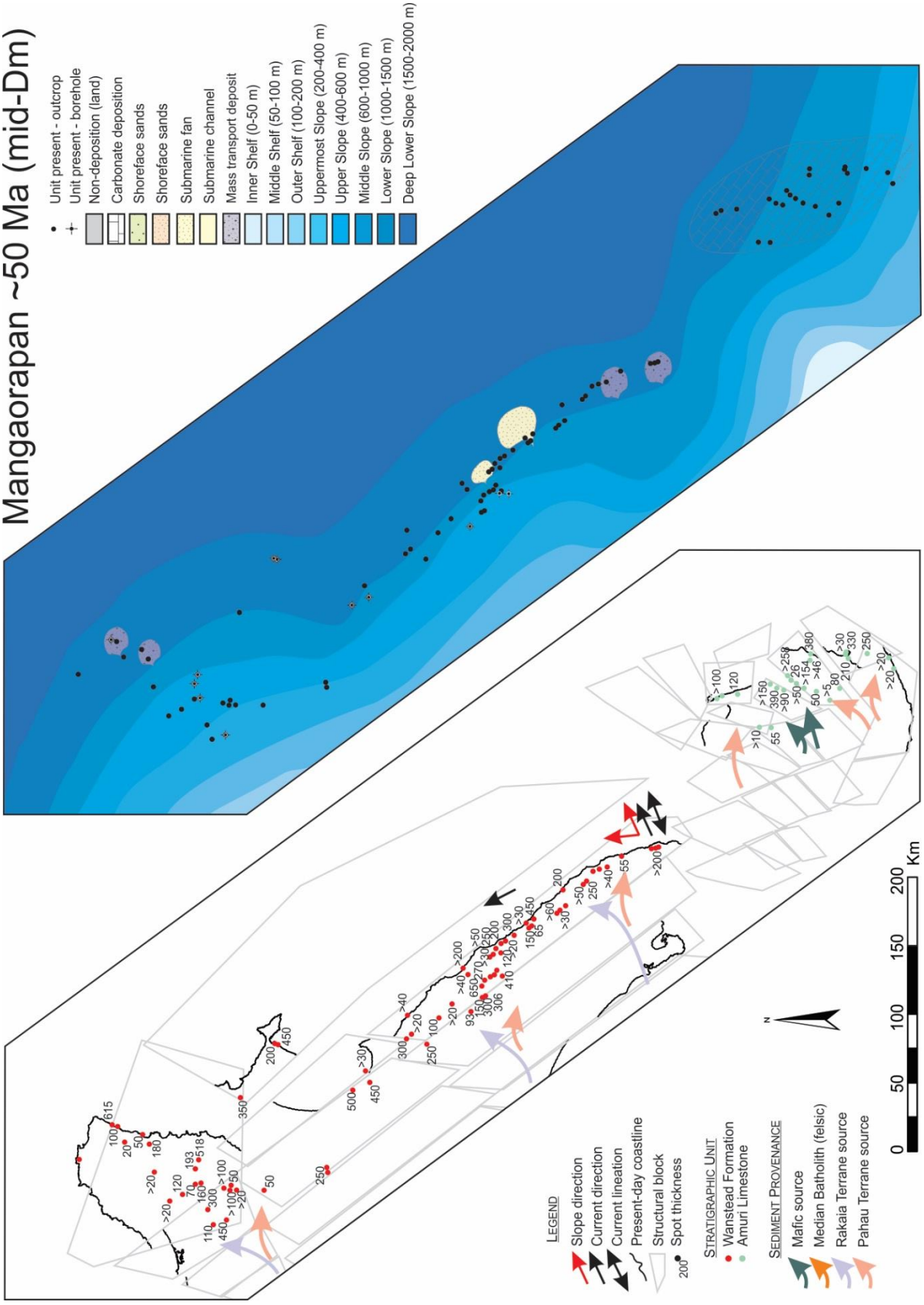

Figure 8.8: Distribution of formations and measured sections spanning the Mangaorapan, and spot thicknesses, alongside interpreted paleobathymetry and paleodepositional settings.

8.3.7 Bortonian (~40 Ma)

The Bortonian Stage preserves the deepest inferred paleodepths identified within the East Coast Basin, representing the ongoing maximum flooding of the Zealandia continent during the late Bortonian to Kaiatan (King, 2000), associated with Paleogene passive margin thermal subsidence.

In the paleo-northwest area of the basin, paleodepths increase to range from upper slope in proximal areas, to lower-slope depths towards the paleo-east. Central, paleo-western areas of the basin (Whangai Range) consistently demonstrate middle-slope depths in benthic foraminiferal faunas (Chapter Four, Appendix 6). Further towards the paleo-east (Eastern Sub-belt), paleodepths are commonly at lower-slope depths, indicated by the lowermost bathyal to abyssal dwelling (>2000 m) benthic foraminifera *Abyssamina poagi* in a number of sections (Porangahau, Tukituki River, Te Mai Stream, Pukemuri Stream; Morkhoven *et al.*, 1986; Hines *et al.*, 2013; FRED; Morgans, Pers. Comms. 2016). Consequently, bathymetric contours are tightly spaced in the intervening area between the Whangai Range and the Eastern Sub-belt. Elsewhere in the basin at this time, paleoecological proxy data inform the placement of broadly spaced bathymetric contours in the paleo-northwest and paleo-southeast.

No change in sediment source is apparent through the Paleogene in bulk-rock geochemical provenance indicators, although sedimentation rates had decreased notably. No paleocurrent data are recorded for the Bortonian Stage in the East Coast Basin.

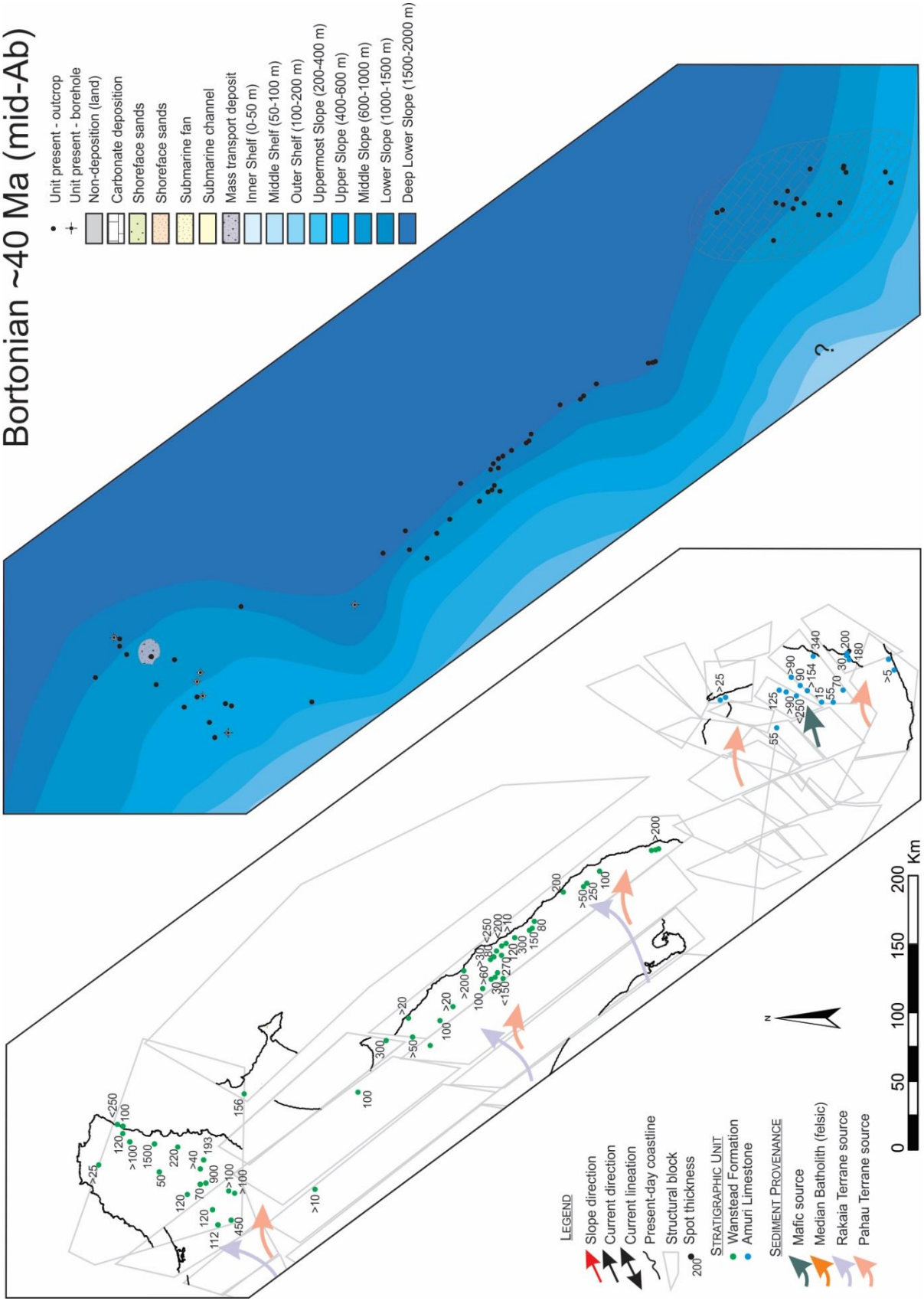

Figure 8.9: Distribution of formations and measured sections spanning the Bortonian, and spot thicknesses, alongside interpreted paleobathymetry and paleodepositional settings.

8.4 Discussion of Paleogeographic Reconstructions

Paleogeographic reconstructions of the East Coast region during the Late Cretaceous indicate a northwest–southeast-trending, linear margin. An interesting observation is that the position of the coastline within the East Coast Basin has not varied substantially between the Cretaceous and present. Likewise, the areas of the basin characterised by Ngaterian–Piripauan submarine fan deposits are the same areas where submarine fans propagate across the K/Pg boundary. Submarine fan development in the same regions implies that the position of the shelf-slope break did not change much during this entire interval from ~95–65 Ma, consistent with a passive margin setting, although surprising considering ~30 Ma of progressive basin fill. This suggests that basin subsidence during this time was equal to, or slightly greater than, the sediment accumulation rate. Additionally, this indicates a strong first-order structural control on the margin, marked by the crustal-scale Mesozoic and Neogene plate boundary zone.

Cretaceous topography is known to have existed in East Cape, Whangai Range and Marlborough areas (e.g., Kenny, 1984, 1986; Laird, 1992; Crampton, 1997; Laird & Bradshaw, 2004), and the rapid deposition of thick sedimentary sequences between the Ngaterian to Haumurian suggests that the mid- to Late Cretaceous was a period of infilling topographic lows and burying of inter-basinal highs (Kenny, 1986). By the Piripauan, much of the relict topography of the eastern margin (Mesozoic subduction trench), and Marlborough portions of the basin had been buried.

The stratigraphic character of the Marlborough region is distinct from trends exhibited elsewhere in the East Coast Basin. Paleo-southwestward-directed marine transgression is evident in the southern parts of the basin, with deposition of shallow-marine strata on top of Pahau Terrane basement during the Piripauan, at Haumuri Bluff, southern Marlborough (Warren & Speden, 1978; Crampton *et al.*, 2003). Further north, in the Clarence Valley area, deposition had been ongoing since the Motuan or Urutawan. Multiple models have been applied to the Marlborough region to explain the different sedimentary and stratigraphic styles. Decreased sedimentation rates in Marlborough during the latest Cretaceous and Paleogene may suggest that the region represents either a separate sub-basin at this time, a deeper more distal aspect of the East Coast Basin, or an isolated paleo-platform (e.g. Crampton *et al.*, 2003). The influx of terrigenous material during the Piripauan and much of the Haumurian suggests that the region was not geographically isolated. The deposition of fine-grained, dominantly micritic limestone through the Muzzle Group from the latest Haumurian to late Eocene is interpreted here as a response to rapid regional deepening of a sub-basin, and a substantially reduced terrigenous sedimentary load, likely from a tectonically quiescent hinterland with subdued topography, rather than an isolated paleo-platform. The

temporal transition towards a significantly reduced terrigenous sediment component is largely restricted to the Marlborough region, although similar facies are deposited in the southern Wairarapa during the late Paleocene (Mungaroa Limestone). This suggests that a terrigenous sediment source continued to supply most of the North Island parts of the East Coast Basin, resulting in the clastic-dominated sedimentary facies of the Whangai Formation. Increased terrigenous influx associated with the Waipawa Formation at Mead Stream, and sandstones associated with the Teredo Limestone Member elsewhere in the Marlborough region, suggest proximity to a terrigenous sediment source.

8.5 Conclusions

Specific Research Questions

1. *Can constraints be placed on paleoenvironmental changes through time, across structural divisions, to assist in the development of paleogeographic reconstructions for the East Coast Basin?*

Application of stratigraphic, sedimentological, paleontological and geochemical data has been particularly informative in resolving paleoenvironmental changes across the basin. The collection of that data, and the integration of it with published datasets, has allowed the resolution of changes in provenance, paleo-redox states, paleodepositional settings, sequence stratigraphies, and paleogeographies of the basin. The retroactive production of a pre-Neogene tectonic and structural framework has allowed these data to be placed in context, and provided a platform for multidisciplinary basin reconstruction. In addition, this study has produced revised age control and correlation of stratigraphic units across the mid-Cretaceous to late Eocene succession of the East Coast Basin.

2. *Can bulk-rock geochemistry be applied to resolve changes in provenance, paleo-redox conditions and paleoenvironmental settings?*

Bulk-rock geochemistry has been particularly useful in resolving paleoenvironmental and ocean/pore water chemical changes during the deposition of the Waipawa Organofacies, enabling the drivers of late Paleocene source rock deposition to be determined. This study has demonstrated that pXRF instrumentation can be applied to the dominantly fine-grained, often lithologically homogenous units of the East Coast Basin to resolve changes in depositional setting and provenance, and corroborate surfaces identified in sequence stratigraphic analysis. Bulk-rock

geochemistry has demonstrated that changes in the supply and sedimentation rate is the strongest driver for organic carbon preservation in the Waipawa Formation. Utilising these data in tandem with source rock analyses, it can be demonstrated that the enriched, and dominantly terrestrial source for organic matter in the Waipawa Formation is associated with increased supply of terrigenous sediment. The increase sediment accumulation is, in turn, associated with a sea-level lowstand, whereby sediment bypassed shelfal settings to be deposited at slope depths. This is then interpreted within a sequence stratigraphic framework (Chapter Seven).

Development of the depositional model for the Waipawa Formation (Chapter Four) involved first producing a pilot study (Chapter Three) to characterise the depositional conditions of 'typical' Waipawa Formation, so that geochemical trends could be correlated with expressions of the Waipawa Organofacies in other depositional settings and differing lithological and facies associations (Chapter Four).

Comparison of bulk-rock major element geochemical trends with heavy mineral assemblages and detrital zircon age-frequency distributions has also identified changes in sediment provenance within different parts of the Cretaceous succession of the East Coast Basin, providing data to support the interpretation of a locally derived, mafic source supplying sediment in the northern Marlborough area during the Late Cretaceous to Eocene. Bulk-rock geochemical analyses indicate a primarily felsic provenance for Motuan to Ngaterian sediments within a restricted area in the southeastern Wairarapa. The Late Cretaceous to Eocene is characterised by a dominantly locally derived sediment source with a consistent composition that varies little across the Hawke's Bay and Wairarapa regions (Chapter Six).

A pilot study, based on relatively high-resolution sampling through the Rakauroa Member (Whangai Formation) at Pukemuri Stream, produced a temporal sampling resolution of ~160 kyr through most of the Haumurian Stage. Variations in major element ratios through this dataset are in good agreement with third-order sequence boundaries identified across the Marlborough and Wairarapa regions, providing an avenue for further research.

3. *Can Neogene deformation be back-stripped to produce a pre-Miocene structural reconstruction of the East Coast Basin?*

The division of the East Coast Basin into a series of well-constrained structural blocks, has produced a micro-plate model that is produced in a repeatable format. The outcome of this is a palinspastic tectonic model that that can be modified relatively easily, extended and adapted for

various applications, or as further data sources become available. Development of the tectonic model has provided a strong platform for paleogeographic data representation, and is used extensively through this study.

4. *Can the signatures of global eustatic sea-level change be discriminated from tectonics in the Cretaceous-Paleogene stratigraphic successions in the East Coast Basin?*

Clearly-resolved second-order sequence stratigraphic patterns are identified across the basin, and furthermore, these data indicate that through much of the succession, a third-order sequence stratigraphic framework can be resolved. Several sequence boundaries can be correlated with records in the Northern Hemisphere (European succession and New Jersey), demonstrating that there is a eustatic sea-level signature that can be resolved in the Late Cretaceous and Paleogene succession of the East Coast Basin. The second- and third-order events identified within this study also identify local, relative sea-level changes associated with regional- and basin-scale tectonism, particularly in the Cretaceous portion of the record.

5. *How has the Paleogeography of the East Coast Basin evolved through the Cretaceous–Paleogene?*

The paleogeographic evolution of the basin is intimately tied to the second-order sequence stratigraphic trends identified in Chapter Seven, overlain on the context of a broadly passive margin from the Late Cretaceous to late Eocene. The series of palinspastic paleogeographic maps presented here are the first such series to consider the entire East Coast Basin and utilize the modified and applied tectonic base model developed in Chapter Five. The resultant paleogeographic maps demonstrate that the relative position of the coastline throughout much of the Late Cretaceous and Cenozoic has remained relatively fixed. Changes in facies are indicative of a broadly fining-upwards trend from the Late Cretaceous to late Eocene, with southern areas of the basin becoming dominated by the deposition of carbonate sediments from the latest Cretaceous onwards, whereas the northern parts of the basin are dominated by terrigenous and hemipelagic sedimentation throughout. Through the reconstructed intervals, sediment supply is primarily derived from local sources. In the northern parts of the basin, there is a transition from distal, likely Western Province basement terrane sources, towards locally derived sediment sources through the mid- to Late Cretaceous.

8.6 Future Work

Tectonic Model

Reconstruction of the East Coast region (and wider southwest Pacific region) was achieved using widely-available open-source software, making it amendable and adaptable to various applications, and facilitating future model iterations and contributions from new and developing datasets. This makes the model suitable for widespread applications in academia and the industry. To promote the use of the model, it will be published as digital source files in an appendix to publications detailing the model development process.

Stratigraphy

Although the Kaikoura earthquake either damaged, destroyed, buried or submerged a number of key sections, there is the likelihood that this has also created a number of new exposures, on the recently uplifted shore platform, in freshly created exposures in landslide scarps, and in rapidly eroding stream sections. Future field work should explore newly exposed successions.

Paleocene Source Rocks (Waipawa Formation)

The application of sulphur isotope studies across high-resolution sample transects of the Waipawa Formation will help substantially in resolving conflicting interpretations of redox states suggested by various trace element and organic proxies. Likewise, thin-section studies of pyrite framboid size distribution will also help this process. Several thin sections through the Whangai, Waipawa and Wanstead formations at the Taylor White, Angora Road section have already been prepared for this purpose. Future work should include a fine, centimetre- to decimetre-scale resolution sampling through the Waipawa Formation to refine the controls on the cyclicity identified in the formation, and determine the reality, or not, of Milankovitch cyclicity-orbital forcing through the unit. Gamma-ray scintillometer and portable X-Ray florescence analysis conducted during this thesis, in tandem with GNS Science, has already begun this avenue of research.

Thermal History

During the course of this research, sixty samples were collected, processed and counted for apatite fission track analysis on basement and cover succession across the Hawke's Bay, Wairarapa and Marlborough. A similar number of zircon mounts were prepared and irradiated and simply remain to be counted.

Apatite fission tracks throughout basement and the cover succession in the North Island and Marlborough reveal that apatites typically have barely entered the partial annealing zone, and are

only partially reset, indicating that there has been less than ~3 km of burial throughout much of the basin (assuming a geothermal gradient of 25°C/km). This has significant implications for thermal history modelling of the basin, and generative and expulsion potential in prospective source rocks. Thermochronological modelling of the thermal history within the basin will provide a useful comparison to models from the basin margin (e.g., Jiao *et al.*, 2014, 2015).

Provenance

The chemistry of garnet and muscovite varies considerably between metamorphic and granitic origins, providing a strong indication of provenance. During preparation of heavy mineral separates for isolating apatite and zircon for fission track analysis, garnet and muscovite separates were also isolated for the specific purpose of determining the major element chemistry of individual grains. In addition, zircon was particularly abundant among the heavy mineral fraction of the samples collected and processed. The zircon fraction from 60 of these samples across basement and cover rocks throughout the basin has been retained for future U/Pb analysis which will add to the dataset considered in Chapter Six of this study.

Sequence Stratigraphy

Better age control and finer lithological/stratigraphic resolution, particularly through the Ngaterian and Bortonian stages would benefit the sequence stratigraphic framework presented here immensely. The identification of sequence stratigraphic surfaces using bulk-rock geochemistry is an approach that should be applied in greater detail, and in tandem with sections with good age control and independent means of sequence stratigraphic interpretation.

Paleogeographic Palinspastic Maps

Future work would benefit through the inclusion of more timeslices for paleogeographic reconstruction. The addition of a paleogeographic map for the Motuan Stage would also be beneficial. Although Motuan outcrop is restricted to discontinuous pockets of strata with poor indices for paleobathymetry, there are abundant paleocurrent and paleo-slope data available. Additionally, the Motuan broadly marks the transition from the cessation of Mesozoic subduction to the development of the Late Cretaceous-Paleogene passive margin, therefore palinspastic reconstruction of this interval will provide important indications of the initial morphology and development of the East Coast Basin. Presently, there is a substantial temporal gap between the Ngaterian (95 Ma) and Piripauan (85 Ma) maps, which could be reduced by the addition of the Raukumara series timeslice. While beyond the scope of this study, additional timeslices through

the Oligocene and Neogene would be a significantly beneficial resource for petroleum exploration, paleobiological, paleotectonic and paleogeographical studies in the basin.

Integration of the paleogeographic map series produced here with correlative reconstructions in the Taranaki, Deepwater Taranaki, Northland, Aotea, Reinga, Canterbury and Great South basins (Arnot & Bland *et al.*, 2016; Strogen *et al.*, 2017; Sahoo & Bland *et al.*, 2017) will enable paleogeographic reconstructions of almost the entire Zealandia region through the mid- to Late Cretaceous to Eocene when applied to the wider regional plate tectonic framework demonstrated in Chapter Five.

REFERENCES

It is not in the nature of things for any one man to make a sudden violent discovery; science goes step by step, and every man depends on the work of his predecessors… Scientists are not dependent on the ideas of a single man, but on the combined wisdom of thousands of men, all thinking of the same problem, and each doing his little bit to add to the great structure of knowledge which is gradually being erected.

-Ernest Rutherford (1906), in *Radioactive Transformations*, Archibald Constable and Company Ltd., London, England.

REFERENCES

Abbott, S. T. (1998). Transgressive systems tracts and onlap shellbeds from mid-Pleistocene sequences, Wanganui Basin, New Zealand. *Journal of Sedimentary Research*, *68*(2).

Adams, A. G. (1985). *Late Cretaceous fauna and sediments of southern Hawke's Bay – New Zealand*. Unpublished PhD thesis lodged at the University of Auckland.

Adams, C. J., & Graham, I. J. (1996). Metamorphic and tectonic geochronology of the Torlesse terrane, Wellington, New Zealand. *New Zealand Journal of Geology and Geophysics*, *39*(2), 157-180.

Adams, C. J., Campbell, H. J., & Griffin, W. J. (2008). Age and provenance of basement rocks of the Chatham Islands: an outpost of Zealandia. *New Zealand Journal of Geology and Geophysics*, *51*(3), 245-259.

Adams, C. J., Mortimer, N., Campbell, H. J., & Griffin, W. L. (2009). Age and isotopic characterisation of metasedimentary rocks from the Torlesse Supergroup and Waipapa Group in the central North Island, New Zealand. *New Zealand Journal of Geology and Geophysics*, *52*(2), 149-170.

Adams, C. J., Mortimer, N., Campbell, H. J., & Griffin, W. L. (2011). Recognition of the Kaweka Terrane in northern South Island, New Zealand: preliminary evidence from Rb–Sr metamorphic and U–Pb detrital zircon ages. *New Zealand Journal of Geology and Geophysics*, *54*(3), 291-309.

Adams, C. J., Mortimer, N., Campbell, H. J., & Griffin, W. L. (2013a). The mid-Cretaceous transition from basement to cover within sedimentary rocks in eastern New Zealand: evidence from detrital zircon age patterns. *Geological Magazine*, *150*(3), 455-478.

Adams, C. J., Mortimer, N., Campbell, H. J., & Griffin, W. L. (2013b). Detrital zircon geochronology and sandstone provenance of basement Waipapa terrane (Triassic–Cretaceous) and Cretaceous cover rocks (Northland allochthon and Houhora complex) in northern North Island, New Zealand. *Geological Magazine*, *150*(1), 89-109.

Adams, C. J., Campbell, H. J., Mortimer, N., & Griffin, W. L. (2017). Perspectives on Cretaceous Gondwana break-up from detrital zircon provenance of southern Zealandia sandstones. *Geological Magazine*, *154*(4), 661-682.

Aitchison, J. (1982). The statistical analysis of compositional data. *Journal of the Royal Statistical Society. Series B (Methodological)*, 139-177.

Aitchison, J. (1986). The statistical analysis of compositional data. *Monographs on Statistics and Applied Probability*, Chapman & Hall Ltd., London.

Aitchison, J. C., Clarke, G. L., Meffre, S., & Cluzel, D. (1995). Eocene arc-continent collision in New Caledonia and implications for regional southwest Pacific tectonic evolution. *Geology*, *23*(2), 161-164.

Aitchison, J., Barceló-Vidal, C., Martín-Fernández, J. A., & Pawlowsky-Glahn, V. (2000). Logratio analysis and compositional distance. *Mathematical Geology*, *32*(3), 271-275.

Algeo, T. J. (2004). Can marine anoxic events draw down the trace element inventory of seawater? *Geology*, *32*(12), 1057-1060.

Algeo, T. J., & Maynard, J. B. (2004). Trace-element behavior and redox facies in core shales of Upper Pennsylvanian Kansas-type cyclothems. *Chemical Geology*, *206*(3), 289-318.

Algeo, T. J., & Maynard, J. B. (2008). Trace-metal covariation as a guide to water-mass conditions in ancient anoxic marine environments. *Geosphere*, *4*(5), 872-887.

Algeo, T. J., & Tribovillard, N. (2009). Environmental analysis of paleoceanographic systems based on molybdenum–uranium covariation. *Chemical Geology*, *268*(3), 211-225.

Allen, P. A., & Allen, J. R. (2013). *Basin analysis: Principles and application to petroleum play assessment*. John Wiley & Sons.

Allibone, A. H., Jongens, R., Scott, J. M., Tulloch, A. J., Turnbull, I. M., Cooper, A. F., ... & Rattenbury, M. S. (2009). Plutonic rocks of the Median Batholith in eastern and central Fiordland, New Zealand: field relations, geochemistry, correlation, and nomenclature. *New Zealand Journal of Geology and Geophysics*, *52*(2), 101-148.

Amorosi, A. (1995). Glaucony and sequence stratigraphy: a conceptual framework of distribution in siliciclastic sequences. *Journal of Sedimentary Research*, *65*(4).

Amorosi, A. (1997). Detecting compositional, spatial, and temporal attributes of glaucony: a tool for provenance research. *Sedimentary Geology*, *109*(1-2), 135-153.

Amorosi, A., Sammartino, I., & Tateo, F. (2007). Evolution patterns of glaucony maturity: a mineralogical and geochemical approach. *Deep Sea Research Part II: Topical Studies in Oceanography*, *54*(11), 1364-1374.

Arnot, M. J. & Bland, K. J. et al. (Compilers). (2016). Atlas of Petroleum Prospectivity, Northwest Province: ArcGIS geodatabase and technical report. *GNS Science Data Series 23b* 34 p. + 1 ArcGIS geodatabase + 5 ArcGIS projects.

Arthur, M. A., Schlanger, S. T., & Jenkyns, H. C. (1987). The Cenomanian-Turonian Oceanic Anoxic Event, II. Palaeoceanographic controls on organic-matter production and preservation. *Geological Society, London, Special Publications*, *26*(1), 401-420.

Arthur, M. A., Dean, W. E., & Pratt, L. M. (1988). Geochemical and climatic effects of increased marine organic carbon burial at the Cenomanian/Turonian boundary. *Nature*, *335*(6192), 714-717.

Arthur, M. A., & Sageman, B. B. (1994). Marine shales: depositional mechanisms and environments of ancient deposits. *Annual Review of Earth and Planetary Sciences*, *22*, 499-551.

Bache, F., Sutherland, R., Stagpoole, V., Herzer, R., Collot, J., & Rouillard, P. (2012). Stratigraphy of the southern Norfolk Ridge and the Reinga Basin: a record of initiation of Tonga–Kermadec–Northland subduction in the southwest Pacific. *Earth and Planetary Science Letters*, *321*, 41-53.

Bache, F., Mortimer, N., Sutherland, R., Collot, J., Rouillard, P., Stagpoole, V., & Nicol, A. (2014). Seismic stratigraphic record of transition from Mesozoic subduction to continental breakup in the Zealandia sector of eastern Gondwana. *Gondwana Research*, *26*(3), 1060-1078.

Bailleul, J., Chanier, F., Ferrière, J., Robin, C., Nicol, A., Mahieux, G., ... & Caron, V. (2013). Neogene evolution of lower trench-slope basins and wedge development in the central Hikurangi subduction margin, New Zealand. *Tectonophysics*, *591*, 152-174.

Ballance, P. F. (1976). Evolution of the upper Cenozoic magmatic arc and plate boundary in northern New Zealand. *Earth and Planetary Science Letters 28*, 356-370.

Ballance, P F. (1993a). The New Zealand Neogene forearc basins. *In:* Sedimentary basins of the world 2. South Pacific sedimentary basins (Ballance, P. F., ed.). Elsevier, Amsterdam: Pp. 177–191.

Ballance, P. F. (1993b). The paleo-Pacific, post-subduction, passive margin thermal relaxation sequence (Late Cretaceous–Paleogene) of the drifting New Zealand continent. *South Pacific Sedimentary Basins of the World*, *2*, 93-110.

Ballance, P. F. (1999). Simplification of the Southwest Pacific Neogene arcs: inherited complexity and control by a retreating pole of rotation. *Geological Society, London, Special Publications*, *164*(1), 7-19.

Ballance, P. F., & Spörli, K. B. (1979). Northland allochthon. *Journal of the Royal Society of New Zealand*, *9*(2), 259-275.

Ballance, P. F., Pettinga, J. R., & Webb, C. (1982). A model of the Cenozoic evolution of northern New Zealand and adjacent areas of the southwest Pacific. *Tectonophysics*, *87*(1-4), 37-48.

Barnes, P. M. (1990). Provenance of cretaceous accretionary wedge sediments: the Mangapokia Formation, Wairarapa, New Zealand. *New Zealand Journal of Geology and Geophysics*, *33*(1), 125-135.

Barnes, P. M., & Lépinay, B. M. (1997). Rates and mechanics of rapid frontal accretion along the very obliquely convergent southern Hikurangi margin, New Zealand. *Journal of Geophysical Research: Solid Earth*, *102*(B11), 24931-24952.

Barnes, P. M., Lépinay, B. M., Collot, J. Y., Delteil, J., & Audru, J. C. (1998). Strain partitioning in the transition area between oblique subduction and continental collision, Hikurangi margin, New Zealand. *Tectonics*, *17*(4), 534-557.

Barnes, P. M., & Audru, J. C. (1999). Quaternary faulting in the offshore Flaxbourne and Wairarapa basins, southern Cook Strait, New Zealand. *New Zealand Journal of Geology and Geophysics*, *42*(3), 349-367.

Barnes, P. M., Nicol, A., & Harrison, T. (2002). Late Cenozoic evolution and earthquake potential of an active listric thrust complex above the Hikurangi subduction zone, New Zealand. *Geological Society of America Bulletin*, *114*(11), 1379-1405.

Barnes, P. M., & Nicol, A. (2004). Formation of an active thrust triangle zone associated with structural inversion in a subduction setting, eastern New Zealand. *Tectonics*, *23*(1).

Bassett, K. N., & Orlowski, R. (2004). Pahau Terrane type locality: Fan delta in an accretionary prism trench-slope basin. *New Zealand Journal of Geology and Geophysics*, *47*(4), 603-623.

Baur, J., Sutherland, R., & Stern, T. (2014). Anomalous passive subsidence of deep-water sedimentary basins: a prearc basin example, southern New Caledonia Trough and Taranaki Basin, New Zealand. *Basin Research*, *26*(2), 242-268.

Beanland, S. (1995). *The North Island Dextral Fault Belt, Hikurangi Subduction Margin, New Zealand: A Thesis Submitted for the Degree of Doctor of Philosophy [in Geology], Victoria University of Wellington* (Doctoral dissertation, Victoria University of Wellington).

Beanland, S., & Haines, J. (1998). The kinematics of active deformation in the North Island, New Zealand, determined from geological strain rates. *New Zealand Journal of Geology and Geophysics*, *41*(4), 311-323.

Beanland, S., A. Melhuish, A. Nicol, and J. Ravens (1998), Structure and deformation history of the inner forearc region, Hikurangi subduction margin, New Zealand. *New Zealand Journal of Geology and Geophysics*, 41, 325 – 342.

Beckmann, B., Wagner, T., & Hofmann, P. (2005). Linking Coniacian-Santonian (OAE3) black shale formation to African climate variability: a reference section from the eastern tropical Atlantic at orbital timescales (ODP Site 959, off Ivory Coast/Ghana). In: Harris N.B (Ed.). *The deposition of organic-carbon-rich sediments: Models, mechanisms, and consequences.* SEPM Special publication No. 82. ISBN 1-56576-110-3 p.125-143

Beckmann, B., Hofmann, P., März, C., Schouten, S., Damsté, J. S. S., & Wagner, T. (2008). Coniacian–Santonian deep ocean anoxia/euxinia inferred from molecular and inorganic markers: Results from the Demerara Rise (ODP Leg 207). *Organic Geochemistry*, *39*(8), 1092-1096.

Beggs, J. M. (1993). Tectono-stratigraphic setting for the clastic rocks of the Torlesse Supergroup/Terrane. *Geological Society of New Zealand Miscellaneous Publication*, v.79A, pp. 39.

Begg, J. G., & Johnston, M. R. (2000). Geology of the Wellington area. 1: 250000 Geological map 10. *Institute of Geological and Nuclear Sciences, Lower Hutt, New Zealand.*

Benson, W. N. (1952). Meeting of the Geological Division of the Pacific Science congress in New Zealand, February, 1949. *International proceedings of the Geological Society of America, 1950*. Pp. 11-13.

Berner, R. A., & Raiswell, R. (1983). Burial of organic carbon and pyrite sulfur in sediments over Phanerozoic time: a new theory. *Geochimica et Cosmochimica Acta*, *47*(5), 855-862.

Bernet, M. (2009). A field-based estimate of the zircon fission-track closure temperature. *Chemical Geology*, 259 (3): 181–189.

Berryman, K.R. (1988). Tectonic geomorphology at a plate boundary: a transect across Hawke's Bay, New Zealand. *In:* The Geomorphology of Plate Boundaries and Active Continental Margins (Williams, P. W., ed.). *Zeitchrift fur geomorphologie supplementband 69:* 69–86.

Berryman, K. R., Ota, Y., & Hull, A. G. (1989). Holocene paleoseismicity in the fold and thrust belt of the Hikurangi subduction zone, eastern North Island, New Zealand. *Tectonophysics*, *163*(3-4), 185-195.

Beu, A. G., Browne, G. H., & Grant-Taylor, T. L. (1980). New Chlamys delicatula localities in the central North Island and uplift of the Ruahine Range. *New Zealand Journal of Geology and Geophysics*, *24*(1), 127-132.

Beu, A. G. (1995). *Pliocene limestones and their scallops: lithostratigraphy, pectinid biostratigraphy, and paleogeography of eastern North Island late Neogene limestone* (No. 68). Institute of Geological & Nuclear Sciences Limited.

Beu, A. G., Marshall, B. A., & Reay, M. B. (2014). Mid-Cretaceous (Albian–Cenomanian) freshwater Mollusca from the Clarence Valley, Marlborough, New Zealand, and their biogeographical significance. *Cretaceous Research*, *49*, 134-151.

Black, R. D. (1980). Upper Cretaceous and Tertiary geology of Mangatu State Forest, Raukumara Peninsula, New Zealand. *New Zealand Journal of Geology and Geophysics*, *23*(3), 293-312.

Bland, K. J. & Kamp, P. J. J. (2006). Geological structure of the forearc basin in central Hawke's Bay, eastern North Island. In: *Proceedings of New Zealand Petroleum Conference 2006*, 6 – 10 March 2006.

Bland, K. J., Kamp, P. J., & Nelson, C. S. (2008). Late Miocene–Early Pleistocene paleogeography of the onshore central Hawke's Bay sector of the forearc basin, eastern North Island, New Zealand, and some implications for hydrocarbon prospectivity. *2008 New Zealand Petroleum Conference Proceedings*, 19 p.

Bland, K. J., Hendy, A. J., Kamp, P. J., & Nelson, C. S. (2013). Macrofossil biofacies in the late Neogene of central Hawke's Bay: applications to palaeogeography. *New Zealand Journal of Geology and Geophysics*, *56*(4), 200-222.

Bland, K. J., Uruski, C. I., & Isaac, M. J. (2015). Pegasus Basin, eastern New Zealand: A stratigraphic record of subsidence and subduction, ancient and modern. *New Zealand Journal of Geology and Geophysics*, *58*(4), 319-343.

Borcard, D., Gillet, F., & Legendre, P. (2011). *Numerical ecology with R*. Springer Science & Business Media.

Boucsein, B., & Stein, R. (2009). Black shale formation in the late Paleocene/early Eocene Arctic Ocean and paleoenvironmental conditions: new results from a detailed organic petrological study. *Marine and Petroleum Geology*, *26*(3), 416-426.

Box, G. E. P. & Draper, N. R. (1987). *Empirical Model-Building and Response Surfaces*, Wiley, p. 424. ISBN 0471810339.

Boyden, J. A., Müller, R. D., Gurnis, M., Torsvik, T. H., Clark, J. A., Turner, M., Ivey-Law, H., Watson, R. J. & Cannon, J. S. (2011). Next-generation plate-tectonic reconstructions using GPlates. In: *Geoinformatics: Cyberinfrastructure for the Solid Earth Sciences*. Cambridge University Press, Cambridge, pp. 95-113. ISBN 9780521897150.

Bradshaw, J. D. (1989). Cretaceous geotectonic patterns in the New Zealand region. *Tectonics*, *8*(4), 803-820.

Bradshaw, J. D., Weaver, S. D. & Muir, R. J. (1996). Mid-Cretaceous oroclinal bending of New Zealand terranes. *New Zealand Journal of Geology and Geophysics 39*, 461-468.

Bradshaw, J. D. (2004). Northland Allochthon: an alternative hypothesis of origin. *New Zealand Journal of Geology and Geophysics*, *47*(3), 375-382.

Breit, G. N., & Wanty, R. B. (1991). Vanadium accumulation in carbonaceous rocks: a review of geochemical controls during deposition and diagenesis. *Chemical Geology*, *91*(2), 83-97.

Briggs, R. M., Okada, T., Itaya, T., Shibuya, H., & Smith, I. E. M. (1994). K-Ar ages, paleomagnetism, and geochemistry of the South Auckland volcanic field, North Island, New Zealand. *New Zealand Journal of Geology and Geophysics*, *37*(2), 143-153.

Briggs, R. M., Middleton, M. P., & Nelson, C. S. (2004). Provenance history of a Late Triassic-Jurassic Gondwana margin forearc basin, Murihiku Terrane, North Island, New Zealand: Petrographic and geochemical constraints. *New Zealand Journal of Geology and Geophysics*, *47*(4), 589-602.

Bromley, R. G. (1990). *Trace Fossils. Biology and Taphonomy*. 280 pp. Un win & Hyman, London.

Bromley, R. G. (1996). Solving problems with trace fossils. In *Trace Fossils* (pp. 275-297). Springer US.

Brothers, R. N. (1959). Heavy minerals from Southland: Part II: Upper cretaceous-lower tertiary coal measures. *New Zealand Journal of Geology and Geophysics*, *2*(4), 788-798.

Browne, G. H., & Field, B. D. (1985). *The lithostratigraphy of Late Cretaceous to early Pleistocene rocks of northern Canterbury, New Zealand* (Vol. 6). Dept. of Scientific and Industrial Research.

Browne, G. H. (1987). In situ and intrusive sandstone in Amuri fades limestone at Te Kaukau Point, southeast Wairarapa, New Zealand. *New Zealand Journal of Geology and Geophysics*, *30*(4), 363-374.

Browne, G. H. (1991). Letters to the Editor. A reassessment of the depositional environment for the conglomeratic facies, Maungataniwha Sandstone, western Hawke's Bay. Comment. *New Zealand Journal of Geology and Geophysics 34*, 563–564.

Browne, G. H. (1992). The northeastern portion of the Clarence Fault: tectonic implications for the late Neogene evolution of Marlborough, New Zealand. *New Zealand Journal of Geology and Geophysics*, *35*(4), 437-445.

Browne, G. H., & Reay, M. B. (1993). The Warder Formation: Cyclic fluvial sedimentation during the Ngaterian (late Albian-Cenomanian) of Marlborough, New Zealand. *New Zealand Journal of Geology and Geophysics*, *36*(1), 27-35.

Browne, G. H. (2004). Late Neogene sedimentation adjacent to the tectonically evolving North Island axial ranges: Insights from Kuripapango, western Hawke's Bay. *New Zealand Journal of Geology and Geophysics*, *47*(4), 663-674.

Browning, J. V., Miller, K. G., & Pak, D. K. (1996). Global implications of lower to middle Eocene sequence boundaries on the New Jersey coastal plain: The icehouse cometh. *Geology*, *24*(7), 639-642.

Brumsack, H. J. (2006). The trace metal content of recent organic carbon-rich sediments: implications for Cretaceous black shale formation. *Palaeogeography, Palaeoclimatology, Palaeoecology*, *232*(2), 344-361.

Burgreen-Chan, B., Meisling, K. E., & Graham, S. (2016). Basin and petroleum system modelling of the East Coast basin, New Zealand: a test of overpressure scenarios in a convergent margin. *Basin Research*, *28*(4), 536-567.

Calvert, S. E., & Pedersen, T. F. (1993). Geochemistry of recent oxic and anoxic marine sediments: implications for the geological record. *Marine Geology*, *113*(1), 67-88.

Calvert, S. E., Bustin, R. M., & Ingall, E. D. (1996). Influence of water column anoxia and sediment supply on the burial and preservation of organic carbon in marine shales. *Geochimica et Cosmochimica Acta*, *60*(9), 1577-1593.

Campbell, K. A. (2006). Hydrocarbon seep and hydrothermal vent paleoenvironments and paleontology: past developments and future research directions. *Palaeogeography, Palaeoclimatology, Palaeoecology*, *232*(2), 362-407.

Campbell, H. J., Andrews, P. B., Beu, A. G., Edwards, A. R., Hornibrook, N. D., Laird, M. G., ... & Watters, W. A. (1988). Cretaceous-Cenozoic lithostratigraphy of the Chatham Islands. *Journal of the Royal Society of New Zealand*, *18*(3), 285-308.

Campbell, H. J., Andrews, P. B., Beu, A. G., Maxwell, P. A., Edwards, A. R., Laird, M. G., Hornibrook, N. d., Mildenhall, D. C., Watters, W. A., Buckeridge, J. S., Lee, D. E., Strong, C. P., Wilson, G. J., & Hayward, B. W. (1993). *Cretaceous-Cenozoic Geology and Biostratigraphy of the Chatham Islands, New Zealand.* Institute of Geological and Nuclear Sciences Monograph, 269 pp.

Cande, S. C., Raymond, C. A., Stock, J., & Haxby, W. F. (1995). Geophysics of the Pitman Fracture Zone and Pacific-Antarctic plate motions during the Cenozoic. *Science*, *270*(5238), 947-953.

Cande, S. C., & Stock, J. M. (2004). Pacific—Antarctic—Australia motion and the formation of the Macquarie Plate. *Geophysical Journal International*, *157*(1), 399-414.

Canfield, D. E. (2001). Biogeochemistry of sulfur isotopes. *Reviews in Mineralogy and Geochemistry*, *43*(1), 607-636.

Canfield, D. E., Farquhar, J., & Zerkle, A. L. (2010). High isotope fractionations during sulfate reduction in a low-sulfate euxinic ocean analog. *Geology*, *38*(5), 415-418.

Caplan, M. L., & Bustin, R. M. (1999). Palaeoceanographic controls on geochemical characteristics of organic-rich Exshaw mudrocks: role of enhanced primary production. *Organic Geochemistry*, *30*(2), 161-188.

Carroll, A. R., & Bohacs, K. M. (2001). Lake-type controls on petroleum source rock potential in nonmarine basins. *AAPG bulletin*, *85*(6), 1033-1053.

Carter, R. T., & Norris, R. J. (1976). Cainozoic history of southern New Zealand: an accord between geological observations and plate-tectonic predictions. *Earth and Planetary Science Letters*, *31*(1), 85-94.

Carter, R. M., & Naish, T. R. (1998). A review of Wanganui Basin, New Zealand: global reference section for shallow marine, Plio–Pleistocene (2.5–0 Ma) cyclostratigraphy. *Sedimentary Geology*, *122*(1-4), 37-52.

Carter, L., Shane, P., Alloway, B., Hall, I.R., Harris, S.E. & Westgate, J.A. (2003). Demise of one volcanic zone and birth of another - A 12 m.y. marine record of major rhyolitic eruptions from New Zealand. *Geology, 31*. 4936–496.

Carter, L., Alloway, B., Shane, P. &Westgate, J. (2004). Deep-ocean record of major late Cenozoic rhyolitic eruptions from New Zealand. *New Zealand Journal of Geology and Geophysics 47*: 481–500.

Cashman, S. M., Kelsey, H. M., Erdman, C. F., Cutten, H. N., & Berryman, K. R. (1992). Strain partitioning between structural domains in the forearc of the Hikurangi subduction zone, New Zealand. *Tectonics*, *11*(2), 242-257.

Catuneanu, O. (2006). *Principles of sequence stratigraphy*. Elsevier.

Catuneanu, O., Abreu, V., Bhattacharya, J. P., Blum, M. D., Dalrymple, R. W., Eriksson, P. G., ... & Giles, K. A. (2009). Towards the standardization of sequence stratigraphy. *Earth-Science Reviews*, *92*(1), 1-33.

Catuneanu, O., Galloway, W. E., Kendall, C. G. S. C., Miall, A. D., Posamentier, H. W., Strasser, A., & Tucker, M. E. (2011). Sequence stratigraphy: methodology and nomenclature. *Newsletters on Stratigraphy*, *44*(3), 173-245.

Challis, G. A. (1966). Cretaceous stratigraphy of the Lookout area, Awatere Valley. *Transactions of the Royal Society of New Zealand,* 4(5). 119 p.

Chambers, L. A., Trudinger, P. A., Smith, J. W., & Burns, M. S. (1975). Fractionation of sulfur isotopes by continuous cultures of Desulfovibrio desulfuricans. *Canadian Journal of Microbiology*, *21*(10), 1602-1607.

Chanier, F. (1991). Le Prisme d'accrretion d'Hikurangi: un temoin de L'evolution geodynamique d'une marge active peripacfique (Nouvelle Zelande), These de Doctorat, Uni. Lille-Flandres-Artois, 321 pp.

Chanier, F., & Ferrière, J. (1991). From a passive to an active margin: tectonic and sedimentary processes linked to the birth of an accretionary prism (Hikurangi margin, New Zealand). *Bulletin*, *162*, 649-660.

Chanier, F., Ferrière, J., & Angelier, J. (1999). Extensional deformation across an active margin, relations with subsidence, uplift, and rotations: The Hikurangi subduction, New Zealand. *Tectonics*, *18*(5), 862-876.

Chang, H., Chu, X., Feng, L., & Huang, J. (2009). Terminal Ediacaran anoxia in deep-ocean: Trace element evidence from cherts of the Liuchapo Formation, South China. *Science in China Series D: Earth Sciences*, *52*(6), 807-822.

Chang, H. J., Chu, X. L., Feng, L. J., & Huang, J. (2012). Progressive oxidation of anoxic and ferruginous deep-water during deposition of the terminal Ediacaran Laobao Formation in South China. *Palaeogeography, Palaeoclimatology, Palaeoecology*, *321*, 80-87.

Claypool, G. E., Holser, W. T., Kaplan, I. R., Sakai, H., & Zak, I. (1980). The age curves of sulfur and oxygen isotopes in marine sulfate and their mutual interpretation. *Chemical Geology*, *28*, 199-260.

Clowes, C. D., Bland, K. J., Morgans, H. E. G. & Hines, B. R. (2016). Record of geological observations and sample collection from the Late Cretaceous-early Miocene strata in southern Hawke's Bay, 04-08 April 2016. *GNS Science Internal Report 2016/14*. 56 p.

Clowes, C.D., *in prep.* Results of a palynological investigation of Taylor White section, Tararua District, with particular emphasis on the Waipawa Formation. *GNS Science Report 2016/55*.

Cluzel, D., Meffre, S., Maurizot, P., & Crawford, A. J. (2006). Earliest Eocene (53 Ma) convergence in the Southwest Pacific: evidence from pre-obduction dikes in the ophiolite of New Caledonia. *Terra Nova*, *18*(6), 395-402.

Cluzel, D., Black, P. M., Picard, C., & Nicholson, K. N. (2010). Geochemistry and tectonic setting of Matakaoa Volcanics, East Coast Allochthon, New Zealand: suprasubduction zone affinity, regional correlations, and origin. *Tectonics*, *29*(2).

Cole, J. W. (1986). Distribution and tectonic setting of late Cenozoic volcanism in New Zealand. In: Smith, I. E. M. (ed). Late Cenozoic volcanism in New Zealand. *Royal Society of New Zealand Bulletin 23*: 7-20.

Cole, J. W. & Lewis; K. B. (1981). Evolution of the Taupo-Hikurangi subduction system. *Tectonophysics 72*, 1-21.

Collot, J., Herzer, R., Lafoy, Y., & Geli, L. (2009). Mesozoic history of the Fairway-Aotea Basin: Implications for the early stages of Gondwana fragmentation. *Geochemistry, Geophysics, Geosystems*, *10*(12).

Cooper, R. A. (2004). The New Zealand geological timescale (Vol. 22). *Institute of Geological & Nuclear Sciences Monograph 19*. Lower Hutt, Institute of Geological & Nuclear Sciences Limited.

Cooper, R. A., & Tulloch, A. J. (1992). Early Palaeozoic terranes in New Zealand and their relationship to the Lachlan Fold Belt. *Tectonophysics*, *214*(1-4), 129-144.

Cox, S. C., & Sutherland, R. (2007). Regional geological framework of South Island, New Zealand, and its significance for understanding the active plate boundary. *A continental plate boundary: tectonics at South Island, New Zealand*, 19-46.

Cox, G. M., Halverson, G. P., Stevenson, R. K., Vokaty, M., Poirier, A., Kunzmann, M., Li, Z., Denyszyn, S. W., Strauss, J. V., & Macdonald, F. A. (2016). Continental flood basalt weathering as a trigger for Neoproterozoic Snowball Earth. *Earth and Planetary Science Letters*, *446*, 89-99.

Coxall, H. K., Wilson, P. A., Pälike, H., Lear, C. H., & Backman, J. (2005). Rapid stepwise onset of Antarctic glaciation and deeper calcite compensation in the Pacific Ocean. *Nature*, *433*(7021), 53.

Crampton, J. S. (1988a). A Late Cretaceous near-shore rocky substrate macrofauna from northern Hawkes Bay, New Zealand. *New Zealand Geological Survey Record*, *35*, 21-24.

Crampton, J. S. (1988b). Stratigraphy and structure of the Monkey Face area, Marlborough, New Zealand, with special reference to shallow marine Cretaceous strata. *New Zealand Journal of Geology and Geophysics*, *31*(4), 447-470.

Crampton, J. S. (1989). An inferred Motuan sedimentary melange in southern Hawkes Bay. *New Zealand Geological Survey Record*, *40*, 3-12.

Crampton, J. S. (1997). The Cretaceous stratigraphy of southern Hawke's Bay-Wairarapa region. *Institute of Geological & Nuclear Sciences Science Report 97/08*. 92 p.

Crampton, J. S. (1998). Ontogenetic variation and inoceramid morphology: a note on early Coniacian Cremnoceramus bicorrugatus (Cretaceous Bivalvia). *Acta Geologica Polonica*, *48*(4), 367-376.

Crampton, J. S., & Moore, P. R. (1990). Environment of deposition of the Maungataniwha Sandstone (Late Cretaceous), Te Hoe River area, western Hawke's Bay, New Zealand. *New Zealand Journal of Geology and Geophysics*, *33*(2), 333-348.

Crampton, J. S., & Laird, M. G. (1997). Burnt Creek Formation and Late Cretaceous basin development in Marlborough, New Zealand. *New Zealand Journal of Geology and Geophysics*, *40*(2), 199-222.

Crampton, J. S., Laird, M., Nicol, A., Hollis, C. J., & Van Dissen, R. J. (1998). Geology at the northern end of the Clarence Valley, Marlborough; a complete record spanning the Rangitata to Kaikoura orogenies. In *Geological Society of New Zealand, New Zealand Geophysical Society 1998 Joint Annual Conference* (Vol. 30).

Crampton, J., Mumme, T., Raine, I., Roncaglia, L., Schiøler, P., Strong, P., ... & Wilson, G. (2000). Revision of the Piripauan and Haumurian local stages and correlation of the Santonian-Maastrichtian (Late Cretaceous) in New Zealand. *New Zealand Journal of Geology and Geophysics*, *43*(3), 309-333.

Crampton, J., Raine, I., Strong, P., & Wilson, G. (2001). Integrated biostratigraphy of the Raukumara Series (Cenomanian-Coniacian) at Mangaotane Stream, Raukumara Peninsula, New Zealand. *New Zealand Journal of Geology and Geophysics*, *44*(3), 365-389.

Crampton, J., Laird, M., Nicol, A., Townsend, D., & Van Dissen, R. (2003). Palinspastic reconstructions of southeastern Marlborough, New Zealand, for mid-Cretaceous-Eocene times. *New Zealand Journal of Geology and Geophysics*, *46*(2), 153-175.

Crampton, J. S., Hollis, C. J., Raine, J. I., Roncaglia, L., Schiøler, P., Strong, P., & Wilson, G. J. (2004a). Cretaceous (Taitai, Clarence, Raukumara and Mata Series). *The New Zealand Geological Timescale*, *22*, pp. 102-122.

Crampton, J. S., Tulloch, A. J., Wilson, G. J., Ramezani, J., & Speden, I. G. (2004b). Definition, age, and correlation of the Clarence Series stages in New Zealand (late Early to early Late Cretaceous). *New Zealand Journal of Geology and Geophysics*, *47*(1), 1-19.

Crampton, J. S., Schiøler, P., & Roncaglia, L. (2006). Detection of Late Cretaceous eustatic signatures using quantitative biostratigraphy. *Geological Society of America Bulletin*, *118*(7-8), 975-990.

Crampton, J. S., Bland, K. J., Hines, B. R., King, P. R., Mortimer, N., Strogen, D. P. (*in prep.*). The end of Cretaceous subduction in Zealandia: the view from the paleo-trench. *In preparation for Gondwana Research.*

Craw, R. C., & Watt, J. C. (1987). An Upper Cretaceous beetle (Coleoptera) from Hawkes Bay, New Zealand. *Journal of the Royal Society of New Zealand*, *17*(4), 395-398.

Croon, M. B., Cande, S. C., & Stock, J. M. (2008). Revised Pacific-Antarctic plate motions and geophysics of the Menard Fracture Zone. *Geochemistry, Geophysics, Geosystems*, *9*(7).

Crouch, E. M., Heilmann-Clausen, C., Brinkhuis, H., Morgans, H. E., Rogers, K. M., Egger, H., & Schmitz, B. (2001). Global dinoflagellate event associated with the late Paleocene thermal maximum. *Geology*, *29*(4), 315-318.

Crouch, E. M., & Brinkhuis, H. (2005). Environmental change across the Paleocene–Eocene transition from eastern New Zealand: a marine palynological approach. *Marine Micropaleontology*, *56*(3), 138-160.

Crouch, E. M., Willumsen, P. S., Kulhanek, D. K., & Gibbs, S. J. (2014). A revised Paleocene (Teurian) dinoflagellate cyst zonation from eastern New Zealand. *Review of Palaeobotany and Palynology*, *202*, 47-79.

Croux, C., Filzmoser, P., & Oliveira, M. R. (2007). Algorithms for Projection–Pursuit robust principal component analysis. *Chemometrics and Intelligent Laboratory Systems*, *87*(2), 218-225.

Curran, J. M. (2013). Hotelling: Hotelling's t-squared test and variants. R package version 1.0–2. https://CRAN.R-project.org/package=Hotelling

Cutten, H. N. C. (1994). Geology of the middle reaches of the Mohaka River. Scale 1:50 000. *Institute of Geological & Nuclear Sciences geological map 6*. Lower Hutt, Institute of Geological & Nuclear Sciences. 1 sheet + 38 p.

Cutten, H. N. C. & Delteil, J. (1993). Neogene transcurrent fault displacements on the east coast, North Island, New Zealand. *Geological Society of New Zealand Miscellaneous Publication 79A*, *58*.

Cutten, H. N. & Delteil, J. E. (1994). The distribution in space and time of transcurrent faults in the emergent Hikurangi subduction margin, North Island, New Zealand. Unpublished GNS Science Report.

Dahl, T. W., Ruhl, M., Hammarlund, E. U., Canfield, D. E., Rosing, M. T., & Bjerrum, C. J. (2013). Tracing euxinia by molybdenum concentrations in sediments using handheld X-ray fluorescence spectroscopy (HHXRF). *Chemical Geology*, *360*, 241-251.

Dallanave, E., Agnini, C., Bachtadse, V., Muttoni, G., Crampton, J. S., Strong, C. P., ... & Slotnick, B. S. (2015). Early to middle Eocene magneto-biochronology of the southwest Pacific Ocean and climate influence on sedimentation: Insights from the Mead Stream section, New Zealand. *Geological Society of America Bulletin*, *127*(5-6), 643-660.

Dallanave, E., Bachtadse, V., Crouch, E. M., Tauxe, L., Shepherd, C. L., Morgans, H. E., ... & Sugisaki, S. (2016). Constraining early to middle Eocene climate evolution of the southwest Pacific and Southern Ocean. *Earth and Planetary Science Letters*, *433*, 380-392.

Davey, F. J., Henrys, S. A., & Lodolo, E. (1995). Asymmetric rifting in a continental back-arc environment, North Island, New Zealand. *Journal of Volcanology and Geothermal Research*, *68*(1), 209-238.

Davey, F. J., Henrys, S., & Lodolo, E. (1997). A seismic crustal section across the East Cape convergent margin, New Zealand. *Tectonophysics*, *269*(3-4), 199-215.

Davidge, S. C. (1982). *A geophysical study of the south Hauraki lowlands*. Unpublished PhD Thesis, University of Auckland.

Davy, B., Hoernle, K., & Werner, R. (2008). Hikurangi Plateau: Crustal structure, rifted formation, and Gondwana subduction history. *Geochemistry, Geophysics, Geosystems*, *9*(7).

Delteil, J., Morgans, H. E., Raine, J. I., Field, B. D., & Cutten, H. N. (1996). Early Miocene thin-skinned tectonics and wrench faulting in the Pongaroa district, Hikurangi margin, North Island, New Zealand. *New Zealand Journal of Geology and Geophysics*, *39*(2), 271-282.

Delteil, J., De Lepinay, B. M., Morgans, H. E. G., & Field, B. D. (2006). Olistostromes marking tectonic events, East Coast, New Zealand. *New Zealand Journal of Geology and Geophysics*, *49*(4), 517-531.

Demaison, G. J., & Moore, G. T. (1980). Anoxic environments and oil source bed genesis. *Organic Geochemistry*, *2*(1), 9-31.

Durance, P., Jowitt, S. M., & Bush, K. (2014). An assessment of portable X-ray fluorescence spectroscopy in mineral exploration, Kurnalpi Terrane, Eastern Goldfields Superterrane, Western Australia. *Applied Earth Science*, *123*(3), 150-163.

Eagle, M. K. (1994). A new Upper Cretaceous species of Isselicrinus (Crinoidea: Articulata) from western Hawkes Bay, New Zealand. *Records of the Auckland Institute and Museum 31*, 175–186.

Ekdale, A. A. (1985). Paleoecology of the marine endobenthos. *Palaeogeography, Palaeoclimatology, Palaeoecology*, *50*(1), 63-81.

Ekdale, A. A. (1988). Pitfalls of paleobathymetric interpretations based on trace fossil assemblages. *Palaios*, 464-472.

Ekdale, A. A., & Mason, T. R. (1988). Characteristic trace-fossil associations in oxygen-poor sedimentary environments. *Geology*, *16*(8), 720-723.

Erdman, C. F., & Kelsey, H. M. (1992). Pliocene and Pleistocene stratigraphy and tectonics, Ohara Depression and Wakarara Range, North Island, New Zealand. *New Zealand Journal of Geology and Geophysics*, *35*(2), 177-192.

Erickson, B. E., & Helz, G. R. (2000). Molybdenum (VI) speciation in sulfidic waters: stability and lability of thiomolybdates. *Geochimica et Cosmochimica Acta*, *64*(7), 1149-1158.

Essa, M. A., Ahmed, E. A., & Kurzweil, H. (2016). Genesis, maturity and weathering of some Upper Cretaceous Egyptian glauconites: Mineralogical and geochemical implications. *Journal of African Earth Sciences*, *124*, 427-446.

Feldmann, R. M. (1993). Additions to the fossil decapod crustacean fauna of New Zealand. *New Zealand Journal of Geology and Geophysics*, *36*(2), 201-211.

Field, B. D. (2005). Cyclicity in turbidites of the Miocene Whakataki Formation, Castlepoint, North Island, and implications for hydrocarbon reservoir modelling. *New Zealand Journal of Geology and Geophysics*, *48*(1), 135-146.

Field, B. D., Browne, G. H., & Davy, B. W. (1989). *Cretaceous and Cenozoic sedimentary basins and geological evolution of the Canterbury region, South Island, New Zealand*. New Zealand Geological Survey.

Field, B. D. & Uruski, C. I., and others (1997). Cretaceous-Cenozoic geology and petroleum systems of the East Coast Region, New Zealand. *Institute of Geological & Nuclear Sciences Monograph 19*. Lower Hutt, Institute of Geological & Nuclear Sciences Limited. 301 p.

Filzmoser, P., Fritz, H., & Kalcher, K. (2014). pcaPP: Robust PCA by Projection Pursuit. R package version 1.9-60. https://CRAN.R-project.org/package=pcaPP.

Fisher, L., Gazley, M. F., Baensch, A., Barnes, S. J., Cleverley, J., & Duclaux, G. (2014). Resolution of geochemical and lithostratigraphic complexity: a workflow for application of portable X-ray fluorescence to mineral exploration. *Geochemistry: Exploration, Environment, Analysis*, *14* (2), 149-159.

Forsyth, P.J., Barrell, D.J.A. & Jongens, R. (2008). Geology of the Christchurch Area. *Institute of Geological & Nuclear Sciences 1:250,000 Geological Map 16*.

Fraley, C. & Raftery, A. E. (2002). Model-Based Clustering, Discriminant Analysis, and Density Estimation. *Journal of the American Statistical Association*, 97: 458, 611-631.

Fraley, C., Raftery, A. E., & Scrucca, L. (2012). Normal mixture modeling for model-based clustering, classification, and density estimation. *Department of Statistics, University of Washington*, *23*, 2012.

Francis, D.A. (1992). Oil seeps and oil impregnations in the Dannevirke-Castlepoint area, southern East Coast Basin. *Petroleum Exploration in New Zealand News 34*: 28–32

Francis, D. (1994). The geology of gas seeps, and oil impregnations in the East Coast of the North Island, New Zealand. Contract report for Ministry of Commerce, Wellington.

Francis, D.A. (1995). Oil and gas seeps of northern and central East Coast Basin. *Petroleum Exploration in New Zealand News 44*: 21–27.

Francis, D. (1999). Oil seeps in Upper Cretaceous rocks, Akitio River, Southern Hawke's Bay, East Coast Basin, New Zealand (PEP 38332). NZP&M, Ministry of Business, Innovation & Employment (MBIE), New Zealand. Unpublished Petroleum Report PR3113.

Francis, D. (2000). Whangai shale distribution report. NZP&M, Ministry of Business, Innovation & Employment (MBIE), New Zealand. Unpublished Petroleum Report PR4310.

Francis, D. (2001). Source and reservoir sequences in the Waipataki-Towai Road area (PEP 38332), and reservoir near Ngahape Road (PEP 38328), Southern Hawke's Bay, East Coast Basin, New Zealand. NZP&M, Ministry of Business, Innovation & Employment (MBIE), New Zealand. Unpublished Petroleum Report PR3110.

Francis, D. (2008). Summary of Prospects and Leads. NZP&M, Ministry of Business, Innovation & Employment (MBIE), New Zealand. Unpublished Petroleum Report PR3889.

Francis, D. A. & Murray, A. P. (1997). Oil and gas generation in the East Coast Basin: an update. *Petroleum Exploration in New Zealand News 51*: 8–17

Francis, D. & Courtney, S. (2002). Remaining potential of PEP38335 Northern East Coast Basin. NZP&M, Ministry of Business, Innovation & Employment (MBIE), New Zealand. Unpublished Petroleum Report PR2675.

Francis, D., Bennett, D., & Courteney, S. (2004). Advances in understanding of onshore East Coast Basin structure, stratigraphic thickness and hydrocarbon generation. *In:* 2004 New Zealand Petroleum Conference Proceedings. 7–10 March 2004. 20 p.

Fujii, N., Yamamoto, T., & Niitsuma, N. (1994). Stratigraphy of the Neogene marine sequence to the east of Dannevirke, southern Hawke's Bay, New Zealand (Memorial volume to the late Professor Teruhiko Sameshima). *Geoscience reports of Shizuoka University*, *20*, 91-113.

Fulthorpe, C. S., Carter, R. M., Miller, K. G., & Wilson, J. (1996). Marshall Paraconformity: a mid-Oligocene record of inception of the Antarctic Circumpolar Current and coeval glacio-eustatic lowstand? *Marine and Petroleum Geology*, *13*(1), 61-77.

Funnell, R., Chapman, D., Allis, R., & Armstrong, P. (1996). Thermal state of the Taranaki basin, New Zealand. *Journal of Geophysical Research: Solid Earth*, *101* (B11), 25197-25215.

Furlong, K.P. & Kamp, P.J.J. (2009). The lithospheric geodynamics of plate boundary transpression in New Zealand: initiating and emplacing subduction along the Hikurangi margin, and the tectonic evolution of the Alpine Fault system. *Tectonophysics 474*, 449-462.

Gaina, C., Müller, R. D., Roest, W. R., & Symonds, P. (1998). The opening of the Tasman Sea: a gravity anomaly animation. *Earth Interactions*, *2*(4), 1-23.

Gale, A. S. (1996). Turonian correlation and sequence stratigraphy of the Chalk in southern England. *Geological Society, London, Special Publications*, *103*(1), 177-195.

Gallego-Torres, D., Martínez-Ruiz, F., Paytan, A., Jiménez-Espejo, F. J., & Ortega-Huertas, M. (2007). Pliocene–Holocene evolution of depositional conditions in the eastern Mediterranean: role of anoxia vs. productivity at time of sapropel deposition. *Palaeogeography, Palaeoclimatology, Palaeoecology*, *246*(2), 424-439.

Garcia, D., Fonteilles, M., & Moutte, J. (1994). Sedimentary Fractionations between Al, Ti, and Zr and the Genesis of Strongly Peraluminous Granites. *The Journal of Geology, 102*(4), 411-422. Retrieved from http://www.jstor.org/stable/30065660.

Gavrilov, Y., Shcherbinina, E., Golovanova, O., & Pokrovsky, B. (2009). A variety of PETM records in different settings, northeastern Peri-Tethys. In *Climatic and Biotic Events of the*

Paleogene [CBEP 2009], Extended Abstracts From an International Conference in Wellington, New Zealand, GNS Science Miscellaneous Series (Vol. 18, pp. 67-70).

Gazley, M. F., Vry, J. K., du Plessis, E., & Handler, M. R. (2011). Application of portable X-ray fluorescence analyses to metabasalt stratigraphy, Plutonic Gold Mine, Western Australia. *Journal of Geochemical Exploration*, *110*(2), 74-80.

Gazley, M. F., & Fisher, L. A. (2014). A review of the reliability and validity of portable X-ray fluorescence spectrometry (pXRF) data. *Mineral Resource and Ore Reserve Estimation–The AusIMM Guide to Good Practice*, 69-82.

Gazley, M. F., Duclaux, G., Fisher, L. A., Tutt, C. M., Latham, A. R., Hough, R. M. de Beer, S.J., & Taylor, M. D. (2015). A comprehensive approach to understanding ore deposits using portable X-ray fluorescence (pXRF) data at the Plutonic Gold Mine, Western Australia. *Geochemistry: Exploration, Environment, Analysis*, *15*(2-3), 113-124.

Gazley, M. F., Vry, J. K., White, A. J. R. & Todd, A. J. (*in submission*.). Considerations for modelling albite in pumpellyite-grade greywacke: South Coast, Wellington, New Zealand. *Submitted to Journal of Metamorphic Petrology*.

George, A. D. (1992). Deposition and deformation of an Early Cretaceous trench-slope basin deposit, Torlesse terrane, New Zealand. *Geological Society of America Bulletin*, *104*(5), 570-580.

Georgiev, S., Stein, H. J., Hannah, J. L., Weiss, H. M., Bingen, B., Xu, G., Rein, E., Hatlø, V., Løseth, H., Nali, M., & Piasecki, S. (2012). Chemical signals for oxidative weathering predict Re–Os isochroneity in black shales, East Greenland. *Chemical Geology*, *324*, 108-121.

Gehlen, M. (2012). *Organofacies variations within the Waipawa Formation (Late Paleocene), East Coast Basin, New Zealand*. MSc Thesis, University of Bremen. 111 p.

Ghisetti, F., Sibson, R. H., & Hamling, I. (2016a). Deformed Neogene basins, active faulting and topography in Westland: Distributed crustal mobility west of the Alpine fault transpressive plate boundary (South Island, New Zealand). *Tectonophysics*, *693*, 340-362.

Ghisetti, F. C., Barnes, P. M., Ellis, S., Plaza-Faverola, A. A., & Barker, D. H. (2016b). The last 2 Myr of accretionary wedge construction in the central Hikurangi margin (North Island, New Zealand): Insights from structural modeling. *Geochemistry, Geophysics, Geosystems*, *17*(7), 2661-2686.

Glaessner, M. F. (1980). New Cretaceous and Tertiary crabs (Crustacea: Brachyura) from Australia and New Zealand. *Transactions of the Royal Society of South Australia 104*, 171–192.

Gordon, R. G., & Cox, A. (1980). Paleomagnetic test of the early Tertiary plate circuit between the Pacific basin plates and the Indian plate. *Journal of Geophysical Research: Solid Earth*, *85*(B11), 6534-6546.

Gradstein, F. M., Ogg, J. G., Schmitz, M., & Ogg, G. (Eds.). (2012). *The geologic time scale 2012*. Elsevier.

Granot, R., Cande, S. C., Stock, J. M., & Damaske, D. (2013). Revised Eocene-Oligocene kinematics for the West Antarctic rift system. *Geophysical Research Letters*, *40*(2), 279-284.

Gray, G. G., & Norton, I. O. (1988). A palinspastic Mesozoic plate reconstruction of New Zealand. *Tectonophysics*, *155*(1-4), 391-399.

Green, P. F., Duddy, I. R., Gleadow, A. J. & Lovering, J. F. (1989). Apatite fission-track analysis as a paleotemperature indicator for hydrocarbon exploration. In *Thermal history of sedimentary basins*. Springer, New York. pp. 181–195.

Grindley, G. W. (1960). Sheet 8 Taupo-Geological Map of New Zealand 1: 250,000. *Department of Scientific and Industrial Research, Wellington, New Zealand*. Hardenbol, J. A. N. (1998). Mesozoic and Cenozoic sequence chronostratigraphic framework of European basins.

Grindley, G. W., Adams, C. J. D., Lumb, J. T., & Watters, W. A. (1977). Paleomagnetism, K-Ar dating and tectonic interpretation of Upper Cretaceous and Cenozoic volcanic rocks of the Chatham Islands, New Zealand. *New Zealand Journal of Geology and Geophysics 20*(3), 425-467.

Grindley, G. W., Mumme, T. C., & Kohn, B. P. (1994). Stratigraphy, paleomagnetism, geochronology and structure of silicic volcanic rocks, Waiotapu/Paeroa Range area, New Zealand. *Geothermics*, *23*(5-6), 473-499.

Grunsky, E. C., Mueller, U. A., & Corrigan, D. (2014). A study of the lake sediment geochemistry of the Melville Peninsula using multivariate methods: Applications for predictive geological mapping. *Journal of Geochemical Exploration*, *141*, 15-41.

Haast, J. (1871a). On the geology of the Waipara district, Canterbury. Geological Survey of New Zealand, *Reports of Geological Explorations during 1870-71*: 5-19.

Haast, J. (1871b). On the geology of the Amuri district, in the Provinces of Nelson and Marlborough. Geological Survey of New Zealand, *Reports of Geological Explorations during 1870-71*: 25–46.

Hall, W. D. M. (1963). The Clarence Series at Coverham, Clarence Valley. *New Zealand Journal of Geology and Geophysics*, *6*(1), 28-37.

Hall, R. (2002). Cenozoic geological and plate tectonic evolution of SE Asia and the SW Pacific: computer-based reconstructions, model and animations. *Journal of Asian Earth Sciences*, *20*(4), 353-431.

Hall, L. S., Lamb, S. H., & Mac Niocaill, C. (2004). Cenozoic distributed rotational deformation, South Island, New Zealand. *Tectonics*, *23*(2).

Hancock, H. J., Dickens, G. R., Strong, C. P., Hollis, C. J., & Field, B. D. (2003). Foraminiferal and carbon isotope stratigraphy through the Paleocene-Eocene transition at Dee Stream, Marlborough, New Zealand. *New Zealand Journal of Geology and Geophysics*, *46*(1), 1-19.

Hardenbol, J. A. N., Thierry, J., Farley, M. B., Jacquin, T., De Graciansky, P. C., & Vail, P. R. (1998). Mesozoic and Cenozoic sequence chronostratigraphic framework of European basins. *SEPM Special Publication 60*, 3-13.

Harris, L. C., & Whiting, B. M. (2000). Sequence-stratigraphic significance of Miocene to Pliocene glauconite-rich layers, on-and offshore of the US Mid-Atlantic margin. *Sedimentary Geology*, *134*(1), 129-147.

Hasegawa, T., Crampton, J. S., Schiøler, P., Field, B., Fukushi, K., & Kakizaki, Y. (2013). Carbon isotope stratigraphy and depositional oxia through Cenomanian/Turonian boundary sequences (Upper Cretaceous) in New Zealand. *Cretaceous Research*, *40*, 61-80.

Haston, R. B., Luyendyk, B. P., Landis, C. A., & Coombs, D. S. (1989). Paleomagnetism and question of original location of the Permian Brook Street Terrane, New Zealand. *Tectonics*, *8*(4), 791-801.

Haston, R. B., & Luyendyk, B. P. (1991). Paleomagnetic results from the Waipapa Terrane, Northland Peninsula, North Island, New Zealand: Tectonic implications from widespread remagnetizations. *Tectonics*, *10*(5), 986-994.

Hatch, J. R., & Leventhal, J. S. (1992). Relationship between inferred redox potential of the depositional environment and geochemistry of the Upper Pennsylvanian (Missourian) Stark Shale Member of the Dennis Limestone, Wabaunsee County, Kansas, USA. *Chemical Geology*, *99*(1), 65-82.

Haq, B. U., Hardenbol, J., & Vail, P. R. (1987). Chronology of fluctuating sea levels since the Triassic. *Science*, *235*(4793), 1156-1167.

Haq, B. U. (2014). Cretaceous eustasy revisited. *Global and Planetary Change*, *113*, 44-58.

Hayes, G. P., Furlong, K. P., & Ammon, C. J. (2009). Intraplate deformation adjacent to the Macquarie Ridge south of New Zealand—the tectonic evolution of a complex plate boundary. *Tectonophysics*, *463*(1-4), 1-14.

Hayward, B. W. (1986). A guide to paleoenvironmental assessment using New Zealand Cenozoic foraminiferal faunas. *New Zealand Geological Survey Paleontology Report*, *109*, 73.

Hayward, B. W., Grenfell, H. R., Sabaa, A. T., Neil, H. L. & Buzas, M. A. (2010). *Recent New Zealand deep-water benthic foraminifera: Taxonomy, ecologic distribution, biogeography and use in paleoenvironmental assessment*. GNS Science Monograph 26, GNS Science, Lower Hutt.

Hector, J. (1874). On the fossil Reptilia of New Zealand. *Transactions and Proceedings of the New Zealand Institute 6*: 333-358.

Helz, G. R., Miller, C. V., Charnock, J. M., Mosselmans, J. F. W., Pattrick, R. A. D., Garner, C. D., & Vaughan, D. J. (1996). Mechanism of molybdenum removal from the sea and its concentration in black shales: EXAFS evidence. *Geochimica et Cosmochimica Acta*, *60*(19), 3631-3642.

Henry, J. D. (1911). Oil Fields of New Zealand. Bradbury, Agnew & Co. Ltd., London.

Heron, D.W. (custodian) (2014). *Geological map of New Zealand 1:250,000*. Lower Hutt, NZ: GNS Science. GNS Science geological map 1. 1 CD.

Herzer, R. H. (1995). Seismic stratigraphy of a buried volcanic arc, Northland, New Zealand and implications for Neogene subduction. *Marine and Petroleum Geology*, *12*(5), 511-531.

Higgs, K. E., King, P. R., Raine, J. I., Sykes, R., Browne, G. H., Crouch, E. M., & Baur, J. R. (2012). Sequence stratigraphy and controls on reservoir sandstone distribution in an Eocene marginal marine-coastal plain fairway, Taranaki Basin, New Zealand. *Marine and Petroleum Geology*, *32*(1), 110-137.

Higgs, K. E., Crouch, E. M., & Raine, J. I. (2017). An interdisciplinary approach to reservoir characterisation; an example from the early to middle Eocene Kaimiro Formation, Taranaki Basin, New Zealand. *Marine and Petroleum Geology*, *86*, 111-139.

Hines, B. R. (2012). *The Early Paleogene Succession at Tora, New Zealand; Stratigraphy and Paeloclimate*. Unpublished MSc Thesis, Victoria University of Wellington.

Hines, B. R. (2015). Paleogene stratigraphy and paleoenvironment of the Tora coast. In: Atkins, C., (ed.) Fieldguides Geosciences 2015, Wellington, Geoscience Society of New Zealand Miscellaneous Publication No. 143b. ISBN: 978-1-877480-50-8.

Hines, B. R., Kulhanek, D. K., Hollis, C. J., Atkins, C. B., & Morgans, H. E. G. (2013). Paleocene–Eocene stratigraphy and paleoenvironment at Tora, Southeast Wairarapa, New Zealand. *New Zealand Journal of Geology and Geophysics*, *56*(4), 243-262.

Hochstein, M. P., & Nixon, I. M. (1979). Geophysical study of the Hauraki Depression, North Island, New Zealand. *New Zealand Journal of Geology and Geophysics*, *22*(1), 1-19.

Hochstein, M. P., & Ballance, P. F. (1993). Hauraki Rift: a young, active, intra-continental rift in a back-arc setting. *South Pacific Sedimentary Basins, Sedimentary Basins of the World*, *2*, 295-305.

Hofmann, P., Wagner, T., & Beckmann, B. (2003). Millennial-to centennial-scale record of African climate variability and organic carbon accumulation in the Coniacian–Santonian eastern tropical Atlantic (Ocean Drilling Program Site 959, off Ivory Coast and Ghana). *Geology*, *31*(2), 135-138.

Holdgate, G. R., & Grapes, R. H. (2015). Wairau Basin and fault connections across Cook Strait, New Zealand: seismic and geological evidence. *Australian Journal of Earth Sciences*, *62*(1), 95-121.

Hollis, C. J. (2002). Biostratigraphy and paleoceanographic significance of Paleocene radiolarians from offshore eastern New Zealand. *Marine Micropaleontology*, *46*(3), 265-316.

Hollis, C. J., Rodgers, K. A., & Strong, C. P. (2000). New Zealand perspective on global change from late Cretaceous to early Eocene: the Cretaceous—Tertiary transition at Flaxbourne River, eastern Marlborough. *GFF*, *122*(1), 73-74.

Hollis, C. J., Rodgers, K. A., Strong, C. P., Field, B. D., & Rogers, K. M. (2003a). Paleoenvironmental changes across the Cretaceous/Tertiary boundary in the northern

Clarence Valley, southeastern Marlborough, New Zealand. *New Zealand Journal of Geology and Geophysics*, *46*(2), 209-234.

Hollis, C. J., Strong, C. P., Rodgers, K. A., & Rogers, K. M. (2003b). Paleoenvironmental changes across the Cretaceous/Tertiary boundary at Flaxbourne River and Woodside Creek, eastern Marlborough, New Zealand. *New Zealand Journal of Geology and Geophysics*, *46*(2), 177-197.

Hollis, C. J., Dickens, G. R., Field, B. D., Jones, C. M., & Strong, C. P. (2005a). The Paleocene–Eocene transition at Mead Stream, New Zealand: a southern Pacific record of early Cenozoic global change. *Palaeogeography, Palaeoclimatology, Palaeoecology*, *215*(3), 313-343.

Hollis, C. J., Field, B. D., Jones, C. M., Strong, C. P., Wilson, G. J., & Dickens, G. R. (2005b). Biostratigraphy and carbon isotope stratigraphy of uppermost Cretaceous-lower Cenozoic Muzzle Group in middle Clarence valley, New Zealand. *Journal of the Royal Society of New Zealand*, *35*(3), 345-383.

Hollis, C.J. & Manzano-Kareah, K. (compilers) (2005). Source rock potential of the East Coast Basin (central and northern regions). Institute of Geological and Nuclear Sciences Client Report 2005/118: 156 pp.

Hollis, C. J., Field, B. D., Crouch, E. M., & Sykes, R. (2006). How good a source rock is the Waipawa (Black Shale) Formation beyond the East Coast Basin? An outcrop-based case study from Northland. In *2006 New Zealand Petroleum Conference Proceedings, Crown Minerals, Ministry of Economic Development, New Zealand*.

Hollis, C. J., Crampton, J. S., Morgans, H. E. G. & Reid, C. (2013). Cretaceous-Paleogene stratigraphy of northeastern South Island. *Geoscience Society of New Zealand Field trip guide*. 52 p.

Hollis, C. J., Tayler, M. J., Andrew, B., Taylor, K. W., Lurcock, P., Bijl, P. K., Kulhanek, D. K., Crouch, E. M., Nelson, C. S., Pancost, R. D., Huber, M., Wilson, G. S., Ventura, G. T., Crampton, J. S., Schiøler, P. & Phillips, A. (2014). Organic-rich sedimentation in the South Pacific Ocean associated with Late Paleocene climatic cooling. *Earth-Science Reviews*, *134*, 81-97.

Hollis, C. J., Stickley, C. E., Bijl, P. K., Schiøler, P., Clowes, C. D., Li, X., & Campbell, H. (2017). The age of the Takatika Grit, Chatham Islands, New Zealand. *Alcheringa: An Australasian Journal of Palaeontology*, 1-14.

Hoolihan, K. (1977). Basement geology of the Motu River mouth area, Raukumara Peninsula. MSc thesis, The University of Auckland, Auckland.

Hunt, T. (1978). Stokes magnetic anomaly system. *New Zealand Journal of Geology and Geophysics*, *21*(5), 595-606.

Hunt, D., & Tucker, M. E. (1992). Stranded parasequences and the forced regressive wedge systems tract: deposition during base-level fall. *Sedimentary Geology*, *81*(1-2), 1-9.

Hutton, F. W. (1874). Report on the geology of the north-eastern portion of the South Island from Cook Strait to the Rakaia. *New Zealand Geological Survey reports of geological exploration during 1872-1873* (8b): 27-58.

Ian Brown Associates Ltd. (2004). Hukarere-1 geochemistry and its implications for PEP38325 prospectivity, Hawke Bay, New Zealand. *Ministry of Economic Development New Zealand, Unpublished Petroleum Report PR2940*. 59 p.

Ingall, E. D., Bustin, R. M., & Van Cappellen, P. (1993). Influence of water column anoxia on the burial and preservation of carbon and phosphorus in marine shales. *Geochimica et Cosmochimica Acta*, *57*(2), 303-316.

Ingall, E., & Jahnke, R. (1994). Evidence for enhanced phosphorus regeneration from marine sediments overlain by oxygen depleted waters. *Geochimica et Cosmochimica Acta*, *58*(11), 2571-2575.

Ingall, E., & Jahnke, R. (1997). Influence of water-column anoxia on the elemental fractionation of carbon and phosphorus during sediment diagenesis. *Marine Geology*, *139*(1-4), 219-229.

Isaac, M. J. (1977). *Mesozoic geology of the Matawai District, Raukumara Peninsula*. Unpublished PhD thesis, University of Auckland.

Isaac, M. J., Moore, P. R., & Joass, Y. J. (1991). Tahora Formation: The basal facies of a Late Cretaceous transgressive sequence, northeastern New Zealand. *New Zealand Journal of Geology and Geophysics*, *34*(2), 227-236.

Isaac, M.J., Herzer, R.H., Brook, F.J. & Hayward, B.W. (1994). Cretaceous and Cenozoic Sedimentary Basins of Northland, New Zealand. Institute of Geological and Nuclear Sciences Monograph, 8.

Isaac, M. J., Isaac, M. J., Rattenbury, M. S., Heron, D. W., & Reay, M. B. (1996). *Geology of the Kaitaia Area: Scale 1: 250 000*. Institute of Geological & Nuclear Sciences.

Jackson, D. A. (1993). Stopping rules in principal components analysis: a comparison of heuristical and statistical approaches. *Ecology*, *74*(8), 2204-2214.

Jarvis, I. A. N., Murphy, A. M., & Gale, A. S. (2001). Geochemistry of pelagic and hemipelagic carbonates: criteria for identifying systems tracts and sea-level change. *Journal of the Geological Society*, *158*(4), 685-696.

Jiao, R., Seward, D., Little, T. A., & Kohn, B. P. (2014). Thermal history and exhumation of basement rocks from Mesozoic to Cenozoic subduction cycles, central North Island, New Zealand. *Tectonics*, *33*(10), 1920-1935.

Jiao, R., Seward, D., Little, T. A., & Kohn, B. P. (2015). Unroofing of fore-arc ranges along the Hikurangi Margin, New Zealand: Constraints from low-temperature thermochronology. *Tectonophysics*, *656*, 39-51.

Jiao, R., Seward, D., Little, T. A., Herman, F., & Kohn, B. P. (2017). Constraining provenance, thickness and erosion of nappes using low-temperature thermochronology: the Northland Allochthon, New Zealand. *Basin Research*, *29*(1), 81-95.

Jenkyns, H. C., Matthews, A., Tsikos, H., & Erel, Y. (2007). Nitrate reduction, sulfate reduction, and sedimentary iron isotope evolution during the Cenomanian-Turonian oceanic anoxic event. *Paleoceanography*, *22*(3).

Joass, Y. J. (1987). The geology of the Tahora district, southern Raukumara Peninsula, New Zealand. Unpublished M.Sc. thesis, lodged in the Library, Victoria University of Wellington.

Johansen, A. (2011), Waitangi Hill Stratigraphic-3 well completion report. NZP&M, Ministry of Business, Innovation & Employment (MBIE), New Zealand. Unpublished Petroleum Report PR4420.

Johansen, A. (2012), Waitangi Hill Stratigraphic-2 well completion report. NZP&M, Ministry of Business, Innovation & Employment (MBIE), New Zealand. Unpublished Petroleum Report PR441.

Johnston, M. R., & Browne, P. D. (1973). Upper Jurassic and Cretaceous conglomerates in the Tinui – Awatoitoi district, eastern Wairarapa (Note). *New Zealand journal of geology and geophysics*, *16*(4), 1055-1060.

Johnston, M. R. (1980). *Geology of the Tinui-Awatoitoi district* (Vol. 94). New Zealand Department of Scientific and Industrial Research.

Jones, B., & Manning, D. A. (1994). Comparison of geochemical indices used for the interpretation of palaeoredox conditions in ancient mudstones. *Chemical Geology*, *111*(1), 111-129.

Jones, R. W., & Charnock, M. A. (1985). Morphogroups" of agglutinating foraminifera. Their life positions and feeding habits and potential applicability in (paleo) ecological studies. *Revue de Paléobiologie*, *4*(2), 311-320.

Kaiho, K. (1994). Benthic foraminiferal dissolved-oxygen index and dissolved-oxygen levels in the modern ocean. *Geology*, *22*(8), 719-722.

Kaiho, K., Arinobu, T., Ishiwatari, R., Morgans, H. E., Okada, H., Takeda, N., ... & Hirai, A. (1996). Latest Paleocene benthic foraminiferal extinction and environmental changes at Tawanui, New Zealand. *Paleoceanography*, *11*(4), 447-465.

Kamp, P. J. (1986). Late Cretaceous-Cenozoic tectonic development of the southwest Pacific region. *Tectonophysics*, *121*(2-4), 225-251.

Kamp, P. J. J. (1987). Age and origin of the New Zealand orocline in relation to Alpine Fault movement. *Journal of the Geological Society*, *144*(4), 641-652.

Kamp, P. J. (1999). Tracking crustal processes by FT thermochronology in a forearc high (Hikurangi margin, New Zealand) involving Cretaceous subduction termination and mid-Cenozoic subduction initiation. *Tectonophysics*, *307*(3), 313-343.

Kamp, P. J. (2000). Thermochronology of the Torlesse accretionary complex, Wellington region, New Zealand. *Journal of Geophysical Research: Solid Earth*, *105*(B8), 19253-19272.

Kamp, P. J., & Nelson, C. S. (1988). Nature and occurrence of modern and Neogene active margin limestones in New Zealand. *New Zealand Journal of Geology and Geophysics*, *31*(1), 1-20.

Kamp, P. J., Vonk, A. J., Bland, K. J., Hansen, R. J., Hendy, A. J., McIntyre, A. P., ... & Nelson, C. S. (2004). Neogene stratigraphic architecture and tectonic evolution of Wanganui, King Country, and eastern Taranaki Basins, New Zealand. *New Zealand Journal of Geology and Geophysics*, *47*(4), 625-644.

Katz, B. J. (2005). Controlling factors on source rock development—a review of productivity, preservation, and sedimentation rate. In: Harris N.B (Ed.). *The deposition of organic-carbon-rich sediments: Models, mechanisms, and consequences*. SEPM Special publication No. 82. ISBN 1-56576-110-3 p.17-33.

Kazians, C. C. (2010). Well completion report for Waitangi Hill Stratigraphic-1. NZP&M, Ministry of Business, Innovation & Employment (MBIE), New Zealand. Unpublished Petroleum Report PR4338.

Kear, D. (1971). Basement rock facies – northern North Island. *New Zealand Journal of Geology and Geophysics 14*: 275–283.

Kear, D. (1993). Reflections on major North Island basement rock assemblages and on megafaults. *Journal of the Royal Society of New Zealand*, *23*(1), 29-41.

Kear, D. (2004). Reassessment of Neogene tectonism and volcanism in North Island, New Zealand. *New Zealand Journal of Geology and Geophysics*, *47*(3), 361-374.

Keller, W. R. (2004). *Cenozoic plate tectonic reconstructions and plate boundary processes in the Southwest Pacific*. Doctoral dissertation, California Institute of Technology.

Kelsey, H. M., Cashman, S. M., Beanland, S., & Berryman, K. R. (1995). Structural evolution along the inner forearc of the obliquely convergent Hikurangi margin, New Zealand. *Tectonics*, *14*(1), 1-18.

Kelsey, H. M., Hull, A. G., Cashman, S. M., Berryman, K. R., Cashman, P. H., Trexler Jr, J. H., & Begg, J. G. (1998). Paleoseismology of an active reverse fault in a forearc setting: The Poukawa fault zone, Hikurangi forearc, New Zealand. *Geological Society of America Bulletin*, *110*(9), 1123-1148.

Kennett, J. P. (1977). Cenozoic evolution of Antarctic glaciation, the circum-Antarctic Ocean, and their impact on global paleoceanography. *Journal of Geophysical Research*, *82*(27), 3843-3860.

Kenny, J. A. (1984). Stratigraphy, sedimentology and structure of the Ihungia decollement, Raukumara Peninsula, North Island, New Zealand. *New Zealand Journal of Geology and Geophysics*, *27*(1), 1-19.

Kenny, J. A. (1986). *Alternating convergent and non-convergent tectonics, 100 million years to present, Puketoro area, northeastern New Zealand*. Unpublished PhD thesis, Auckland University.

Keyes, I. W. (1977). Records of the northern hemisphere Cretaceous sawfish genus Onchopristis (order Batoidea) from New Zealand. *New Zealand Journal of Geology and Geophysics 20*, 263–272.

Killops, S. (1996). A geochemical perspective of oil generation in New Zealand basins. In *New Zealand Petroleum Conference Proceedings* (Vol. 1, pp. 179–187).

Killops, S. D., Cook, R. A., Sykes, R., & Boudou, J. P. (1997). Petroleum potential and oil-source correlation in the Great South and Canterbury Basins. *New Zealand Journal of Geology and Geophysics*, *40*(4), 405-423.

Killops, S. D., Hollis, C. J., Morgans, H. E. G., Sutherland, R., Field, B. D., & Leckie, D. A. (2000). Paleoceanographic significance of Late Paleocene dysaerobia at the shelf/slope break around New Zealand. *Palaeogeography, Palaeoclimatology, Palaeoecology*, *156*(1), 51-70.

Kimbrough, D. L., Mattinson, J. M., Coombs, D. S., Landis, C. A., & Johnston, M. R. (1992). Uranium-lead ages from the Dun Mountain ophiolite belt and Brook Street terrane, South Island, New Zealand. *Geological Society of America Bulletin*, *104*(4), 429-443.

King, P. R. (2000a). Tectonic reconstructions of New Zealand: 40 Ma to the present. *New Zealand Journal of Geology and Geophysics*, *43*(4), 611-638.

King, P. R. (2000b). New Zealand's changing configuration in the last 100 million years: plate tectonics, basin development, and depositional setting. In *2000 New Zealand Petroleum Conference Proceedings* (Vol. 15).

King, P. R., Browne, G. H., & Slatt, R. M. (1994). Sequence architecture of exposed late Miocene basin floor fan and channel-levee complexes (Mount Messenger Formation), Taranaki Basin, New Zealand. *Submarine fans and turbidite systems: sequence stratigraphy, reservoir architecture and production characteristics of Gulf of Mexico and international. Houston, Gulf Coast Section, Society of Economic Paleontologists and Mineralogists Foundation*, 177-192.

King, P. R., & Thrasher, G. P. (1996). *Cretaceous Cenozoic geology and petroleum systems of the Taranaki Basin, New Zealand* (Vol. 2). Institute of Geological & Nuclear Sciences.

King, P. R., Naish, T. R., Browne, G. H., Field, B. D. & Edbrooke, S. W. (1999). Cretaceous to Recent sedimentary patterns in New Zealand. *Institute of Geological and Nuclear Sciences Folio Series*, *1*: 35 p.

King, P. R., & Browne, G. H. (2001). Miocene turbidite reservoir systems in the Taranaki Basin, New Zealand: established plays and analogues for deep-water exploration. *In*: Hill, K.C., and Bernecker, T., eds., Proceedings of East Australian Basins Symposium (EABS), The Australasian Institute of Mining and Metallurgy: Petroleum Exploration Society of Australia, Special Publication, p. 129–139

King, P. R., Ilg, B. R., Arnot, M., Browne, G. H., Strachan, L., Crundwell, M., & Helle, K. (2011). Outcrop and seismic examples of mass-transport deposits from a late Miocene deep-water

succession, Taranaki Basin, New Zealand. *Mass-Transport Deposits in Deep-Water Settings: SEPM, Special Publication*, *96*, 311-348.

Kingma, J. T. (1959). The tectonic history of New Zealand. *New Zealand Journal of Geology and Geophysics*, *2*(1), 1-55.

Kingma, J. T. (1971). *Geology of Te Aute Subdivision* (No. 70-71). New Zealand Dept. of Scientific and Industrial Research.

Klinkhammer, G. P., & Palmer, M. R. (1991). Uranium in the oceans: where it goes and why. *Geochimica et Cosmochimica Acta*, *55*(7), 1799-1806.

Kominz, M. A., Browning, J. V., Miller, K. G., Sugarman, P. J., Mizintseva, S., & Scotese, C. R. (2008). Late Cretaceous to Miocene sea-level estimates from the New Jersey and Delaware coastal plain coreholes: An error analysis. *Basin Research*, *20*(2), 211-226.

Kondo, Y., Abbott, S. T., Kitamura, A., Kamp, P. J., Naish, T. R., Kamataki, T., & Saul, G. S. (1998). The relationship between shellbed type and sequence architecture: examples from Japan and New Zealand. *Sedimentary Geology*, *122*(1-4), 109-127.

Kulhanek, D. K., Crouch, E. M., Tayler, M. J. S. & Hollis, C. J. (2015). Paleocene calcareous nannofossils from East Coast, New Zealand: biostratigraphy and paleoecology. *Proc. 14th INA Conf. Reston, VA, USA. Journal of Nannoplankton Research* 35 (2) 155–176.

Kurtz, A. C., Kump, L. R., Arthur, M. A., Zachos, J. C., & Paytan, A. (2003). Early Cenozoic decoupling of the global carbon and sulfur cycles. *Paleoceanography*, *18*(4).

Laird, M. G. (1992). Cretaceous stratigraphy and evolution of the Marlborough segment of the East Coast region. *In:* 1991 New Zealand Oil Exploration Conference proceedings. Wellington, Petroleum and Geothermal Unit, Energy and Resources Division, Ministry of Commerce. Pp. 89–100.

Lamb, S. H. (1988). Tectonic rotations about vertical axes during the last 4 Ma in part of the New Zealand plate-boundary zone. *Journal of Structural Geology*, *10*(8), 875-893.

Lamb, S. (2011). Cenozoic tectonic evolution of the New Zealand plate-boundary zone: A paleomagnetic perspective. *Tectonophysics*, *509*(3), 135-164.

Lamb, S. H., & Bibby, H. M. (1989). The last 25 Ma of rotational deformation in part of the New Zealand plate-boundary zone. *Journal of Structural Geology*, *11*(4), 473-492.

Lamb, S., Mortimer, N., Smith, E., & Turner, G. (2016). Focusing of relative plate motion at a continental transform fault: Cenozoic dextral displacement> 700 km on New Zealand's Alpine Fault, reversing> 225 km of Late Cretaceous sinistral motion. *Geochemistry, Geophysics, Geosystems*, *17*(3), 1197-1213.

Landis, C. A., Campbell, H. J., Begg, J. G., Mildenhall, D. C., Paterson, A. M., & Trewick, S. A. (2008). The Waipounamu Erosion Surface: questioning the antiquity of the New Zealand land surface and terrestrial fauna and flora. *Geological Magazine*, *145*(2), 173-197.

Leckie, D. A., Morgans, H. E. G., Wilson, G. J. & Uruski, C. I. (1992). *Stratigraphic framework and source-rock potential of maastrichtian to paleocene marine shale: East coast, North Island, New Zealand: hydrocarbon prospects* (Vol. 92). Institute of Geological and Nuclear Sciences Science Report 92/5, 1-35 p.

Leckie, D. A., Morgans, H., Wilson, G. J., & Edwards, A. R. (1995). Mid-Paleocene dropstones in the Whangai Formation, New Zealand – evidence of mid-Paleocene cold climate? *Sedimentary Geology*, *97*(3), 119-129.

Lee, J. M. (1995). *A Stratigraphic, Biostratigraphic and Structural Analysis of the Geology at Huatokitoki Stream, Glenburn, Southern Wairarapa, New Zealand.* Unpublished MSc Thesis, Victoria University of Wellington.

Lee, J. M., Begg, J. G., & Forsyth, P. J. (2002). *Geology of the Wairarapa area*. Institute of Geological & Nuclear Sciences.

Lee, J. M., Bland, K. J., Townsend, D. B., & Kamp, P. J. J. (2011). Geology of the Hawkes Bay Area, QMAP 1: 250,000 Geological Map. *GNS Sciences, Lower Hutt, New Zealand*, *97*.

Leonard, G. S., Begg, J. G. & Wilson, C. J. N. (2010). *Geology of the Rotorua area*. QMAP 1: 250,000 Geological Map. *GNS Sciences, Lower Hutt, New Zealand.*

Lewis, D. W. (1992). Anatomy of an unconformity on mid-Oligocene Amuri Limestone, Canterbury, New Zealand. *New Zealand Journal of Geology and Geophysics*, *35*(4), 463-475.

Lewis, K. B. (1994). The 1500-km-long Hikurangi Channel: trench-axis channel that escapes its trench, crosses a plateau, and feeds a fan drift. *Geo-Marine Letters*, *14*(1), 19-28.

Lewis, K.B. & Pettinga, J.R. (1993). The emerging, imbricate frontal wedge of the Hikurangi Margin. *In: South Pacific sedimentary basins* (Ballance, P. F., ed.). Sedimentary basins of the world 2. Amsterdam, Elsevier Science Publishers B.V: Pp. 225–250.

Lewis, K. B., Carter, L., & Davey, F. J. (1994). The opening of Cook Strait: interglacial tidal scour and aligning basins at a subduction to transform plate edge. *Marine Geology*, *116*(3-4), 293-312.

Lillie, A. R. (1953). The Geology of the Dannevirke Subdivision. *New Zealand Geological Survey Bulletin 46*: 156 p. + 10 enclosures.

Lillie, A. R. (1980). *Strata and structure in New Zealand.* Tohunga Press, Auckland. ISBN: 0473000385. 441 p.

Little, T. A., & Roberts, A. P. (1997). Distribution and mechanism of Neogene to present-day vertical axis rotations, Pacific-Australian plate boundary zone, South Island, New Zealand. *Journal of Geophysical Research: Solid Earth*, *102*(B9), 20447-20468.

Little, T. A., & Jones, A. (1998). Seven million years of strike-slip and related off-fault deformation, northeastern Marlborough fault system, South Island, New Zealand. *Tectonics*, *17*(2), 285-302.

Little, T. A., & Mortimer, N. (2001). Rotation of ductile fabrics across the Alpine Fault and Cenozoic bending of the New Zealand orocline. *Journal of the Geological Society*, *158*(5), 745-756.

Love, H., LeGood, M., Stuart, G., Reyners, M., Eberhart-Phillips, D. E., & Gubbins, D. (2015). Fast P-wave precursors in New Zealand: high velocity material associated with the subducted Hikurangi Plateau. *Geophysical Journal International*, *202*(2), 1223-1240.

Lückge, A., Ercegovac, M., Strauss, H., & Littke, R. (1999). Early diagenetic alteration of organic matter by sulfate reduction in Quaternary sediments from the northeastern Arabian Sea. *Marine Geology*, *158*(1), 1-13.

Lyle, M., Gibbs, S., Moore, T. C., & Rea, D. K. (2007). Late Oligocene initiation of the Antarctic circumpolar current: evidence from the South Pacific. *Geology*, *35*(8), 691-694.

Lyons, T. W., & Severmann, S. (2006). A critical look at iron paleoredox proxies: new insights from modern euxinic marine basins. *Geochimica et Cosmochimica Acta*, *70*(23), 5698-5722.

MacDougall, D., & Crummett, W. B. (1980). Guidelines for data acquisition and data quality evaluation in environmental chemistry. *Analytical Chemistry*, *52*(14), 2242-2249.

Malahoff, A., Feden, R. H., & Fleming, H. S. (1982). Magnetic anomalies and tectonic fabric of marginal basins north of New Zealand. *Journal of Geophysical Research: Solid Earth*, *87*(B5), 4109-4125.

Martín-Fernández, J. A., Hron, K., Templ, M., Filzmoser, P., & Palarea-Albaladejo, J. (2012). Model-based replacement of rounded zeros in compositional data: classical and robust approaches. *Computational Statistics & Data Analysis*, *56*(9), 2688-2704.

Mason, B. H. (1941). The geology of the Mount Grey district, North Canterbury. *Transactions of the Royal Society of New Zealand 71*: 103-127.

Maurizot, P. (2011). First sedimentary record of the pre-obduction convergence in New Caledonia: formation of an Early Eocene accretionary complex in the north of Grande Terre and emplacement of the 'Montagnes Blanches' nappe. *Bulletin de la Société Géologique de France*, *182*(6), 479-491.

Mazengarb, C. (1993). *Cretaceous stratigraphy of Raukumara Peninsula*. Institute of Geological & Nuclear Sciences.

Mazengarb, C. (1994). Estimating actual displacement along the Alpine Fault; time for a test. *Geological Society of New Zealand Newsletter 105*, 58.

Mazengarb, C., & Harris, D. H. M. (1994). Cretaceous stratigraphic and structural relations of Raukumara Peninsula, New Zealand: stratigraphic patterns associated with the migration of a thrust system. In *Annales Tectonicae* (Vol. 8, pp. 100-118).

Mazengarb, C., & Speden, I. G. (Eds.). (2000). *Geology of the Raukumara area* (Vol. 6). Institute of Geological & Nuclear Sciences *1:250 000 geological map 6*. Lower Hutt, Institute of Geological & Nuclear Sciences. 1 sheet + 60 p.

Meyers, S. R., Sageman, B. B., & Lyons, T. W. (2005). Organic carbon burial rate and the molybdenum proxy: Theoretical framework and application to Cenomanian-Turonian oceanic anoxic event 2. *Paleoceanography and Paleoclimatology*, *20*(2).

McKay, A. (1877a). Report on Kaikoura Peninsula and Amuri Bluff. Geological Survey of New Zealand, *Report of Geological Explorations during 1874-76*: 172-184.

McKay, A. (1877b). Report on Weka Pass and Buller districts. Geological Survey of New Zealand, *Report of Geological Explorations during 1874-76*: 36-42.

McLernon, C.R. (1978). Indications of petroleum in New Zealand. *New Zealand unpublished openfile petroleum report 839*. Ministry of Commerce, Wellington.

McManus, J., Berelson, W. M., Klinkhammer, G. P., Hammond, D. E., & Holm, C. (2005). Authigenic uranium: relationship to oxygen penetration depth and organic carbon rain. *Geochimica et Cosmochimica Acta*, *69*(1), 95-108.

Meadows, D. J. (2009). *Stable isotope geochemistry of Paleocene to Early Eocene strata around southern New Zealand*. Unpublished MSc thesis, Victoria University of Wellington.

Miller, W. (1995). Examples of Mesozoic and Cenozoic Bathysiphon (Foraminiferida) from the Pacific Rim and the taxonomic status of Terebellina Ulrich, 1904. *Journal of Paleontology*, *69*(4), 624-634.

Miller, W. (2005). Giant Bathysiphon (Astrorhizina: Foraminifera) from the Late Cretaceous Hunters Cove Formation, southwestern Oregon. *Journal of Paleontology*, *79*(2), 389-394.

Miller, K. G., Sugarman, P. J., Browning, J. V., Kominz, M. A., Hernández, J. C., Olsson, R. K., ... & Van Sickel, W. (2003). Late Cretaceous chronology of large, rapid sea-level changes: Glacioeustasy during the greenhouse world. *Geology*, *31*(7), 585-588.

Miller, K. G., Sugarman, P. J., Browning, J. V., Kominz, M. A., Olsson, R. K., Feigenson, M. D., & Hernández, J. C. (2004). Upper Cretaceous sequences and sea-level history, New Jersey coastal plain. *Geological Society of America Bulletin*, *116*(3-4), 368-393.

Miller, K. G., Kominz, M. A., Browning, J. V., Wright, J. D., Mountain, G. S., Katz, M. E., ... & Pekar, S. F. (2005). The Phanerozoic record of global sea-level change. *Science*, *310*(5752), 1293-1298.

Mitchum Jr, R. M., & Van Wagoner, J. C. (1991). High-frequency sequences and their stacking patterns: sequence-stratigraphic evidence of high-frequency eustatic cycles. *Sedimentary Geology*, *70*(2-4), 131-160.

Molnar, R. E. (1981). A dinosaur from New Zealand. In: *Gondwana Five*, M.M. Cresswell & P. Vella, eds, Fifth International Gondwana Symposium, Wellington, New Zealand, February 1980. Rotterdam, AA Balkema, pp. 91–96.

Molnar, R. E. & Wiffen, J. (1994). A Late Cretaceous polar dinosaur fauna from New Zealand. *Cretaceous Research 15*, 689–706.

Molnar, R. E. & Wiffen, J. (2007). A presumed titanosaurian vertebra from the Late Cretaceous of North Island, New Zealand. *Arquivos do Museu Nacional 65*, 505–510.

Montague, T. G. (1981). Cretaceous stratigraphy of the Mt. Lookout area and its relation to the proposed regional unconformity at the end of the Rangitata orogeny. Unpublished PhD thesis, University of Canterbury.

Moore, P. R. (1978). Geology of western Koranga Valley, Raukumara Peninsula. *New Zealand Journal of Geology and Geophysics 21*: 1–20.

Moore, P. R. (1980). Late Cretaceous-Tertiary stratigraphy, structure, and tectonic history of the area between Whareama and Ngahape, eastern Wairarapa, New Zealand. *New Zealand Journal of Geology and Geophysics*, *23*(2), 167-177.

Moore, P.R. (1987a). Stratigraphy and structure of the Te Hoe-Waiau River area, western Hawkes Bay. *New Zealand Geological Survey Record 18*: 4–12.

Moore, P. R. (1987b). Terebellina-sponge or foraminiferid. *A comparison with Makiyama and Bathysiphon. New Zealand Geological Survey Record*, *20*, 43-50.

Moore, P. R. (1988a). Stratigraphy, composition and environment of deposition of the Whangai Formation and associated Late Cretaceous-Paleocene rocks, eastern North Island, New Zealand. *New Zealand Geological Survey* Bulletin 100: 82p.

Moore, P. R. (1988b). Structural divisions of eastern North Island. *New Zealand Geological Survey Record,* 30: 24 p.

Moore, P. R. (1988c). Dolomite concretions in the Whangai Formation (Late Cretaceous-Paleocene) at Mara Quarry, northern Wairarapa. *New Zealand Geological Survey Record*, *40*, 52-54.

Moore, P. R. (1989a). Stratigraphy of the Waipawa Black Shale (Paleocene), Eastern North Island, New Zealand. *New Zealand Geological Survey Record* 38: 19 p.

Moore, P. R. (1989b). Kirks Breccia: a late cretaceous submarine channelised debris flow deposit, Raukumara Peninsula, New Zealand. *Journal of the Royal Society of New Zealand*, *19*(2), 195-203.

Moore, P. R. (1989c). Lithological changes across the Cretaceous-Tertiary boundary in eastern North Island. *New Zealand Geological Survey Record*, *40*, 41-47.

Moore, P. R., & Speden, I. (1979). Stratigraphy, structure, and inferred environments of deposition of the Early Cretaceous sequence, eastern Wairarapa, New Zealand. *New Zealand Journal of Geology and Geophysics*, *22*(4), 417-433.

Moore, P. R., & Speden, I. G. (1984). *The Early Cretaceous (Albian) sequence of eastern Wairarapa, New Zealand* (Vol. 97). New Zealand Geological Survey Bulletin 97.

Moore, P. R., Adams, A. G., Isaac, M. J., Mazengarb, C., Morgans, H. E. G. & Phillips, C. J. (1986a). A revised Cretaceous-Early Tertiary stratigraphic nomenclature for eastern North Island, New Zealand. *New Zealand Geological Survey Report*, G104: 31 p.

Moore, P. R., Braithwaite, R. L., & Roser, B. P. (1986b). Correlation of Early Cretaceous volcanic-sedimentary sequences at Red Island and Hinemahanga Rocks, southern Hawke's Bay. *New Zealand Geological Survey Record 18*, 27-32.

Moore, P. R., & Morgans, H. E. G. (1987). Two new reference sections for the Wanstead Formation (Paleocene-Eocene) in southern Hawkes Bay. *New Zealand Geological Survey Record*, *20*, 81-87.

Moore, P. R., Snowdon, L. R., & Osadetz. K. G. (1987). Maturation and petroleum source rock potential of the Whangai and Waipawa Formations (Late Cretaceous–Paleocene), Eastern North Island. *New Zealand Geological Survey Record*, 20 (1987), 17–23 p.

Moore, P. R., Isaac, M. J., Crampton, J. S., & Mazengarb, C. (1988). Late Cretaceous sediments west of Lake Waikaremoana, Urewera National Park. *New Zealand Geological Survey Record 35*: 55–60.

Moore, P. R., Isaac, M. J., Mazengarb, C., & Wilson, G. J. (1989). Stratigraphy and structure of Cretaceous (Neocomian-Maastrichtian) sedimentary rocks in the Anini-Okaura Stream area, Urewera National Park, New Zealand. *New Zealand Journal of Geology and Geophysics 32*: 515–526.

Morris, J. C. (1987). *The stratigraphy of the Amuri limestone group, east Marlborough, New Zealand.* Unpublished PhD thesis, University of Canterbury.

Morford, J. L., Russell, A. D., & Emerson, S. (2001). Trace metal evidence for changes in the redox environment associated with the transition from terrigenous clay to diatomaceous sediment, Saanich Inlet, BC. *Marine Geology*, *174*(1), 355-369.

Morgans, H. E. G. (2001). Foraminiferal biostratigraphy of Waitaria-2 onshore petroleum exploration well, Poverty Bay, East Coast, New Zealand. *Institute of Geological and Nuclear Sciences client report 2000/*23.

Morgans, H. E. G. (2009). Late Paleocene to Middle Eocene foraminiferal biostratigraphy of the Hampden Beach section, eastern South Island, New Zealand. *New Zealand Journal of Geology and Geophysics*, *52*(4), 273-320.

Morgans, H. E. G. (2016). The Weber Formation at its type location in Southern Hawke's Bay, and its distribution through the East Coast, North Island, New Zealand. *GNS Science Report 2015/38*. 95 p.

Mortimer, N. (1993). Metamorphic zones, terranes, and Cenozoic faults in the Marlborough Schist, New Zealand. *New Zealand Journal of Geology and Geophysics*, *36*(3), 357-368.

Mortimer, N. (1995). Origin of the Torlesse Terrane and coeval rocks, North Island, New Zealand. *International Geology Review 36*: 891–910.

Mortimer, N. (2004). New Zealand's geological foundations. *Gondwana Research 7*: 261–272.

Mortimer, N. (2014). The oroclinal bend in the South Island, New Zealand. *Journal of Structural Geology*, *64*, 32-38.

Mortimer, N., & Roser, B. P. (1992). Geochemical evidence for the position of the Caples–Torlesse boundary in the Otago Schist, New Zealand. *Journal of the Geological Society*, *149*(6), 967-977.

Mortimer, N., Tulloch, A. J., Spark, R. N., Walker, N. W., Ladley, E., Allibone, A., & Kimbrough, D. L. (1999). Overview of the Median Batholith, New Zealand: a new interpretation of the geology of the Median Tectonic Zone and adjacent rocks. *Journal of African Earth Sciences*, *29*(1), 257-268.

Mortimer, N., Herzer, R. H., Walker, N. W., Calvert, A. T., Seward, D., & Chaproniere, G. C. H. (2003). Cavalli Seamount, Northland Plateau, SW Pacific Ocean: a Miocene metamorphic core complex? *Journal of the Geological Society*, *160*(6), 971-983.

Mortimer, N., Rattenbury, M. S., King, P. R., Bland, K. J., Barrell, D. J. A., Bache, F., ... & Edbrooke, S. W. (2014). High-level stratigraphic scheme for New Zealand rocks. *New Zealand Journal of Geology and Geophysics*, *57*(4), 402-419.

Mortimer, N., Kohn, B., Seward, D., Spell, T., & Tulloch, A. (2016). Reconnaissance thermochronology of southern Zealandia. *Journal of the Geological Society*, *173*(2), 370-383.

Morton, A. C., & Hallsworth, C. (1994). Identifying provenance-specific features of detrital heavy mineral assemblages in sandstones. *Sedimentary Geology*, *90*(3-4), 241-256.

Mueller, U. A., & Grunsky, E. C. (2016). Multivariate spatial analysis of lake sediment geochemical data; Melville Peninsula, Nunavut, Canada. *Applied Geochemistry*, *75*, 247-262.

Müller, D., Qin, X., Sandwell, D., Dutkiewicz, A., Williams, S., Flament, N., ... & Seton, M. (2017, April). The GPlates Portal: Cloud-based interactive 3D and 4D visualization of global geological and geophysical data and models in a browser. In *EGU General Assembly Conference Abstracts* (Vol. 19, p. 4194).

Mumme, T. C., Lamb, S. H., & Walcott, R. I. (1989). The Raukumara paleomagnetic domain: Constraints on the tectonic rotation of the east coast, North Island, New Zealand, from paleomagnetic data. *New Zealand Journal of Geology and Geophysics*, *32*(3), 317-326.

Murphy, R. P., & Seward, D. (1981). Stratigraphy, lithology, paleomagnetism, and fission track ages of some ignimbrite formations in the Matahana Basin, New Zealand. *New Zealand Journal of Geology and Geophysics, 24*(3), 325-331.

Murphy, A. E., Sageman, B. B., Hollander, D. J., Lyons, T. W., & Brett, C. E. (2000). Black shale deposition and faunal overturn in the Devonian Appalachian basin: Clastic starvation, seasonal water-column mixing, and efficient biolimiting nutrient recycling. *Paleoceanography*, *15*(3), 280-291.

Musgrave, R. J. (1989). A weighted least-squares fit of the Australian apparent polar wander path for the last 100 Myr. *Geophysical Journal International*, *96*(2), 231-243.

Naeser, C. W. (1979). Fission-track dating and geological annealing of fission tracks. *In*: Jager, E. and Hunziker, J. C. (Eds), *Lectures in Isotope Geology*. Springer, Berlin Heidelberg. 154–169.

Naish, T., Kamp, P. J., Alloway, B. V., Pillans, B., Wilson, G. S., & Westgate, J. A. (1996). Integrated tephrochronology and magnetostratigraphy for cyclothemic marine strata, Wanganui Basin: implications for the Pliocene-Pleistocene boundary in New Zealand. *Quaternary International*, *34*, 29-48.

Naish, T., & Kamp, P. J. (1997). Sequence stratigraphy of sixth-order (41 ky) Pliocene–Pleistocene cyclothems, Wanganui basin, New Zealand: a case for the regressive systems tract. *Geological Society of America Bulletin*, *109*(8), 978-999.

Naish, T. R., & Wilson, G. S. (2009). Constraints on the amplitude of Mid-Pliocene (3.6–2.4 Ma) eustatic sea-level fluctuations from the New Zealand shallow-marine sediment record. *Philosophical Transactions of the Royal Society of London A: Mathematical, Physical and Engineering Sciences*, *367*(1886), 169-187.

Nalin, R., Nelson, C. S., Basso, D., & Massari, F. (2008). Rhodolith-bearing limestones as transgressive marker beds: fossil and modern examples from North Island, New Zealand. *Sedimentology*, *55*(2), 249-274.

Naqvi, S. W. A., Yoshinari, T., Jayakumar, D. A., Altabet, M. A., Narvekar, P. V., Devol, A. H., ... & Codispoti, L. A. (1998). Budgetary and biogeochemical implications of N2O isotope signatures in the Arabian Sea. *Nature*, *394*(6692), 462-464.

Naqvi, S. W. A., Yoshinari, T., Brandes, J. A., Devol, A. H., Jayakumar, D. A., Narvekar, P. V., Altabet, M. A., & Codispoti, L. A. (1998). Nitrogen isotopic studies in the suboxic Arabian Sea. *Proceedings of the Indian Academy of Science* 107, 367–378.

Neef, G. (1984). *Late Cenozoic and early Quaternary stratigraphy of the Eketahuna District* (No. 153). New Zealand Geological Survey.

Neef, G. (1992). Turbidite deposition in five Miocene, bathyal formations along an active plate margin, North Island, New Zealand: with notes on styles of deposition at the margins of east coast bathyal basins. *Sedimentary Geology*, *78*(1-2), 111-136.

Neef, G. (1995). Cretaceous and Cenozoic geology east of the Tinui Fault Complex in northeastern Wairarapa, New Zealand. *New Zealand Journal of Geology and Geophysics*, *38*(3), 375-394.

Nicol, A. (2011). Landscape history of the Marlborough Sounds, New Zealand. *New Zealand Journal of Geology and Geophysics*, *54*(2), 195-208.

Nicol, A., & Campbell, J. K. (1990). Late Cenozoic thrust tectonics, Picton, New Zealand. *New Zealand Journal of Geology and Geophysics*, *33*(3), 485-494.

Nicol, A., & Van Dissen, R. (2002). Up-dip partitioning of displacement components on the oblique-slip Clarence Fault, New Zealand. *Journal of Structural Geology*, *24*(9), 1521-1535.

Nicol, A., VanDissen, R., Vella, P., Alloway, B., & Melhuish, A. (2002). Growth of contractional structures during the last 10 my at the southern end of the emergent Hikurangi forearc basin, New Zealand. *New Zealand Journal of Geology and Geophysics*, *45*(3), 365-385.

Nicol, A., & Beavan, J. (2003). Shortening of an overriding plate and its implications for slip on a subduction thrust, central Hikurangi Margin, New Zealand. *Tectonics*, *22*(6).

Nicol, A., & Uruski, C. (2005). Structural Interpretation and Cross Section Balancing, East Coast Basin, New Zealand. *Open-File Petroleum Report*, *3184*, 14.

Nicol, A., Walsh, J., Berryman, K., & Nodder, S. (2005). Growth of a normal fault by the accumulation of slip over millions of years. *Journal of Structural Geology*, *27*(2), 327-342.

Nicol, A., & Wallace, L. M. (2007). Temporal stability of deformation rates: Comparison of geological and geodetic observations, Hikurangi subduction margin, New Zealand. *Earth and Planetary Science Letters*, *258*(3), 397-413.

Nicol, A., Mazengarb, C., Chanier, F., Rait, G., Uruski, C., & Wallace, L. (2007). Tectonic evolution of the active Hikurangi subduction margin, New Zealand, since the Oligocene. *Tectonics*, *26*(4).

Nicolo, M. J., Dickens, G. R., & Hollis, C. J. (2010). South Pacific intermediate water oxygen depletion at the onset of the Paleocene-Eocene thermal maximum as depicted in New Zealand margin sections. *Paleoceanography*, *25*(4).

Ohneiser, C., Wilson, G. S., Field, B. D., & Crundwell, M. P. (2008). A new high-resolution, middle Miocene magnetostratigraphy from western Southland, New Zealand. *New Zealand Journal of Geology and Geophysics*, *51*(3), 261-274.

Oksanen, J., Blanchet, F. G., Kindt, R., Legendre, P., Minchin, P. R., O'hara, R. B., ... & Oksanen, M. J. (2013). Package 'vegan'. *Community Ecology Package, Version*, *2*(9).

Oliver, P. J., Grindley, G. W., Mumme, T. C., & Vella, P. (1979). Paleomagnetism of the Upper Cretaceous Mount Somers Volcanics, Canterbury, New Zealand. *New Zealand Journal of Geology and Geophysics*, *22*(2), 199-212.

Olsson, R. K., Miller, K. G., Browning, J. V., Wright, J. D., & Cramer, B. S. (2002). Sequence stratigraphy and sea-level change across the Cretaceous-Tertiary boundary on the New Jersey passive margin. *Geological Society of America Special Papers*, *356*, 97-108.

Ongley, M. (1941). Type Sections. *New Zealand Geological Survey 35th Annual Report.* Pp. 8-9.

Ongley, M. & Willianson, J. H. (1931). Eketahuna Subdivision. *New Zealand Geological Survey 25th Annual Report.* Pp. 3-5.

Ozolins, V. & Francis, D. (2000). Whakatu-1 well completion report PEP38328. NZP&M, Ministry of Business, Innovation & Employment (MBIE), New Zealand. Unpublished Petroleum Report PR2476. 498 p.

Parrish, J. T., Daniel, I. L., Kennedy, E. M., & Spicer, R. A. (1998). Paleoclimatic significance of mid-Cretaceous floras from the middle Clarence Valley, New Zealand. *Palaios*, *13*(2), 149-159.

Pearson, M. J., Grosjean, E., Nelson, C. S., Nyman, S. L., & Logan, G. A. (2010). Tubular concretions in New Zealand petroliferous basins: Lipid biomarker evidence for mineralisation around proposed miocene hydrocarbon seep conduits. *Journal of Petroleum Geology*, *33*(3), 205-219.

Pedersen, T. F., & Calvert, S. E. (1990). Anoxia vs. productivity: what controls the formation of organic-carbon-rich sediments and sedimentary Rocks?. *AAPG Bulletin*, *74*(4), 454-466.

Pettinga, J.R. (1982). Upper Cenozoic structural history, coastal Southern Hawke's Bay, New Zealand. *New Zealand Journal of Geology and Geophysics 25*: 149–191.

Phillips, C. J. (1985). Upper Cretaceous and Tertiary geology of the upper Waitahaia River, Raukumara Peninsula, New Zealand. *New Zealand Journal of Geology and Geophysics*, *28*(4), 595-607.

Piercey, S. J., & Devine, M. C. (2014). Analysis of powdered reference materials and known samples with a benchtop, field portable X-ray fluorescence (pXRF) spectrometer: evaluation of performance and potential applications for exploration lithogeochemistry. *Geochemistry: Exploration, Environment, Analysis*, *14*(2), 139-148.

Piper, D. Z. (1994). Seawater as the source of minor elements in black shales, phosphorites and other sedimentary rocks. *Chemical Geology*, *114*(1), 95-114.

Piper, D. Z., & Perkins, R. B. (2004). A modern vs. Permian black shale—the hydrography, primary productivity, and water-column chemistry of deposition. *Chemical Geology*, *206*(3), 177-197.

Pole, M. (2008). The record of Araucariaceae macrofossils in New Zealand. *Alcheringa 32*, 405–426.

Pondard, N., & Barnes, P. M. (2010). Structure and paleoearthquake records of active submarine faults, Cook Strait, New Zealand: Implications for fault interactions, stress loading, and seismic hazard. *Journal of Geophysical Research: Solid Earth (1978–2012)*, *115*(B12).

Qin, X., Müller, R. D., Cannon, J., Landgrebe, T. C. W., Heine, C., Watson, R. J., & Turner, M. (2012). The GPlates geological information model and markup language. *Geoscience Instrumentation, Methods & Data Systems Discussions 2*, 365-428.

R Core Team (2017). R: A language and environment for statistical computing. R Foundation for Statistical Computing, Vienna, Austria. URL https://www.R-project.org/.

Raine, J. I. (1990). Late Cretaceous plant macrofossils from Mangahouanga stream. In: *Geological Society of New Zealand Annual Conference Napier 1990: programme and abstracts*, H.J. Campbell, B.W. Hayward & D.C. Mildenhall, eds, Geological Society of New Zealand Miscellaneous Publication 50b, 189–202.

Raine, J.I., Beu, A.G., Boyes, A.F., Campbell, H.J., Cooper, R.A., Crampton, J.S., Crundwell, M.P., Hollis, C.J., Morgans, H.E.G. & Mortimer, N., (2015). New Zealand geological timescale NZGT 2015/1. *New Zealand Journal of Geology and Geophysics*, *58*(4), 398-403.

Raiswell, R., Buckley, F., Berner, R. A., & Anderson, T. F. (1988). Degree of pyritization of iron as a paleoenvironmental indicator of bottom-water oxygenation. *Journal of Sedimentary Research*, *58*(5), 812-819.

Rait, G. J., Chanier, F., & Waters, D. W. (1991). Landward-and seaward-directed thrusting accompanying the onset of subduction beneath New Zealand. *Geology*, *19*(3), 230-233.

Rait, G. J. (2000). Thrust transport directions in the Northland allochthon, New Zealand. *New Zealand Journal of Geology and Geophysics*, *43*(2), 271-288.

Randall, K., Lamb, S., & Mac Niocaill, C. (2011). Large tectonic rotations in a wide zone of Neogene distributed dextral shear, northeastern South Island, New Zealand. *Tectonophysics*, *509*(3), 165-180.

Rattenbury, M. (2006). Kaikoura Sheet, 1: 250,000 QMAP series. *Geological and Nuclear Sciences, New Zealand.*

Rattenbury, M. S., & Isaac, M. J. (2012). The QMAP 1: 250 000 geological map of New Zealand project. *New Zealand Journal of Geology and Geophysics*, *55*(4), 393-405.

Reay, M. B. (1980). *Cretaceous and Tertiary stratigraphy of part of the middle Clarence Valley, Marlborough*. Doctoral dissertation, University of Canterbury.

Reay, M. B. (1987). The lower part of Branch stream, Marlborough and implications for the Early Cretaceous geology of the Clarence Valley. *New Zealand Geological Survey Record*, 20, 35-42.

Reay, M. B. (1993). Geology of the middle part of the Clarence Valley. Scale 1: 50 000. *Institute of Geological & Nuclear Sciences Geological Map*, *10*.

Reay, M. B., & Strong, C. P. (1992). The Branch Sandstone, Clarence valley, and implications for latest Cretaceous paleoenvironments and geological history of central Marlborough. *New Zealand Geological Survey Record*, *44*, 43-49.

Reyners, M. (2013). The central role of the Hikurangi Plateau in the Cenozoic tectonics of New Zealand and the Southwest Pacific. *Earth and Planetary Science Letters*, *361*, 460-468.

Reyners, M., Eberhart-Phillips, D., & Bannister, S. (2011). Tracking repeated subduction of the Hikurangi Plateau beneath New Zealand. *Earth and Planetary Science Letters*, *311*(1-2), 165-171.

Reyners, M., Eberhart-Phillips, D., Upton, P., & Gubbins, D. (2017). Three-dimensional imaging of impact of a large igneous province with a subduction zone. *Earth and Planetary Science Letters*, *460*, 143-151.

Ridd, M. F. (1967). Miocene transcurrent movement on the Pongaroa fault, Wairarapa, New Zealand. *New Zealand Journal of Geology and Geophysics*, *10*(1), 209-216.

Rimmer, S. M. (2004). Geochemical paleoredox indicators in Devonian–Mississippian black shales, central Appalachian Basin (USA). *Chemical Geology*, *206*(3), 373-391.

Ritchie, D. D. (1986). Stratigraphy, structure and geological history of mid-Cretaceous sedimentary rocks across the Torlesse-like/non Torlesse boundary in the Sawtooth Range-Coverham area, Marlborough.

Rogers, K. M., Collen, J. D., Johnston, J. H., & Elgar, N. E. (1999). A geochemical appraisal of oil seeps from the East Coast Basin, New Zealand. *Organic Geochemistry*, *30*(7), 593-605.

Rogers, K. M., Morgans, H. E., & Wilson, G. S. (2001). Identification of a Waipawa Formation equivalent in the upper Te Uri Member of the Whangai Formation-implications for depositional history and age. *New Zealand Journal of Geology and Geophysics*, *44*(2), 347-354.

Röhl, H.-J., & Schmid-Röhl, A. (2005). Lower Torarcian (Upper Liassic) black shales of the central European epicontinental basin: a sequence stratigraphic case study from the SW German Posidonia Shale. In: Harris N.B (Ed.). *The deposition of organic-carbon-rich sediments: Models, mechanisms, and consequences.* SEPM Special publication No. 82. ISBN 1-56576-110-3 p. 165-189.

Rohlf, F. J. (1985). *NT-SYS—Numerical Taxonomy System of Multivariate Statistical Programs*. Department of Ecology and Evolution, State University of New York.

Roncaglia, L., & Schiøler, P. (1997). *Dinoflagellate biostratigraphy of Piripauan-Haumurian sections in southern Marlborough and northern Canterbury, New Zealand* (Vol. 97). Institute of Geological & Nuclear Sciences Limited.

Roncaglia, L., Field, B. D., Raine, J. I., Schiøler, P., & Wilson, G. J. (1999). Dinoflagellate biostratigraphy of Piripauan-Haumurian (Upper Cretaceous) sections from northeast South Island, New Zealand. *Cretaceous Research*, *20*(3), 271-314.

Roser, B. P., & Korsch, R. J. (1986). Determination of tectonic setting of sandstone-mudstone suites using content and ratio. *The Journal of Geology*, *94*(5), 635-650.

Roser, B. P., & Korsch, R. J. (1988). Provenance signatures of sandstone-mudstone suites determined using discriminant function analysis of major-element data. *Chemical Geology*, *67*(1-2), 119-139.

Roser, B. P., & Korsch, R. J. (1999). Geochemical characterization, evolution and source of a Mesozoic accretionary wedge: the Torlesse terrane, New Zealand. *Geological Magazine*, *136*(5), 493-512.

Ross, P. S., Bourke, A., & Fresia, B. (2014). Improving lithological discrimination in exploration drill-cores using portable X-ray fluorescence measurements: (1) testing three Olympus Innov-X analysers on unprepared cores. *Geochemistry: Exploration, Environment, Analysis*, 2012-163.

Rowan, C. J., Roberts, A. P., & Rait, G. J. (2005). Relocation of the tectonic boundary between the Raukumara and Wairoa Domains (East Coast, North Island, New Zealand): implications for the rotation history of the Hikurangi margin. *New Zealand Journal of Geology and Geophysics*, *48*(1), 185-196.

Rowan, C. J., & Roberts, A. P. (2006). Magnetite dissolution, diachronous greigite formation, and secondary magnetizations from pyrite oxidation: Unravelling complex magnetizations in

Neogene marine sediments from New Zealand. *Earth and Planetary Science Letters*, *241*(1), 119-137.

Rowan, C. J., & Roberts, A. P. (2008). Widespread remagnetizations and a new view of Neogene tectonic rotations within the Australia-Pacific plate boundary zone, New Zealand. *Journal of Geophysical Research: Solid Earth*, *113*(B3).

Rowe, H. D., Loucks, R. G., Ruppel, S. C., & Rimmer, S. M. (2008). Mississippian Barnett Formation, Fort Worth Basin, Texas: Bulk geochemical inferences and Mo–TOC constraints on the severity of hydrographic restriction. *Chemical Geology*, *257*(1), 16–25.

Rowe, H., Hughes, N., & Robinson, K. (2012). The quantification and application of handheld energy-dispersive x-ray fluorescence (ED-XRF) in mudrock chemostratigraphy and geochemistry. *Chemical Geology*, *324*, 122-131.

Sageman, B. B., Lyons, T. W., Ji Joo, Y. (2003a). Geochemistry of fine-grained sediments and sedimentary rocks. *In: Treatise on Geochemistry*. Second edition. pp. 115 – 158. Elsevier Ltd.

Sageman, B. B., Murphy, A. E., Werne, J. P., Ver Straeten, C. A., Hollander, D. J., & Lyons, T. W. (2003b). A tale of shales: the relative roles of production, decomposition, and dilution in the accumulation of organic-rich strata, Middle–Upper Devonian, Appalachian basin. *Chemical Geology*, *195*(1), 229-273.

Sahoo, T.S. & Bland, K.J., et al. (Compilers), 2017. Atlas of Petroleum Prospectivity, Southeast Province: ArcGIS geodatabase and technical report. *GNS Science Data Series 23c*. 50 p. + 1 ArcGIS geodatabase + 5 ArcGIS projects.

Saul, G., Naish, T. R., Abbott, S. T., & Carter, R. M. (1999). Sedimentary cyclicity in the marine Pliocene-Pleistocene of the Wanganui basin (New Zealand): Sequence stratigraphic motifs characteristic of the past 2.5 my. *Geological Society of America Bulletin*, *111*(4), 524-537.

Savrda, C. E. (1991). Ichnology in sequence stratigraphic studies: An example from the Lower Paleocene of Alabama. *Palaios*, 39-53.

Savrda, C. E., Browning, J. V., Krawinkel, H., & Hesselbo, S. P. (2001). Firmground ichnofabrics in deep-water sequence stratigraphy, Tertiary clinoform-toe deposits, New Jersey slope. *Palaios*, *16*(3), 294-305.

Scarlett, R. J. & Molnar, R. E. (1984). Terrestrial bird or dinosaur phalanx from the New Zealand Cretaceous. *New Zealand Journal of Zoology 11*, 271–275.

Schellart, W. P., Lister, G. S., & Toy, V. G. (2006). A Late Cretaceous and Cenozoic reconstruction of the Southwest Pacific region: tectonics controlled by subduction and slab rollback processes. *Earth-Science Reviews*, *76*(3), 191-233.

Schellart, W. P. (2007). North-eastward subduction followed by slab detachment to explain ophiolite obduction and Early Miocene volcanism in Northland, New Zealand. *Terra Nova*, *19*(3), 211-218.

Schiøler, P., & Wilson, G. J. (1998). Dinoflagellate Biostratigraphy of the Middle Coniacian: Lower Campanian (Upper Cretaceous) in South Marlborough, New Zealand. *Micropaleontology*, 313-349.

Schiøler, P., Crampton, J. S., & King, P. R. (2000). *Palynostratigraphic analysis of a measured section through the Karekare, Owhena and Whangai formations (Upper Cretaceous) at Waitahaia River:" Owhena Stream"(Raukumara Peninsula)*. Institute of Geological & Nuclear Sciences.

Schiøler, P., Crampton, J. S., & King, P. R. (2001). Palynostratigraphic analysis of a measured section through the Karekare, Tahora and Whangai formations (Upper Cretaceous) at Koranga Stream (Raukumara Peninsula). *Institute of Geological & Nuclear Sciences Science Report 2001/27*. 15 p.

Schiøler, P., Crampton, J. S., & Laird, M. G. (2002). Palynofacies and sea-level changes in the middle Coniacian–late Campanian (Late Cretaceous) of the East Coast Basin, New Zealand. *Palaeogeography, Palaeoclimatology, Palaeoecology*, *188*(3), 101-125.

Schiøler, P., Rogers, K., Sykes, R., Hollis, C. J., Ilg, B., Meadows, D., ... & Uruski, C. (2010). Palynofacies, organic geochemistry and depositional environment of the Tartan Formation (Late Paleocene), a potential source rock in the Great South Basin, New Zealand. *Marine and Petroleum Geology*, *27*(2), 351-369.

Schiøler, P., & Crampton, J. S. (2014). Dinoflagellate biostratigraphy of the Arowhanan Stage (upper Cenomanian–lower Turonian) in the East Coast Basin, New Zealand. *Cretaceous Research*, *48*, 205-224.

Schröder, S., & Grotzinger, J. P. (2007). Evidence for anoxia at the Ediacaran–Cambrian boundary: the record of redox-sensitive trace elements and rare earth elements in Oman. *Journal of the Geological Society*, *164*(1), 175-187.

Schoepfer, S. D., Tobin, T. S., Witts, J. D., & Newton, R. J. (2017). Intermittent euxinia in the high-latitude James Ross Basin during the latest Cretaceous and earliest Paleocene. *Palaeogeography, Palaeoclimatology, Palaeoecology*, *477*, 40-54.

Schmitz, B., Pujalte, V., Molina, E., Monechi, S., Orue-Etxebarria, X., Speijer, R.P., Alegret, L., *et al.*, (2011). The global stratotype sections and points for the bases of the Selandian (Middle Paleocene) and Thanetian (Upper Paleocene) stages at Zumaia, Spain. *Episodes*, *34*(4), 220-243.

Schulte, P., Schwark, L., Stassen, P., Kouwenhoven, T. J., Bornemann, A., & Speijer, R. P. (2013). Black shale formation during the Latest Danian Event and the Paleocene–Eocene Thermal Maximum in central Egypt: Two of a kind? *Palaeogeography, Palaeoclimatology, Palaeoecology*, *371*, 9-25.

Seebeck, H., Nicol, A., Giba, M., Pettinga, J., & Walsh, J. (2014). Geometry of the subducting Pacific plate since 20 Ma, Hikurangi margin, New Zealand. *Journal of the Geological Society*, *171*(1), 131-143.

Seton, M., Müller, R. D., Zahirovic, S., Gaina, C., Torsvik, T., Shephard, G., ... & Chandler, M. (2012). Global continental and ocean basin reconstructions since 200 Ma. *Earth-Science Reviews*, *113*(3-4), 212-270.

Shanmugam, G. (1985). Significance of coniferous rain forest and related organic matter in generating commercial quantities of oils, Gippsland Basin, Australia. *Bulletin of American Association of Petroleum Geologists*, 69 (1985), pp. 1241-1254.

Sherwood, G. J. (1988). Paleomagnetism and magnetostratigraphy of Miocene volcanics in eastern Otago and Banks Peninsula, New Zealand. *New Zealand Journal of Geology and Geophysics*, *31*(2), 207-224.

Silberling, N. J., Nichols, K. M., Bradshaw, J. D., & Blome, C. D. (1988). Limestone and chert in tectonic blocks from the Esk Head subterrane, South Island, New Zealand. *Geological Society of America Bulletin*, *100*(8), 1213-1223.

Sim, M. S., Bosak, T., & Ono, S. (2011). Large sulfur isotope fractionation does not require disproportionation. *Science*, *333*(6038), 74-77.

Simandjuntak, T. O., & Barber, A. J. (1996). Contrasting tectonic styles in the Neogene orogenic belts of Indonesia. *Geological Society, London, Special Publications*, *106*(1), 185-201.

Simandl, G. J., Paradis, S., Stone, R. S., Fajber, R., Kressall, R. D., Grattan, K., ... & Simandl, L. J. (2014). Applicability of handheld X-Ray fluorescence spectrometry in the exploration and development of carbonatite-related niobium deposits: a case study of the Aley Carbonatite, British Columbia, Canada. *Geochemistry: Exploration, Environment, Analysis*, *14*(3), 211-221.

Slotnick, B. S., Dickens, G. R., Nicolo, M. J., Hollis, C. J., Crampton, J. S., Zachos, J. C., & Sluijs, A. (2012). Large-amplitude variations in carbon cycling and terrestrial weathering during the latest Paleocene and earliest Eocene: The record at Mead Stream, New Zealand. *The journal of geology*, *120*(5), 487-505.

Slotnick, B. S., Dickens, G. R., Hollis, C. J., Crampton, J. S., Percy Strong, C., & Phillips, A. (2015). The onset of the early Eocene climatic optimum at branch stream, Clarence River valley, New Zealand. *New Zealand Journal of Geology and Geophysics*, *58*(3), 262-280.

Smale, D. (1978). The composition of a Torlesse conglomerate—Ethelton, North Canterbury. *New Zealand Journal of Geology and Geophysics*, *21*(6), 699-711.

Smale, D. (1983). *Heavy Minerals from Cretaceous and Tertiary Sandstones, Waipara and Oxford, North Canterbury*. New Zealand Geological Survey.

Smale, D. (1987a). *Heavy minerals in Cretaceous-Cenozoic sandstones in Canterbury*. New Zealand Geological Survey, Department of Scientific and Industrial Research.

Smale, D., & Morton, A. C. (1987b). Heavy mineral suites of core samples from the McKee Formation (Eocene—lower Oligocene), Taranaki: implications for provenance and diagenesis. *New Zealand Journal of Geology and Geophysics*, *30*(3), 299-306.

Smale, D. (1988a). Detrital pumpellyite and epidote group minerals in Cretaceous and Tertiary sandstones in the South Island, New Zealand. *Journal of Sedimentary Research*, *58*(6).

Smale, D. (1988b). Heavy minerals in Cretaceous and Tertiary sandstones from Northland. *New Zealand Geological Survey report SL18*. 41 p.

Smale, D. (1989). Leaching of heavy minerals above and below the Mid-Cretaceous unconformity in the Ohuriawa Gorge area of the Waipara River, North Canterbury, New Zealand. *Journal of Sedimentary Research*, *59*(6).

Smale, D. (1990). Distribution and provenance of heavy minerals in the South Island: a review. *New Zealand Journal of Geology and Geophysics*, *33*(4), 557-571.

Smale, D. (1997). Heavy minerals in the Torlesse Terrane of the Wellington area, New Zealand. *New Zealand Journal of Geology and Geophysics*, *40*(4), 499-506.

Smale, D. (2007). Sediment trails in tectonically active islands: heavy minerals in use in New Zealand. *Developments in Sedimentology*, *58*, 569-585.

Smale, D., & Laird, M. G. (1995). Relation of heavy mineral populations to stratigraphy of Cretaceous formations in Marlborough, New Zealand. *New Zealand Journal of Geology and Geophysics*, *38*(2), 211-222.

Smiley, R. (2014). Ngapaeruru-1 Well Completion Report. NZP&M, Ministry of Business, Innovation & Employment (MBIE), New Zealand. Unpublished Petroleum Report PR4943.

Sorrentino, L., Cas, R. A., & Stilwell, J. D. (2011). Evolution and facies architecture of Paleogene Surtseyan volcanoes on Chatham Islands, New Zealand, Southwest Pacific Ocean. *Journal of Volcanology and Geothermal Research*, *202*(1), 1-21.

Sorrentino, L., Stilwell, J. D., & Mays, C. (2014). A model of tephra dispersal from an early Palaeogene shallow submarine Surtseyan-style eruption (s), the Red Bluff Tuff Formation, Chatham Island, New Zealand. *Sedimentary Geology*, *300*, 86-102.

Speden, I. G. (1973). Distribution, stratigraphy and stratigraphic relationships of Cretaceous sediments, western Raukumara Peninsula, New Zealand. *New Zealand Journal of Geology and Geophysics*, *16*(2), 243-268.

Speden, I. G. (1975). Cretaceous stratigraphy of Raukumara Peninsula. Part 1: Cretaceous stratigraphy of Koranga (parts N87 and N88); part 2: Geology of the Lower Waimana and Waiotahi Valleys (part N78). *New Zealand Geological Survey Bulletin 91*. 70 p.

Spörli, K. B. (1989). Tectonic framework of Northland, New Zealand. *R. Soc. NZ Bull*, *26*, 3-14. *In:* Spörli, B., & Kear, D. (1989). Geology of Northland: Accretion, allochthons and arcs at the edge of the New Zealand micro-continent. *Royal Society of New Zealand.* 26.

Spörli, K. B., & Aita, Y. (1994). Tectonic significance of Late Cretaceous Radiolaria from the obducted Matakaoa Volcanics, East Cape, North Island, New Zealand (Memorial volume to the late Professor Teruhiko Sameshima). *Geoscience reports of Shizuoka University*, *20*, 115-133.

Stagpoole, V., & Nicol, A. (2008). Regional structure and kinematic history of a large subduction back thrust: Taranaki Fault, New Zealand. *Journal of Geophysical Research: Solid Earth*, *113*(B1).

Stern, T. A. (1985). A back-arc basin formed within continental lithosphere: the Central Volcanic Region of New Zealand. *Tectonophysics*, *112*(1-4), 385-409.

Stern, T. A. (1987). Asymmetric back-arc spreading, heat flux and structure associated with the Central Volcanic Region of New Zealand. *Earth and Planetary Science Letters 85*, 265-276.

Stern, T. A., Stratford, W. R., & Salmon, M. L. (2006). Subduction evolution and mantle dynamics at a continental margin: Central North Island, New Zealand. *Reviews of Geophysics*, *44*(4).

Stilwell, J. D., Consoli, C. P., Sutherland, R., Salisbury, S., Rich, T. H., Vickers-Rich, P. A., ... & Wilson, G. J. (2006). Dinosaur sanctuary on the Chatham Islands, Southwest Pacific: first record of theropods from the K–T boundary Takatika Grit. *Palaeogeography, Palaeoclimatology, Palaeoecology*, *230*(3), 243-250.

Stilwell, J. D., & Consoli, C. P. (2012). Tectono-stratigraphic history of the Chatham Islands, SW Pacific—The emergence, flooding and reappearance of eastern 'Zealandia'. *Proceedings of the Geologists' Association*, *123*(1), 170-181.

Stilwell, J. D., Vitacca, J. J., & Mays, C. (2016). South polar greenhouse insects (Arthropoda: Insecta: Coleoptera) from the mid-Cretaceous Tupuangi Formation, Chatham Islands, eastern Zealandia. *Alcheringa: An Australasian Journal of Palaeontology*, *40*(4), 502-508.

Stoneley, R. (1968). A lower Tertiary decollement on the east coast, North Island, New Zealand. *New Zealand Journal of Geology and Geophysics*, *11*(1), 128-156.

Strogen, D. P., Seebeck, H., Nicol, A., & King, P. R. (2017). Two-phase Cretaceous–Paleocene rifting in the Taranaki Basin region, New Zealand; implications for Gondwana break-up. *Journal of the Geological Society*, jgs2016-160.

Strong, C. P. (1977). Cretaceous-tertiary boundary at woodside creek, north-eastern Marlborough. *New Zealand Journal of Geology and Geophysics*, *20*(4), 687-696.

Strong, C. P. (2000). Cretaceous-Tertiary foraminiferal succession at Flaxbourne River, Marlborough, New Zealand. *New Zealand Journal of Geology and Geophysics*, *43*(1), 1-20.

Strong, C. P., Hollis, C. J., & Wilson, G. J. (1995). Foraminiferal, radiolarian, and dinoflagellate biostratigraphy of Late Cretaceous to middle Eocene pelagic sediments (Muzzle group), Mead Stream, Marlborough, New Zealand. *New Zealand Journal of Geology and Geophysics*, *38*(2), 171-209.

Suggate, R.P. (1963). The Alpine Fault. *Royal Society of New Zealand Transactions (2),* 105-129.

Sutherland, R. (1995). The Australia-Pacific boundary and Cenozoic plate motions in the SW Pacific: Some constraints from Geosat data. *Tectonics*, *14*(4), 819-831.

Sutherland, R. (1999a). Cenozoic bending of New Zealand basement terranes and Alpine Fault displacement: a brief review. *New Zealand Journal of Geology and Geophysics*, *42*(2), 295-301.

Sutherland, R. (1999b). Basement geology and tectonic development of the greater New Zealand region: an interpretation from regional magnetic data. *Tectonophysics*, *308*(3), 341-362.

Sutherland, R., Davey, F., & Beavan, J. (2000). Plate boundary deformation in South Island, New Zealand, is related to inherited lithospheric structure. *Earth and Planetary Science Letters*, *177*(3), 141-151.

Sutherland, R., King, P., & Wood, R. (2001). Tectonic evolution of Cretaceous rift basins in south-eastern Australia and New Zealand: implications for exploration risk assessment. *Eastern Australian Basins Symposium.* 3-13.

Sutherland, R., Stagpoole, V., Uruski, C., Kennedy, C., Bassett, D., Henrys, S., ... & Barker, D. (2009). Reactivation of tectonics, crustal underplating, and uplift after 60 Myr of passive subsidence, Raukumara Basin, Hikurangi-Kermadec fore arc, New Zealand: Implications for global growth and recycling of continents. *Tectonics*, *28*(5).

Sutherland, R., Collot, J., Lafoy, Y., Logan, G. A., Hackney, R., Stagpoole, V., ... & Wood, R. (2010). Lithosphere delamination with foundering of lower crust and mantle caused permanent subsidence of New Caledonia Trough and transient uplift of Lord Howe Rise during Eocene and Oligocene initiation of Tonga-Kermadec subduction, western Pacific. *Tectonics*, *29*(2).

Sutherland, R., Collot, J., Bache, F., Henrys, S., Barker, D., Browne, G. H., ... & Mortimer, N. (2017). Widespread compression associated with Eocene Tonga-Kermadec subduction initiation. *Geology*, *45*(4), 355-358.

Sykes, R., Zink, K. G., Rogers, K. M., Phillips, A., & Ventura, G. T. (2012). New and updated geochemical databases for New Zealand petroleum samples, with assessments of genetic oil families, source age, facies and maturity. *GNS Science Consultancy Report 2012*, *37*, 29.

Tagami, T., Carter, A. & Hurford, A. J. (1996). Natural long-term annealing of the zircon fission-track system in Vienna Basin deep borehole samples: constraints upon the partial annealing zone closure temperature. *Chemical Geology,* 130: 147–157.

Tanaka, H. G. M. T., Turner, G. M., Houghton, B. F., Tachibana, T., Kono, M., & McWilliams, M. O. (1996). Palaeomagnetism and chronology of the central Taupo volcanic zone, New Zealand. *Geophysical Journal International*, *124*(3), 919-934.

Tayler, M. J. S. (2011). *Investigating stratigraphic evidence for Antarctic glaciation in the greenhouse world of the Paleocene, eastern North Island, New Zealand* (Doctoral dissertation, University of Waikato).

Taylor, P. D., & Gordon, D. P. (2007). Bryozoans from the Late Cretaceous Kahuitara Tuff of the Chatham Islands, New Zealand. *Alcheringa*, *31*(4), 339-363.

Thomson, J. (1913). Results of field work. *New Zealand Geological Survey 7th annual report*. 122-123.

Thomson, J. A. (1920). The Notocene geology of the Middle Waipara and Weka Pass district, North Canterbury, New Zealand. *Transactions of the New Zealand Institute 52*: 322-415.

Tjalsma, R. T., & Lohmann, G. P. (1983). Paleocene-Eocene bathyal and abyssal benthic foraminifera from the Atlantic Ocean. *Micropaleontology*, *4*, 94.

Townsend, D. B., & Little, T. A. (1998). Pliocene-Quaternary deformation and mechanisms of near-surface strain close to the eastern tip of the Clarence Fault, northeast Marlborough, New Zealand. *New Zealand Journal of Geology and Geophysics*, *41*(4), 401-417.

Trewick, S. A., & Bland, K. J. (2012). Fire and slice: palaeogeography for biogeography at New Zealand's North Island/South Island juncture. *Journal of the Royal Society of New Zealand*, *42*(3), 153-183.

Tribovillard, N., Ramdani, A. & Trentesaux, A. (2005). Controls on organic accumulation in Upper Jurassic shales of northwestern Europe as inferred from trace-metal geochemistry. In: Harris N.B (Ed.). *The deposition of organic-carbon-rich sediments: Models, mechanisms, and consequences*. SEPM Special publication No. 82. ISBN 1-56576-110-3 p. 145-163.

Tribovillard, N., Algeo, T. J., Lyons, T., & Riboulleau, A. (2006). Trace metals as paleoredox and paleoproductivity proxies: an update. *Chemical Geology*,*232*(1), 12-32.

Tribovillard, N., Algeo, T. J., Baudin, F., & Riboulleau, A. (2012). Analysis of marine environmental conditions based on molybdenum–uranium covariation—Applications to Mesozoic paleoceanography. *Chemical Geology*, *324*, 46-58.

Tulloch, A. J., & Kimbrough, D. L. (1989). The paparoa metamorphic core complex, New Zealand: cretaceous extension associated with fragmeotation of the Pacific margin of Gondwana. *Tectonics*, *8*(6), 1217-1234.

Tulloch, A. J., Ramezani, J., Mortimer, N., Mortensen, J., van den Bogaard, P., & Maas, R. (2009). Cretaceous felsic volcanism in New Zealand and Lord Howe Rise (Zealandia) as a precursor to final Gondwana break-up. *Geological Society, London, Special Publications*, *321*(1), 89-118.

Tulloch, A. J. & Mortimer, N. (2017). A new basement map of Taranaki Basin. *Second Petroleum Basin Workshop, 28-29th September 2017*, GNS Science, Lower Hutt.

Turchyn, A. V., & Schrag, D. P. (2006). Cenozoic evolution of the sulfur cycle: insight from oxygen isotopes in marine sulfate. *Earth and Planetary Science Letters*, *241*(3), 763-779.

Turgeon, S., & Brumsack, H. J. (2006). Anoxic vs dysoxic events reflected in sediment geochemistry during the Cenomanian–Turonian Boundary Event (Cretaceous) in the Umbria–Marche Basin of central Italy. *Chemical Geology*, *234*(3), 321-339.

Turnbull, R., Weaver, S., Tulloch, A., Cole, J., Handler, M., & Ireland, T. (2010). Field and geochemical constraints on mafic–felsic interactions, and processes in high-level arc magma chambers: an example from the Halfmoon Pluton, New Zealand. *Journal of Petrology*, *51*(7), 1477-1505.

Turner, G. M., Roberts, A. P., Laj, C., Kissel, C., Mazaud, A., Guitton, S., & Christoffel, D. A. (1989). New paleomagnetic results from Blind River: Revised magnetostratigraphy and tectonic rotation of the Marlborough region, South Island, New Zealand. *New Zealand Journal of Geology and Geophysics*, *32*(2), 191-196.

Turner, G. M., Michalk, D. M., & Little, T. A. (2012). Paleomagnetic constraints on Cenozoic deformation along the northwest margin of the Pacific-Australian plate boundary zone through New Zealand. *Tectonics*, *31*(1).

Tyson, R.V., Pearson, T.H., (1991). Modern and ancient continental shelf anoxia: an overview. In: Tyson, R.V., Pearson, T.H. (Eds.), *Modern and Ancient Continental Shelf Anoxia.* Geological Society Special Publication No. 58, London, pp. 1–24.

Tyson, R. V. (2001). Sedimentation rate, dilution, preservation and total organic carbon: some results of a modelling study. *Organic Geochemistry*, *32*(2), 333-339.

Tyson, R. V. (2005). The "productivity versus preservation" controversy: cause, flaws and resolution. In: Harris N.B (Ed.). *The deposition of organic-carbon-rich sediments: Models, mechanisms, and consequences*. SEPM Special publication No. 82. ISBN 1-56576-110-3 p.17-33.

Uruski, C. I. (1992). Sedimentary basins and structure of Cook Strait, Institute of Geological and Nuclear Sciences Report 92/3.

Uruski, C. I. (2010). New Zealand's deepwater frontier. *Marine and Petroleum Geology*, *27*(9), 2005-2026.

Uruski, C., & Wood, R. A. (1993). The Hikurangi Triangle and its effect on the petroleum geology of the East Coast Basin. *Pet. Expl. NZ News*.

Uruski, C. I., Field, B. D., & Funnell, R. (2005). The East Coast Basin of New Zealand, an emerging petroleum province. *The APPEA Journal*, *45*(1), 563-580.

Uruski, C. I., Field, B. D., Funnell, R., Hollis, C., Nicol, A., & Maslen, G. (2006). Developments in the central and northeastern East Coast Basin, North Island, New Zealand. *The APPEA Journal*, *46*(1), 215-236.

Uruski, C. I., & Bland, K. (2010). Pegasus Basin and the prospects for oil and gas. *Unpublished petroleum report PR4326, GNS Science Consultancy Report*, *291*.

Vajda, V., & Raine, J. I. (2010). A palynological investigation of plesiosaur-bearing rocks from the Upper Cretaceous Tahora Formation, Mangahouanga, New Zealand, *Alcheringa: An Australasian Journal of Palaeontology*, 34:3, 359-374,

Van den Heuvel, H. B. (1960). The geology of the Flat Point area, eastern Wairarapa. *New Zealand Journal of Geology and Geophysics*, *3*(2), 309-320.

Van der Lingen, G. J. & Pettinga, J. R. (1980). The Makara Basin: a Miocene slope-basin along the New Zealand sector of the Australian-Pacific obliquely convergent plate boundary. *Sedimentation in Oblique-slip Mobile Zones (Special Publication 4 of the IAS)*, *34*, 191.

van der Meer, Q. H., Storey, M., Scott, J. M., & Waight, T. E. (2016). Abrupt spatial and geochemical changes in lamprophyre magmatism related to Gondwana fragmentation prior, during and after opening of the Tasman Sea. *Gondwana Research*, *36*, 142-156.

Van Dissen, R. J. (1989). *Late Quaternary faulting in the Kaikoura region, southeastern Marlborough, New Zealand.* Unpublished PhD Thesis, Oregon State University.

Van Dissen, R., & Yeats, R. S. (1991). Hope fault, Jordan thrust, and uplift of the seaward Kaikoura Range, New Zealand. *Geology*, *19*(4), 393-396.

van Hinsbergen, D. J., & Koymans, M. R. (2017, April). An online tool on Paleomagnetism. org to test kinematic restorations against paleomagnetic data. In *EGU General Assembly Conference Abstracts* (Vol. 19, p. 10343).

Van Morkhoven, F. P., Berggren, W. A., Edwards, A. S., & Oertli, H. J. (1986). *Cenozoic cosmopolitan deep-water benthic foraminifera* (Vol. 11). Elf Aquitaine.

Van Wagoner, J. C., Posamentier, H. W., Mitchum, R. M. J., Vail, P. R., Sarg, J. F., Loutit, T. S., & Hardenbol, J. (1988). *An overview of the fundamentals of sequence stratigraphy and key definitions*. The Society of Economic Paleontologists and Mineralogists (SEPM).

Vail, P. R. & Mitchum, R. M. Jr (1977). Seismic stratigraphy and global changes of sea level, Part 1: overview. In: *Seismic Stratigraphy – Applications to Hydrocarbon Exploration* (Ed. by C.E. Payton), *American Association of Petroleum Geology Memoirs, 26*, 51–52.

Vella, P., & Collen, J. D. (1998). McLeod Fault: associated monocline and Pliocene angular unconformity, Point Range and Mangaopari Stream, Wairarapa, New Zealand. *Journal of the Royal Society of New Zealand*, *28*(1), 157-164.

Ventura, G.T.; Field, B.D.; Sykes, R. (2013). East Coast Basin Source Rock Properties. GNS Science Data Series 22a.

Ventura, G.T., Scadden, P.G., Heron, D.W., Strogen, D.P., Martin, C., Sykes, R. (2014). An ArcGIS project on petroleum occurrences in New Zealand basins, GNS Science Consultancy Report 2014/226. 43 p. + portable hard drive.

Vetö, I., Demény, A., Hertelendi, E., & Hetényi, M. (1997). Estimation of primary productivity in the Toarcian Tethys—a novel approach based on TOC, reduced sulphur and manganese contents. *Palaeogeography, Palaeoclimatology, Palaeoecology*, *132*(1), 355-371.

Vető, I., Hetényi, M., Hámor-Vidó, M., Hufnagel, H., & Haas, J. (2000). Anaerobic degradation of organic matter controlled by productivity variation in a restricted Late Triassic basin. *Organic Geochemistry*, *31*(5), 439-452.

Vető, I., Ozsvárt, P., Futó, I., & Hetényi, M. (2007). Extension of carbon flux estimation to oxic sediments based on sulphur geochemistry and analysis of benthic foraminiferal assemblages: A case history from the Eocene of Hungary. *Palaeogeography, Palaeoclimatology, Palaeoecology*, *248*(1), 119-144.

Vickery, S., & Lamb, S. (1995). Large tectonic rotations since the Early Miocene in a convergent plate-boundary zone, South Island, New Zealand. *Earth and Planetary Science Letters*, *136*(1-2), 43-59.

Walcott, R. I. (1984). Reconstructions of the New Zealand region for the Neogene. *Palaeogeography, Palaeoclimatology, Palaeoecology*, *46*(1-3), 217-231.

Walcott, R. I. (1987). Geodetic strain and the deformational history of the North Island of New Zealand during the late Cainozoic. *Philosophical Transactions of the Royal Society of London 321*(1557), 163-181.

Walcott, R. I. (1989). Paleomagnetically observed rotations along the Hikurangi margin of New Zealand. In *Paleomagnetic rotations and continental deformation* (pp. 459-471). Springer Netherlands.

Walcott, R. I. (1998). Modes of oblique compression: Late Cenozoic tectonics of the South Island of New Zealand. *Reviews of Geophysics*, *36*(1), 1-26.

Walcott, R. I., Christoffel, D. A., & Mumme, T. C. (1981). Bending within the axial tectonic belt of New Zealand in the last 9 Myr from paleomagnetic data. *Earth and Planetary Science Letters*, *52*(2), 427-434.

Mumme, T. C., & Walcott, R. I. (1985). *Paleomagnetic studies at geophysics division, 1980-1983*. Geophysics Division, Department of Scientific and Industrial Research.

Wallace, L. M., Beavan, J., McCaffrey, R., & Darby, D. (2004). Subduction zone coupling and tectonic block rotations in the North Island, New Zealand. *Journal of Geophysical Research: Solid Earth*, *109*(B12).

Wallace, L. M., Beavan, J., McCaffrey, R., Berryman, K., & Denys, P. (2007). Balancing the plate motion budget in the South Island, New Zealand using GPS, geological and seismological data. *Geophysical Journal International*, *168*(1), 332-352.

Wallace, L. M., Ellis, S., & Mann, P. (2009). Collisional model for rapid fore-arc block rotations, arc curvature, and episodic back-arc rifting in subduction settings. *Geochemistry, Geophysics, Geosystems*, *10*(5).

Wallace, L. M., Barnes, P., Beavan, J., Van Dissen, R., Litchfield, N., Mountjoy, J., ... & Pondard, N. (2012). The kinematics of a transition from subduction to strike-slip: An example from the central New Zealand plate boundary. *Journal of Geophysical Research: Solid Earth*, *117*(B2).

Waterhouse, J. B., & Bradley, J. (1957). Redeposition and slumping in the Cretaceo-Tertiary strata of SE Wellington. In: *Transactions of the Royal Society of New Zealand* (Vol. 84, No. 3, pp. 519-548).

Webb, P. N. (1966). *New Zealand Late Cretaceous foraminifera and stratigraphy*. Utrecht, Schotanus and Jens NV. 19 p.

Webb, P. N. (1971). New Zealand Late Cretaceous (Haumurian) foraminifera and stratigraphy: A summary. *New Zealand Journal of Geology and Geophysics 14*: 795-828.

Webby, B. D., & Van Den Heuvel, H. B. (1965). Note on glauconitic sandstones in the Wairarapa, New Zealand. *New Zealand Journal of Geology and Geophysics*, *8*(1), 81-84.

Webby, B. D. (1969). Trace fossils Zoophycos and Chondrites from the tertiary of New Zealand. *New Zealand Journal of Geology and Geophysics*, *12*(1), 208-214.

Wedepohl, K. H. (1971). Environmental influences on the chemical composition of shales and clays. *Physics and Chemistry of the Earth*, *8*, 305-333.

Wehausen, R., & Brumsack, H. J. (1999). Cyclic variations in the chemical composition of eastern Mediterranean Pliocene sediments: a key for understanding sapropel formation. *Marine Geology*, *153*(1), 161-176.

Wellman, H. W. (1959). Divisions of the New Zealand Cretaceous. *Transactions of the Royal Society of New Zealand 87*: 99-163.

Wellman, H. W. 1971: Age of the Alpine Fault, New Zealand. *Proceedings of the 22nd International Geological Congress (India 1965) 4*: 148-162.

Welles, S. P. & Gregg, D. R. (1971). Late Cretaceous marine reptiles of New Zealand. *Records of the Canterbury Museum 9*: 1-111.

Westech Energy Ltd (2001). Hukarere-1 Well Completion Report. PEP38325 *Ministry of Economic Development New Zealand, Unpublished Petroleum Report PR2656*. 385 p.

Whattam, S. A., Malpas, J., Ali, J. R., Lo, C. H., & Smith, I. E. (2005). Formation and emplacement of the Northland ophiolite, northern New Zealand: SW Pacific tectonic implications. *Journal of the Geological Society*, *162*(2), 225-241.

Wiffen, J. (1980). Moanasaurus, a new genus of marine reptile (Family Mosasauridae) from the Upper Cretaceous of North Island, New Zealand. *New Zealand Journal of Geology and Geophysics 23*, 507– 528.

Wiffen, J. (1981). The first Late Cretaceous turtles from New Zealand. *New Zealand Journal of Geology and Geophysics 24*, 293–299.

Wiffen, J. (1983). The first record of Pachyrhizodus caninus Cope (Order Clupeiformes) from the Late Cretaceous of New Zealand. *New Zealand Journal of Geology and Geophysics 26*, 109–119.

Wiffen, J. (1990a). *Moanasaurus mangahouangae* or *Mosasaurus mangahouangae*? *New Zealand Journal of Geology and Geophysics 33*, 87–88.

Wiffen, J. (1990b). New mosasaurs (Reptilia; Family Mosasauridae) from the Upper Cretaceous of North Island, New Zealand. *New Zealand Journal of Geology and Geophysics 33*, 67–85.

Wiffen, J. (1991). *Valley of the Dragons: the Story of New Zealand's Dinosaur Woman*, Random Century, Auckland, 128 pp.

Wiffen, J. (1996). Dinosaurian palaeobiology: a New Zealand perspective. *Memoirs of the Queensland Museum 39*, 725–731.

Wiffen, J. (2003). The Mangahouanga Stream fossil site. *Geological Society of New Zealand Newsletter 131*, 5–13.

Wiffen, J., & Moisley, W. L. (1986). Late Cretaceous reptiles (Families Elasmosauridae and Pliosauridae) from the Mangahouanga Stream, North Island, New Zealand. *New Zealand Journal of Geology and Geophysics 29*: 205–252.

Wiffen, J. & Molnar, R. E. (1988). First pterosaur from New Zealand. *Alcheringa 12*, 53–59.

Wiffen, J. & McKee, J. W. A. (1990). Mangahouanga Stream – Cretaceous vertebrate site. In: *Geological Society of New Zealand Annual Conference, 26–30 November 1990, Napier, New Zealand: Conference Field Trips*, H.J. Campbell, B.W. Hayward & D.C. Mildenhall, eds, Geological Society of New Zealand Miscellaneous Publication 50b, 189–202.

Wiffen, J., De Buffrinil, V., De Ricqls, A. & Mazin, J. M. (1995). Ontogenetic evolution of bone structure in Late Cretaceous Plesiosauria from New Zealand. [Modifications ontogenetiques de la structure osseuse chez les plesiosaures du Cretace terminal de Nouvelle-Ze1ande]. *Geobios 28*, 625–640.

Wignall, P. B. (1991). Test of the concepts of sequence stratigraphy in the Kimmeridgian (Late Jurassic) of England and northern France. *Marine and Petroleum Geology*, *8*(4), 430-441.

Wilson, D. D. (1963). Geology of Waipara subdivision. *New Zealand Geological Survey Bulletin 64*. 122 p.

Wilson, G. J. (1988). *Paleocene and Eocene dinoflagellate cysts from Waipawa, Hawkes Bay, New Zealand* (No. 57). New Zealand Geological Survey.

Wilson, G. J. (1989). Dinoflagellate assemblages from the Urewera Group. *New Zealand Journal of Geology and Geophysics 32*: 525–526.

Wilson, A. (2004). Geology of the coastal hills of Ward, Marlborough. BSc Honors thesis submitted to Trinity College. 45 p.

Wilson, G. J., & Moore, P. R. (1988a). Cretaceous–Tertiary boundary in the Te Hoe River area, western Hawkes Bay. *New Zealand Geological Survey Record*, *35*, 34-37.

Wilson, G. J., Moore, P. R., & Isaac, M. J. (1988b). Age of greywacke basement in the Urewera Ranges, eastern North Island. *New Zealand Geological Survey Record 35*: 29–33.

Wilson, G. J., Morgans, H. E. G., & Moore, P. R. (1989). Cretaceous-Tertiary boundary at Tawanui, southern Hawkés Bay, New Zealand. *New Zealand Geological Survey Record*, *40*, 29-40.

Wilson, G. J., Schiøler, P., Hiller, N., & Jones, C. M. (2005). Age and provenance of Cretaceous marine reptiles from the South Island and Chatham Islands, New Zealand. *New Zealand Journal of Geology and Geophysics*, *48*(2), 377-387.

Wilson, C. J. N., Houghton, B. F., McWilliams, M. O., Lanphere, M. A., Weaver, S. D., & Briggs, R. M. (1995). Volcanic and structural evolution of the Taupo Volcanic Zone, New Zealand: a review, *Journal of Volcanology and Geothermal Research* 68, 1–28.

Wilson, C. J., & Rowland, J. V. (2016). The volcanic, magmatic and tectonic setting of the Taupo Volcanic Zone, New Zealand, reviewed from a geothermal perspective. *Geothermics*, *59*, 168-187.

Wing, B. A., & Halevy, I. (2014). Intracellular metabolite levels shape sulfur isotope fractionation during microbial sulfate respiration. *Proceedings of the National Academy of Sciences*, *111*(51), 18116-18125.

Wood, R., Lamarche, G., Herzer, R., Delteil, J., & Davy, B. (1996). Paleogene seafloor spreading in the southeast Tasman Sea. *Tectonics*, *15*(5), 966-975.

Wood, R. A., & Stagpoole, V. M. (2007). Validation of tectonic reconstructions by crustal volume balance: New Zealand through the Cenozoic. *Geological Society of America Bulletin*, *119*(7-8), 933-943.

Wright, I. C. (1993). Pre-spread rifting and heterogeneous volcanism in the southern Havre Trough back-arc basin. *Marine Geology*, *113*(3-4), 179-200.

Wright, I. C. (1994). Nature and tectonic setting of the southern Kermadec submarine arc volcanoes: An overview. *Marine Geology*, *118*(3-4), 217-236.

Wright, I. C., & Walcott, R. I. (1986). Large tectonic rotation of part of New Zealand in the last 5 Ma. *Earth and Planetary Science Letters*, *80*(3-4), 348-352.

Yamada, R., Tagami, T., Nishimura, S. & Ito, H. (1995). Annealing kinetics of fission tracks in zircon: an experimental study. *Chemical Geology,* 122: 249–258.

Young, M. (1999). Dating the dinosaurs: palynology of the Maungataniwha Sandstone, northwestern Hawke's Bay. In: *Geological Society of New Zealand Inc 1999 Annual Conference, 29 November–1 December, Massey University, Palmerston North: Programme and Abstracts*, C. WALLACE, ed., Geological Society of New Zealand Miscellaneous Publication 107A, 178.

Young, M. D. & Hannah, M. J. (2010). Dinoflagellate biostratigraphy of the vertebrate fossil-bearing Maungataniwha Sandstone, northwest Hawke's Bay, New Zealand. *New Zealand Journal of Geology and Geophysics 53*, 81–87.

Zheng, Y., Anderson, R. F., van Geen, A., & Fleisher, M. Q. (2002). Remobilization of authigenic uranium in marine sediments by bioturbation. *Geochimica et Cosmochimica Acta*, *66*(10), 1759-1772.

Zhou, L., Wignall, P. B., Su, J., Feng, Q., Xie, S., Zhao, L., & Huang, J. (2012). U/Mo ratios and δ 98/95 Mo as local and global redox proxies during mass extinction events. *Chemical Geology*, *324*, 99-107.

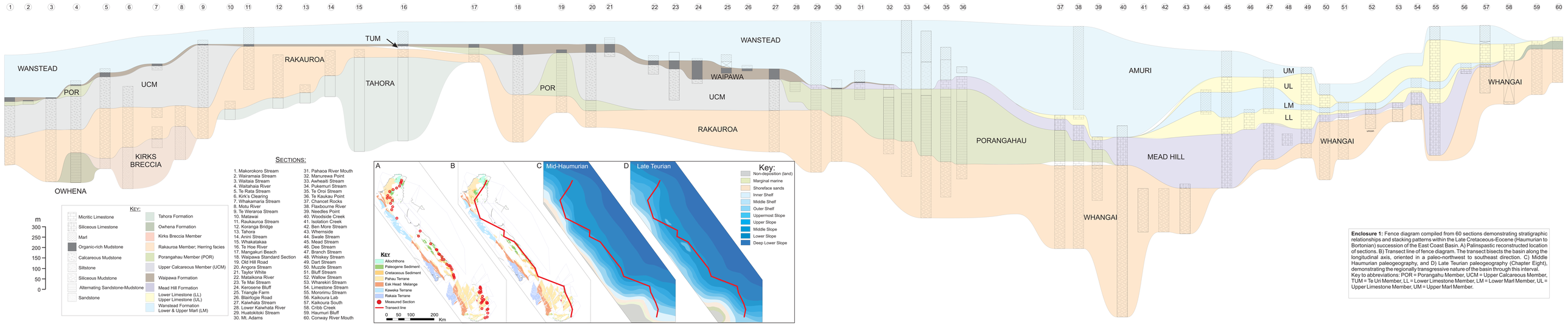

Enclosure 1: Fence diagram compiled from 60 sections demonstrating stratigraphic relationships and stacking patterns within the Late Cretaceous-Eocene (Haumurian to Bortonian) succession of the East Coast Basin. A) Palinspastic reconstructed location of sections. B) Transect line of fence diagram. The transect bisects the basin along the longitudinal axis, oriented in a paleo-northwest to southeast direction. C) Middle Haumurian paleogeography, and D) Late Teurian paleogeography (Chapter Eight), demonstrating the regionally transgressive nature of the basin through this interval. Key to abbreviations: POR = Porangahu Member, UCM = Upper Calcareous Member, TUM = Te Uri Member, LL = Lower Limestone Member, LM = Lower Marl Member, UL = Upper Limestone Member, UM = Upper Marl Member.